

Open Research Online

The Open University's repository of research publications and other research outputs

Patterns of Foraminiferal Micro-evolution and Enviromental Change in the Lower Chalk

Thesis

How to cite:

Johnston, Russell (2005). Patterns of Foraminiferal Micro-evolution and Enviromental Change in the Lower Chalk. PhD thesis The Open University.

For guidance on citations see [FAQs](#).

© 2005 The Author



<https://creativecommons.org/licenses/by-nc-nd/4.0/>

Version: Version of Record

Link(s) to article on publisher's website:

<http://dx.doi.org/doi:10.21954/ou.ro.0000e8d6>

Copyright and Moral Rights for the articles on this site are retained by the individual authors and/or other copyright owners. For more information on Open Research Online's data [policy](#) on reuse of materials please consult the policies page.

oro.open.ac.uk

UNRESTRICTED

Patterns of Foraminiferal Micro-evolution and Environmental Change in the Lower Chalk

A thesis submitted for the degree of Doctor of Philosophy

Russell Johnston
BSc. (Hons) Geology
Manchester University

Department of Earth Science
The Open University

AUTHOR NO M7137842

DATE OF SUBMISSION 7 OCTOBER 2004

DATE OF AWARD 16 JUNE 2005

ABSTRACT

Patterns of Foraminiferal Microevolution and Environmental Change in the Lower Chalk

The research tests Sheldon's *Plus ça change* model by tracking a single fossil lineage through a succession of marine environments showing geological-scale differences in background stability. Orbitally driven cyclic sediments of Cenomanian age, predominantly recording a 20 kyr precessional shift, provide both the time-frame and the main engine of environmental variability, although transgressive pulses and other events are also superimposed. The cyclicity provides spectacular geographical and temporal control, allowing a million-year sequence to be sampled at 100 kyr intervals at three laterally adjacent sites, and partially sampled at 20 kyr and 2 kyr intervals at one of these sites. The lineage of interest is a benthic agglutinated foraminiferan, *Tritaxia pyramidata*, which occurs in prolific numbers; additional ecological evidence comes from a large microfossil database recovered from the same samples.

The Lower Chalk benthic microfauna have very stable patterns of relative abundance, with the same species occurring in similar proportions for at least a million years. Analysis of *Tritaxia*'s ecology identifies it as an *r*-selected generalist playing a keystone role in the community. During development, *Tritaxia* exhibits a persistent tendency to uncoil, but this tendency is strongly manifest only after average life expectancy, leading to its interpretation as a construction mistake rather than a product of design. This developmental quirk sheds light on the grain and texture of the morphospace through which *Tritaxia* is forced to navigate, significantly limiting its evolutionary potential. The result is a lineage that achieves a million years' worth of wobbly stasis, largely because it is boxed into a small corner of morphospace by the joint influence of a narrow developmental channel and competitive interference from other species.

The dynamics of this process predominantly support the *Plus ça change* model, even though not all the predicted patterns are found.

Acknowledgements

This project has been a vast personal odyssey and it would be impossible to remember all the people along the way who have contributed in some form or another. I shall do my best.

For professional help both in the field and in getting the project up and running, thanks go to Andy Gale, Malcolm Hart, David Horne, Simon Mitchell, Chris Paul, Paul Pearson, Norman Peake, Iain Slipper, and Chris Wood; Ed Hathorne helped me take the SEM shots. Many, many thanks go to my supervisors, Peter Sheldon and Peter Skelton, along with numerous other people within the OU's administrative framework who supported my work, even when it had passed well outside the bounds of any normal research studentship.

Peter Sheldon deserves particular acclaim for the role he played; in many ways this project is as much his success as it is mine. I've heard it said that British PhDs are somewhat like traditional apprenticeships, with the student gradually soaking up their supervisor's attitudes and values as the research progresses. I sincerely hope it is true. Peter is the epitome of the gentleman scientist: honest, generous, scrupulously fair, and utterly dedicated to the quality of work he produces. If any of that has rubbed off on me, I am deeply grateful. His support has been unwavering; without it I would have given up long ago. Peter, thank you so much.

Equal thanks go to those who have given me emotional support throughout the years. The way this project was accomplished required a good deal of waywardness on my part, and an absolute determination not to give in to naysayers. Whenever the lowing herd had worn me down, the love of a small core of people (they know who they are) would re-inflate me and have me grinning mischievously to myself. My true friends: I'll never know what I did to deserve even one of you, let alone the whole bunch. I love you dearly and I miss you all.

Now, in various categories and starting to name some names: thumbs up to the Newts (Treez, Em, Mike, Rob); cheers to the awesome foursome (Phil, Mike, and Ben being the other three); praise be for the babes (Kirstein, Butts, Elric, Claire, Jane, Nickers, and the lovely Liz Kennedy); commiserations to all the other poor buggers who've had to live with me over the years (H, Monty, Adele, Allister, Rufus, John, Chris, Ness, Aaron, Mingers, Mino, Mozzer, Margo, and Muttley); a shiver from my liver to the party animals (Mikey B, Chez, the Vic Crew, the Sopha People, the Sensorialites).

Thanks also to all those who have engaged me in earnest discussion about just what on earth is going on on Earth —yup, it spins me out as much as it does you (Aaron, Arun, Ayres, Blando, Deborah, Johnny-no-shoes, Littlewood, Monty, Peter, and Zig). Particular acknowledgement goes to Yvette Evans, who has unquestionably contributed more to the thinking in this project than any other person. This is your philosophy too, Yvette, and though we're pushing at different boundaries now, we're still pushing in the same direction. Good luck.

To the various loves (all categories) who have teased me apart and spread me across the world (Emma P., Emma D., Yvette, and Nessie), thank you sweethearts. Thanks especially to Caitlin, who represents an opening of the future rather than a closing of the past, and who therefore shouldn't really be part of a retrospective at all. Caitlin introduced me to the poem overleaf, and all that goes with it. Lastly, thanks to my long-suffering parents who had no idea what *K*-strategy entailed before they found out the hard way. It's every parent's wish to want something better for their kids; the life I've lead has surpassed (okay, sometimes bypassed) all expectations, largely because of the care and trust I was given in my early years. Thanks for teaching me how to see the world; I'll try to help others to see it too.

This project was sponsored by NERC, the DSS, and my Mum.

WINTERGREEN RIDGE

Where the arrows
of the roadsigns
lead us

Life is natural
in the evolution
of matter

Nothing supra-rock
about it
simply

butterflies
are quicker
than rock

Man
lives hard
on this stone perch

by sea
imagines
durable works

in creation here
as in the centre
of the world

let's say
of art
We climb

the limestone cliffs...

Excerpt from a poem by Lorine Niedecker (1903-1970).

TABLE OF CONTENTS

Part I Context

Thesis Introduction - 1

Chapter 1 History and Opinion

Introduction - 2

1.1 Established Perspectives - 3

1.1.1 The Status of Palaeontology in Modern Biology - 3

1.1.2 Punctuated Equilibrium: an Alternative to Phyletic Gradualism? - 4

1.1.3 An Introduction to the Straw Man - 9

1.1.4 Plain Tales from the Field - 13

1.1.5 Mechanisms of Morphological Control - 18

1.2 A New Perspective - 25

1.2.1 *Plus ça change* - 25

1.2.2 Predictions of the Model - 29

1.2.3 Testing *Plus ça change* - 31

1.2.4 Thesis Structure - 33

Summary - 34

Part II Ecology

General Introduction - 36

Chapter 2 Environment and Organism

Introduction - 38

2.1 A Physical Context for *Plus ça change* - 38

2.1.1 The Sediment - 38

2.1.2 Bedding Style - 40

2.1.3 Causes of Cyclicity - 41

2.1.4 Correlation and Stratigraphy - 46

2.1.5 Palaeogeography - 49

2.1.6 Palaeoceanography - 51

2.2 A Biological Context for *Plus ça change* - 54

2.2.1 Ecological Structure-Top Down - 54

2.2.2 Ecological Structure-Bottom Up - 56

2.2.3 Foraminifera in the Food Chain - 62

2.2.4 Niche Partitioning - 64

2.2.5 From Ecology to Palaeoecology - 66

2.2.6 Paleocological Events in the Mid-Cenomanian Chalk Sea - 71

Summary - 74

Chapter 3 Fossils from the Lower Chalk

Introduction - 76

3.1 Method - 77

3.1.1 Location of Sampling Points - 77

3.1.2 Sampling - 78

3.1.3 Sample Preparation - 79

3.1.4 Collection and Identification of Specimens - 80

3.2 Analysis - 82

3.2.1 Relative Abundance - 82

3.2.2 Absolute Abundance - 82

3.2.2.i Compensation in a single couplet - 83

3.2.2.ii Compensation between couplets - 86

3.2.3 Measures of Diversity - 88

3.2.4 Timeseries Analysis - 89

3.2.4.i Measures of Irregularity and Variation - 89

3.2.4.ii Correlations - 91

3.2.5 Preservational Noise - 91

3.2.6 Presentation of Results - 96

3.3 Results: Presentation and Discussion - 100

3.3.1 2 kyr Resolution: A Single Couplet - 100

3.3.1.i Physical Characteristics - 100

3.3.1.ii Community Structure - 101

3.3.1.iii General Diversity - 104

3.3.1.iv Absolute and Relative Abundances per Taxon - 106

3.3.2	20 kyr Resolution: A Short Transect - 108
3.3.2.i	Physical Characteristics - 108
3.3.2.ii	Community Structure - 109
3.3.2.iii	General Diversity - 110
3.3.2.iv	Absolute and Relative Abundances per Taxon - 110
3.3.3	100 kyr Resolution: Three Long Transects - 113
3.3.3.i	Physical Characteristics - 113
3.3.3.ii	Community Structure - 113
3.3.3.iii	General Diversity - 114
3.3.3.iv	Absolute and Relative Abundances per Taxon - 115
3.3.4	Combined Scales - 119
3.3.4.i	Physical Characteristics - 120
3.3.4.ii	Community Structure - 121
3.3.4.iii	General Diversity - 122
3.3.4.iv	Absolute and Relative Abundances per Taxon - 122
	Summary - 123

Chapter 4 A Palaeoecological Reconstruction

Introduction - 125

4.1 The Geometry of the Chalk Sea Micro-community - 125

- 4.1.1 Axis 1: r and K - 126
- 4.1.2 Axis 2: Specialists and Generalists - 131
- 4.1.3 Axis 3: Competition and Co-operation - 135
- 4.1.4 A Periodic Table of Niches - 141
- 4.1.5 Universal Niche Structure - 146

4.2 Ecological Control: Inside or Out? - 151

- 4.2.1 Assemblages or Communities? - 151
- 4.2.2 External Control - 153
- 4.2.3 Internal Control - 156
- 4.2.4 Scaling and Stability - 160
 - 4.2.4.i. Scaling - 160
 - 4.2.4.ii. Stability - 165

4.3 Stability Regimes in the Lower Chalk - 173

4.3.1 Milankovitch Cyclicality and Primary Productivity - 173

4.3.2 Distribution of Variations in Cyclicality - 177

4.3.3 Distribution of Aperiodic Events - 181

4.3.4 Faunal Response - 183

Summary - 189

Part III Development

General Introduction - 191

Chapter 5 Living Matter

Introduction - 192

5.1 Foraminifera - 192

5.1.1 The Living Foraminiferan - 192

5.1.2 Reproduction - 194

5.1.3 Functions of the Test - 195

5.1.4 Test Construction - 197

5.2 Aboutness and Context - 198

5.2.1 One Domain, Two Descriptions - 198

5.2.2 Functional Context - 202

5.2.3 Compression and Representation - 205

5.2.4 Resource Granularity - 208

5.3 Two Landscape Concepts - 210

5.3.1 State Spaces - 210

5.3.2 Fitness Landscapes - 214

5.3.3 Epigenetic Landscapes - 216

5.3.4 Zeroing-in - 221

5.4 Information and Economy - 224

5.4.1 The Cost of Information - 224

5.4.2 Information Hierarchy - 226

5.4.3 External Offloading - 229

5.4.4 Internal Offloading - 231

5.5 The Shape of Life - 233

5.5.1 Progress and Directionality - 233

5.5.2 The 'Open' End to Life - 237

5.5.3 Melting Metaphors - 241

5.5.4 A Theory in Search of a Metaphor - 244

Summary - 248

Chapter 6 *Tritaxia pyramidata*

Introduction - 249

6.1 Morphology in 3 Dimensions - 249

6.1.1 *Tritaxia* in the Literature - 249

6.1.2 Choice of Characters - 251

6.1.3 Character Measurements - 253

6.1.3.i Exotic Growth Types - 253

6.1.4 The Platonic Foram - 266

6.2 *Tritaxia* in 4 Dimensions - 270

6.2.1 Growth and the Problem of Age Dependency - 270

6.2.2 Character Correlations in General - 272

6.2.2.i Association of Continuous Variables - 274

6.2.2.ii Association of Categorical Variables - 277

6.2.2.iii Associations Between Both Variables - 282

6.2.3 Allometry: Separating Constants from Magnitudes - 283

6.2.4 Visualising Morphological Spaces - 288

Summary - 296

Chapter 7 A Lifeline

Introduction - 297

7.1 Growth Sequence in *Tritaxia* – 297

7.2 Some Bones of Contention - 308

7.2.i One or More Species? - 308

7.2.ii One or More Generations? - 311

7.3	Distribution in Morphospace - 312
7.3.i	Continuity: A Single Species - 313
7.3.ii	Discontinuity: Teratism - 316
7.4	A Mechanism for Chamber Formation - 318
7.5	The Fabric of Morphospace - 323
	Summary - 331

Part IV Evolution

	General Introduction - 332
--	----------------------------

Chapter 8 Changes Through Time

	Introduction - 333
--	--------------------

8.1	Method and Analysis - 333
-----	---------------------------

8.1.1	Sample Populations - 333
-------	--------------------------

8.1.2	Summarising Data - 335
8.1.2.i	Sizes - 335
8.1.2.ii	Shapes - 336
8.1.2.iii	Trajectories - 336
8.1.2.iv	Categories - 336

8.1.3	Measuring Difference - 337
8.1.3.i	Size and Shape - 337
8.1.3.i.a	<i>t</i> tests - 338
8.1.3.i.b	<i>F</i> tests - 339
8.1.3.i.c	<i>haldanes</i> - 339
8.1.3.ii	Trajectories - 341
8.1.3.ii.a	<i>Z</i> tests - 341
8.1.3.iii	Categorical Variables - 341
8.1.3.iii.a	Statistical tests - 341
8.1.3.iii.b	Percentage similarity - 342

8.1.4	Statistical Summaries - 343
8.1.4.i	<i>t</i> , <i>F</i> and <i>Z</i> tests: Appendix Tables - 343
8.1.4.ii	Fields of Possible Combination - 346
8.1.4.iii	Rates of Change - 348
8.1.4.iv	Similarity Scores - 350

8.1.5	Presentation of Results - 351
8.1.5.i	Evolutionary Timeseries - 351
8.1.5.ii	Presentation Format - 352
8.1.5.iii	'Scalar' and 'Vector' Values - 354
8.1.5.iv	Correlations - 355
8.1.6	Presentation Sequence - 362
8.1.7	Preservational Noise - 363
8.2	Results - 365
8.2.1	2 kyr Resolution: A Single Couplet - 365
8.2.1.i	Individual patterns - 365
8.2.1.i.a	Size - 365
8.2.1.i.b	Shape - 367
8.2.1.i.c	Trajectory - 368
8.2.1.i.d	Categorical - 369
8.2.1.ii	Systematic patterns - 370
8.2.1.iii	Environmental patterns - 371
8.2.2	20 kyr Resolution: A Short Transect - 375
8.2.2.i	Individual patterns - 375
8.2.2.i.a	Size - 375
8.2.2.i.b	Shape - 377
8.2.2.i.c	Trajectory - 378
8.2.2.i.d	Categorical - 378
8.2.2.ii	Systematic patterns - 379
8.2.2.iii	Environmental patterns - 380
8.2.3	100 kyr Resolution: Three Long Transects - 382
8.2.3.i	Individual patterns - 382
8.2.3.i.a	Size - 382
8.2.3.i.b	Shape - 387
8.2.3.i.c	Trajectory - 389
8.2.3.i.d	Categorical - 391
8.2.3.ii	Systematic patterns - 393
8.2.3.iii	Environmental patterns - 395

8.2.4 Combined Scales - 400

8.2.4.i Individual patterns - 400

8.2.4.i.a Size - 400

8.2.4.i.b Shape - 402

8.2.4.i.c Trajectory - 403

8.2.4.i.d Categorical - 403

8.2.4.ii Systematic patterns - 405

8.2.4.iii Environmental patterns - 408

Summary - 409

Chapter 9 Flexibility and the Fabric of Morphospace

Introduction - 411

9.1 A Summary of Morphological Change - 411

9.1.1 Growth Curves Reconsidered - 411

9.1.2 Parameter Malleability - 416

9.2 Morphometric Correlations - 419

9.2.1 Signal or Noise? - 419

9.2.2 Heterochrony and Heterotopy - 423

9.2.2.i Size Shifts - 423

9.2.2.ii Shape Shifts - 427

9.2.2.iii Trajectory Shifts - 433

9.2.2.iv Category Shifts - 453

9.3 Timeframes - 436

9.3.1 Stasis and Change on Different Scales - 436

9.3.2 The Tension Between Stasis and Change - 442

9.4 Macroscopic Pattern - 446

9.4.1 Time: The Long-term Signal - 446

9.4.2 Space: The Basin-wide Signal - 450

9.5 Summing Up - 460

9.5.1 Age (or Stage) Dependency Again - 460

9.5.2 Tritaxia in the Round - 470

Summary - 474

Chapter 10 The Mechanics of Morphological Change

Introduction - 476

10.1 Causes of Change - 476

10.1.1 Ecophenotypic Change - 476

10.1.2 Cline Shifts - 479

10.1.3 Directional Selection - 483

10.1.4 Neutral Drift - 486

10.2 Causes of Stasis - 490

10.2.1 Development Constraint - 490

10.2.2 Stabilizing Selection - 493

10.2.3 Coordinated Stasis - 496

10.2.4 Ecological Locking - 498

10.3 *Plus ça change* - 500

10.3.1 Whither *Plus ça change*? - 501

10.3.2 A Suggestion - 505

Summary - 508

References – 510

Appendix – Separate Volume

List of Text Figures

1.1 Fisher's Microscope in schematic form. 10

1.2 *Plus ça change* diagram. 25

1.3 *Plus ça change* prediction for a single lineage. 29

2.1 Sketch of a typical chalk-marl couplet. 41

2.2 Gale's Stratigraphic Scheme for the Cenomanian. 48

2.3 Ocean current systems in the Chalk Sea. 49

2.4 Isopach map of the Lower Chalk. 50

2.5 Important boundary points in an organism's environment. 57

2.6 One, two and three dimensional niche spaces. 58

2.7 Ecological granularity. 59

2.8 Ecological patterns at different temporal resolutions. 68

2.9 Palaeoecological translation between space and time. 70

2.10 Reconstruction of Cenomanian benthic environment. 72

3.1 Conversion of initial numbers of specimens to absolute numbers via the within couplet method. 85

3.2 Conversion of initial numbers of specimens to absolute numbers via the between couplet method. 87

3.3 Polarity, Irregularity and Range (after McShea 1991). 90

3.4 Taphonomy and deposition rate compensation. 94

3.5 Various methods of presenting relative abundance data. 103

3.6 Various end points of diversity metrics. 105

4.1 Simulated faunal response to an input of resources. 127

4.2 Simulated faunal response to variations in the input of resources. 129

4.3 Theoretical yearly floral and faunal response to Milankovitch cyclicity and their time averaged empirical counterparts. 130

4.4 Irregularity index values for foraminiferal relative abundance. 134

- 4.5 A network showing ecological correlations found in the Lituolacean corner of Text Table 4.1. 140
- 4.6 One small corner of the network shown in Text Figure 4.5. 140
- 4.7 The whole network of ecological correlations for foraminifera shown in Text Table 4.1 as a matrix of absolute versus relative abundances. 142
- 4.8 Specialists and generalists in a 2 dimensional niche space. 146
- 4.9 The hub-model: an extra dimension is added to Figure 4.8. 147
- 4.10 Correlation between ecological 'connectedness' (correlated ecological behaviour) and 'specialism' (irregularity score). 149
- 4.11 Absolute abundance of *Dorothia gradata* versus relative abundance of *Tritaxia pyramidata*: a negative ecological correlation. 157
- 4.12 Irregularity index values for foraminifera across a range of sampling points at different sampling resolutions. 161
- 4.13 Polarity index values for foraminifera across a range of sampling points at different sampling resolutions. 163
- 4.14 Distribution of relative abundance values for *Tritaxia pyramidata*. 164
- 4.15 Distribution of relative abundance values for various (other) foraminiferal taxa. 166
- 4.16 A positive correlation between carbonate and clay. 175
- 4.17 The relationship between nutrient availability (clay), precessional effects and productivity (carbonate). 176
- 4.18 Several measures of sedimentary variation in the chalk-marl cycles. 177
- 4.19 Fine detail A.I.R. profile of the Folkestone study section. 179
- 4.20 Spindle diagrams of variability in cycle strength and thickness. 180
- 5.1 Cross section of an infaunal agglutinating foraminiferan in life position. 193
- 5.2 Two set theoretic representations of isomorphic overlap. 202
- 5.3 Two versions of a three dimensional binary state space. 211
- 5.4 A five place holder binary 'hypercube'. 212
- 5.5 Causal arrows marked on a state space – convergence. 213
- 5.6 Causal arrows marked on a state space – divergence. 213
- 5.7 Two state space situations transformed to landscape. 214
- 5.8 Waddington's epigenetic landscape. 218

- 5.9 An epigenetic landscape between two points in state space. 219
- 5.10 The system of interactions underlying the epigenetic landscape. 220
- 5.11 Seilacher's Triangle. 233
- 5.12 Conceptual architecture of a replicator. 238
- 5.13 Two ways of avoiding ecological overlap. 240

- 6.1 Schematic drawing of Tritaxia plus its measured characteristics. 252
- 6.2 Categories for non-metric variables. 256
- 6.3 Various sub-species of Tritaxia reproduced from Jefferies 1962. 258
- 6.4 Growth types: Phase I, type 1— standard triserial growth. 260
- 6.5 Growth types: Phase II, Group A, types 2, 3, & 4— single chamber deviations along the w' dimension. 262
- 6.6 Growth types: Phase II, Group B, types 1.5, 2.5 & 3.5— single chamber deviations along the l' dimension. 263
- 6.7 Growth types: Phase III, types 8, 9 & 10— non-triserial growth incorporating more than one deviant chamber. 265
- 6.8 The 'Platonic Foram'. 268
- 6.9 Model Tritaxia composed of measured character dimensions alone. 269
- 6.10 A positive correlation: H versus W for the entire data set. 275
- 6.11 Chi (square?) plot for *ind.* (indentation) versus *tw.* (twist) in visual format. 280
- 6.12 Curves for different values of allometric parameter. 285
- 6.13 H and W are indeed allometrically related. 287
- 6.14 i & ii The basic measurements can be used to construct even simpler geometric figures. 291
- 6.15 The geometric figures can be used to illustrate various shape ratios. 292
- 6.16 How to interpret a bivariate scatter in terms of shape change. 293
- 6.17 Higher dimensional shapes in their appropriate parts of morphospace. 295

- 7.1 a, b & c Mean character values per chamber number cohort (growth stage), including profiles predicted by growth rate. 299
- 7.2 a-f Comparison between empirical data and derived growth rate extrapolation. 301-303

7.3	Overlay of mean character values and calculated growth rates showing the sigmoidal pattern of the former disguised in the latter.	305
7.4 i - iii	Higher dimensional growth sequences by chamber number.	306
7.5	Relationship between growth type and chamber number.	318
7.6 i - vi	Chamber formation in <i>Tritaxia</i> .	320
7.7	<i>Tritaxia</i> , in situ, building its test.	321
7.8	<i>Tritaxia</i> 's developmental plinth.	326
7.9	Regions of higher dimensional morphospace explored by successive phases of <i>Tritaxia</i> 's development.	328
8.1	Idealised versions demonstrating well-defined patterns on the statistical test grids.	345
8.2	Idealised versions demonstrating the <i>Plus ça change</i> model as a well-defined pattern on the statistical test grids.	346
8.3	A standard method of visualising the relationship between germ-line and phenotype.	352
8.4	The method for statistically assessing timeseries pattern.	357
8.5	Different relationships between size and shape in different halves of the 20 kyr transect.	381
8.6	How the 100 kyr transects split into upper and lower fields.	396
9.1	How size, shape and trajectory parameters relate to one another in terms of an evolutionary timeseries with w' versus h' in C13 as the example.	413
9.2	The trajectory parameters untethered.	415
9.3	Idealised correlations between timeseries patterns.	422
9.4	Mapping shape correlations between bivariate and multi-dimensional morphospaces.	428
9.5	Distribution of evolutionary trajectories in higher dimensional morphospace.	430
9.6	Developmental versus evolutionary trajectories for the l'/w' vs. w'/h' shape ratios.	432
9.7	A negative correlation for trajectory values in the pairing l'/w' vs. w'/h' .	433
9.8	Showing the relationship between the three principle final chamber dimensions.	434
9.9	Rates of change across all three sites and three scales.	437
9.10	Range of values in i) size and ii) shape.	440
9.11	Range of morphological shift in the chamber parameter, h' .	444
9.12	H at all three sites and all three scales.	445

- 9.13 Various interpretations of the relationship between sampled and background changes in morphology. 448
- 9.14 Basin-wide series for sizes. 451
- 9.15 Basin-wides series for shapes. 453
- 9.16 Basin-wide series for trajectory *a* values. 455
- 9.17 Basin-wide series for categorical characters. 456
- 9.18 Character/Ch ratios. 464
- 9.19 Relationship between some aspects of *Tritaxia*'s morphology and ecology. 469
- 9.20 Correlation between exotic growth forms and other morphological parameters. 472

- 10.1 Correlations between exotic growth forms and other species. 489
- 10.2 The sliding puzzle illustration of ecological locking. 500
- 10.3 Macroevoolutionary patterns ripe for *Plus ça change*. 507

List of Text Tables

- 1.1 Patterns of change in the fossil record (From Erwin and Anstey, 1995). – 13
- 1.2 Four key differences in morphological response to environments of varying stability. – 30
- 2.1 Types of ecological interaction. – 55
- 2.2 Distribution and duration of Lower Chalk pulse faunas. – 74
- 3.1 Derivation of absolute specimen numbers via the within couplet method. – 85
- 3.2 Derivation of absolute specimen numbers via the between couplet method. – 87
- 3.3 The relationship between breakage and shape in foraminifera. – 93
- 3.4 Summary of Text Sections and Appendix Figures used to display ecological data. – 97
- 3.5 Sample points labelled by Gale's notation and the temporal notation relevant to this survey. – 98
- 3.6 Taxa exhibiting peaks at different points of a chalk-marl cycle (C13). – 107
- 3.7 Classification of foram absolute abundance patterns across the short (20 kyr) transect. – 111
- 3.8 Summary of pattern classification for ecological fluctuations at 100 kyr resolution. – 117
- 4.1 Correlation matrix for ecological relationships between taxa in the Lower Chalk. – 138
- 4.2 Percentage of correlations found in various subfields of Text Table 4.1. – 139
- 4.3 Classification of taxa according to broad (universal) niche axes. – 144
- 4.4 A selection of placeholders from the 'Periodic Table of Niches'. – 145
- 4.5 Correlation values for various interaction styles as shown in Text Figure 4.10. – 149
- 4.6 Measures of variation in cycle strength and depositional rate between the upper and lower halves of the study section at Folkestone. – 178
- 6.1 Character values for the 'Platonic Foram'. – 268
- 6.2 Correlation coefficients and *t*-statistics for all combinations of metric variables. – 276
- 6.3 Worked example of a chi square test for *ind* versus *tw*. – 278

6.4 Chi square values and confidence levels for all combinations of categorical variables. –	281
6.5 Linear and Disordered cases of significant association in categorical characters. –	282
6.6 Trajectory <i>a</i> and <i>b</i> values for triserial and exotic versions of the Platonic Foram. –	294
7.1 Mean values for size and shape per chamber number cohort. –	298
7.2 Calculated growth rates for size changes during growth. –	300
8.1 Specimen numbers per sample population. –	334
8.2 Generic formats for timeseries correlation grids. –	359
8.3 Specimen numbers per sample for the non-zero category g.dist populations. –	363
8.4 Location of morphometric information for the 2 kyr scale transect. –	365
8.5 Timeseries correlations for size parameters in the 2 kyr transect. –	366
8.6 Timeseries correlations for shape parameters in the 2 kyr transect. –	367
8.7 Timeseries correlations for trajectory parameters in the 2 kyr transect. –	368
8.8 Timeseries correlations for category parameters in the 2 kyr transect. –	369
8.9 Significant differences in the 2 kyr transect –	371
8.10 Summary of statistical tests for lithological sub regions of C13. –	372
8.11 Summary of statistical tests for sub-regions of the 2 kyr and 20 kyr transects. –	373
8.12 Average standard deviation scores in the 2 kyr transect. –	374
8.13 Location of morphometric data for the 20 kyr scale transect. –	375
8.14 Timeseries correlations for size parameters in the 20 kyr transect. –	376
8.15 Timeseries correlations for shape parameters in the 20 kyr transect. –	377
8.16 Timeseries correlations for trajectory parameters in the 20 kyr transect. –	378
8.17 Timeseries correlations for category parameters in the 20 kyr transect. –	379
8.18 Significant differences in the 20 kyr transect. –	380
8.19 Averages for standard deviation scores in the 20 kyr transect. –	381
8.20 Location of morphometric information for the 100 kyr scale transect. –	382
8.21 Timeseries correlations for size parameters in the 100 kyr transects. –	384
8.22 Directions and divergence of change in mean values in the 100 kyr transects. –	385

8.23	Directions and divergence of change in standard deviation in the 100 kyr transects.	– 386
8.24	Timeseries correlations for shape parameters in the 100 kyr transect.	– 388
8.25	Timeseries correlations for trajectory parameters in the 100 kyr transect.	– 390
8.26	Timeseries correlations for category parameters in the 100 kyr transect.	– 392
8.27	Summary of statistical tests for the 100kyr resolution transects.	– 394
8.28	Summary chart showing the distribution of statistical shifts between upper and lower halves of the 100 kyr transects.	– 397
8.29	Summary chart for all statistical findings in the 100 kyr resolution transect.	– 398
8.30	Average standard deviation scores for the 100 kyr transects.	– 399
8.31	Location of morphometric information for the Combined Scales transect.	– 400
8.32	Timeseries correlations for size parameters in the Combined Scales transect.	– 401
8.33	Timeseries correlations for shape parameters in the Combined Scales transect.	– 402
8.34	Timeseries correlations for trajectory parameters in the Combined Scales transect.	– 403
8.35	Timeseries correlations for category parameters in the Combined Scales transect.	– 404
8.36	Summary table showing the density of correlations for morphological measurement parameters from each transect represented in the text.	– 405
8.37	Summary of statistical tests for Folkestone 2 kyr, 20 kyr and 100 kyr transects.	– 407
8.38	Summary table of results for the combined scales split into upper and lower halves.	– 408
9.1	Different patterns in various parameter types.	– 416
9.2	Correlation grids of five overlapping transects.	– 421
9.3	Summary of Text Table 9.4.	– 438
9.4	Ranges of morphological exploration at three sampling scales.	– 439
9.5	Site by site versus amalgamated series statistical differences.	– 458
9.6	Correlations between exotic growth and other morphological parameters.	– 471
10.1	Correlations between exotic growth and other species.	– 487
10.2	Timeseries showing the predicted pattern for <i>Plus ça change</i> .	– 502

Thesis Introduction

Life is not a thing but a process: it is intrinsically dynamic. Fossils, on the other hand, are things—traces of life's endless reworking of the physical matrix. Because processes are fleeting and ever changing, we must often infer the rules that govern them from the things they leave behind. Fossils are virtually the only evidence of life's long history that we have access to, and these are what we must use if we are to infer the rules behind the process of evolution.

Peter Sheldon's *Plus ça change* model (Sheldon, 1996) is a theory about some of those rules; specifically, it is a theory about the rate of evolutionary change in environments of varying stability. It can be tested by using the fossil record to track a species lineage through a succession of environments of differing background stability, where the stability in question is operant on a geological timeframe. The model is somewhat counter-intuitive, claiming that evolution actually proceeds *more slowly* in geologically unstable settings than in environments exhibiting long-term stability. It stands in marked contrast to standard biological explanations of stasis and change, which normally invoke environmental stability to account for the former and environmental instability for the latter. It also stands in contrast to many palaeontological theories; these often appeal to hazily defined 'internal constraints' as the primary engine of morphological transformation, assuming these to be present wherever there is stasis and to have dissolved whenever there is change.

Plus ça change is non-committal about mechanism, being principally a theory about the distribution of things—fossils, and the sedimentary indicators of environmental stability—rather than processes. As such it is a prime candidate for theoretical expansion as well as empirical investigation, and in this document I try to show that an information-theoretic approach can provide a first step on the road to an integrated account of internal and externally driven processes.

As an empirical work, this project tests the *Plus ça change* model by tracking a fossil lineage through three different timeframes, the longest representing a million years of residence in an environment exhibiting both geological-scale stability and instability. The lineage is a benthic, agglutinated foraminiferan called *Tritaxia pyramidata*, and the environment that of a shallow shelf sea, as recorded by the cyclic, chalk-marl sediments of the Cenomanian aged Lower Chalk.

Part I Context

Chapter 1 History and Opinion

Introduction

Psychologist Julian Jaynes (1976) once classified language as “an organ of perception”, and I can think of no clearer way to emphasise the guiding role played by theoretical frameworks than to liken them to mental sense organs whose function it is to filter empirical pattern. Like most palaeontologists, I was initially trained as a geologist, and my first serious appreciation of ‘evolution’ came through the vast panoramas afforded by phylogenetic trees of diversification across the Phanerozoic. I was at least lucky enough to have studied biology at college; goodness knows what my perception of ‘ecology’ would have been had my first introduction come through the kind of staged dioramas used in museums to display Palaeozoic faunal assemblages! I sympathise fully with the confusion felt by students to whom ‘evolution’ means the process of gene replacement in laboratory-bred fruitflies, and ‘ecology’ means metre square grid counts of daisies in meadows, on their first introduction to the fossil record.

Nowadays we all have a much richer appreciation of commonly shared and widely used biological terms, partly because of the realisation that modern scientific disciplines are so swollen that anyone working even marginally outside of a given narrow field is effectively just another educated member of the general public. But the struggle for common understanding is ongoing, and is manifested acutely in the gulf which still exists between palaeontology and neontology (i.e. biology). The principle issue is that well understood and experimentally observable processes occurring over human timespans become nigh inconceivable as explanations when scaled up to a geological framework. Those working at either end of the evolutionary spectrum now appreciate that there is a substantial problem with scaling, but the realisation was slow to dawn and caused a good deal of antagonism on both sides before it was finally acknowledged.

Section 1.1 Established Perspectives

1.1.1 The Status of Palaeontology in Modern Biology

In a 1984 *Nature* article, theoretical biologist John Maynard Smith welcomed palaeontology back to the High Table after an absence of almost a century. Prior to that auspicious event it was probably not clear to most palaeontologists that there even was a High Table at which they should be yearning to sit, but in retrospect it appears that Maynard Smith had a point. In an odd fate for a theory whose originator felt would stand or fall on the basis of fossil evidence (Eldredge, 1995), the first hundred years of Darwinian thinking had been completely swamped by population level mechanics. The centenary of *The Origin* saw a Modern Synthesis dominated by the findings of Mendelian heredity and the ensuing statistical theory of population genetics which was so successfully promoted by Fisher, Haldane and Wright, and later extended to the ecology of natural populations by the likes of Dobzhansky, Mayr and Simpson. The main input from palaeontology was Simpson's early (1944) demonstration that the fossil record was mostly consistent with Darwinian thinking, although he did attempt to outline some major inconsistencies concerning the extrapolation of rates. Later, the identification of DNA as the molecular seat of heritable traits, and the subsequent blossoming of biochemistry, eclipsed most other biological concerns throughout the fifties and sixties.

During this course of developments palaeontologists had indeed been far more frequently on the receiving end of a flow of information and ideas than they had been in a position to contribute; but by the mid-nineteen seventies the tide was finally beginning to turn—a change which Maynard Smith attributes, at least in part, to the notion of *punctuated equilibrium* and the erstwhile work of its creators, Niles Eldredge and Stephen Jay Gould (1972). Punctuated equilibrium was primarily a theory about the appearance of speciation in the fossil record and, as the authors themselves pointed out in a 1977 progress review, “scarcely a revolutionary proposal” (Gould and Eldredge, 1977). This frank admission aside, the zeal with which they set about exorcising the spectre of *gradualism*, a figure which some (e.g. Dawkins, 1986) denounced as a ‘straw man’ but which most took to mean the modern synthesis as a whole, could only beget one result. Fuelled by comments such as

Gould's (in hindsight, foolhardy) assertion (1980a) that Darwinism was "effectively dead", the biological community rose up in wrath and came down heavily on punctuated equilibrium, which one British geneticist dubbed "evolution by jerks" (Turner, 1986).

Even Maynard Smith's benevolent mood was not to last. Using Peter Sheldon's (1987b) report on gradualistic patterns in Ordovician trilobites, he launched a rather scalding attack on the excesses of palaeontology (Maynard Smith, 1987). Focusing on the notion of 'species selection' he concluded that, "there never was much sense in the idea anyway". Naturally this provoked a response (Eldredge and Gould, 1988), and a retort (Maynard Smith, 1988), followed by a 'last word' (Gould and Eldredge, 1988). Nowadays the dinner guests are distinctly sulky: Eldredge (1995) and Gould (2000, 2002) caricature the neontological position as 'Ultra-Darwinism', a form of unremitting reductionism which acknowledges no meaningful entities beyond the gene; Maynard Smith, by comparison, has claimed "Gould ... is a man whose ideas are so confused as to be hardly worth bothering with ..." (quoted from Andrew Brown's Guardian article, March 4th, 1999).

From the perspective of an onlooker with a sympathetic foot in both camps, this is a miserable state of affairs. There is only one history of life, a history that looks like neontology in the short term and palaeontology in the longer; there *must* be a way of reconciling these disparate approaches. This thesis provides a palaeontological contribution to evolutionary thinking by testing the *Plus ça change* model of Sheldon (1996). It presents an integrated theoretical framework based on the idea that life is "the control of matter by information" (Williams, 1992), and examines the topic of evolutionary rate with a data set designed to keep track of processes operating on different timescales. Let us start with Eldredge and Gould's initial claim (1972) about phyletic gradualism versus punctuated equilibrium.

1.1.2 Punctuated Equilibrium: an Alternative to Phyletic Gradualism?

The theory of punctuated equilibrium made its debut in a rather unremarkable guise. Eldredge and Gould's 'Punctuated Equilibria: an alternative to Phyletic Gradualism' (1972) was a topical Kuhnian complaint against the "cloven hoofprint of theory"—a tendency for explanation to generate expectation—and an exhortation for students of palaeontology to record what they saw of evolution, rather than what they thought they

should see. With examples drawn from their own work on Devonian trilobites and Pleistocene land snails, Eldredge and Gould argued that a pattern of morphological stasis, occasionally punctuated by the rapid appearance of new and distinct forms, is what the fossil record really holds, and, indeed, what we should expect given the mechanics of allopatric speciation, the prevailing explanation of lineage splitting.

In Mayr's allopatric model (1963) speciation occurs in peripheral isolates, small demes of a widespread race temporarily partitioned from the main body, perhaps by some geographic barrier. Cut off from the gene pool at large, probably bearing a disproportionate frequency of alleles (the founder effect), and subject to the alien selective pressures of a very insular environment, these strangers in a strange land would speedily evolve to suit the local optimum, thereby achieving ecological differentiation and reproductive isolation, and thus able to form a new species. Irrespective of the timespan involved in this transition (assumed in any case to be short), the majority of the sedimentary, fossil-bearing sequences across the region would record no evidence of it; only if the new species reinvaded large portions of its ancestral range could palaeontologists in years to come expect to see any traces. Thus, the pattern preserved *should* be one of morphological change occurring in bursts, as the fruits of evolution-accomplished-elsewhere spread across broad geographic zones. The new species might or might not replace the old, depending on how sundered the two had become in terms of ecological distance; but whether it did so or not the pattern would be one of stasis with punctuation, and not the gradual and unidirectional picture, a steady transition from ancestor to descendant, expected from a straightforward extrapolation of the Darwinian mechanism alone.

There are a number of separate claims involved in the punctuated equilibrium theory, which, as Lister (1984) pointed out, do not necessarily stand or fall together. The issues of whether evolutionary change occurs mostly in relation to small population size, lineage splitting, or genuine saltation, are distinct from the notion of a particular characteristic transformational rate throughout the history of a single lineage. The various components of Eldredge and Gould's initial mechanism, along with their suggested extrapolations of 'decoupled' macroevolution and species sorting (Gould and Eldredge, 1977; Stanley, 1979; Vrba and Eldredge, 1984; Vrba and Gould, 1986), are still the subject of intense debate (Gould, 2002), but none have been so readily accepted as a genuine problem in biological thinking as the existence of *stasis* (Williams, 1992; Gould and Eldredge, 1993).

Unlike the punctuational elements, stasis can often be demonstrated by fossil material, and whether 'gradualism' as depicted by the palaeontologists had ever existed in the minds of neontologists or not, there has been considerable difficulty in explaining how evolution can be *restrained* over geological timescales. The problem is not that there are a variety of rates, an element anticipated by Darwin himself (4th edition, see Rhodes, 1983), nor even that there is no way within the modern synthesis of accounting for stasis, but rather that the standard mechanism, stabilizing selection, requires a constant environment in order to produce zero change over long periods—and it is hard to envisage an environment, biotic or physical, remaining adequately stable for vast spans of time.

Of course, fossil evidence will always be insufficient to demonstrate that there was absolutely no evolutionary transformation occurring across a species' temporal range: we are rarely ever left with anything other than skeletal material, and so there could have been a wealth of adaptive selection going on in the soft tissues (Schopf, 1982; and see Stanley and Yang, 1987 for evidence that the two can occur independently). But an objection like this misses the real point. At any period in history, organic form, over and above the continuous geographic and environmental variation shown within a species, is distributed among discrete portions of morphological space. This is as true for the hard parts as it is for the entire organism: museum drawers the world over are stuffed with discretely differing skeletons. And so the problem can be cast, if necessary, entirely in terms of hard parts: how did the skeletons, shells, tests and kernels of modern organisms get into such discrete clumps? Darwin gave us a simple and elegant answer which had eluded earlier thinkers, and there is no doubt that he was, by and large, correct. But what had not been anticipated, if Eldredge and Gould are to be believed, is the large portion of its history that a skeleton lineage tends to remain in one discrete state, relative to the amount of time spent transforming between such states. In fact, a rough measure of these relative periods was later advanced by suggesting that speciation (and thus presumably morphological change, since in Eldredge and Gould's model the two are concurrent) should comprise only a percentage or two of a species' total duration, somewhere in the region of 10 000 to 100 000 years (Gould, 1982).

Thinking about evolution in terms of modern species also gives us an indication of the *amounts* of morphological change that should be involved. If there is some degree of transformation across a temporal span, how do we tell if that amount is a little or a lot? There are formal methods of assessing absolute rates of metric transformation (e.g. the units

called *haldanes*) which we shall come to in due course, but as a rule of thumb we can use the measure of variation between modern species as a standard. If the forms seen in a fossil community fall into the kind of discrete clumps we expect modern organisms to, then these are probably all different species; and if a species clump cannot be clearly differentiated from a similar clump which is a million years older or younger, then that obviously amounts to very little change.

This kind of approach has been criticised for reflecting the habits of taxonomists rather than genuine patterns of morphological transformation; but taxonomists as much as anybody else strive to ‘carve nature’ at appropriate and meaningful joints. This is not to confuse the rather separate issues of collection from numerous horizons for the purposes of description (Sheldon, 1993), or the misleading partition of phyletic transformations into arbitrary chunks to fit them onto range charts (Fortey, 1985)—no serious analyst should use those data as a primary source (including Steven Stanley, 1979)—but as Sheldon (1987a) soberly pointed out, if fossil species did not really exist as discrete entities across broad geographic zones and for long periods of time, the Natural History Museum’s popular identification guides to fossils would be useless.

Unfortunately, the ‘alternative’ to punctuation and stasis *has* no meaningful joints to carve at because those joints were exactly the features Darwin had to dissolve in order to convince his contemporaries of the validity of gradual adaptive transformation. Whilst lineage splitting permits us to apply Mayr’s biological species concept as a non-arbitrary ‘joint’, true phyletic speciation does not (Kellogg, 1983). Indeed, it is for precisely this reason that Eldredge and Gould identified speciation with the morphological punctuation they saw in the fossil record.

At this point we need to acknowledge the problem of scaling. During the now famous, 1980 Chicago conference on Macroevolution, one of the main bones of contention concerned what was meant by ‘rapid’ since, as Jones (1981) diplomatically phrased it, “one man’s punctuation is another man’s phyletic gradualism”. In fact, the scale issue bites deep into both aspects of punctuated equilibrium: with regards to punctuation, there is clearly a difference between genuine saltation and a geologically rapid event which in fact takes thousands of generations to complete; and, with regards to equilibrium, there is similarly a difference between true or absolute stasis and approximate or average stasis, in which a continuing sequence of small transformations is repeated over and over but ends up by going nowhere.

To what extent its various proponents see *punctuation* as occurring at a particular scale is, as suggested earlier, a topic of continuing debate, and one which does not much concern this thesis. Apart from the more extreme perspectives (Gould, 1980a, for example, edged towards genuine saltation for a while), the idea of punctuation, if it is allowed to take neontologically acceptable lengths of time, is hardly a contentious issue; but what comes after, morphological stasis for millions of years, certainly is.

Stasis is a phenomenon which only truly appears at a geological resolution, and it should be acknowledged that even hardcore punctuationalists do not insist on absolute stasis, but rather on the approximate or average version. Typically, stasis involves “zero sum net change” (e.g. Lieberman *et al.*, 1995) or the same amount of variation through long periods as a modern species shows throughout its geographic range (e.g. Stanley and Yang, 1987). A comparison of evolutionary rates measured across widely differing timescales shows a very convincing negative correlation (Gingerich, 1983; but see Gould’s criticism, 1984), most plausibly reflecting a tendency for continuous oscillation around a restricted set of morphologies which generates little overall novelty. Indeed, Sheldon (1993) is so convinced of the ubiquity of evolutionary reversal, even within strong directional trends, that he suggests a failure to find one is simply an indication of too coarse a sampling resolution.

The difference between stasis and gradualism (traditional phyletic evolution), therefore, is that whilst both allow for a bit of free movement and oscillatory behaviour, gradualism should achieve the kind of morphological transition typical of speciation (i.e. the distance between most modern species), without there being two highly distinct rates involved, whereas stasis should involve no such transition and consist, most of the time, of only one rate (zero). It is useful, for the purposes of this thesis, to cast this distinction in terms of rates alone because speciation, as we shall see (Chapter 2), is not a necessary component of the *Plus ça change* model. That said, it should also be noted that in many respects it is rather hard to determine whether an organism is exhibiting wobbly stasis or weak gradualism until it has changed sufficiently to decisively rank as two species.

In order to set the *Plus ça change* model in an explanatory context, I shall review some of the attempts to find a satisfactory mechanism behind stasis; but before doing that it will be instructive to examine a bit of classic gradualistic thinking and its extrapolation through time, and then see what patterns the fossil record actually reveals.

1.1.3 An Introduction to The Straw Man

A popular launch-pad for gradualistic thinking is Sir Ronald Fisher's foundational piece of reasoning on the likely magnitude of adaptive change (Fisher, 1930—available as an extract in Ridley, 1997). His starting point is the average organism, which everyone accepts is already quite well adapted to its current setting:

“An organism is regarded as adapted to a particular situation, or to the totality of situations which constitute its environment, only in so far as we can imagine an assemblage of slightly different situations, or environments, to which the animal would on the whole be less well adapted; and equally only in so far as we can imagine an assemblage of slightly different organic forms, which would be less well adapted to that environment.” [But note that the term ‘slightly’ was introduced twice.]

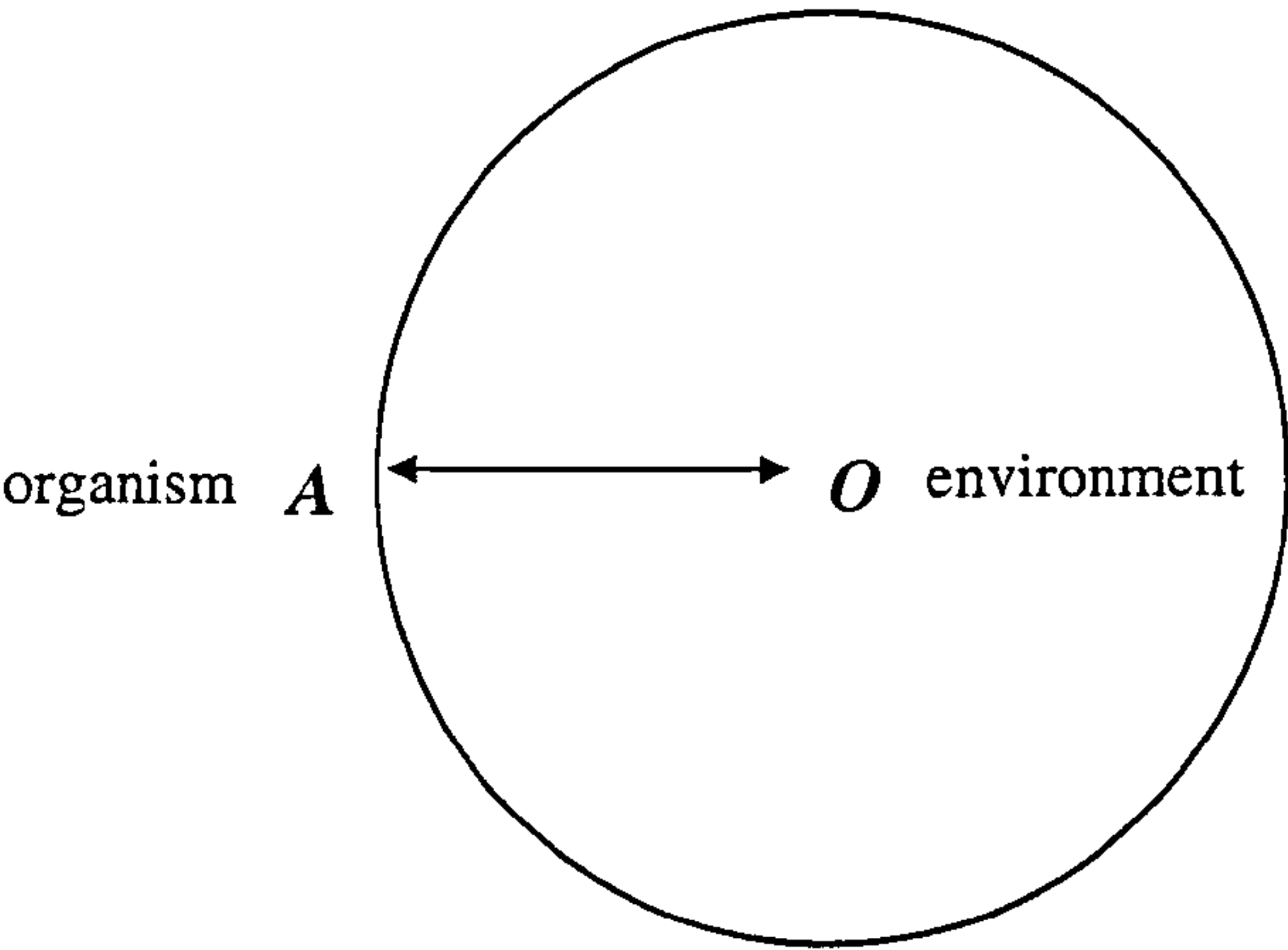
From there he goes on to argue in terms of adaptation, which is metaphorised into a distance between two points, a fixed one corresponding to the environment (which he labels *O*), and a movable one corresponding to the organism (which he labels *A*); the shorter the distance, the greater the degree of adaptation (Text Fig 1.1). For a single dimension of variability, a gene or character, the point *A* can only move in two directions, either towards *O* or in the other direction; but for multiple dimensions, say three, the point will lie on a sphere, with the distance between *A* and *O* being its radius, and it can move to any point, either away from, within, or, significantly, across to the other side of this sphere. If there is an equal probability of *A* spontaneously moving to any other location (an event representing random mutation), the topography of the adaptive sphere allows us to assign a further probability, this time for the chances of such a random move leading to better adaptation (a shorter radius). For infinitesimally small shifts in position the probability of moving inside the sphere is almost 50:50, but as the distance of relocation increases, the probability of a superior adaptive move becomes ever smaller, until, for distances greater than the diameter, the prospects for improvement are zero.

This is great logic, but we should be careful about the propositions, especially the ones which have been introduced implicitly. Why is *A* allowed to move in any direction with an equal probability, for example?; and do the small changes correspond to small changes in adaptation, small changes in phenotype or small changes in genotype, since there is no necessarily linear relationship between the three? Also, small relative to what?

Nevertheless, the reasoning is very persuasive, and to help it along he gives us a more homely metaphor:

“The conformity of these statistical requirements with common experience will be perceived by comparison with the mechanical adaptation of an instrument, such as the microscope, when adjusted for distinct vision. If we imagine a derangement of the system by moving a little each of the lenses, either longitudinally or transversely, or by twisting through an angle, by altering the refractive index and transparency of the different components, or the curvature, or the polish of the interfaces, it is sufficiently obvious that any large derangement will have a very small probability of improving the adjustment, while in the case of alterations much less than the smallest of those intentionally effected by the maker or the operator, the chance of improvement should be almost exactly one half.”

—the elegance of good design, relegated in the last two lines to fine tuning by an agentless cause; no wonder it was revived by Richard Dawkins in *The Blind Watchmaker* (1986), where it appears in the index under ‘Fisher, Sir R. A.—necessity of gradualism’.



Text Figure 1.1 *The relationship between an organism and its environment according to Fisher.*

Fisher’s argument allowed him to translate the complex phenotype-mediated interaction between genes and environment into a single factor, the genetic load or *lag load*. The genetic load is the difference between the mean fitness of the population (comprising all existing genotypes) and that of the optimum genotype available (given the variation present in the total accessible gene pool), and is rendered as a proportion of the optimum.

The ensuing 'fundamental theorem' (a tautology) implies that the rate of evolution will increase as the lag load increases, and as the population average falls behind the optimum (Stenseth, 1985; or see Ridley, 1993 Chapter 7 for further discussion). In terms of the 'adaptive sphere' scenario, the lag load is that portion of the population further away from *O* than the optimum at *A*. Every time a tiny new improvement is found, shifting *A* and *O* closer together, the lag increases and needs to be mopped up by selection.

More important than the argument itself is its fallout in biological attempts to extrapolate through time. Since the feature of interest is simply the distance between Fisher's *A* and *O*, changes in the environment are as likely to be bad as changes in the organism; and since a large part of the environment from any organism's perspective consists of other organisms, we should thus expect a never-ending cascade—the runaway system which Van Valen (1973) likened to the frenetic behaviour of Lewis Carroll's loopy Red Queen. Van Valen used this reasoning to formulate his Law of Constant Extinction, a law which Stenseth and Maynard Smith tried to capture as a formalisation in 1984.

Building on the lag load concept but applying it (at three different timescales) to an entire population of similar loads, Stenseth and Maynard Smith derived two intelligible outcomes. One of them was the Red Queen result in which a species-rich system never settled down but just kept on evolving, and the other was a 'stationary' mode in which a species-poor system eventually ground to a halt; this second feature they tentatively identified with palaeontological stasis. Significantly, their models assumed a constant physical environment. When the physical setting was modelled as unstable there was nothing like a stationary mode, although the species-poor scenario did yield a system which settled down quickly and had to be nudged back into activity by physical changes (Stenseth, 1985).

What is most striking in this train of gradualistic thinking is that it tells us nothing whatsoever about the organism. The model of Stenseth and Maynard Smith is cast entirely in terms of the magnitude of lag loads, with an implicit assumption that the constant mopping up is also driving morphological change. Poor Alice (the argument goes), she can't stop running; all that exertion must have paid off somehow; after all, marathon runners constantly jostle for the lead, often without gaining much on their rivals, *but at least they cover ground*. Surely our Alice is too smart to spend millions of years running in a circle!

Ridley (1993), virtually opens his very self-conscious, 19th Chapter on 'Rates of Evolution' with this illuminating explanation of Gingerich's (1983) inverse correlation between evolutionary rates and the timescale upon which they were measured:

"The inverse relationship found by Gingerich is therefore probably an artefact, reflecting some kind of preselection of the fossil series used to measure evolutionary rates ... the most likely reason is that the evolutionary rate of a character can only be measured if the character is recognizably the same character throughout the measuring period. Once a character changes more than a certain amount, it will start to look like a different character [thus confusing the palaeontologists!]; it may then not be possible to measure its evolutionary rate in the same way."

He apparently harbours no suspicion that the pattern is genuine and that evolution measured in the lab proceeds in the wild with much oscillation and frequent reversals, and thus normally leads to stasis in the long term.

The conclusions are clear: biologists expect evolution to be gradual (Fisher and Dawkins), inevitable and perpetual (Van Valen, Stenseth and Maynard Smith), and they generally expect it to go somewhere (Ridley). It seems there is life in the Straw Man yet. When first I owned a car I used it mostly to drive into town or thereabouts, and then one day I packed all my belongings into it and relocated somewhere hundreds of miles away. The car was the vehicle with which I moved, but no-one would really want to say it was the *reason*. Confusion about the level at which an appropriate explanation should be pitched is a constant area of inflammation in modern biology, and although it is not always easy to be enthusiastic about their calls for revolution, it seems that Eldredge and Gould do indeed have a point when they bemoan the neontologists' resistance to accepting the basic data of palaeontology.

1.1.4 Plain Tales from the Field

So what *are* the basic data of palaeontology? More than thirty years on from Eldredge and Gould’s provocative call to arms, they are, to say the least, diverse. The expertly written opening chapter in Erwin and Anstey’s edited compendium *New Approaches to Speciation in the Fossil Record* (1995) provides as good an overview as any (but see Gingerich, 1985; and Jackson & Cheetham, 1999, for alternative reviews). Erwin and Anstey’s survey of case studies, based on 58 fossil lineages and categorised in terms of stasis or gradualism, branching or non-branching behaviour, reveals a variety of patterns (Text Table 1.1).

<i>Pattern</i>	Gradualism	Stasis and gradualism	Punctuation and stasis
Non-branching	13	13	6
Limited branching	2	2	6
Multiple branching	2	0	14

Text Table 1.1 *Number of case studies showing lineages whose evolutionary behaviour fits into each category. From Erwin and Anstey, 1995, Chapter 1.*

There are entries in almost every category, but the most striking feature is the distribution: punctuation and stasis are more commonly associated with multiple branching events whereas lineages showing gradualistic phases do not normally branch at all. This is very much in line with Eldredge and Gould’s original prediction concerning a rate increase associated with speciation, although the diversity of phenomena, including instances showing both stasis and gradualism in a single lineage, is much richer than initially suggested.

An important consideration to be borne in mind when assessing the relative frequency of patterns, is that case studies are not always directly comparable to one another, differing as they do in the timescales involved, the numbers of specimens and characters measured, the geographic spread of the data, the types of organism studied, and the manner in which the initial measurements have been analysed. Take the difference between Ozawa (1975) and Bell *et al.* (1985) as an example: the first examines a Permian foraminiferan across tens of millions of years, with a huge geographic spread but only six sampling levels, and it employs nine character measurements drawn from a very respectable number of

specimens; the second concerns a Miocene stickleback from a single quarry, sampled twenty six times across a hundred thousand year span, but with only six measured features. The distribution of evolutionary variables seen in Text Table 1.1 may reflect methods of analysis as well as frequency of occurrence, to say nothing of the way in which reasons for embarking upon a particular investigation can bias the outcome (it must, for example, be easier to find branching patterns if one specifically sets out to study cladogenesis rather than phyletic change).

Even more insidious and unobservable are the beliefs, attitudes and interpretational biases of researchers themselves. As Gould and Eldredge's 1977 critique demonstrated, authors can disagree on the patterns shown by a particular morphological signal, even when viewing the same data set presented in the same way. Their re-evaluation of Gingerich's mammal data (1974, 1976) argued for stasis and punctuation from the same patterns he interprets as being gradualistic, and, to be fair, the dotted guidelines included in the original figures are highly influential additions to what would otherwise be an incoherent and uninspiring cloud of markers. It is rare indeed to come across a report of stasis from Gingerich, or an interpretation of gradualism in the personal work of Eldredge, Gould or Stanley; and it is worth considering that a major role played by the fossil record is as a Rorschach test, amplifying theory's cloven hoofprint to conspicuous proportions—an interpretation in line with the work of Raup and Crick (1981) who failed to decide upon a category of pattern for their twice-examined ammonite data despite (or perhaps because of) a thorough statistical analysis.

From the examples I find most convincing, Stanley and Yang (1987) stands out as one of the best expositions of stasis. They use various methods of inquiry, including two multivariate techniques, based on a large number of characters in, 19 lineages of Neogene bivalve from the Caribbean. The measurements are drawn from populations ranging from 17 million years old to extant forms, and geographic spread is also considered. The results demonstrate that morphology, especially external shell form, is extremely conservative, and that the range of variation across large stretches of time (4 million years) is of a similar magnitude to the variation seen in geographically separated living populations (but see Roopnarine, 1995, for a challenge to this simple interpretation). Evolutionary rates are found to vary inversely with the measurement timespan, in accordance with Gingerich's (1983) evaluation, and the authors conclude that either "evolution has followed a weak

zigzag course, yielding only trivial net trends” or that “haphazard sampling of anastomosing populations gives this pattern”.

Williamson's (1981) much discussed study of Cenozoic molluscs from the Turkana Basin in East Africa also demonstrated stasis, even if the status of his punctuations is disputed (see Mayr, 1982, and others in the same issue). This time it was a multivariate assessment of 13 lineages, of which 10 could be tracked for over 4-5 million years and up to the present day. They exhibited no net morphological change, but showed environmentally correlated, short-term synchronised excursions of a cryptic nature, which Williamson claimed were punctuated speciation events.

The series of studies conducted on Neogene bryozoans by Cheetham and Jackson (Cheetham, 1986; Jackson and Cheetham, 1994; Cheetham and Jackson, 1995) provide further convincing evidence of widespread morphological stasis, along with punctuation similar in character to that predicted by Eldredge and Gould. Their data involves good stratigraphic control, wide geographical coverage, and, impressively, information on genetic differences between the various extant species to support their morphological classification. According to Jackson and Cheetham (1999), eleven of the nineteen species examined originated fully formed with no evidence of morphological intermediates, and then persisted unchanged for 2-16 million years.

Cronin's (1985) study of several Cenozoic ostracods, and Lieberman *et al.*'s (1995) example of two Devonian brachiopods are also good demonstrations of what is meant by stasis; but in fact the majority of other cases also show their subject lineages exhibiting long periods with no substantial change. Even when the object of the exercise has been to document a known transformation, the events of interest are often sandwiched between what are evidently multi-million year periods with no substantial morphological alteration; examples include the studies of cladogenesis by Kellogg, 1983; and Lazarus, 1986; or of anagenesis by Reymont, 1982, 1985; and Geary, 1990.

At the other extreme, generally accepted examples of gradual transformation include Sheldon's (1987b) celebrated presentation of parallel evolution in Ordovician trilobites from the Builth inlier of Central Wales. Eight lineages underwent changes in the number of ribs they possessed, within a block of sediment that spanned 3 million years. Rib number is considered a diagnostic feature in trilobite taxonomy, and many of the lineages made the transition between species designations without a sharp boundary. The fact that

eight separate lineages showed a net increase in rib number suggests that the changes were not random but rather reflect some common selective influence, although the restricted sampling location also makes shifting geographic gradients a plausible alternative.

Geary (1990) has documented gradual anagenesis in a gastropod clade from the Pannonian Basin of Eastern Europe. Following the extinction of the resident marine gastropod fauna in the Late Miocene, a freshwater species which had spent the last 7 million years in stasis colonised the area, and underwent a period of gradual anagenetic change which lasted 2 million years. Thereafter the lineage rapidly split in two to produce a daughter species and a smattering of intermediates which persisted for another million years until the lineages finally parted for good (Geary, 1992).

Some particularly impressive evidence on evolutionary change has come from a growing database on Cenozoic planktonic foraminifera as a result of the Deep Sea Drilling Program. The *Globorotalia (Globoconella) conoidea* clade has been shown to exhibit both gradualistic anagenetic change and a punctuational split. A rounded, many-chambered morph transformed anagenetically into a series of keeled species with fewer chambers, and then underwent a punctuational split at the Miocene-Pliocene boundary. One branch retained the keel, flattened and enlarged, whilst the other lost the keel and shrank, but then started, once again in anagenetic steps, to become increasingly rounded and enlarged. Malmgren and Kennett (1981) reported on the anagenetic branch of this process in what has become a textbook example of phyletic gradualism: the *G. conoidea* root transformed successively into *G. conomiozea*, *G. sphericomiozea*, *G. puncticulata* and finally into the extant form *G. inflata*; some characters changed at a fairly constant rate (e.g. chamber no.), some at variable rates (e.g. overall size) and some catastrophically (e.g. the keel which was said to disappear upon passing an architectural threshold). Subsequent investigation has revealed evidence that the anagenetic trend was driven by climatic changes (Schneider and Kennett, 1996), and that certain transitions occurred via heterochronic developmental shifts (Wei, 1994a, 1994b).

Regarding cladogenesis, *G. conomiozea*, the species in place immediately prior to the Miocene-Pliocene boundary, seems to have existed as a geographic cline which stretched across some 2500 km, from the warm subtropics to the temperate region off the coast of New Zealand (Wei and Kennett, 1988). When the cline was partitioned and separated by the formation of the oceanic Tasman Front it collapsed into two distinct species, the keeled, larger *G. pliozea* in the peripheral subtropics, and the rounded, smaller

G. sphericomiozea which formed the temperate central stock; it thus constitutes a good example of speciation via the allopatric method and demonstrates that “the two “alternative” evolutionary models complement each other rather than being mutually exclusive” (Wei and Kennett, 1988). If further work involving different branches of the *Globoconella* lineage is forthcoming, this an interesting area to watch.

Malmgren *et al.* (1983) coined the term ‘punctuated gradualism’ for cases of anagenetic evolution with a discontinuous rate, although the fact that these periods of slow anagenesis are so close to stasis means that Eldredge and Gould’s original term would be more appropriate if it was not so laden with cladogenetic associations. It is fair to say that the majority of the cases I have encountered basically record patterns in this mode, with substantial zones of almost stasis interrupted by stretches of rather more rapid (though hardly instantaneous) change, some of which is associated with lineage splitting, but quite as often not. What is truly remarkable is just how sluggish evolution in the fossil record seems to be, even when it is going flat out. Lande (1976) provided an insight into exactly how slow with some theoretical calculations, and when these were applied to empirical data (Gingerich’s mammal teeth) he concluded that in the cases examined the observed trends could be achieved by a single selective death per million individuals per generation!; or, alternatively, by random drift in interbreeding populations with tens to hundreds of thousands of individuals. Reyment (1982a, 1982b, 1985) has since applied the same calculations with similar conclusions. Clearly, unless the world abounds with far more neutral morphology than one would expect, the kind of ubiquitous direction changes championed by Sheldon (1993) must be rife, and indeed when studies are conducted with finer sampling resolutions and over shorter periods (Bell *et al.*, 1985; Chiba, 1996, 1998) the magnitude of fluctuation seems to be similar to that seen over longer fossil sequences, again in line with Gingerich’s inverse plot. Nevertheless, as Geary (1990) points out: “given that past studies were assumed complete only if gradual change was apparent, it seems somewhat ironic that unseen mechanisms or events, however realistic, must now be invoked in order to explain an instance of gradual change.” ✓

1.1.5 Mechanisms of Morphological Control

Since it is abundantly clear that even (or especially) in well established cases of gradual change, the rates apparent in the fossil record are many orders of magnitude lower than their observed modern equivalents, there has been an urgent need to account for the discrepancy. Explanations for the lack of structural change can be divided into those which postulate an *internal* mechanism, a constraint of some sort, and those which suggest that the control was *external*. External mechanisms must cope with the supposedly high malleability of organic form, and so they have tended to emphasise, by various means, the stabilising influence of the environment. But let us start with the internal options since this is the route Eldredge and Gould originally took.

Given the furore which followed, the 1972 paper was remarkably offhand about the mechanism for stasis. Sidestepping a different kind of internal mechanism—conflicting selection pressure between demes, which is internal to the species if not the individual—Eldredge and Gould casually suggested developmental or genetic ‘homeostasis’, referring primarily to a book of the same name by Lerner (1954). Lerner’s book deals with the general phenomenon of higher fitness in multiple heterozygotes than in multiple homozygotes, and is aimed towards artificial selection for livestock and crops. He is quite clear about the limited applicability of the mechanism across evolutionary timescales, however, and in the last three chapters explains that the generally higher fitness of the heterozygote results from genetic variation maintained as a buffer against environmental variation. The artificial breeding of extreme phenotypes runs into fertility problems because the requisite genetic variation is not present in the short term, after years of canalization by natural stabilizing selection (and see Bradshaw, 1991 for similar examples in the wild).

This cannot seriously be what Eldredge and Gould had in mind to account for millions of years’ worth of morphological stability, and sure enough by the time their 1977 (Gould and Eldredge) progress review was published, they had sharpened their ideas somewhat:

“We applaud the burgeoning emphasis on change in regulatory genes as the stuff of morphological evolution..., if only because one of us has written a book to argue that the classical, and widely ignored, data on evolution by heterochrony should be exhumed and valued as a primary demonstration of regulatory

change. We do not see how point mutations in structural genes can lead, even by gradual accumulation, to new morphological designs. Regulatory changes in the timing of complex ontogenetic programs seem far more promising—and potentially rapid, in conformity with our punctuational predilections.”

It seems that in 1977, Gould and Eldredge envisaged some kind of command constraint at the genetic level; indeed, just a few years later Gould (1980a) talks of the triplet code as “machine language” and says that “the program resides at a higher level of control and regulation—and we know virtually nothing about it.” Gould has gone on to promote the idea of ‘constraint’ in a number of different contexts (e.g., 1980b; Gould & Lewontin, 1979; and in a series of papers on *Cerion*, his favourite snail: Gould, 1984a, 1984b, 1988, 1989, 1992; Gould, Young & Kasson, 1985; Gould & Woodruff, 1990), although normally it is more clearly a property of phenotypic development than a programming constraint *per se*.

The idea of constraints on evolution has enjoyed a considerable revival in the last few decades, and has a diverse range of supporters. Brian Goodwin is the high priest of the hard-line approach (see Goodwin, 1982, 1984, 1994; also Webster, 1984; Webster & Goodwin, 1996) which has variously been termed ‘Structuralism’ (Hull, 1998) and ‘Neo-Rationalism’ (Smith, 1992), territory which Stuart Kauffman (1993), amongst others, has converged upon from a different direction. Per Alberch (1982), by contrast, champions a softer perspective (see also Alberch & Oster, 1982; and Smith, 1992 for reviews); Gould, too, qualifies as a soft structuralist (especially 2002).

One of the major problems with the notion of constraint is that it is often rather hard to understand what constitutes an example, a feature which has caused considerable confusion in the literature (Antonovics & van Tienderen, 1991). Maynard Smith *et al.* (1985; and the identity of the co-authors is well worth a look) provide the now classic definition:

“A developmental constraint is a bias on the production of variant phenotypes or a limitation on phenotypic variability caused by the structure, character, composition, or dynamics of the developmental system.”

The paper goes on to explain the difference between *universal* and *local* constraints (discussed later in Part IV) and suggests some research strategies for distinguishing instances of constraint from those of selection.

A common objection to the notion of constraints is that they imply a limit to variation; Ridley (1993) makes the following complaint:

“The question of whether evolutionary constancy is caused by stabilizing selection or constraint is a particular form of the general question of what causes phenotypic patterns in nature, and the same general points can be made. The hypothesis that a [variable, phenotypic] character is not changing because it has no genetic variation can be tested. It predicts that the character’s heritability is zero... Stabilizing selection is well documented, whereas a lack of genetic variation has never been shown to be the reason why any character remains unchanged. Most characters show significant heritability; those that do not are puzzling, because the nature of the constraint is not understood.”

The great failing of this argument is that it apparently takes into consideration only single characters: variation towards the end of a character’s normal range does not guarantee that there will be variation available in the furthest ends of the ranges of a large number of such characters simultaneously. An organism must constitute an integrated whole, and factors such as pleiotropy and allometry really do impose limitations on the range of variation available, by limiting the number of truly independent characters. Tugging a character in a particular direction generation after generation may well mean dragging whole batch of other unobserved characters along with it, which is fine in the lab, but not in the wild. A neo-Darwinian defender might say that the element constituting a ‘character’ has simply been mis-diagnosed, to which a structuralist would retort, “precisely, that’s the *point!*”

The better understood and more traditional internal mechanism rejected by Eldredge and Gould in their 1972 paper, is the effect of gene flow between sub-populations of a widespread species. In this case, selection in a particular location acts to unravel other work, achieved elsewhere under different selective regimes. This counts as ‘internal’ because it is the cosmopolitan nature of the species itself, and its preference for wide dispersal, which guarantees overall stability: in effect the species becomes a generalist across its heterogeneous geographic range. Stasis is maintained not because the environment remains stable, but because it is pulling in many different directions all at once, and thus effectively ‘cancels out’.

This idea was challenged by Ehrlich and Raven (1969), the paper Eldredge and Gould originally cited against it. According to them, gene flow can be conspicuously

lacking between populations which nevertheless remain morphologically identical, and equally be surprisingly strong between populations which are undergoing significant adaptation to local conditions. But Stanley (1979) and more recently Eldredge (1995) have promoted the idea again, suggesting that it was anticipated by Sewall Wright's shifting balance theory. Interestingly, some palaeontologists are keen to distance themselves from the idea that this process could be interpreted as a form of space-averaged stabilizing selection, and are prepared to tie themselves in any number of knots to avoid it (e.g. Lieberman and Dudgeon, 1996).

Whether gene flow overwhelms local selection or vice versa seems to depend on the relative strengths of each; for neutral features, for example, drift can apparently be overcome if a single migrant enters a local population every other generation (Charlesworth *et al.*, 1982). Furthermore, in cases where there is a persistent selective tension between populations, evolution should work to erect barriers to gene flow, as Bradshaw (1991) discovered when his spoil heap and natural grass populations began to modify their flowering times. So in cases where evolution *can* occur, it seems, from many modern examples, to do so extremely rapidly; thus, the only way in which local selection pressures can keep a population in long term stasis is if they themselves are constantly changing, providing a signal so fleeting that it cannot be tracked. What this argument manifestly fails to explain, however, are examples of stasis in the face of long-term environmental shifts such as ice ages, which are imposed across all local environments simultaneously.

We thus come to a third internal mechanism, the idea of habitat tracking, in which species are recognised as active homeostatic agents with the ability to select their own comfortable circumstances. A frequently quoted vindication of this process is Coope's (e.g., 1994) demonstration that numerous species of beetles have maintained the same morphology and, apparently, physiological preferences, by migrating back and forth as they followed specific temperature zones throughout the last bout of Quaternary glacial oscillation. Not everyone is convinced. Williams (1992), for one, considers it a "fable" and suggests instead that "the physical changes are probably of minor importance compared to biological differences in community composition"; and certainly there are many cases of migration in which the species composition of the communities concerned changes dramatically (e.g. Bennett, 1997). Nevertheless, Eldredge is happy with the idea (1989, 1995a), and claims that to vapidly postulate evolution or extinction in the face of

environmental degradation, rather than the obvious alternative of migration, constitutes “imagination colliding with common sense” (1995a). Whether common sense stands up to imagination when the two are pitted against one another over millions of years remains to be seen.

The stock biological explanation for stasis is *stabilizing selection* (Charlesworth *et al.*, 1982). The biggest problem here is that once the *potential* for evolution has been conceded, all control is passed on to the environment, which must then be argued to remain static for millions of years. In what way the environment must be stable is not entirely clear; geologists are well aware that all physical aspects of the Earth’s surface are in constant flux, and for them that fact alone is enough to discourage reliance on stabilizing selection (e.g. Gould, 1982). Then there is Red Queen reasoning, which implies that biological interactions alone are sufficient to keep organic form constantly on the move, even in perfectly stationary physical settings (Stenseth and Maynard Smith, 1984).

The most common strategy adopted by biologists faced with these difficulties is to completely ignore them. Charlesworth *et al.* (1982), Dawkins (1986) and Ridley (1993), all vehemently maintain that stabilizing selection is vastly preferable to developmental constraint as a method of maintaining stasis, without so much as hinting that there could be some gaps in the explanation. Williams (1992) adopts a much more reasonable approach, devoting an entire chapter to the issue. Recognising that natural populations are extremely malleable, and that there is no prospect of genuine stability in either the physical environment or the biotic one, he looks for a way of soaking up or cancelling out all the evolution he thinks should be occurring. His solution is ‘normalizing clade selection’, roughly what Eldredge (1995b) means when he appeals to “differential probability of survival in taxa of varying niche widths” (and see also Vrba’s, 1985, ‘effect hypothesis’ for an explicitly macroevolutionary version). The suggestion is that species with long-lasting, wide niches persist for long periods but constantly give rise to smaller branches of specialist daughters. Specialist environments are spatially restricted and do not last for geologically significant periods, so these stenotopic offspring leave a very scattered fossil record, contributing no more than a few odd outliers to that of the long lived and widespread, generalist parent. Williams calls this a “desperation hypothesis”, but it has all the hallmarks of fine palaeontological thinking, acknowledging, as it does, that high resolution processes can seem very different from a geological perspective.

Other endeavours to account for the spectrum of evolutionary patterns by invoking extrinsic environmental or ecological factors have generated some very stimulating suggestions. To explain why entire communities of organisms should exhibit 'co-ordinated stasis', keeping not only their morphological identities but also the same relative abundances, Morris *et al.* (1992) have proposed a mechanism of 'ecological locking'. The normal justification for community inertia is incumbency, which accounts for the persistence of resident species by sheer numerical abundance: rare immigrants are wiped out for purely random reasons before they have a chance to gain the kind of foothold necessary to compete in the usual way. Instead, ecological locking is more a case of fluid tessellation. It occurs when an ecological mosaic is sorted, and naturally selected, by physical disturbance on a variety of scales, eventually resulting in a community winnowed into a hierarchically ordered, highly stable pattern (Ivany, 1996; Miller, 1996). The result is a hub-centred configuration which both soaks up most physical disturbance and obviates the need for a lot of evolution. Generalist species forming the hubs are adapted to small scale, high frequency physical disturbance and respond ecologically without needing to evolve; meanwhile, when a large scale, low frequency event does finally occur, the specialists which respond to it are out in the tendrils or spokes, buffered from other specialists by the mediating presence of the hub, and thus do not propagate the effects of any evolutionary or ecological changes they may be undergoing. In effect the model posits a form of *ecological homeostasis* to explain why physical changes are not transformed into evolutionary ones.

Johnson (1982) and Fortey (1985), by contrast, have emphasises the fact that evolution is expected to be *driven* by change in an organism's physical surroundings, and so we ought to see gradualism in pelagic settings where the environment is simpler, more predictable, and any changes slow; a punctuational pattern should then be associated with benthic ecology where abrupt shifts are more likely. This is the pattern one might naively expect if morphological transformation was seen as a simple linear correlate of the pattern of environmental disturbance.

The argument for stasis as well as punctuation in unpredictable settings gains some support from Parsons (1991, 1994) who notes an inverse correlation between fitness and environmental stress. Organisms subjected to circumstances far outside their normal range

of preference, as might occur towards the edge of a species' geographical distribution, tend to suffer greatly reduced fitness because of higher metabolic costs, which waste resources otherwise channelled into reproduction. If evolution is to proceed it will do so only where physical parameters are changing rather slowly. The natural extension of this argument is that in gradually changing environments evolutionary change will be permitted, whereas in stressful situations with disturbance rife the only options are to weather the storm or go extinct.

This reasoning takes us right up to Peter Sheldon's *Plus ça change* model (1996) which is the main topic of the next section.

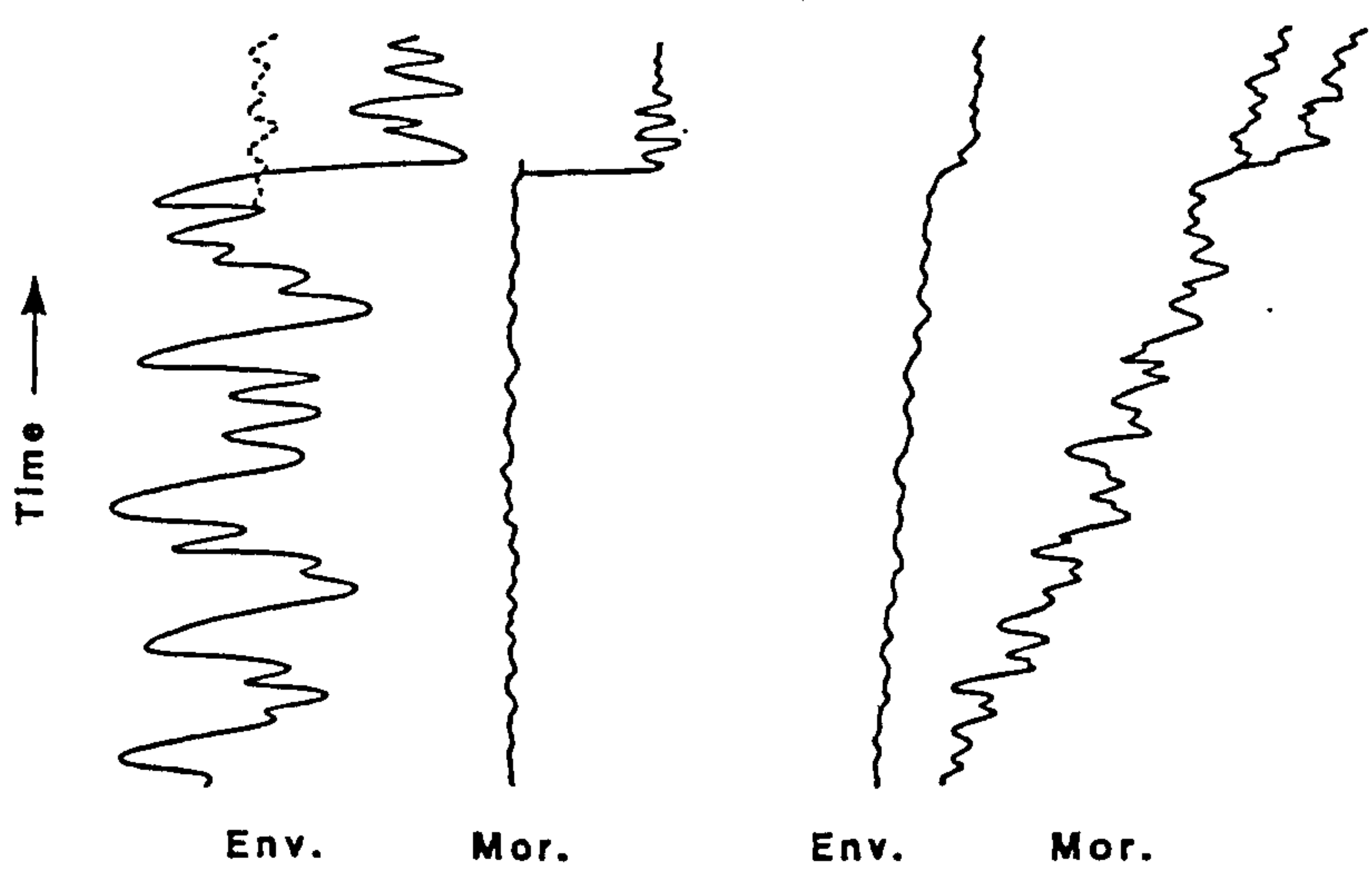
Section 1.2 A New Perspective

1.2.1 *Plus ça change*

The first glimmerings of *Plus ça change* appeared in the penultimate paragraph of Peter Sheldon’s 1987b *Nature* article, reporting parallel gradualistic trends in Ordovician trilobites. He concluded:

“Perhaps this kind of gradual phyletic evolution can only be sustained by organisms living in or able to track narrowly-fluctuating, slowly changing environments, whereas stasis, almost paradoxically, tends to prevail in more widely-fluctuating, rapidly changing environments.”

The suggestion was reiterated three years later (Sheldon, 1990) and the phrase ‘*Plus ça change, plus c’est la même chose*’ offered to portray the attitude of a morphologically static species to its apparently unsettled environment; a diagram demonstrated the type of patterns he had in mind (Text Figure 1.2). A fuller exposition came in 1996, in the form of the *Palaeogeography, Palaeoclimatology, Palaeoecology* paper, ‘*Plus ça change—a model for stasis and evolution in different environments*’.



Text Figure 1.2 *The pattern of morphological response to environmental stability predicted under the Plus ça change model as depicted in the 1996 PPP paper. Env. = ‘environment’, Mor. = ‘morphology’.*

The PPP account is by far the most detailed, and stands as the best reference point for Sheldon's views to date (although see also Sheldon, 1997 and the e-text, Sheldon, 2000). After a few preliminary remarks concerning the perception of evolutionary patterns in the fossil record, we are treated to a variety of observations and quotes from the wider literature, coupled with some delicious metaphors, which gradually flesh out what Sheldon has in mind. From early on it is apparent that it is not just stasis and gradualism he wishes to address, but (as is fitting for a general model of evolution) global patterns of diversity, life history strategy and ecological specialization, all in relation to the stability of the physical environment—but stability on a geological scale:

“The kind of environmental stresses for which this generalization is proposed are physical (abiotic) variables that can be studied over geological timescales, such as changing sea level, substrate, salinity and climate (e.g. mean temperature). It is crucial to realise that the timescales of change involved here are orders of magnitude longer than those usually studied by biologists and ecologists.”

He recognises that stability can be viewed at different resolutions and that instability on an ecological scale can be extremely predictable within a longer timeframe. Events which are cyclic in nature, such as tides, are obvious cases of orderliness and regularity in spite of their incessant movement. But more erratic events can be predictable features of an organism's environment too, and he cites as an example the case of plant species whose niches entail re-colonisation in forests regularly thinned by fire. Conversely, while tidal effects are a case of long term stability despite their everyday variation, wholesale changes in water depth, which may take hundreds of thousands of years to occur, and which are invisible on an ecological scale, are just the sort of instability he is interested in.

He is keen to point out that the stasis predicted to accompany geological scale instability is not a case of time-averaged, short-duration directional selection, where frequent reversals undo each evolutionary move:

“An important feature of the model is that net long-term stasis in more widely fluctuating environments is *not simply a case of major morphological shifts that keep getting cancelled out* [his italics]; the morphological response has become damped compared with the environmental shifts, and of less amplitude than typical responses in a narrowly fluctuating environment.”

So the underlying cause is altogether more fundamental—a diminishment of the *capacity* (or need) to evolve in lineages subjected to geological scale environmental perturbation.

In the final paragraph of the explanation section we discover that:

“Perhaps the most important (and perhaps most controversial) mechanism I am suggesting here is a type of lineage selection with two stages: (1) if an established or an incipient species experiences a widely fluctuating environment on geological timescales, the evolutionary response (morphological change) tends to become damped with time, and (2) those species that are least sensitive to environmental change (the most “generalised” in a long-term sense) are the ones that tend to persist, remaining in morphological stasis until a threshold is reached.”

Consequently, Sheldon also wants to emphasise that the circumstances are relative, not just in terms of magnitude but in terms of their temporal relationships:

“In the model it is change *relative to pre-existing conditions* [his italics again] that is important: the impact of an event is entirely contingent on history. If a system has been subjected many times to large disturbances, yet another one may yield no response at all [... or send the species over a threshold—as the 2000 document adds]. After a while, nothing is perceived to change, just as in a human society rebellion can become conformity. In contrast, a medium magnitude disturbance in a system that has experienced only low magnitude events for a long time may have a large effect, like a loud sneeze in a hushed library.”

So we glean from this the idea that an evolving species should grade in and out of evolutionary tempo, through periods of curtailed and enhanced morphological malleability, depending upon the way the present environment is acting upon them, and given that they are what they are *in virtue of the way their history has shaped them*.

What are the mechanisms behind this behaviour? Thus far it seems rather impressionistic, a fact he candidly admits in saying, “The most likely causal mechanisms of stasis in the context of the model remain to be established”. But there are some hints of what he has in mind:

“A greater amplitude of morphological responses in a narrowly fluctuating environment can be expected because selection probably has the chance to act on a greater range of variation tolerated (and perhaps produced) in a stable environment under relaxed selection pressures.”

We are also given an assortment of related processes, any or all of which may be involved, although none of them quite meets the demands of the model. With regards to stasis in fluctuating environments we are reminded of the versatility of ‘all-purpose’

organisms adapted to temperate climates, an argument which “can be scaled up to geological intervals’ to produce long term generalists.” Such geological generalists (and their specialist counterparts) “are related to but distinct from the ecological division into eurytopes and stenotopes”. In a similar vein he invokes the *r-K* dichotomy but warns that “the ecologist’s ‘unpredictable environment’ may, experienced over the long term, be *more* predictable until a threshold is reached”, so that “disturbance-adapted species with short-lived populations may thus have longer species durations.” The tendency for hierarchical ordering and homeostatic, disturbance-minimising behaviour (of the kind suggested by Morris *et al.*, 1992) in ecosystem structuring is also mentioned.

When it comes to stable settings the ecological comparison is even stronger, and he suggests that one of the features behind gradualistic evolution is specialisation into narrow niches. This is what lies behind the long term specialist’s tendency to be “more sensitive to minor environmental nudges” so that (with respect to cladogenesis) “another factor contributing to high tropical and deep sea diversities could be a higher frequency of such events there”. A further suggestion, attributed to Dobzhansky, is that “organisms living in narrowly fluctuating physical environments may be especially sensitive to biotic interactions”. This, of course, ties into the Red Queen conception of evolution.

All in all, this sounds like fairly standard ecology, but the fact that it operates over such huge timescales makes it distinct. There is also the lurking impression that something altogether more arcane is going on, as the references to ‘lineage selection’ suggest. Rather disappointingly (or wisely) he is cautious and does not go all out for this line of argument, but there are several cryptic references to macroevolutionary mechanisms, for example:

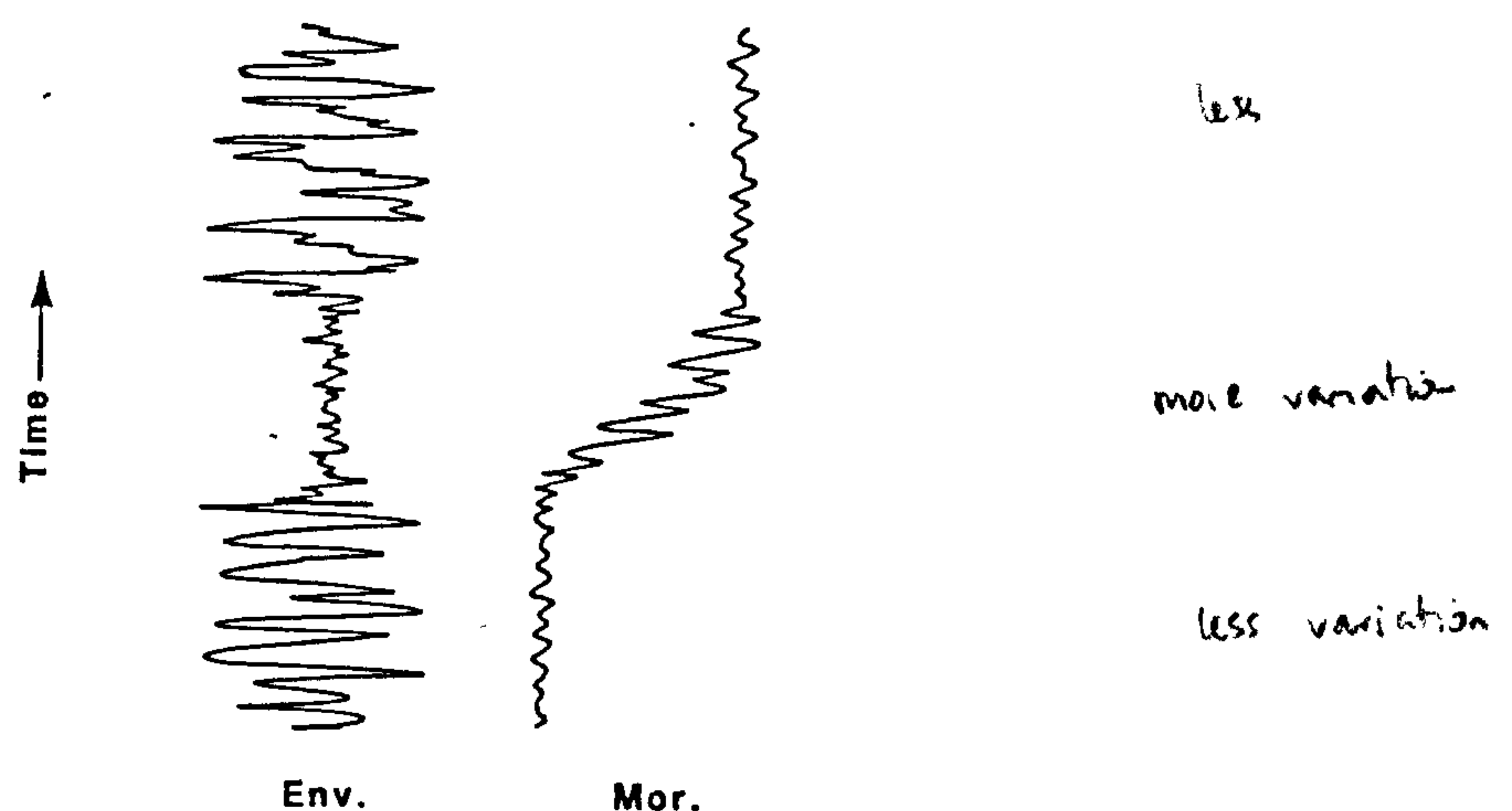
“Presumably lineages that produce a wider range of variation “when the going is good” are more likely to survive severe new environmental perturbations. If so, this could be an important mechanism for ‘lineage selection’ i.e. the preferential sorting of species, especially fledgling species.”

His vagueness about this part of the process is easy to forgive since he is clearly trying to convey a general idea without committing to one mechanism or another, at least before the jury has returned. The pattern is what Sheldon is interested in—however it happens to come about—and one of the great virtues of the *Plus ça change* model is that it generates well-defined endpoint predictions of pattern, and thus gives an empirical worker plenty to focus on. But it is also significant (to this worker at least) that the underlying mechanism of the model remains ambiguous, because the theoretical framework through

which the empirical material will be interpreted will thus also be a contribution in its own right.

1.2.2 Predictions of the Model

In fact there are so many predictions in the PPP paper that we are spoilt for choice when selecting which ones to test. Fortunately, one of Sheldon's main motivations is not only to promote his explanation of pattern, but also to prompt palaeontologists to look for it, and perhaps even set up circumstances to test it explicitly. To make this process as easy as possible he provides a second diagram (reproduced below Text Figure 1.3) explaining exactly what he thinks we should look for in order to confirm his predictions.



Text Figure 1.3 *Sheldon's suggestion of what an empirical test should focus on: The morphological response of a single lineage as it experiences a succession of different environmental stability regimes (from Sheldon, 1996).*

He sensibly chooses to emphasise environmental effect on tempo rather than mode (i.e. patterns of speciation), which he could just as well have done since the model provides an equal number of predictions concerning cladogenesis. Mode, however, is notoriously hard to demonstrate in the fossil record (Fortey, 1985; Gingerich, 1987; Gould and Eldredge, 1993) and in any case his macroevolutionary predictions are still being honed. Instead, he suggests tracking a single lineage across changing environmental stability regimes. Shown in Text Figure 1.3, these pass from widely fluctuating to narrow, and back

again; the morphology of the single lineage is expected to remain relatively static for the first part, oscillating a little around a mean, and then to become gradually more dynamic as the environment settles down. This second phase is characterised by having both a higher overall rate and a net trend, albeit muted by frequent reversals. Finally, to drive the point home, the diagram shows a resumption of stasis when the environment begins to fluctuate again, although it could as easily have shown extinction. What is not included in the figure, but is clear from the accompanying text, is that standing variation (variation in the population or species at any particular moment), in addition to rapid morphological change, is expected to increase during the stable periods.

The nature and number of the environmental and morphological features is left open, and presumably could be equally applied to one or many separate examples. He is also non-committal about any kind of absolute rate, either in the environment or in morphology. The strength of the test is in its juxtaposition of situations—the stability regimes butt onto one another, and so we can define a *relative* status, using each as a comparison for its counterpart, and similarly for morphology.

Environment	Unstable	Stable
Effect no. 1	Stasis (irrespective of reversals)	Net change (irrespective of reversals)
Effect no. 2	Diminishing response to any but the most extreme events	Increasingly strong response to even the smallest events
Effect no. 3	Low rate of change (irrespective of reversals)	High rate of change (irrespective of reversals)
Effect no. 4	Decreasing variation in morphology in any one sample	Increasing variation in morphology in any one sample

Text Table 1.2 *Four key differences in morphological response to environments of varying stability.*

Some major predictions of the model are summarised in the table above (Text Table 1.2; and see Sheldon 1996, 1998 & 2000 for others), but there are also a host of other connections which would provide support for Sheldon’s hypothesis if they could be demonstrated. He expects “long term generalism” to be correlated to some extent with ecological generalism or eurytopy, and long term specialism with stenotopy; if someone could demonstrate that a lineage changed its ecological role in response to environmental stability then that would be support. Similarly with the suggested connection to *K*- and *r*-selection: if a species shrank in the mean volume of its individuals (a proxy for biomass)

during unstable geological sequences and expanded in stable ones, that too might be an interesting link. There are also his passing comments about the length of time it might take for such patterns to emerge, and his suspicion of ‘fractal’ evolution (whatever that might be), both of which are worth keeping an eye open for (both predictions in Sheldon, 1996).

1.2.3 Testing *Plus ça change*

Retrieving and demonstrating evolutionary patterns from palaeontological data is by no means a straightforward task. The fact that palaeontologists work with natural data, unconstrained by experimental procedure and subject to a multitude of unguessed influences—and highly contingent, one-off historical influences at that—means it is especially hard for us to justify any causal account we wish to provide. Discrimination of repeated correlations goes some way towards providing statistical arguments for the validity of pattern, but the real problem lies in the very large combination of plausible alternatives capable of *explaining* any data set one might produce. We are thus compelled to anticipate the likely objections in advance, and to set up our sampling procedure in a way that will allow us to answer our critics with the same data we use to present our case.

In their critique of reported examples of gradualism, Gould and Eldredge (1977) give an insight into the types of judgement one can expect, and list some of the criteria sought from fossil data: “good geographical coverage, long sequence of closely spaced samples, unambiguous definition of taxa, and adequate biometrical testing on sufficiently large samples”.

To these requirements we can add many others. When Williamson (1981) published his account of mollusc punctuation in Lake Turkana, the chief criticism was that the pattern could just as easily be ecophenotypic; so data and counter arguments to fend off a charge of developmental plasticity had better be available, too. Numerous authors (e.g. Erwin and Anstey, 1995) have acknowledged the need for ecological data to supplement and provide a context for any evolutionary story; thus, a full scale ecological reconstruction would also be worthwhile. And this is all before any reference has been made to the supporting geological arguments for environmental interpretation, stratigraphic correlation and evenness of preservation.

As a specific argument, *Plus ça change* has its own peculiar blend of requirements, in addition to any of the more general demands. At the very least, from Sheldon's stipulations as shown here in Text Figure 1.3, we need an environment which was demonstrably more stable at one time than at another, plus a lineage which persists throughout. Since the question is one of rates, we also need a time-frame against which to measure them. Clearly, finding material which will make everyone happy is going to be impossible; but I believe that the chosen environment, the mid-Cenomanian succession of the Anglo-Paris Basin, and the chosen lineage, a benthic foraminiferan species from a diverse and abundant fauna, permit a surprisingly large number of these desiderata to be fulfilled.

In particular, the following circumstances hold:

- The Cenomanian sediments of the Anglo-Paris Basin (the Lower Chalk in Southern England) were formed from a combination of phytoplankton debris and terrestrial runoff. The precise composition of this mixture was affected by climate, resulting in a rhythmic sedimentation pattern which records Milankovitch cycles, and which can thus be used to measure time. The cyclicity can also be used to accurately correlate between distant areas, allowing fairly synchronous sampling across a broad geographic spread.
- The sediment has undergone little compaction or cementation, affording good three dimensional preservation to many of the fossils, and permitting them to be recovered easily. The abundance of microfossils means that a few grams of bulk sediment is sufficient to provide a representative sample of the fauna, so that the community structure can also be examined.
- The microfossils (mostly benthic foraminifera) respond in an ecologically unambiguous way to the cyclic variations in sedimentation, permitting an ecological reconstruction which fleshes out the biological character of many species and relates them to the changes occurring in their physical environment.
- Cyclicity can be demonstrated or inferred on a variety of scales, ranging from the seasonality of phytoplankton blooms to various orders of Milankovitch cyclicity and up to the eustatic rhythms of transgressive systems tracts. The way in which such cycles interact and interfere with one another provides ample evidence that the environment was more unsettled at some times than others, again at a variety of scales.

- By measuring a range of characters on the chosen lineage (fourteen in fact) a good three dimensional representation of the organism is developed. And because foraminifera grow in a series of discrete chambers, such measurements can be related to stages of ontogeny, allowing a model of the developmental process to be constructed, and related to its inferred environment.

1.2.4 Thesis Structure

Inspired by Van Valen's (1973) astute observation that "evolution is the control of development by ecology", the thesis from here onwards is split into three functionally specific parts.

Part II concerns the environment. It introduces a physical setting, an orbital timeframe, and a sequence of geological-scale events. Together these are used to argue that the criteria for testing the *Plus ça change* model are met. It also considers the biological matrix in terms of both its association with the physical setting and the ecological relationships existing between its constituent species. A model of the community structure is advanced to account for its probable short term fluidity and evident long term stability; especially close attention is paid to the issue of scaling in time and space. The aim is to build an impression of the environment as 'perceived' by the focus lineage that will later provide a framework for interpreting its evolutionary behaviour. The model is also used as device for interpreting the ecological response of the microfauna to both predictable and unpredictable environmental fluctuations alike.

Part III concerns the developmental sequence of the focus lineage, *Tritaxia pyramidata*, an infaunal, agglutinating foraminiferan. The aim in this portion of the thesis is to develop a thorough appreciation of its morphology and growth sequence, to 'get inside' the building program responsible for its agglutinated test, and to try to imagine *how* the creature organised its own construction. Ultimately, the goal is to acquire an understanding of the developmental materials on which natural selection, under the guidance of ecology, was able to work. Part III also operates as a bridgehead between Parts II and IV, and is thus a conduit for translating ecology into evolution. As such, its theoretical section is the conceptual anchor of the whole thesis. The approach adopted here is inspired by another aphorism, this one from Williams (1992): "[life] is the control of matter by information". Information thinking is hardly new to biology, but sometimes it is

less explicit than it might be: Chapter 5 makes it fully explicit. An information theoretic approach is outlined and then extrapolated into a number of contexts relevant to the chapters to come. After that, an argument is made for considering *Tritaxia* as a single lineage, and some important developmental quirks are highlighted for the insight they provide on the growth sequence. Eventually the growth sequence is mapped out in good detail.

Part IV examines changes to *Tritaxia*'s morphology over the course of a million years as the organism passes through an appropriate suite of environmental conditions. The penultimate Chapter 9 is dedicated to summarising these patterns in preparation for Chapter 10, which offers some interpretations. A range of standard theoretical models is considered first before applying the accumulated data set to *Plus ça change* itself.

The overall structure of the thesis can (obviously) best be appreciated by consulting the contents list. One benefit of an exposure to taxonomic practice is good mental hygiene, and the reader will find both the data and the argument split into a series of hierarchically nested categories designed to shoulder as much of the organisational burden as possible. After working with this format for a little while it should become very familiar, with the consequent advantage of intuitively knowing where to look when something needs to be found.

Summary

Despite their common subject matter, palaeontology and biology (neontology) are still largely separate disciplines. A major factor in this persistent and long-standing division (but by no means the only one) is the issue of scaling. Extrapolation from known biological phenomena up to geological timeframes routinely results in thwarted expectation; conversely, the explanation of macroscopic phenomena in terms of commonly understood, directly observable biological process seems equally incredible, because these are normally too unstable to exercise long term control. On a human timescale, species are extremely fluid; on a geological timeframe they are manifestly viscous; squaring these two perspectives is no mean feat. Stasis has thus emerged as a major problem of translation between disciplines at either end of the temporal hierarchy.

Models accounting for long term morphological stability can be partitioned into those which posit an internal source of control and those which posit an external one.

Internal candidates include either genetic or phenotypic constraints, eurytopic population structure, and habitat tracking; external candidates are normalizing clade selection, ecological homeostasis, and environmental stability.

1 Into this morass comes *Plus ça change*, which offers a new perspective. I shall argue (gradually, throughout the text) that a well-developed information-theoretic paradigm is one of the most saliently missing pieces in modern biology and palaeobiology. Since information is abstract enough to be substrate neutral (to be unconstrained by the medium), it also has the right profile to be scale independent. *Plus ça change* is couched in implicit information processing terms from the beginning, even though its author is not explicit about that fact: it concerns the sensitivity of an organic receiver to various frequencies and amplitudes in signal strength, against a background containing various degrees of noise; hence the metaphor of the sneeze in the hushed library.

The thesis tests a range of predictions from the *Plus ça change* model using an information theoretic approach to understand a mass of empirical material which comes partitioned into the categories of environment (external source), development (internal receiver) and evolution (interpretative response).

Part II The Environment

General Introduction

Britain of old was named Albion on account of the gleaming white chalk cliffs which rise so imposingly on the nearest approach from the mainland. These buttressed walls cut a transect through the Upper Cretaceous sediments on the northern rim of the Anglo-Paris Basin, stretching between Champagne and Wiltshire, and from the Loire to the Thames. From the Martello Tower at Copt Point, Folkestone, it is possible to view the cliffs from a distance. Here, one can see that their base does not end sharply, but fades downward to a haze of blue-grey. The darker section is the Cenomanian aged Lower Chalk, traditionally divided into the Chalk Marl and Grey Chalk members. It underlies the dazzling Mesozoic deposits of the Middle and Upper Chalk across much of the basin, and represents a transition between the ocean-born biogenic sediments above and land derived material, the Gault Clay, which came before. On closer inspection this apparently smooth gradation becomes a myriad of alternating grey and white bands stretched out along the shoreline. These are cycles of darker, muddy limestones or 'marls' and paler, often harder 'chalks'. The bands can be arranged in pairs or 'couplets' of each, and the variation in shade shown to be a consequence of differences in composition of the primary sediment.

These cycles are the background setting within which the *Plus ça change* model is to be tested. In accordance with the strategy and requirements laid out in Part I, the next three chapters aim to demonstrate how they fulfil the necessary criteria: namely, that they represent differing regimes of environmental stability, can be correlated across the sections under study, and form a time frame against which to assess rates of evolution.

Within and above the detritus which formed the regular mid-Cenomanian cycles, thrived a host of creatures, that lived, reproduced and died over a million year span. When the time comes to imagine how an evolving lineage interacted with its surroundings, the details of these processes will become particularly relevant; but quite apart from such considerations, *Plus ça change* is about rates of evolution in fluctuating and stable environments, and, as Van Valen (1973) insisted, "the most important part of the environment from any organism's point of view are the other organisms in it". Since the dynamic interactions of a community can in themselves constitute stability or change for

any component species, a demonstration that the fauna was undergoing a compositional shift is a weighty argument for environmental variability. In addition, the dynamics of the fossil record normally shed a little extra light on any sedimentary evidence, so a palaeoecological survey will be useful in helping to reconstruct the physical environment too. Before embarking on a detailed assessment, however, it is necessary to provide a context.

Chapter 2 Environment and Organism

Introduction

The context to be established has two components: the geological nature of the physical setting, and the biological character of the organisms which inhabited it. Since this part of the text is merely an attempt to introduce those elements and general mechanisms required to begin thinking about the data, treatment of most topics will be fairly superficial. At this stage, physical considerations include a general appreciation of the sediment type, its behaviour through time, and what this has to say about the regional setting, including some historical remarks relevant to the area. The biological portion opens with a framework for understanding relationships between organisms, then develops the theme by providing examples from studies of modern foraminifera, and their translation into palaeoecology.

Section 2.1 A Physical Context for *Plus ça change*

2.1.1 The Sediment

The beds of the Lower Chalk are predominantly a mixture of two components, clay and carbonate, in variable amounts; and it is the variation between these two elements which underpins the suitability of the section for this investigation.

The carbonate consists mostly of stable, low Mg calcite, a primary feature and the main reason there has been so little subsequent alteration. The particles range in size from 0.5-1000 μ m with a bimodal frequency distribution centring on 0.5-4 and 10-100 μ m (Hancock, 1975). These two size concentrations reflect the biological origin of the material: the larger portion representing shell fragments, echinoderm prisms and the like, mixed with tiny foraminifera (at about 70-20 μ m); and the smaller the nanno-flora. These are the coccoliths for which the Chalk is so famous, and they totally dominate the sediment, constituting some 75-90% of the carbonate fraction in a typical chalk sample. While many are still whole rings yet more are broken, and it is the dimensions of individual coccolith laths that define the sharp cut-off point on the lower end of the size range.

These components are jumbled haphazardly together with a large amount of pore space, 42% on average in white chalks according to Hancock (1975). Because the low Mg form of calcite is so stable at near surface temperatures and pressures, and because the whole of the Upper Cretaceous sequence in this region has been subjected to relatively little overburden, diagenesis, aside from special cases such as hardgrounds, is limited to the infilling of foraminiferal chambers. Ditchfield (1990), after a thorough petrological examination involving acetate peels and SEM analysis, describes “a ‘spot welded’ framework of coccolith grains... characteristic of chalks that have undergone initial dewatering during early diagenesis but little subsequent compaction due to burial.” This matrix, hosting a variable amount of clay, seems fairly representative of the original sediment in which the Cenomanian benthic community lived.

The clay portion of the chalk is a mixture of clay grade quartz, illite and smectite, with lesser amounts of kaolinite and chlorite, an overall conclusion of Jeans (1968), and more recently supported by Ditchfield (1990). Although Jeans felt there was room for some authigenic illite and smectite, Ditchfield reasons that the clay at Folkestone is detrital and the most probable sources are the London-Brabant High and the Rhenish Massif to the southeast. Since the Armorican Massif in the south and the Cornubian Massif to the southwest are also known to have been emergent during the Cenomanian, they may thus have made their own contributions to the terrigenous supply.

Pyrite is a minor but common component in many beds. It occurs as minute crystals dispersed throughout the rock giving it a grey colour when fresh or yellowish hue when weathered. It also occurs, more prominently, as globular or cylindrical clusters of blade-like crystals, sometimes forming nodules an inch or so in diameter. Pyrite in this nodular form often occurs around burrows where the organic material within them may have encouraged growth by locally altering the oxidation potential (e.g. Ekdale and Bromley, 1984). In these cases the nodules are normally small, less than half a centimetre in diameter, and they occur in winding lines as they track the course of the burrow. Larger nodules occur with no equivalent association, suspended freely in the sediment. My own subjective impression of these distributions is that the large nodules are much more common in the very soft clay rich beds at the bottom half of the section, and the burrow lining type in harder, cleaner chalks toward the top.

Glaucinite is also present throughout the Chalk (Hancock, 1975), but in such minute quantities that it can rarely be seen in the field. Sieved residues occasionally reveal

green crystal fragments which are probably glauconite, and there are green grains incorporated in the tests of several species of agglutinating foraminifera, the focus group included, but it does not form a major component of the rock. Phosphates can occur as brown streaks and rings where they coat surfaces and 'pebbles' of partly consolidated sediment which have remained unburied for a significant period. The hardgrounds and pebble beds of the Turonian are especially rich in phosphatic deposits and replacement minerals but such things are largely absent from the Cenomanian sections under study.

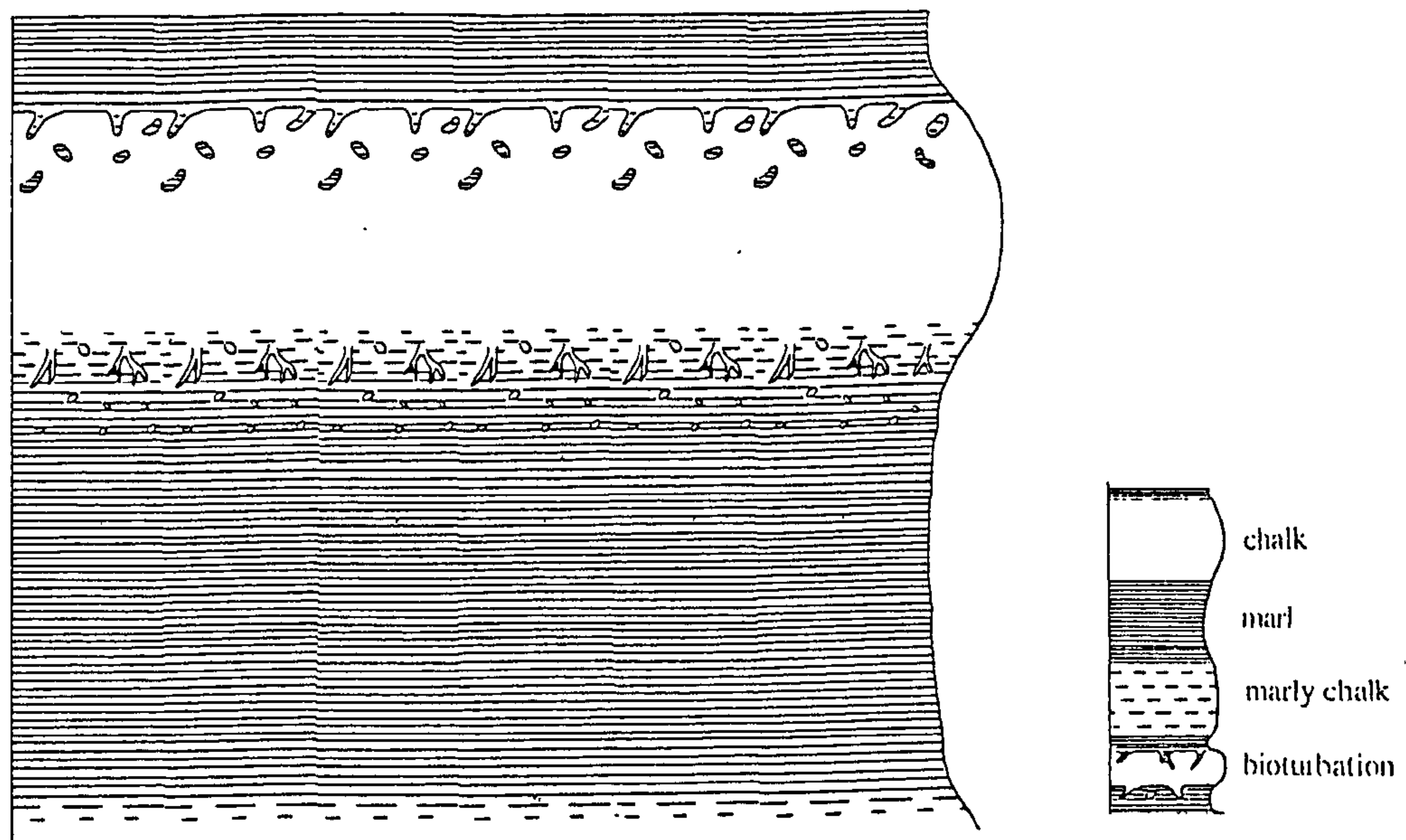
2.1.2 Bedding Style

The rhythmic alternation in colour reflects differences in the composition of the sediment, mainly variations in the clay-carbonate mix. Gale (1990) views the banding in terms of couplets, each couplet consisting of one bed of carbonate-rich 'chalk' and another of clay-rich 'marl' (Text Fig. 2.1). These lithological designations are relative: there is no absolute threshold of proportion defining either half of a couplet; indeed it will be apparent in the sections to come that a marl from a couplet high in the succession may be as chalky as a chalk nearer the base.

Bed boundaries show a variable range of intergradation from softly diffuse to relatively abrupt, but there is rarely evidence of the genuinely sharp contact which would accompany a prolonged break in deposition. Even the most defined transitions are interrupted by a ubiquitous bioturbation which is best seen at these points, piping sediment betwixt the contrasting adjacent layers. Styles of boundary are not random: the gradational variety is most commonly encountered in the upwards transition from marl to chalk, and the sharper type when the ascent involves a passage from a chalk to an overlying marl. Thus the couplets might be viewed as miniature versions of the whole successional trend with chalk overlying marl, and the cycles they represent as somewhat asymmetric.

Because there is an overall decrease in the amount of clay upward through the sequence the clay contribution eventually wanes so much that the banding dies out almost entirely to leave long stretches of apparently homogeneous chalk as the Cenomanian draws to a close. This is probably a case of subtlety rather than absence, however, because after the commotion of the Plenus Marls and Melbourne Rock, with the normal background accumulation of white chalk (now Turonian in age) once more well underway, the cycles

reappear albeit in a very muted form (e.g. Cottle, 1990). Turonian sections at St Margaret's Bay show faint regular variations in colour on a good day, looking more like a poorly washed window pane than the magnificent cycles of the Lower Chalk; but they are present nonetheless and show the same asymmetry, with maximum contrast between the top part of a chalk and lower boundary of a marl.



Text Figure 2.1 *Sketch of a Cenomanian chalk-marl couplet. Typically, the chalk will have a relatively sharp upper boundary indicative of a firm substrate, often with well developed Thalassanoides bioturbation and sometimes accompanied by a gritty texture. The upper boundary of a marl, by contrast, will normally grade into the chalk above, and most frequently be accompanied by flattened Planolites and thin Chondrites style traces. Sizes of couplets range from over a metre to around 10 cm for the smallest. Compare with Appendix Figure 2.1.*

2.1.3 Causes of Cyclicity

Cyclicity in sedimentary sequences is common on a variety of scales, and in the Mesozoic strata of the British Isles rhythmic alternations of clay and carbonate are especially prevalent. The origin of such cycles has a long history of debate (see Einsele, 1982 and Fischer, 1986 for reviews) and the theories generated fall into two categories: either the cycles are a primary feature of the depositional process, or they are secondary, resulting from diagenesis.

A purely secondary origin is apparently rejected by most authors (see Ditchfield, 1990) and can confidently be discarded in the case of the Lower Chalk for several reasons. Firstly, bioturbation is rife, routinely cutting bed boundaries and transporting sediment of different colour and composition between layers; secondly diagenetic activity of any description seems conspicuously lacking; and finally diagenetic unmixing of previously homogeneous sediment would be expected to produce randomly scattered nodules rather than even rhythmic layers: at the very least there must have been some primary feature to co-ordinate such a pattern (Ditchfield, 1990).

There are several theories concerning cyclicity in primary depositional processes, and many revolve around the shared theme of climatic fluctuation due to semi-periodic alterations in the Earth's orbit. The most regular of such oscillations is in *axial obliquity*, the tilt of the planet's axis away from a position normal to the plane of orbit. At present the Earth's tilt is 23.5° but it can range from 22.1° to 24.5° and it does so at a regular frequency of 41 000 years (House, 1995). *Precession* is a wobble on the axis so that it sweeps out a cone, an effect perhaps better initially envisaged with reference to a spinning top or coin than to an orbiting planet. In this the Earth varies with a rather more complex frequency than the obliquity cycle, but has major components repeating at, 19 000 and 23 000 years. At low resolution these subtleties can often appear combined as a single frequency of 21 000 years (House, 1995). There are also variations in the *eccentricity* of the orbit, i.e. changes in the major and minor axes of the ellipse. Frequencies here are more complicated still, but there is a major peak at 413 000 years, and others between 138 000 - 95 000. Once again, at low resolutions these blur, this time into a signal with a pulse of approximately 100 000 years. All three major effects are caused, to a greater or lesser degree, by the gravitational drag of other planets in the solar system.

Eccentricity is important because it is the only one of the Earth's foibles to have an effect on the *overall* flux of solar energy to the surface, but within this scheme the latitudinal energy *distribution* and certain aspects of seasonality can be affected by both obliquity and the interaction of the precessional cycle with the eccentricity cycle.

The transportation and distribution of solar energy by the oceans and atmosphere is not very well understood, but several mechanisms have been advanced to link orbital variations and the accumulation of rhythmic deposits. Arthur *et al.* (1986) review the possibilities, and Ditchfield (1990) distils them into five main categories, three of which he rejects as major factors in the generation of Cenomanian couplets. Dissolution, redox and

scour cycles do not stand up to investigation for a wide variety of reasons, although the factors involved in each probably accompany the genuine causes to some extent; productivity and dilution cycles are considerably more promising and both seem certain to have played a major role in the formation of chalk/marl couplets.

Productivity cycles are changes in the origination rate of biogenic carbonate which, when superimposed on a steady rain of detrital clay, could be responsible for the observed lithologic alternation: in this case the cycles would result from phytoplankton blooms of one sort or another. Perhaps 'bloom' is misleading because given the long timespan represented by an average bed of chalk, productivity might have increased only slightly overall, or alternatively the effect may have been due to a tendency toward genuine blooms, red tide-like events which flooded the sea floor with organic matter and which became more frequent or widespread on a periodic basis. Physical inducements to such phenomena include an increase in the availability of limiting factors, specifically nutrients, or an amelioration of environmental conditions from the perspective of the carbonate producers. There is some evidence for the second of these. In 1989 Ditchfield and Marshall reported a $\delta^{18}\text{O}$ isotope signal from a fine-scale transect through three Cenomanian rhythms which seemed to indicate that surface water temperatures reflected in the two lithologies may have differed by as much as 4.5°C . Given the apparent absence of cement in their samples they concluded that the most likely reason for the fluctuations was that the coccolith groundmass of the sediment had formed in surface waters which were on average 2°C warmer in chalks than in the marls. Recent analysis of the 'concealed' cement which can be found within the tests of foraminifera has raised concerns that primary temperature signals such as these may be somewhat spurious (Mitchell *et al.* (including Marshall), 1997). However, it still seems probable that the original conclusions of Ditchfield and Marshall, as well as the associated reports which came later (Leary, Cottle & Ditchfield, 1990; Leary and Hart, 1992), containing several other lines of evidence, are generally correct and make a strong case for a productivity component in the cycles.

Dilution cycles are a reversed version of the productivity scenario in which periodically increased contributions of terrigenous material to a steady supply of carbonate cause a pulse of marl to appear at the expense of normal chalk. An improved supply of detrital material could arise quite simply from additional terrestrial runoff, and Einsele (1982) estimated that the enhanced availability of clay needed to create a rhythmically bedded sequence is considerably less than the variation in carbonate necessary to generate

productivity cycles. Perhaps significantly, models of climatic variation resulting from changes in insolation level point to an intensified monsoonal period as one of the major effects (Rossignol-Strick *et al.*, 1983; Prell *et al.*, 1988).

An essential and important difference between the dilution and productivity models is that each sees an alternative material (and hence lithology) involved in accelerating the pace of deposition. Dilution by clay adds extra impetus to the normal sea floor buildup of carbonate; production of carbonate swells the steady rain of detrital clay. The significance of this becomes apparent when one considers that each lithology also represents a different amount of time (per unit volume), but that which is which depends upon the model.

Paul (1992) tackles this problem with considerable success. Using data from Ditchfield (1990) and assuming (because of the suspected Milankovitch origin) that every chalk/marl couplet represents the same duration, he calculates the amount of time each lithology is expected to represent depending on whether a productivity or dilution model is used. This is achieved by assuming that one of the components accumulates at a variable rate but that the other is steady, thus acting as either a siliciclastic or carbonate 'clock' by which to assess relative rates of deposition for the other lithology. Multiplying the rates obtained by bed thicknesses to calculate the length of time represented by each, he managed to compare the results from a series of fifteen laterally equivalent couplets in four widely spaced locations. Whilst figures generated by the dilution model vary considerably between sites and cycles, those predicted by productivity are remarkably consistent, despite the differences in insoluble residue content and sediment thickness from site to site. The calculations indicate that marls contribute something like 70% of the time represented by a couplet.

Paul makes his point but cautions that the values are not to be taken too literally; specifically, he notes that differential compaction between the contrasting sediments would affect the calculations. Since diagenesis generally occurs early in carbonates, however, and clay grade siliciclastic sediments are inclined to dewater significantly, any difference in compaction will tend to enhance the pattern. Thus the calculations for chalk deposition should be treated as maxima and those for marls as minima.

But this is evidently not the whole story. If the basal rate of siliciclastic accumulation assumed by the productivity model remained constant, and the couplets always represent the same amount of time, then the rhythms should thicken up-section as

the chalk takes over. In fact the reverse occurs, which implies that the siliciclastic contribution waned as time went on.

Hart (1987) attempted to construct a timescale for the Cenomanian succession based on the exposures at Culver Cliff in the Isle of Wight. He very reasonably made the 'bold assumption' that obliquity cycles of 41 000 year duration were likely to have had the greatest effect on phytoplankton and, using this value as the foundation, calculated that the Cenomanian should span some 6.5 million years. Culver Cliff was an unfortunate choice because it is rather condensed; Hart was aware of this and selected the site on the grounds of accessibility. Nevertheless, his efforts to compensate for the absent rhythms missed the mark and he guessed at 143 instead of the 212 later recognised by Gale (1995). Had he appreciated just how much of the sequence was unaccounted for he would have realised that 41 kyr is far too long a period, assigning the stage a term twice as long as the most recent radiometric estimate of 4.0 - 4.5 million years (Hallam *et al.*, 1985).

Gale (1990) tried a slightly different approach by identifying a secondary bundling effect of the basic chalk/marl couplets. His suggestion was that couplets tended to occur in aggregates of five as 100 000 year eccentricity cycles incorporating 20 000 year precessional ones. Where there is lateral condensation, as at Culver Cliff, bundles of five couplets are often replaced by a single rhythm. Gale has since lost confidence in the ubiquity of this secondary bundling (e.g. Gale, 1995) but I have seen enough evidence to convince me that there is some such effect in the couplets of the Channel sections. Even so, the original conception worked well enough for him to postulate forty four 100 kyr bundles, averaging five cycles each, in the most complete representations of the Cenomanian, giving the stage a duration of 4.4 Myr. Since then he has refined the scheme a little and works entirely by individually characterised couplets; this has recently lead to the 212 band plan of his, 1995 paper.

Acceptance that chalk/marl rhythms in the Cenomanian represent orbital forcing by roughly 20 kyr precessional cycles is now fairly unanimous (e.g. Jenkyns *et al.*, 1994; Paul *et al.*, 1994; Owen, 1996; Robaszynski *et al.*, 1998; Moghadam & Paul 2000 etc.). This time scale provides an outstanding base line by which to assess rates of morphological change.

2.1.4 Correlation and Stratigraphy

As with most British geology, the Lower Chalk has a long history of research, and there are stratigraphic schemes dating back for well over a century. Only in the last few decades, however, has correlation been possible on anything other than a million year scale, and only in the latter half of the, 1990s did it approach the resolution necessary for research of the kind needed to test *Plus ça change*.

The present stratigraphy is based on ammonite faunas with the foundation set in, 1960 when Hancock split the French Cenomanian into three parts. Kennedy (1969) used this plan to define a further six sub-zones, three in each of Hancock's two lowest divisions, and in 1984 Wright and Kennedy refined the divisions still further. These were not the only zonal schemes attempted: Carter and Hart (1977) erected a system based on both planktonic and benthonic foraminifera which probably only works for the south of England, but Sliter (1989) refined a broader planktonic version designed to work world-wide, and which has since been followed in the French Cenomanian (Robaszynski and Caron, 1995).

The scheme followed here is that developed by Gale (1995) who identifies zones by means of an 'integrated stratigraphy'. This revolves around the ammonite work of Wright & Kennedy (1984) into which Gale has introduced further divisions of his own, but it is also bound together with a wide range of other correlating features including sedimentary and faunal marker horizons (often the result of 'pulse faunas') and the topography of $\delta^{13}\text{C}$ curves (e.g. those in Jenkyns *et al.*, 1994). Since the recognition of prominent Milankovitch cyclicity in the European Cenomanian, this framework is being used in the ambitious but thoroughly impressive aim of correlating across several basins on a *bed by bed* scale! (e.g. Gale, 1995; Owen, 1996). The work has some way to go but looks promising, and, whether or not it succeeds completely, sufficient progress has already been made to match individual couplets across one rim of the Anglo Paris Basin.

Gale's strategy has been to log in detail the most complete successions, looking all the while for marker horizons as well as the characteristic zonal faunas, and to count the number of couplets between regionally recognised levels. Tackled in this way the distinctive nature of individual beds soon becomes obvious. Frequently there are a consistent number of chalk-marl couplets between marker horizons and where there are not it is normally possible to observe beds thinning to extinction, amalgamating and/or gradually forming condensed horizons. There are some rare instances of widespread

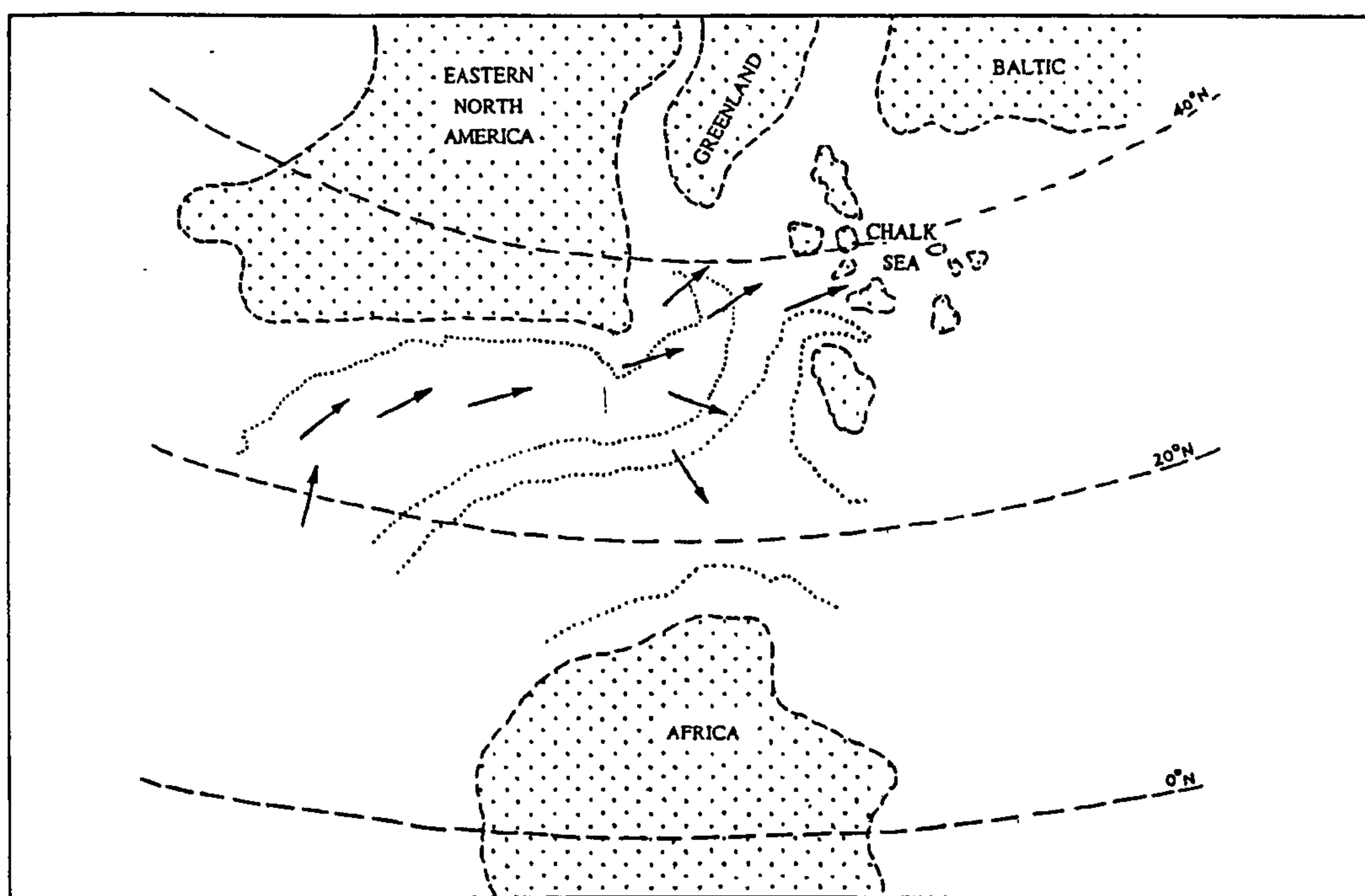
erosion in which only the minimum number of couplets lost can be estimated (from their occurrence elsewhere), but these erosion surfaces can themselves be used as marking points. More problematic is tracing couplets where the cyclicity is not well developed, and as a consequence the stable part of the study section, because of the lower degree of contrast between chalk and marl, is less well correlated across even the local sections of southern England. Precision to within a few tens of thousands of years is still possible, however, and in comparison with typical geological sequences this resolution is outstanding.

Gale's stratigraphy (1989, 1990 and especially 1995) has been followed for this project because it exploits the distinctive identity of individually numbered couplets, rather than relying on the collection of rare zone fossils every time orientation becomes problematic; consequently his numbering system has also been employed. I believe (and hope) it will become increasingly conventional to adopt this scheme for the Cenomanian in Europe, despite occasional quibbles concerning nomenclature (e.g. Bristow *et al.*, 1998), because Gale's work is extremely detailed and very competent. On the rare occasions my own initial observations have conflicted with those of his published logs, further (normally more widespread) examination has always vindicated him and proved me wrong. And there can be no doubt that a basin-wide nomenclature is considerably more meaningful than one restricted to exposures on the Channel coast.

Gale's scheme splits the Cenomanian sequence into four main blocks, labelled A-D, each with around 50 couplets in them, plus an additional block, E, with 17 couplets to account for the Plenus Marls (Text Fig. 2.2, column 3). The study section covers all of block C and the top few couplets of block B (more of this in Section 4.1.1), this being roughly the transition from upper Chalk Marl to lower Grey Chalk in the traditional scheme, and the upper part of the *Mantelliceras dixonii* and all of the *Acanthoceras rhotomagense* ammonite zones in Kennedy's (1969) scheme. Recent work on sequence stratigraphy in the Cenomanian deposits of the Anglo-Paris Basin (Robaszynski *et al.*, 1998) suggests that Gale's numbering scheme reflects transgressive system tracts, the boundaries to each of the numbering blocks corresponding with a sequence boundary. As will become apparent, it is significant that the transition from B to C block occurs in the purportedly variable part of the succession.

2.1.5 Palaeogeography

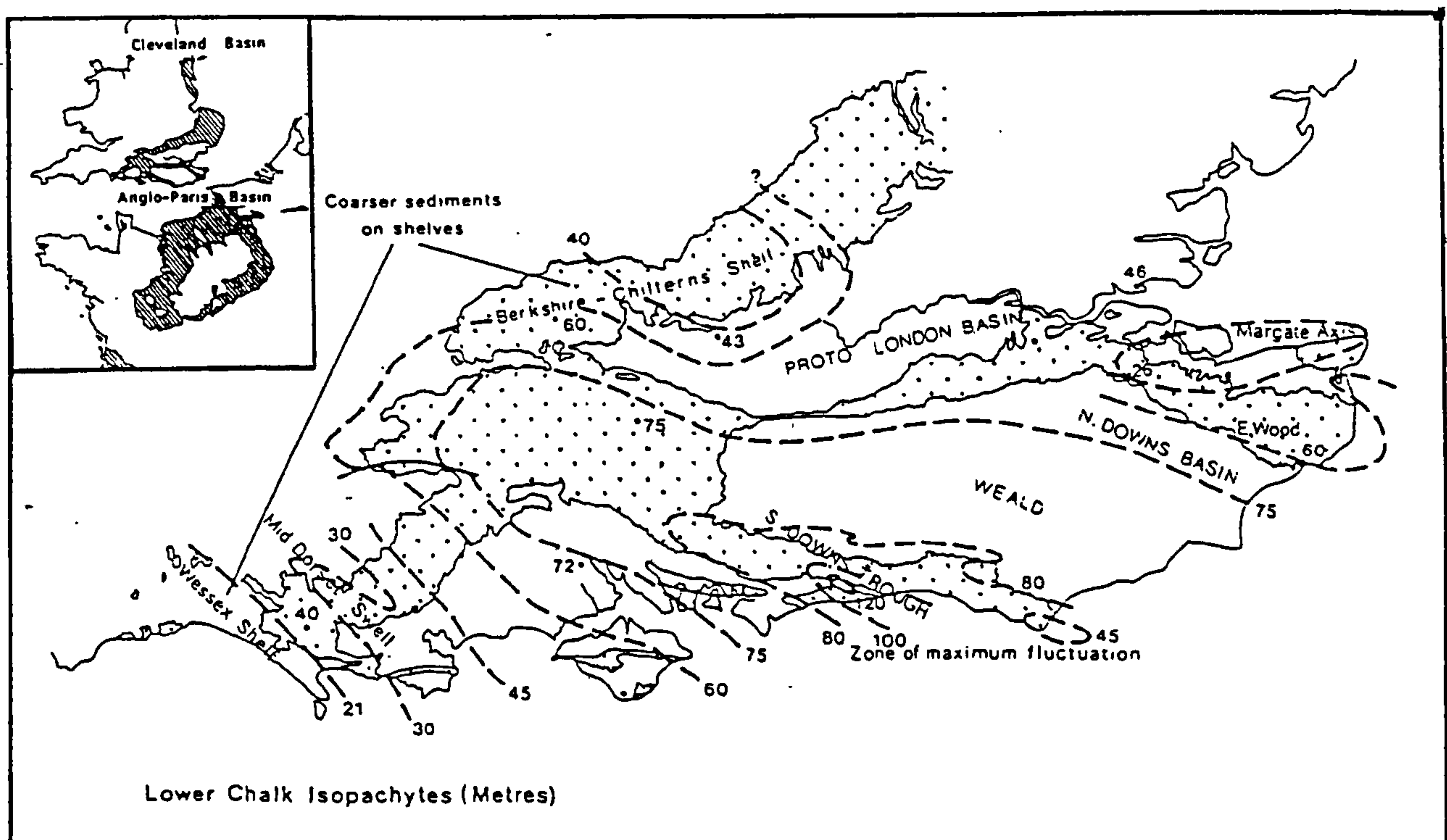
Some 95 million years ago the Anglo-Paris Basin was at a latitude of between 35 and 40°N, putting it on an equivalent level to present day southern Spain and Portugal. The opening of the Atlantic was well underway, but the ocean was not yet wide. Major current systems are supposed to have run poleward along the eastern coast of the North American mass and swept across the narrow sea, closing on Europe from the west (Hart and Tarling, 1973: Text Fig. 2.3).



Text Figure 2.3 *Ocean current systems approaching the Chalk Sea from the early Atlantic. Compare this broad context with Text Fig. 2.4. After Hart and Tarling 1973.*

The area had been a shallow embayment ringed by islands, hovering between land and sea for the previous 35 million years, but the expanding and active Mid-Atlantic Ridge system eventually provided the impetus for an overwhelming transgression. Wealden lagoons gave way to banks of shallow marine sand which were swept clockwise around the gulf by interchanging currents from the North Sea and the Atlantic. The shoreline migrated landward as the water level rose and muds took over in the centre of the basin as the Albian progressed. To the south and west both Brittany and Cornwall remained

uncovered, shielding the region from strong ocean currents; to the north the Pennines and Cambrian Mountains, and the Rhenish Massif in the east completed the bulwark (Anderton *et al.*, 1990). By early Cenomanian times the sea had flooded Dorset, but muddy basinal sedimentation stretched no further west than Bournemouth. Beyond, a topographic high known as the Mid-Dorset Swell collected exotic mineral sands eroded from the Hercynian granites of Cornwall (Hancock, 1969; Drummond, 1970). The beach at this time would have lain somewhat west of Bridport, running southeast to northwest, parallel to the offshore swell, and, thus set, the situation seems to have changed little throughout the middle of the Cenomanian. Despite an erratic but persistent transgression, chalk was slow to overwhelm the shelf, and the islands were probably not entirely swallowed, nor their sediment supply choked, for another five million years (Hancock, 1969, 1989). The northern shores of this Cenomanian sea are now obliterated but the southern and eastern edges of the province tell a very similar story (Robaszynski, 1981).



Text Figure 2.4 Contours of equal thickness reveal the geography of the northern portion of the Cenomanian Chalk Sea. Shaded areas (cross-hatched or stippled) show the outcrop of the Chalk series. Compare these maps with Text Fig. 2.3 for a wider context. Modified from Mortimore 1983.

Within the basin, slabs of Hercynian basement controlled deposition. Predominantly east-west trending graben and half graben structures offset by northwest to southeast wrench faults carved the terrain into a number of roughly rhomboidal blocks and troughs, which jostled each other as the region subsided (Robaszynski, 1981, Lake and Karner, 1987, Ditchfield, 1990). Throughout Lower Chalk deposition the overall geography across the northern edge of the province was that of an elongate southeast sloping shelf, bounded by structural highs to the north and west. Locally the South Downs Trough and Brighton Dome provided maximum vertical relief, accumulating, over the whole period, a difference in 80 metres of sediment across a separation of about 50 kilometres (Mortimore, 1983). Although submerged, the London-Brabant platform remained a structural high throughout the era, separating the depression of the Anglo-Paris Basin from that of the Cleveland Basin to the north (Text Fig. 2.4).

2.1.6 Palaeoceanography

Local events aside, global sea level rose across the Cenomanian, although it did not do so smoothly, and evidence of temporary regression has long been recognised. In an effort to construct a west European sea level curve, Hancock (1989) used condensed horizons and zones of widespread erosion as an index of water depth. These were applied in the absence of marginal sequences and taken as signs of lowstand, with a rough assumption that highstands should be midway between. Two transgressive peaks were identified in this way, separated by an extensive period of regression or persistent lowstand that spanned virtually the whole of the middle Cenomanian, including most of the study section.

Gale (1990, 1995) and Paul *et al.* (1994) suggest that there is a period of transgression within Hancock's continuous lowstand. Deep water in the *M. dixonii* Zone, Gale's B band couplets, was succeeded by a stepped regression around B41 - C2; this is the base of Hancock's lowstand and it is a level of widespread erosion: in the Chilterns a large segment of the sequence is missing between this point and the overlying Totternhoe Stone. Paul *et al.* (1994) argue in favour of a double or stepped lowstand at this point, one part at the base of B41, the *arlesiensis* bed, and another at the base of the *primus* bed, C1. Following these, all indications are of deeper water until the sandy chalks of Jukes-Browne

Bed VII, possibly contiguous with the Totternhoe Stone, mark the reappearance of shallower conditions.

Carter and Hart (1977), Hart and Bailey (1979) and Hart (1980) reported a mid-Cenomanian shift in the proportion of planktonic (P) to benthonic (B) foraminifera which they called the P/B break. The percentage contribution of the plankton increases dramatically up section from around 0-10% to a typical 50% of the >250 μ m fauna; the change takes place over a small number of rhythms (see Paul *et al.*, 1994), and there is no prolonged break in deposition, although the phenomenon is often associated with a rather condensed couplet (C10). According to the original interpretation, all of this indicates a rapid deepening in the basin, which fits in well with the present opinion that a transgression was well underway by that point.

The Cenomanian-Turonian boundary at the upper end of the Lower Chalk is represented by the Plenus Marls, which record a well established global catastrophe, very sensibly (if rather unimaginatively) dubbed CTBE—the Cenomanian-Turonian Boundary Event (Paul *et al.*, 1994). Sepkoski (1986) ranked the faunal turnover associated with this occurrence in the top ten post-Palaeozoic marine mass extinctions, and it is thought to have been driven by an expansion of the oxygen minimum layer to a point where it intersected large portions of continental shelf and offshore platform (Schlanger and Jenkyns, 1976; Jarvis *et al.*, 1988). An expanded low oxygen layer, starting 100-300m below the mixing zone of the surface and extending to more than 2 kilometres depth, is believed to have formed on at least two occasions in the Cretaceous when, associated perhaps with tectonic events in the South Atlantic (e.g. Summerhayes, 1987), nutrient-rich deep water is thought to have welled into the photic zone and spurred phytoplankton blooms on an unprecedented scale. High surface productivity always creates a low oxygen layer in the water column below due to the breakdown of organic matter as it sinks, and when the layer of deoxygenated water swells enough to intersect the shelf, the result is an aerobically hostile environment which discourages many organisms and allows an organic rich sediment to accumulate (Schlanger and Jenkyns, 1976; Jarvis *et al.*, 1988).

The CTBE in the Plenus Marls is marked by a peak in the $\delta^{13}\text{C}$ trace, and isotopic investigations lower in the succession have revealed a similar, though smaller hump from the beds of the putative lowstand at B41 - C2 (Jenkyns, Gale and Corfield, 1994; Paul *et al.*, 1994; Text Fig. 2.2). Like the regression it coincides with, the peak is also stepped, with a

minor shift at B41 and a rather larger one between C1 and C2; unlike the CTBE in the Plenus Marls it initiates no obvious extinctions, but it is associated with the same transient faunas as CTBE (Paul *et al.*, 1994) and present opinion holds that it represents a similar oxygen depletion event, prompted by upwelling waters and perhaps the shallowness of the sea.

Section 2.2 A Biological Context for *Plus ça change*

2.2.1 Ecological Structure - Top Down

In any ecosystem there is a finite input of energy and matter per unit of time and all organisms compete for their share of it. The hierarchy of consumption is the food chain and the various stages trophic levels. Because energy transfer from stage to stage inevitably involves a great deal of wastage, there are rarely more than half a dozen or so trophic levels in any ecosystem, and because interaction between levels is always a variety of predator-prey (or grazer-grazed) relationship the links in the chain tend to regulate one another by negative feedback. Apart from such 'vertical' connections there are 'lateral' relationships along the same trophic level, and also situations where potentially vertical relationships are actually laterally offset, because although one organism could perhaps feed on the other, in practice it never does. One way of understanding this network is to focus on top carnivores which can be thought of as 'sinks' into which the energy and material from lower levels are funnelled, although in reality the ultimate sink is inevitably the lowest level of detritivores. In fact, any organism can be viewed this way so that the whole ecosystem network is seen as a series of energy 'drainage basins' arranged as anastomosing, nested sets.

Direct relationships between organisms in such a network might be considered to fall into one of three categories depending upon whether they are beneficial, detrimental or totally neutral, so that between any pair of organisms there are just six possible styles of interaction (Text Table 2.1). Situations involving perfectly neutral interaction are probably fairly rare in nature and are not particularly interesting anyway, but mutualism, competition and predation are extremely significant. In this way the set of all species interactions can be represented as a community matrix (Levins, 1968) with the direct vertical component constituted by a (+ -) 'predation' symbol. Direct interactions, however, become far less important once indirect ones are taken into consideration. For example, consider two prey species with a common predator. If either of the prey increases in number the predator will tend to follow suit, to the detriment of the second prey species—a kind of indirect competition! It is clear, then, that the final sign of any direct interaction depends upon all the other indirect relationships in the matrix, which, according to Pianka (1987) is one of the reasons why good experimental community ecology is so difficult to do.

Interaction	A	B	Nature of the interaction
Competition	-	-	A and B inhibit each one another
Predation	+	-	A exploits B
Mutualism	+	+	A and B both benefit from each other
Neutralism	o	o	A and B do not affect one another
Commensalism	+	o	A benefits, B is unaffected
Amensalism	-	o	A is inhibited, B is unaffected

Text Table 2.1 *Styles of interaction between a pair of species (after Pianka, 1994).*

If predator-prey relationships involve negative feedback then mutualistic ones are a form of positive feedback, with each species encouraging its partner. By contrast, competitive (- -) interactions can go either way, depending upon the strength of the interaction (represented by a competition coefficient) and the population sizes of each species relative to the other. In simple models (e.g. the original Lotka-Volterra version) there are regions in the range of possible values which will inevitably push one of a pair of species into extinction, configurations in which either species can win depending upon the relative density of the populations when the model begins, and versions where neither species can eliminate the other so that some stable equilibrium is eventually reached. This kind of thinking has led to the idea that in the long term communities tend to settle into stable states in which the population densities of all the species regulate one another; the community matrix can then be seen as possessing ‘attractors’ in terms of the distribution of population densities, so that if the system is nudged out of equilibrium (by a change in the physical environment perhaps) it will wander for a while and then either settle back into the original state or, if pushed far enough, find a new equilibrium. Equilibria come in a variety of types including ‘cyclic’ stabilities and ‘trajectory’ stabilities (such as ecological successions) as well as the more obviously static ‘point’ equilibria (Pianka, 1994).

Not all positions in the community matrix hold equal importance: some have a keystone role in which the abundance of a particular species is responsible for regulating the densities of a large number of others (e.g. Paine, 1974). The specific organisation of the food chain is of vital importance to the keystone function. Pimm (1991) has modelled the effects of species removals from hypothetical trophic networks to demonstrate the impact of a loss, and his overriding conclusion is that prediction of an outcome is very difficult unless the whole food chain is understood.

The issue of experimental prediction is irrelevant to the retrospective gaze of a palaeontologist, but the fact that ecosystems can be both sensitive and robust is an important one. Peripheral species might come and go in an almost modular fashion, whereas loss of those more integral to the whole can precipitate a comprehensive collapse. The ample benefits of hindsight provide an opportunity to analyse what transpired long after the event, and it may well be that the ecological character of a particular species can be more accurately understood by watching its fossil pattern of invasion and retreat.

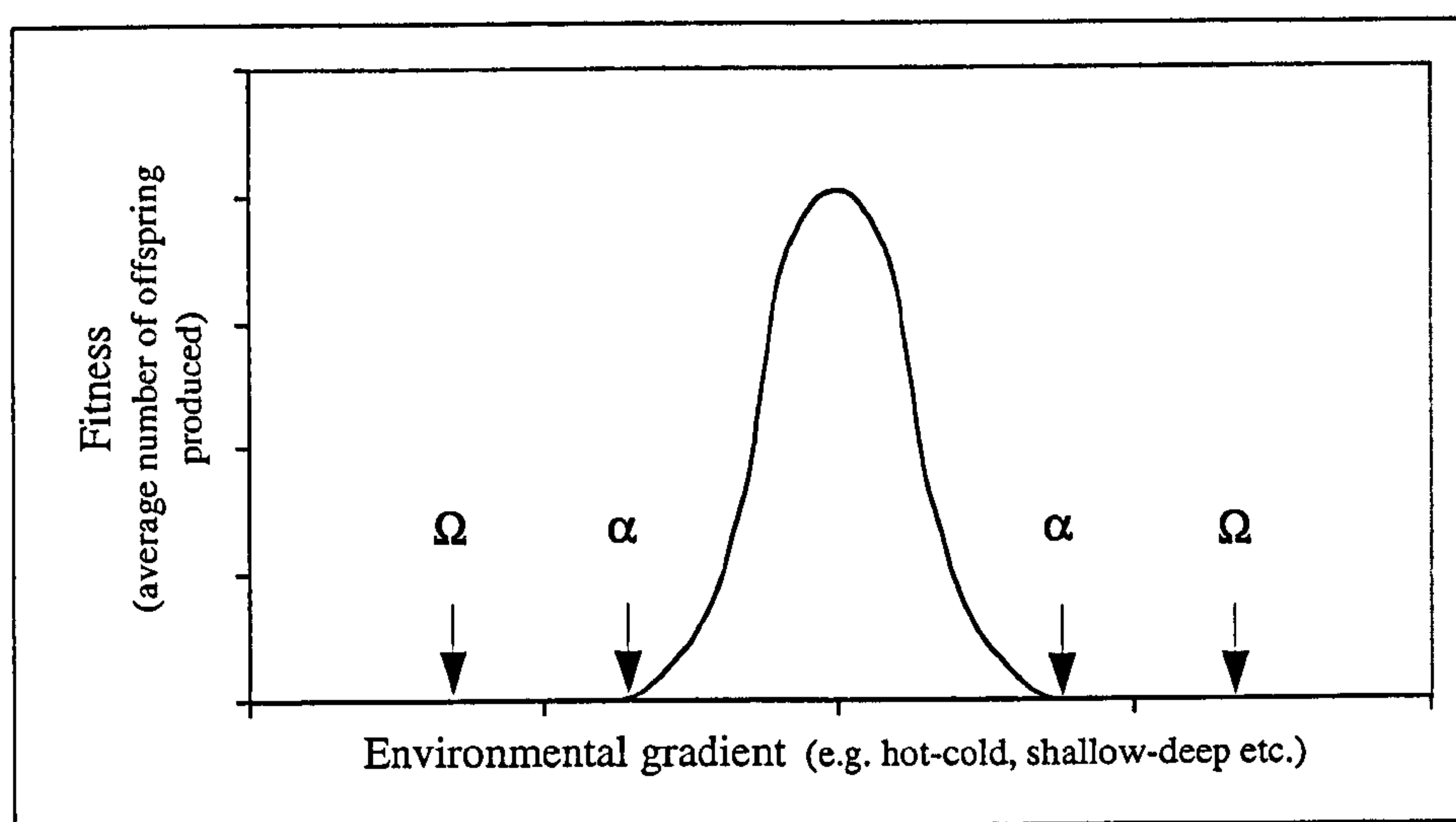
2.2.2 Ecological Structure - Bottom Up

Given its design, there are a set of environmental requirements which must be met in order for any living thing to survive long enough to successfully reproduce. Because the world is not homogeneous but varies in its range of conditions, there are four particularly significant points linking an organism to relevant scales of physical variation: two are outer limits beyond which survival is impossible, and there are two inner gradients within which reproduction is progressively encouraged. For a population on any resource or habitat gradient the relationship between the number of offspring generated (fitness) and environmental conditions is generally thought of as a roughly normal distribution, with an optimal point midway between the limits of tolerance. For a large number of variables the distribution is an n -dimensional 'hypervolume' (Text Fig.'s. 2.5 & 2.6).

A hypervolume encompassing the entire set of physical conditions under which the organism can live and replace itself constitutes its *fundamental niche*, a hypothetical idealised hyperspace in which the organism encounters no predators or competitors and is limited only by the quantity of resources. No environment is infinite and so a point will always be reached, even under ideal conditions, when the limitations of the fundamental niche are met. At that point the species will come under internal (*intraspecific*) competition, so that when novelties are produced the result will be a natural selection of new ways to broaden the fundamental niche and exploit hitherto untapped regions in the space of possible resources.

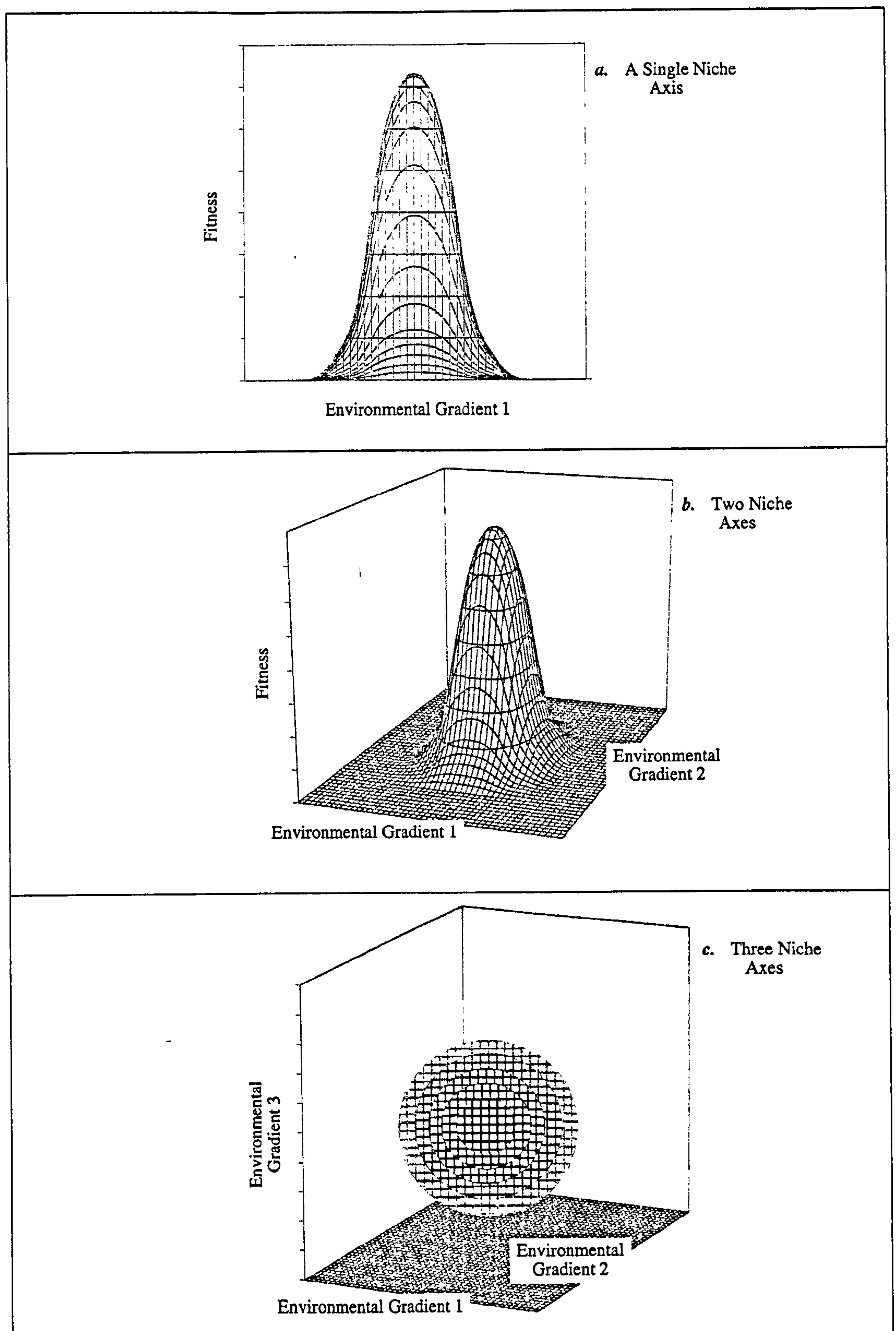
The actual set of conditions under which most organisms exist is far less than the total possible range and is termed the *realized niche*. A fundamental niche may be restricted because of limitations in the physical environment, but more commonly the

limitation comes from interference with other species whose fundamental niches overlap, in which case the competition will also be *interspecific*. One ‘aim’ or endpoint of interspecific competition is the elimination of any rival in the occupied zone so that the organism can fill its fundamental niche, and this is what the competition coefficient (mentioned in the paragraphs above) is supposed to measure. But it is equally advantageous to avoid competition if at all possible and so, where exploration has permitted it, the fundamental niche will tend to be shifted into unoccupied zones of resource space. The ideal stable state is one in which the component species have spread their fundamental niches out through resource space in such a way as to avoid overlaps, and indeed evolution can be thought of as a process by which the fundamental niche is nudged, or forces its way, into a realized niche of the same dimensions.

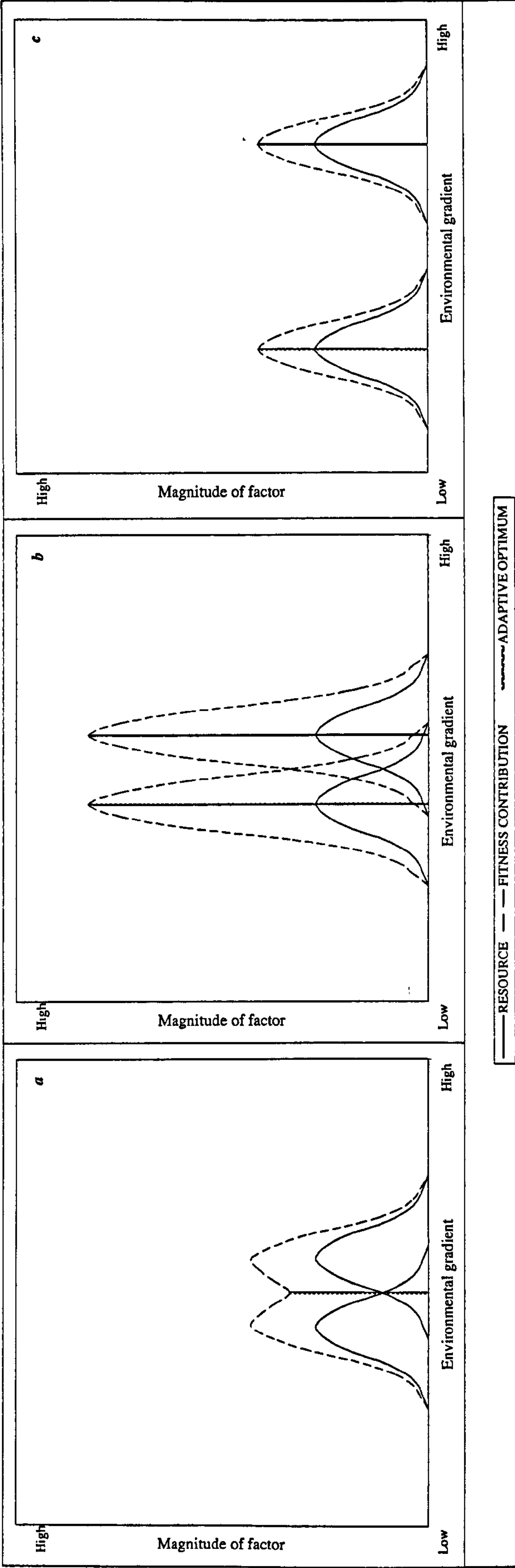


Text Figure 2.5 *Important boundary points in an organism's world. α marks the onset of conditions allowing reproduction to occur, Ω marks the point beyond which survival is impossible.*

Different species spread themselves through different ‘volumes’ of resource space: some occupy relatively small regions and are thus specialists, and others occupy much broader zones and are therefore generalists. Whether a species adopts a generalist or specialist approach to exploiting a portion of any resource gradient depends upon the ‘granularity’ of that resource relative to the needs of the organism. Granularity is a kind of pay-off between the patchiness of a resource and the contribution it makes to fitness. Relatively homogeneous resources will encourage generalism, as will less homogeneous ones with a lower contribution to fitness, whereas resources with a spatially heterogeneous distribution will foster specialism, particularly if the clumps each make a large contribution to fitness (Text Fig. 2.7).



Text Figure 2.6 A standard textbook (e.g. Pianka, 1994) way of depicting one, two and three-dimensional niche spaces. Note that in c, because all three dimensions are taken to represent habitat gradients, fitness is shown with greyscale shading. Further dimensions can be taken into account so that the final configuration for any species is an n -dimensional hypervolume. See text for discussion.



Text Figure 2.7 The relationship between resource distribution, fitness contribution and adaptive strategy (drawing and argument adapted from Pianka, 1987). Panel a: Resources conferring only a modest contribution to fitness overlap along an environmental gradient. The organism 'perceives' them as effectively homogeneous and adopts a generalist strategy. Panel b: Again, resources overlap somewhat, but because of the significant fitness contribution conferred by each, specialist adaptive strategies are adopted allowing two species to co-exist. Panel c: Resources do not overlap at all. Perceived as heterogeneous, they have become the focus of specialist adaptation in spite of their modest contribution to fitness. As an easy example to bear in mind, the two resources might represent seeds of different sizes available for exploitation by Darwin's Finches of the Galapagos (see Weiner, 1987, for an accessible account). Panel a then depicts a situation in which a pair of seed types overlap in size and also offer only a modest energy yield, thus supporting only a single generalist species with a beak size optimised to the middle of that range; although the beak cannot cope with seeds at the furthest ends of either seed range, there is a sufficient density of middle range material to keep the species going. Panel b depicts a situation in which two seed types overlap in size but offer such high energy yields that they have become the focus of specialisation, thus supporting two specialist species. Panel c depicts a situation in which two seed types of modest yield have nevertheless resulted in specialization because there is no beak size which can handle both of them. Note that the designation of whether or not a resource is of sufficient 'granularity' to be exploited one way rather than another is a function not just of the resource itself, but also of the species in question. For instance, with a larger organism altogether, the situation in Panel c might be perceived to be a situation more similar to Panel a. (See Section 5.2.4 for a continuation of this argument.)

Species which opt for generalism may do so either by constructing a range of slightly different phenotypes which are each adapted to some specific aspect of the available resource, or by constructing an all-purpose phenotype able to exploit wide zones of the gradient. Which of these strategies is adopted will probably depend upon how constant any heterogeneities in the resource gradient are: if they can be relied upon for long periods then the species may well have time to discover a range of distinct phenotypes (or ecophenotypes which mask an all-purpose genome behind a variety of expressions), which would then tend to cut down on intraspecific competition.

Constancy of environment, or 'temporal patchiness', in terms of the abundance of resources available over any particular period, exerts a very important control on the variety of lifestyles possible. Given a finite amount of any resource—matter, energy, space etc.—there are a correspondingly limited number of individuals, for any particular design of organism, which can be maintained. The overall limitation is the 'carrying capacity' of the environment (a factor generally termed K) and it can be subject to fluctuations of its own. When an environment's carrying capacity first increases, receptive populations will tend to grow exponentially until the newly available resources are all used up, and while this happens there will be positive selection for a plexus of reproductive characteristics associated with fast breeding: short generation times, single reproductive bursts, and large numbers of fast growing, short lived offspring. Species adapted to regularly fluctuating resources by employing these features are termed r -strategists (because they have a high intrinsic rate of natural increase, r) and they are contrasted with species which are limited instead by the constancy of their environment's carrying capacity. Such K -selected species are rarely in circumstances where their fitness is maximised by mass manufacturing, and tend to end up adopting the opposite range of characteristics as they dig in for a war of attrition. The important point is that the terms K - and r -selected are *relative* designations and that the characteristics which define them are *adaptations to a gradient of resource stability*; K - and r -selection then becomes the process of adaptive motion along such an axis.

Temporal resource patchiness can now be compared with spatial habitat homogeneity. By extending the arguments presented above it seems that whether or not a temporally fluctuating resource can be assimilated into the life strategy of an organism once again depends upon its 'granularity'. This time, however, granularity means frequency (the temporal analogue of spatial homogeneity), along with the contribution a resource makes to

fitness, which are the controlling factors. We can see that it is only worth 'specialising' in (i.e. *r*-adapting to) truly intermittent resources when they make a large contribution to fitness, and that an 'opportunist' organism which is fussy about its habitat range (i.e. one which is a specialist in the normal sense of restricted niche breadth) will be seriously reducing its chances of finding suitable opportunities to exploit. We thus expect opportunism and generalism to go together, and equilibrium strategy to be correlated with specialism. It should also be stressed that the adaptations will be to some massively time-averaged expectation of temporal variability, with various bet-hedging strategies thrown in to help cope with the unevenness of the patchiness itself. Once again, this should be less important, and less apparent, to the retrospective gaze of a palaeontologist than it would be to an ecologist working with organisms over short timescales.

Without taking into consideration the character of any particular setting we have models here for predicting how *all* ecosystems should be structured, along what might be termed *universal* niche axes. The process of natural selection is hugely dependent upon chance events and random directions of exploration (Eble, 1999), with individual cases apparently dominated by their idiosyncratic histories, a fact which has lead some to deny that biological laws exist at all (e.g. Popper, 1959). But even highly contingent events, if performed time and time again, can yield statistical patterns, and this is what the universal niche axes represent. They are features so general and non-specific that they can be expected to occur in any setting at any time, and also for local faunas to have become adapted to them over and over again. We can envisage a community to always be strung out along such universal axes, irrespective of how the specific resources and opportunities are actually distributed.

In fact, there are many ways in which the gross statistical results of this ecological distribution process tend to be remarkably similar (otherwise there would be no talk of guilds and trophic levels). One of the most ubiquitous is the so-called 'log-normal' distribution of species, in which there are a small number of very abundant types and a large number of very rare ones. The standard 'broken stick model' explanation for this is that in an empty environment the total range of any resource gradient might originally be exploited by a single pioneer species, but as new species arrive (or evolve), sequestering randomly allotted portions for themselves (i.e. breaking bits of the original stick), the total volume becomes progressively more partitioned. Effectively the argument hinges on the fact that for any given axis there are more ways to partition it narrowly than broadly, or in

other words there are more ways to be specialised than there are to be generalised. In this reading, specialism necessarily squares with low resource volume and therefore low species abundance. With sufficient time the outcome will be a log-normal distribution, a result so ubiquitous and expected that it is sometimes used as a calibration point to gauge how accurately a community has been surveyed.

2.2.3 Foraminifera in the Food Chain

Their good fossilization potential means that foraminifera probably always appear more ecologically significant to the palaeontologist than they would have done to a contemporary biologist. They are, however, widespread, often prolific, and an important biological element of any environment in which they occur. Standing crops vary enormously depending not only on the type of environment and general stability of the setting but also on a very local level as individuals track specific micro-habitats. Murray (1991) summarises an impressively large list of published surveys and suggests that values for the Atlantic seaboard of Europe and NW Africa range from 10 living individuals per 10cm² to 550, with an inverse relationship between sediment grain size and patch density. Numbers between size fractions reflect this too, with <125 µm gradings typically recording hundreds of individuals, whereas >125 µm ones often contain only tens.

The main ecological 'role' of foraminifera is in rescuing energy from the lowest trophic level and redistributing it back up the food chain (Lipps and Valentine, 1970; Gooday *et al.*, 1992). This is achieved by occupancy of a cluster of adjacent and overlapping niches concentrated around detrital scavenging, bacterial 'grazing' and suspension feeding, and, in turn, being the choice food of specialist predators as well as the chance victims of unselective deposit feeders. Lipps (1983) listed "flatworms, polychaetes, chitons, gastropods, nudibranchs, bivalves, crustaceans, holothurians, asteroids, echinoids, crinoids, tunicates and fish" as incidentally swallowing foraminiferal tests. These are all organisms which at some time or another have been found with tests within their guts; they by no means ingest only live foraminifera, nor may they derive much nutrition from those living specimens which they do. However, it seems fair to assume that given the impressive and unexpectedly large contribution of meiofaunal elements (mostly tiny nematodes, polychaetes and crustaceans but also including representatives from the majority of phyla)

to productivity in the sediment from shelf areas (Platt, 1981), foraminifera should be a significant factor in the feeding strategies of many deposit feeding creatures. In addition to these there is a smaller range of organisms, mainly larger polychaetes, molluscs and crustaceans, which have been found to feed selectively on foraminifers (Lipps, 1983), sometimes choosing only particular benthic species from a broader foraminiferal population (Bilyard, 1974).

For the foraminifera themselves, the main criterion for a potential food source, it seems, is that the target must be small enough to cope with (Murray, 1991). Apart from that forams cover as wide a range of feeding styles as any group of heterotrophs: there are herbivores, carnivores, omnivores and detritivores; cannibalism, parasitism, and osmotrophy have also been demonstrated in certain species (Lipps, 1983). This is not to say that foraminiferal species are unspecific feeders; laboratory tests have demonstrated that when suitable varieties of algae and bacteria are present in their environment these are preferentially consumed, leading to enhanced growth among those species that favour the food sources available (Lee and Muller, 1973).

The primary source of energy rich organic material in the Cenomanian Chalk Sea must have been the coccolithophorid debris and associated faecal material drifting down from above. This would have been primarily consumed by both foraminifers, their meiofaunal companions, and such detritivorous organisms as bacteria, and these in turn secondarily consumed by more foraminifers along with other minute predators and anything which vacuumed the sea bed. Below the sediment-water interface the process would presumably continue with a range of infaunal detritivores picking over the remains: the whole of this microcosm would then be available as food for the menagerie of Lipps' list. Of the many predatory taxa listed, gastropods, asteroids, crinoids and especially bivalves and echinoids have some fossil presence in the Lower Chalk (Owen and Smith, 1987). And of those leaving no body fossils to mark their existence, the abundance of traces including *Planolites*, and *Thalassinoides* testify to the mass of worms and crustaceans which must have squirmed in the soft debris of the sea floor.

Modern analogues for this idealised fossil ecosystem certainly exist. The bacterial reproductive response to phytoplankton blooms has been documented by Lochte and Turley (1988), and the foraminiferal response by Gooday and others (Gooday, 1988, Gooday and Lambshead, 1989, Gooday and Turley, 1990, Lambshead and Gooday, 1990).

The speed of such responses has been assessed by Graf (1989) who suggests it could be as little as eight days after a major fall of material. This is not so surprising in the case of bacteria since they can reproduce sometimes in a matter of hours, but with foraminifera such a rapid reaction is quite impressive.

2.2.4 Niche Partitioning

Although Gooday (1988) was not able to pin the speed of response down to less than two months he does present fascinating evidence on the nature of the fauna. The phytodetritus from his samples harboured an abundance of only three species, none of which were present in large numbers in the sediment below. The size distribution histograms from this prolific, low diversity fauna suggested that at least two of the species had responded reproductively to the influx of material, generating population curves which were skewed towards the juvenile end or obviously bimodal; the remaining species may well merely have migrated in from the underlying sediment. In addition to this, two of the species had greenish protoplasm suggesting they had ingested the phytoplankton itself, and all three (from a study of epifluorescence) had been consuming the blooming prokaryotes which accompanied the fall. While other species were more common in the sediment below, some seemed to fare equally well in both the new detritus and the old.

An obvious conclusion from this information, previously supported by authors such as Murray (1991) and Lipps (1983), and even exploited for palaeontological purposes (e.g. Koutsoukos and Hart, 1990; Koutsoukos, Leary and Hart, 1990), is that even foraminifera can exhibit the range of life strategies commonly explained by models of *K*- and *r*-selection: adaptation to a *relatively* opportunistic role is evident even amongst these short lived and semelparous creatures. A fauna dominated by unusually small, thin-shelled individuals is often taken as evidence of *r*-strategy (Koutsoukos, Leary and Hart, 1990, Leary and Hart, 1992) and in a situation where the main energy source is seasonally available detritus, those species living an epibenthic existence at the sediment-water interface might be more likely to encounter selection for opportunism.

Vertical partitioning within the sediment was reported by Corliss (1985) in deep water samples from the North Atlantic. In this case the distinction was not due to a phytoplankton bloom which encouraged opportunistic species but a natural segregation of the community into infaunal and epifaunal modes of existence. Recognition of the characteristic test shapes associated with different lifestyles has given rise to the morphogroup method of ecological classification (e.g. Severin, 1983; Kitazato, 1984; Jones and Charnock, 1985; Bernhard, 1986). In general, forms which are planar, plano-convex, concavo-convex or biconvex (i.e. disc like and flattened in some way) are thought to be epifaunal. Those which are elongate, tapered, fusiform or globular are normally considered infaunal. The rationale for this distinction comes primarily from modern distributions coupled with a consideration of the shapes best suited for floating on a two dimensional environment, or lodging within a three dimensional one (e.g. Corliss, 1985).

On a rather broader scale, Corliss and Chen (1988) reported on the distribution of numerous morphotypes along a depth profile in the Norwegian Sea. Most of the groupings have well defined peaks of relative abundance which change with depth, although it is less clear what is responsible for such variation. Several physical parameters change across the transect including the grain size and percentage of carbonate and organic carbon in the sediment; presumably also the temperature and hydrostatic pressure change since the depths ranged between 150 - 4000m. Most authors agree that benthic foraminifera are sensitive to a variety of features in their physical environment. The characteristics of the substrate and temperature of the setting seem to be particularly important, but salinity, oxygen levels, current velocity, the availability of calcium carbonate and even light intensity may be crucial factors (best found in general reviews of foraminiferal ecology e.g. Murray, 1991; Haynes, 1981; Brasier, 1979).

All organisms are patchily distributed across their total range (e.g. Hanski and Gilpin, 1991) and local clumping is thought partially to reflect sensitivity to small differences in the immediate surroundings. With foraminifera these environmental heterogeneities may not be obvious to casual inspection, but there is no doubt the organisms themselves are aware of them. They may be chemical, physical or biological - any of the elements listed in the pages above - and although subtle they are presumed to provide comfortable circumstances and a competitive advantage to appropriately adapted species.

2.2.5 From Ecology to Palaeoecology

Major discontinuities between standard ecological data and its palaeontological equivalent arise through two factors: differential preservation and temporal scaling. Both must be accounted for in order to produce an accurate portrayal of an environment some 95 million years gone.

The preservational element concerns a distinction between the organisms present in the original community and those recorded in the fossil record. No entirely soft-bodied organism can be expected to endure for long; in addition there are many shelled species whose hard parts might have survived intact had the conditions of preservation been more favourable, but which have since been lost due to the vagaries of their setting. These subtler taphonomic criteria, the breakage by transport of delicate features and the subsequent dissolution of others, may vary on a bed to bed basis. Thus, we are presented with two sets of problems. Firstly, what portion of the fauna had a shelly skeleton, and to what extent does it represent the whole? Secondly, within this subgroup of fossilizable creatures, to what extent is their preservation uniform?

The first issue must be addressed on a largely theoretical basis by examining the preserved portion of the fauna and identifying an equivalent extant ecosystem which has a similar mix of shelly creatures. This should reveal a number of ecological roles played by soft bodied taxa, and the extent to which they are represented in a modern community. There is no guarantee that the same mix of organisms, or even types of organisms, were present in the past; but it is not unreasonable to postulate that something of the sort occupied a similar community role because ecosystems at certain resolutions can be remarkably conservative. For example, faced with a predominance of some shelly form which demonstrates a particular feeding type, it seems logical to assume that creatures occupying the food source role once also existed, regardless of preservational evidence; furthermore, given the regularity of energy transfer between trophic levels, we can guess that the biomass of the missing food source was five to ten times greater than that of the consumers (Crame, 1990). Models based on modern ecosystems and their recently preserved inhabitants suggest that around 50-75% of the total fauna may be entirely unpreservable, but that within certain restricted portions (for example when considering only the foraminiferal fauna) the proportion of unpreserved elements is likely to be as low as 5% (Murray, 1991). Thus, it is possible to construct a gappy community structure from

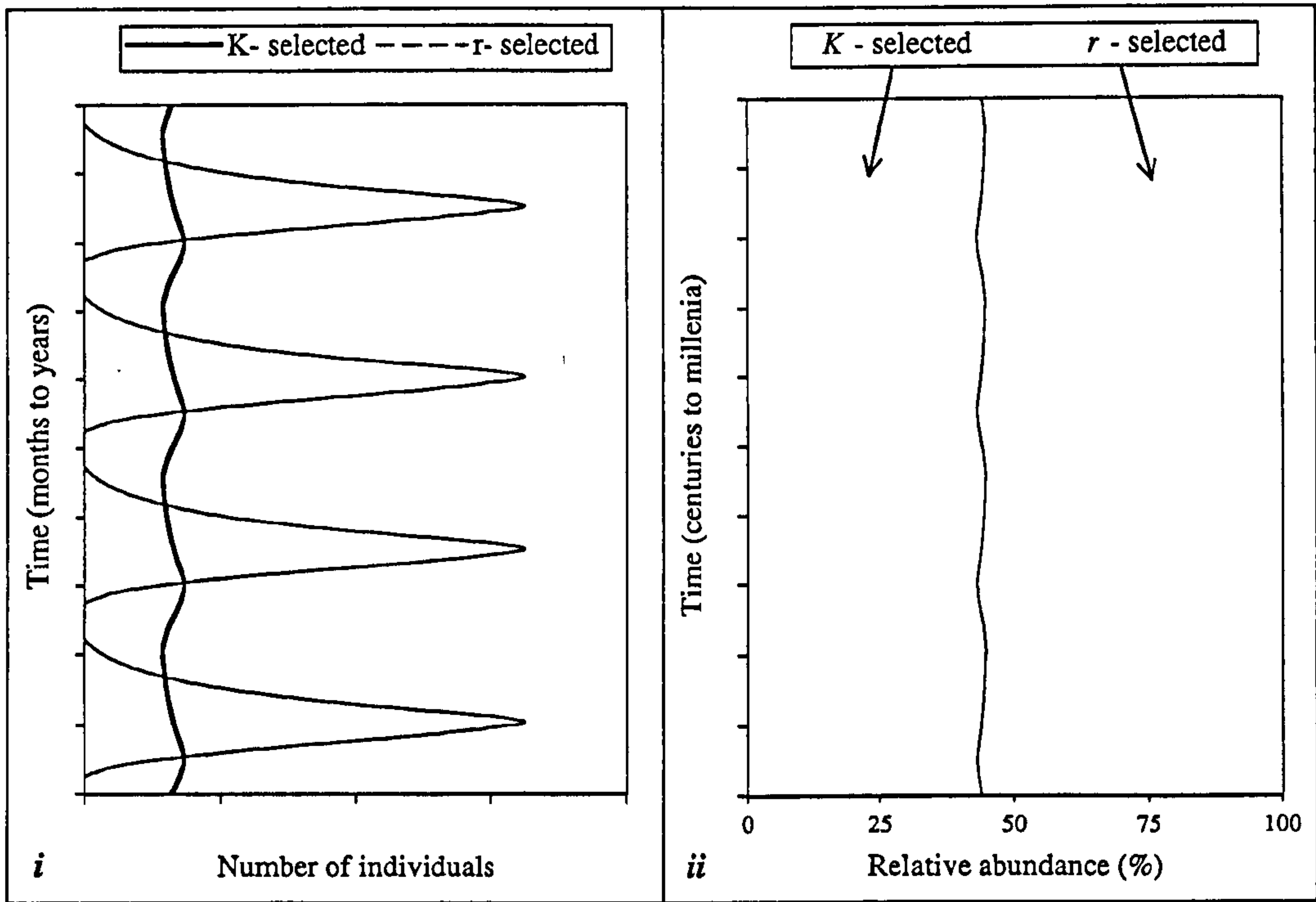
fossils, and then guess what occupied the remaining holes. Trace fossils often provide a deluge of evidence in this department: burrows, trackways, resting places; borings, gnawings and nibblings; open tunnel systems, sweep searches and even subterranean 'farm' complexes can all be ample testament to the anonymous perpetrators. Finally, Scott (1978) sensibly warns that the conclusions of the analysis must be related to the environment. For example, systems dominated by deposit feeders inhabit muddy substrates not hardgrounds; if the geological evidence is at odds with a faunal extrapolation, then it is probably the latter which is at fault.

The second set of problems, the issue of differential preservation between sampling points, may be tackled using the available fossil material. Shells which have been transported for any period tend to become worn and broken, but the effect is not sudden: there is a gradual build-up of wear and tear which is itself preserved in the remaining specimens. Analysis of the extent of breakage allows an index of transportation to be drawn up, and the same goes for dissolution. While the specimens to hand may provide little indication of the *absolute* levels of damage and loss (that information has probably gone forever), they at least allow some idea of the *relative* amounts from horizon to horizon, which, in the given context, is more important. As long as we know to what extent the data are comparable with each other we are in with a fighting chance.

The effects of temporal scaling are much more interesting, and there can even be beneficial side effects (e.g. Schindel, 1982, Kowalewski *et al.*, 1998). A bulk sample from the cliff face will generally represent several thousand years worth of sediment deposition, and a corresponding faunal accumulation over the same amount of time. This may be problematic with regards to the fine detail, but it is advantageous when assessing how an ecosystem works long term. Events which are atypical and local in time and space should be blurred together to give an averaged picture—one which may better reflect the scale of selective forces operative in the system. Among the vagaries which can be avoided this way are the normally patchy distribution of most organisms, so that species which appear rare probably are rare, rather than merely absent from the present site but locally abundant a few kilometres distant; and one can also expect age distributions to be fairly representative, rather than skewed by short term founder effects. At the same time, however, much of the data on heterogeneity has been lost. Spatial distributions are concealed except on a very broad scale, faunal tracking of local conditions is no longer so apparent, and phenomena

such as depth segregation within the sediment are superimposed and can only be inferred from the shapes of fossils.

Fine resolution events separated in time are equally confused. Hallam (1972) has suggested how patterns of opportunist and equilibrium species should look in the fossil record (Text Fig. 2.8.i). I think this is almost certainly wrong. Opportunists peak and trough over months to years, whereas the mixing and time-averaging so characteristic of most depositional settings conspire to obscure processes operating at much less than several hundreds of years (e.g. Kowalewski *et al.*, 1998). Individual beds, and the fossils distributed throughout, represent times far in excess of those needed to reveal such fine ecological detail. A more realistic version of Hallam's diagram would show both opportunists and equilibrium strategists blurred into a continuous presence, with relative abundances indicative of their time-averaged proportions (Text Fig. 2.8.ii).

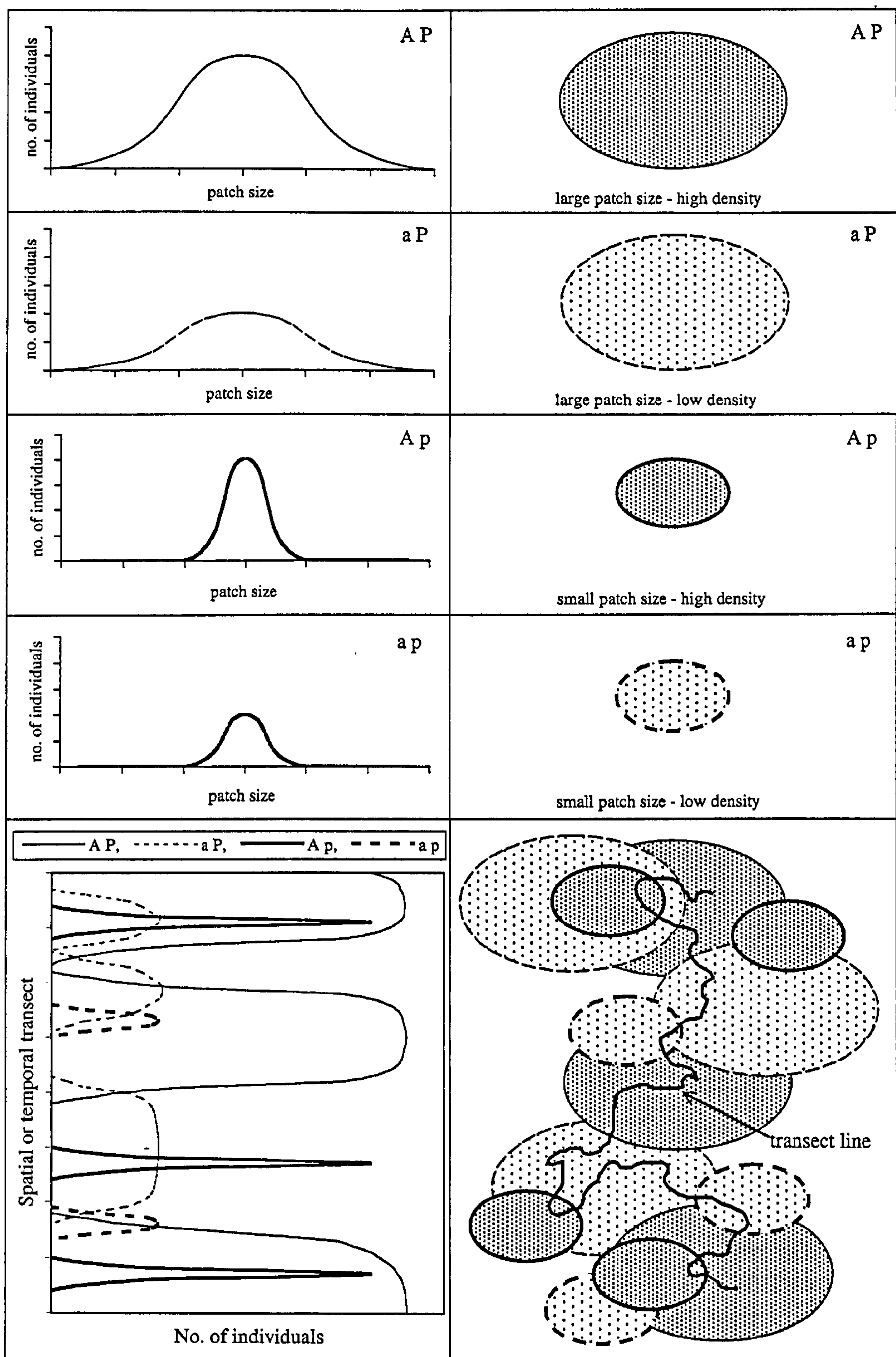


Text Figure 2.8 *Ecological patterns at different temporal resolutions. Differences in faunal behaviour at an ecological resolution (i) blur into a single indivisible signal on a palaeoecological scale (ii). The model in panel i is based on a diagram from Hallam (1972) purporting to show how opportunist and equilibrium strategy behaviour might appear in the fossil record. In panel ii the oscillations are time averaged and have coalesced into a single value corresponding to each species' proportional abundance. Absolute abundances at the palaeoecological scale will normally be influenced more by sedimentation rate and preservational factors than by short term biological processes.*

The same kind of argument applies to predator-prey cycles and probably ecological successions too. It also implies that palaeoecological 'events' such as pulse faunas, which are scattered throughout a bed or beds recording accumulation over several thousands of years, probably represent fairly profound and long term ecological shifts and faunal migrations, perhaps on the scale of glacial and interglacial phenomena.

In an attempt to salvage some of the blurred information on spatial distributions McKinney and Allmon (1995) have adapted the metapopulation model of Levins (1969; see also recent developments, e.g. Hanski and Gilpin's 1991 review) to work in a palaeoecological context. A metapopulation is a scale of spatial organisation somewhere between the extent of a normal ecological population and the entirety of a species' geographic range. There is no definitive size for a metapopulation, and with respect to palaeoecological analysis that is a strength. Natural populations normally exist in a statistically fractal-like arrangement (Allen and Hoekstra, 1992; Hanski and Gilpin, 1991), being roughly self-similar on a variety of scales, so the size at which a palaeoecological pattern is detected will depend partly upon the rate of deposition, and thereafter on the sampling resolution of the survey (McKinney and Allmon, 1995).

Invoking Walther's Law of temporal and spatial symmetry, McKinney and Allmon point out that vertical sampling is equivalent to spatial sampling across a wandering community of patchily distributed species: the wandering of population patches across the sampling point then replaces a randomly moving sample point amongst static patches (Text Fig. 2.9). A patch can be described by two parameters: the spatial extent (its diameter, say) and the density of organisms within it (the standing crop). If we assume that the taphonomy and sedimentation rate did not vary significantly within the time-averaged resolution of a single bulk sample, then all specimens from that sample can be treated alike. With these conditions McKinney and Allmon take the abundance of preserved organisms to be directly proportional to some combination of patch size and standing crop. Patch size and standing crop cannot be disconnected within a single time-averaged sample because they just combine to signify either 'rare' or 'common', but so long as the taphonomic and depositional factors remain constant, comparison *between* samples does provides a means of separation. Small patches show rapid transitions and relatively large spaces between major peaks; large patches, by comparison should provide a fairly constant input.



Text Figure 2.9 Connection between spatial and temporal distribution of patch size and standing crop.

Upper page: end-point combinations of the variables patch size and standing crop; left side - abundance histograms, right side - bird's eye perspective. A, a = abundance, P, p = patch size; capitals and lowercase indicate high and low respectively.

Lower page: showing how a spatial transect translates into a temporal one. ii is a spatial distribution of patches which either wander over a set point or have a wandering transect throughout them; i is a sampling pattern, either by spatially sampling along the transect line, or by allowing the patches to drift across the static point and then sampling up through time. (After McKinney and Allmon 1995.)

Adding the standing crop parameter gives us four combinations (Text Fig. 2.9), each of which leaves a distinctive signal along a vertical sampling transect, although special care should be taken with low density populations because in these the patch size signals are inherently prone to sampling errors.

As a sedimentological setting, the Chalk Sea would have enjoyed relatively invariant depositional rates (Schindel, 1980; Anders *et al.*, 1987), recording most periods of a thousand years or more. And with an average depositional rate 25 mm/kyr (25 Bubnoff units), samples spaced more widely than 2.5 vertical centimetres apart should have avoided the kind of complete homogenisation documented by Kowalewski *et al.* (1998), although there is extensive bioturbation. Samples incorporating a vertical thickness of 15 cm represent about 6 000 years of history (or 3 000 for 7.5 cm sample thicknesses; see Section 3.1.2 for discussion). A benthic foraminiferal patch which moves at a metre per month, say 10 m per year—a reasonable estimate according to McKinney and Allmon (1995)—can travel 60 000 metres (60 km) in 6 000 years. If it drifts randomly with the square root of twice its velocity $((2 \times 60\,000)^{1/2}$ - *ibid*) then it will shift some 350 m on average during the 6 000 years of that sampling period (or 250 m for 7.5 cm samples). Given such a resolution within any single sample, we can expect to be working with metapopulation patches of a 250-500 metre diameter.

These are the idealised limits of spatial and temporal resolution for ecological processes at work in the Lower Chalk: we cannot expect to *directly view* any event which took place in under a thousand years, or operated over less than 250 m. In all likelihood the resolution is poorer still, given the bioturbation and migration of sediments around the basin, but these minimal figures at least provide us with a kind of standard to bear in mind.

2.2.6 Palaeoecological Events in the Mid-Cenomanian Chalk Sea

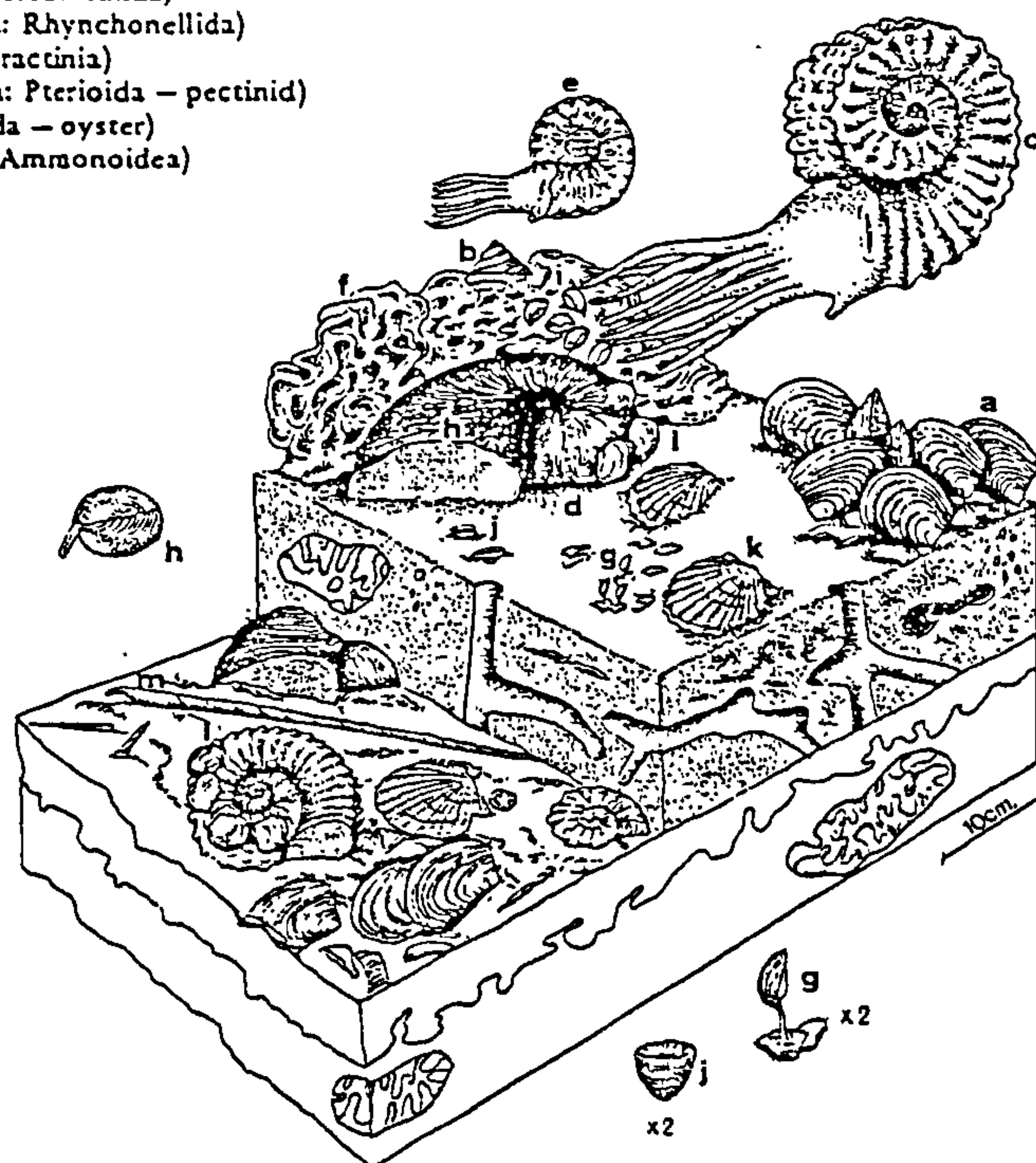
The most comprehensive and (relatively) high resolution assessment of the Lower Chalk macro-fauna comes from Kennedy (1969), although more recently some narrow zones have been documented in greater detail (e.g. Gale, 1989; Paul *et al.*, 1994). The general story, as one might expect, is of a mixed suspension and deposit feeding community which gradually changes from shallow to deeper water throughout the course of

the Cenomanian. The hexactinellid sponges and occasional decapods found towards the base gradually give way to a higher proportion of echinoderms, mostly echinoids (e.g. *Holaster trecencis*) and occasionally a brittle star or two, as the terrigenous sediment waned and the bottom currents reduced with deeper water. Throughout, the most common (fossilised) benthic elements are bivalves, mostly inoceramids (e.g. *Inoceramus crippsi*) and small oysters (e.g. *Pycnodonte vesicularis*), especially lower in the sections, and then brachiopods (e.g. *Concinnithyris*, *Terebratula*) once the water was deeper (Kennedy, 1969). Altogether the middle reaches of the Lower Chalk sport at least forty-one fossil species of bivalve, twenty-one brachiopods, nine echinoderms, a dozen gastropods and half as many crustaceans, plus a motley assortment of other echinoderms, solitary corals, sponges and serpulid worms (Smith, 1987). The nekton is represented by no less than twenty species of shark, a similar number of ammonites, and some rare belemnites. We can also guess that there must also have been a variety of worms and soft crustaceans to account for the *Planolites* and *Thalassinoides* trace fossils (Bromley, 1990).

Mid-Cenomanian Argillaceous Chalk Community

Fig. 103 Mid-Cenomanian Argillaceous Chalk Community

- a *Inoceramus crippsi* (Mollusca: Bivalvia: Pterioidea)
- b *Bathrotomaria perspectiva* (Mollusca: Gastropoda: Archaeogastropoda)
- c *Acanthoceras rhotomagense* (Mollusca: Cephalopoda: Ammonoidea)
- d *Cymatoceras elegans* (Mollusca: Cephalopoda: Nautiloidea)
- e *Schloenbachia coupei* (Mollusca: Cephalopoda: Ammonoidea)
- f *Exanthesis labrosus* (Porifera: Hyalospongia)
- g *Terebratulina striatula* (Brachiopoda: Articulata: Terebratulida)
- h *Cocinnithyris albensis* (Brachiopoda: Articulata: Terebratulida)
- i *Orbiryhynchia mantelliana* (Brachiopoda: Articulata: Rhynchonellida)
- j *Micrabacia coronula* (Coelenterata: Anthozoa: Scleractinia)
- k *Chlamys (Aequipecten) beaveri* (Mollusca: Bivalvia: Pterioidea – pectinid)
- l *Pycnodonte vesicularis* (Mollusca: Bivalvia: Pterioidea – oyster)
- m *Sciponoceras baculoide* (Mollusca: Cephalopoda: Ammonoidea)



Text Figure 2.10 Reconstruction of a Cenomanian benthic environment showing some of the common macro-organisms present in the fossil record. From McKerrow (1978).

The emerging picture is of a smooth, dimly-lit, gently undulating plane of wholly biogenic carbonate plus a little clay. Although easily agitated at the surface, the sediment must have been solid enough at some times and places to support a bivalve or brachiopod of visible dimensions, and to maintain open burrow systems, but soft enough at others for an irregular echinoid to move through. The main input of productive material, apart from the occasional fish corpse, was a seasonally swollen rain of phytoplankton debris forming an even, gelatinous, flocculating mass only millimetres deep on the seabed (e.g. Gooday, 1988). Gentle currents across the plane would have agitated this material into patches, perhaps even shallow drifts, and swept them from place to place to feed the scattered community of bivalves and brachiopods. At the top of the food chain, vagrant echinoderms and crustaceans roamed to and fro, or ploughed the sediment, picking up whatever they could from the dead swimmers and the sickly and vulnerable among the shellfish. Somewhere in all of this, at a level between the foodchain's bacterial sump and the macrofaunal deposit-feeding backbone were the meiofauna, a mass of tiny nematodes, polychaetes, amphipods, ostracods and foraminifera.

Superimposed upon these general background conditions, and interrupting the overall transgression, were the cyclic sequences reflected in Gale's alphabetical labelling system (Gale, 1995, Robaszynski *et al.*, 1998; Text Fig. 2.2, Appdx. Fig. 1.1). The sea lapped onto the land and partially off again five times throughout the Cenomanian, with the study sections encompassing not only an entire cycle (C block), but also its passage from an earlier phase (B block). Apart from the Plenus Marls, the B-C block transition is the most intensively studied of these sequence boundaries, and also the most distinctive because it coincided with the $\delta^{13}\text{C}$ peak documented by Paul *et al.* (1994). From an ecological perspective, one particularly interesting feature about the whole episode is its accompanying suite of 'pulse' faunas, briefly but regionally abundant organisms which are otherwise rare or absent from the sequence. The same species appear in the Plenus Marls some two million years later where they accompany another lowstand and an even larger $\delta^{13}\text{C}$ anomaly. In the mid-Cenomanian they are arranged concentrically around the lowstand with a characteristic pattern (Text Table 2.2), immediately reminiscent of migrating faunal zones sweeping across the site and then back out into the basin as the water level changed. On encountering these species in the Plenus Marls, Jefferies (1962, 1963) originally

concluded the bivalves and belemnite faunas were indicative of cold water conditions, but Mitchell and Carr (1998) favour a depth based interpretation, and I am inclined to agree with them.

Horizons	Duration	Organism
C2-C11	~200 kyrs	<i>Orbirhynchia mantelliana</i> (Brachiopod)
C1-C2	~20-40 kyrs	<i>Oxytoma seminudum</i> (Bivalve)
C1	<20 kyrs	<i>Actinocamax primus</i> (Cephalopod - a belemnite)
B41	<20 kyrs	<i>Lyropecten arlesiensis</i> (Bivalve)
B40-B42	~20-40 kyrs	<i>Oxytoma seminudum</i> (Bivalve)
B36-B41	~120 kyrs	<i>Orbirhynchia mantelliana</i> (Brachiopod)

Text Table 2.2 *Distribution and duration of pulse faunas around the B-C block boundary. The data are from both Folkestone and Southerham and this table does not distinguish between sites. See Paul et al. 1994 for the original data.*

Summary

The cyclic sediments of the Lower Chalk predominantly record precessional scale episodes of orbital forcing imposed upon a sedimentary system poised between the influences of land and sea. The mid-Cenomanian Chalk Sea was a shallow marine embayment separated into a number of distinct basins, ringed by islands, and receiving currents from the young North Atlantic. Periods of enhanced solar flux to the northern hemisphere prompted greater phytoplankton blooms in this sea, overwhelming the terrestrial input to the muds of the basin and substituting a layer of chalk in place of clay-rich marl. The rhythms so formed are chalk-marl couplets and have been organised into exceptionally detailed stratigraphic schemes providing both a fine resolution timescale and bed by bed correlation across large geographic zones. Overlaying this background sedimentary activity were regional transegression cycles, one of which, at Gale’s B-C block sequence boundary, was associated with prolific algal blooming and an episode of widespread anoxia on the seafloor.

Within this setting, yearly spring blooms of phytoplankton contributed the primary resource input. Solar energy, initially captured by tiny floating plants, thus drove the biological network of the seafloor, streaming through each trophic level until it was finally all dissipated. Organisms consume energy and materials in order to reproduce, but the

resources are finite and eventually competition ensues. In competing for their portion of these vital resources, the benthic organisms must have formed networks of competition and collaboration, just as they do elsewhere. Competition occurs when two or more species are able to exist and reproduce in the same circumstances (a niche) but rely on a common pool of finite resources; it drives evolution until the species in question are sufficiently specialised that one of them regularly out-competes the other in a narrow suite of circumstances (the realised niche). It is possible to describe ecological networks and niche allocation in either very general or very specific terms; neither approach is any more or less real than the other, they simply each capture different levels of biological organisation.

The role of extant foraminifera in such ecological networks has been well documented, and, by using modern analogues, it is possible to imagine a wide range of biologically and physically tailored niches to which fossil species might be adapted. Recovering such information from the fossil record is no mean feat, however, and particular care must be taken with issues of temporal scaling. Some palaeoecological evidence is already available for both the Lower Chalk macrofauna, and the microfauna with which this study is primarily concerned.

Chapter 3 Fossils from the Lower Chalk

Introduction

This chapter examines microfossil data derived from Lower Chalk sediment samples. After explaining what kind of material was obtained, how, and where from, a range of transformation procedures are introduced. These are intended to gauge or emphasise relevant characteristics of the available data set; some give absolute measures of single variables, some give contextual, relative measures, and others describe the global, emergent parameters of multi-variable groups. In all cases, considerable care is taken to explain exactly how particular metrics relate to or transform the initial data. Preservation issues are also succinctly dealt with in a catch-all section, culminating in a page of figures which is intended to be a reference point on this matter for the rest of the document.

The palaeoecological data set has proved extremely flexible, and has generated an enormous number of charts and figures. Over a hundred of these appear as a standard sequence in the Appendix. The text, by comparison, consists of a series of short descriptions which aim to pick out and categorise noteworthy patterns in the graphical data. The goal of this chapter is simply to display those patterns from the data set which will be pertinent to the interpretation, and verify their status as signals rather than artefacts of preservation, practice or sampling. In order to facilitate easy cross-referencing between the text and the figures, the presentation of both has been arranged in the same standard format, a sequence which will be relaxed in later chapters when the emphasis is on the mechanisms underlying particular patterns, rather than similarities in the type or derivation of data.

Section 3.1. Method

3.1.1 Location of Sampling Points

Three sites were chosen for study. These were at Southerham Grey Pit near Lewes in Sussex (National Grid reference TQ426090); Abbot's Cliff, Folkestone, Kent (TR277387); and Escalles, Cap Blanc Nez, France (Sheet 50: 50° 50.5' N, 1° 40.2' E).

From each of these, 10 or 11 samples were initially taken to conduct a faunal analysis, starting at the marl of B31 (Gale's scheme, 1995) at Folkestone and Southerham, and B36 at Escalles (B31 could not be identified at Escalles because the cliff face was so frost-shattered and degraded). B31 was succeeded by B36, B41, C5, C10, C15, C21, C29, C35, C40 and, finally, C45 at each site (see Appdx. Fig. 1.1). All samples were taken from the marly portion of the couplet if there was one, or from the place it should have been in cases of condensation (i.e. C15 at Southerham). These beds were chosen because they are at approximately every fifth 21 kyr couplet, and thus should represent horizons *roughly* one hundred thousand years apart. They also come from the most strongly developed marls at the base of the 100 kyr mega-cycles described by Gale (1989). He no longer thinks the whole of the Cenomanian is so simply ordered (pers. comm.), but the upper C block at Folkestone and Escalles certainly seems (to me) to be, and so the samples come from equivalent parts of both 21 kyr and 100 kyr cycles. The ordering in places is rather rough, however, and an exact 100 kyr separation is not always achieved. This is largely because in some places, especially the upper parts of the sequence where the cyclicity is less developed, a need for well-defined and easily recognisable points of correlation over-rode my aesthetic desire to separate the samples evenly. Nevertheless, the interval is always 100 kyr to within a few tens of thousands of years, and for the sake of simplicity these transects are referred to as 100 kyr transects in the text.

In addition to these, a single rhythm, C13 from Folkestone, was chosen to assess the faunal response on a smaller timescale. There are 11 sampling points across the whole rhythm, plus one from the top of the last and one from the base of the next, which thus have an average separation of roughly two thousand years. C13 was picked because there was an unusually clear distinction between the chalk and marl portions, and because it was a large, relatively expanded couplet from the middle part of the middle section.

Finally, to bridge the scales of resolution, marls from C11, C12, C14, C16, C17, C18, C19 and C20 (each unsampled marl between C10 and C21) at Folkestone were also analysed. This selection effectively spans the central part of the central site and forms a link between C13 and the longer, geographically correlated transects. As with the 100 kyr samples, for the sake of style (to emphasise the regular slicing of larger units), this short transect is referred to as being at 20 kyr resolution (rather than 21 kyrs) in the text.

Further samples were taken from the middle of every bed (both chalks and marl) at Folkestone but these were used only for assessing the clay/carbonate ratio.

The three sites are perched on the edge of the London-Brabant Platform, and represent a transect across the north-western rim of the Anglo-Paris Basin. Folkestone and Escalles are a little closer together than either are from Southerham, and over the interval sampled they also accumulated a little more sediment. However, referring back to Text Figure 2.3 (last chapter), we can see that the Southerham site would have been situated somewhat closer to centre of the basin's elongate, northwest-southeast axis, and so to differentiate these variations in location, Southerham is normally referred to in the text as 'basinal' and Folkestone and Escalles as 'marginal'. Appendix Figures 1.1 and 1.2 show how the sampling horizons relate to one another both laterally and vertically.

3.1.2 Sampling

Bulk samples were collected from all sites by chiselling parallel grooves some 15 cm apart and hammering all the weathered crust from the top; half a kilogram or so of the sediment was then gouged from the cleared area and placed in a sample bag. The sampling points were selected carefully after a thorough investigation of the site using unpublished logs drawn and supplied by Andy Gale. I also logged the sections myself (admittedly rather roughly) to ensure that I understood them well enough. Gale's logs are superb and there is virtually no point at which I would be inclined to disagree with them, even in fine detail. All samples were taken from the middle of beds, the exception being the fine resolution transect which runs across a whole rhythm and necessarily includes bed boundaries and so forth. Whilst normally the collection zones were wide to allow for the extensive bioturbation, and to provide a rather generalised signal from the middle of each bed, in the case of C13 smaller intervals (7.5cm—roughly half the normal size) were used in

order to fit a sensible number of sampling horizons into the single cycle. It is likely that there is contamination due to bioturbation from vertically adjacent points, but that is the price paid for attempting a higher temporal resolution.

3.1.3 Sample Preparation

A portion of each bulk sample was randomly selected (they were all in 1-5 centimetre sized chunks and thoroughly jumbled in the bags), crushed further and spread in metal trays to dry. Drying took place in an oven at about 100°C and the samples were often left for several days. They were then taken, still warm from the oven, and 50.0g was weighed and placed in a beaker where it was immersed in industrial grade paraffin. They stood like that for at least 24 hours, and often longer, before the excess liquid was decanted and replaced by water. In many cases the samples disintegrated immediately, but, whether or not, they were left for another 24 hours before being agitated several times to break up any persistent lumps, and then they were sieved.

Sieving was conducted through three grades of mesh: 500µm, 250µm and 125µm (a further 63µm mesh was used for most of the Folkestone samples but it eventually ripped and was not replaced because it made the process painfully slow). Pieces which had not broken down and failed to make it through the 500µm sieve were washed back into a tray, dried thoroughly again, and picked through briefly to ensure there was nothing of interest, before being weighed and discarded. The weight of the discarded material was deducted from the 50.0g standard of the original sediment so that it was possible to calculate absolute abundances per unit weight. The residues from each of the sieves was weighed again and stored in a separate sample bottle with all the relevant information concerning location, mesh size and weight diligently recorded on the label as it was filled to avoid any mix-ups.

In addition to these proceedings, a much smaller portion was taken from all the main sampling horizons and from every single bed at Folkestone. This material was used to determine the proportion of acid insoluble residue, an indicator of the clay/carbonate ratio. The bulk sediment was ground to powder, dried, and 0.200g of it was covered in excess 0.1mol HCl and left to react completely. Thereafter, the residue was filtered, washed, dried again and weighed.

3.1.4 Collection and Identification of Specimens

The >250µm portion was picked clean of all microfossils, the absolute abundance per 50g of original sediment (for this size fraction) being simply the number of specimens amassed. Both whole and broken fossils were collected so the abundance results indicate the *maximum* possible number of specimens. There were always more than the 300 individuals required for most standard counts, and often in excess of a thousand per sample. All microfossil specimens were picked from a 100 square grid and glued straight onto the slide. They were identified in the process and arranged carefully into groupings which reflect taxonomy.

In total 82 benthonic groups were identified (48 forams, 34 ostracods), some of them to species level, some only to genera. They were identified using a number of standard texts: Loeblich and Tappan (1987) for up to generic level classification in the forams, and also the more Cenomanian specific Jefferies (1962), Carter and Hart (1977) Jarvis *et al.* (1988) and Mitchell and Carr (1998) for some species level distinctions. Weaver (1982) was consulted for the identification of ostracods. Although there is a broad overlap, almost all of these sources show some of the same species with different names or the same names for obviously different species. To avoid too much ambiguity about what the names used here refer to, SEM photographs of the most common forms listed are shown in Appdx. Figures 2.2.1 - 2.2.3. In any case, the interpretations given are rather broad and should never exceed the taxonomic resolution; where particular species are mentioned they normally belong to common, monospecific genera, and all the major arguments revolve around well established and easily identifiable types.

The identification, to species level, of various smoothly carapaced ostracods surpassed my skills, particularly when the shells were broken and complete outlines and hinge areas could not be seen. Consequently they are dealt with mostly at the generic level. The absolute abundance values of these genera are *estimates* based on the whole specimen counts plus a number of unidentifiable fragments the allotment of which simply mirrors the proportions of known specimens: no differences in breakage rate between shell types were taken into consideration. It follows that their relative abundance counts are grounded entirely in the ratios of *identifiable* specimens (not *all* specimens) and that taphonomic information is only available for the set of smooth ostracods *as a whole* and cannot be reliably extended to individual types.

Planktonic foraminifera, too, were not resolved to the level of species for a variety of reasons. Firstly, the mid-Cenomanian hosts a number of forms which are rather similar and therefore difficult and time-consuming to distinguish; secondly, the fact that planktonic forams predominate only in the chalky upper part of the section means they tend to be encased in carbonate debris, making recognition even more tenuous; and finally, since in life they occupied a zone somewhat removed from the sea bed, ecological information from such a source was considered to be of limited value anyway. Where appropriate they will be presented merely as a bulk planktonic group on the grounds that the planktonic/benthonic (P/B) ratio is presumed to reflect depth changes, and because as a mass they must have contributed something to the trophic web.

The 125 - 250 μm portion has been largely ignored although it was collected and retained throughout. A complete survey would have included smaller size fractions as well (which host a variety of extra species in addition to miniature versions of those encountered), but there is no attempt here to present a truly comprehensive picture. Most of the necessary points concerning environmental stability can be made using only the larger microfossils.

Section 3.2 Analysis

3.2.1 Relative Abundance

Relative abundance, rather than the absolute, is a tool much used by micro-palaeontologists and students of recent foraminifera alike. Modern biologists use relative abundance because foraminiferal populations are often very patchy and absolute numbers of all groups can vary over short distances whilst the overall composition of the fauna remains unchanged. Although palaeontologists have less to worry about from local patchiness, absolute counts often provide more information on the rate of sedimentation than they do on the community dynamics. However, relative abundance must be used with discretion; Murray (1991) and Paul (1992) have both dedicated fairly large tracts of text to the warning that *all* ratios in a relative count will vary when *any* component changes. Thus, it is possible for the relative abundance of some uniform species to shift passively, simply because of a change in the numbers of another. Nevertheless, the percentage contribution of individual species to a larger grouping is a useful piece of information and will be used extensively.

3.2.2 Absolute Abundance

Because of problems entailed in the interpretation of proportion it would be easier all round if absolute abundances could be examined. Unfortunately, variable rates of accumulation, which plague even the most constant of depositional environments, normally make this practice somewhat suspect: all things being equal, slower sedimentation concentrates fossil specimens, producing spuriously larger counts. But the Milankovitch cyclicity of the Lower Chalk and the bipartite composition of the sediment provide methods of partial compensation.

Since each cycle represents 21 000 years of accumulation, the average depositional rate within a single rhythm must have been the couplet thickness divided by 21 kyrs. And if it is assumed that each couplet was a productivity cycle with a carbonate bloom imposed

on a constant background input rate for the clay, then the clay will act as a detrital 'clock' against which to measure sedimentation rate within the rhythm. In reality the situation was more complex; the various orbital influences must have overlapped to merge or miss some of the cycles, condensation may have destroyed others, and there is no concrete guarantee that the clay accumulation across a single cycle did not wax and wane as the carbonate seems to have done. All the same, since the horizons under study span the era of strongest cyclicity, most orbital variations should have been recorded, and there are many methods of detecting condensation and omission taken into consideration by Gale's stratigraphy (e.g. 1995). Also, the calculations of Paul (1992; refer back to Section 2.1.3 for discussion) provide some firm support for a simple productivity model.

Once rates of deposition are known, either between rhythms or between samples within a rhythm, it is simple to calculate how many specimens there should have been if the rates had been constant. Note that the data obtained in this way are not absolute in the normal sense since fossil material is rarely ever more than a small fraction of the original existing numbers over any span. But the method does standardise data between samples so that it can be taken *as if* it were absolute, clearing the way for other methods of tackling taphonomic variation. There are two ways of calculating such 'absolute' abundance.

3.2.2.i Compensation in a Single Couplet

With the assumption that there was a constant rate of deposition for the clay component, and also that the acid insoluble residues provide a fairly reliable impression thereof, it follows that the total amount of insoluble material derived from a vertical transect can be used to represent the total amount of time encompassed by the couplet. It also follows that differences in the amount of residue between samples represent the differences in times taken for those samples to accumulate (so long as each came from an equal weight and thickness of original sediment, which for C13 they did), since the clay was being deposited at a constant rate.

In this situation it is not the clay/carbonate ratio that is important, it is *the amount of residue from each sample as a proportion of the total residue taken from throughout the cycle*. It is also unimportant how long the cycle really took to form; each sample point is effectively rendered as a percentage of the total amount of time, and by transforming data

by the relevant factors it becomes possible to compare information from different horizons as though it were equivalent. Text Table 3.1 is a worked example from C13 using the total number of benthic foraminifera per sample.

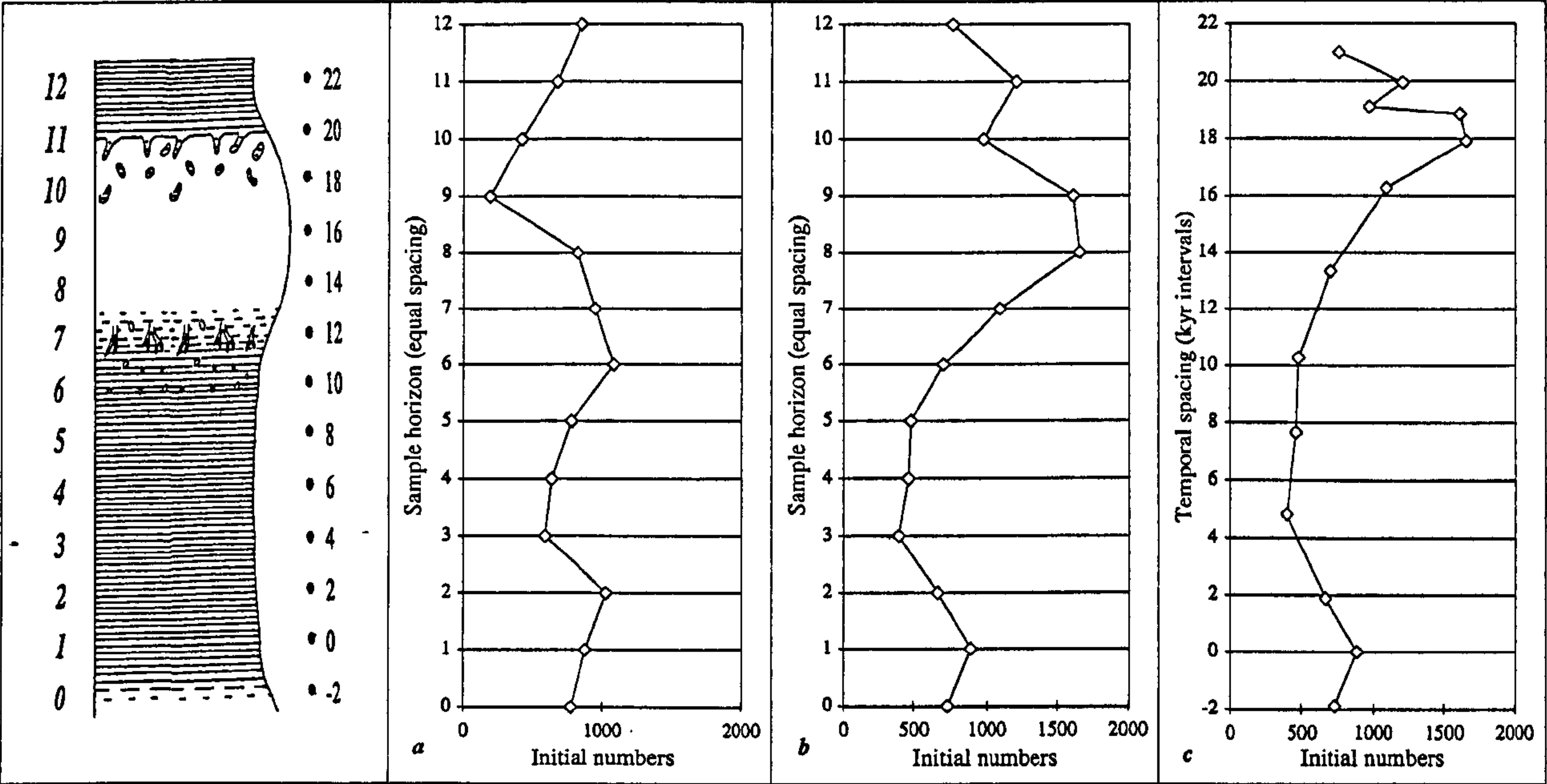
The technique can also be extended to calculate the amount of time which elapsed between sampling points. Since the samples all come from an equal thickness of sediment which accumulated at a variable rate, the mean duration per sample, 1750 years (21 000 yrs/12 samples), can be multiplied by the relevant conversion value to give an absolute duration for the deposition of that thickness at each part of the cycle (e.g. $1750 \times 0.12 = 210$ yrs; $1750 \times 1.596 = 2793$ yrs etc.). By taking on board only an assumption of steady insoluble residue input this procedure generates some startling but very intelligible results (Text Table 3.1 and Text Fig. 3.1).

Chris Paul (pers. comm.), having unearthed cidarid sea urchins with spines still intact in British chalks of Campanian age, has expressed some scepticism regarding the evenness of chalk sedimentation. His urchins would have needed to be covered quickly in order to escape the borings and encrustations common to exposed hard surfaces, and so he believes they were rapidly swamped by up to 30 cm of sediment, implying that the chalk was highly mobile and cannot be assumed to represent a steady pace of deposition.

He has a good point, and there is certainly enough evidence of scouring in the Lower Chalk to convince me that the sediment could indeed exhibit significant mobility; but I think that on a 21 000 year scale most local, short term patchiness would cancel out to leave an effectively continuous rate of accumulation (e.g. Anders *et al.*, 1987). In addition, there is a world of difference between a metre of chalk in a cliff-face and the soft deposit from which it was formed, since a drift of several centimetres might be compressed by up to 50% of its original volume with the overburden of half a kilometre of rock (e.g. Schindel, 1980), in contrast to the hard skeleton it concealed. But quite apart from these factors, anyone who has watched a bit of drift wood nucleating a sand dune knows that burial by current action is not just a case of passively piling sediment on top of something; currents around a protruding object normally exhume a hole before burying the thing once it has fallen in, without much disturbance to the surroundings. There are more ways than one to bury an echinoid.

Horizon (couplet)	gms of residue per 100g sediment	...as a % of total residue..	...as a proportion of an equal share...	...gives a con - version value.	Initial no. of specimens per sample	...are then converted to...	'absolute' abundance per 50g of sediment.
C13-12	18	10.1	10.1/9.09	1.112	850	850/1.112	764
C13-11	9	5.1	5.1/9.09	0.556	675	675/0.556	1214
C13-10	7	3.9	3.9/9.09	0.433	421	421/0.433	973
C13-9	2	1.1	1.1/9.09	0.124	199	199/0.124	1610
C13-8	8	4.5	4.5/9.09	0.494	818	818/0.494	1654
C13-7	14	7.9	7.9/9.09	0.865	949	949/0.865	1097
C13-6	25	14.0	14.0/9.09	1.545	1086	1086/1.545	703
C13-5	26	14.6	14.6/9.09	1.607	775	775/1.607	482
C13-4	22	12.4	12.4/9.09	1.360	635	635/1.360	467
C13-3	24	13.5	13.5/9.09	1.483	591	591/1.483	398
C13-2	25	14.0	14.0/9.09	1.545	1026	1026/1.545	664
C13-1	16	9.0	9.0/9.09	0.989	877	877/0.989	887
C13-0	17	9.6	9.6/9.09	1.051	771	771/1.051	734
	178	100	Totals for the	middle 11	samples.		

Text Table 3.1. Derivation of conversion values via the *within couplets method*, and its application to the conversion of 'absolute' abundance for the total number of benthic specimens. Conversion values are produced by taking the 21 kyr couplet to be split into 11 equal segments, with two values from the edges of adjacent couplets (C13 - 0 and C13 -12) which are patched on afterwards by assuming they relate in an equivalent way to the others.



Text Figure 3.1 Conversion of initial numbers of specimens (a) to absolute numbers (b & c) via the *within couplet compensation method* (see text for details). Initial data are for the total numbers of benthic specimens (both forams and ostracods) from couplet C13 at Folkestone. Notice that there are two scales on the ordinate axes of these charts. The first is simply an even spacing of samples reflecting the basic sample numbering scheme; the second (in panel c) is a temporal scale in kiloyears. For C13, because of a great variability in deposition rate (see Section 2.1.3), the samples are not evenly spaced through time; panel c shows that fact clearly. When charts of this type are shown in the Appendix Figures, however, they assume that there is a perfectly even 2 kyr temporal gap between samples, a useful simplification reflecting the practice of referring to the transect as 2 kyr resolution. Translations between labelling systems based on sample number and temporal spacing are presented in Section 3.2.6 (Text Table 3.5).

3.2.2.ii Compensation Between Couplets

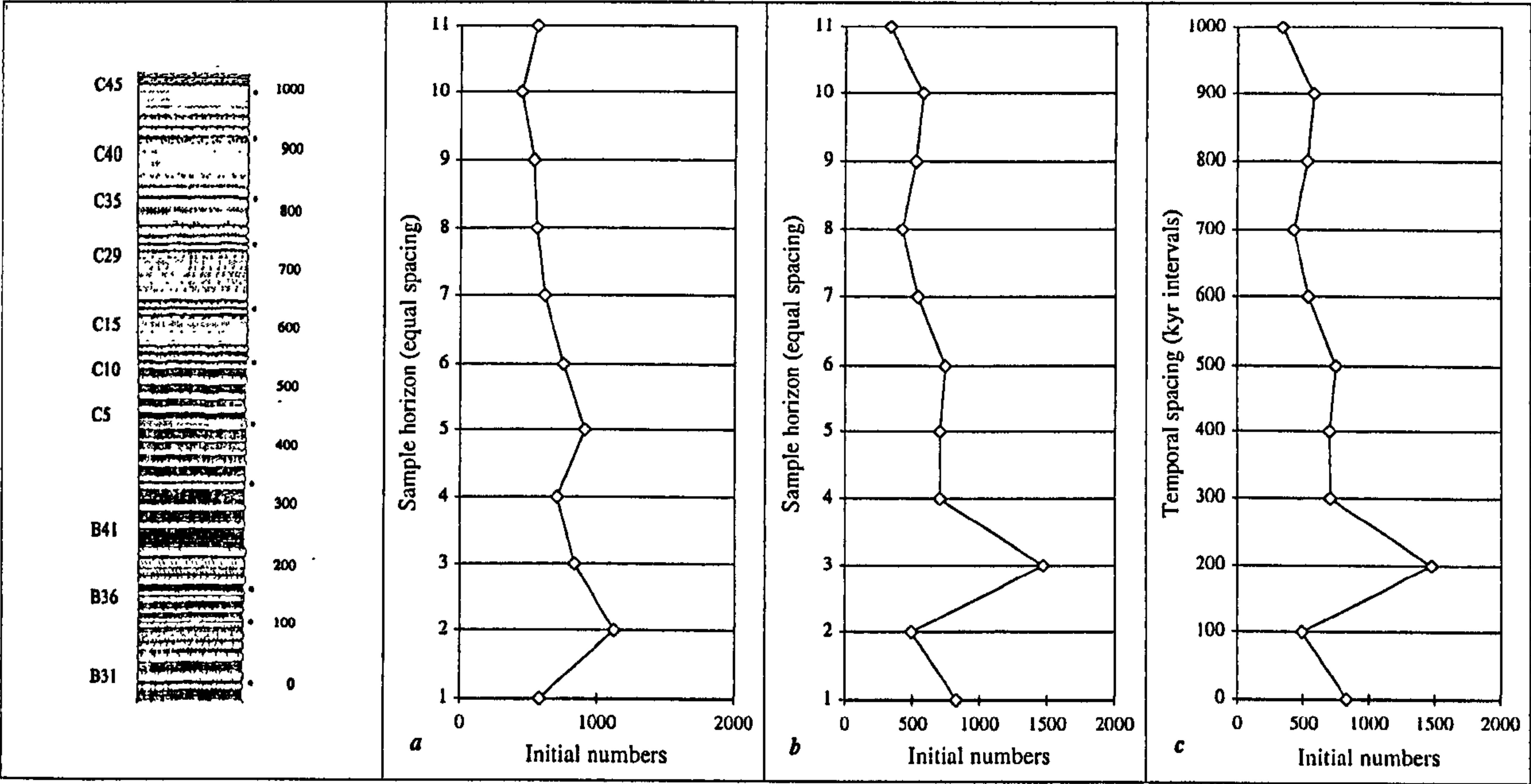
Once outside the confines of a single rhythm, the two component system can be abandoned as a means of transforming initial data, and with it the assumption of clay deposition at a constant rate. In the Lower Chalk, sedimentation varies considerably across wider tracts of time, certainly enough to invalidate the previous method as a means of correcting for differences between widely spaced rhythms. Instead, another assumption must be carried—that each rhythm itself is of a constant duration. This is not an unfair proposition for a variety of reasons, some of them outlined immediately above, and others in Section 2.1.3.

If each cycle does represent an equal portion of time, then the total thickness of that cycle provides the overall rate of accumulation, carbonate and clay, during each equivalent period. As long as the samples from each horizon were from equal vertical thicknesses of the cliff, the same part of each cycle, and the data come from an equal weight of sediment—all of which are satisfied in this case—it should be possible once again to standardise the samples and iron out idiosyncrasies. The method this time is to find a mean rhythm thickness (values from Gale's logs) from all horizons sampled and then divide individual couplet thicknesses by this average to find a compensation value. Thereafter observed abundances need merely be multiplied by the relevant rhythm's compensation factor to bring them into line—a process analogous to that for a single rhythm but substituting bed thickness for residue content (Text Table 3.2, below and see Text Fig 3.2 for a graphic display). The conversion factors used for all the sections can be found in the Appendix (Appdx. Table 1.6).

One further point might be made concerning both methods of data transformation: since the whole fauna from each sample receives an equivalent transformation, relative abundances remain exactly the same. In any case, where the modified values are presented they will normally be accompanied by the original data for comparison, so doubtful readers can make their own judgements.

Horizon (couplet name)	Rate of deposition (cm/20kyrs)	...as a proportion of the mean	...gives a conversion value.	Initial number of specimens per sample	...are converted to...	'absolute' abundance per 50g of sediment.
C45 [1000]	30	30/45.5	0.66	556	556 x 0.66	337
C40 [900]	60	60/45.5	1.32	443	443 x 1.32	583
C35 [800]	45	45/45.5	0.99	538	538 x 0.99	533
C29 [700]	35	35/45.5	0.77	558	558 x 0.77	430
C21 [600]	40	40/45.5	0.88	618	618 x 0.88	544
C15 [500]	45	45/45.5	0.99	756	756 x 0.99	748
C10 [400]	35	35/45.5	0.77	913	913 x 0.77	703
C5 [300]	45	45/45.5	0.99	713	713 x 0.99	706
B41 [200]	80	80/45.5	1.76	838	838 x 1.76	1475
B36 [100]	20	20/45.5	0.44	1126	1126 x 0.44	495
B31 [0]	65	65/45.5	1.43	583	583 x 1.43	834

Text Table 3.2 *Derivation of conversion values via the between couplets method and its application to the conversion of 'absolute' abundance for the total number of benthic specimens. The example is drawn from 100 kyr spaced samples at Folkestone.*



Text Figure 3.2 *Conversion of initial numbers of specimens (a) to absolute numbers (b & c) via the between couplet compensation method (see text for details). Unlike Text Fig. 3.1, the assumption of equal durations for cycles does not distort the ordinate when an axis which simply records sample spacings (a & b) is swapped for one which reflects time (c). Please see the legend of Text Figure 3.1 for more information about axis labelling. Section 3.2.5 has a discussion of the preservational issues involved with variable rates of sedimentation. As with Text Table 3.2, the example is from the 100 kyr data at Folkestone.*

3.2.3 Measures of Diversity

Ecologists interested in the number and proportion of species in a community generally employ three measures. *Species richness*, usually denoted S , is simply the number of species present. *Equitability* (E) is an overall measure of the relative proportions of those species. *Diversity* in the form of the Shannon index is a combination value that includes both the variety and relative abundance within the community and is termed H . A system which has four species is more diverse than one with three, and the four species system is (intuitively) more diverse if those species each occupy an equal portion of the community than if one organism dominates to the near exclusion of all the others.

The Shannon function was developed by communications engineers to take both heterogeneity (S) and homogeneity (E) into account, the goal being to make a statistical prediction of the next letter in an unknown incoming message. H depends on the number of letters (or species) and the relative frequency of each, the idea being that the more letters with higher frequencies there are the less easy it is to predict the next in the sequence; analogously, high equitability in a large number of species makes the identity of the next in the sample harder to anticipate. The Shannon function can be found in any standard ecology text (see Krebs, 1994, or Ricklefs and Miller, 1999, for example) and reads:

$$H = -\sum_{i=1}^S p_i \log_2 p_i$$

where

H = index of species diversity (information content of the sample in bits/individuals)

S = number of species

p_i = proportion of total sample belonging to the i th species.

\log_2 = log to base 2

Equitability is calculated against a theoretical maximum which would come about when all the component species were present in the same proportions: for example, the community with four species would have 25% of each.

$$H_{\max} = \log_2 S; \text{ so } E = H/H_{\max}$$

H again being the diversity index illustrated above, S the number of species, and H_{\max} the maximum equitability.

H , E and S are all standard ecological measures providing useful summaries of a sample. They should, however, be used with caution because they can be very dependent upon sample size; with species richness in particular, the addition of a few rare taxa can greatly alter the value.

3.2.4 Timeseries Analysis

All the ecological data are presented as one-dimensional, one-directional timeseries charts. Two single metric methods are used to assess the patterns generated by this mode of presentation.

3.2.4.i Measures of Irregularity and Variation

Because a central concern of the project is the relative magnitude of environmental stability at different times, some kind of measurement would be helpful. Here I have co-opted and modified a method devised by Dan McShea (e.g. 1992), originally used to quantify complexity (variability) in sequential, homologous, morphological elements. McShea (1991, 1993) examined the complexity of backbones in various mammals, and employed a number of metrics, some of which are very useful. Spinal columns and stratigraphic successions have in common the fact that they are composed of a one dimensional series of homologous elements, vertebrae on the one hand and 'time slices' or horizons on the other. For any given group of (time averaged) measurements from a number of time slices, we could do with a metric to tell us how much the magnitude of the measurement fluctuates both between them and within the group as a whole. The *range* of measurement values is an obvious metric, as is what McShea calls *polarization*, the average amount of fluctuation around the mean (basically the standard deviation); but most useful of all is his *irregularity* index, which involves sequential relationships in a given direction between adjacent values. To find this one must measure the magnitude of shift that has occurred *between sequential values* (Text Fig. 3.3). Irregularity is a particularly handy metric because it is comparable to an organism's-eye (or species'-eye) perspective on an environment, as it moves along a temporal trajectory.

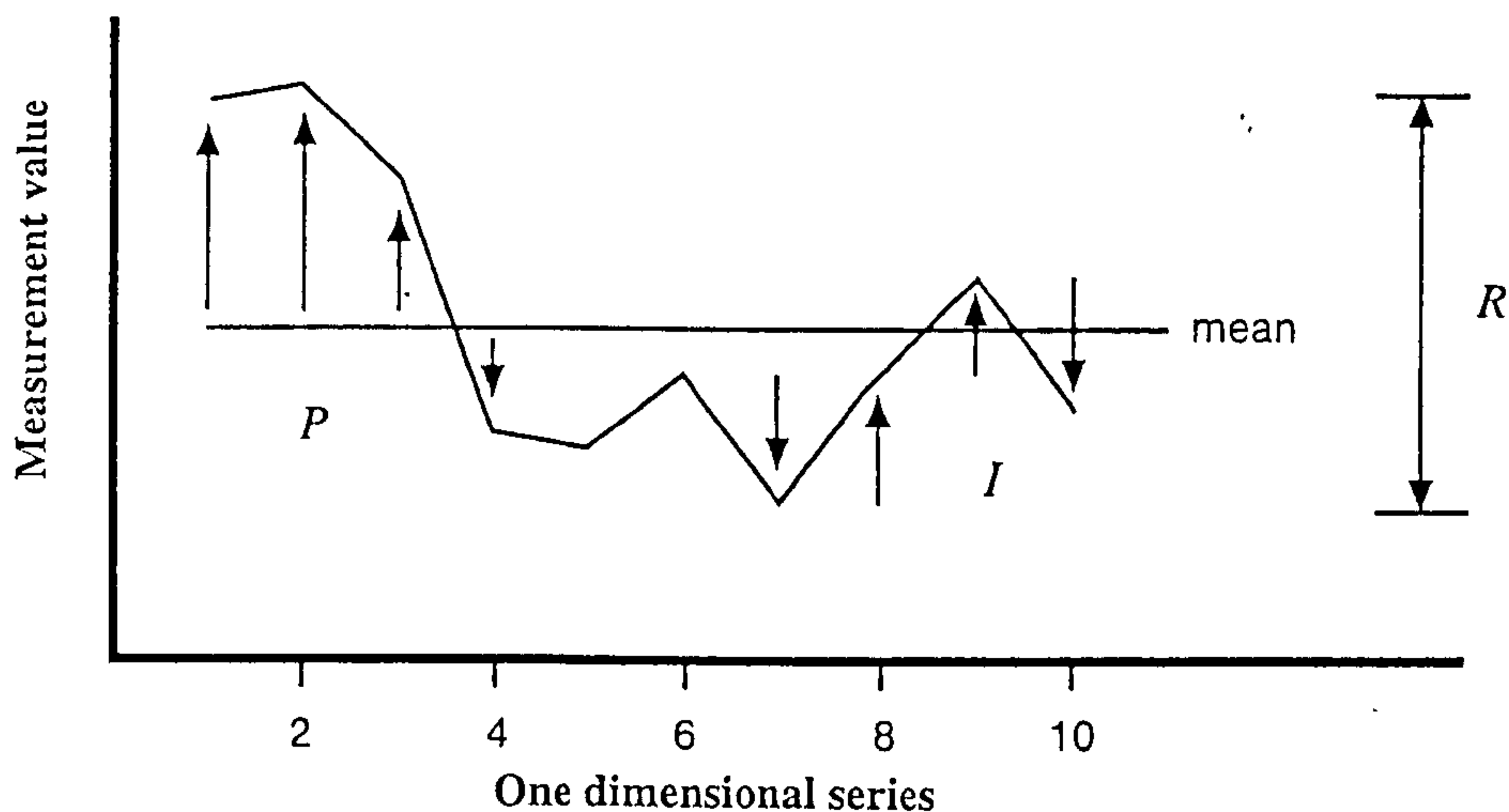
Range, polarity and irregularity (R , P and I) are:

$$R = X_{\max} - X_{\min}$$

$$P = \sum |X_i - \bar{X}| / N$$

$$I = \sum |X_{i+1} - X_i| / [N-1]$$

where X_i is the measured variable at the i th level, N is the number of levels and \bar{X} is the mean measurement for the variable in question.



Text Figure 3.3 *Plot showing an artificial series and the way in which R , P and I are calculated. (Modified from McShea 1991.)*

Polarity and irregularity are sometimes standardised against a mean for the whole series so that fluctuations at different magnitudes can be compared in terms of variability alone. This is important for two reasons. One is that the environment in Sheldon's model is defined in relativistic terms: there is no absolute magnitude of variation which would suffice to count as 'stable' or 'unstable'; rather these must be quantified relative to the history of the system and thus to something playing the role of a local central tendency. Secondly, in a world of biological diversity, cross-species metrics often have to be scaled in order to make any sense at all. A millimetre difference in the length of two fruitflies is of far more significance than a millimetre difference in the length of two whales. Since the indices here will be used to assess variations in species relative abundance, they will need to be scaled to an average in order to be comparable between cases. We also need to be careful about statistical 'walls' (such as proximity to 0 or 100 percent) which will tend to skew the variables.

The ideal depiction of a one-dimensional variable timeseries is muddled somewhat by the fact that real environments vary from place to place as well as time to time, so that what we really need are transects or grids measured in the same terms and then converted to timeseries sequences. The lateral information available here is limited to a one dimensional transect composed of just three data points (or almost, the sites are actually triangularly arranged), so the spatial series has not been given the same treatment as the temporal one. If there was ever a need or opportunity, however, the variability indices could easily be converted to a multidimensional measurement.

3.2.4.ii Correlations

Use is frequently made of correlations between different measurements. In all cases the relationships analysed in this chapter are between continuous variables, so the standard Pearson correlation coefficient (r) is the appropriate measure, along with a t -test for statistical significance. However, because the notion of correlation is so central to any understanding of morphology, and specifically to defining and measuring regions of 'morphospace', an in-depth discussion on the topic is deferred until the more appropriate context of Part III (Chapter 6). If necessary, the calculation of r and t , along with a sample statistical test, can be previewed in Section 6.2.2.i without disrupting the present flow of the text.

3.2.5 Preservational Noise

To save space, taphonomic issues are dealt with here rather than alongside the fossil elements from which the data are derived; a separate treatment in the results section for each of the sampling scales is unnecessary and far too lengthy.

Text Table 3.3 shows the breakage rates of the various taxa and, unsurprisingly, reveals that delicate, filamentous forms (e.g. *Ramulina*, *Dentalina*, *Dorothia*) fragment much more readily than equidimensional, rounded ones (e.g. *Oolina*, *Eggerellina*, *Gyroidinoides*).

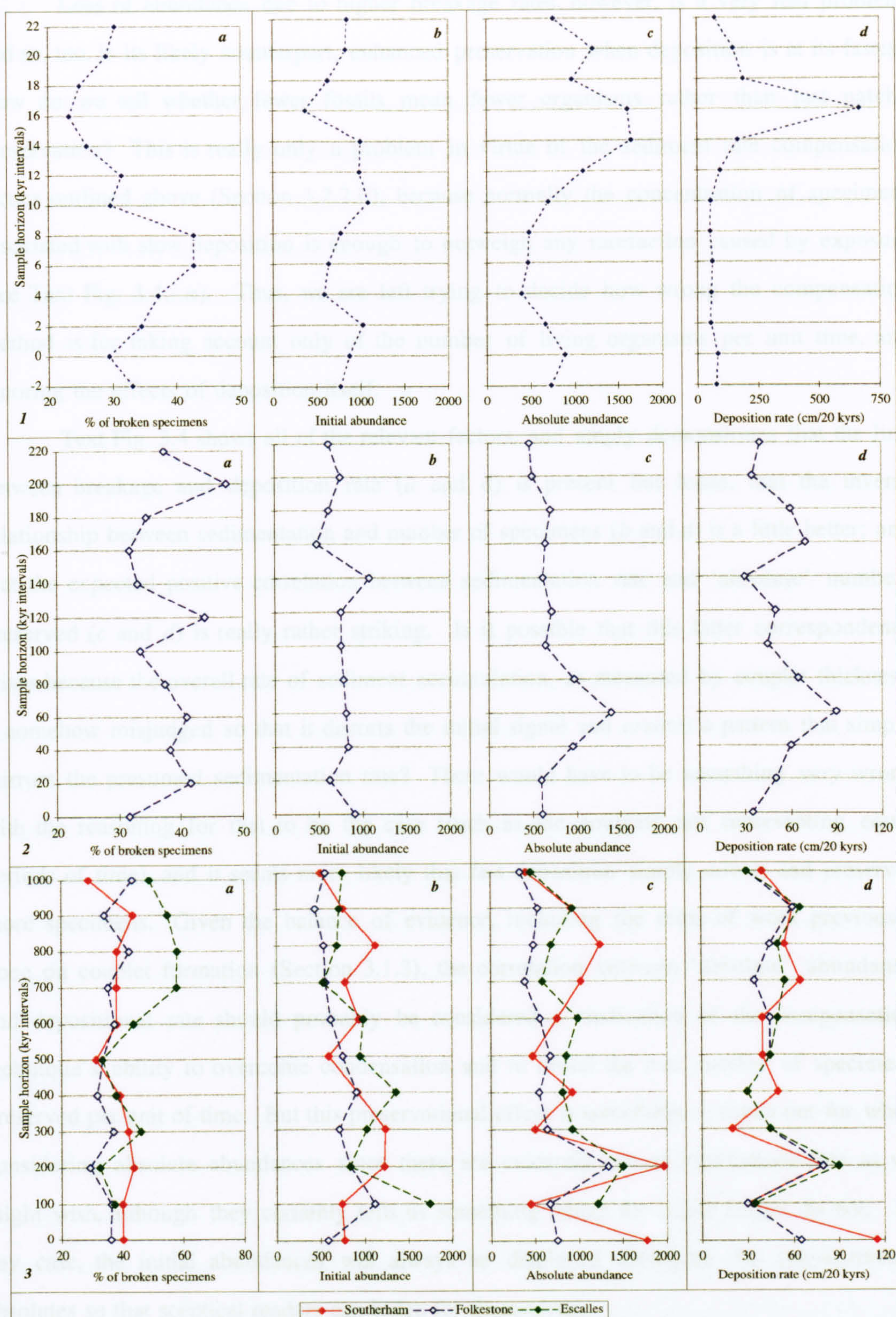
Across C13 the breakage rate is, on average, twice as high in the marl as it is in the chalk (Text Fig. 3.4.i.a), most plausibly because of a longer residence time in near surface sediments, and very much in keeping with the interpretation of depositional rates advanced above (Sections 3.2.2 and 2.1.3).

The effect also extends to wider intervals where the breakage rate is sometimes highest in thin, condensed marls (e.g. C5 - Text Fig. 3.4.iii.a, time horizon 300). When breakage is not obviously associated with low depositional rate, one alternative is that a scour was accidentally sampled (small pockets filled with debris are particularly common in the shallow water portions, but do occur sporadically throughout the section). Post-burial effects such as dissolution may well account for some of the enigmatic preservational failure seen in Escalles samples C29, C35 and C40 [time horizons 700-900]. Escalles had portions of extensively frost shattered rock, and its westerly facing aspect means that it also bears the brunt of Channel storms, which must drive carbonate-undersaturated rain and seawater deep into the porous rock.

The really important issue is the extent to which taphonomic effects have smothered genuine biological signals. There are two ways in which this might happen: either higher breakage produces lowered abundance counts because more specimens are destroyed, or it produces higher abundance counts because some specimens are spuriously 'created' (recall that the values represent the *total* number of cases—broken plus whole). The first scenario may well be correct and an argument along those lines will be examined next. The second scenario is much more likely for some groups than others (Text Table 3.3), but on the whole the impact is probably trivial. The vast majority of breakages involve a corner knocked off or a missing final chamber, and in no way could the missing piece be identified as another individual specimen; almost all of them would have passed straight through the sieves, and would probably be unidentifiable even if they had not. But some of the filamentous forms (*Ramulina* especially; perhaps also *Vaginulina* and *Dentalina*; conceivably *Dorothia*) might break in such a way that both halves are candidates for an individual count. To be cautious we can check surges in these genera against each other and against the overall breakage rate, and be suspicious if they correlate; but in all likelihood, the effect will be so insignificant, especially at the resolution of interpretation employed here, that we can all but ignore it.

Species	Total	Broken	% Broken	General shape
<i>Ramulina</i> sp.	420	420	100.0	round filamentous
<i>Planularia</i> sp. B	2	2	100.0	discoidal
<i>Bulbophragmium</i> sp.	21	20	95.2	round filamentous
<i>Nodosaria</i> sp. A	41	36	87.8	round filamentous
<i>Dentalina</i> sp.	123	100	81.3	round filamentous
<i>Vaginulina</i> sp. A	377	300	79.6	flattened filamentous
<i>Pseudospiroplectinata plana</i>	22	17	77.3	flattened filamentous
<i>Vaginulina</i> sp. B	6	4	66.7	flattened filamentous
<i>Frondicularia</i> sp. A	134	88	65.7	flattened filamentous
<i>Lenticulina rotulata</i>	3754	2189	58.3	discoidal
<i>Planularia</i> sp. A	35	18	51.4	discoidal
<i>Marginulina</i> (smooth)	16	8	50.0	round filamentous
<i>Dorothia gradata</i>	1145	569	49.7	round filamentous
<i>Gavelinella baltica</i>	1606	772	48.1	discoidal
<i>Gavelinella cenomanica</i>	3188	1487	46.6	discoidal
<i>Spiroloculina papyracea</i>	60	26	43.3	discoidal
<i>Gavelinella intermedia</i>	2091	873	41.8	discoidal
<i>Pseudotextulariella cretosa</i>	1028	394	38.3	conical
<i>Ammodiscus cretaceus</i>	25	9	36.0	discoidal
<i>Arenobulimina advena</i>	3649	1277	35.0	fusiform-spheroidal
<i>Gavelinella reussi</i>	995	346	34.8	discoidal
<i>Plectina mariae</i>	314	108	34.4	flattened filamentous
<i>Nodosaria</i> sp. C	3	1	33.3	fusiform
<i>Quinqueloculina antiqua</i>	3	1	33.3	discoidal
<i>Tritaxia pyramidata</i>	11096	3678	33.1	fusiform
<i>Marginulina</i> (striated)	47	15	31.9	fusiform
<i>Saracenaria</i> sp.	92	29	31.5	uncoiled/discoidal
<i>Tristix</i> sp.	35	9	25.7	fusiform
<i>Labrospira latidorsa</i>	4	1	25.0	discoidal
<i>Nodosaria</i> sp. B	4	1	25.0	round filamentous
<i>Marssonella trochus</i>	1239	293	23.6	conical
<i>Palmula</i> sp.	5	1	20.0	discoidal
<i>Gyroidinoides parva</i>	1105	217	19.6	spheroidal
<i>Ataxophragminum deprressum</i>	154	27	17.5	spheroidal
<i>Textularia</i> spp.	2341	401	17.1	conical
<i>Flourensina intermedia</i>	322	45	14.0	fusiform
<i>Guttulina</i> sp.	28	3	10.7	fusiform
<i>Lingulogavelinella globosa</i>	130	11	8.5	spheroidal
<i>Plectina cenomana</i>	24	2	8.3	fusiform
<i>Eggerellina mariae</i>	712	57	8.0	spheroidal
<i>Lingulogavelinella jarvezii</i>	80	6	7.5	spheroidal
<i>Oolina</i> sp.	103	6	5.8	spheroidal
<i>Pseudonodosaria</i> sp.	4	0	0.0	fusiform
<i>Pyrulina</i> sp.	2	0	0.0	fusiform
<i>Frondicularia</i> sp. B	1	0	0.0	flattened filamentous
<i>Vaginulina</i> sp. C	1	0	0.0	flattened filamentous

Text Table 3.3 The relationship between breakage rate and shape in foraminifera.



Text Figure 3.4 *Taphonomy and deposition rate compensation.*

Row 1 C13 at Folkestone, a 20 kyr single couplet at 2 kyr sampling resolution.

Row 2 C10-C21 at Folkestone, a 200 kyr transect at 20 kyr sampling resolution.

Row 3 C31-C45 at Southerham, Folkestone and Escalles, three 1000 kyr transects at 100 kyr resolution.

Initial and absolute abundances of specimens calculated according to the procedures outlined in Section 3.2.2. Consult the supporting text for a fuller explanation. Note that the ordinate is labelled as a temporal scale. See Text Table 3.5 for translation into sample locations.

Loss of abundance due to higher breakage rates, however, is a very real problem, and so, too, is its likely counterpart, enhanced preservation when deposition is at its fastest. How do we tell whether fewer fossils mean fewer organisms rather than just patchy preservation? This is really only a problem in virtue of the sediment rate compensation tactics outlined above (Section 3.2.2.ii), because normally the concentration of specimens associated with slow deposition is enough to outweigh any rarefaction caused by exposure (see Text Fig. 3.4.i.a). Thus, we are left trying to decide how wrong the compensation method is for taking account only of the number of living organisms per unit time, and ignoring the effects of deposition itself.

Text Fig. 3.4 shows all of the relevant factors, and amply demonstrates that the link between breakage and deposition rate (a and d) is present but loose; that the inverse relationship between sedimentation and number of specimens (b and d) is a little better; and that the expected positive correlation between sedimentation rate and ‘absolute’ numbers preserved (c and d) is really rather striking. Is it possible that this latter correspondence arises because the overall rate of sediment accumulation, as measured by couplet thickness, is somehow misjudged so that it distorts the initial signal and *creates* a pattern that simply mirrors the presumed sedimentation rate? There would have to be something *very* wrong with the reasoning for that to be the case (such as the couplets not representing equal periods of time), and it seems more likely that fast deposition simply covers and preserves more specimens. Given the balance of evidence, including the mass of work previously done on couplet formation (Section 3.1.3), the correlation between ‘absolute’ abundance and depositional rate should probably be considered a vindication of the compensation technique’s ability to overcome condensation and to reveal the true number of specimens preserved per unit of time. But this preservational effect is something to watch out for when considering absolute abundances since these are evidently not as interference-free as we might wish, although they certainly tells us something which the initial counts do not. In any case, the initial abundances will always be displayed alongside the rate-corrected absolutes so that sceptical readers can judge for themselves.

Text Fig. 3.4 stands as a reference point for the examination of patterns shown by individual taxa, and, since fast deposition almost certainly records more rare species of small patch size, for comparison with the community structure and diversity plots too.

3.2.6 Presentation of Results

The presentation of results will take a fairly standard sequence. The single rhythm, sampled across a 21 000 year precessional cycle, C13 from Folkestone, will be addressed first; then the short transect through C10-C21, also at Folkestone; these are followed by the three longer sections at Southerham, Folkestone and Escalles. Each part constitutes a sampling regime with its own characteristic scale of temporal resolution: roughly 2 000 years for the first, 20 000 years for the second and 100 000 years for the latter. From here on, these intervals will simply be referred to as 2 kyr, 20 kyr and 100 kyr without any further justification of precision. Finally, the Folkestone data are presented all over again but in a format specifically designed to address the issue of scaling: the Combined Scales charts have their finer sampling resolutions nested within the coarser ones.

For each of the four presentation sections (2 kyr, 20 kyr, 100 kyr and Combined Scales), the data are split and arranged into a further four subdivisions which focus on different facets of ecological identity. The first of these is concerned with physical data such as sedimentary logs, deposition rate and proportions of acid insoluble residue. The second touches on the general stability and wholesale composition of the benthic community. The third addresses standard global measures of community structure by examining the diversity metrics. And finally there is a chance to see the community split up into its component parts: the patterns exhibited by specific groups. The entire sequence of presentations comes in the form of both Appendix Figures and supporting text (Section 3.3 below); its general structure can be conveniently viewed in the contents lists, and is also summarised below in Text Table 3.4.

While each of the main parts—at 2 kyr, 20 kyr, 100 kyr and Combined Scales—is split into roughly the same four subdivisions, not all of the categories have an identical internal configuration. In those dealing with the community structure, for example, a different series of diagrams is used in each case because certain features are only present at particular scales. The data set is very flexible and the same information can be viewed and re-considered over and over again, in such a bewildering variety of ways that the number of available combinations soon becomes overwhelming. This will be particularly apparent in the portion dealing with individual groups: the fauna comprises more than eighty species or higher taxa (with the ostracods included), which is far too many to present individually, and many of them are very rare. Larger groupings are often used, and only split into

component species for the more common forms. Occasionally, to save space, quite significant faunal elements are neglected (the ostracods often are); some are mentioned once to make a particular point but then never again. All the missing data can be found in the appendices (Appdx. Tables 1.1 - 1.5).

I have tried to arrange as much overlap between the numbering schemes for Appendix Figures and Text Sections as possible; that way the number of the section provides the key to charts relevant to that section, and vice versa (See Text Table 3.4, below).

Text Sections are labelled with a 3 (denoting Chapter 3), a 3 (denoting Section 3: Results), a number from 1 to 4 depending on which scale is being referred to, and finally a *Roman numeral* depending upon the *topic* (e.g. Overall Diversity is *iii*).

Appendix Figures are not labelled with a Chapter heading (they miss the first 3 out) but they do have a section heading (3), a number from 1 to 4, again denoting the scale, and also a *Roman numeral* which refers to the *topic*. Finally, some of these figures possess a letter, which has no equivalent role in the Text headings, to label an individual case (because there are no text sections dealing specifically with a single species, but there are charts which do).

<i>Topic / Scale</i>	2 kyr	20 kyr	100 kyr	All Scales
<i>Physical Characteristics</i>	Text Section 3.3.1.i. Appdx. Figs. 3.1.i.	Text Section 3.3.2.i. Appdx. Figs. 3.2.i.	Text Section 3.3.3.i. Appdx. Figs. 3.3.i.	Text Section 3.3.4.i. Appdx. Figs. 3.4.i.
<i>Community Structure</i>	Text Section 3.3.1.ii. Appdx. Figs. 3.1.ii. a-e.	Text Section 3.3.2.ii. Appdx. Figs. 3.2.ii. a-b.	Text Section 3.3.3.ii. Appdx. Figs. 3.3.ii. a-d.	Text Section 3.3.4.ii. Appdx. Figs. 3.4.ii. a-g.
<i>Overall Diversity</i>	Text Section 3.3.1.iii. Appdx. Figs. 3.1.iii.	Text Section 3.3.2.iii. Appdx. Figs. 3.2.iii.	Text Section 3.3.3.iii. Appdx. Figs. 3.3.iii.	Text Section 3.3.4.iii. Appdx. Figs. 3.4.iii.
<i>Abundances of Individual Taxa</i>	Text Section 3.3.1.iv. Appdx. Figs. 3.1.iv. a-y.	Text Section 3.3.2.iv. Appdx. Figs. 3.2.iv. a-y.	Text Section 3.3.3.iv. Appdx. Figs. 3.3.iv. a-y.	Text Section 3.3.4.iv. Appdx. Figs. 3.4.iv. a-y.

Text Table 3.4 *Summary of the Text Sections and Appendix Figures used to display ecological data. The structure of both the text and the supporting figures has been kept as similar as possible to facilitate easy cross-referencing.*

Not all data types can be plotted equally well by the drawing program (Excel 5) and so bed names (like B41) have generally been replaced by a *time* (like 200 kyrs); we have already seen this in Text Figure 3.4. Some graphs (histograms and line charts for example) do permit letters and irregular numbers to be plotted on the abscissa, and, when appropriate, these will normally bear the Gale scheme numbering; those which do not (x-y scatters) are listed with a number referring to an appropriate time interval. For the record, and to assist with translation, these two methods of identifying sample points are presented together in Text Table 3.5 above. Certain time listings bear alternative numbers because for some charts they need to be shoehorned in between a pair of 100 kyr points. All of this will (hopefully) become clear from viewing the charts themselves. Whenever a sampling point is mentioned in the text its Gale number will be used; and if it is mentioned with reference to a specific chart, the corresponding time horizon will also appear beside it in square brackets.

Long Transects (100 kyr)		Short Transect (20 kyr)		Single Couplet (2 kyr)	
Gale scheme	Time slice	Gale scheme	Time slice	My scheme	Time slice
C45	1000	C21	220 or 200	C13-12	22
C40	900	C20	200 or 180	C13-11	20
C35	800	C19	180 or 160	C13-10	18
C29	700	C18	160 or 140	C13-9	16
C21	600	C17	140 or 130	C13-8	14
C15	500	C16	120	C13-7	12
C10	400	C15	100	C13-6	10
C5	300	C14	80	C13-5	8
B41	200	C13	60	C13-4	6
B37	100	C12	40	C13-3	4
B31	0	C11	20	C13-2	2
		C10	0	C13-1	0
				C13-0	-2

Text Table 3.5 *Sample points labelled by Gale’s notation (e.g. Gale 1995) and by an alternative label designed to reflect temporal resolution. See text for explanation.*

Irregularity measures do not appear in the results section immediately below but are used to make certain points when summing up in Chapter 4. They are used to assess the properties of entire timeseries of points, rather than to provide a single reading per sample (as the diversity metrics are), so we need the timeseries to be fairly long if we are to have much conviction in whatever a variability metric is telling us. Working *within* the confines of a particular scale, for example by asking whether the upper half of the single couplet is more variable than the lower, is requiring an index to compare variation across just a

handful of points, in this case six or seven, which is far too small a number. But we can have more confidence when comparing *between* scales (e.g. in asking whether behaviour is more variable at the 2 kyr or 20 kyr scale wherein a string of 13 is compared with a string of 12), and quite a lot of confidence in assessing *overall* behaviour (whether one taxon is generally more variable than another) in which there would be 31 to 53 points to consider, depending upon the data set. Consequently, indices of variation are unavailable for examining fluctuations in signal throughout a single scale, and they are not presented alongside the other measures (e.g. diversity) as a standard index, but are kept instead for the interpretation sections (particularly Sections 4.1.2, 4.2.3, 4.2.4 and 4.3.2) where they can be applied more appropriately. A similar reasoning restricts the use of correlations, although these at least have a significance test to support our intuitions.

Section 3.3 Results

3.3.1 2 kyr Resolution

This survey was conducted to examine the behaviour of the benthic micro-community at a high resolution. Precessionally driven chalk-marl cycles form the basic sedimentary unit of the study sections, and it is useful to consider the effect they have on the fauna. In many respects C13, the host of the 2 kyr transect, is not a typical couplet because it is so thick and has such a strongly developed cyclicity; but since this part of the project is subsidiary to the main goal of establishing an environmental setting suitable for testing the *Plus ça change* model, only a single cycle has been investigated. Complete transects across other couplets are available in the literature, and these will be drawn into the discussion in due course; but it is necessary to have available some material, no matter what its limitations are in terms of geographical spread, which has been sampled and analysed in an identical way (and is thus directly comparable) to that employed in the coarser resolution surveys.

3.3.1.i Physical Characteristics (Appdx. Figs. 3.1.i)

The cycle itself is 90 cm thick, some 25 cm of it being 'chalk' and the rest 'marl' (Appdx. Fig. 3.1.i). As one might expect, the results show the maximum concentration of acid insoluble material in the marly part of the cycle where the clay portion is assumed to be at its highest. The peak value is at 26% but there is a plateau of over 20% throughout the marl. Correspondingly, the lowest proportion of residue comes right in the middle of the chalk.

3.3.1.ii Community Structure (Appdx. Figs. 3.1.ii.a-d)

Appendix Figure 3.1.ii.a shows the ranked distribution of the fifty five species recognised from C13 when data from *all* of the sampling horizons are clumped together. As one might expect (see Section 3.2.3), the distribution of abundances is severely lopsided: the top three species account for 50% of the total number of specimens, the most abundant ten for 77%, whilst the rarest half of the fauna comprise just 5.5% in total. The inset shows this data plotted on a log₂ scale; it does not quite have the ubiquitous log normal distribution that ecologists expect (Section 2.2.2), perhaps because the ostracod fauna is undersampled, but it is close. Appendix Figs. 3.1.ii.b and 3.1.ii.c show the benthic microfossil community separated into ostracod and foraminiferal faunas.

When these data are decomposed into a time series, the emerging picture is both dynamic and stable, depending on how it is viewed. To illustrate this fact, I have chosen to present the material in a rather unusual way, and so considerable care must be taken when interpreting the charts. Text Figure 3.5 shows how the presentation formats relate to each other.

Fig 3.5.a is simply a ranked abundance histogram, similar to Appendix Figures 3.1.ii.a-c, with values showing *amalgamated* data from all the horizons in C13 but displaying only the ten most abundant foraminiferal species (for the sake of clarity). Text Figure 3.5.a has two components: the abundances and the ranking; Text Figures 3.5.b & 3.5.c show these values separately, and also show how they vary *between* sampling horizons across the rhythm.

In Figure 3.5.b we can see that *Tritaxia pyramidata* (white squares, left hand side) always ranks highest in abundance; that *Lenticulina*, which is next to it, always ranks second, except at horizon 4 where it is displaced by *Arenobulimina*; and that *Dorothia gradata* (black squares), which is the least abundant overall, reaches fifth in the ranking order at horizon 5.

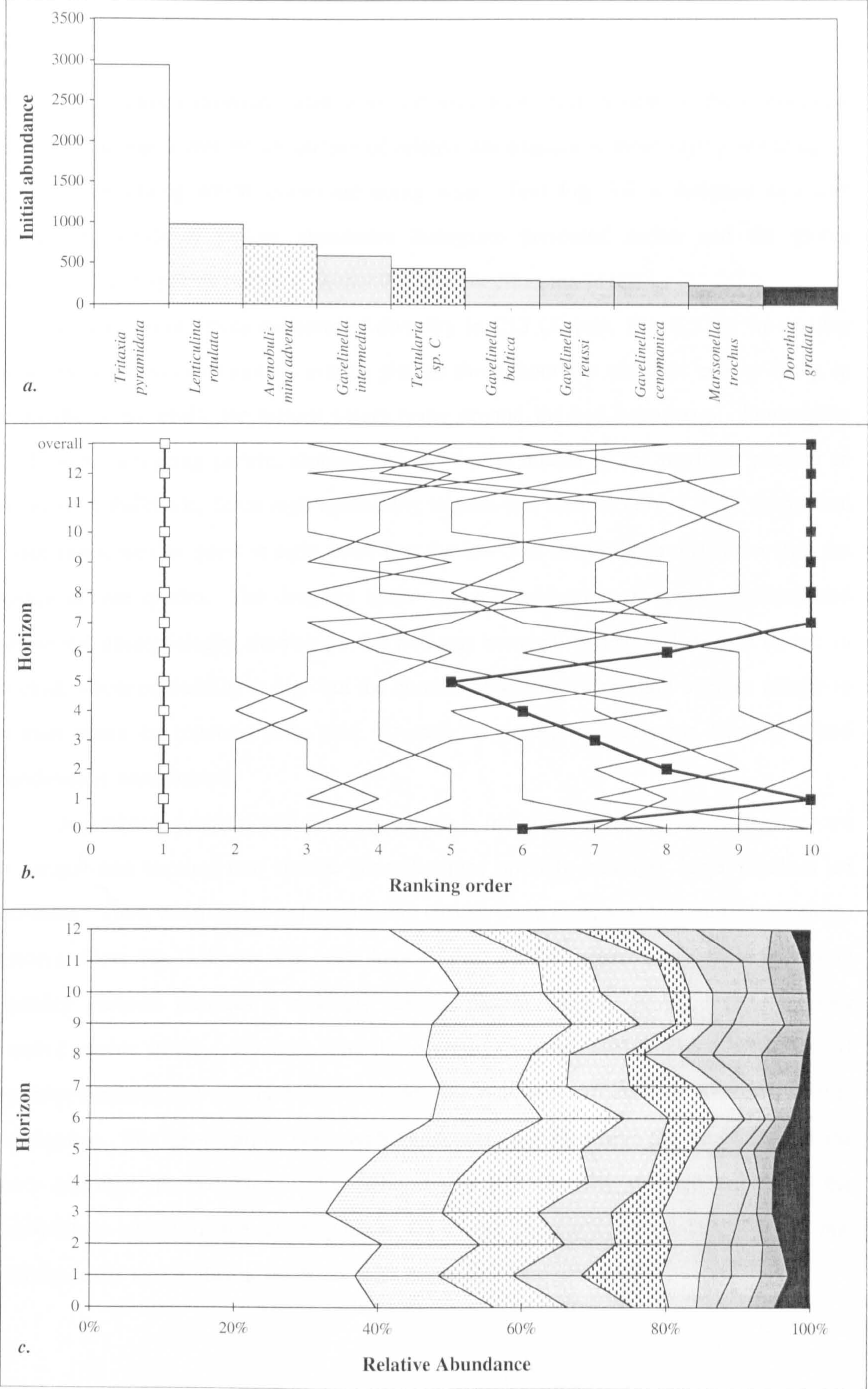
By contrast, Text Figure 3.5.c uses *relative abundances*, as opposed to the initial counts shown in Fig. 3.5.a, in order to emphasise the community *structure*, rather than any wholesale changes caused by, for example, variations in sedimentation rate. The immediate impression is of highly co-ordinated behaviour between the different species, but in this the chart is simply misleading because most of the synchronicity is caused by passive oscillations in relative abundance. Concentrate instead on how much the relative

abundances do *not* change, and notice that *Lenticulina*, for example, is always roughly one third as abundant as *Tritaxia*, and roughly four times as abundant as, say, *Marssonella*. All that jostling for position in the ranking order seen in Figure 3.5.b translates to almost no real change at all in the relative abundance of most taxa: the common species are always by far the most common and the rarer ones the most rare.

Appendix Figure 3.1.ii.d & 3.1.ii.e shows essentially the same set of charts but for the entire community (foraminifera and ostracods). None of the categories are labelled because with fifty five species to account for, the labelling just gets too confusing. To some extent the placeholders can be identified by cross checking with the ranked abundance chart of Appdx. Fig. 3.1.ii.a. since d. has a layer at the top which corresponds to the amalgamated overall abundances, and e. has the species arranged in the same rank order. The figures are designed to be impressionistic—but what different impressions they give! Should we view the changes in community structure across C13 as dynamic variations in ranked abundance, or as rather invariant patterns of relative abundance? I for one was rather surprised to see just how stable community structure can apparently be across the course of 20 000 years.

To be fair, attention should be drawn to the fact that randomness becomes increasingly important as specimen numbers drop, and that much of the tangle in the lower end of chart Appdx. Fig. 3.1.ii.d must be statistical noise. We should also note that although there are no really striking changes in relative abundance there are still species (such as the ostracod genera *Macrocypris* and *Pontocyprilla*, 14th and 17th in overall ranking) whose relative abundances vary by at least an order of magnitude between chalk and marl (samples C13-9 to C13-11 [16 to 20] versus C13-2 to C13-5 [2 to 8], respectively).

In general, the marly part of the cycle is extremely stable, and where disturbances in relative abundance do occur they tend to be at the lithological boundaries (C13-0 to C13-1 [-2 to 0], C13-6 to C13-7 [10 to 12], C13-11 to C13-12 [20 to 22]). The mid-chalk sample (C13-9 [16]) had many fewer specimens than the other samples and will be prey to a higher degree of sampling error.



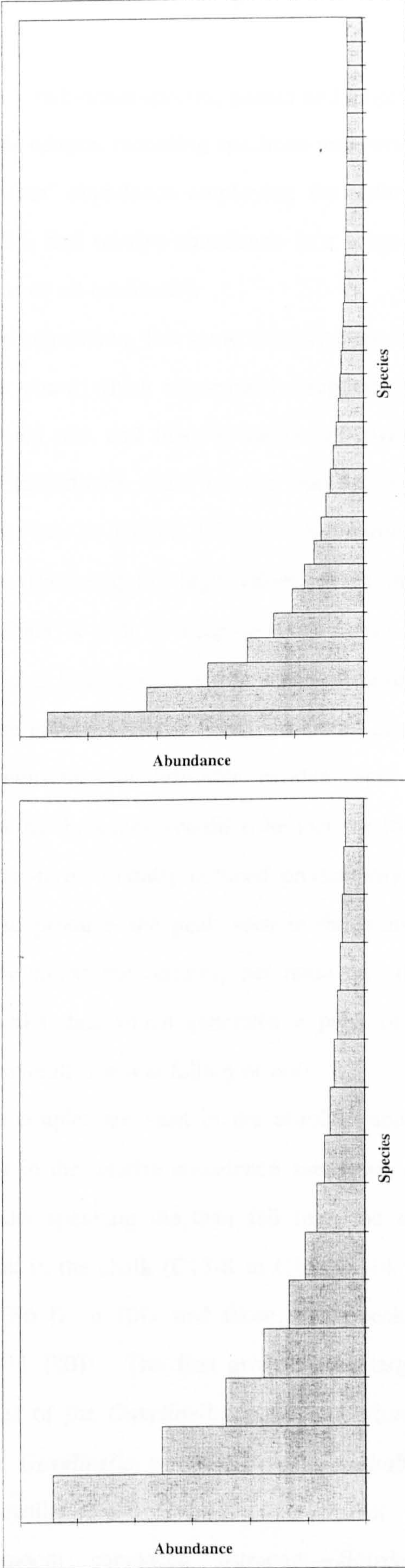
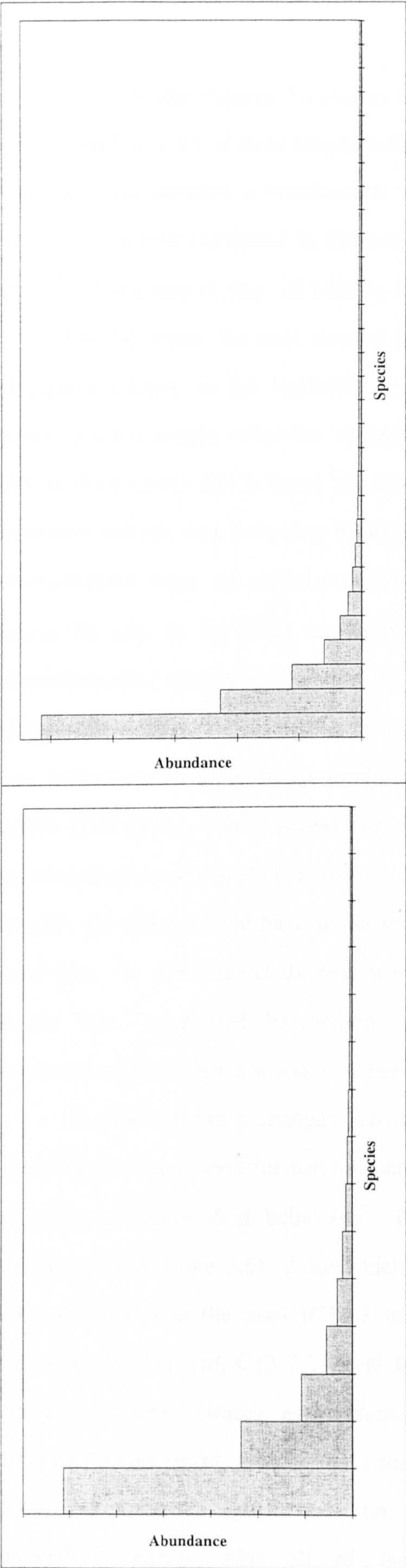
Text Figure 3.5 Demonstrating the relationships between various methods for presenting relative abundance data.(See text Section 3.3.2.ii. for an explanation.)

3.3.1.iii Diversity (Appdx. Figs. 3.1.iii)

The Shannon diversity index is an indiscriminate measurement of the community structure, painting a very broad picture of relative abundances without saying anything in particular concerning which species are doing what. Text Fig. 3.6 is designed as a link between the kinds of ranked abundance histogram presented earlier and the global measurements of species richness, equitability and the Shannon index.

Looking at our three measures of diversity in C13 (Appdx. Fig. 3.1.iii), we see that species richness (S) maintains a wavering plateau throughout the marl but crashes badly in the middle of the chalk, the highest values being around the bed boundaries. Equitability (E) shows a contrasting pattern, dipping strongly in the middle of the marl but peaking in the centre of the chalk. Since high equitability implies that there is only a small proportion of rare types, we can guess straight away that the low S in the chalk probably records the absence of rare species. The diversity index (H), a combination of species richness and equitability, unsurprisingly, shows a pattern mid-way between the two. There is a trough in the chalk where equitability is high but the number of species is low, and another trough in the marl where the converse is the case. Overall, the pattern of maximum diversity at bed boundaries is accentuated.

A persistent problem with diversity indices is that they tend to be very dependent on the sample size because rare species generally turn up only amongst large numbers of specimens. Thus, the richness and equitability curves, when compared to a plot of specimen numbers (Text Fig. 3.4 row 1.b, and Appdx. Fig. 3.1.iii), reveal more than a passing similarity: richness provides a strikingly parallel pattern whereas equitability is a rather distorted mirror image. Concern that the diversity patterns are simply a reflection of specimen numbers, and thus probably sedimentation rate, was sufficient to prompt a further investigation. The rarest half of the overall fauna, were removed from the data base and the curves replotted (dashed lines). The richness plot is necessarily subdued but, while the equitability is higher and the diversity lower, the overall patterns remain intact: it seems that diversity really *was* higher at the boundaries between lithological types.



Text Figure 3.6 *Shapes of abundance curves for various parameters of global diversity*

3.3.1.iv Absolute and Relative Abundances per Taxon (Appdx. Figs. 3.1.iv.a-y)

In Appendix Figures 3.1.iv.a to 3.1.iv.y individual species, genera and larger groups are presented as a set of three charts: initial abundance, recording specimen numbers as they came out of the samples, a transformed ‘absolute’ abundance employing the sediment rate conversion method explained in Section 3.2.2.i, and relative abundance as a proportion of some sensible category (e.g. all benthic forams or all ostracods).

On the whole, the total benthic faunal abundance has some similarity but does not correspond closely to the insoluble residue chart, which immediately suggests that the pattern is not a simple reflection of depositional rate, and that the fauna underwent some kind of fluctuation; this is borne out by the (admittedly often minor) changes in relative abundance and the rank swapping behaviour we saw in Section 3.3.1.ii. The within-couplet transformation alters the signal considerably, flattening the high values in the marl and turning the dip in the chalk inside out. This is well in keeping with Paul’s (1992) sedimentological reasoning (Section 2.1.3), and is almost certainly a much more honest representation of real faunal dynamics than the picture available from the initial data alone. Even if there is an error by assuming the constancy of insoluble residue input (Paul’s rhythm, C14, the one above, is only two thirds the thickness—could it be that the long-term clay contribution was declining even as shorter-term orbitally induced productivity was on the up?), the effect would have to be huge to produce the peak seen in the transformed faunal data. At worst, the chalk peak would be muted, but certainly not removed. (Besides, the fact that I have tried the method on Paul’s data which generates a peak of similar magnitude suggests that it works whether the overall rate was falling or not).

The most striking changes across the couplet are seen in the absolute abundance, but it is important to look for parallel patterns in the relative abundance scores too because that suggests independent behaviour. Broadly speaking the taxa fall into one of three categories (Text Table 3.6): those which peak in the chalk (C13-8 to C13-10 [14 to 18]), those which peak in the marl (C13-2 to C13-6 [2 to 10]), and those which peak at bed boundaries (C13-1, [0], C13-7 [12] & C13-11 [20]). The first group is the largest and obviously includes *Tritaxia pyramidata*, most of the *Gavelinella* group and *Marssonella trochus* as broad peaks, *Lenticulina rotulata*, *Gavelinella cenomanica* and *Arenobulimina advena* as narrower spikes and, on a smaller scale, *Gyroidinoides parva*, perhaps *Eggerellina mariae*, plus all of the smooth carapaced ostracods—*Bairdoppilata*,

Macrocypris, *Pontocyprrella* and *Cytherella*. The undifferentiated planktonic foraminifera also fall spectacularly into this category.

Convincing bed boundary forms are *Textularia* sp C, *Pseudotextulariella cretosa*, *Flourensina intermedia* and maybe *Plectina mariae*, and some individual species within both the minor nodosarian and ornamented ostracod groups also qualify (but are not presented as graphs). Of those which crash badly in the chalk but fare rather better in the marl *Dorothia gradata* is the most persuasive, but the rare agglutinated forams and *Lingulogavelinella* might also be considered, as might some components of the mixed pattern shown by the minor nodosarian group.

It should be noted that the absolute abundance patterns are highly sensitive to fluctuations in the clay content, and that some of the erratic behaviour across the chalk can be attributed to error in the estimation of insoluble residue. The narrow spike shown by *Arenobulimina*, for example, might well be an artefact. Furthermore, no amount of sedimentation rate compensation can alter a zero count, so ‘no specimens present’ might equally be regarded as ‘no data available’, in deference to the maxim that absence of evidence is not evidence of absence (although that makes it hard to say what *would* be considered evidence of absence). We must always keep in mind that smaller numbers are so much more prone to chance fluctuations that it is unwise to read too much into the specific distributions of the rarer groups (which is why many are clumped into larger categories).

Chalk Peak	Boundary Peak	Marl Peak
<i>Tritaxia pyramidata</i> <i>Lenticulina rotulata</i> <i>Marssonella trochus</i> <i>Gyroidinoides parva</i> <i>Gavelinella baltica</i> <i>Gavelinella intermedia</i> <i>Gavelinella reussi</i> <i>Gavelinella cenomanica?</i> <i>Arenobulimina advena?</i> <i>Eggerellina mariae</i> <i>Bairdoppilata</i> spp. <i>Cytherella</i> spp. <i>Pontocyprrella</i> spp. <i>Macrocypris</i> spp.	<i>Textularia</i> sp. C <i>Pseudotextulariella cretosa</i> <i>Flourensina intermedia</i> <i>Plectina mariae?</i> Ornamented ostracods	<i>Dorothia gradata</i> Rare agglutinated forams (esp. <i>Ataxophragmium</i>) <i>Lingulogavelinella globosa?</i> Rare nodosarian forams

Text Table 3.6 *Taxa exhibiting peaks at different points of a chalk-marl cycle (C13).*

3.3.2 20 kyr Resolution

This short transect across the middle part of the study sections (and the middle site) serves to link the small scale, high resolution 2 kyr survey of C13 with the large scale, low resolution 100 kyr survey which is the main focus of the project. It does so by providing samples *from the marls* of every couplet between C10 and C21, effectively resolving patterns to the roughly 20 000 year resolution of Milankovitch precessional frequency.

When the 100 kyr resolution sampling points were originally selected I did not have access to Gale's (1995) numbering scheme, and was rather uncertain about the status of C17 as a complete rhythm. Consequently, C21 (which appears on the 100 kyr timeseries charts as time slice 600) was chosen to be a 100 kyr representative rather than C20 (in large part this was also to help close the gap across the homogeneous sediments between C21 and C29). It now seems that C17 is indeed a complete cycle, and its subsequent inclusion means that there are now 11 samples across the short transect rather than the ideal 10; nevertheless, so long as there are no cycles missing, the spacing between samples should still be the promised interval of 20 kyr.

Because its principal purpose is to serve as a link, the transect incorporates samples from both the coarse and fine resolution surveys, and thus includes some duplication of material. Specifically, the samples from C10, C15 and C21 are later used in the coarse resolution analysis of the Folkestone site (they appear there as time horizons [400], [500] & [600], but in this transect as time horizons [0], [100] & [220], respectively), and the data representing C13 is an amalgamation (employing mean specimen numbers) of horizons C13-3, C13-4 and C13-5 [4 to 8] which are mid-marl and therefore equivalently placed to the samples from other couplets.

3.3.2.i Physical Characteristics (Appdx. Figs. 3.2.i)

As with C13, the insoluble residue values (here available for both marl and chalk components of each couplet—Appdx. Fig. 3.2.i.) closely reflect the pattern suggested by the sedimentary log, and therefore also the visual impression available in the field. A wider-scale oscillation in the lower part of the sequence where the rhythms are well defined gives

way to a more subtle difference between chalky and marly halves in the upper portion, especially across C17 to C19 [140 to 180]. Bed thickness also varies across the section with two peaks of high sedimentation rate, one at C13 to C14 [60 to 80] and another at C18 to C19 [160 to 180]. Initial abundance counts are to some extent reflected in this variation although the association is not perfect (see Text Fig. 3.4. row 2 for comparison).

3.3.2.ii Community Structure (Appdx. Figs. 3.2.ii.a-b)

The overall community structure in this set of rhythms is very similar to that seen across C13, with *Tritaxia* persistently dominating the fauna, most of the nodosarian and ornamented ostracod groups strung out at the bottom end, and the others clustered in roughly the same order (Appdx. Fig. 3.2.ii.a.). This ranked distribution graph represents the combined foraminiferal and ostracod faunas, with specimens drawn from all of the horizons at the relevant resolution. Although there is one less sample in the 20 kyr array than there was in the 2 kyr one (12 instead of 13), there are only 345 specimens less. Consequently, the greater departure from a perfect log normal arrangement seen in Appdx. Fig. 3.2.ii.a. is likely to be due to small differences in community structure between couplets rather than a case of comparative undersampling.

Appendix Figure 3.2.ii.b is set up in the same way as its equivalent in C13 (Appdx. Fig. 3.1.ii.e), and shows that the community maintains the same general structure in every sample of the transect. Again it is possible to identify some of the commoner taxa by counting along from the left and comparing with the ranked abundance graph since the chart is arranged with placeholders in the same order. No counterpart to Appendix Figure 3.1.ii.d. is included for the C10-C21 transect because the diagram delivers so little in the way of specific information: we can be confident that the species jostled for ranking order just as chaotically as they did in C13 without having to view the ensuing tangle, and the relative abundance figure shown is demonstration enough that such small scale shifts never amounted to much. Where slight changes in community structure do occur, they are best viewed as individual cases.

3.3.2.iii General Diversity (Appdx. Figs. 3.2.iii)

Starting off on a relative high, the number of species dips somewhat in samples C11 and C12 [20 & 40], and again in C15 [100]. Comparison with the sample size and sedimentation rate (Text Fig. 3.4) shows that although the correlation with initial sample size is weak, there is some evidence that higher depositional rates (especially in the thick couplet of C13 [60]) did preserve rarer species. As with the transect across C13, diversity scores are displayed with and without the rarest half of the amalgamated fauna. The equitability plot has an overall high across the middle of the transect (C14, C16 and C17 [80, 120 & 140]) and a spike at C11 [20]. The global diversity signal, as always, mirrors aspects of both species richness and equitability and is just as hard to generalise about, although it does appear to flatten out towards the top of the transect. The magnitude of difference between the highest and lowest points in all three plots is similar to that seen across the single rhythm.

3.3.2.iv Absolute and Relative Abundances per Taxon (Appdx. Figs. 3.2.iv.a-y)

The initial total number of benthic specimens (Text. Fig. 3.4 line 2*b*) shows a rough inverse correlation with bed thickness across the top half of the transect, but a rather poorer one across the bottom. The deposition rate compensation method outlined in Section 3.2.2.ii. was designed to correct condensation associated with slow burial, but in this case the between-couplets method seems to have spuriously turned a static abundance pattern at C12-C14 [40-80] into a peak, which is obviously controlled entirely by the bed thickness values at that point. It is not clear why initial abundance over these few couplets should have varied so little, in spite of the changes in sedimentation rate; enhanced preservation through fast burial is one option (but then why did the same thing not happen at C18-C19 [160-180]?), and chance sampling of fossil-filled scours is another. It is also possible that the standing crop really *was* higher across these couplets than it normally would have been. Whatever the reason, it seems wise to take the absolute abundance peak at C12-C14 [40-80] with a pinch of salt. I suspect that there really was a peak of some sort (like the hump at C18-C19 [160-180]), but that it was smaller than the absolute abundance signal suggests.

When the whole fauna is split into individual groups a number of contrasting patterns emerge. It is clear, for example, that it is the foraminifera which tend to show a correlation with deposition rate (Appdx. Figs. 3.2.iv.a. - 3.2.iv.t.) rather than the ostracods which follow a very different plan (Appdx. Figs. 3.2.iv.u. - 3.2.iv.y.). But even within the foraminiferal group, behaviour can be split into those which do and those which do not show a deposition rate correlation. These are summarised in Text Table 3.7.

Average Relative Abundance	Deposition Rate Correlation	Independent Pattern
R.A. >5%	<i>Tritaxia pyramidata</i> <i>Lenticulina rotulata</i> <i>Arenobulimina advena</i> <i>Gavelinella baltica</i> <i>Gavelinella intermedia</i> ? Minor Nodosarian group	<i>Gavelinella cenomanica</i> <i>Textularia</i> spp.
R.A. 1-5%	<i>Dorothia gradata</i> ? <i>Gavelinella reussi</i> ? <i>Gyroidinoides parva</i> ?	<i>Marssonella trochus</i> ? <i>Eggerellina mariae</i> <i>Pseudotextulariella cretosa</i>
R.A. <1%	<i>Plectina</i> spp.?	<i>Flourensina intermedia</i> <i>Lingulogavelinella</i> spp. Minor agglutinating group Porcellaneous group

Text Table 3.7 *Classification of foraminiferal absolute abundance patterns across the short (20 kyr resolution) transect at Folkestone (see text above for discussion).*

The deposition rate pattern is found much more commonly in the abundant taxa than in the rarer ones, and we can assume that this is at least partly to do with sampling error since any statistical effect becomes swamped by noise at low frequency. In support of this interpretation is the minor nodosarian category, a clumping of a dozen or so rare species, none of which show the pattern in themselves, but which preserve it remarkably well as a group (Appdx. Fig. 3.2.iv.r).

What is more interesting is that in *every* abundance category there are at least some examples in which the depositional pattern is *not* followed. *Gavelinella cenomanica* and the *Textularia* group (predominantly one species, C), both of which average several dozen individuals in an initial count, are particularly clear. *Marssonella*, *Eggerellina* and *Pseudotextulariella* are also fairly convincing: they are abundant enough to show some signs of a deposition rate controlled pattern, but they depart from it substantially.

This finding is important because it suggests that deviation from the depositional pattern is not simply a consequence of small sample numbers. If that is true then it can

only mean that there were genuine fluctuations in abundance which have been superimposed upon the passive depositional effect, and which drown it. If we do take the depositional style pattern to be misleading, and say that the abundances of *Tritaxia*, *Arenobulimina* and the like were totally static throughout the section, then, by comparison, the abundances of *G. cenomanica*, *Textularia* sp. C, *Marssonella*, *Eggerellina* and *Pseudotextulariella must* have fluctuated. Consequently, the effect can also be seen in the relative abundance values: taxa which correlate with the sedimentation rate tend to have rather invariant relative abundances, whereas those which show an independent pattern often have a strongly fluctuating signal.

Apart from this general observation on erratic fluctuation in some species and likely stability in others, there is little to say about the foraminiferal fauna. There are a few cases which look like trends: *Tritaxia pyramidata* gradually increases in relative abundance across the section while *Textularia* sp. C and *Pseudotextulariella cretosa* decline; *Dorothia gradata* shows a dip in the most carbonate rich horizons (C18-C20 [160-200]) just as it did in C13, but then so does *Gavelinella reussi* which peaked in the single couplet chalk.

The ostracods show almost entirely unrelated patterns. *Bairdoppilata* spp. is the only one to exhibit anything like a deposition rate correlation. *Pontocyprilla* spp. appears to generally increase in abundance up section, as does *Macrocypris* spp.; *Cytherella* spp. would be utterly chaotic if it were not for the fact that all the smooth genera exhibit a fairly close correspondence in the sequence of positive and negative steps. The ornamented ostracods as a group are rare in the early couplets, peak in horizon 80 (C14 [80]) and then level out to a plateau. Individual genera within the group show no greater regularity nor any convincing correspondence with the physical data.

3.3.3 100 kyr Resolution

These sections are the main emphasis of the study because they span a timescale suitable for testing the predictions of the *Plus ça change* model. In addition to their million year temporal range, they form a lateral transect across the northern edge of the basin so that the geographical distribution of events can also be investigated. Folkestone and Escalles are considerably closer together than either of them are to Southerham (Appdx. Fig. 1.1) and they represent, certainly in the lower half of the succession, a somewhat shallower, more proximal setting. The data for the Folkestone section duplicates material already presented in the short transect, namely, samples from C10 [0/400], C15 [100/500] & C21 [220/600].

3.3.3.i Physical Characteristics (Appdx. Figs. 3.3.i)

Acid insoluble residue data from the samples alone (i.e. only the marls of the sampled couplets) reveals a similar pattern for each of the three sites: all show a gradual decline in residue content up-section and all exhibit the pronounced peak at couplet B41 [200] (Appdx. Fig. 3.3.i.). In addition, it is clear that the marginal sites of Folkestone and Escalles are extremely similar to one another, whereas more distant Southerham is distinct.

Likewise with the couplet thicknesses: the patterns are similar in all three sites, but Folkestone and Escalles are most alike. Sequential variation too tends to diminish up-section, being somewhat erratic in the first half, but levelling out to a fairly even 50 cm per cycle for the latter.

3.3.3.ii Community Structure (Appdx. Figs. 3.3.ii.a-d)

The ranked distribution chart for an amalgamated data set at 100 kyr intervals (Appdx. Fig. 3.3.ii.a) shows that the overall community structure remained very similar to that already seen across the shorter durations, albeit somewhat less even as the log2 inset shows. The lack of evenness is again presumably due to small changes in structure from

place to place and time to time, and apart from one notable exception these are best viewed as individual cases (Section 3.3.3.iv, below). When the data are separated into locations and time series, and presented as relative abundances, this general uniformity is clear, especially in the light of the only noteworthy exception—a marked excursion at horizon B41 [200] (Appdx. Fig. 3.3.ii.b). As usual the placeholders in this diagram are unlabelled for the sake of simplicity, but the identities of the more abundant species can be deduced by counting left along the abscissa of the ranked distribution chart. *Tritaxia*'s role in the excursion is clear: its relative abundance plummets in B41 [200].

To illustrate this occurrence more clearly Appdx. Figs 3.3.ii.c and 3.3.ii.d show the ranked abundance chart from B41 [200] (the data are drawn from all three sites but only that level) and the relative abundance diagrams replotted with the first placeholder, *Tritaxia*, removed. It is clear that *Tritaxia* plays a major role in controlling the relative abundance patterns, but that its scarcity in B41 [200] does not wholly account for the differences in community structure. B41 [200] is associated with a substantial restructuring whereby normally medium abundance species such as *Gyroidinoides parva* and *Dorothia gradata* rise high in the ranking order. It is also worth recalling at this point that B41 (the *arlesiensis* bed) sits at the onset of the $\delta^{13}\text{C}$ excursion documented by Paul et al. (1994; see Section 2.1.6) just below Gale's B-C block sequence boundary; it also lies at the epicentre of the concentric macrofossil zoning described in Section 2.2.6.

3.3.3.iii General Diversity (Appdx. Figs. 3.3.iii)

Wholesale measures of community structure show several noteworthy features (Appdx. Fig. 3.3.iii). Firstly, the sequence of values in all three cases is, like the physical data, more similar for the shoreward and closely spaced sites of Folkestone and Escalles than for the distant, basinal section at Southerham. Also, the range of variation across the million year span is similar to that seen across shorter durations. And finally, the highest peak in overall diversity, at least in the proximal sites, is at B41 [200] with its unusual community structure, a feature which arises not only because of high equitability (presumably related to the loss of *Tritaxia*) but also because of a large number of species in those samples.

Although the effect is markedly more pronounced at Southerham, all three sites show a general decline in overall diversity. In the case of Southerham the diversity drop is mostly due to a lowering of equitability, whilst at Folkestone and Escalles it is due to a decline in the number of species.

There are no really striking similarities between general diversity patterns and the sedimentary data (compare Appdx. Fig. 3.3.iii with Text Fig. 3.4 row 3.d), suggesting that there is unlikely to be much interference from deposition. Some caution might be exercised in viewing the values from samples at B41 [200] and C10 [400] where the sedimentary rates were high and low respectively, and all three diversity measurements follow suit, but otherwise the deposition-diversity correlation is fairly poor.

3.3.3.iv Absolute and Relative Abundances per Taxon (Appdx. Figs. 3.3.iv.a-y)

Across the 100 kyr resolution sections the benthic foraminifera show some very striking patterns (Text Table 3.8). The most impressive of these are associated with horizon 200 (B41 [200]) in cases where an imposing shift interrupts an otherwise rather stable plateau. In reality this is two opposing styles of behaviour: *Tritaxia pyramidata* (3.3.iv.a) and *Gavelinella reussi* (3.3.iv.p) (and *Gavelinella intermedia?* -3.3.iv.o) show a sharp dip; *Dorothia gradata* (3.3.iv.d), *Gyroidinoides parva* (3.3.iv.k) plus, less strikingly, *Gavelinella baltica* (3.3.iv.n), *Lingulogavelinella* spp. (3.3.iv.l), and *Plectina mariae* (3.3.iv.g) all exhibit a peak. In the case of *Lingulogavelinella* the peak is due almost entirely to the brief appearance of *L. jarzevae* while the rest of the graph records the more widespread and constant *L. globosa*. Note also that *G. baltica* peaks maximally at Southerham whilst *L. jarzevae* peaks least there.

A twin tipped peaking pattern with surges at B41 [200] and C10 [400] is the characteristic signal shown by *Textularia* sp. C. (3.3.iv.e), *Pseudotextulariella cretosa* (3.3.iv.b) and *Marssonella trochus* (3.3.iv.c). At this sampling resolution, *P. cretosa* positively crashes after C10 [400], although it recovers towards the end of the succession; *Textularia* sp. C and *M. trochus* decline more slowly but remain down and out for the count.

There also appears to be a third, less well-defined suite of patterns. *Arenobulimina advena* (3.3.iv.i) and *Eggerellina mariae* (3.3.iv.f) share a number of similarities in their

sequence of positive and negative steps, most notably in the middle and upper half of the succession. Two of the grouped rare species, the minor nodosarian taxa (3.3.iv.r) and the agglutinating ones (3.3.iv.j), are also similar to one another. In this latter case we can see that there are two humps in the pattern, one centred on B41 [200] and a second spanning C15-C21 [500-600]. Comparing the *Arenobulimina-Eggerellina* pattern with the one shown by the grouped taxa reveals a general likeness between them all, and prompts the suspicion that they may represent different facets of the same phenomenon. *Arenobulimina* lacks the B41 [200] peak shown in the others, but when its signal is set beside that of *Lenticulina rotulata* (3.3.iv.q) and *Gavelinella cenomanica* (3.3.iv.m) there are resemblances once again and a suggestion that this behaviour might be found even further afield.

In cases as general and hazy as this one, the most obvious explanation is that the similarities result, as in the short transect, from some kind of shared sedimentary effect. Curiously, however, this time it is the rarest taxa which exhibit the pattern most strongly, flying in the face of statistical rules for signal clarity. Examine the agglutinated group, *Eggerellina*, the nodosarians, *Arenobulimina*, *Lenticulina* and *G. cenomanica*, in that order (Appdx. Figs 3.3.iv.j, f, r, i, q, & m), and watch the double humped arrangement gradually fade away as the relative abundance climbs. There are no obviously comparable patterns in the sedimentary data, or even in the diversity and community plots. Whether this apparent correlation is a genuine pattern at all is not clear to me, but it is certainly intriguing.

Teasing the grouped taxa into their component strands reveals little internal homogeneity to support the more general pattern, which tends to confirm that the latter arises through some kind of statistical accumulation (see Appendix Tables 1.3, 1.4 & 1.5 for these, they are not shown as graphs). Within the minor agglutinated group, the peak at B41 [200] is mostly due to the elsewhere uncommon genus *Bulbophragmium*, whereas that between levels C15-C21 [500-600] records an increase in the much commoner *Ataxophragmium*. The minor nodosarian group is similar inasmuch as the peak it shows at B41 [200] is enhanced by an unusual turnout from normally rare (e.g. *Dentalina*) or otherwise absent (e.g. *Guttalina*) groups, whereas that between C15-C21 [500-600] merely involves an increase in the abundance of much commoner genera (e.g. *Vaginulina* and *Ramulina*).

Major Excursions	Taxa
B41 [200] only	<i>Tritaxia pyramidata</i> <i>Gavelinella reussi</i> <i>Gyroidinoides parva</i> <i>Dorothia gradata</i> <i>Lingulogavelinella jarvezeae</i> <i>Gavelinella baltica?</i> <i>Plectina</i> spp?
B41 & C10 [200 & 400]	<i>Textularia</i> sp. C <i>Pseudotextulariella cretosa</i> <i>Marssonella trochus</i>
B41 [200] & C15 - C21 [500 - 600]	Rare agglutinating taxa <i>Eggerellina mariae</i> Rare nodosarian taxa <i>Arenobulimina advena?</i> <i>Lenticulina rotulata?</i> <i>Gavelinella cenomanica?</i>
Other	<i>Flourensina intermedia</i> Planktonic foraminifera Porcellaneous taxa

Text Table 3.8 Summary of pattern classification for fluctuations at 100 kyr resolution.

Apart from those mentioned above, the only discernible order amongst the other foraminifera is a general decrease up-section within the porcellaneous group, and increases in abundance in *Flourensina intermedia* (3.3.iv.h) and the planktonic group (3.3.iv.t). The dramatic take-off in relative abundance (as a proportion of total foraminiferal abundance) of the planktonic species above C10 [400] is the well-documented P/B break (see Section 2.1.6).

Among the ostracods there is little to report. *Bairdoppilata* spp. (3.3.iv.u) seems to suffer a general decline up-section, whereas *Pontocyprrella* (3.3.iv.w) tends to be more abundant. *Cytherella* spp. (3.3.iv.x) has a *Tritaxia* style dip at B41 [200] but also between C15 [500] and C21 [600] (those horizons again!), while the ornamented group as a whole (3.3.iv.y) shows an impressive co-ordinated peak at B41 [200]. Breaking the ornamented group into its component genera reveals that the B41 [200] signal is primarily the result of appearances from unusual taxa such as *Cythereis* and the very rare *Planileberis*, combined with peaks in the commoner *Mandocythere*, *Rehacythereis*, *Protocythere* and *Bythoceratina*; which oscillate in an effectively random way throughout the rest of the succession.

In general, one feature which stands out about the individual data as a whole is the close correspondence between signals from Folkestone and Escalles when compared with those from Southerham. This is a regularity which appears consistently and which cannot

be caused by data transformation (e.g. by the process of calculating absolutes) because it occurs in both the initial data set and in the relative abundances too. The other really striking and noteworthy feature is the large number of elements which show basin wide co-ordination, both in the signals of individual taxa (e.g. in the up-section increase in *Flourensina intermedia*), and also between them (e.g. the co-ordinated peaks of numerous species at B41 [200]).

3.3.4 Combined Scales

Given that the Folkestone sections have similar data available at different temporal resolutions, it is useful to see each of these in the context of the others. This section once again examines material from the 2 kyr resolution survey over C13, the 20 kyr transect between C10-C21, and the 100 kyr resolution transect at Folkestone, but this time as a single timeseries. The purpose here is simply an exploration of how the various sampling resolutions relate to one another to help make interpretations based on scaling more robust. The issues mostly concern how best to fill gaps in the coarser scale survey, and the commentary will primarily be directed toward that goal.

In the plots for diversity and individual taxa (Appdx. Figs. 3.4.iii & 3.4.iv.a-y), the temporal scale is presented as distance along the ordinate in the usual manner; this analogue representation is more or less to scale, which means there is a loss of resolution in the single couplet data, but one which is more than made up for by being able to glimpse the magnitudes accurately. (There is still *some* distortion in spacing along the time axis: an extra 20 kyr sample, C17, is placed unevenly [at 530] within the 100 kyr markers between C15 [500] and C21 [600], and twelve of the thirteen single-couplet samples are shoehorned, again unevenly, into a gap of 20 kyrs. See Section 3.2.7. Text Table 3.5.)

The same abscissa is used for all three resolutions, and consequently the vastly swollen ‘absolute’ abundances present for some taxa in the single-couplet chalk tend to overwhelm the individual taxon signatures across all other scales. Absolute abundances have been left as a combination of the ‘within’ and ‘between’ couplet compensation methods. Again this causes a small distortion in terms of equivalence between the data at different scales, but at least they are then directly comparable with material presented in earlier sections; it also avoids a need for the lengthy demonstration and justification required to explain how the two methods can be combined. At the level of analysis required, the differences between a ‘patched-together’ and ‘integrated’ approach are negligible. I experimented with an integrated version for several taxa and the plots looked almost identical, so in the end I gave up and adopted the simpler patchwork option instead.

The time axis on the community structure chart (Appdx. Figs. 3.4.ii.b, d,e & g) is, unfortunately, not to scale. This is simply because I could not coax the drawing package (Excel 5) into producing relative abundance plots in a style similar to those used for the

diversity and individual taxon data. Consequently, the region taken up by the single rhythm and short transect are much larger than they should be—an advantage in some ways because at least the patterns are more easily seen.

3.3.4.i Physical Characteristics (Appdx. Figs. 3.4.i)

Appendix Figure 3.4.i shows the insoluble residue and depositional rate variations at the three sampling scales used at Folkestone. Insoluble residue data are presented for the marls only (i.e. only the sampling points themselves) at 100 kyr resolution, but for both halves of each of the 20 kyr couplets from the middle zone and from each of the 2 kyr single couplet sampling points which are at a finer resolution than the beds themselves. This sets the scale and extent of the cyclic oscillations against the steady decline in terrigenous material which is evident from the 100 kyr spacings.

When deposition speed is considered, the pace of sedimentation in the single couplet chalk vastly outstrips the kind of time-averaged rates typical across an entire 20 kyr span. The rate data in Appendix Figure 3.4.i are the same as those already presented in Text Figure 3.4 row 1, where sedimentation within the single couplet was calculated as an extrapolation per unit of time. Text Figure 3.4 row 1 *d* shows how the time taken to accumulate a 7.5 cm vertical stretch of sediment varies if we assume a regular clay clock, and it gives us a rate for the chalk which, if left to run constantly for 20 kyrs, would produce 6 m of sediment (only 2% of it clay). Whether this is a deceptive result, derived from a spuriously low insoluble residue count in the mid-chalk sample, is not clear; but even if it is an exaggeration we can be certain that rates of sedimentation (and thus of carbonate production) during chalk formation were considerably higher than they were during the accumulation of marls. Thus, we can see that differences in overall rate between whole 20 kyr rhythms are likely to be trivial in comparison to the variations across a single cycle, and that if fluctuations in clay input really *were* minor within the timescale of couplet formation, the more pronounced the chalk-marl rhythmicity, the more marked such deposition rate variations would have been over the course of a 20 kyr cycle.

3.3.4.ii Community Structure (Appdx. Figs. 3.4.ii.a-g)

The earlier sections have already told us that with the exception of couplet B41 [200], the mix and relative abundance of species in the Lower Chalk microfossil community remained roughly constant across every resolution investigated. Appendix Figures 3.4.ii.b, d, & g allow us to see this constancy in a scaled context for the whole fauna, and for the separated foraminiferal and ostracod faunas. Clearly the predominance of foraminifera in the samples is primarily responsible for the stability, because the ostracods behave erratically at all scales! Ostracods rarely constitute more than 20% of the total benthic fauna—in fact, it is normal for *Tritaxia* alone to comprise at least twice the proportion of the entire ostracod group—but the ostracods seem to be subject to their own dynamics, over and above the sampling issues, as a comparison between the three relevant charts should demonstrate.

Set against the coarser resolution behaviour, and recalling that the temporal axes on these charts are larger than true scale, the oscillations in the short transect, and particularly in the single rhythm, begin to look considerably more dynamic. The kinks across the upper, chalky half of the single couplet are accentuated and start to look more like rapid and substantial shifts once they are set against the background of more widely spaced marl samples, and especially when the foraminiferal fauna is singled out (Appdx. Fig. 3.4.ii.d). Nor is this a passive effect controlled by the behaviour of *Tritaxia* alone because the other foraminifera show it too (Appdx. Fig. 3.4.ii.e).

Even during the 200 000 years of the short transect the fauna appears to be oscillating relatively rapidly in comparison to the stability across the whole million year backdrop. The 100 kyr samples are no more time-averaged, as samples, than are those at 20 kyr, and so the coarser resolution pattern must be considered as a series of snapshots taken from a system which was constantly undergoing metamorphoses at a speed and magnitude equal to that seen across the directly comparable marl samples of the 20 kyr resolution transect. Obviously, this diminishes the significance we are willing to accord to most peaks and troughs at 100 kyr resolution, making them look far more like noise than signal (an issue dealt with at length in Section 9.4.1). Most impressive, however, is the fact that in the long term, the continuous sequence of transformation amounts to very little: panning back, we see all those accumulated millennia of fluctuation, gradually crystallise into a million years of dynamic stability.

The chalk of C13 and the marl of B41, are clearly exceptions to the background scale of oscillation. The gross faunal structure wandered hither and thither, but these two events are quite definitely departures from the general behaviour. We cannot say how many other B41 magnitude events lie hidden between the uninvestigated 100 kyr markers, nor to what extent the patterns seen in the chalk of C13 are typical of other chinks in the sequence, but we can be certain that in these two examples, both occurrences constitute disruptions to community structure which are over and above that expected between equivalent marly phases of the sedimentary cycle.

3.3.4.iii Diversity Measures (Appdx. Figs. 3.4.iii)

The gross information structure of the community is also pushed outside its normal bounds during the C13 chalk and in B41. Equitability, species richness and hence overall diversity, reach their lowest levels in the single couplet chalk; conversely, they achieve their highest values in B41, although only just. The extent to which these effects are produced by one taphonomic artefact or another is not entirely clear—I suspect that a lot of the small shifts in both diversity and many other measures of ecological behaviour will turn out to be noise rather than signal—but in defence of a straightforward interpretation in these two cases, the background physical conditions seem to be more striking reasons for unusual diversity parameters than any sedimentary effect *per se*.

3.3.4.iv Absolute and Relative Abundances per Taxon (Appdx. Figs. 3.4.iv.a-y)

As with the other indices of faunal behaviour, the individual taxon signatures confirm the importance of the transition from marl to chalk, and the change in community structure at B41 [200], as events which stand out against a lower level of background variability.

With the chalk signature, the effect is seen most strongly in the absolute abundances: *Tritaxia pyramidata*, *Marssonella trochus*, *Arenobulimina advena*, *Lenticulina rotulata*, *Gyroidinoides parva*, most of the gavelinellids, the planktonic foraminifera and all of the

ostracod groupings show very strong peaks in absolute abundance in the chalk. These are also the commonest taxa, and in almost every case the huge swell in absolute numbers is *not* matched by an equally large disturbance in their relative abundance.

The shift in community structure at B41 [200], by contrast, is also reflected in changes of relative abundance; here the fauna is qualitatively different, certainly far more so than in normal marls, and also more distinctively than in the single couplet chalk. As already noted, *Tritaxia pyramidata* crashes badly in B41 [200] while *Dorothia gradata* and *Gyroidinoides parva*, in particular, peak. Of the others showing change associated with B41, the alteration in absolute, and especially relative, abundance is rather less dramatic when set against fluctuations at finer resolution; but the fact that the B41 signals are normally coordinated across all three sites suggests that whatever happened there was still an event worth remarking upon, rather than some kind of sampling bias or idiosyncratic ecological oddity.

Summary

The sections have been introduced and the range of techniques for assessing ecological factors explained. Various factors relevant to a taphonomic assessment were presented in the series of charts comprising Text Figure 3.4.

Acid insoluble residue (AIR), as an indicator of the primary depositional signal, tends to support the impression given by the graphic logs. Diversity as measured by S, E and H to some extent reflects the depositional setting (i.e. higher rates of deposition preserve more specimens per unit time, condensed horizons preserve more specimens overall simply because they represent longer units of time), but also captures an element of the genuine ecological signal as shown by individual species abundances.

Once a deposition rate correction method has been applied to the 2 kyr resolution transect of C13, it becomes apparent that there was a huge surge in absolute faunal abundance during the influx of phytoplankton associated with the formation of the chalk. While almost all species respond to this event, different species respond in different ways, as shown by their relative abundance profiles. Most of the normally common species become even more abundant, and many of the rarer species become less. A third suite of species tended to peak at the chalk-marl boundaries instead.

The 20 kyr transect between successive marl bands reveals a distinction between species whose abundance changes passively alongside sedimentation rate, versus those showing an element of independence. It is not easy to say what causes this independent behaviour, but the fact that some elements of the fauna are active over and above the sedimentary dynamics is a significant finding.

The three long transects at 100 kyr resolution reveal a good deal of ecological correlation between the three geographically separated sections, particularly between the marginal sites of Folkestone and Escalles. This coarse resolution million year sequence is utterly dominated by an event at horizon B41 in which the relative (and absolute) abundance of *Tritaxia pyramidata*, usually the most prolific of components, is radically diminished, while several other species peak in its stead. There are also some abundance shifts around C10 and in the upper parts of the sequence around C15 - C21, plus idiosyncratic behaviour exhibited by various faunal elements (e.g. *Flourensina intermedia*).

With the exception of its response to B41 and the chalk of C13, the Cenomanian micro-fauna is remarkably consistent throughout at all three sites and all three scales investigated. It shows the same 'decay curve' distribution of taxa, in which the same species maintain roughly the same relative abundances, regardless of whether the period of observation is 20 kyrs at 2 kyr intervals, 200 kyrs at 20 kyr intervals, or 1000 kyrs at 100 kyr intervals. Furthermore, the size of the fluctuations is similar across all three transects, suggesting that with the exception of obvious excursions from background behaviour in B41 and the C13 chalk, much of the variation between successive marl samples may be better regarded as noise rather than signal.

Chapter 4 Life In The Cenomanian Chalk Sea: A Palaeoecological Reconstruction

Introduction

Chapter 3 introduced the palaeoecological data set. Preservational interference seems to be minimal, allowing patterns that have been buried for the last 95 million years to fight their way free from the inevitable background noise and enjoy a second lease of life. This chapter aims to incorporate those patterns into a broad theoretical framework, an ecology of conceptual relationships, one might say, to discipline and manage the empirical material itself. Section 4.1 will advance a very general interpretation of the micro-faunal structure, drawing on both empirical and theoretical material presented in the previous chapters, and occasionally focusing on specific taxa to flesh out their ecological character more fully. Then, building on this understanding of the gross faunal structure, issues relevant to its dynamic nature will be considered in Section 4.2. Finally, in Section 4.3, the maturing body of explanation will be let loose on those issues that have a particular significance to the project, to demonstrate that the study sections provide the kind of setting in which the *Plus ça change* model may be tested. There is no attempt in this chapter to address the data in the sequence or category in which it was originally presented; from here on, the dimensions of the conceptual configuration itself will define the order of discussion.

Section 4.1 The Geometry of the Chalk Sea Micro-community

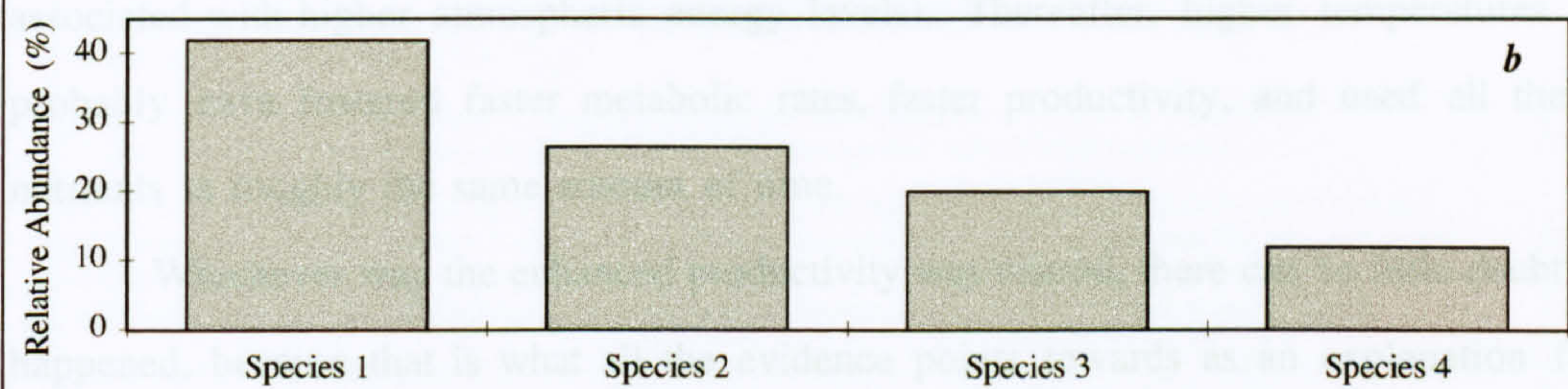
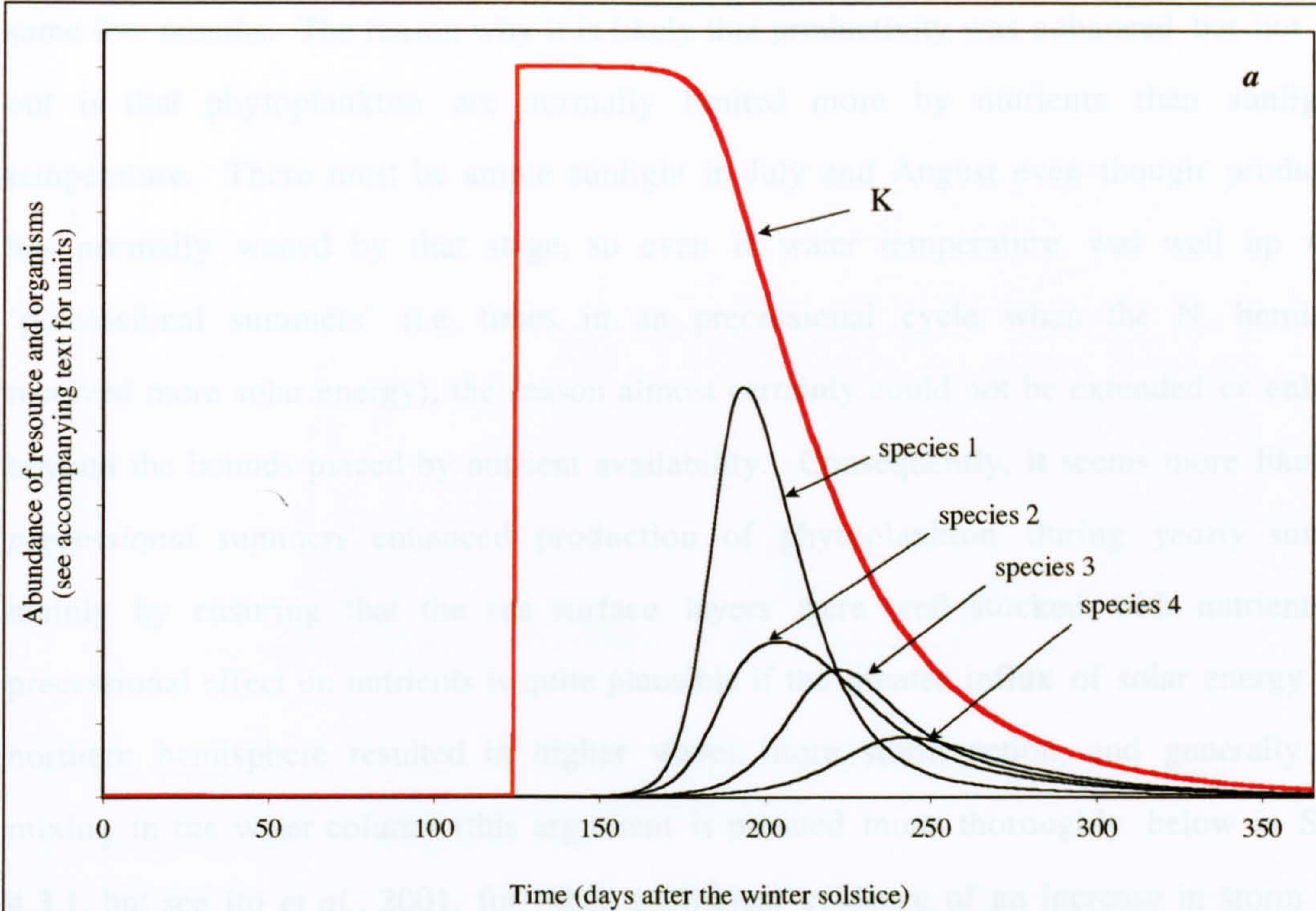
Sections 2.2.1 and 2.2.2 were descriptions of ecosystem structure in the most general terms, including such features as trophic levels, community interaction matrices and universal niche axes. Interpretation of the Lower Chalk micro-fauna will begin by matching patterns in the empirical data to these theoretical constructs, sketching out a broad geometry within which particular taxa are placed on the basis of fluctuations in their abundance. We can start with the dominant axis of organisation, and then work down from there.

4.1.1 Axis 1: K and r

The productivity-variation explanation for chalk-marl cyclicity is now generally accepted (Section 2.2.3; e.g. Ditchfield and Marshall, 1989; Leary, Cottle and Ditchfield, 1990; Gale, 1989, 1995; Paul, 1992; Paul *et al.*, 1994; Mitchell and Carr, 1998), and we can be fairly confident that the main source of energy and material for the mid-Cenomanian benthic community was the input of phytoplankton and associated faecal debris. In latitudes as high as the Anglo-Paris Basin must have been, even during the Cenomanian (~40° N; Section 2.1.6), modern phytoplankton productivity has a strong seasonal component (Harris, 1986; Boney, 1989). Plankton productivity is normally restricted by two factors, the influx of solar energy, and the availability of limiting nutrients. During a typical yearly cycle, the low temperatures, cloud cover and weather-driven turbulence in the winter sea will ensure that plankton growth is slow and erratic, and that mixing and replenishment of the surface layer with deeper, nutrient rich waters is effective. But as the year progresses, the sea warms and becomes successively more stratified, allowing plankton to proliferate in the stable surface layers until they become limited by a depletion of the raw materials they need (typically N, P, S and Fe). Peak productivity occurs some 40 to 100 days after the spring equinox, and tails off thereafter when resources run short (Harris, 1986). Since there is no reason to believe that May in the Cenomanian was any less vibrant than the month we are familiar with, or had any less of an effect on the phytoplankton of the Chalk Sea, I shall adopt the structure of these modern floras wholesale and just transport them back in time.

From the perspective of the Cenomanian foraminifera, the rain of detritus probably started to pick up around May and to peak during June and into July. Throughout the winter months, food would presumably have been limited mainly to rotten detritus left over from the previous summer, and competition amongst the micro-benthos would have been fairly high, favouring economical and specialized equilibrium (K -selected) species. With the spring blooms, a sudden reappearance of large quantities of fresh material must have allowed overwintering r -selected opportunists the chance to proliferate, as the observations of Gooday and co-workers suggested (Gooday, 1988 and others by same author—see Section 2.2.4; Text Fig. 4.1 below).

The effect of precessional cyclicity on this seasonal rhythm seems to have been either to prolong the growing season, or, more likely, to enhance productivity across those



The faunal abundance curves in **a** were calculated using the Lotka-Volterra competition equations which are found and explained in any standard ecology text (e.g. Pianka 1994). The variables are an intrinsic rate of increase (r) and a carrying capacity (K) for the entire community, plus a set of competition coefficients which define the impact each individual of a particular species has on the other species.

In this case the carrying capacity for each species is considered to be equal, so that abundances are determined purely by the number of individuals spread throughout the community, the distribution and weighting of competition coefficients between them, and the stage of growth with respect to the overall carrying capacity, K , (represented by the thick green line, but at one fifth the magnitude so it would fit on the chart).

What does vary between species are the rates of increase and the magnitude of competition coefficients. These are set such that species with *high* rates of increase (r) had a small competitive impact on species with *low* r values; conversely, those with low rates of natural increase had a high competitive impact on those with higher rates. The high r - low r , low competition - high competition axis is a classic r - K distinction. In this model it runs from Species 1 to Species 4.

The chart shows an instantaneous input of resources representing an early summer fall of phytoplankton and the variegated response of a handful of species which compete with one another for it. The species curves denote population sizes and are measured in 'numbers of individuals'; the curve for K shows the amount of available resource and in this case might be labelled 'calories of energy' or 'biomass of phytoplankton' although it could equally stand for other kinds of resources in different circumstances (such as 'area of barren ground' in a recently fire scorched prairie).

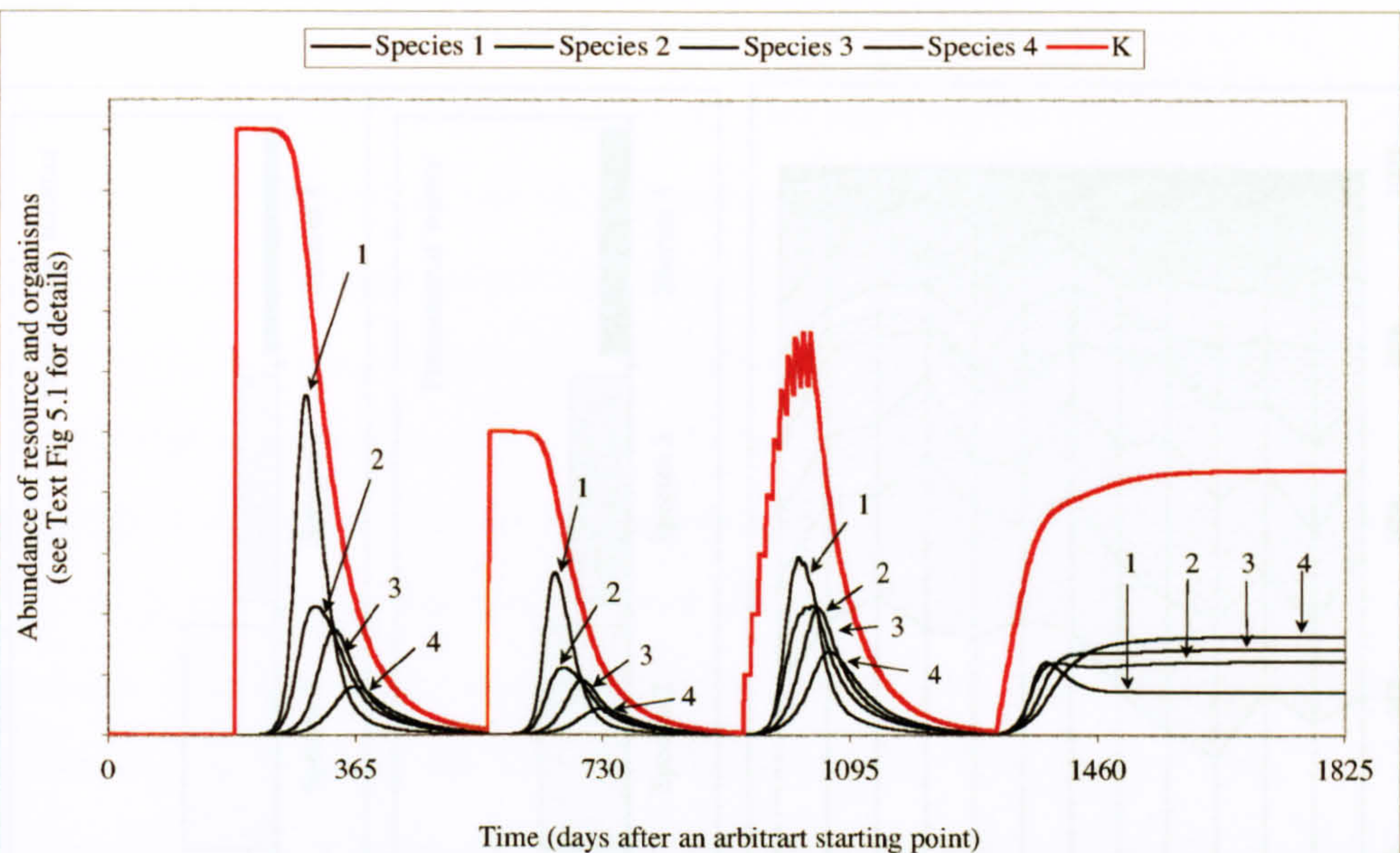
The histogram (**b**) shows ranked proportions of each species accumulated over the entire year (the area under each curve), and thus indicates the relative abundances which would have been available for fossilization.

Text Figure 4.1 *Simulated faunal response to an input of resources*

same few months. The reason why it is likely that productivity was enhanced but not drawn out is that phytoplankton are normally limited more by nutrients than sunlight or temperature. There must be ample sunlight in July and August even though productivity has normally waned by that stage, so even if water temperature was well up during 'precessional summers' (i.e. times in an precessional cycle when the N. hemisphere received more solar energy), the season almost certainly could not be extended or enhanced beyond the bounds placed by nutrient availability. Consequently, it seems more likely that *precessional* summers enhanced production of phytoplankton during *yearly* summers, mainly by ensuring that the sea surface layers were well stocked with nutrients. A precessional effect on nutrients is quite plausible if the greater influx of solar energy to the northern hemisphere resulted in higher waves, more storm action, and generally better mixing in the water column (this argument is pursued more thoroughly below in Section 4.3.1, but see Ito *et al.*, 2001, for other geological evidence of an increase in storm action associated with higher atmospheric energy levels). Thereafter, higher temperatures would probably have fostered faster metabolic rates, faster productivity, and used all the extra nutrients in roughly the same amount of time.

Whichever way the enhanced productivity was caused, there can be little doubt that it happened, because that is what all the evidence points towards as an explanation for the cyclicity of the Lower Chalk (see Section 2.1.3). But the effect that such precessional summers would have had on the biota does depend on how long the yearly summer crop lasted. Extra energy and material poured into the bottom of the benthic food chain would probably have boosted standing crops all round, but which elements of the fauna were favoured most, the opportunist spring bloomers or the die-hard winter specialists, would have depended on *how* the additional resources were distributed over time. A season of equal length but greater instantaneous input would benefit the opportunists, whereas one in which the extra resources were introduced at the same rate but over a longer period, would presumably favour equilibrium strategists (Text Fig. 4.2).

An explanation of chalk-marl cyclicity as enhanced productivity squeezed into the normal 1-2 month window of a summer bloom, fits well with data from the single couplet. Section 2.2.5 explained how time-averaged patterns of opportunist and equilibrium strategy should appear in the fossil record, and Text Figure 4.2 demonstrates how variation in the magnitude and rate of resource input translates into them. This behaviour is exactly what the absolute abundance data from the single couplet shows (Text Fig. 4.3).



Growth curves were plotted using the same method employed in Text Fig 5.1; see the accompanying text of that figure for details.

As before the sequence tracks the input of new material to a community of four competing species over the course of a year. This time the process has been repeated for four consecutive years but the resource magnitude and rate of introduction are variable to demonstrate the effect this has on species relative abundances. The four species and their properties (rates of increase, competition coefficients) are the same throughout and the same as those used in Text Fig 5.1.

In the first year the resource input is instantaneous and the same magnitude as it was in Text Fig. 5.1 (it does not matter what the 'magnitude' actually is, it is just a number representing a resource).

In the second year the resource input is again instantaneous but this time its magnitude is half what it was the previous year. Note that Species 1 which employs the most opportunistic strategy performs far less well on this occasion because its fast rate of increase is its main competitive advantage: it increases exponentially (at its natural rate) while resources are still largely unused, but suffers a decline when it has to compete with the others.

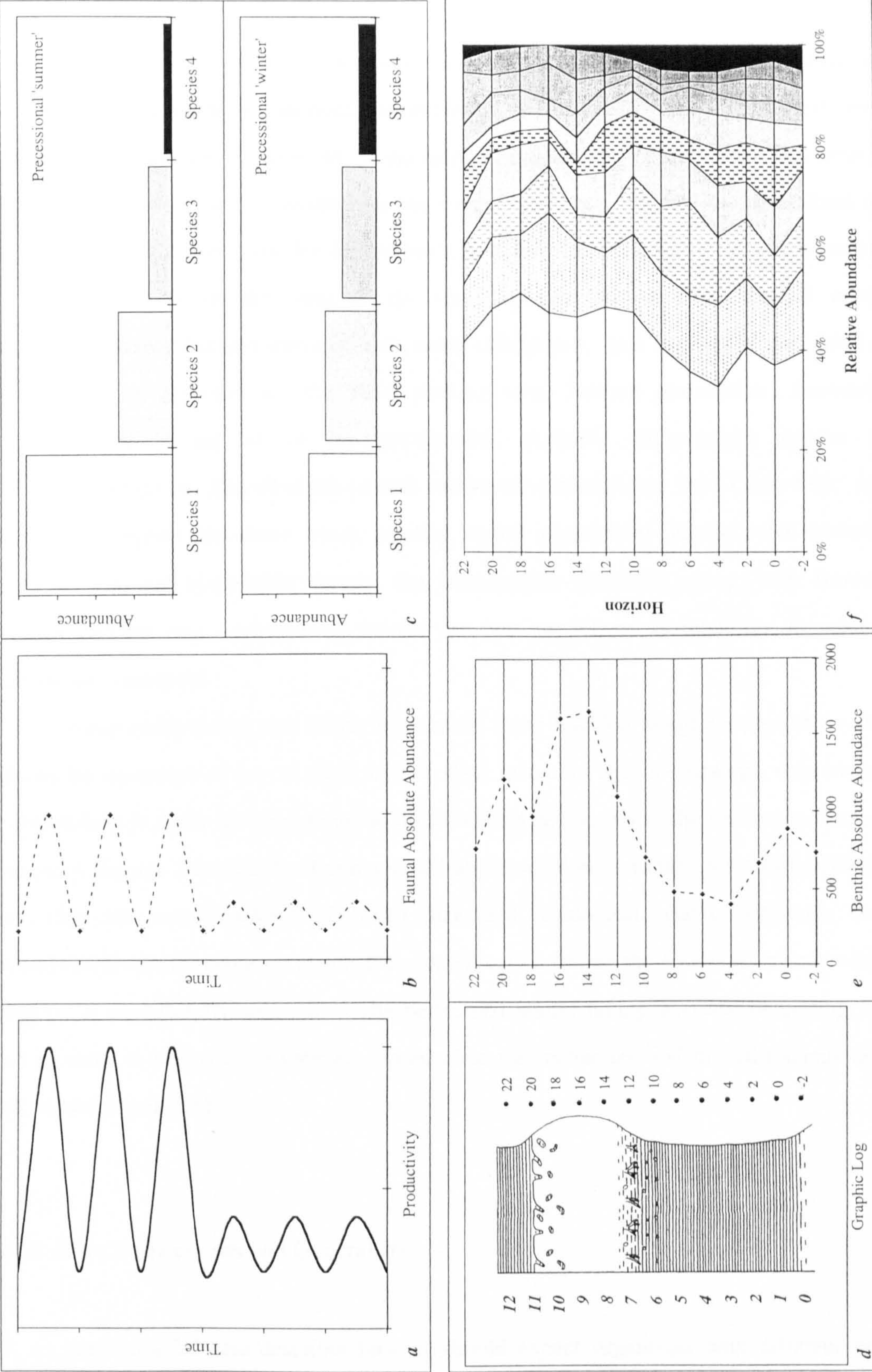
In the third year the magnitude of resource available is the same as it was in the first year, but this time it was introduced in staggered weekly doses over the course of two and a half months (each week another tenth is instantaneously added). As with the reduced volume, staggered introduction favours the *K* - strategists more than the opportunists, although the intantaneous batches are of some advantage to those higher intrinsic rates.

In the final year the resource introduction reaches its logical extreme and is added effectively 'continuously', which means that a hundredth dose of the standard allocation is added every day. In this situation the *r* - strategist's advantage (high *r*) is severely reduced and the competition coefficients becomes very important. Unsurprisingly the most *K* - selected species come to dominate, and are still winnowing away at the opportunist when the sequence ends; presumably the most competitive species (4) will eventually win or else the system reaches a multispecies equilibrium.

Below are relative abundance values for each of the species in each of the four scenarios, plus an additional range of values corresponding to different magnitudes of instantaneous resource input and its effect on the community. Note that the distribution is most top heavy (has the lowest equitability and global diversity) when resource input is large and instantaneous, corresponding to situations in which opportunism is at its premium and also, at least on an ecological timescale, to when the environment is most variable.

<u>Speed</u>	<u>Volume</u>	<u>Species 1</u>	<u>Species 2</u>	<u>Species 3</u>	<u>Species 4</u>
Staggered	Standard	26.9	27.2	25.3	20.5
Continuous	Standard	17.4	25.3	27.9	29.4
Instant	x 0.125	34.5	27.5	22.2	15.8
Instant	x 0.25	36.9	27.2	21.4	14.4
Instant	x 0.5	39.5	26.9	20.6	13.0
Instant	Standard	41.9	26.5	19.9	11.8
Instant	x 2	44.2	26.0	19.1	10.7
Instant	x 4	46.4	25.5	18.4	9.7
Instant	x 8	48.6	25.0	17.6	8.8

Text Figure 4.2 *Simulated response to varying inputs*



Text Figure 4.3 *Theoretical yearly floral and faunal response to Milankovitch cyclicity (upper row), and their time averaged empirical counterparts (lower row).*
a. Expected magnitude of yearly phytoplankton blooms during precessional summers (upper) and winters (lower); *b.* Faunal response; *c.* Faunal community structure.
d. Sedimentary signature - field log; *e.* Faunal signature - deposition rate corrected absolute abundance e.g. Text Fig. 3.1; *f.* Community structure - ten most common foraminifera e.g. Text Fig. 3.5.

Overall absolute abundance counts were well up in the chalk of C13, in line with an increase in phytoplankton volume, and the community was more top-heavy than that from the marl, i.e. the relative abundance of rare species was suppressed, and the most common forms were the ones showing the most enhanced and persistent peaks: exactly as the ecological model in Text Fig 4.2 predicts. Conversely, in the marl, where summer blooms were less dramatic and the fauna was closer to equilibrium for longer, all those competitive, specialized and rare species seem to have won for themselves a relatively greater share of the yearly budget.

It is mainly on the basis of the single couplet data and the ranked relative abundance charts, but nevertheless with some confidence, that I propose the label of opportunistic *r*- strategist for the chalk peaking taxa, *Tritaxia pyramidata*, *Lenticulina rotulata*, most if not all of the gavelinellids, probably *Marssonella trochus* and *Gyroidinoides parva*, plus all of the smooth carapaced ostracods (see Text Table 4.6). And, conversely, suggest that those which reached higher proportions in the marl, including many of the rare nodosarian species, the ornamented ostracods, along with *Dorothia gradata* and the rare agglutinating forams, are best considered as relatively *K*- selected, equilibrium strategists.

As an independent test of this hypothesis, Peter Sheldon suggested that the various species be measured to see if their relative sizes match *r*- and *K*- strategy expectations; unfortunately, it never occurred to me to do so while I had access to the microscope (but see Appendix Figures 2.2.1-2.2.3). From a visual appraisal alone I cannot tell whether there is any clear-cut correspondence between size and ecological status, although some foraminiferal species certainly match their classification (while the ostracods mainly violate theirs!). A thoughtfully and statistically performed study, taking account of coiling style and so forth to estimate bio-volume, should clear the matter up, and this still stands as an option worth pursuing.

4.1.2 Axis 2: Specialists and Generalists

Section 2.2.5 also describes how we should expect organisms with different patch sizes and densities of standing crop to appear in time-averaged palaeontological data sets. The suggestion was that species with small patches leave a gappy record whereas those with large ones are more continuous. *Textularia* sp C, for example, exhibits peaks at B41 [200],

C10 [400], and at the chalk-marl boundaries in C13 (Appdx. Figs. 3.[1, 2, 3 & 4].iv.e); it frequently changes its relative abundance from less than five to nearly fifteen percent of the fauna between adjacent sampling points, some of them spaced at only 2 kyrs. This kind of behaviour seems somewhat more erratic than that shown by, say, *Gavelinella cenomanica*, which varies across a similar range but tends to do so over a number of sequential steps (Appdx. Fig. 3.4.iv.m). Are these taxa really so very different, and, if so, how different? Situations like these are what the irregularity index (Section 4.2.4) was recruited to measure: it provides a more objective assessment of how irregularly a variable is behaving across a time series (Text Fig. 4.4, below).

Rare taxa are normally specialists, their specialism being the cause of their rarity; but this is not always the case. One of the benefits of being specialized, and therefore highly competitive, must be the ability to out-perform other species within your niche, and so it is perfectly plausible that we can find specialists at quite high densities. I suggest that the mark of a specialist foraminiferan is small patch size (specific local conditions exploited to the exclusion of other species; failure outside the narrow niche) rather than rarity *per se*, and that the mark of a small patch is temporal irregularity in signal strength, in accordance with the suggestions of McKinney and Allmon (1995).

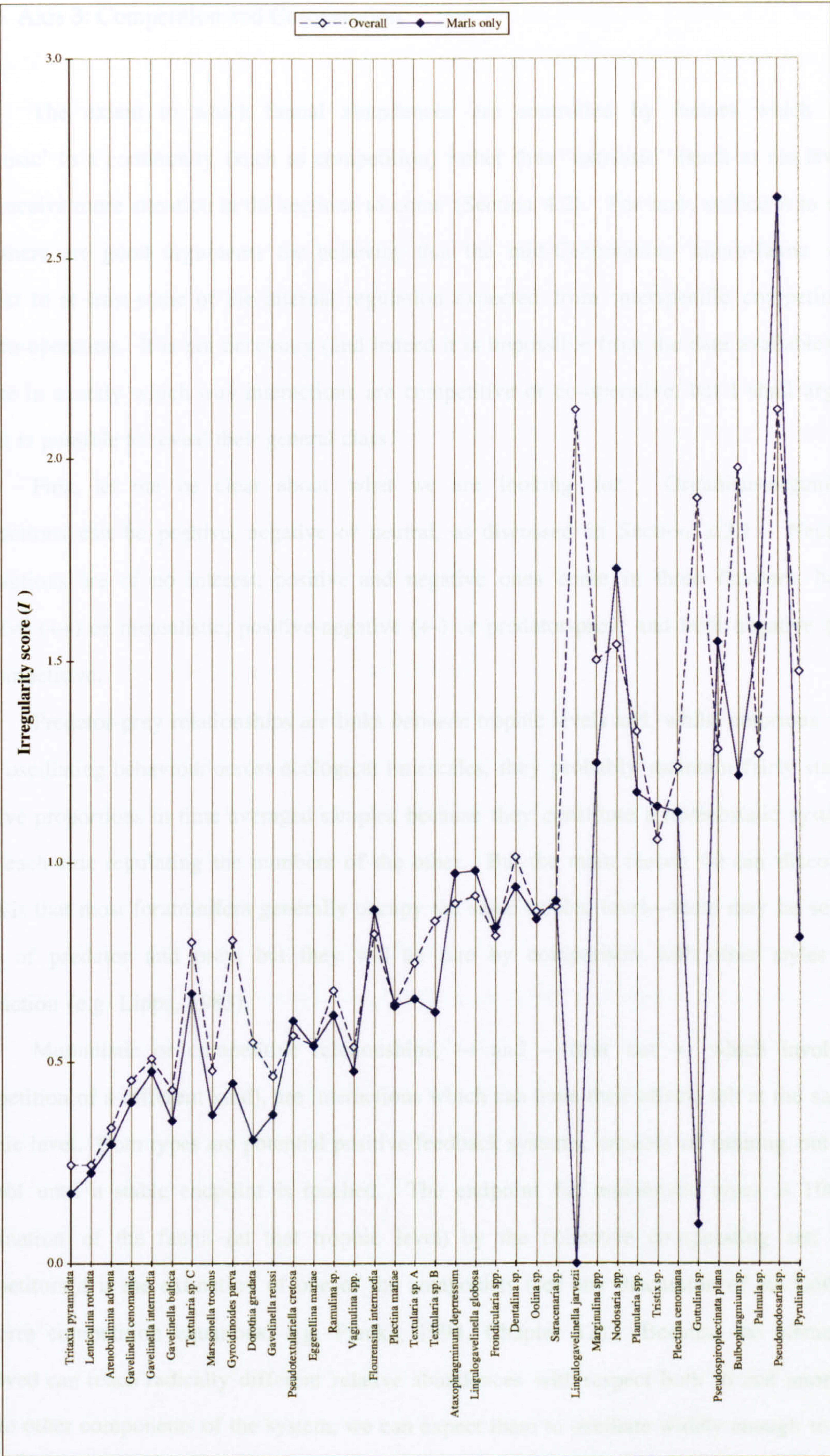
Irregularity in faunal signals is best measured in relative abundance where there is no interference from sedimentary and preservational processes. Relative abundance, of course, is subject to internal interference of its own, but since we are comparing the *entire set* of foraminiferal taxa with one another, rather than looking at a single case, the effects of passive disturbance in proportionality should cancel out. Rare species certainly tend to absorb more passive variability than they give back in return (Section 4.3.4, below), but that is a general tendency, and it is idiosyncratic behaviour we are interested in here.

Rare taxa are also subject to greater disruption from statistical noise, and we must be wary about their variability scores for that reason, too. The taxa in Text Figure 4.4 are arranged in order of overall relative abundance (*Tritaxia* being the commonest), and probably only the leftmost dozen or so are really dependable; certainly values for groups any rarer than *Flourensina* should be treated with considerable caution, and irregularity scores for the ostracods are not presented at all for the same reason (along with the fact that many of them are available only to generic resolution). There is also a boundary to be aware of. Some of the taxa are sufficiently rare that they register a zero percentage in many horizons, and therefore their distribution is skewed. Indices are normalised against the

mean (see Section 2.2.4 for method), and since most species are unlikely to be truly absent from any sampling period, the index values generated will be higher than they really should be (see Section 4.2.4 for further discussion). Occasional zero percentages are present from anywhere to the right of *Pseudotextulariella*, but only amount to more than 10% of the sample in the rightmost fifty percent of the list.

Text Figure 4.4 shows irregularity values for all the foraminiferal species in samples representing general background marl conditions. Data from B41 [200 - Appdx. Figs 3.3.iv.a-y) and three mid-chalk samples (8, 9 and 10) from C13 have been excluded from one of the data sets on the grounds that they are atypical. Events at those horizons represent breaks with normality from the perspective of other marl samples (Section 3.3.4), and since it is a species' intrinsic tendency towards irregularity (i.e. its 'normal' patch size) that we are looking for, the data should be as comparable as possible. This is not a cover up: the other trace on the chart represents the irregularity scores from the entire data set, including specimens from B41 and the chalk, by way of a comparison. The contribution made by B41 is particularly obvious in the signal for the likes of *Gyroidinoides parva*. Normally this species has a rather modest irregularity score, but it seems to behave as erratically as *Textularia* sp. C with the B41 data included. A glance back at the original relative abundance signals (e.g. Appdx. Figs. 3.4.iv.e and 3.4.iv.k) is a convincing demonstration that B41 [200] data entirely skews the normal signal, and that values from the background marls alone are fairer and much more in keeping with an intuitive appraisal.

The values in Text Figure 4.4 rise in magnitude from the most common species to the least, a tendency which is without doubt due mostly to increasing contamination by statistical noise (especially zero counts and passive imprinting), but which is also a trend we should expect, since rarer species are likely to be more specialized. Imposed upon this general trend are impressive idiosyncratic peaks and troughs: *Textularia* sp. C does indeed have a very high irregularity score considering its relative abundance, as do *Gavelinella intermedia*, *Flourensina intermedia*, and perhaps *Pseudotextulariella cretosa* and *Eggerellina mariae*, too. By contrast *Tritaxia pyramidata*, *Lenticulina rotulata*, *Gavelinella baltica*, *Marssonella trochus* and *Dorothia gradata* have low scores. There is no attempt in this section to differentiate between sites or scales (see the discussion in Section 4.2.4, below), so these variability ratings concern 'general' or overall patchiness.



Text Figure 4.4 Irregularity index values for foraminifera across a range of sampling points. See text Section 4.1.2 for discussion.

4.1.3 Axis 3: Competition and Co-operation

The extent to which faunal abundances are controlled by factors which are 'intrinsic' to a community (such as competition) rather than 'extrinsic' (such as sea level) will receive more attention in the sections to come (Section 4.2). For now, suffice it to say that there are good arguments for believing that the mid-Cenomanian micro-fauna was subject to at least some of the internal regulation expected from interspecific competition and co-operation. It is not necessary (and indeed it is impossible from the data available) to isolate in exactly which way interactions are competitive or co-operative, but I shall argue that it is possible to reveal their general class.

First, let me be clear about what we are looking for. Organism-organism interactions can be positive, negative or neutral, as discussed in Section 2.2.1. Neutral interactions are of no interest; positive and negative ones come in three flavours: both positive (++) or mutualistic, positive-negative (+-) or predator-prey, and both negative (--) or competitive.

Predator-prey relationships are links *between* trophic levels and, whilst notorious for their oscillating behaviour across ecological timescales, they probably maintain fairly stable relative proportions in time averaged samples because they constitute a homeostatic system, with each side regulating the numbers of the other. But the main reason we can discount them is that most foraminifera generally occupy the same trophic level—there may be some cases of predator and prey, but they will be rare by comparison with other styles of interaction (e.g. Lipps, 1983).

Mutualistic or competitive relationships, ++ and -- (but not +- which involves competition of a different kind), are interactions which can have their effects felt at the same trophic level. Both types are potential positive feedback systems, capable of running out of control until a stable endpoint is reached. The endpoint for mutualistic types is 100% domination of the fauna (at that trophic level) by the collective co-operating set; for competitors it is the extinction of one of the antagonists (see any discussion of the Lotka-Volterra competition equations, e.g. Pianka, 1994, Chapter 12). Because the elements involved can reach radically different relative abundances with respect both to one another and to other components of the system, we can expect them to oscillate widely enough to be visible even between extensively time averaged sampling points. These are the features which I believe can be identified in the Lower Chalk micro-community.

So where and how will these patterns of behaviour be revealed? I think they can be glimpsed in positive and negative correlations between the abundances of various species. In the short term, ecology is a zero sum game (in the long run evolution is non-zero sum, opening up the possibility of exploiting new resources or exploiting the old ones more economically), which is why relative abundance is often a very reasonable guide as to how the various components of a community are faring with respect to one another. Clearly, we cannot look for positive and negative correlations in the patterns of *relative* abundance because these are linked necessarily: when one species obtains a greater proportion in the community, at least one other must suffer a corresponding fall. Negative and positive correlations will drop out of this situation as definitional artefacts and we will learn nothing from them. Conversely, if the fauna is linked to a common pool of resources (anything from phytoplankton input to space), then an expansion in some limiting factor, or even simply a rise in the likelihood of preservation, could easily produce all-round increases in *absolute* abundance, and thus give us meaningless positive correlations, at least from the perspective of discriminating mutualistic interactions.

But there is no necessary connection between the *relative* abundance of one species and the *absolute* abundance of another. For example, resource expansion could swell the absolute abundances of a pair of species without any change in their proportions. For unspecified causes of change in absolute abundance (e.g. preservational factors, widely used resources such as phytoplankton, and even random mixes of narrowly utilised 'resources' such as specific habitat regimes), we expect there to be *no* correlation between the absolute abundance of one species and the relative abundance of another. Consequently, if there *is* a good correlation we need to know why. I suggest that by far the most likely explanation for a good negative correlation is competition, and that a very likely explanation for good positive correlations is mutualism, since in these cases there are reasons why an increase in the relative abundance of one species *should* result in a higher or lower absolute abundance for another.

These are the most likely explanations, but not the only ones. Positive correlations could easily arise between a pair of species simply because the two of them were tracking the same physical variable, a point which will be discussed below (Section 4.2.2). Conversely, there is no guaranteed connection between an increase in the proportion of some competitor and a decrease in a species' absolute abundance, because the absolute abundance of both could increase in spite of the fact that the loser was suffering a

proportionally heavier toll. Nevertheless, correlations between these factors are highly intriguing and are more than likely to represent interspecific interactions.

Appendix Tables 1.2.3, 1.2.4, and Text Table 4.1, each show positive and negative correlations for all microfossil species across a large number of sampling horizons. Appdx. Table 1.2.3 is for correlations with all sampling points included ($n = 53$), Appdx. Table 1.2.4 is similar but does not include the three samples from the marl of horizon B41 ([200]: the *arlesiensis* bed; see Sections 3.3.3.ii, 2.1.6 & 2.2.6), and Text Table 4.1 does not include the three B41 samples *or* three samples (8, 9 & 10) from the chalk of C13. As with the irregularity charts in the last Section (4.1.2.), data from B41 was removed because the events at that level were certainly connected with some kind of a physical disturbance and are thus likely to yield positive correlations because elements of the fauna were tracking similar, unusual physical conditions; chalk data were removed for similar reasons (just in case). Thus, Text Table 4.1 comes from the most restricted data set and reveals the extent of interspecific correlations during ‘normal’ background, marl-forming conditions. It is this chart that I shall focus most attention upon, the other two being lodged in the Appendix so that they are available for comparison. Furthermore, to ensure that we are analysing ‘good’ correlations, the discussion will be limited to those cases which can be identified at a 99% confidence level, although the results are very similar at 95% and many correlations even make it to 99.9% (in other words the results are robust and there is a fairly sharp boundary between cases which do and do not correlate).

These correlation charts make most sense when read from the top row down each column, that is, by comparing the relative abundance of a particular taxon with the absolute abundances of another one. This is effectively asking what happens to the absolute abundance of species *B* when the relative abundance of species *A* changes, a question which makes more ecological sense than the alternative, since relative abundance suggests performance in a proportionality competition, whereas absolute abundance may be measuring something else entirely.

The chart as a whole forms the space of all possible interactions (at this taxonomic resolution—many entries are only to generic level). In all three charts the entire field is subdivided into four sub-fields, three of them foraminiferal groups, the other comprising the ostracods. The foraminiferal groupings represent three major ‘Superfamilies’: the Lituolacea (headed by *Tritaxia*), the Cassidulinacea (headed by *Gyroidinoides*), and the Nodosariacea (headed by *Lenticulina*)—these are the groups more commonly referred to in

B41 and C13 chalk excluded		A B U N D A N C E																																																																																																																																																																																																																																																																																																																																																																																																																																																																																																																																																																																																																																																																																																																																																																																																																																																																																																																																																																																																																																																																																																																																																																																																																																																																																																																																																																																																																																																																																																																																																																																																																																																																																																																																																																																					
n = 47																																																																																																																																																																																																																																																																																																																																																																																																																																																																																																																																																																																																																																																																																																																																																																																																																																																																																																																																																																																																																																																																																																																																																																																																																																																																																																																																																																																																																																																																																																																																																																																																																																																																																																																																																																																							
99% confidence																																																																																																																																																																																																																																																																																																																																																																																																																																																																																																																																																																																																																																																																																																																																																																																																																																																																																																																																																																																																																																																																																																																																																																																																																																																																																																																																																																																																																																																																																																																																																																																																																																																																																																																																																																																							
		1	2	3	4	5	6	7	8	9	10	11	12	13	14	15	16	17	18	19	20	21	22	23	24	25	26	27	28	29	30	31	32	33	34	35	36	37	38	39	40	41	42	43	44	45	46	47	48	49	50	51	52																																																																																																																																																																																																																																																																																																																																																																																																																																																																																																																																																																																																																																																																																																																																																																																																																																																																																																																																																																																																																																																																																																																																																																																																																																																																																																																																																																																																																																																																																																																																																																																																																																																																																																																																		
	<i>Tritaxia pyramidalis</i>	1	0																																																																																																																																																																																																																																																																																																																																																																																																																																																																																																																																																																																																																																																																																																																																																																																																																																																																																																																																																																																																																																																																																																																																																																																																																																																																																																																																																																																																																																																																																																																																																																																																																																																																																																																																																																																				
	<i>Pseudotextulariella cretosa</i>	2		0																																																																																																																																																																																																																																																																																																																																																																																																																																																																																																																																																																																																																																																																																																																																																																																																																																																																																																																																																																																																																																																																																																																																																																																																																																																																																																																																																																																																																																																																																																																																																																																																																																																																																																																																																																																			
	<i>Marssonella trochus</i>	3					+																																																																																																																																																																																																																																																																																																																																																																																																																																																																																																																																																																																																																																																																																																																																																																																																																																																																																																																																																																																																																																																																																																																																																																																																																																																																																																																																																																																																																																																																																																																																																																																																																																																																																																																																																																																
	<i>Dorothia gradata</i>	4	-		0								+																																																																																																																																																																																																																																																																																																																																																																																																																																																																																																																																																																																																																																																																																																																																																																																																																																																																																																																																																																																																																																																																																																																																																																																																																																																																																																																																																																																																																																																																																																																																																																																																																																																																																																																																																																										
A	<i>Textularia</i> sp. A	5	-				0					-																																																																																																																																																																																																																																																																																																																																																																																																																																																																																																																																																																																																																																																																																																																																																																																																																																																																																																																																																																																																																																																																																																																																																																																																																																																																																																																																																																																																																																																																																																																																																																																																																																																																																																																																																																											
B	<i>Textularia</i> sp. B	6		+			0	+																																																																																																																																																																																																																																																																																																																																																																																																																																																																																																																																																																																																																																																																																																																																																																																																																																																																																																																																																																																																																																																																																																																																																																																																																																																																																																																																																																																																																																																																																																																																																																																																																																																																																																																																																																															
S	<i>Textularia</i> sp. C	7	-	+	+	+	+	0																																																																																																																																																																																																																																																																																																																																																																																																																																																																																																																																																																																																																																																																																																																																																																																																																																																																																																																																																																																																																																																																																																																																																																																																																																																																																																																																																																																																																																																																																																																																																																																																																																																																																																																																																																															
O	<i>Eggerellina mariae</i>	8	-						0																																																																																																																																																																																																																																																																																																																																																																																																																																																																																																																																																																																																																																																																																																																																																																																																																																																																																																																																																																																																																																																																																																																																																																																																																																																																																																																																																																																																																																																																																																																																																																																																																																																																																																																																																																														

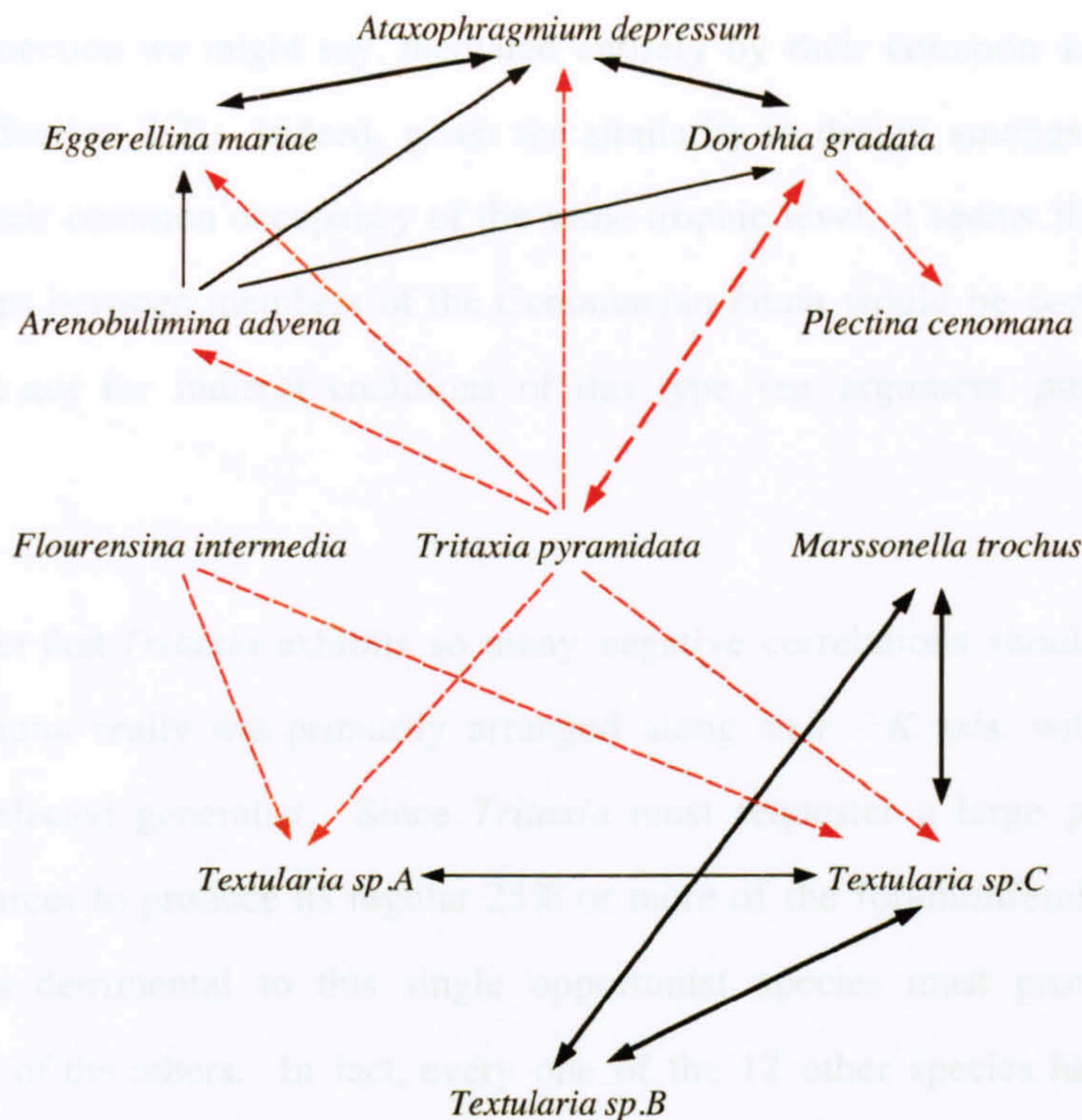
the text and appendix tables as ‘agglutinated’, ‘calcareous’ and ‘nodosarian’; technical names are used here to cement the impression of genealogical proximity. Each subfield also has a set of possible interactions, for example the set of interactions between Lituolacean relative abundances and Cassidulanacean absolute abundances, and we can ask what proportion of such possible interactions turn out to form correlations. Text Table 4.2 summarises the results from Text Table 4.1 and shows us that Lituolacean foraminifera show a higher percentage of correlations with other Lituolaceans, Cassidulinacea with other Cassidulinaceans, and Nodosariacea with other Nodosariaceans. The results are similar for the ostracods which correlate better with other ostracods than with the forams: exactly what we should expect from organisms whose similarity in design specification has them treading on one another’s toes (or pseudopods!).

A.A. \ R.A.	Lituolacea	Cassidulinacea	Nodosariacea	Ostracods
Lituolacea	10.4	4.5	1.3	9.2
Cassidulinacea	7.1	9.5	2.9	6.7
Nodosariacea	3.3	3.8	5.7	3.1
Ostracods	5.4	3.8	3.1	14.3

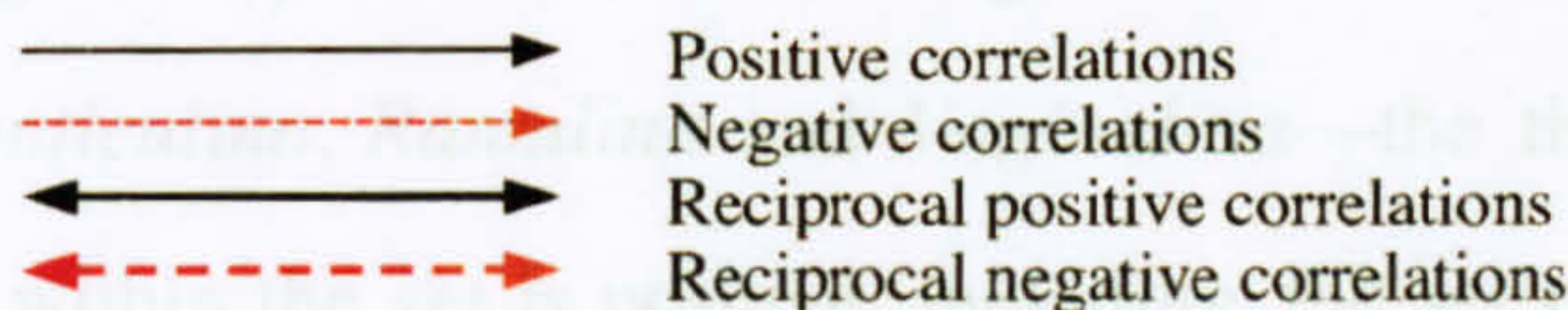
Text Table 4.2 Percentage of positive and negative correlations between absolute (A.A.) and relative (R.A.) abundance found in various subfields of Text Table 4.1.

Let us now consider a small zone in this ensemble of correlations by examining interactions among the agglutinating foraminifera. Text Figure 4.5 (below) shows eleven species and their interactions with each other according to Text Table 4.1. As we can see, *Tritaxia* has negative correlations with six of the others, one of which, *Dorothia*, is reciprocal; in fact *Ataxophragmium* is also reciprocally negative with *Tritaxia* once the three chalk samples are included (Appdx. Table 1.9). Hardly any of the species besides *Tritaxia* have negative correlations with one another, but several of them exhibit positive ones, many of which are again reciprocal.

Focusing in on the triad of *Tritaxia*, *Dorothia* and *Ataxophragmium* (Text Fig. 4.6) we can see that the positive correlation between *Ataxophragmium* and *Dorothia* could arise entirely out of the fact that both are negatively correlated with *Tritaxia*. If both have niches that overlap somewhat with that of *Tritaxia*, whether they overlap one another or not, *Tritaxia*’s success means a failure for each of them. The corollary, however, is that if one of them wins at the expense of *Tritaxia* and keeps *Tritaxia*’s numbers down, both stand to benefit. They form a complementary set and have an indirect mutualistic arrangement



Key - style and orientation of correlations:

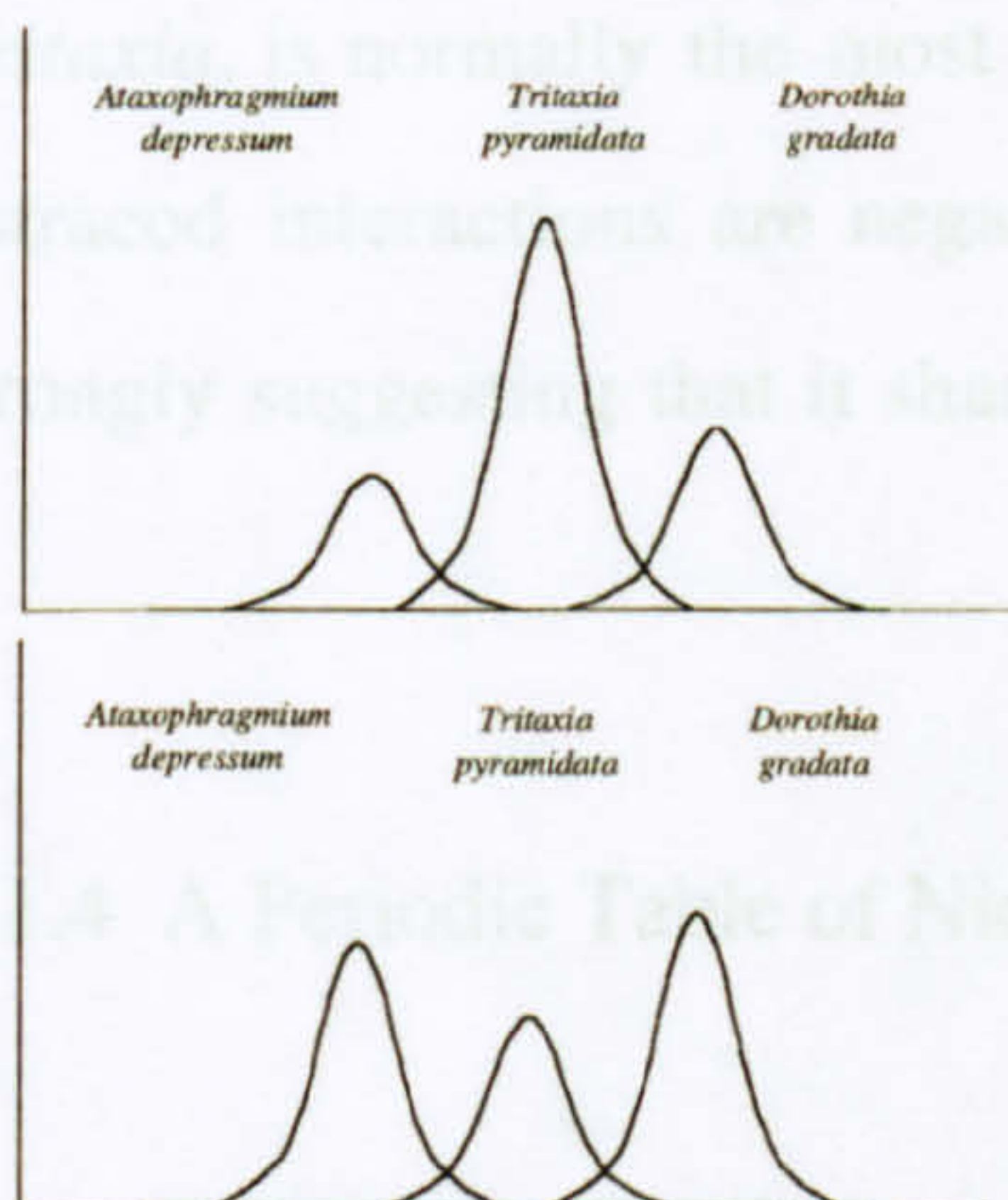


Arrows run from *relative* abundance to *absolute* so that

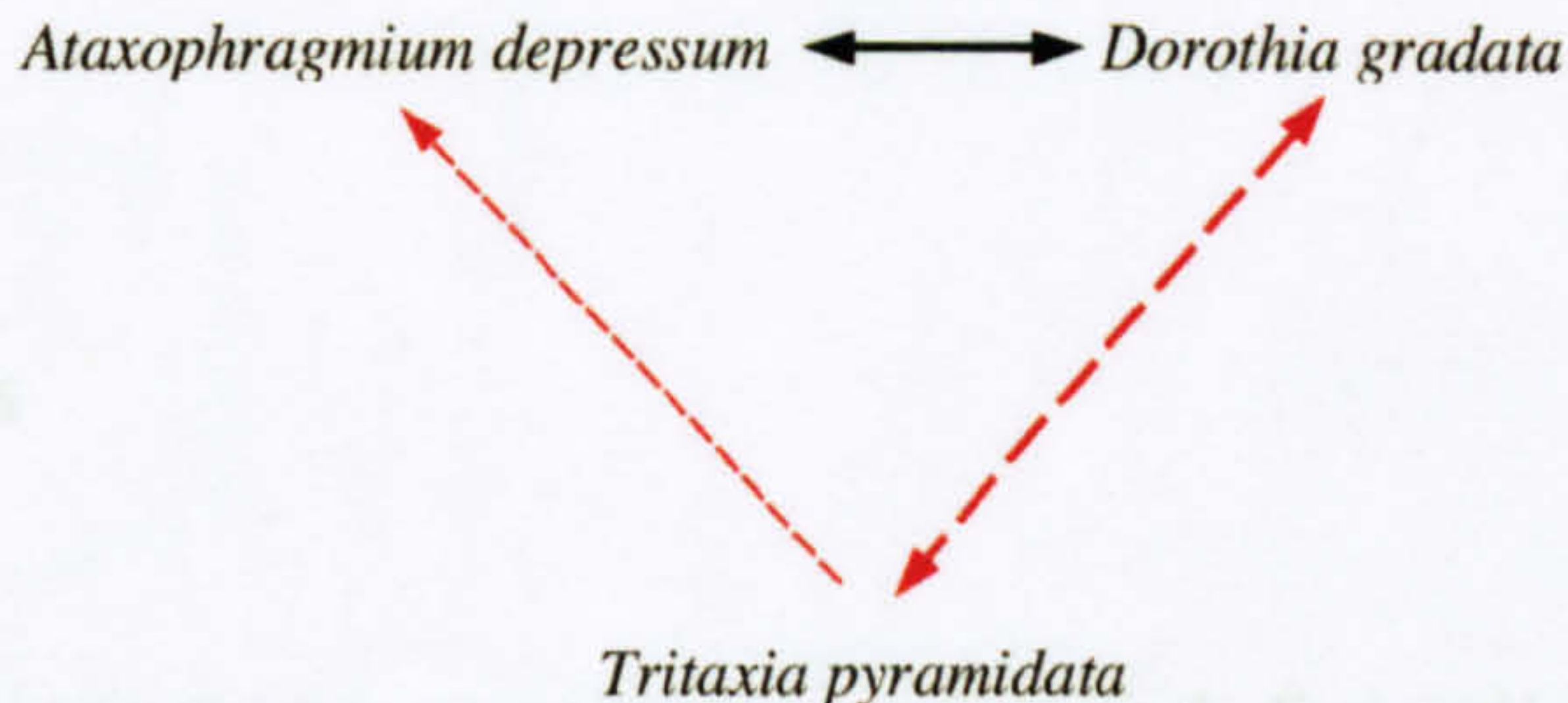


means 'the *relative* abundance of A correlates positively with the *absolute* abundance of B'; or in other words, 'when the relative abundance of A increases, the absolute abundance of B does too'.

Text Figure 4.5 Network of relationships in the Lituolacean corner of the correlation chart (See Text Table 4.1 and main text for discussion.)



Do *Dorothia* and *Ataxophragmium* have an indirect positive relationship with one another in virtue of having a real negative relationship with *Tritaxia*, as the side charts suggest?



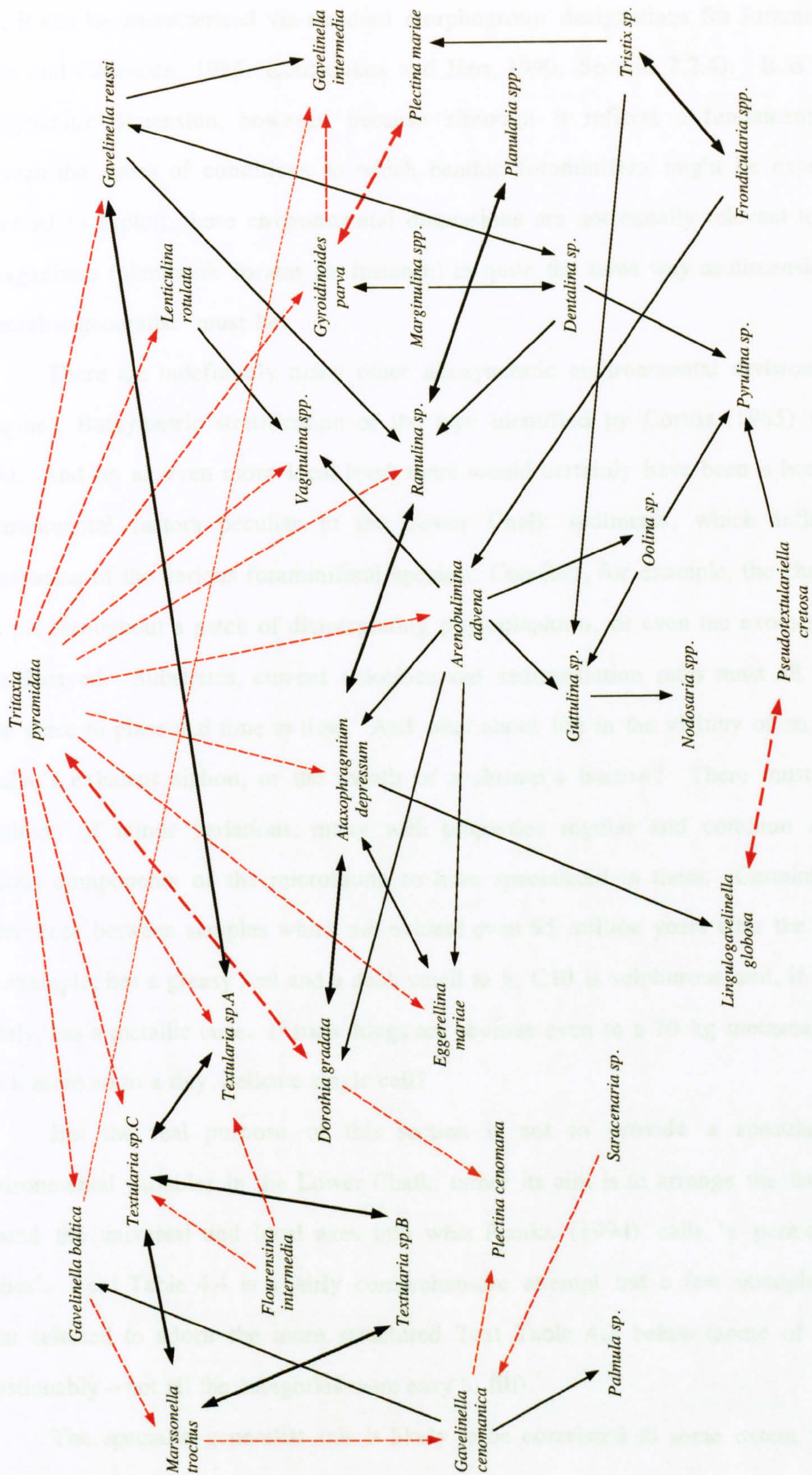
Text Figure 4.6 One small part of the network shown in Text Fig. 4.5

a ‘virtual’ connection we might say, mediated entirely by their common antagonism with a third species (Section 2.2). Indeed, given the similarity in design amongst foraminifera in general, and their common occupancy of the same trophic level, it seems likely that most of the relationships between members of the Cenomanian fauna would be competitive to some extent, were it not for indirect coalitions of this type (an argument pursued in Section 4.2.3).

The fact that *Tritaxia* exhibits so many negative correlations should not surprise us if the micro-fauna really was primarily arranged along an $r - K$ axis, with *Tritaxia* as the dominant r -selected generalist. Since *Tritaxia* must sequester a large proportion of the available resources to produce its regular 25% or more of the foraminiferal population, any event which is detrimental to this single opportunist species must provide a wealth of potential to all of the others. In fact, every one of the 12 other species having an absolute abundance which correlates directly with *Tritaxia*’s relative abundance does so negatively. By contrast the generally rarer nodosarian genera have three direct negative correlations with *Tritaxia* (*Lenticulina*, *Ramulina* and *Vaginulina*—the three most common) and every other correlation within the set is positive, including the set of nodosarians correlating with other nodosarians in which they score 12 out of 12. Text Fig. 4.7 is a summary of all inter-foraminiferal correlations clearly showing *Tritaxia* in a kind of keystone role: the whole fauna appears to be largely held together by a shared direct or indirect tension with this one species. Interestingly, and in support of this conclusion, is the fact that the ostracod fauna has a similar structure, albeit to a lower taxonomic resolution. The genus *Cytherella*, like *Tritaxia*, is normally the most abundant in the set, and sure enough all of its 8 ostracod to ostracod interactions are negative (becoming 11 out of 12 when the forams are included), strongly suggesting that it shares an equivalent role in the ostracod community.

4.1.4 A Periodic Table of Niches

The ‘ $r-K$ ’, ‘specialist-generalist’ and ‘competitor-co-operator’ distinctions are what I have termed *universal* niche axes (Section 2.2.2)—dimensions along which the fauna or flora from *any* ecosystem can be differentiated. They are powerful ways of talking about ecology precisely because they depend upon global, statistical features and avoid any



Text Figure 4.7 Network of relationships for the entire foraminiferal fauna (see Text Fig. 4.5 for a key and the text for discussion).

mention of particulars. However, there are other, more idiosyncratic dimensions for discriminating niches in the mid-Cenomanian micro-fauna. The infaunal-epifaunal axis is one; it can be characterised via standard morphogroup designations for foraminifera (e.g. Jones and Charnock, 1985; Koutsoukos and Hart, 1990; Section 2.2.4). It is a relatively idiosyncratic dimension, however, because although it reflects a fundamental division between the suites of conditions to which benthic foraminifera might be exposed, or be expected to exploit, those environmental dimensions are not equally relevant to all groups of organisms (planktonic forams for instance) in quite the same way as dimensions such as 'specialist-generalist' must be.

There are indefinitely many other idiosyncratic environmental divisions we might imagine. Bathymetric stratification of the type identified by Corliss (1985) is a case in point. And on an even more local level, there would certainly have been a host of micro-environmental factors peculiar to the Lower Chalk sediments, which influenced the distribution of the various foraminiferal species. Consider, for example, the changes in Eh and pH throughout a patch of disintegrating phytoplankton, or even the exothermic output as it decayed. Substrates, current velocities and sedimentation rates must all have varied from place to place and time to time. And what about life in the vicinity of an inoceramid bivalve's exhalant siphon, or the mouth of a shrimp's burrow? There must have been hundreds of minor variations, many with properties regular and common enough for various components of the microfauna to have specialized in them. Certainly there are differences between samples which are evident even 95 million years after the event: B41, for example, has a greasy feel and a dank smell to it; C10 is sulphurous and, if I remember rightly, has a metallic taste. If such things are obvious even to a 70 kg metazoan, then how much more so to a tiny, delicate single cell?

But the real purpose of this section is not to provide a speculative list of environmental variables in the Lower Chalk; rather its aim is to arrange the fauna roughly around the universal and local axes into what Pianka (1994) calls 'a periodic table of niches'. Text Table 4.4 is a fairly comprehensive attempt but a few examples have also been selected to adorn the more structured Text Table 4.3 below (some of them rather questionably—not all the categories were easy to fill).

The specialist-generalist axis is likely to be correlated to some extent with the *r-K* axis (discussed below), but this arrangement is by no means rigid and the categories are at least semi-independent. It is plausible to claim that *Dorothia gradata*, for instance, pursued

Classification	Total no.	% R.A.	r	K	spec	gen	+	-	inf	epi
Foraminifera										
Agglutinated										
<i>Tritaxia pyramidata</i>	11096	30.3	r			g	0	12	i?	
<i>Pseudotextulariella cretosa</i>	1028	2.8		K?	s?		2	1		e?
<i>Marssonella trochus</i>	1239	3.4	r			g?	2	2	i	
<i>Dorothia gradata</i>	1145	3.1		K		g	1	4	i?	
<i>Textularia</i> sp. A	323	0.9		K?		g?	4	0	i?	
<i>Textularia</i> sp. B	247	0.7		K?		g?	2	0	i	
<i>Textularia</i> sp. C	1769	4.8	r		s		3	1	i	
<i>Eggerellina mariae</i>	712	1.9	r?		s?		2	0	i	
<i>Plectina mariae</i>	314	0.9		K?			0	1	i	
<i>Plectina cenomana</i>	24	0.1		K?			0	0	i?	
<i>Flourensina intermedia</i>	322	0.9		K?	s		1	2	i	
<i>Arenobulimina advena</i>	3649	10.0		K?		g?	6	1	i	
Rare agglutinated species	201	0.5		K	s		8	1		
<i>Ataxophragmium depressum</i>	154	0.4		K	s?		4	1	i	
<i>Bulbophragmium</i> sp.	21	0.1		K		g?	3	0	i	
<i>Pseudospiroplectinata plana</i>	22	0.1		K?			1	0		e?
<i>Labrospira latidorsa</i>	4	0.0		K?			0	0		e?
Calcareous										
<i>Gyroidinoides parva</i>	1105	3.0	r				0	2	i?	
<i>Lingulogavelinella globosa</i>	130	0.4		K?	s?		1	1		e
<i>Lingulogavelinella jarvezae</i>	80	0.2					4	0		e
<i>Gavelinella cenomanica</i>	3188	8.7	r?		s?		3	1		e
<i>Gavelinella baltica</i>	1606	4.4	r?			g?	2	2		e
<i>Gavelinella intermedia</i>	2091	5.7	-r?		s		0	0		e
<i>Gavelinella reussi</i>	995	2.7	r?			g?	5	0		e
<i>Lenticulina rotulata</i>	3754	10.3	r			g	2	0		e
Rare nodosarian species	1479	4.0		K	s		21	2		
<i>Dentalina</i> sp.	123	0.3		K?			4	0	i?	
<i>Fronicularia</i> spp.	135	0.4		K?			2	0		e?
<i>Marginulina</i> spp.	63	0.2		K?			2	0	i	
<i>Nodosaria</i> spp.	48	0.1		K?			1	0	i	
<i>Oolina</i> sp.	103	0.3		K?			3	0	i	
<i>Ramulina</i> sp.	420	1.1	r?		s?		2	0	i	
<i>Saracenaria</i> sp.	92	0.3		K?			0	1		e
<i>Tristix</i> sp.	35	0.1		K?			4	0	i	
<i>Vaginulina</i> spp.	384	1.0	r?			g	0	1		e?
<i>Planularia</i> spp.	37	0.1		K?			1	0		e?
<i>Pseudonodosaria</i> sp.	4	0.0		K?			0	0	i	
<i>Palmula</i> sp.	5	0.0		K?			0	0		e?
<i>Guttulina</i> sp.	28	0.1		K?			1	0	i	
<i>Pyrulina</i> sp.	2	0.0		K?			1	0	i	
Porcellaneous species	88	0.2	r?		s?					e?
Ostracods										
Smooth carapaced										
	4287	79.7	r			g	20	14		
Miscellaneous spp.	49	0.9								
<i>Bairdoppilata</i> spp.	907	16.9		K?			5	1	i?	
<i>Macrocypis</i> spp.	195	3.6	r?				8	0	i?	
<i>Pontocyprilla</i> spp.	766	14.2	r				6	2	i?	
<i>Cytherella</i> spp.	2370	44.1	r				1	11	i?	
Ornamented										
	1091	20.3	K/r	K/r	s		27	5		
<i>Bythoceratina</i> spp.	285	5.3	r?				2	1		e
<i>Monoceratina longspina</i>	29	0.5		K?			1	0		e
<i>Pterygocythereis robusta</i>	121	2.2	r?				3	1		e
<i>Phyloptera reducta</i>	1	0.0		K?			4	0		e
<i>Mandocythere</i> spp.	176	3.3	r?				1	0		e
<i>Oertliella</i> spp.	126	2.3	r?				2	3		e
<i>Neocythere vanveeni</i>	33	0.6		K?			8	0		e
<i>Rehacythereis</i> spp.	134	2.5	r?				2	0		e
<i>Cythereis</i> spp.	92	1.7		K?			3	0		e
<i>Cornicythereis larivourensis</i>	3	0.1		K?			1	0		e
<i>Cytherelloidea</i> spp.	29	0.5		K?			0	0	i?	
<i>Patellacythere parva</i>	3	0.1		K?			0	0		e
<i>Protocythere lineata</i>	57	1.1		K?			0	0		e
<i>Planileberis scrobicularis</i>	2	0.0		K?			0	0		e
Text Table 4.3 Classification of taxa according to broad niche axes										
<i>r/K = r or K selected, spec/gen = specialist or generalist, +/- = no. of positive and negative correlations, respectively; inf/epi = infaunal or epifaunal morphotype</i>										
<i>See text Section 4.1.4 for details.</i>										

a rather generalist equilibrium strategy, whilst *Textularia* sp. C was a relatively *r*- selected specialist. *Tritaxia pyramidata* and the various species of *Nodosaria* amongst the rare nodosarian group, form the corollary—taxa which correlate in the expected fashion. Interestingly, in terms of abundance, *Tritaxia* (*r*- selected generalist) is most common, followed by *Textularia* (*r*- selected specialist), then *Dorothia* (*K*- selected generalist), and finally *Nodosaria* (*K*- selected specialist). Furthermore, my guess is that although *Tritaxia* is bigger than *Textularia* on average, *Dorothia* is almost certainly larger than either, but smaller than *Nodosaria* (see Appendix Figures 2.2 for a partial confirmation).

r- strategist								K- strategist							
generalist				specialist				generalist				specialist			
infaunal		epifauna l		infaunal		epifauna l		infaunal		epifauna l		infaunal		epifauna l	
-	+	-	+	-	+	-	+	-	+	-	+	-	+	-	+
<i>T.</i>	<i>M.</i>	<i>V</i>	<i>L.</i>	<i>G.</i>	<i>T</i>	<i>G.</i>	<i>G.</i>	<i>D.</i>	<i>A.</i>	<i>P</i>	<i>F</i>	<i>N</i>	<i>A.</i>	<i>L.</i>	<i>P.</i>
<i>p</i>	<i>t</i>	<i>a</i>	<i>r</i>	<i>p</i>	<i>e</i>	<i>i</i>	<i>c</i>	<i>g</i>	<i>a</i>	<i>a</i>	<i>o</i>	<i>d</i>	<i>d</i>	<i>g</i>	<i>c</i>
<i>y</i>	<i>r</i>	<i>g</i>	<i>o</i>	<i>a</i>	<i>x</i>	<i>n</i>	<i>e</i>	<i>r</i>	<i>d</i>	<i>n</i>	<i>n</i>	<i>o</i>	<i>e</i>	<i>l</i>	<i>r</i>
<i>r</i>	<i>o</i>	<i>i</i>	<i>u</i>	<i>r</i>	<i>t</i>	<i>t</i>	<i>n</i>	<i>a</i>	<i>v</i>	<i>u</i>	<i>d</i>	<i>s</i>	<i>p</i>	<i>o</i>	<i>e</i>
<i>a</i>	<i>c</i>	<i>u</i>	<i>u</i>	<i>v</i>	<i>l</i>	<i>e</i>	<i>o</i>	<i>d</i>	<i>e</i>	<i>l</i>	<i>i</i>	<i>a</i>	<i>r</i>	<i>b</i>	<i>t</i>
<i>m</i>	<i>h</i>	<i>l</i>	<i>a</i>	<i>a</i>	<i>a</i>	<i>r</i>	<i>m</i>	<i>a</i>	<i>n</i>	<i>a</i>	<i>c</i>	<i>r</i>	<i>e</i>	<i>o</i>	<i>o</i>
<i>i</i>	<i>u</i>	<i>i</i>	<i>a</i>		<i>r</i>	<i>m</i>	<i>a</i>	<i>t</i>	<i>a</i>	<i>r</i>	<i>u</i>	<i>i</i>	<i>s</i>	<i>s</i>	<i>s</i>
<i>d</i>	<i>s</i>	<i>n</i>	<i>a</i>		<i>i</i>	<i>e</i>	<i>a</i>			<i>i</i>	<i>a</i>	<i>a</i>	<i>s</i>	<i>a</i>	<i>a</i>
<i>a</i>		<i>a</i>			<i>a</i>	<i>d</i>				<i>a</i>	<i>a</i>	<i>sp.</i>	<i>u</i>		
<i>t</i>		<i>sp.</i>			<i>sp.</i>	<i>i</i>				<i>sp.</i>	<i>r</i>		<i>m</i>		
<i>a</i>					<i>C.</i>	<i>a</i>					<i>a</i>				

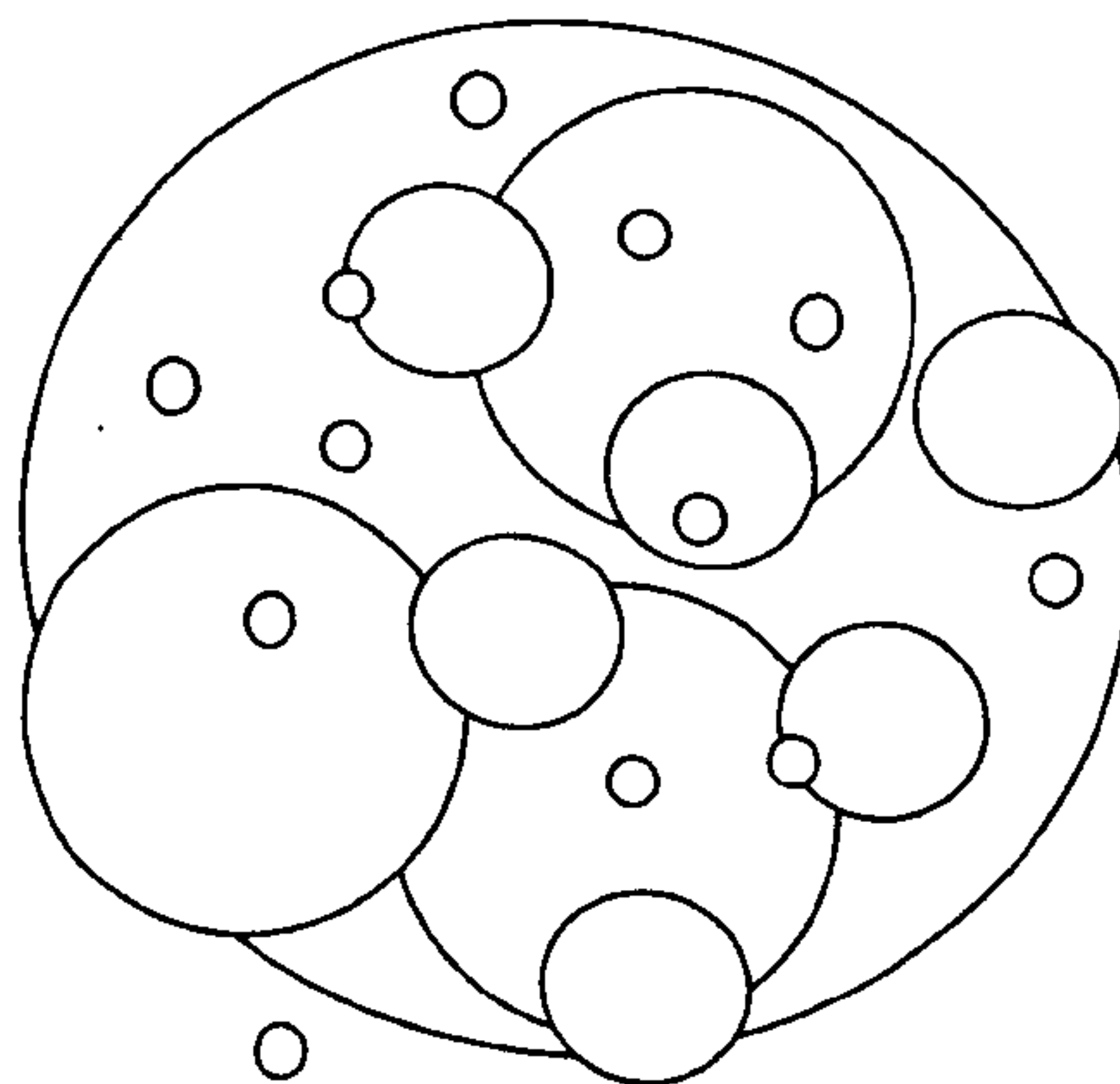
Text Table 4.4 Examples drawn from sets at the intersection of the four main niche axes for the foraminiferal fauna.

Once again, the aim is not to find a specific pigeonhole for each taxon but simply to spread the fauna out across a structured ecological space. Nevertheless, it should be apparent by now that some species can be very confidently assigned to their appropriate corners. Notable amongst them is *Tritaxia pyramidata*, an *r*- selected, probably semi-infaunal generalist, which maintains a host of competitive relationships with its neighbours. This species forms the evolutionary focus of the thesis and will be our test case for the *Plus ça change* model.

4.1.5 Universal Niche Structure

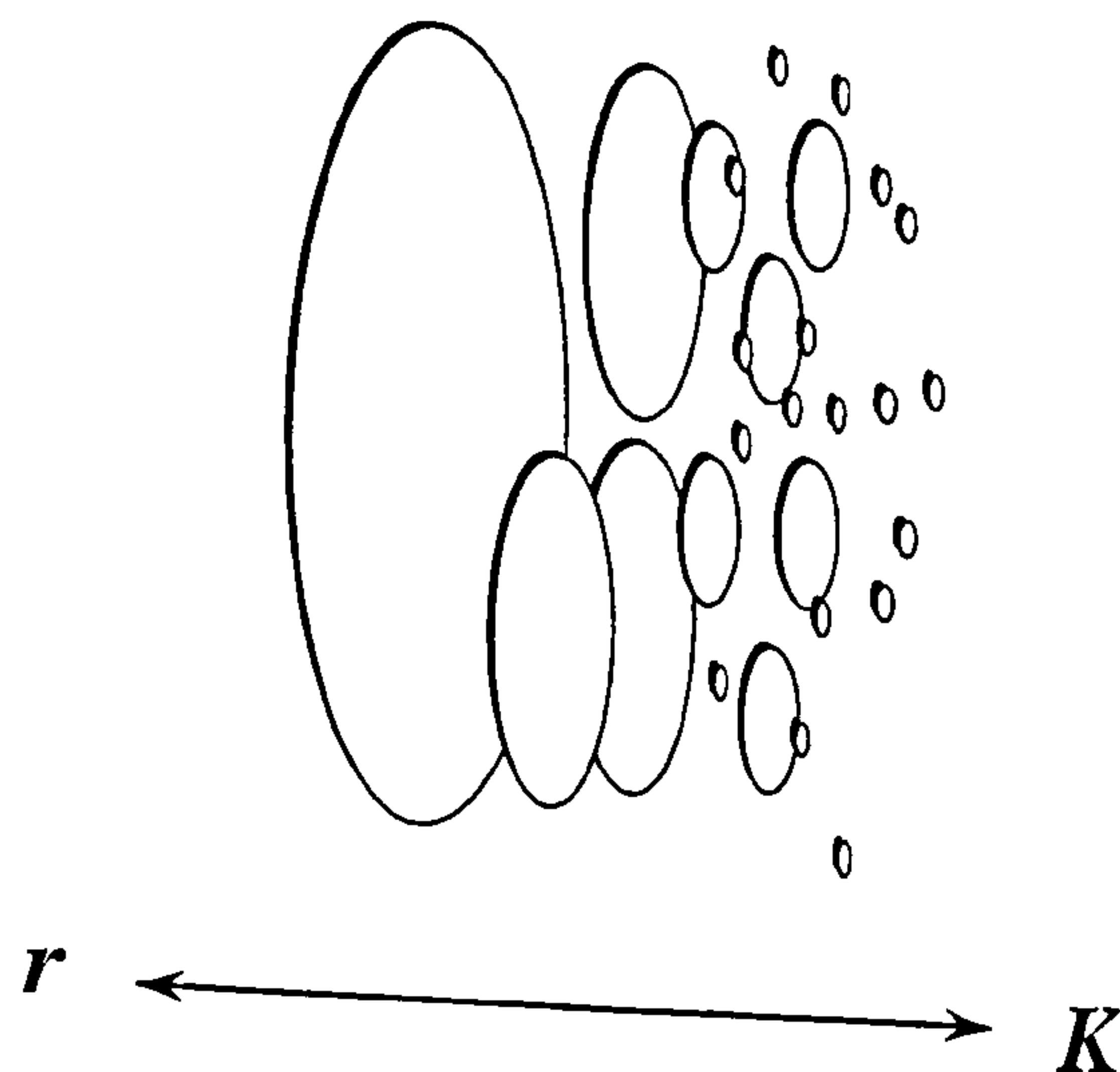
But periodic tables aside, the universal axes *are* linked with one another to some extent. Over and above the pigeonholing of individual species there is undoubtedly a kind of global structure to the community. This framework can be understood in rather abstracted terms and is expected to apply to any ecosystem; so a thorough exploration is a worthy investment.

As mentioned in Section 2.2.2, the log normal species distribution is ubiquitous, and the Lower Chalk micro-community proves no exception. The standard explanation for this configuration is the broken stick model, in which a universal resource axis is randomly broken into ever smaller fragments through time; as the number of random breakages increases, the distribution of piece lengths approaches a log normal distribution. It is clear that the potential number of fragments of a particular length will be inversely proportional to their size, and that if the process occurs in several dimensions at once, the number of fragments will increase exponentially with the number of dimensions. What this boils down to is that there are many more ways to occupy small volumes of resource and habitat space than there are to occupy large ones—or in other words, that there are many more potential specialists than there are generalists. No matter how many trades there are to master, there is only one way to be a jack of them all (Text Fig. 4.8).



Text Figure 4.8 *A series of specialists nested within the fundamental niches of more generalized species. The diagram depicts only two niche dimensions so that the hypervolumes appear as circles, but in reality these should be n-dimensional as suggested in Section 2.2.2, Text Fig. 2.6. In the present figure, the largest circle represents a 'jack of almost every trade', the one trade-exception being that of a small niche-volumed specialist which lies outside its range (towards the bottom); apart from that it can exist in the habitats of any of the others but it is unlikely to be particularly competitive. See text for discussion.*

The 'purpose' of specialization is to avoid competition by reducing the overlap between occupied niches, but generalists must be hard-pressed not to overlap both with each other and with the numerous specialists. There is no point in being a specialist unless you are better at what you do than a jack of all trades, so in a head-to-head fight, the generalists will tend to lose out to their specialist competitors. As they age, and the organisms in them evolve, we might expect ecosystems to tend towards greater partitioning and a reduction in the number of generalists. But generalists manage to keep a toe-hold anyway (a very substantial one) because the world is never entirely static and new opportunities are always arising. So it seems likely that the way a generalist persists is to routinely be in the right place at the right time, which is why generalism and opportunism (normally *r*-selection) often occur together. Text Figure 4.9 summarises this arrangement.



Text Figure 4.9 *Showing the same arrangement as Fig. 4.8 but with an extra dimension added. This dimension might be labelled 'transient - permanent' or 'unexpected - expected' but here it is called *r* - *K* to denote the life-history strategy of the species at either end. In this dimension there is less niche overlap and we can see how a generalist manages to outperform a specialist within its preferred range—by doing the same thing faster, albeit poorly. The generalist's advantage is simply in getting there first and accomplishing whatever it can, as fast as it can, before a specialist arrives and displaces it.*

If volume of niche space translates into quantity of individuals, for example by correlating with the number of places one can live or the range of foodstuffs one can survive on, then Text Fig. 4.9 shows something very like a log normal distribution. More impressively, it also looks uncannily like the web of interactions shown in Text Fig. 4.7, where numerous negative correlations appear to link *Tritaxia* to a layer of a dozen or so

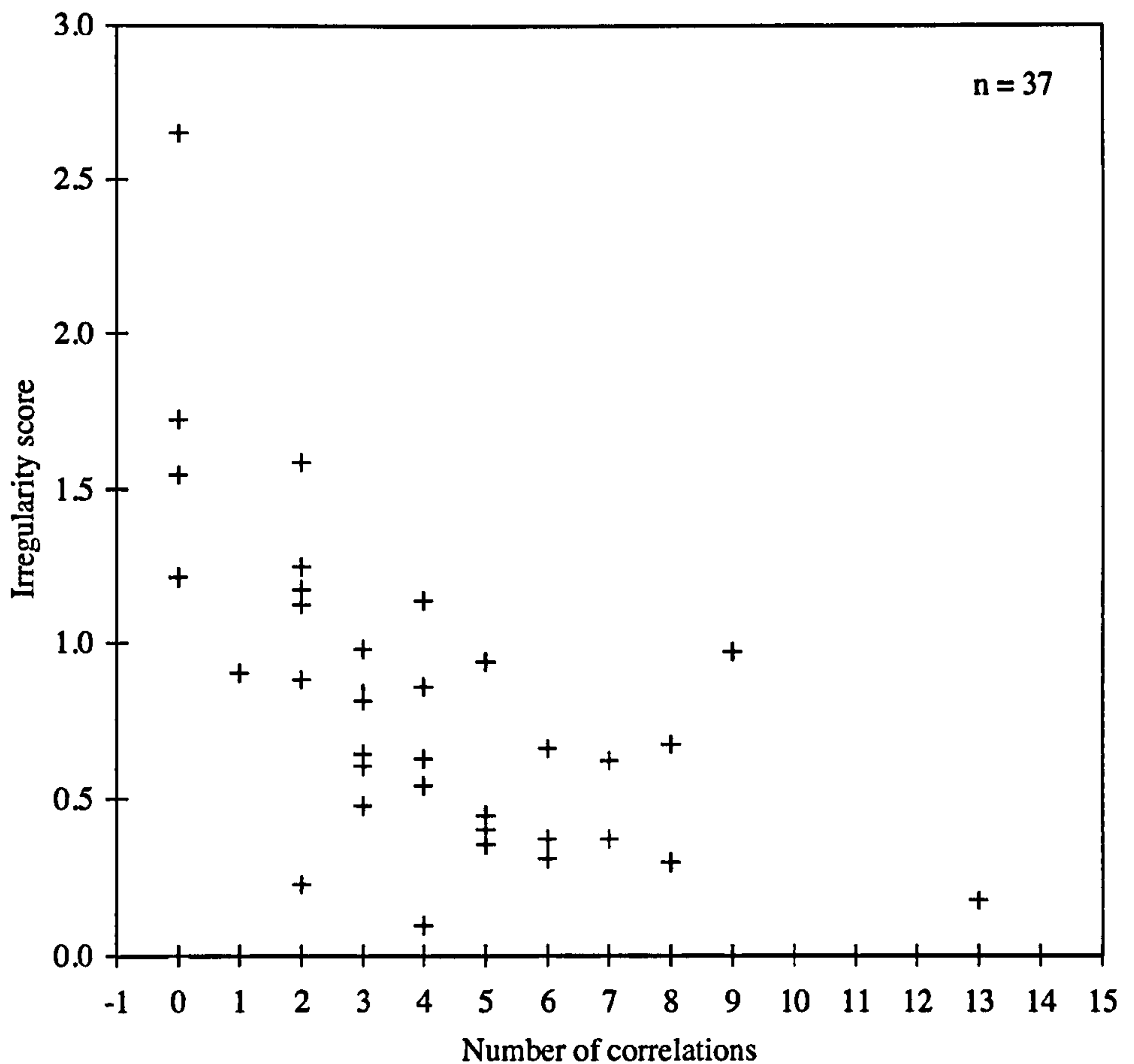
species which are often mutually co-operative and which effectively ‘shield’ the other two-thirds of the fauna. In the depiction above, the generalist is a kind of template for indirect co-operation precisely *because* it overlaps with so many other species; conversely, the specialists have normally achieved the kind of compartmentalisation which liberates them from direct competition with one another. There is a very strong correspondence here with the kind of community structure advocated by enthusiasts of ecological locking (Section 1.1.5), with *Tritaxia* as the ‘hub’ and the rarer groups (e.g. the minor nodosarians) as the ‘tendrils’.

If the reasoning advanced so far is sound, we should expect the *number of interactions* a species maintains (i.e. how many positive or negative correlations it has) to scale inversely with the *volume of niche space occupied* (i.e. with its degree of specialization as shown by an irregularity score)—and it does: to a confidence of 99% (Text Fig. 4.10)!

The main objection I can envisage to this series of interpretations is that the patterns could depend more on rarity and sample size than on any kind of ecological consideration. For example, it might be that the reason we do not see so many correlations among the rare taxa is because such regularities are masked by sampling effects. But note from Text Table 5.2, that the rare nodosarian groups correlate better with one another than they do with the more abundant calcareous (cassidulinarian) or agglutinated (lituolacean) taxa; this is not at all what one would expect of a noisy system, where the chances of degrading a correlation between a pair of species must surely be even higher if *both* groups are rare.

Perhaps, then, we are seeing a burial-rate effect in which correlations between the rare taxa are enhanced when they all appear together due to the deposition rate being slow enough to include them in the fossil record (or, alternatively, fast enough to catch them while they last—the argument could be spun either way). But the evidence weighs against this explanation, too: rather than surging in unison when the deposition rate goes either up *or* down, the rare taxa actually show no consistent tendency to correlate with sedimentation at all. The minor nodosarian group, for instance, correlates with couplet thickness (a good measure of the background sedimentation rate over a 20 kyr span) at only $r = -0.14$ (Appdx. Tab. 1.10), which would fail to be significant even if we were prepared to accept a confidence level of less than 75%.

Finally, the sample size argument does nothing to explain why certain species are rare in the first place. A log normal distribution might arise for purely statistical reasons



Text Figure 4.10 Relationship between the number of correlations (interactions) shown by a species versus its irregularity score.

Data are from Text Fig 4.4 and Text Table 4.1 and are for foraminifera only. The figure is for all styles of interaction. Interactions come as 'competitive' (negative correlations) and 'cooperative' (positive correlations). Because there are two variables, A.A. and R.A., there are also two different ways of arranging a correlation. I have chosen to call these 'inputs', when another species' R.A. correlates with the given species' A.A. (i.e. reading a grid like Text Table 4.1 from the side), and 'outputs' when another species A.A. correlates with the given species R.A. (i.e. reading a grid like Text Table 4.1 from the top down). Text Table 4.1 itself was calculated as 'outputs'. With regards to interpretation, it does not matter which of these methods is used since they both give comparable results. In both cases, negative correlations correlate significantly with irregularity score and positive ones do not; taken on mass, all correlations together do correlate significantly, as Text Table 4.5 (below) demonstrates.

	Negative	Positive	Both
Input	-0.418	-0.226	-0.393
Output	-0.391	-0.220	-0.391
Both	-0.380	-0.264	-0.508

Text Table 4.5 Correlation values for various combinations of interaction style. For n = 37, significant correlations are >0.271 at 0.05, >0.375 at 0.01, & >0.483 at 0.001.

(for example in the grain size distribution of a sediment), but if so then we should expect different taxa to have different relative abundances in different samples. Clearly, this is not the case: the common taxa are always common and the rare ones are always rare (which is like discovering that quartz grains are always big and olivines small—it tells you that *something* must be going on). The probability of such repeated patterns forming by chance alone is infinitesimal, and can safely be ignored. In fact, so far as I can tell, the only explanation which can account for the static relative abundances, the irregularity of certain signals, and the distribution of correlations, is the ecological one advanced above. If anyone should wish to test it further then the way to do so would be to stagger the sampling procedure: When fifty of the most common individuals have been found, their proportions relative to the rarer ones are noted and they are not collected any further; collection then continues on this pattern until there are equal numbers of all species. This would produce an equal probability of finding or losing a signal, irrespective of the intrinsic rarity of the species carrying it. But I have no doubt that the general outcome would be exactly the same, and that the conclusion would have to be that the community was spread out over a series of universal and local niche dimensions.

Section 4.2 Ecological Control: Inside or Out?

One of the features stressed in the results section is just how stable the configuration of Lower Chalk micro-fossils was. The extent to which a community is a genuine structure, over and above a collection of its individual parts, is an issue of considerable interest in the palaeoecological literature (e.g. DiMichele, 1994; Jackson, 1994; Ivany, 1996; Schopf, 1996; Jablonski and Sepkoski, 1996). This section examines some factors which contribute to community cohesion, and then attempts to explain how they might relate to one another across a range of temporal scales.

4.2.1 Assemblages or Communities?

Thus far I have simply referred to the assemblage of fossils as a 'community', and sometimes talked of the foraminiferal and ostracod communities as separate things; but I have never explained what it all amounts to in biological terms, a practice not at all unusual in palaeontology. Jablonski and Sepkoski (1996) identify the palaeontologist's operational notion of community as 'a spatially and temporally recurrent association of species, without implying that those species behaved as a functional unit or that biotic interactions determined the structure of that association'. This, however, is not at all what an ecologist would mean by community. Drake (1990) defines a community as 'the ensemble of species in some area whose limits are determined by the practical extent of energy flow' and states that 'the key to determining community limits is to identify boundaries...where the population dynamics...are unaffected by each other'.

This is actually a modern manifestation of a debate that was running continuously throughout the 20th Century. The two poles are defined by their architects, F. E. Clements, who believed that ecosystems were 'superorganism'-like coherent wholes, bound together by mutual dependencies, and H. A. Gleason who viewed the lack of specificity in many ecological reactions (e.g. the fact that if foxes don't catch rabbits, they'll eat mice instead) as evidence that 'community' is just a convenient notion for ecologists to work with, but actually represents little more than an assemblage of species with similar physical tolerances (Ricklefs and Miller, 2000). The debate has resurfaced most recently in palaeobiological

literature around the issue of co-ordinated stasis and its community counterpart, ecological locking (Morris et al., 1992; Ivany, 1996; Miller, 1996; Section 1.1.5)

Reasoning and evidence along Gleasonian lines has led workers to question whether there is really any such thing as a community at all; and as Jablonski and Sepkoski note, the Quaternary records are replete with examples of species that change their associations regularly, and appear to migrate hither and thither quite independently of one another (e.g. Graham and Grimm, 1990; Overpeck *et al.*, 1992; Bennett, 1997). If we accept that what happened in the Quaternary was typical across timescales on the order of thousands and tens of thousands of years, and that epiphenomenal interpretations of community structure are a valid explanation at that temporal resolution, there is a substantial scaling problem involved in accounting for the stable pattern seen in a million years of chalk-marl rhythmicity. Sterelny, 2001, responding to claims of co-ordinated stasis and ecological locking, calls this the 'Pleistocene paradox'.

A much discussed report from Buzas and Culver in 1994 further compounds the problem. It involves benthic foraminifera across truly geological timescales, and thus provides a *wider* temporal envelope for faunal dynamics. Sedimentary sequences recording six episodes of transgression and regression into a Cenozoic epeiric sea on the North American Atlantic Coastal Plain apparently reveal no community coherence between benthic foraminiferal species. Typically, each episode of transgression produced a different mix of species, some of which occurred in the local transgression below, but many of which did not and had instead emigrated in from different associations in other locations. Buzas and Culver's conclusion is that species associations are a mix and match affair, rather than a co-ordinated enterprise with strict functional rules for members; but that is not at all the picture afforded us by the Lower Chalk community.

Buzas and Culver's report concerned a scale above that seen in this study: their sequences were often several million of years in duration, and the changes in association occurred *between* such blocks. They gave little information on the internal dynamics of each sequence, so the pattern is not directly comparable to abundances and associations at the scale seen here. Nevertheless, the fact that species seem to behave individualistically at both lower and higher temporal resolutions does not bode well for an interpretation of community cohesion in the Lower Chalk microfauna. Worse still, an interpretation of individualism means that the faunal dynamics of the Cenomanian provide far less information about their environment than we might wish. If the species present were merely

an ‘assemblage’—a more or less random bag of taxa, perhaps thrown together by repeated directionless sampling—then neither the community structure, nor the changes it underwent, would tell us a great deal about how the organisms within that assemblage were experiencing their environment, or experiencing each other.

It is quite possible that each organism is controlled by individualistic aspects of the physical environment, and by those alone; in which case a species’ presence or absence in a sample simply corresponds to the presence or absence of some appropriate set of physical factors. Since we are unlikely to have much idea of which particular physical factors control an extinct organism, we will be hard pressed to say in what way the environment was or was not changing. Furthermore, there is nothing of ecological substance in such an account: there would have to be a separate story for each organism, and the community behaviour would be highly contingent, and therefore effectively random.

At the other end of the scale, Drake (1990, 1991; Drake *et al.*, 1993), in his search for assembly rules, documents some rather sensitive ecological systems (at experimental timescales), which, depending upon small random fluctuations in their past, can be flipped between a multitude of stable configurations (see also references in Drake, 1990). If the patterns documented by Buzas and Culver are just rampant individualism or Drake’s contingency writ large, then there is little meaningful to say about foraminiferal dynamics in the Cenomanian, or indeed in any period. We might as well submit to a tidal wave of historicism, give up, and go home.

The distinction at stake is whether or not the community was controlled from ‘outside’, by the physical environment, or from ‘inside’, by some sort of interspecific ecological rule following (e.g. Ivany, 1996). I have suggested that there are at least *some* general internal rules at play, and this argument will be revisited shortly; but first, let us review evidence for the alternative: individualistic habitat tracking.

4.2.2 External Control

The tension between internal versus external mechanisms of community structuring is not as strained as is often made out (for example by Jackson, 1994, who used Buzas and Culver’s article in the same issue to apply some fairly forceful rhetoric). In every ecological association we expect there to be *both* internal factors and external ones; after all,

the fundamental relationship is between an individual species and its environment, and other organisms are simply a particular class of environmental variable (at the very least, heterotrophs have to eat, and what they eat are other organisms). But the extent to which a community is merely a reflection of the component organisms' overlapping physical tolerances, versus a highly integrated biological system, is important for a wide variety of reasons, for example because it affects what we are willing to call an 'individual' and thus impinges on the levels of selection debate. But a more proximal concern is that the *Plus ça change* model concentrates explicitly on organism-environment relationships, and specifically on relationships with the physical environment over geological timescales. If we are going to make any statement about the effects of those environmental components at that particular scale, we had better be able to distinguish them from the effects of other components at other scales.

Students of micropalaeontology have suffered a near obsession for linking foraminifera with physical variables, most notably water depth, substrate and latitude (see Murray, 1991, for example, then read Lipps' plea for more biology to be introduced to the discipline - Lipps, 1981). In the Lower Chalk, we have recent contributions from Mitchell and Carr (1998) who explain changing faunal composition in terms of temperature and water depth, and Graff (2000) who explains it in terms of sequence stratigraphy. In the present data set there are numerous intriguing patterns which suggest a broad physical control to abundance. *Pseudotextulariella cretosa*, for instance, (and to a lesser extent *Plectina* spp.) is at its highest absolute and relative abundance early in the succession, during the run-up to Gale's B-C block sequence boundary, and then again towards the top of the sequence, this time on the run-up to the C-D block boundary (Appdx. Figs. 3.3.iv.b. & g. and 3.4.iv.b & g). Is it tracking water depth or some equivalent facies association?: the substrate seems different in each case but it may be that grain size or current activity were similar. *Marssonella trochus* and *Textularia* sp. C are both markedly more abundant in the early half of the section (Appdx. Figs. 3.3.iv.c & e and 3.4.iv.c & e). Is this a correlation with water depth, strength of cyclicity, sediment composition or current activity?

And what about the cryptic suite of patterns shown by the rare nodosarian and agglutinated species groups? (Appdx. Figs. 3.3.iv.j & r and 3.4.iv.j & r); or the similar ones shown by *Eggerellina mariae* and *Arenobulimina advena*? (Appdx. Figs. 3.3.iv.f & i and 3.4.iv.f & i). In Section 4.3.3.iv I discussed this pattern in terms of its being a depositional

artefact of one sort or another, and concluded that it probably was not, on the grounds that the rarer groups showed it most clearly. In fact it turns out that *Arenobulimina advena*, the rare nodosarian group and the rare agglutinating species all correlate positively, to a high degree of confidence (> 99.9% for the first two, only to 99% for the latter) with the proportion of acid insoluble residue (Appdx. Table 1.10). Astonishingly, but seemingly correct, despite the apparent similarity of pattern between *Eggerellina mariae* and *Arenobulimina advena* in the 100 kyr transects, *Eggerellina* correlates only weakly (0.09!) with insoluble residue count (as do *Lenticulina rotulata* and *Gavelinella cenomanica*, also mentioned in Section 4.3.3.iv.). Still, it is tempting to suppose that the groups which do correlate with insoluble residue were tracking a physical feature, in this case substrate composition or consistency (but see Section 4.3.4. for an alternative story). In fact there are a wide variety of taxa which correlate with the percentage of acid insoluble residue (Appdx. Table 1.10); only *Tritaxia pyramidata* amongst the forams correlates negatively, although some of the ostracod groupings do too.

The samples at B41, from all three sites, provide an insight into a ‘community’ which has either undergone a substantial restructuring, or is on the brink of doing so. What can we learn from it? Two species, *Tritaxia pyramidata* and *Gavelinella reussi*, are depressed way beyond their usual proportions and come close to constituting what Brett and Baird (1995) called ‘outages’ (Appdx. Figs. 3.3.iv.a & p), while a large number of others, most notably *Dorothia gradata* and *Gyroidinoides parva* (Appdx. Figs. 3.3.iv.d & k), exhibit a corresponding peak. And there is an accompanying guest appearance (or ‘incursion epibole’ in the terminology of Brett and Baird) from *Lingulogavelinella jarveae*, *Bulbophragmium* sp., *Pyrulina* sp. and *Guttalina* sp. among the forams, and from a number of ostracod species, too.

Is this a biological event in the sense of a community breakdown, or simply a case of habitat tracking in a number of species with different preferences? Grist for the habitat tracking mill is easy to come by. The fauna could have been following sea level (which was low), oxygenation (also low), water temperature (probably low), organic input (definitely high), clay content of the substrate (also high) or sedimentation rate (fairly high), to mention only the most prominent: B41—the *arlesiensis* bed—is an ‘event’ horizon for good reason (see Section 2.1.6 for discussion). But no matter what we choose to say the fauna is reacting to—and it is certainly reacting to something—the question still remains as to whether it was behaving in an individualistic, or community co-ordinated manner.

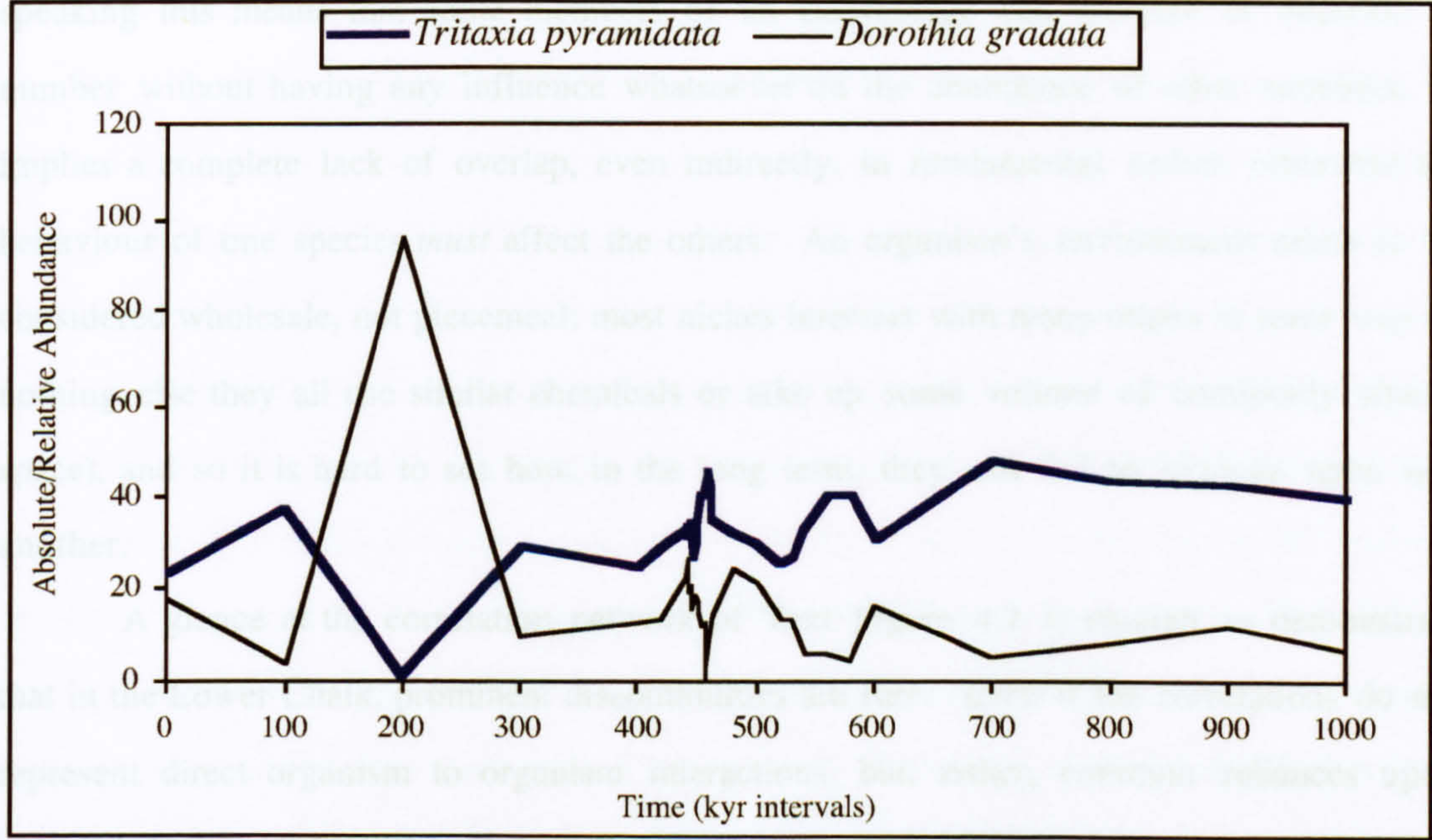
4.2.3 Internal Control

The problem with the habitat tracking explanation, although undoubtedly correct to some extent, is that it fails to engage the organism-environment relationship in a biologically meaningful way. The ever important ecological question to ask is: ‘Why aren’t there more of them?; What limits their number?’ Organisms of any species should, over geological timescales and barring substantial geographic barriers, be ubiquitous within the confines of their fundamental niche: that is their nature. In tracking preferred habitats, are foraminifera really just following the boundaries of their *fundamental* niches? If so, why are their fundamental niches so narrow, and why have they not found ways to broaden them?—an evolutionary question rather than an ecological one; but then we are talking about a million year span.

Given the similarity in form and lifestyle among the vast majority of foraminiferal species, it seems highly implausible to me that the reason species *A* is found in water fifty metres deep while species *B* lives a hundred metres deeper is because they simply fail to survive in each others’ habitats. Rather, I would argue, in those settings they out-compete one another. I am not claiming that there is a total overlap in fundamental niche between species: some, especially the equilibrium strategists, are guaranteed to have non-overlapping fundamental niches as a result of specialization. But *I am* suggesting that most habitat tracking behaviour involves the pursuit of *realized* niches rather than fundamental ones, and that if the niches *are* fundamental, they achieved that status as a result of interspecific competition in the past. Or, to put it another way, since the constant decay of genetic material by copying errors and other mutations virtually guarantees that phenotypic features are retained on a use it or lose it basis (Section 5.4), I am suggesting that the only thing which could possibly keep organisms so phylogenetically and ecologically similar from overlapping one another’s niches is a constant pressure from interspecific competition. Here is an example from the Lower Chalk.

Tritaxia pyramidata and *Dorothia gradata* descended from a common verneuliid ancestor sometime in the Early Cretaceous (Haynes, 1981; Tappan and Loeblich, 1988). Both have agglutinated tests which typically start with a triserial coil (occasionally

multiserial for *Dorothia*), but while *Dorothia* switches to a biserial arrangement after just a few whorls, *Tritaxia* often remains triserial to the end (Appdx. Figs. 2.2.1.i, 2.2.1.x, 2.3.9 & 2.3.10). We might almost call *Dorothia* an uncoiled form of *Tritaxia*, although it is also more granular and the chambers are rounded instead of sharp. According to the morphotype theory, however, the pair of them should occupy broadly similar life positions, and they do indeed occur in sediments from the same (admittedly time-averaged) samples. We can also see from the correlation data that a rise in the relative abundance of *Tritaxia* closely corresponds with lower absolute abundances of *Dorothia* (Text Fig. 4.11), and vice versa. Is this not *clearly* a case of competitive exclusion?—because the alternative seems to require the claim that these two morphologically and phylogenetically proximal life forms had utterly non-overlapping fundamental niches, and that the appearance of co-habitation is simply a time-averaged illusion of the fossil record.



Text Figure 4.11 Absolute abundance of *Dorothia gradata* versus relative abundance of *Tritaxia pyramidata*. The ordinate is in numerical abundance of specimens for *Dorothia* and percentages for *Tritaxia*. The material is from Folkestone - Combined Scales so the abscissa is linear but the points are not equally spaced.

If this kind of situation is typical (many figures such as the one above could be shown; see Text Table 4.1)—and we should expect it to be, given the commonality of descent and structure amongst the foraminiferal species of the Lower Chalk—then biological inter-dependencies must have been rife. Habitat tracking would certainly have gone on, but it can hardly have occurred in a vacuum.

I explained the kind of structure the fauna seems to exhibit in Section 4.1, employing descriptions that relied only on broad statistical generalities, and which thus avoided the problems of unknown detail (such as in precisely what way an organism was specialized, or exactly which features qualified it as an opportunist). In the section to come, I use similar reasoning in an attempt to bypass the difficulties of historicism, and explain how the fauna managed to remain so stable over a million-year span. But as a run up to the topic of stability I first want to press one of the universal niche axes outlined in Section 4.1 into service and explore some broad features of the community's internal structure.

In Drake's definition (1990; Section 4.2.1.), 'boundary structures' are said to occur in a community when elements of a fauna do not affect one another. Strictly speaking this means that some members of an assemblage can increase or decrease in number without having any influence whatsoever on the abundance of other members. It implies a complete lack of overlap, even indirectly, in fundamental niches, otherwise the behaviour of one species *must* affect the others. An organism's environment needs to be considered wholesale, not piecemeal; most niches intersect with many others in some way (if nothing else they all use similar chemicals or take up some volume of commonly shared space), and so it is hard to see how, in the long term, they can fail to impinge upon one another.

A glance at the correlation network of Text Figure 4.7 is enough to demonstrate that in the Lower Chalk, prominent discontinuities are rare. Even if the correlations do not represent direct organism to organism interactions, but, rather, common reliances upon physical factors, there are still very few boundaries to be found. Obvious cases would appear as gaps in the network of connections—clusters of taxa which failed to connect, even indirectly, with other such clusters. In Text Figure 4.7 there are none: every single taxon which has an input can be traced to every other. Care should be taken with Text Figure 4.7, however, because the arrows do not denote *directions* of causality, but simply correlations of behaviour from the *perspective* of a chosen species' relative abundance. Nevertheless, there are still grounds for insisting upon common causal threads of some sort, even if the direction of causal flux cannot be demonstrated, otherwise there would be no significance to a 'significant' correlation.

Fortunately, in order to say something sensible about the community, we do not need to know the direction and style of interactions—whether an increase in the abundance of *Tritaxia* caused a decrease in the abundance of so many others, for example, or whether it was the other way around—we merely need to know that there was *some* connection. Stuart Kauffman (1993) has trailblazed the route to biological understanding in empirically impoverished circumstances by modelling situations in which the average properties of complex systems alone suffice to tell us interesting facts. One of the tools frequently used is the random Boolean network (see Kauffman, 1993), in which an array of switches is linked together by logical commands telling one another what to do. Any switch can, theoretically, be linked to any or all of the other switches, with a specific wiring diagram as the result. (A useful endpoint to consider is a situation in which each switch is linked to every other, because there is then only one possible wiring diagram: fewer connections generally means a larger space of possible wiring diagrams.) The significance of a Boolean network to ecology is not entirely obvious, but for the present purposes let us just suppose that the logical states ‘on’ and ‘off’ correspond with more continuous features such as increase and decrease in relative abundance (from Kauffman’s discussion it doesn’t seem to matter what the elements do to one another so long as they do something).

The statistical nature of the models means that general properties emerge without us having to know any details. One major theoretical result, touted by Kauffman as a universal property of dynamical systems, is that out of the list of possible connections (K) between elements, ranging from $K=1$ to $K=N$ (N being the total number of elements), an average of just two connections per element routinely produces arrays which can adapt to a given optimum most effectively. $K=2$ networks persistently evolve out of arrays which start from higher or lower connectivities, when these are allowed to change their number of connections throughout repeated cycles, whilst optimizing to a given task. The explanation for this is that $K=2$ networks have an intrinsic tendency to form self-stimulating causal loops—positive feedback systems which freeze into particular states. Such frozen connections tend to ‘percolate’ across the array, and because they are stuck such that their values cannot change, they serve as ‘walls’ which partition the remaining free elements. Changes of state or connection in the free elements are then isolated and incapable of spreading throughout the array, hindered as they are by the walls of frozen clusters; thus, they effectively form modular units which can be tweaked independently of one another, allowing the network to fine tune itself without too much disruption taking place.

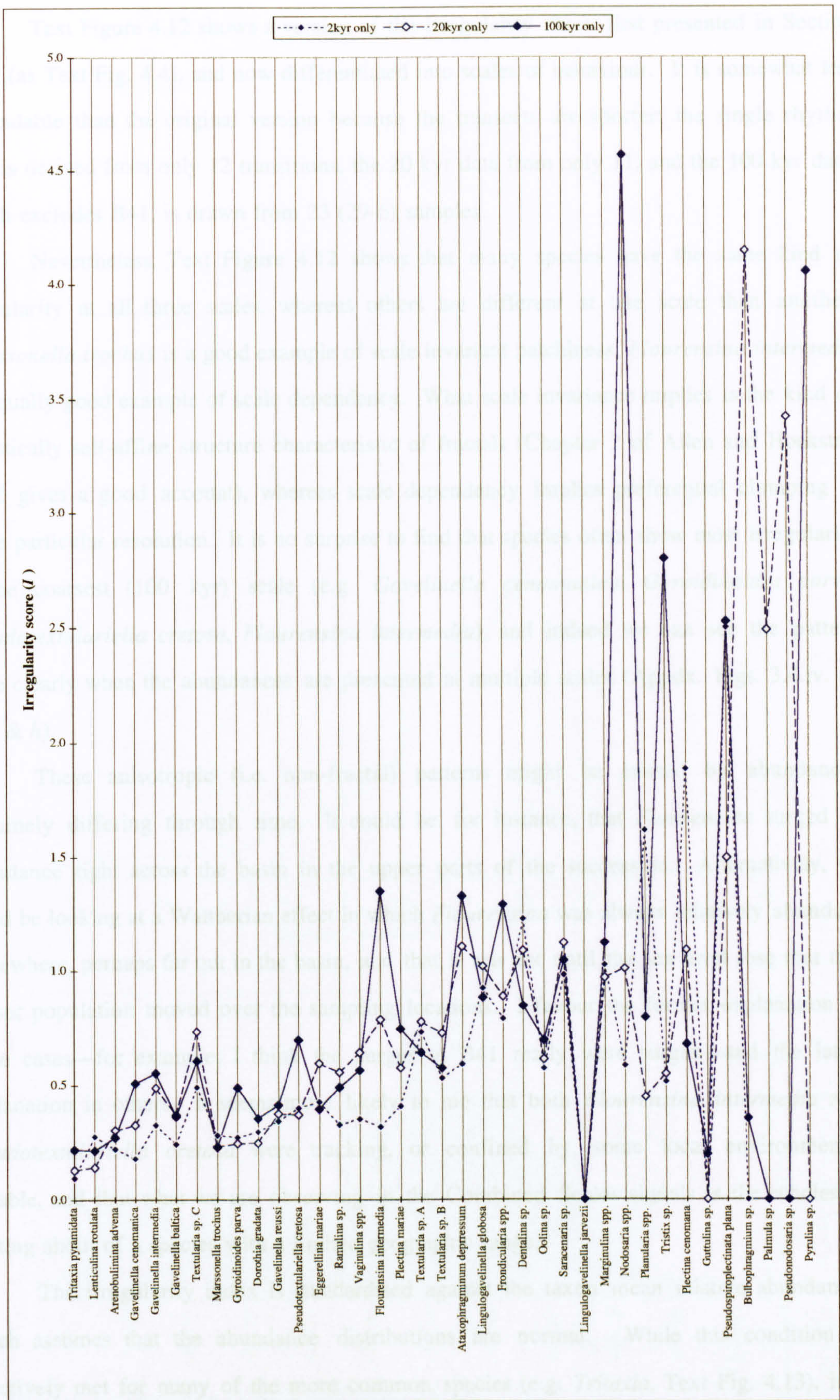
The result is a system which is both stable and adaptable, and which is capable of 'maximising inclusive fitness'; unsurprisingly ecologists have started to become very interested in such hierarchically buffered systems (e.g. Allen and Hoekstra, 1992), and the expectation is that natural networks of dependency will tend to stumble onto such configurations and remain there.

Are Kauffman's *walls* (his 'percolating frozen structures and homogeneity clusters') the dynamic equivalent to Drake's *boundaries*? Logic arrays are rigid and discontinuous in ways that natural systems are not; but, even so, the idea that dynamic networks exhibit a phase of connectivity in which threads and walls of feedback carve the system into isolated fragments is very attractive, especially when its global features can be predicted. Does the tangled layer of species which interact directly with *Tritaxia* in Text Figure 4.7 constitute a such a wall or a series of percolating threads? Most of them have reciprocal relationships, and it is easy to see how an increase in the abundance of one would propagate across the whole layer so as to form a buffer between *Tritaxia* and the other two thirds of the fauna. Of course, almost all the relationships in that layer are mutualistic and it is likely that most of the connections are indirect and arise through a common antagonism with generalists like *Tritaxia*. If so, can networks have *virtual* connections? Most intriguing of all, is it coincidence or confirmation that the 37 foraminiferal species in the network have just 72 correlations (connections) between them, an average of almost exactly $K=2$ per element?

4.2.4 Scaling and Stability

4.2.4.i Scaling

Scaling is a central issue in ecology (Levin, 1992) and it is also a major concern of this work. Section 2.2.5 was aimed at general purpose scaling between ecological patterns and geological ones, with Section 4.3.4 demonstrating some of the scaling data available from this study. I now want to top-up with a few additions that will hopefully help to explain the structuring and stability of the Cenomanian micro-fauna.



Text Figure 4.12 Irregularity index values for foraminifera across a range of sampling points at different sampling resolutions. See text Section 4.2.4 for discussion.

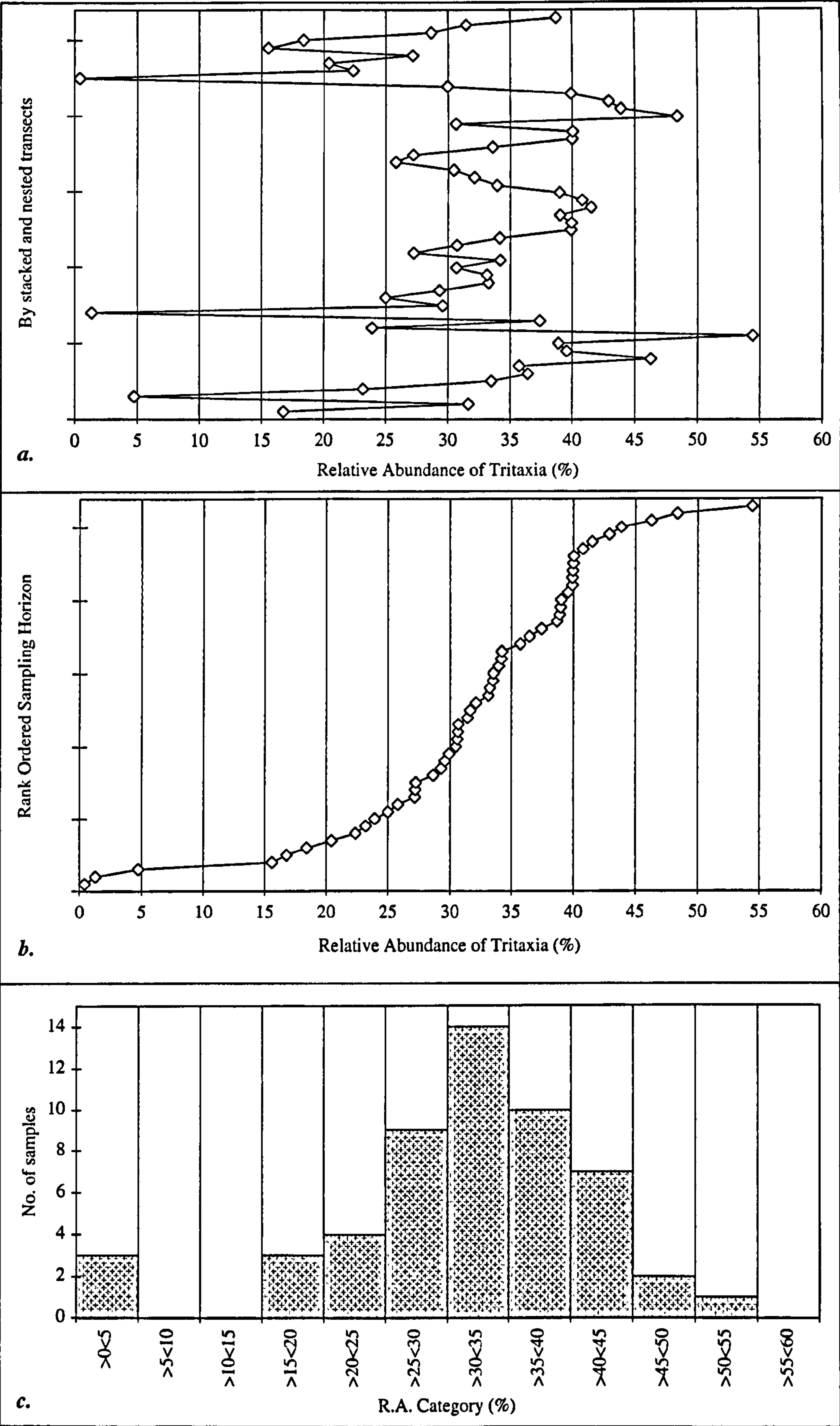
Note that the value for 100 kyr resolution does not include the data from B41.

Text Figure 4.12 shows a version of the irregularity chart, first presented in Section 4.1.2 (as Text Fig. 4.4), and now differentiated into scales of behaviour. It is somewhat less dependable than the original version because the transects are shorter; the single rhythm data is derived from only 12 transitions, the 20 kyr data from only 11, and the 100 kyr data, which excludes B41, is drawn from 23 (29-6) samples.

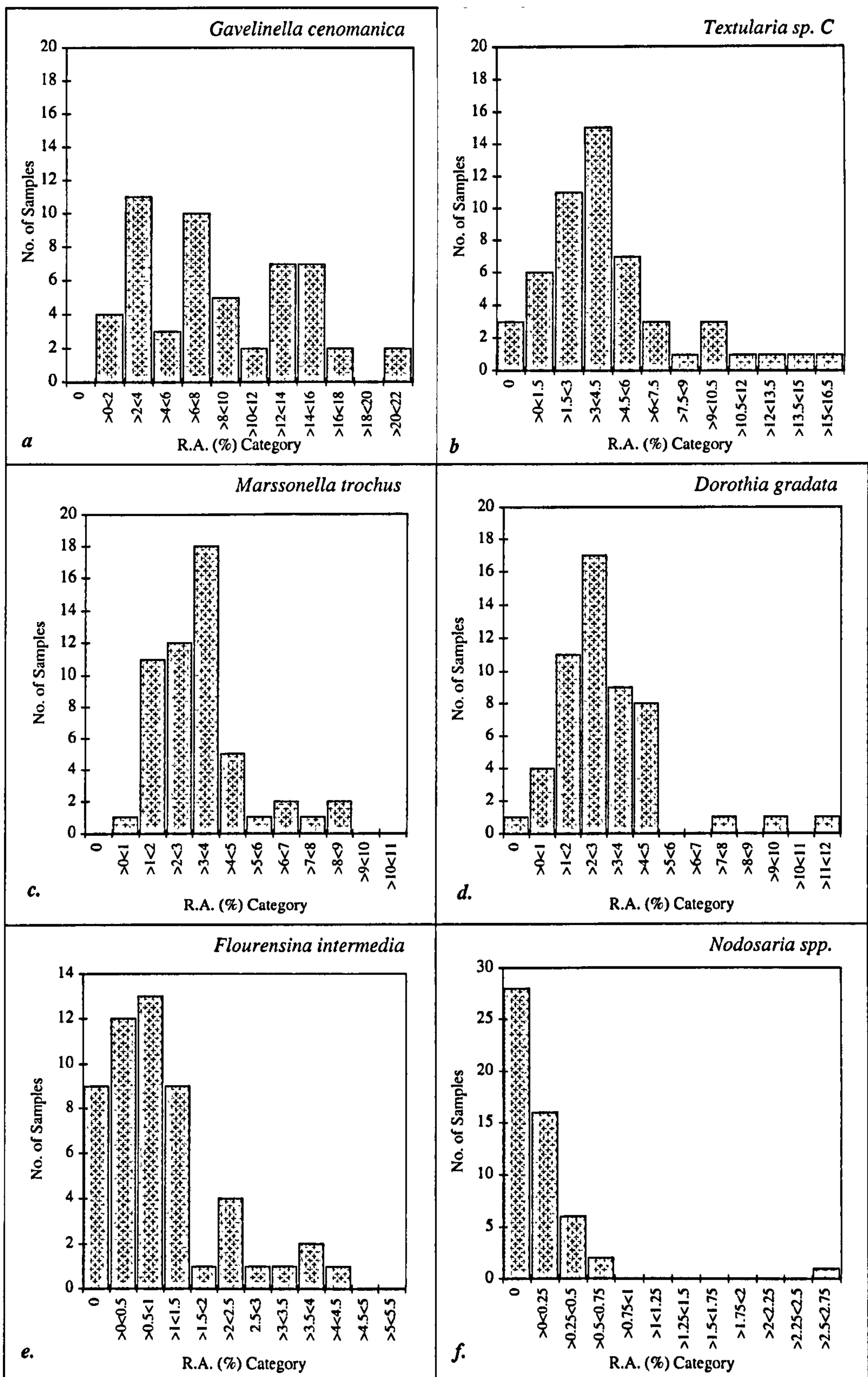
Nevertheless, Text Figure 4.12 shows that many species have the same kind of irregularity at all three scales, whereas others are different at one scale than another. *Marssonella trochus* is a good example of scale invariant patchiness, *Flourensina intermedia* an equally good example of scale dependency. What scale invariance implies is the kind of statistically self-affine structure characteristic of fractals (Chapter 2 of Allen and Hoekstra, 1992 gives a good account), whereas scale dependency implies preferential clumping at some particular resolution. It is no surprise to find that species often show most irregularity at the coarsest (100 kyr) scale (e.g. *Gavelinella cenomanica*, *Gyroidinoides parva*, *Pseudotextulariella cretosa*, *Flourensina intermedia*), and indeed we can see the pattern quite clearly when the abundances are presented at multiple scales (Appdx. Figs. 3.4.iv. *m*, *k*, *b*, & *h*).

These anisotropic (i.e. non-fractal) patterns might be caused by abundances genuinely differing through time. It could be, for instance, that *Flourensina* surged in abundance right across the basin in the upper parts of the succession. Alternatively, we could be looking at a Waltherian effect in which *Flourensina* was always relatively abundant somewhere, perhaps far out in the basin, and that it was not until the sea level rose that this denser population moved over the sampling locations. I favour the former explanation in some cases—for example, I think the surges at B41 really were surges—and the latter explanation in others. It seems more likely to me that both *Flourensina intermedia* and *Pseudotextulariella cretosa* were tracking, or confined by, some local environmental variable, and that what we are observing in the Combined Scales signals is the wholesale shifting about of a species with a limited geographic range.

The irregularity index is standardised against the taxon mean relative abundance, which assumes that the abundance distributions are normal. While this condition is effectively met for many of the more common species (e.g. *Tritaxia*, Text Fig. 4.13), it is clearly an oversimplification for the rarer ones (e.g. Text Fig. 4.14 *a* & *f*). Text Figure 4.14 provides a selection of distributions as examples; most of the groups shown are towards the abundant end of the scale and exhibit a more or less normal spread, as do most



Text Fig 4.13 *Distribution for the Relative Abundance values of Tritaxia pyramidata.*
a. R.A. values distributed by sampling horizon.
(sequence in panel a: S 100, F nested 100-20-2, E 100, stacked sequentially).
b. R.A. values distributed according to value, smallest first.
c. Histogram for distribution of R.A. values (mean 30.3, std dev. 10.7).



Text Figure 4.14 *Distribution of Relative Abundance values some foraminiferal taxa*

- a. *Gavelinella cenomanica* : multimodal distribution as suggested by the variability plot (Text Fig. 4.12)
b. *Textularia sp. C*: unimodal and even but with a skew.
c. *Marssonella trochus* : unimodal, slightly uneven and slightly skewed.
d. *Dorothis gradata* : unimodal, slightly uneven and slightly skewed.
e. *Flourensina intermedia* : unimodal?, skewed, zero scores a significant component.
f. *Nodosaria spp.*: unimodal, extremely skewed, zero scores predominate.
in all cases n = 53.

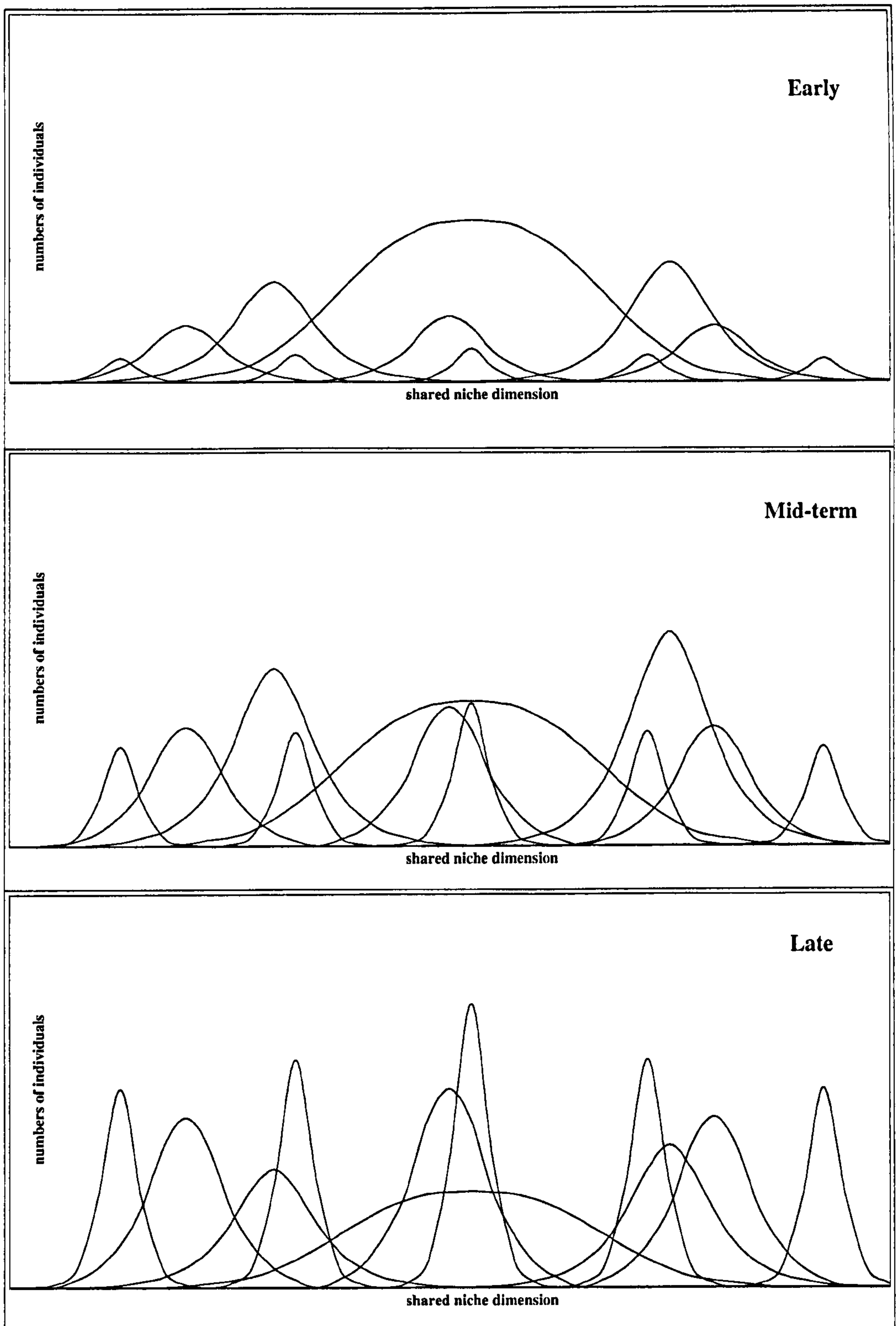
of the unshown groups at that end; most of the rare groups have distributions more like that of *Nodosaria* (4.14 *f*). *Gavelinella cenomanica* is unusual in Text Fig. 4.14, because it apparently displays multimodality, probably because of its scale dependent clumping, as the irregularity scores indicate (Fig. 4.12). But the most important deviation from a normal spread clearly arises because of sampling bias in low abundance groups (Text Fig. 4.14 *d* & *e*). As discussed in Section 4.1.2, this is probably a major contributing factor to the overall trend across the irregularity chart.

According to the story so far, then, the community appears to be a shifting montage of species, with roughly scale invariant distributions, probably resulting in the kind of statistically fractal pattern that often emerges from multiple independent controlling forces. Superimposed were some scale dependent elements, perhaps due to habitat tracking of geographic ranges and other broadly distributed heterogeneous features. And within this quivering mosaic, relative abundances were evidently free to oscillate back and forth within certain limits, generating normal distributions.

4.2.1.ii Stability

As we saw in Section 4.1, the benthic community seems to have been broadly adapted to a yearly input of phytoplankton, and probably reacted in the kind of sequence of species-specific surges depicted in Text Figure 4.1. Text Figure 4.15 (below) shows a different version of the same event. To get the best out of this picture, imagine that it is what one might see by standing next to the Ghost of Christmas Yet To Come in Text Figure 4.1 and watching the wave of sequentially peaking species come crashing towards you through time. It can also be compared to Text Figures 4.9, a static version, as looking along the *K-r* axis from the *K* end, and to Text Fig. 4.8, a bird's eye view, showing a pair of shared niche dimensions rather than just one.

The sequence depicts a standard ecological *succession*, with opportunists like *Tritaxia* colonising a new phytoplankton fall first and being gradually displaced by wave after wave of more specialized taxa, until the new spate of phytoplankton falls again next spring. But experimental work on the process of community assembly has apparently shown that community composition is a fragile affair, highly sensitive to starting configuration and historical effects. Drake's review (1990) of over two dozen empirical



Text Figure 4.15 *The peaking and declining proportions of species with different niche breadths during the course of an ecological succession.*

Early on, the single r -strategic generalist surges in huge numbers, taking advantage of the lack of competition to spread profusely; by the late stage, the generalist has been out-competed by the ascendant multitude of narrowly adapted specialists. There is no specific time period over which this ecological event is to occur - it could take place over a matter of days (for bacteria and protists) or years (for a woodland to mature). The figure is also deliberately evocative, recalling a fluid in wave form, a splash from a single droplet, or a bucket full of water thrown across the ground. Fluidity is part of the image I want to suggest. An ecological succession should have different species peaking in different mixtures on different occasions. The basic form, however, is fairly universal, and would emerge clearly from a statistical overlay of many individual succession events. See text for discussion.

studies demonstrates that slightly different assembly sequences result in alternative or multiple steady states. Since the data seem consistent for that scale we should accept them and ask instead how more stable patterns can be generated over the longer period.

Like the individual patterns of relative abundance, ecological succession is not a rigidly deterministic affair (no biological process ever is), but rather an emergent behaviour appearing as a statistical generality; and there is plenty of room in such a conception for transitive cases of sensitive dependence on sequence, because the scenario is set and run time after time. Drake's experimental work (Drake, 1991; Drake *et al.*, 1993), whilst demonstrating the range of possible outcomes, also paradoxically serves to illustrate the subtly deterministic nature of these systems. For example, the only way Drake and co. can get their experiments to show any sensitivity at all, is to ensure they add what are obviously *r*-selected species before the equilibrium ones, otherwise the opportunists fail to take and the outcome is a forgone conclusion. Sensitive though it is, the process clearly has a directional preference.

An explanation of community structure in terms of ecological succession is already starting from a time averaged perspective. While Drake's work suggests that community assembly is like a game of 'paper-scissors-stone', the successional component argues strongly for a weighting or skew hidden somewhere behind this superficially contingent process, a weighting that only manifests itself as a long-term emergent property. We know that it is not impossible to grow a forest from bare ground, just that in all likelihood the weeds will get in there first. The weighting behind such a skew on otherwise contingent outcomes is a classic example of an attractor—in this case a trajectory attractor which causes not just individual elements, but rather the entire system to settle through a sequence, though that sequence appears to be deterministic only over a large number of runs. The obvious question to ask next is whether there are any other attractors at larger and longer scales, which work to crystallise orderly behaviour out of individually sensitive, but iteratively run sequences, because these might help to account for the stability seen in the Lower Chalk microfauna. It seems the answer is yes, but the attractors are similarly subtle ones.

If the correlations shown in Text Figure 4.7 really are network connections in the style of Kauffman's Boolean grids, there is no reason why they should be static. I am sure

there are some predictable aspects—similar morphotypes will be in conflict more often than dissimilar ones, for instance—but absolute rigidity is not required for stability. Returning to Text Fig. 4.7 we might ask whether there would be a sign change in the connection between *Textularia* sp. C and *Marssonella trochus* if *Textularia* sp. B disappeared? The link between *Tritaxia pyramidata* and *Gavelinella intermedia* seems to be neutral, balanced on one side by an indirect negative connection via *Gavelinella reussi* and an indirect positive one via *Gyroidinoides parva*; does that mean that the sign of the *Tritaxia pyramidata* and *Gavelinella intermedia* relationship depends on which of the *intermediary* species is present, or even locally most abundant? Connections both direct and indirect can be made or broken, depending upon the presence or absence of individual species on a local or regional scale. What happens to the array when such events take place, as they are likely to do only too often? One can envisage changes in sign and connectivity cascading through the network and transiently or permanently altering large portions of the array.

This is where the concept of internal self-organization is at its most useful. Kauffman's claim is that large and permanent changes happen only rarely in networks as modestly connected as the Lower Chalk forams appear to be, although they are more common when the connectivity is higher (see his Chapter 5 p 201-202). Typically $K=2$ systems have about \sqrt{N} attractors (N being the number of elements) created by the freezing of self-reinforcing elements and subsequent 'percolation by frozen structures'. This means there are about six (which may be point attractors, sequences or limit cycles) if the foraminiferal fauna alone is considered, seven if the ostracods are added, and perhaps two dozen if the entire Cenomanian macrofauna were included. So any amount of sign changing or connection switching leads into one of only six to two dozen possible attractors, and then the system settles down again; in fact, according to the theory, for 80 to 90 percent of such perturbations the system should settle into the *same* attractor! (ibid. p202).

The next question concerns how different the alternative attractors are? The answer is that 70% or more of the elements fall into a state which is *identical* on *all* the attractors—in other words, most of the time species connections should form the same positive or negative reinforcing relationships, no matter how much the network is stirred up. Spontaneous order indeed!

If this is true then it is good news for fans of stability; but how does it square with the empirical data? I think it is not inconsistent because whether a dynamical system is viewed as stable or unstable depends partly upon how it is measured. Consider the difference in perception between the tangled thicket of species rank-order shifts in Text Figure 3.5 (Appdx. Fig. 3.1.iii.d & e) against the stately wobble of their actual relative abundances. If we imagine stirring up the Cenomanian forams in Text Figure 4.7 to generate a new ensemble of connections but with a self-organising 70% of them still the same (e.g. *Tritaxia* still directly at odds with a similar cluster of other species, those species forming a ring of mutual collaboration which buffers the rest of the fauna etc.)—would that constitute a big difference or a small one?

It is not terribly easy to wring information from the Buzas and Culver (1994) paper, but my impression is that if the data had been presented differently the conclusions might have followed suit. There are many examples in the literature where I suspect a perception of variability and interspecific individuality could be substituted for one of uniformity and interspecific community cohesion if either the format or the expectations of those involved in the discussion were changed. Overpeck *et al.* (1992), for instance, claim ‘no modern analogue’ for glacial tree associations when their Figure 2 clearly shows half a dozen species that maintained very similar proportions over the last 18 kyrs and into the present day, with birch as the only one to change its relative abundance to any significant degree (see also Bennett, 1997, for many similar examples). In view of the kind of loose construction dynamics demanded by Kauffman’s attractors, the mix and match pattern shown by Buzas and Culver’s forams might be a perfectly acceptable case of stability, and perhaps there is little wonder that Brett and Baird (1995) interpret their faunas as exhibiting 65-80% persistence across geological timespans.

There is thus room for both statistically stable *and* idiosyncratically dynamic elements in the community behaviour, and this is the sense in which history and contingency can both be both incorporated by an appropriate perspective on system stability. To wrap the section up I want to summarise by explaining how I think attractors operating at varying scales could plausibly relate to one another.

On a year by year basis we can expect chance effects and assembly-rule sensitivity to have had a strong effect. I envisage years in which *Tritaxia* was almost absent and others in which it fairly dominated the foraminiferal fauna (like a ladybird plague), with the

regular 25-30% contribution being an average over repeated episodes. The more or less static relative abundances might be considered as loosely constrained point attractors, of the type normally depicted, via analogy to gravity, by balls in concave cups or the resting points of pendula. If so, then the constraining cups are interactions with other species in the community, and the free play is Drake's element of contingency at that scale. Foraminifera almost certainly have rather broadly overlapping fundamental niches, and we can expect them to be boxed into realized corners of such zones by competitive exclusion (Section 4.2.3, Text Fig. 4.11). This boxing process is again a statistically emergent feature which crystallises out from highly contingent short term ecological events, and that is one reason why the relative abundance values have a normal distribution (Text Figures 4.13 & 4.14).

Whatever caused the point attractors was evidently no more than a weighting that tended to focus the outcome of species interactions in certain proportions; it was certainly nothing like a rigid rule. But while it is quite likely that a fair amount of stability would be found if the proportions of species were tracked over the course of a few tens of years, that is not what we are seeing in the fossil relative abundances. I suspect that what we find in the fossil record are *variations in the attractors themselves*, so that on a month-by-month basis the community behaviour was biased by certain tendencies, but on a century-by-century scale the tendencies themselves changed, again more or less 'randomly' (that is, in response to a multitude of independently varying factors). This is a case of vague influences stacked on top of one another, but I think that is all we need to account for stability in a community of billions of individual organisms which were playing an ecological game together with some rules, but also requiring a large dose of luck, over millions of iterative rounds.

The kind of self-organizing networks suggested by structural biologists could be working at a variety of scales. Firstly, it may be that *sensitive assembly rules themselves* generate the kind of self-reinforcing threads sufficient to partition a community into buffered zones. In this case it is the proliferation of random mixes of antagonistic species which inevitably results in a locked-up framework, causing the system to settle onto one of a small number of very similar states. Alternatively, the percolating 'walls' are altogether more diffuse, being properties which emerge from iterative episodes in much the way that the realized niches and relative abundances do. This time it could be *fine tuning by natural selection*, which biases the strength of various interactions, and thus promotes certain outcomes; but which, despite repeated selective tinkering, fails to do more than shift the community between a handful of stable states. And finally, there is the long-term *restriction*

of interactions (the setting for Kauffman's K parameter) which results in a community with the kind of connectivity capable of exhibiting spontaneous order in the first place.

Each of these self-organizing scenarios operates at a different scale: seasonally for the first, in decades or more for the second, and over the course of a handful of millennia for the third. Throwing a unique fauna together would involve many seasons of experimentation, with niches shifting around due to selection until the fauna reached a long term stable configuration with an average of two dimensions of niche overlap per species, at which point the whole community structure is securely in place, robust to perturbation, and does not shift for a very long time. It is this longer term configuration which I find most interesting, and which the Lower Chalk foraminiferal fauna has the most bearing upon, and my guess is that the universal niche structure outlined in Section 4.1.5 represents the kind of flexible but stable configuration that any ecological community can be expected to assume over evolutionary timescales, without it depending too much on the identities of the taxa involved. *Tritaxia* was evidently the keystone player in this case; but with a different mix of species the community might still have been winnowed into the same configuration, and simply used different actors with different specific niches to play the same, broad functional roles.

A prominent absence in all of Kauffman's theories is the specific structure of the external environment. Computer models of self-organization tend to lack a coherent setting; instead, selection is judged according to 'arbitrary optima'. In nature optima are *not* arbitrary: they reflect the physical structure of the world, and by neglecting this important facet one can hardly fail to uncover 'self-organization', since everything else capable of doing the job has been removed. (It doesn't take a genius to realise that if you *define* external influence as arbitrary, then the only possible source of 'non-arbitrary' order left must be internal.) Environmental structure impinges on the micro-fauna of the Lower Chalk in different ways. Specifically, the fundamental and realized niches are adapted not only to the other organisms present but also to the relatively inert physical setting. It may well be that species A has an advantage over species B in water of a certain depth, but the variable depth of water is at least as important in the distinction as those differences in structure on which the advantage proximally hinges. In more general terms, and as we saw in the earlier section (4.1), there are ways in which the environment conspires to partition the community that can be understood without us knowing anything at all about the

particulars. If the correlations presented in Section 4.1.3 really are telling us about the strength and sign of species interactions, then it seems that the community had indeed attained roughly the kind of critical state required for spontaneous order and maximum stability. But as we have seen, the correlations are not 'arbitrarily' assigned—they are distributed according to niche breadth, which in turn depends upon location along an r - K axis (Section 4.1.4, Text Figs. 4.7, 4.8 & 4.9).

Section 4.3 Stability Regimes in the Lower Chalk

Plus ça change hinges upon environmental stability within a geological timeframe; the factors which operate at this scale need to be isolated, so we can consider the effect they had on processes operating across shorter or longer spans. ‘Geological’ time encompasses anything from millennia to the age of the Earth, but for a survey spanning only a million years in total something on the order of tens to hundreds of thousands of years is appropriate: it needs to be of sufficient duration for us to resolve it into a manageable number of instances, and there need to be a sufficient number of instances to identify variation between batches. The most obvious target is the Milankovitch scale precessional cyclicality, precisely the reason the section was chosen for study, and to a lesser extent the variations in water depth which seem to be cyclic on a scale of several hundreds of thousands of years (Robaszynski *et al.*, 1998; Mitchell and Carr, 1998).

Since the phytoplankton played an important role in couplet formation, were a primary component of the sediment, and were also a major determinant of benthic ecosystem structure, we can start by developing a better understanding of geological scale controls on productivity in the Chalk Sea.

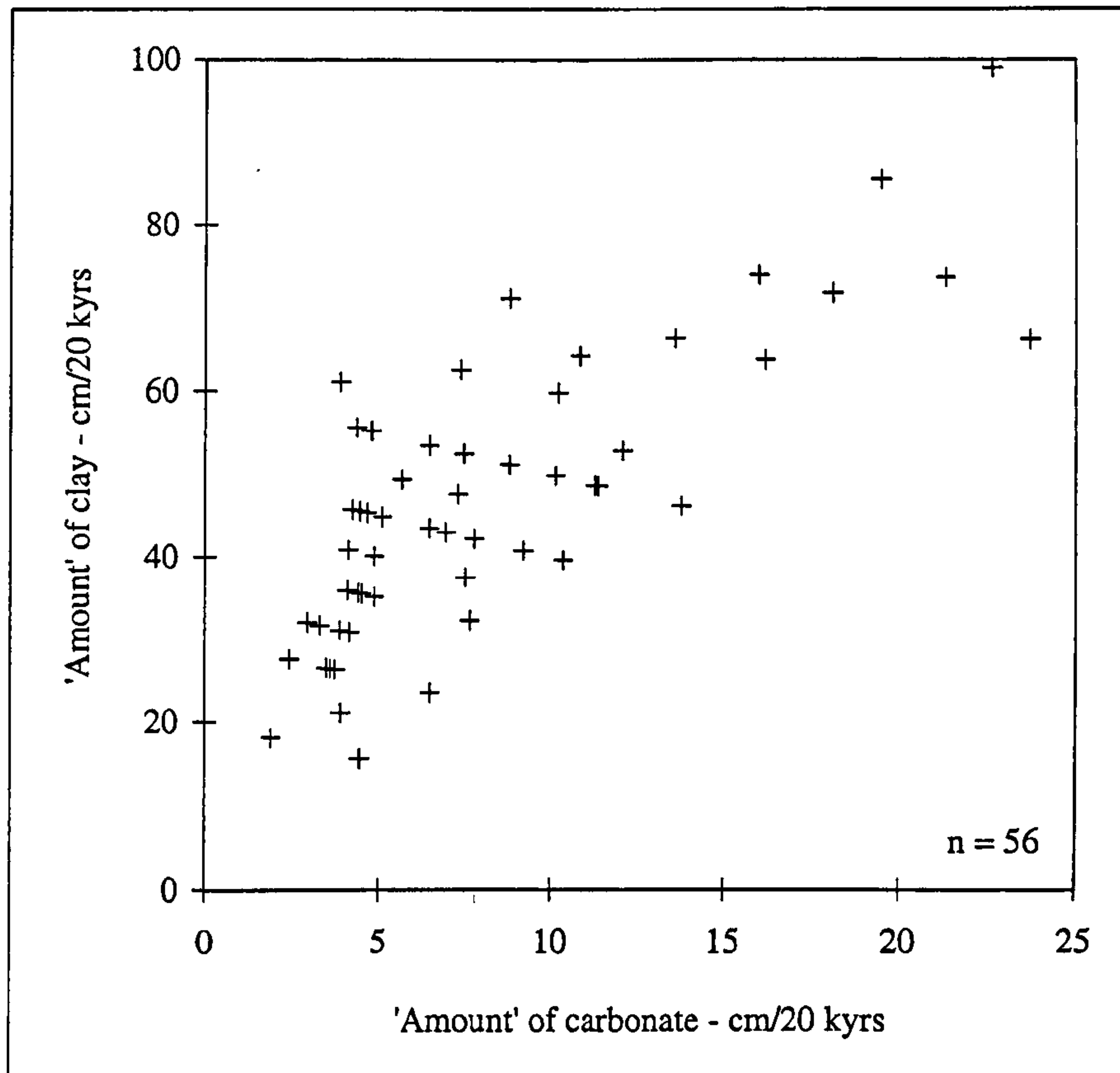
4.3.1 Milankovitch Cyclicality and Primary Productivity

The graphic logs for all three sites (Appdx. Fig. 1.1) and acid insoluble residue data for every couplet at Folkestone (Text Fig. 4.19, in Section 4.3.2, below) are evidence that the sedimentary cyclicality varied across the succession: specifically, that the cycles were stronger in the lower half and weaker in the upper. If the interpretation based on modern phytoplankton studies, advanced in Section 4.1.1, is correct, then the main limiting factors to chalk production would have been water temperature and the availability of nutrients. Surface water conditions must have been governed by a seasonal interplay of currents, sunshine and wind, just as they are today, with solar flux clearly being the main variable on the scale of chalk-marl cyclicality. Precessional cycles, as astronomical phenomena, are virtually invariant, so while changes in solar flux may well have controlled the cycle

formation itself, they cannot have been directly responsible for the *differences* in cycle strength between upper and lower halves of the succession. So what else could?

One major change occurring across the sequence was a progressive deepening of the water, with a lowstand centred on the B-C block boundary and a highstand somewhere in the middle to upper Cs (e.g. Paul *et al.*, 1994; Robaszynski *et al.*, 1998; Section 2.1.6.). Depth could have influenced productivity cycles in three ways, two of which are consistent with a maximum distinction between chalk and marl in the shallower part of the succession. Firstly, it could be that the shallower water was easier to warm so that the average water temperature was higher; this does not really explain a difference in composition between couplet halves, however, since the temperature would have been higher in precessional winters too. Secondly, and more plausibly, it could be that runoff from the surrounding uncovered land was providing nutrients for the phytoplankton. And finally, it could be that the shallower water was more easily agitated and thus brought more nutrients up into the photic zone (Mitchell and Carr, 1998, advanced a similar model to account for the distribution of planktonic forams, albeit for short transgressive cycles on a 100 kyr scale).

The amount of clay coming into the basin was quite definitely linked to the amount of carbonate produced. By using the insoluble residue data from each bed in the Folkestone section it is possible to calculate roughly 'how much' carbonate and clay was accumulated over a given 20 kyr span. The method is to multiply the *thickness* of each *bed* (not couplet) by the *proportion* of insoluble residue, and then add the values from either half of a couplet to one another. This kind of calculation should not be taken too literally because bed thicknesses vary laterally from place to place; and, since there is only one datum from each bed, the method assumes an unrealistic instantaneous transition from chalk to marl. Nevertheless, it does provide us with *some* information about the amounts of clay per unit of time. The same procedure for the carbonate (or simply subtracting the value for the clay from the total couplet thickness) gives an amount of both clay and carbonate in 'vertical cm per 20 kyr cycle'. Text Figure 4.16 presents these values plotted against one another, and demonstrates that they were highly correlated; in fact they correlate at $r = 0.777$, which in this case is significant to a confidence level of 0.001. I can think of no better reason why carbonate and clay should be so correlated than that terrestrial runoff (plausibly linked to temperature driven climate change) was enhancing productivity.

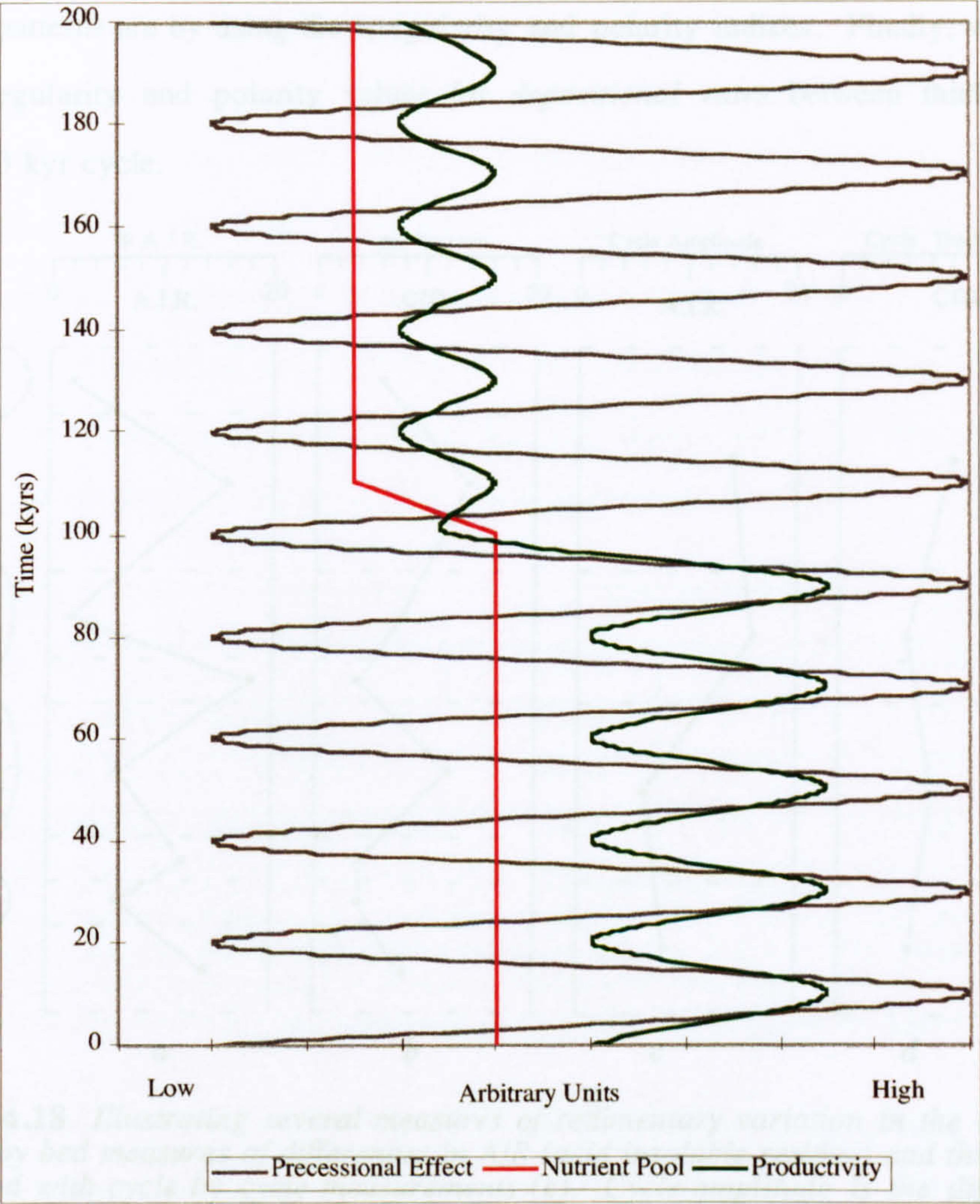


Text Figure 4.16 *A positive correlation between carbonate and clay. Note that abscissa and ordinate scales are unequal. See text above for method and discussion. $r = 0.777$, $t = 9.058$; 0.001 significance for $v = 54$ is $t > 3.232$.*

The runoff and agitation hypotheses advanced above both involve the kind of events which might plausibly be linked to precessional climate change, and Text Figure 4.16 illustrates the strong link between clay input and productivity. But Paul's (1992) use of carbonate versus insoluble residue clocks to calculate equivalent couplet thicknesses between different sites (see Section 2.1.3. for discussion), shows us that the change of composition involved an input of carbonate to a rather steady supply of clay. So while total couplet *thickness* is a function of the amount of clay introduced to the basin, the *strength of cyclicity* cannot have been. The input of clay remained roughly constant throughout the duration of a single cycle (otherwise Paul's calculations wouldn't have worked), which relegates a simple runoff (dilution) scenario to second place when it comes to explaining the couplets, and supports the contention already made (Section 4.1)—that cyclicity had more to do with mixing by violent seasonal storms in the precessional summers.

The kind of process I have in mind for linking a runoff associated increase in nutrients with cyclic productivity invokes a loosening of the limiting factors connected with

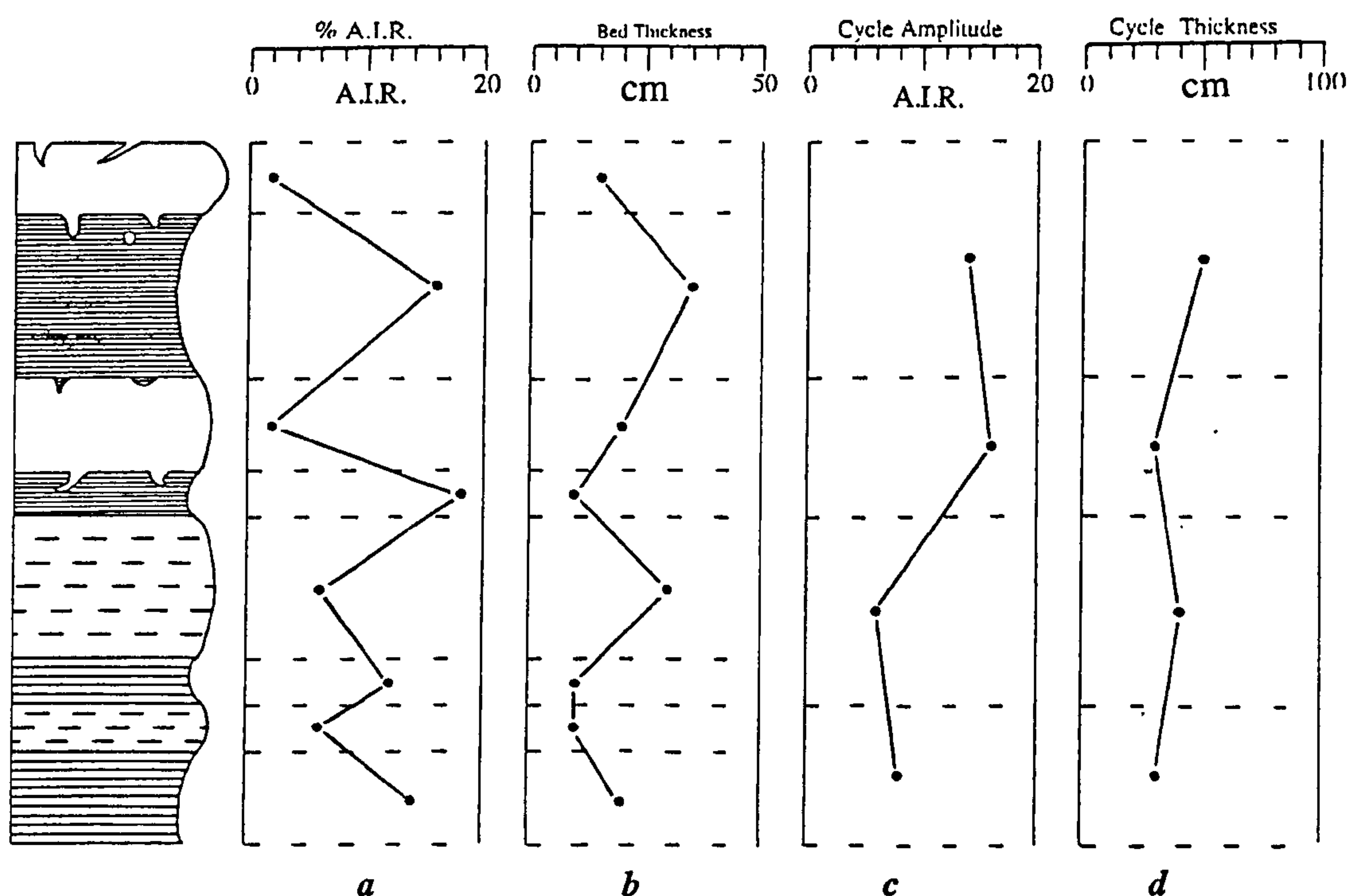
normal phytoplankton blooms. Given the increase in temperature suggested by Ditchfield and Marshall (1989) and mixing suggested by Ito *et al.* (2001), productivity could occur a little faster in precessional summers if, and *only* if, there were sufficient nutrients available. Without the extra nutrients, that difference in solar energy had a very limited effect on the rate of phytoplankton production. No matter how much the yearly winter storms blew during those energetic ‘precessional summers’, the turbulence could only bring enriched waters to the surface if they were there in the first place. And the nutrient pool seems to have been related to the overall input of clay, itself a function of sea level and terrestrial exposure. These factors are summarised in Text Fig 4.17 below.



Text Figure 4.17 Relationship between nutrient availability, precessional effects and productivity. Nutrients are the limiting factors to phytoplankton production. Productivity will rise when more nutrients are available, but the availability also depends upon mixing, which is enhanced by the extra energy available during precessional summers.

4.3.2 Distribution of Variations in Cyclicity

Whatever the precessional forces were, be they temperature or mixing effects, there is little doubt that they were driving the productivity cycles, and that the magnitude of the effect varied at different parts of the succession. There are a number of ways we could measure sedimentary properties to assess how they are distributed across the study sections. Firstly, and most straightforwardly, we can consider the *magnitude of compositional difference between adjacent beds* (expressed as the carbonate to non-carbonate ratio); but we might also take the *amplitude of change across a single couplet*, and compare it with the amplitude of change across others (Text Fig 4.18). For each of these we can consider how variable the patterns are by using the irregularity and polarity indices. Finally, we can also calculate irregularity and polarity values for *depositional rates* between thicknesses of equivalent 20 kyr cycle.



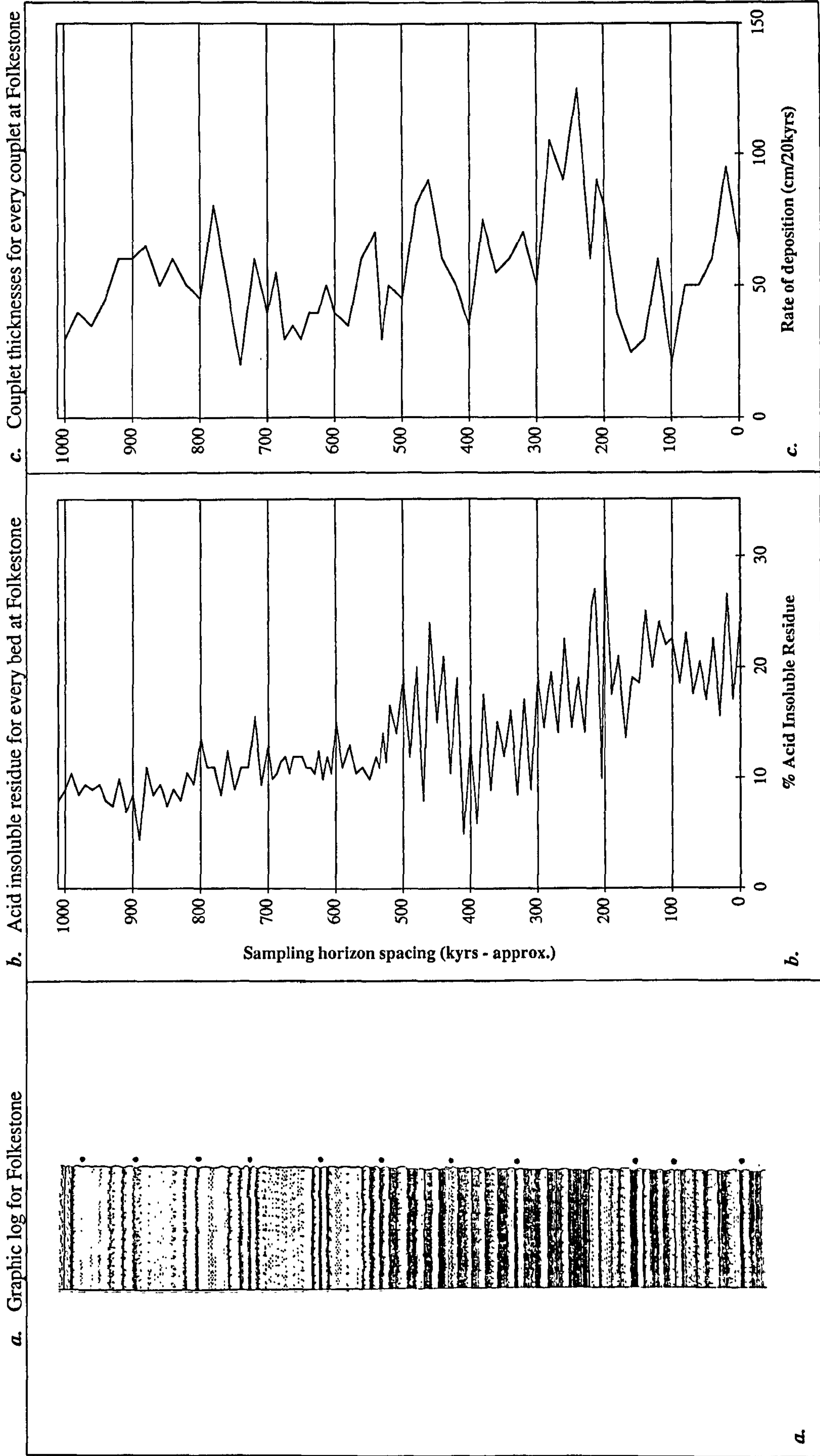
Text Figure 4.18 Illustrating several measures of sedimentary variation in the chalk-marl cycles. Bed by bed measures of differences in AIR (acid insoluble residue) and thickness (a) are contrasted with cycle by cycle measurements (c). Cycle amplitude is the difference in AIR (clay content) across a single couplet; it gives a measure of how dramatic the change from marl to chalk was. Bed by bed thickness (b) and cycle by cycle thickness (d) are self-evident. Each of these variations can be measured as polarity (deviation from the mean) or irregularity (sequential variation in absolute magnitude), as explained in Section 3.2.4.i); note, however, that this time we are interested in absolute magnitudes so it is not necessary to relativise the values to the sequence mean. Unlike the change in composition associated with AIR (a), the relevance of bed thickness (b) is uncertain: sedimentation never really stops, and rates cannot be measured to better than a bulk value per 20 kyrs; so, although it is a potential factor, the thickness of individual beds has not been used in the assessment of variability and is shown here for explanatory purposes only.

As explained in Section 3.2.4.i, irregularity is a most important measure because it captures the temporal trajectory, the ‘perspective’, of any species passing through the environment in question. Cycles can be extremely predictable despite the fact that they oscillate, and polarity alone fails to capture that fact. Cycles can also occur at a variety of scales; but, whilst a hierarchy of rhythms at different wavelengths may well be present in the Lower Chalk, only the precessional scale is considered here since it is the clearest and the one at the most appropriate scale for testing *Plus ça change*. There is not enough insoluble residue data from either Southerham or Escalles to perform a detailed study of the sequence at those sites, so this section will concentrate on the transect from Folkestone where an insoluble residue reading is available for every bed. The aim is to make a case for taking the suggestive appearance of the Folkestone graphic log at face value, so that the same impressionistic strategy can then be extended to the other two sites (see Text Fig. 4.19 and compare with Appdx. Fig. 1.1). To quantify this impression, the succession was split into two halves around couplet C15 [500] (which is included in both data sets) and the measurements explained above in Text Figure 4.18 were calculated separately for each half. The results are summarised in Text Table 4.6 and clearly show that *the magnitude of variation is always larger in the lower half of the succession*.

Variability Metric	Polarity		Irregularity	
Sequence Portion	Lower	Upper	Lower	Upper
a) Between Bed Cyclicity (% AIR)	5.64	2.39	7.13	2.08
c) Between Couplet Cyclicity (% AIR)	4.16	1.71	4.59	1.76
d) Between Couplet Depn. Rate (cm/20 kyr)	25.1	13.7	23.8	14.6

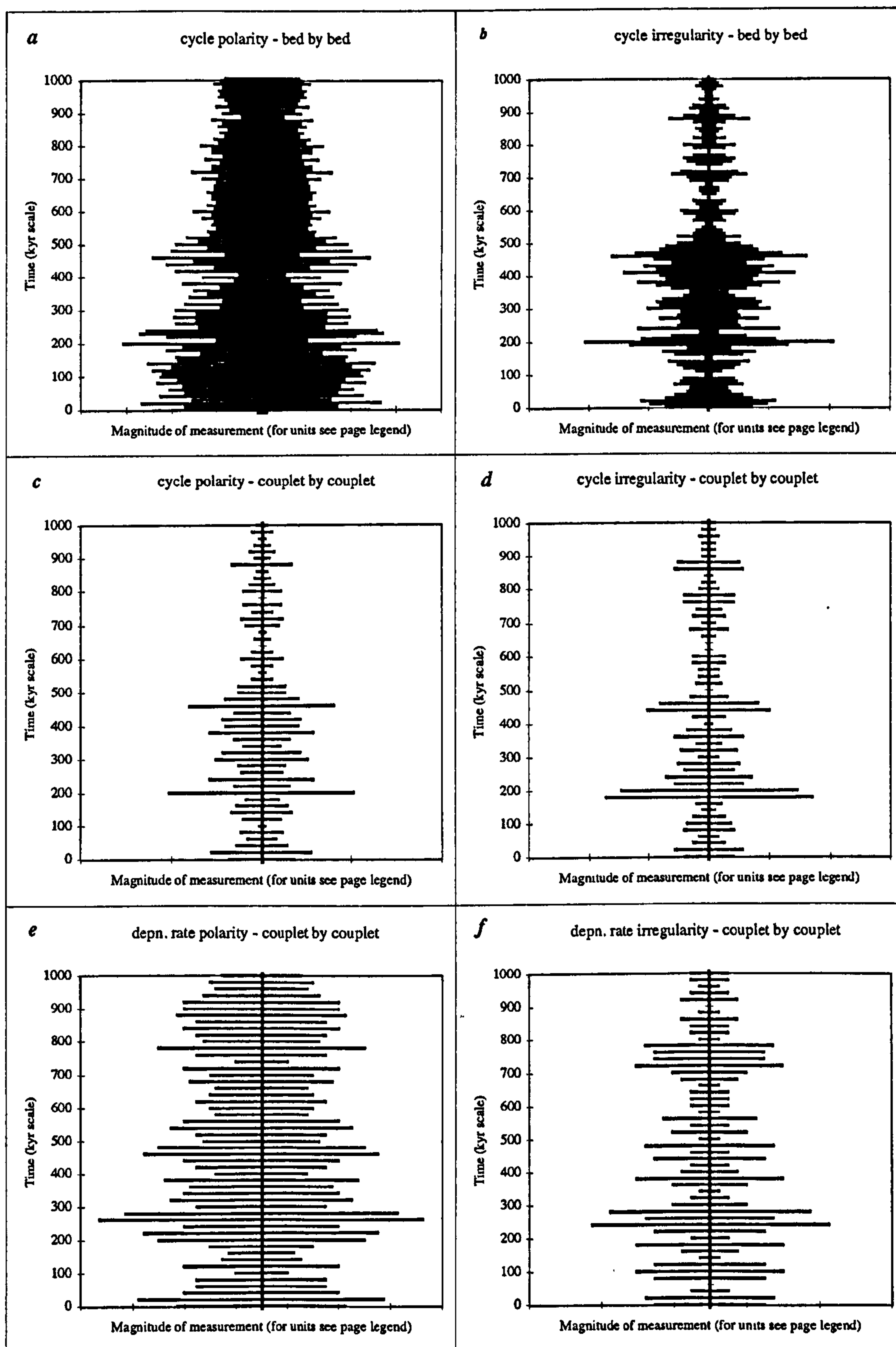
Text Table 4.6 *Measures of variation in cycle strength and depositional rate between the upper and lower halves of the study succession at Folkestone. Polarity and Irregularity are calculated according to the specifications given in Section 3.2.4.i. The three measures of sedimentary variability correspond to features depicted in Text Fig. 4.18. Note that in every case, the values are larger for the lower half of the sequence than for the upper.*

Text Figure 4.20 shows the data which generated these results plotted as timeseries ‘spindle’ diagrams: the pattern intuitively matches that seen in the graphic log for Folkestone, and consequently it is reasonable to suppose that such logs can be taken at face value. Cycle strength and regularity, and also fluctuations in depositional rate, are markedly more variable in the lower half of the succession than they are in the upper, forming two quite distinct stability regimes. This is true for all three sites investigated (Appendix



100 kyr time lines are approximations only; they correspond to the 100 kyr resolution sampling points, which are not perfectly evenly spaced. Extra beds are 'shoehorned' in between the marked horizons.

Text Figure 4.19 *Fine detail physical characteristics of the Folkestone study section.*



Text Figure 4.20 Spindle diagrams for variability in cycle strength and thickness. The absolute value for each measurement is split in two and distributed evenly about an arbitrary reference point (the vertical line, in this case the mean). The diagrams are designed to show the relative magnitude of sequential signals and so absolute values are unimportant (they can be found in Appdx. Table 1.7). As usual Polarity records the absolute magnitude of some value as a deviation from the mean, Irregularity records the difference between adjacent values up-section. Units of measurement are: a & b - absolute value of % AIR; b & d - differences in value of % AIR; e & f - differences in value for deposition rate (in vertical cm/20 kyrs).

Figure 1.1), and probably extends across the whole of the relic Chalk Sea (as Andy Gale's other work suggests e.g. 1995), although we can perhaps expect the distinction to be muted towards the middle of the basin. The variation occurs on a scale of tens to hundreds of thousands of years and thus matches the requirements of the *Plus ça change* model remarkably well.

4.3.3 Distribution of Aperiodic Events

In addition to variations in the pervasive background cyclicity, there are also a small number of one-off events which are not repeated over the interval in question. By far and away the most impressive of these occur at the B-C block boundary, exemplified in the data set by samples from B41 [200]. In reality there are probably a number of partly independent events at work here and these were discussed in Section 2.1.6. (for sources see refs. therein). There was the general lowstand and sequence boundary with its widespread erosion, odd rhythmicity and deposition rate fluctuations; there was also the phenomenon represented by the $\delta^{13}\text{C}$ isotope excursions at B41 (the *arlesiensis* bed) & C1 (the *primus* bed), probably eutrophication events with associated dysaerobic conditions.

The only event remotely like the B-C block anoxia episode is shown by a hump in the $\delta^{13}\text{C}$ trace, around two million years earlier at the Albian-Cenomanian boundary (see Text Fig. 2.2). Nor does a phenomenon of this type occur again until some two million years later, where it had a most impressive effect on the fauna of the well documented Plenus Marls (Jarvis *et al.*, 1988; Hart, 1996). With regards to the sequence boundary, there were certainly others, for example, the A-B and C-D block boundaries, which do not coincide with $\delta^{13}\text{C}$ peaks. Such events are frequently repeated during transgressive sequences, and are therefore fairly predictable, albeit on a timescale which is long by the standards of the interval under scrutiny. But the real significance of a sequence boundary occurring roughly 200 000 years into the study section is that it constitutes a major disruption in the lower half of the succession, and hence an irregularity or instability of some sort. That it was linked with an unusual anoxic episode only serves to highlight the effect; but any period of shallow water is intrusive to the marine realm in a way that a period of deep water is not: it brings with it markedly different sedimentological conditions, variable current regimes, more terrestrial material and, all in all, a taste of that most alien of

worlds—the land. When Sheldon (1996) suggests that shallow marine sequences are more variable than deepwater facies, this is the sort of thing he means; but even *within* a particular class of marine setting there will be periods of shallow and deep, with the shallower ones representing relatively more variable conditions; and that was the reason for arranging the unstable zone around the B-C block boundary.

There is a further one-off event of which much has been made: the P/B break at couplet C10 [400]. Carter and Hart (1979) devote a substantial portion of their text to explaining, in terms of rapid sea-level rise, the sudden appearance of a large proportion of planktic foraminifera (Section 2.1.6). Weaver (1982) followed them by organising his ostracod range charts around that level; and in fact the P/B break has been mentioned in most of the subsequent mid-Cenomanian (Lower Chalk) literature. There is not enough data available here to validate Weaver's claims, but from this study there certainly appears to be a considerable increase in the proportion of planktic foraminifera (mostly the genus *Hedbergella*) sometime after C10 [400] (Appdx. Figs. 3.[3, 4].iv.t). Unfortunately, there was almost no effect on the benthic foraminiferal fauna. Couplet C10 [400] was deliberately selected because of its reputation, and C11-C20 picked at least partly in the hope of finding something interesting going on; but there is nothing. Nevertheless, events higher in the water column may have had some kind of effect on the sea-bed, and the P/B break can be tentatively entered as an aperiodic fluctuation.

These noteworthy episodes both occur in the lower half of the study sections, but not a single published study, that I have been able to find, proclaims an 'event' of any kind between C15 [500] and D1, the base of the next sequence block. There are studies of single couplets in this zone (e.g. Ditchfield and Marshall, 1989; Leary, Cottle & Ditchfield, 1990; Leary and Hart, 1992; Paul, 1992), but they are all taken to be representative of steady background conditions. As a further example, in his monograph on the stratigraphy of the Lower Chalk, Kennedy (1969) split the lower half of the study section (B31-C15), 28 couplets over a vertical span of 20m, into six zones on the basis of faunal and sedimentological marker horizons; by contrast, he encapsulated the upper portion (C16-C45), 30 couplets spanning 12m of sediment and 500 000 years worth of time, into a single stratigraphic unit because it bore no distinctive internal features. So in terms of both variations in cyclicity *and* one-off aperiodic events, the lower half of the section fluctuates more than the upper.

4.3.4 Faunal Response to Orbital Variation

A good case has been made for a particular kind of faunal response to the yearly productivity cycle (Sections 2.2.4 & 4.1.1; Text Fig. 4.1), along with an argument that the effect should scale up to precessional cyclicity, especially if the process occurred by increasing the volume of phytoplankton *delivered rapidly or unexpectedly* to the system, rather than by simply extending its duration (Sections 2.2.5 & 4.1.1; Text Figs. 4.2 & 4.3). The fauna exhibits a characteristic response in couplet C13 that includes a massive surge in ‘absolute’ abundance throughout the chalk, but also associated changes in the relative abundance of certain taxa. Notably, many of the taxa which increase in relative abundance in carbonate rich samples are those which are very common normally; conversely, most of the taxa which decrease in proportion during the chalk, and are correspondingly more common in the marl of that cycle, are those which are generally rare: this prompted the designations of *r*- and *K*- strategist, respectively, to each type.

What has not yet been demonstrated, and indeed is undemonstrable given the data to hand, is that the response of the benthic fauna in C13 was typical across chalk-marl cycles in general. Whilst other workers (e.g. Leary, Cottle & Ditchfield, 1990; Leary and Hart, 1992; Paul, 1992; Mitchell and Carr, 1998) have published results which seem to be in broad agreement with my conclusions, none of them has presented data in a format that enables the link between cyclicity and relative abundance to be clearly seen. The closest is Paul (1992) who showed initial abundances (deposition rate uncorrected) for various taxa across C14, allowing a rough estimate of relative abundance, and they at least seem to confirm the pattern.

But what is really wanting is an illustration that the absolute and relative abundance patterns are repeated cycle after cycle, and preferably that their expression is proportional to cycle strength. A direct empirical demonstration along these lines would require the sampling of several couplets, with different degrees of cycle development, to the same resolution as C13—an endeavour well beyond the scope of this project.

Fortunately, an indirect alternative *is* available from the present data set. Cycle strength is a function of how much the carbonate percentage differs across a particular couplet, and what *can* be shown is that at least some of the fauna are strongly correlated with the clay/carbonate ratio. The effect is seen in the disparate changes to relative abundance in those elements previously identified as *r*- or *K*- strategists. As suggested by

the *r*-*K* faunal model, the relative abundance of certain opportunists tends to increase, along with the percentage of carbonate, so as to form a positive correlation; whilst that of the *K*-strategists tends to diminish, producing a negative correlation.

To avoid this pattern simply being a reiteration of the one already claimed in connection with C13, correlations were carried out using a number of different data bases. The most restricted is composed only of those samples spaced more widely than 2 kyr, i.e. the amalgamated 100 kyr samples from Southerham, Folkestone and Escalles, along with the 20 kyr ones from Folkestone (the averaged marl sample drawn from horizons 7, 8 & 9 in C13 seems fair game so it is included in this set), but *not* those from B41, which is again regarded as atypical (so $n = 38: 32-3+9$). Other combinations of sample horizons give results which are broadly comparable. The values I shall focus on can be found in Appendix Table 1.10.

Considerable care should be taken when interpreting this series of correlations because although there is no reason why the sediment composition should not, in principle, be entirely independent of particular relative abundance patterns, the same cannot be said of relationships between the taxa themselves. Consequently, a correlation between sediment type and just one faunal element is likely to generate other correlations as a passive side effect. A clear example of this is seen in the total benthic foraminifera and ostracod correlations in Appdx. Table 1.10: they have the same values, but opposite signs. Since these groups are expressed as relative abundances of a two group system, a correlation between the insoluble residue and just one of them necessitates an equivalent but opposite correlation with the other. One of the correlations could be an entirely passive effect, and we have no way of knowing which one.

But wait a moment, what does it mean to say that *one* of the correlations could be a passive effect? If we are treating the fauna as a set of players in a zero-sum game, then there is no such thing as a passive effect. Think about comparing winning football teams with their home and away matches: if the team which won was always the one playing at home, would it make sense to ask whether it was 'playing at home' that correlated with winning or 'playing away' that correlated with losing? Although the matter under consideration—the ubiquity of the *r*-*K* axis—rather assumes that the fauna was in a zero-sum arrangement around phytoplankton input, we should nevertheless acknowledge the potential for different elements to exhibit free play (for example by tracking factors

additional to phytoplankton availability). The situation is less clear in the long term because then the game is probably *non-zero* sum, and the faunal elements truly independent. But the point is that by artificially forcing species into percentage contributions we are treating them *as though* they were involved in a zero-sum game, and passive correlations can easily arise as a consequence.

Since I can think of no way around this problem, I shall just limit my claim: the correlations show us that *something* in the benthic microfossil community was correlating with sediment composition. In order to investigate the conditions under which active patterns are imprinted on passive recipients, I constructed several makeshift model communities with similar parameters to those in the foraminiferal fauna (log normal distributions, equivalent variation around relative abundance means etc.), and which incorporated both active (independently variable) elements and passive ones. It turns out that a large relative abundance for the pattern donor, along with a very strong signal (i.e. high polarity and irregularity), are, unsurprisingly, the most important factors in causing an unvarying element to passively pick a pattern up. Any active pattern is spread evenly throughout the rest of the set, so in a highly partitioned community there needs to be a lot of signal to go around; thus, the element with the highest abundance, or the largest amplitude of oscillation, generally tends to be the one which overcomes the noise of other active parties to clearly impose itself upon the passive set.

Among those members of the foraminiferal community which show a correlation with carbonate content, only *Tritaxia* is abundant enough to pass it on to all the others. It is also virtually the only species oppositely correlated to most of the others in this respect. So we can be fairly sure that *Tritaxia* at least was actively affected by the sediment composition, even if all the other *apparently* correlating species were, in actuality, totally indifferent.

Tritaxia correlates positively with carbonate content, and so do two other major groupings: the ostracods as a proportion of the total benthic fauna, and the planktonic forams as a proportion of the total foraminiferal fauna (Appdx. Table 1.10). I find this surprising; certainly I would have expected the ostracods to be outstripped by foraminifera when food became abundant. The best explanation I can think of is that both the plankton and the ostracods, being mobile, could track the shifting coccolithophorid clouds more effectively, whether on the surface or the sea bed; and, who knows, perhaps this was *Tritaxia's* secret too.

Note that it is not the *amount* of carbonate ($\text{CaCO}_3/20$ kyr cycle) that the fauna correlates so well with, nor is it the overall rate of deposition: it is the *proportion* of carbonate in the sediment (% AIR). We know that clay and carbonate go together, and that when the input of clay to the basin was high, the input of carbonate was too (Text Figure 5.16). The percentage of acid insoluble residue, by contrast, measures something like ‘the amount of carbonate *more than would be expected* from a given input of clay’. For a given input of terrestrial material, the yearly productivity would generally constitute some roughly determinate and thus predictable volume; the fauna is correlating with the amount more or less than that determinate and predictable volume. The percentage of acid insoluble residue is a measure of the *unexpectedness* of the phytoplankton input. It is thus highly relevant to the *Plus ça change* model, which operates around the biological perspective to whom such predictability might be a matter for concern.

As an alternative to the productivity-based explanation, I suppose we might hypothesise that these correlations actually concern more proximal aspects of sediment composition, its texture and porosity perhaps. Whereas *Tritaxia* and the ostracods tended to avoid clay-rich sediments, the other foraminifera flourished in them. Why this should be so is not entirely obvious, but it is not beyond the bounds of credibility, either, and should not be rejected out of hand; the literature, after all, is crammed with accounts of correlations between benthic foraminifera and the sediment type in which they are found (e.g. Murray, 1991), although I suspect that this largely reflects the fact that sediment type is such an easy variable to measure. My guess is that sediment composition as a physical variable may account for a small proportion of the behaviour we observe, but not a whole lot of it; and without a better understanding of the biological motives behind a passion for clay, I am unwilling to grant the idea too much importance.

A much more likely scenario, I maintain, is that the community really *was* arranged around a zero-sum response to phytoplankton (carbonate) input. Some species obviously *were* free to vary more or less independently, or at least to buck the trend, because they were tracking other conditions alongside phytoplankton availability; thus, we see major elements correlating only weakly with the gross composition of the sediment (e.g. *Lenticulina rotulata*, *Gavelinella cenomanica*), not to mention those whose distribution patterns shift markedly through time (e.g. *Pseudotextulariella cretosa*) suggesting they were habitat tracking on a grand scale (Sections 4.2.2 & 4.2.4). Indeed, it may even be the case that some species were free to vary independently of the phytoplankton input precisely *because*

Tritaxia was so tightly correlated with it; that would be in line with ecological locking models which posit a stable community hierarchically organized around a generalist hub, whose 'function' within the system is to soak up short-term variation and stop it translating throughout (Section 1.1.5).

But, by and large, the community seems to have been aligned along a resource availability axis which bore *Tritaxia* as the prow and the rare nodosarian species as the stern. We can imagine the entire fauna pitching back and forth along waves in this r - K axis, depending upon the irregularity of food input. Text Figure 4.15 depicts the yearly succession of species peaking sequentially, and from the model presented in Text Figure 4.2, we can readily see how any increase in the magnitude of instantaneously delivered phytoplankton would enhance the r -strategist end, while any increase in slowly delivered or constantly available foodstuffs would enhance the K -strategist end. Insofar as the irregularity or unexpectedness of phytoplankton input is reflected by the clay/carbonate ratio, the community structure can be expected to have swung from a strongly lop-sided, low diversity arrangement to a more equitable, high diversity pattern, in accordance with the sediment composition (see Text Fig 3.6 for diversity patterns).

Sadly, this effect is *not* reflected by the overall diversity metric itself (Appdx. Table 1.10, probably because there was so much noise from the independently behaving species (especially the ostracods), and from preservational factors like the overall deposition rate. I have no doubt that a good correlation could be found if we were to prepared to selectively assemble a community of 'carbonate responsive species' and measure its shifting diversity patterns through time, although that would basically be cheating, and would certainly not constitute good science.

Happily, with respect to the rich narrative licensed by such a wonderful data set, the structure of the argument required for *Plus ça change* permits a certain amount of leeway: it actually does not matter *why* some elements of the fauna were correlated with sediment type, the fact is that they were, and to a very significant degree. *All* of the explanations put forward can turn out to be wrong without there being any doubt about this empirical fact: that *Tritaxia* at least was correlated with sediment composition. Since correlation implies a causal connection, and causality requires a transmission of information structure, the fact that carbonate content varied in the way shown in Section 4.3.2 means those elements which actively correlate with it *must* have followed suit (with a one part in a thousand probability

that the correlation is by chance). Strictly speaking, the correlations shown apply only to differences in carbonate content between *marls*, but there is no reason why they should not be taken as a general result and extended to differences within couplets; in which case faunal oscillation can be mapped, in a fairly literal way, onto the insoluble residue chart and spindle diagrams of Text Figures 4.19 & 4.20, and from there onto the graphic logs themselves. From *Tritaxia*'s perspective, there were undoubtedly variable stability regimes in the Lower Chalk—instability for the first half-a-million years, and relative stability for the second.

4.3.5 Faunal Response to Aperiodic Variation

When it comes to aperiodic disturbances there is no problem whatever in demonstrating that the fauna was affected. The events at B41 have dominated the data set throughout, and this horizon is only a representative of the general zone (Mitchell and Carr, 1998, document the rest). Was the fauna reacting to low sea-level, low oxygen, low water temperature, high organic input, high clay content or high sedimentation rate (Paul *et al.*, 1994; Jarvis *et al.*, 1988; Mitchell and Carr, 1998)? We are spoilt for choice. Again, and quite importantly from the perspective of *Plus ça change*, it does not really matter which of these influences was involved in the faunal commotion at B41, as long as something unusual happened—and there can be no doubt that it did. But it would be a shame to pass over the opportunity of another neat interpretation.

Mitchell and Carr (1998) demonstrate that the peculiarities of B41 extend throughout couplets B42 and B43 (a period of 60 kyrs), and perhaps even across the erosion surface (B44 and B45 are absent along the Channel exposures) and into C1 at the start of the next sequence. The most obvious explanation for this pattern would be the existence of something like a faunal gradient associated with water depth. Paul *et al.* (1994) document concentric layers of macrofossils arranged around the B-C block boundary (Section 2.2.6), and Mitchell (1996) showed a similar effect with foraminiferal assemblages around the same level but in the Cleveland Basin, claiming that the Anglo-Paris Basin fauna remains relatively homogeneous by comparison! Translation via Walther's Law makes this an obvious documentation of gradients in the community composition sweeping back and

forth across an area. If this is true then we can identify *Tritaxia* as a relatively deep-water form, and many of those peaking in B41 as shallow water equivalents.

But the features associated with the B-C block transition are much stronger than at any level outside the Plenus Marls, which is why there has been so much interest in this zone; and it seems likely that there were elements at play which do not routinely occur in other shallowing events (such as in the 'Jukes-Browne Bed VII' sequence at the base of D block). All indications are that productivity was spectacularly high at the time of B41: apart from producing a sequence of very thick couplets around a time of low sea level and maximum erosion, the $\delta^{13}\text{C}$ peak suggests an expanded oxygen minimum layer in the style of Schlanger and Jenkyns (1976; Section 2.1.6).

It occurs to me that in a situation of very low sea level, with maximum terrestrial exposure, and where waves could continuously disturb the sea bed—perhaps even during the summer months—that the distinct changes associated with spring in the open water might have become somewhat blurred. This is not to suggest that productivity was equally high all the year round, but rather that stratification was perhaps less pronounced, and, instead of being arranged around boom and bust periods, the phytoplankton were able to keep up a more continuous presence than usual. Without a spring bloom there is no selective advantage to being *r*-selected, and *Tritaxia*'s opportunistic approach would have failed. *K*-selected species should have filtered into the gap, and indeed that is more or less what we seem to see. Without any need to invoke multiple responses to a variety of external forces, we can explain both the physical (e.g. $\delta^{13}\text{C}$) and faunal changes in B41 by tuning out a single environmental variable (the spring bloom) and simply allowing the community structure to re-set itself.

Summary

Without specifying any environmental properties beyond a seasonal input of phytoplankton, the patterns seen in the Lower Chalk microfauna can be understood in terms of their distribution among a series of universal niche dimensions. These combine to form a hub-centred arrangement with a main axis running from *r*-strategists at one end to *K*-strategists at the other. *Tritaxia pyramidata* constitutes the *r*-selected, keystone generalist of

the whole arrangement, while behind it the rest of the fauna feathers out into an architecture of shifting alliances and conflicts.

The arrangement is meta-stable, reacting fluidly to short-term environmental fluctuations, by far the most important of which concern the seasonal influx of phytoplankton; but it plausibly owes its long-term stability to the perpetual rediscovery of a restricted set of relationships that crystallise out from the dynamic flux of more idiosyncratic ecological preferences. It has very likely been winnowed into the stable configuration it exhibits by constant exposure to a repeating set of environmental circumstances, and it is robust enough to persist or reassemble in the face of individualistic habitat tracking by various of its components.

The phytoplankton input to which this ecology is primarily adapted varies according to both orbital forcing and nutrient input, with the latter tending to amplify the former. The graphic logs of the study sections thus provide a good analogue representation of variations in the environment's primary resource over geological timeframes. While sediment thickness provides data on how much energy and material was available to the system per unit of time, the proportion of carbonate in the sediment reflects its predictability, and this in turn correlates well with shifts in faunal abundance along the central axis of the ecological edifice.

A one-off episode of environmental disruption associated with lowstand conditions around the B-C block boundary was superimposed upon this system. While well adapted to predictable variations in the wider environment, the community appears to have been pushed beyond its normal limits in this event by deletion of the seasonal component to its resource input. The hub species, *Tritaxia pyramidata*, lost a vital element of its broad niche and was thus displaced from its central location in the ecological framework. With the original hub no longer in place, the rest of the microfauna reconfigured itself to a new setting, permitting a successful invasion by several alien species. The event seems to have lasted for at least 60 000 years.

Part III Development

Introduction

The middle reaches of the Lower Chalk across the northern edge of the Anglo-Paris Basin have proved to be an admirable location for testing the *Plus ça change* model. All the necessary environmental criteria have been met; the fauna yields its ecological structure to a mix of careful observation and surmise; and there are several foraminiferal species occurring consistently and in sufficient quantity to meet most statistical needs. Among them, *Tritaxia pyramidata* is particularly suitable since it is almost always present in large numbers, of which a fair proportion are generally well preserved. In addition, its ecology is relatively clear. According to the story so far, it seems to have been an infaunal, *r*-selected generalist which held a keystone role in the community; it responds vigorously and fairly straightforwardly to resource fluctuations and larger scale environmental events alike; and it appears to have dominated the fauna ever more with time, suggesting that it was gradually out-competing other members of the ecosystem, either because the environment was shifting in its favour or because *Tritaxia* itself was discovering new strategies for survival.

The empirical aims of Part III are to describe and explain the form and growth sequence of *Tritaxia pyramidata* in order to produce a model that can later be used to examine morphological change within the sedimentary sequence. But this middle part of the thesis also explains its main theoretical foundations. After opening with a few general remarks about foraminiferal biology, Chapter 5 introduces the information theoretic paradigm; this is adopted as a bridge between ecology and development, and it will eventually provide a framework for interpreting the evolutionary material of Part IV. After this theoretical discussion, the empirical material on development is examined. A methodology for the morphological measurement of *Tritaxia* appears in Chapter 6, where the whole morphological data set is used to form a general representation of the fossil itself. Finally, in Chapter 7, the data presented in Chapter 6 is brought to life to give a dynamic interpretation of *Tritaxia*'s passage through morphospace during the course of development. This is the model carried over into Part IV.

Chapter 5 Living Matter

Introduction

In his elegant little book, 'What is Life?', Erwin Schrödinger (1944) mused on the physics of biology and concluded that living systems are those arrangements of matter which persist far from thermodynamic equilibrium by 'feeding on negative entropy'. Negative entropy is any orderly or dense concentration of matter and energy that can be expected to decay to a more disorderly state over time. According to Schrödinger, such thermodynamic decay provides the solution to life's problem of existence by fuelling its endless cycle of rebirth. Much of what follows owes a huge debt to Schrödinger's conception, albeit cast in the slightly more topical terms of information theory. Living systems are those which encode and deploy *information*, a term given some backbone in this chapter before being pressed into service as the conceptual interface between ecology, development and evolution. But before defining life in abstraction, we should start with a more earthy look at the alien lives of foraminifera themselves.

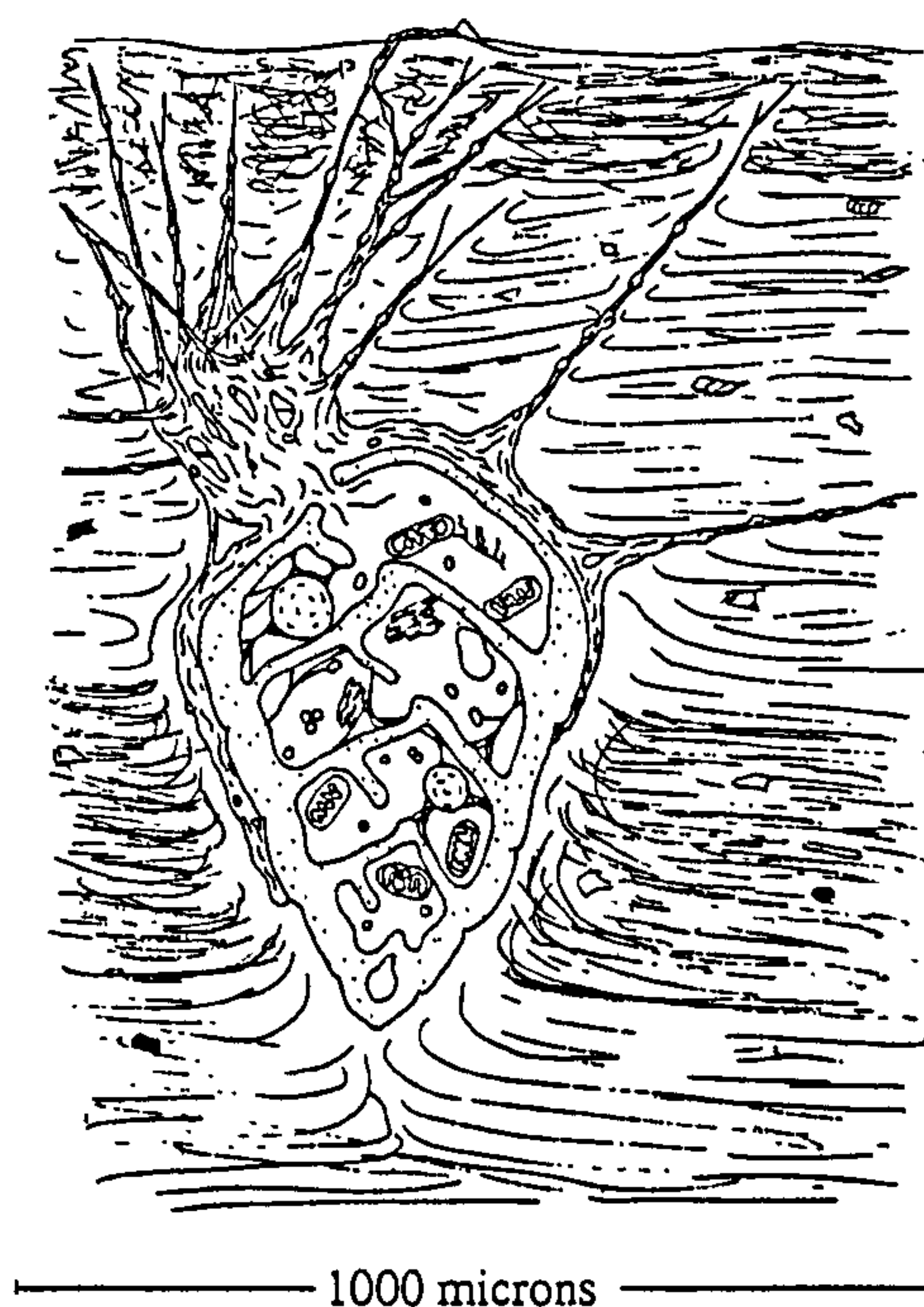
Section 5.1 Foraminifera

5.1.1 The Living Foraminiferan

Foraminifera are single celled amoeba-like eukaryotes (Phylum Protozoa, Class Rhizopoda) incorporating an internal, apertured test that separates the outermost cytoplasm from the inner. The main body of the cell is composed of dark, dense sol-like endoplasm which houses the usual organelles common to eukaryotes, and in which the main metabolic processes take place. These are co-ordinated by the nuclear material, and if the nucleus is removed the cell becomes disorganised, fails to digest and eventually dies (Haynes, 1981). The test itself is a gelatinous (proteinaceous mucopolysaccharide or 'tectin') bag which can either be naked or covered in a hard, mineralised or agglutinated chamber, or series of chambers, each of which is connected to the previous one with an opening—a foramen. These gaps in the structure allow access from chamber to chamber in multichambered

forms; the cell body is normally distributed between several chambers, sometimes with multiple nuclei scattered throughout. The test also incorporates one or more openings (apertures) through which the cytoplasm can extrude, these being created secondarily by dissolution around chamber sutures in multilocular forms or by maintaining a terminal aperture in the end wall of the final chamber of unilocular types, a feature which is preserved as a sequence of internal foraminae as the test develops (e.g. Loeblich and Tappan, 1964; Haynes, 1981; Lee, 1990; Murray, 1991).

The cytoplasm which issues from these apertures is clear, and forms a thin coating to the outside of the test. It gives rise to numerous branching granular threads which create a web of filaments, often reaching to several times the length of the main body. This 'ectoplasm' can be sticky and moves in a curious fashion, streaming in alternate directions along the length of a filament. By this method it is possible for the cell to collect food which adheres to the pseudopods and also to move at rates of a few millimetres per hour by shooting out threads which anchor to the substrate and then contract. When the organism is living within the sediment, the pseudopods tend to coalesce into robust bundles rather than spreading out, probably to push aside and probe through the surrounding detrital grains. It has been suggested that the granules in the pseudopods are mitochondria and stercomata, vacuoles full of waste. Collected food is normally digested outside the test in vacuoles housed in a temporary feeding cyst made of detrital material, and the digestion products passed inside through an aperture (Haynes, 1981).



Text Figure 5.1 *Cross section of an infaunal agglutinating foraminiferan in life position within a seasonally bedded sediment. Adapted from Haynes (1981).*

5.1.2 Reproduction

Foraminiferal life cycles seem to be extremely varied; so much so that it is difficult even to generalise (Lee, 1990). The 'classical' version is a plant-like alternation of generations between a haploid, sexually reproducing 'A' stage and a diploid, asexual 'B' stage. These two generations are often sufficiently distinct in morphology to be recognised as *A* or *B* forms, with the sexual *A* phase individuals being uninucleate and smaller, but with a larger first chamber or proloculus (they are said to be *megalospheric*). The mature *A* phase typically produces numerous tiny flagellate gametes which are released to swim free until they meet and fuse to form the minuscule, *microspheric* proloculus of the next stage. These mature into *B* phase forms which, by contrast, are multinucleate, diploid, and despite the small initial chamber, tend to grow to a larger overall size. When their time comes, they undergo meiosis and schizogony (nuclear and cytoplasmic division) and spew forth a further generation of haploid *A* forms. (Loeblich and Tappan, 1964; Haynes, 1981; Lee, 1990).

Many other combinations of sexual and asexual behaviour are also to be found, including species in which the gametes are not released but fuse to form zygotes within a single parental test, species in which the gametes of different parents combine only when those individuals themselves fuse together, asexual reproduction by diploid individuals, and single or multiple binary fission (Lee, 1990).

Reproduction will occur when an individual has amassed sufficient resources to do so and when conditions are ripe, rather than at some preordained stage of maturity. This is an important point to remember from the developmental standpoint because it introduces an environmental component to the lifecycle in place of a rigidly deterministic set of genetic instructions. Murray (1991) claims that the prompt for reproduction can be any one of a plexus of interacting factors such as temperature or light intensity, and that there is evidence to suggest that the presence of large amounts of food may override many of the others.

Elphidium crispum, provides a good example of this 'classic' life cycle. The species is apparently seasonally tuned: in the English Channel in winter the proportion of *A* forms to *B* is ~30:1; this changes to 1:1 or less in the spring as schizogony reaches a peak (Lee, 1990).

5.1.3 Functions of the Test

Numerous functions have been suggested for the foraminiferal test. Murray (1991) lists the following as commonly encountered examples: to protect the cell against predation; to provide shelter from unfavourable physical or chemical conditions; to assist in the growth of the cell; to control buoyancy; and to serve as a receptacle or concentration of excreted matter.

Dealing with the various suggestions in reverse order: Brasier (1986) suggested that biomineralization may be necessary to remove toxic Ca^{2+} ions from the cell body, but this does not explain why agglutinated tests are so common, particularly since they are probably less energy efficient than calcitic ones (Murray, 1991).

Buoyancy control is a fairly obvious function for species with a planktonic lifestyle but Marszalek et al. (1969) also noted that the benthic allogromiid *Iridia* stores low density lipids and suggested that in this case the test may be necessary as a compensation device, although the same effect could presumably be had by simply gathering sediment together without the need to arrange it into the elaborate structure of a test.

Arguments against the test as a means of support revolve around the fact that the cell itself needs to encyst and enclose the newly forming chambers: since the cell must support the chambers, the chambers cannot support the cell (Murray, 1991). This reasoning hinges on the misplaced notion that the cell itself is a static system with properties which do not alter. Cells have a cytoplasmic skeleton of microtubules which will change configuration when necessary as, for example, during cell division when spindle fibres form across the cell body to assist in chromosomal splitting. Since the cytoskeleton can form rigid structures on these occasions, it can presumably do so when a cyst is created for the purposes of construction—but that does not mean such temporary support structures remain, or that more permanent support is not needed during the everyday running of the cell. Besides, the temporary support offered by a cyst can hardly provide the compressive resistance of a mineralised test.

Unless a cell does incorporate some type of scaffolding, as plant cells do, it tends to have a very low compressive strength (Ingber, 1998). Being strung from the inside of a rigid calcite chamber must open up a number of possibilities otherwise denied to a naked protist, of which increased biomass and the option of an infaunal ecology are the most

obvious. It is no coincidence that forams are the largest single celled organisms, often growing to visible dimensions.

Although, according to Murray (1990), there is no evidence that the test can protect against predation, neither is there any reason to suppose that it cannot. Just because foraminifera have been observed to be eaten whole, test and all, does not necessarily imply that this is always the case, or that some individuals do not come out unscathed at the other end. And the test can certainly protect against unfavourable physical or chemical conditions. Marszalek *et al.* (1969) noted that many foraminifera can close off test openings for several hours by sealing them with debris, and Bradshaw (1961) demonstrated that *Ammonia tepida*, a species with a calcareous test, survived at a pH of 2.0 for over an hour, albeit mostly due to the test's organic component, and was later able to repair the dissolution which took place. Such strategies almost certainly give a foraminiferan the chance to pass through a deposit feeder's gut unscathed, and a test shape with ridges and spines could even hasten the procedure by irritating the gut-lining. (Having recently watched a small pond snail scour a petri dish clear of thousands of paramecii, rotifers and other single celled micro-organisms, leaving a tough-cuticled unicellular alga, *Closterium*, as the only eukaryote to emerge intact from its faecal pellets, I have no doubt at all that the possession of a test confers a massive selective advantage to foraminifera). And as for the organisms which have found a way to get inside the foram test (Lipps, 1983), these are specialist predators which have been selected, at least in part, for their ability to overcome the protective barrier and reach the morsels within. Many other organisms will not have evolved such an ability and so, although not 100% effective, the test must at least prevent foraminifera from being food for all.

Another way in which the test might be useful in the everyday running of a foraminiferan is by providing a means of splitting up the endoplasm. A unicellular organism must accomplish in a single workspace many of the processes which are distributed among several specialized organs in a metazoan. A multichambered test provides the opportunity of dividing up that workspace, and hence of assisting in the division of labour too. Certain agglutinated species from the Lower Chalk, *Arenobulimina advena*, for example, and *Pseudotextulariella cretosa* (see Carter and Hart, 1977, for the first and Barnard, 1963, for the second), have dozens of intricately partitioned

chambers—too much internal detail, one would think, to be a useless fluke of the building process.

But, all things considered, although some of the test's other proposed applications may play a minor role in the lifestyle of a foraminiferal cell, or even a major one depending on the species, as a general rule it seems likely that skeletal support and protective armoury are by far the most important. In accepting this, the main function of the foraminiferal test is brought into line with the function of hard parts in the vast majority of other shelled or test-bearing organisms.

5.1.4 Test Construction

DNA is the focus of much organisation in the daily running of any living system. The fact that digestion stops in foraminifera whenever the nucleus is removed implies that genetic material is responsible for orchestrating a supply of enzymes and other metabolic products in a process of continual consultation with the rest of the cell. But one of the things that makes single-celled organisms so fascinating is that they also display kinetic behaviour with a marked functionality. When the pseudopod of a foram touches something unpleasant and recoils from danger, does the logic of that reflex have to pass back to a central decision making unit within the nucleus? It seems unlikely and cumbersome that it should; but if not then presumably the reflex is confined to a more local level of decision-making, with behaviour as a whole distributed throughout the cell body.

Chamber formation provides a particularly interesting intersection between distributed behavioural co-ordination and the centralised decision-making of the nuclear DNA. Here, we know for sure that there must be at least *some* genetic guidance, because overall test form is a species specific trait, repeated generation after generation. Comprehending exactly how an inherited pattern of nucleotide bases gets translated into the three dimensional configuration of a freshly minted foraminiferal test, however, is an altogether more challenging project.

In its most primitive manifestation the test is no more than a pliable tectin membrane separating two zones of cytoplasm. The addition of randomly oriented detrital grains is the first step of a process which reaches its peak of development in beautifully

sculpted agglutinated structures composed of carefully selected and arranged grains of one specific mineral or another, bound together with a calcareous or ferruginous cement. In truly calcareous forms even the adventitious material is done away with and the test is composed only of the ‘cement’, which is secreted directly onto the tectin membrane as structured layers of minute crystals (e.g. Hemleben et al., 1989).

This process occurs within the confines of a protective cyst, normally gathered from surrounding sediment. According to Jepps (1942; quoted in Haynes, 1981; also consistent with Hemleben et al., 1989), within the cyst:

... “an unusually dense fan-shaped mass of anastomosing pseudopodia make their appearance, radiating from the terminal apertures of the last chamber of the shell”. [In time] “these arch over in a reticulum which outlines the cavity of a future chamber” ... [and] ... “gradually swell at their bases and merge into one another there, whilst a fluid wells out amongst them and comes to fill up a space they enclose ... This comes to have a clear cut surface, fashioned in the shape of the new cavity even to the retral processes and the projections at the future foramina ... As soon as the surface is available, a collection of shining granules may be seen there which gradually form a thin layer of shell. This seems to be laid down in patches like the pieces of a jigsaw puzzle, which unite, losing their separate outlines more or less completely as the shell thickens.”

Jepps was describing the process in the calcareous species, *Elphidium crispum*, and the details would obviously be different for other designs of calcareous test, and especially for cases of agglutination where specific types of particle must be gathered and added to the growing creation. But it does hint at the degree of organisation required for a single cell to build such a structure. How on earth is it all orchestrated? How does the “dense, fan-shaped mass of anastomosing pseudopodia” *know* to “arch over in a reticulum outlining the future chamber”?—and a specific size and shape of chamber at that!

Section 5.2 Aboutness and Context

5.2.1 One Domain, Two Descriptions

The question of control at a cellular level is part of a more general problem concerning ‘teleological’, apparently goal-directed agency, and the origin of smart

behaviour from essentially stupid components. If the enterprise to naturalise life processes, by shifting them from the ethereal realm of vital spirits and dualistic essences and onto the solid turf of physics and chemistry, is to succeed at all, it had better do so smoothly and convincingly, with no conjuring tricks along the way. But it is no mean feat to explain how a 'proteinaceous mucopolysaccharide bag' with a bit of DNA inside it could possibly 'know' anything at all; the complexity of a bottom-up causal account must be absolutely staggering. Consequently, answers to the questions posed in the section above can best be met through a more abstract, top-down framework which spans from cybernetics to linguistics and deep into the social sciences, branching into all manner of philosophical debate along the way. Fortunately, this is such a fascinating and compelling field that the theoretical literature is large, comprehensive, and has a well-defined common core, even though many biological details still remain obscure. The account I shall give is necessarily sparse; but still useful I hope.

First, I want to start with an example that highlights the difference between 'bottom-up' and 'top-down' approaches. Many organisms come partitioned into two distinct sexes, the proportions of which are generally 1:1. There are different strategies to explaining why this should be. Some explanations are case specific: in mammals, a distinct pair of sex chromosomes segregate in equal proportions during meiosis; in *Drosophila*, it depends on the ratio between female-determining X-chromosomes and the number of sets of autosomes, which are collectively male-determining; in addition to genetic factors, some species rely on environmental features such as the presence of pheromones or other externally variable prompts; in crocodiles, for example, sex is strongly influenced by the temperature of the nest (Gilbert, 1997).

These are all 'bottom-up', *causal/historical explanations*. They contrast strongly with the 'top-down' *equilibrium explanation* first provided by Ronald Fisher—'the singles bar effect'. Fisher's answer, put simply, was this: if either males or females start to outnumber the other, there is an immediate advantage to being the less numerous sex, so that selection quickly evens the balance. A 1:1 sex ratio is self-righting; it is an attractor of the type known as an evolutionarily stable strategy (Dawkins, 1976).

The important point is that specific causal/historical accounts are actually quite irrelevant to the equilibrium model: it doesn't matter *how* the 1:1 ratio is produced, so long as it is produced *somehow* (this is an attitude generally referred to as 'functionalism' in the cognitive sciences). Note how tempting it is to say that the equilibrium account is the 'real'

explanation: it seems to appeal to something ‘deeper’ than any of the specific bottom-up versions. Note also that the equilibrium account targets an element of repetition in the various individual examples: if they hadn’t all tended towards the same result, we would have had no reason to search for a ‘deeper’ rationale ‘behind’ the multitude of idiosyncratic mechanisms. Finally, (and self-reflexively) note how the language used to distinguish these two types of explanation relies heavily on spatial metaphor—‘top-down’, ‘bottom-up’, ‘deeper’, ‘behind’—to identify relationships that are otherwise totally abstract. All these noteworthy factors are related to one another, as we shall see in due course.

Life is about information—or “the control of matter *by* information”, to deploy George Williams’s felicitous phrase (Williams, 1992). Information is a slippery topic, however, and the way biologists themselves talk about it often leads to misunderstanding. In 1996, Williams (along with Dawkins) was accused of dualism by creationist lawyer Philip Johnson for claiming that the ‘codical domain’ was separate from the ‘material domain’. The codical domain is certainly *distinct* from the material domain (though perhaps not separate) and Williams was right to say that the distinction rests on how we describe the two of them. I shall try a tangential approach to illustrating what this means.

Once upon a time, messages were sent between London and naval ports like Portsmouth via the semaphore system. Men occupying hilltop lookouts would spot an incoming signal and pick up their telescope to watch another man on a different hilltop performing a ritual dance with some flags; then, they would fire up a warning beacon of their own, pick up their flags, and perform the same complicated structural manoeuvre for the next position down the line. But what was actually being ‘sent’? No single material item could be said to pass along the whole route: only the message itself reached the final destination.

Information is about pattern, not stuff. Patterns are structural relationships between parts. They are *substrate neutral* in that the same pattern can exist in many different types of medium, but they are *not substrate independent*, and thus they are not dualistic, either. A spiral galaxy, a hurricane and a cephalopod shell all have in common a spiral pattern, but it is realised on very different material substrates. Many different media can play host to the same message, but the message is always dependent on a causal, material medium of some kind.

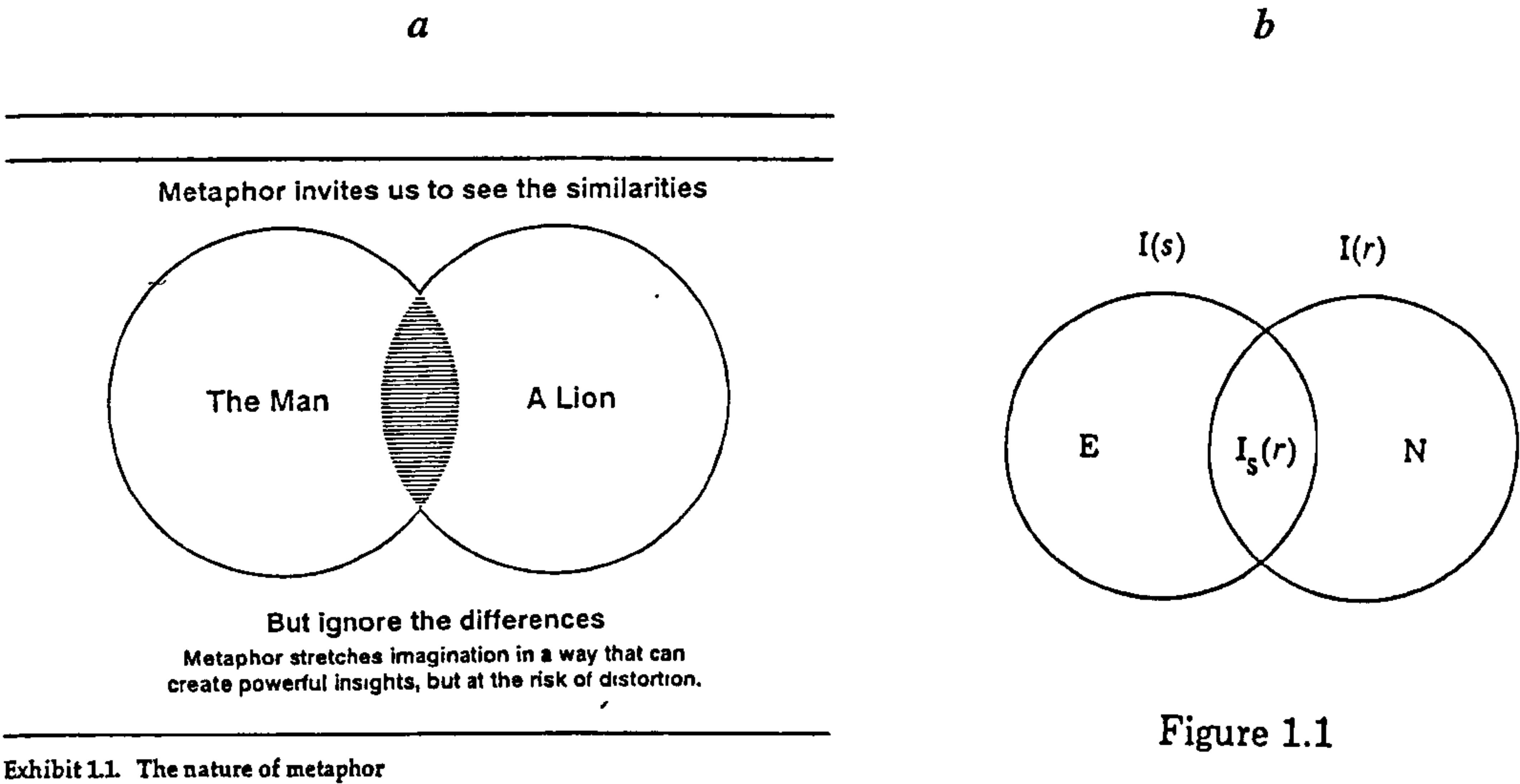
Material and codical descriptions differ in roughly the same way that a sample population differs from its average. The average is a summary; it captures a certain aspect of the population structure—its centre of gravity, let's say—at the expense of omitting all the other detail. Furthermore, different combinations of data can conspire to give the *same* average, so averages do not correspond to sample populations with an exclusive one to one mapping. However, an average is not something which exists independently, over and above the sample population it summarises. The notion of an average floating out there in the ether, waiting for a sample population to turn up, is simply nonsensical.

Regarding the example of the galaxy, the hurricane and the mollusc shell, I shall call what they all have in common an 'isomorphism'—literally, an equivalence of shape. Now let us try a different line of approach: metaphor. By saying that Richard I was a lion in battle, we are not literally suggesting that he was a big cat: rather, what we mean is that he and a lion might be said to share certain behavioural properties, in this case fierceness. Like averages, metaphors are always simultaneously revealing *and* obscuring; they capture abstraction at the expense of ignoring some material detail. In fact, the word 'metaphor' itself is particularly revealing in this sense. It comes from two Greek roots: *meta*, meaning to change, and *pherein*, which is to carry or hold, as in a vessel of some kind. With a metaphor, something changes between vessels (and to this day Greek removal vans have 'μεταφορά' written on their side); but what are the vessels carrying? Like the galaxy, the hurricane and the shell, a metaphor carries a kind of isomorphism—a 'conceptual shape'—which is preserved regardless of the medium it is carried by. Text Figure 5.2.a employs a set theoretic diagram to show the relationship between the two 'vessels' involved in a metaphor.

Now let us switch back to information. When information is transmitted, it is said to pass from a source to a receiver. The diagram used to convey this transfer is normally also presented in set theoretic terms (Text Figure 5.2.b). Information (or structure) present at the source $[I(s)]$ which does not transmit to the receiver is known as *equivocation* $[E]$; information present in the receiver $[I(r)]$ which was not transferred from the source is *noise* $[N]$; the rest $[I_s(r)]$ is the information we are interested in.

In what follows I shall argue that an organism is something like a 'metaphor for its environment'—a florid extrapolation, it might seem, but one which I hope to make good in due course. At this point it will suffice to have argued that information is about pattern

rather than stuff, and that it often depends on the preservation of a rough or average isomorphism rather than on exact detail; also, that it is always carried by a material medium of some kind. Information is unquestionably physical, and is thus a suitable topic for scientific enquiry.



Text Figure 5.2 *Two set theoretic representations of isomorphic overlap: a. the relationship between an original and its extension in metaphor (taken from Gareth Morgan’s 1997 bestseller on management practice, ‘Images of Organization’); b. the overlap between source and receiver in information transmission (from Fred Dreske’s now classic 1981 treatise on epistemology, ‘Knowledge and the Flow of Information’). Note that in both publications the figure is the first one shown because it plays such a foundational role in understanding the rest of the text.*

5.2.2 Functional Context

Gregory Bateson (1972) had a neat slogan for information: he held that “information is a difference that makes a difference”—in other words, a physical configuration of the world which causes something to happen that would never have happened otherwise. Bateson’s definition is probably the one a physicist would use (e.g. Von Bayer, 2003), but it fails to separate anything of biological distinction from a general background of matter in flux. The crucial distinction between merely physical versus biological accounts of information is *semantic content*, an issue sidestepped by classical information theory which presupposes the existence of a receiver having all the requisite qualities to contribute a semantic interpretation. Semantic content is *meaning*, and meaning

only ‘means’ something when it means something to *someone*. For biological information we require a theory of agency, and the naturalistic tradition readily supplies it.

Living systems are continually faced with the same fundamental problem: they need to decide what to do next (Dennett, 1991). Thus, information in the biological sense is any difference which makes a difference between getting life’s crucial decisions right and getting them wrong; between succeeding and failing; between living and dying; ultimately, between persisting and going extinct. Such distinctions as ‘right’ and ‘wrong’ can only be judged relative to a ‘locus of interest’, a party to whom such designations actually matter: the *someone* that information is meaningful *to*. This factor is manifestly lacking in the physical account which is thus totally neutral. Note, however, that objectively speaking (i.e. adopting a ‘view from nowhere’) the neutral account of information *must* be true, and the biological version illusory, since the latter yields contradictions. Biologically, the same information can be both ‘right’ *and* ‘wrong’ depending on whose perspective it is judged from: a camouflaged stick insect, for instance, is sending the right message only when a predatory bird receives the wrong one!

For semantics, the information patterns we are interested in are those which can be described as functional. Happily, ‘function’ has about the sharpest definition one could ask for:

The *function* of *x* is to do *F*

x exists *because* it does *F*

This is a version of Larry Wright’s (1973) classic explication and it has reached a virtual unanimity of acceptance among philosophers of biology (Millikan, 1984, 1989; Neander, 1991). It is worth trying out a few times, just to get a feel for: e.g. ‘The function of a heart is to pump blood; hearts exist *because* they pump blood’. It carries all the way down to the fundamental causes of organic existence: ‘The function of an organism is to make more organisms; organisms exist *because* they make more organisms’. And it sharply divides organic features which are properly functional from those which are not: human hearts may weigh about a half a kilo, but that is *not* their function. (The weight of a heart, by the way, is probably best thought of as a ‘spandrel’ (Gould and Lewontin, 1979), which, as Pinker and Bloom (1990) rightly observe, comprises “anything [organic] that can be talked about in non-functional terms.” For what it’s worth, ‘the fact that human hearts recoil more than

two inches but less than a foot when thrown hard at an unyielding surface' is also a spandrel. In the definition I am proposing, spandrels are not actually parts of organisms at all; they are simply parts of the environment that happen to be correlated with parts of organisms.)

Wright's definition of function is deeply context specific. A heart is only functional by pumping blood when it is part of a circulatory system feeding a body which requires blood to be constantly circulated in order to perform its primordial function of making more bodies to that design. And the context does not end there. The bodies themselves have to be in environments conducive to functionality; which is to say, they must at all times be somewhere between the two omegas in Text Figure 2.5, and somewhere between the two alphas when performing their primordial function.

The result of all this contextual embedding is a *hierarchy* of reference frames, each depending on the one further 'outside' to provide it with a semantic 'sense'; the outermost frame is simply a physical setting which does not depend on functionality for its existence. This context dependency explains another feature of semantic content in biological information: the fact that it is always information *about* something.

'Aboutness' is a quality known to philosophers as 'intentionality', not implying deliberateness as such, but deriving from the same Latin verb, *intendio*, meaning to 'aim at' or 'point towards' (Gregory, 1987). Biological information certainly points towards something, and that something is its frame of reference. For example, with respect to the nested set of contexts suggested above, we might say that a wing is *about* flying because:

- i) flying requires structures which provide lift,
- ii) given the laws of physics, aerofoils, which is what wings are, are structures capable of providing lift,
- iii) wings (aerofoils) are found in the context of flying (and here we are simply talking about function, and therefore of adaptation, though only in the proximally adaptive sense so far and with a historical component clearly missing).

And within this argument we can nest a further one by saying that genes for wings are genes *for* wings because:

iv) the absence of such genes would result in no wings in the context of that organism's developmental system, and

v) the organism in question (and thus its developmental system) has a fundamental niche which includes flying, and a realized niche which (given competition) positively demands it.

In other words, in order to persist and reproduce in a particular niche, the organism requires wings as an output product, and hence also requires genes which 'code for' and thus cause them.

Does some part of the information 'content' of bird genes 'point', via the bird phenotype, to an ultimate reference frame in the physics of aerofoils? I would say yes, although there is undoubtedly a historical component missing from this basic argument, as one soon discovers by asking what the wing genes in flightless birds are 'about'. The important point is that a particular kind of regularity or stable correlation can be seen to exist between a set of genes, their phenotype, and the kind of environmental pocket described in Chapter 3 as a niche.

5.2.3 Compression and Representation

So *perspectivity* and nested functional *context* help to define the semantic content of biological information. Bateson's 'difference that makes a difference' gives it causal influence. The correlation between environment and organism is actually none other than the familiar phenomenon known as *adaptation*, and clearly the definition of function given above, in conjunction with a process of natural selection, suffices to explain why such correlations exist. But there is a further element of information we must consider, especially with the *Plus ça change* model in mind; I shall call it *representational acuity*.

The reason George Williams was keen to separate the codical and material domains is because there are indeed two completely different ways to talk about them. Every item that 'contains' information about something is both a thing in its own right and a representation (a 're-presentation') of the thing it is about. Consider a guide book to London. Here, we have a stack of pages composed of mashed and set cellulose strands, unevenly coated with ink. It weighs about 200 grammes and if you burned it would release some 2000 kilojoules of heat. At the same time it is a book *about* London, despite the fact that it is sitting on a bookshelf many miles away from the city itself. What makes it a book

about London, and not *just* a pile of paper covered in ink, is a certain type of functional correlation between the physical layout of London and the patterns of ink on the book's pages (it also requires a *reader*, but we will get to that in due course). Where the ink is organised into maps, the nature of that correlation is particularly obvious; we can call this kind of correspondence literal or analogue: it simply uses scaled-down spatial relationships to represent the real-scale spatial relationships of London itself. Where the ink is organised into text, the nature of the correlation is far less obvious, but we can still see that it must exist. This mode of correlation depends on other, older, pre-existing correlations between spoken sounds or written characters and those features of the environment they 'represent'—correlations so ancient, contextually embedded and irretrievably buried by their own history that the relationship now seems arbitrary. Francis Crick (1968) once referred to this kind of correlation in the genetic code as a 'frozen accident'; we can call it symbolic or digital.

Now, whether we are dealing with literal *or* symbolic representations (the same point can be made in either case), they will always be somewhat imperfect. In fact, like the average of a sample population, representations will always capture something at the expense of losing virtually everything else. Imagine a map that was a *comprehensive* analogue representation of London: it would have to be at least as large as the city itself and detailed down to the cracks in the pavement. You simply couldn't make one. More importantly, there would be *no point* in making one. The whole reason for having a representation is that it uses only the most salient bits, leaving all the irrelevant detail out. Representations, like averages, are economical devices. They preserve a kind of correlation between whoever is using them (the agent-like perspective that cares about getting it right or wrong) and the referent itself—the object to be manipulated, dodged or navigated—but with a huge amount of naturally occurring redundancy squeezed out, or *compressed*.

Straightforward comparison to an average is probably the easiest and most accessible way to explain compression, which is why I used a similar characterisation for information in the introductory paragraphs of Section 5.2.1, above. Think of the information conveyed by a single noun, 'dog'. What breed of dog? How big is it? How old? None of these factors feature in the term. The meaning of a word like 'dog' (its function) is simply to pick out a general class of physical objects which share a more or less definable common core. As with the use of an average to summarise a sample population,

the term captures only the centre-of-gravity of dog-hood, at the expense of jettisoning all the glorious doggy details. That ‘centre-of-gravity’ defines a cluster of properties common to all dogs—quite literally, their *isomorphism*—which is highly redundant in the sense of being repeated over and over again in all the multiple instances of individual dogs. (Classicists will see a battle between Plato and Aristotle here; I side with Aristotle, as a good biologist should.)

Let us put things more formally. Take a string of characters (numbers in this case) with a lot of repetition among them, such as:

3777777773

This sequence can be compressed by turning it into another, shorter sequence, thus:

3(7x9)3

Here, compression clearly amounts to replacing the repetitive section with different elements that nevertheless ‘stand for’ or ‘provide information about’ the features they replace. In this example, the symbol ‘x’ denotes the mathematical function of multiplication. Like any function, multiplication is a process—an algorithm—which bridges a temporal sequence—a before and after—according to *rules*. In this instance, the output is achieved by manipulating symbols according to a convention so as to get from a ‘starting point’ (9x7) to a ‘destination’ (77777777) in a deterministic and thus dependable fashion.

The formal (mathematical) definitions of ‘redundancy’, ‘orderliness’ and ‘pattern’ are all framed alike in terms of algorithmic compression: a regular pattern is one that can be replaced by a compressed, shorthand version with minimal loss of information (Chaitin, 1975). By comparison, ‘randomness’ is defined as maximal incompressibility, like a symbol string with no internal pattern, whose actual sequence is its own shortest description. And note, as a corollary, that the compression of a sequence is necessarily *less* redundant and thus *more* internally random than was the original.

How much information loss is a *minimal* loss? How much detail can be omitted by a compression—a representation—before it becomes meaningless? Mathematics is an exact science, so, formally speaking, a redundant mathematical pattern should be *totally* recoverable: there should be zero loss of information. But the real world is messier than that. Will a sketch map get you to your destination, or do you require more detail? If the example used above had been a different string, 37777775773, say, then we would have been stumped. It could be rendered as 3(7x6)5(2x7)3, but, counting the brackets, this is

longer than the original sequence. Alternatively, we could have roughly (or pseudo-) compressed it to $3(7 \times 9)^3$ and simply lost some information. This is what 'representational acuity' amounts to; the issue concerns how much information loss can be tolerated before a representation becomes useless (i.e. non-functional).

The key to compressibility is redundancy: the more redundancy a feature has, the more compressible it will be. Ultimately, what this boils down to is Schrödinger's assertion that living systems are those which feed on negative entropy, meaning any orderly or dense concentration of matter and energy. My basic thesis is that evolution allows living systems to discover redundancy in their environments, which they then represent in compressed form, thus turning the original redundancy, via the second law of thermodynamics, into a more disorderly arrangement. And this in turn brings us back to the idea, first aired in Section 2.2, of *resource granularity*.

5.2.4 Resource Granularity

The earlier account of resource granularity in Section 2.2 was rather spare, but Text Figure 2.7 provided a fleshed-out example that we can use again. Finches eat seeds because seeds provide the energy and materials required to make more finches. More specifically, seeds are high density concentrations of matter and energy relative to their surroundings (an objective fact) which occur in a form accessible to finches of a particular morphology (an objective fact centred on a subjective point of view, i.e. depending on the finch in question).

As Text Figure 2.7 explained, the distribution of seed size and the contribution a seed makes to the fitness of an individual finch will determine whether or not finches adopt specialist or generalist strategies. If the seeds come in two distinct and homogeneously distributed size ranges, representable as the notation 111111111 & 999999999, then this will tend to foster specialism; if the seeds are of a similar size, say 444444444 & 555555555, or if they have broad range of sizes, 221323234 & 546475465, albeit centred on two distinct average values, then these arrangements will tend to foster generalism. (I take it that the use of symbolic notation is not too obscure a way of connecting redundancy in seed size to the formal definition of algorithmic compression.)

In terms of ‘aboutness’, the size of a finch beak becomes a literal or analogue (or *proximal*) representation of seed size when natural selection fosters a specialism that mirrors a redundancy in the seeds themselves. Likewise, the genes responsible for orchestrating different finch beaks constitute a digital or symbolic (or *distal*) representation of the seeds, because their genetic functionality is lodged within, and is thus only meaningfully translated through, the complexities of a finch developmental system. (The terms proximal and distal refer to the nested hierarchy of functional context outlined above in Section 5.2.2.)

In terms of the notation used above, we might usefully think of as the genes for two specialist finches as (1x9) and (9x9), coding for beaks of type 111111111 and 999999999, respectively, each of which handles a distinct size of seed. Note that the crucial area of overlap between the formal definition of compression and representation, and its mapping onto development and adaptation, is the notion of an algorithm as *any causal sequence capable of generating a specific output from a specific input* in a more or less deterministic, or a least functionally competent, kind of way (also note that ‘more or less deterministic’ acknowledges the environmentally sensitive genome-as-recipe metaphor rather than the rigidly set genetic-program version more suited to a formal definition of compression). The fact that both the formal and organic versions of compression depend crucially on algorithmic (i.e. causal) mediation between an input and an output brings us full circle to Bateson’s definition of information as ‘a difference that makes a difference.’

The broad point is that environmental redundancy of one sort or another is a prerequisite for adaptation. The information in an organism, its method of getting decisions right rather than wrong, must also represent something regular in the layout of the world. Whether or not the information is detailed and specialized or sketchy and generalized will in part depend on the distribution of redundant features available for organic representations to discover and exploit in the first place. Like a random string, a world with no regularity is its own shortest description: organisms can find no purchase under totally chaotic circumstances, or at the very least they will need to generalize by ‘panning back’ from the chaos of detail until they find an exploitable average (like a gas law) to use.

This is the real utility to the *Plus ça change* model of an information theoretic approach. It allows us to see, in mechanistic terms, how a very generalised aspect of the environment—its bulk redundancy along one or more measurement axes—could be mirrored (represented) in an organism. This is what I meant in Section 5.2.1 when I said

that an organism can be thought of as a metaphor for its environment—a distorted and filtered reflection, but a reflection nonetheless, of the regularity present in the world it inhabits.

Plus ça change concerns redundancy through time. It is not concerned with static pattern as such, but about whether what regular patterns there are can be predictably tracked for a suitable duration. Evolution is a random search process, and that search takes time. To be ‘found’ and successfully ‘incorporated’ into an organism, an environmental signal needs to be both strong and consistent, providing positive feedback for natural selection.

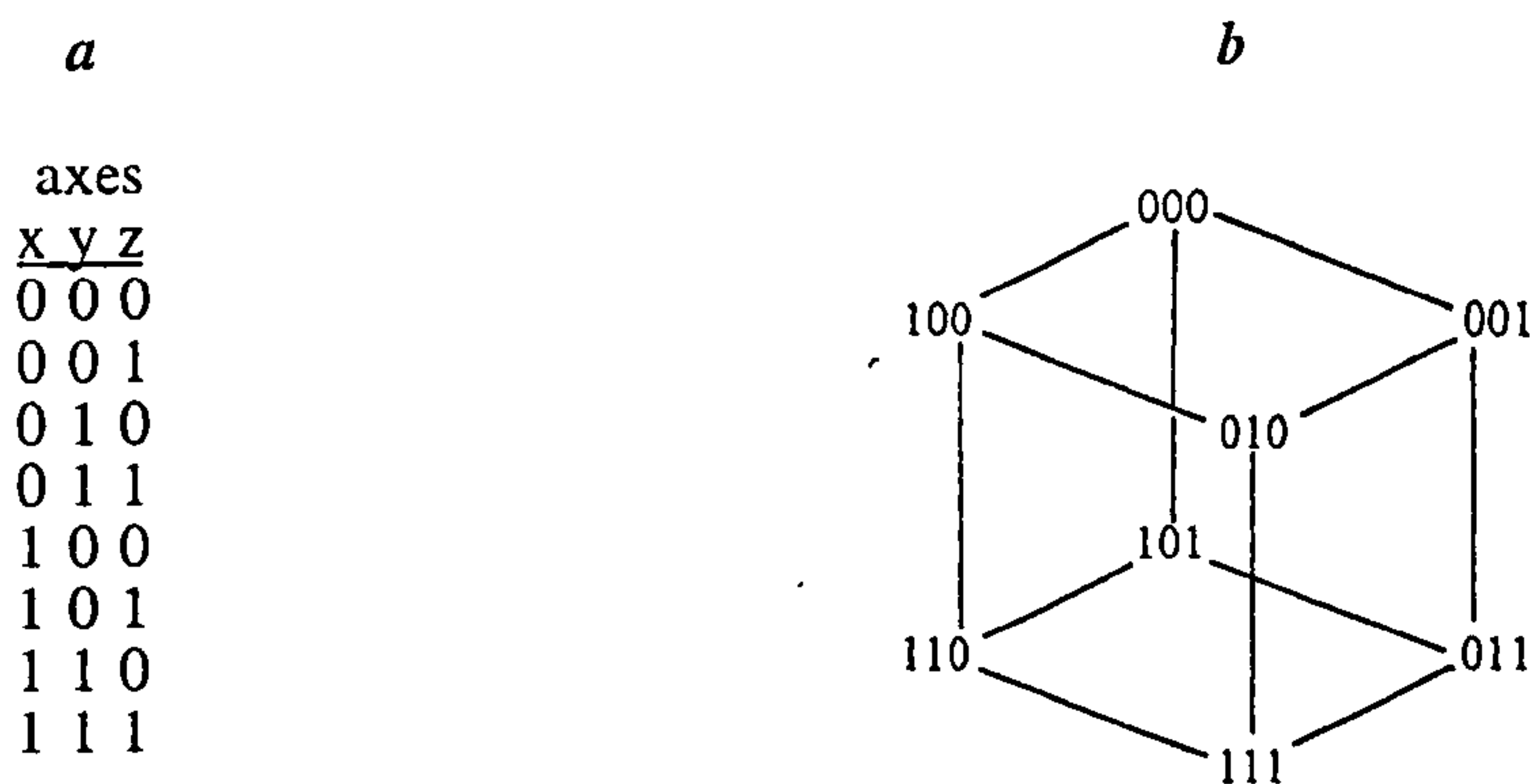
But environmental stability is not the only factor of significance. Signals can only be picked up by receivers of a suitable kind, and not all organisms provide the right template to bear a particular environmental stamp. In addition to the environmental component, therefore, *Plus ça change* demands a theory about developmental malleability. Fortunately, the information theoretic conception provides this, too, permitting enough of an insight on the underlying dynamics to help us appreciate how environmental redundancy might be transferred from the ‘outside’ to the ‘inside’.

Section 5.3 Two Landscape Concepts

5.3.1 State Space

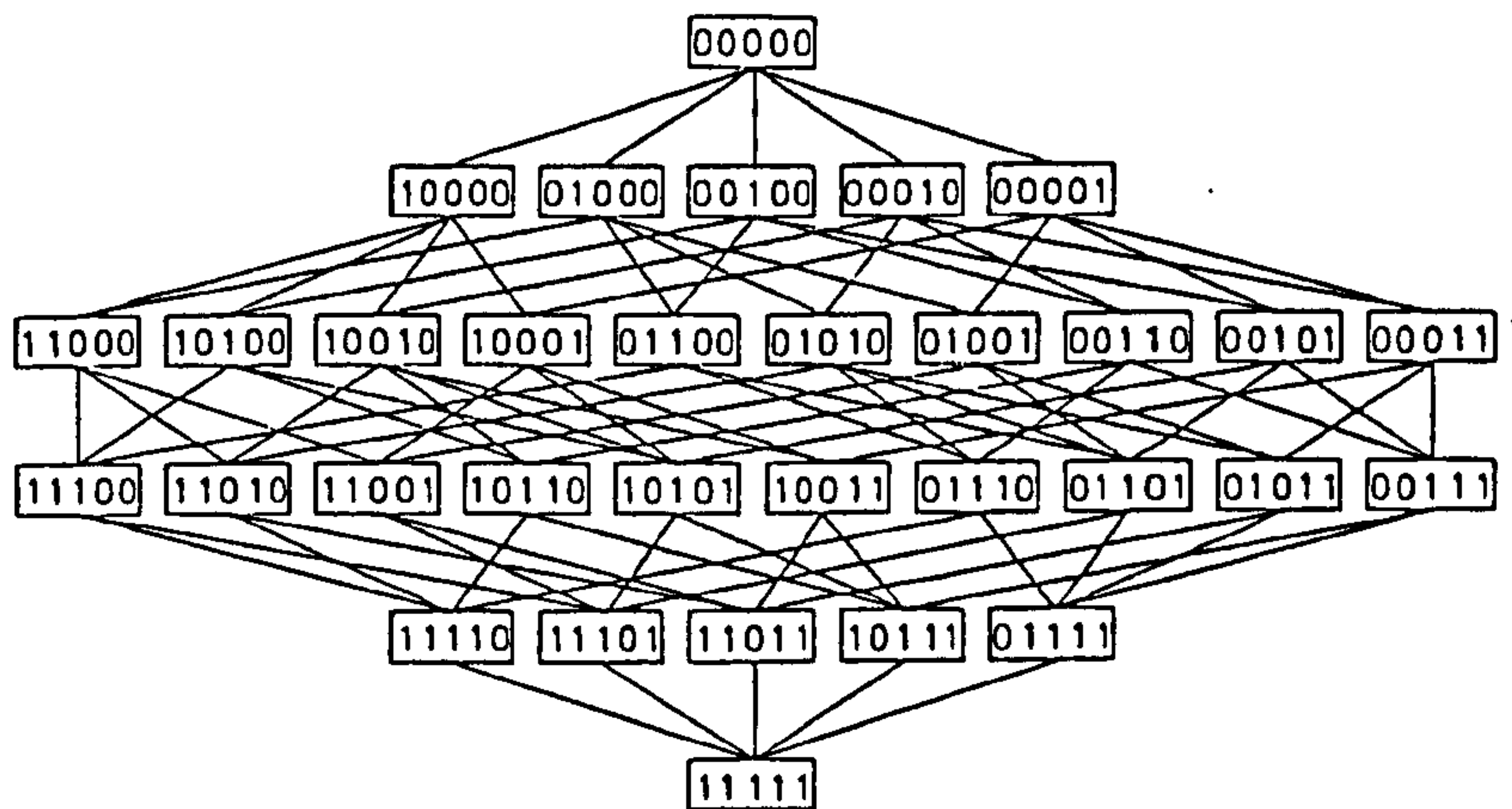
It is a deeply plausible contention that metaphor lies at the very heart of human cognition (Jaynes, 1976; Hofstadter, 2001; Lakoff and Johnson, 1980). Certainly it often proves easier to explain an unfamiliar or abstract thing by comparing it to something else entirely, so long as that something else is more tangible or already well understood. Bohr’s early attempt to model the atom by using the solar system as a template is an absolutely classic example. Agency talk, for instance, abounds in biology, even when the ‘agents’ are shreds of DNA. Most discussions of communication make use of container metaphors in which information is a substance and ideas are things to be packed up in the removal van of language and transported to a new destination. But on the whole, spatialization has to be the all time favourite metaphorical tool, for humans at least.

Biology is full of spatial metaphors, perhaps even more so than other sciences, although the ability to calibrate a variable almost inevitably goes hand in hand with its transposition to a one dimensional measurement axis. We already met niche ‘volumes’ in Chapter 2; in this chapter we shall consider two landscape concepts, the fitness landscape and the epigenetic landscape. But first we need a notion of *state space* in general and how to navigate through it by using ‘string’ descriptions. Text Figure 5.3 shows a three dimensional binary state space, the smallest and simplest one within which the necessary points can be made. Each corner corresponds to a ‘state’, a unique combination of elements; the array as a whole serves to define the entire range of possible states. Next to it is a string version which simply displays the same range of combinations as a list. The two versions are isomorphic: they map on to one another perfectly and exhaustively.



Text Figure 5.3 *Two versions of a three dimensional binary state space: 5.3.b is a ‘space’; 5.3.a is a list of ‘strings’.*

Binary characters have only two possible states, 1 or 0; there is nothing in between. The binary notation reflects the two ends to each spatial dimension while the three dimensions themselves reflect the fact that there are only three such binary characters in each of the possible strings. More generally the rule is E^p , where E is the number of elements available (for binary, two), and p is the number of placeholders among which these can be distributed (in this case three). Text Figure 5.4 shows a five placeholder binary hypervolume which has $2^5 = 32$ possible states. There is theoretically no upper limit to either the number of elements we could consider, or the number of placeholders. A state space with an infinite number of elements and three placeholder dimensions, for instance, would correspond to a continuous volume like a sphere, or that of the three dimensional niche space shown in Text Figure 2.6.

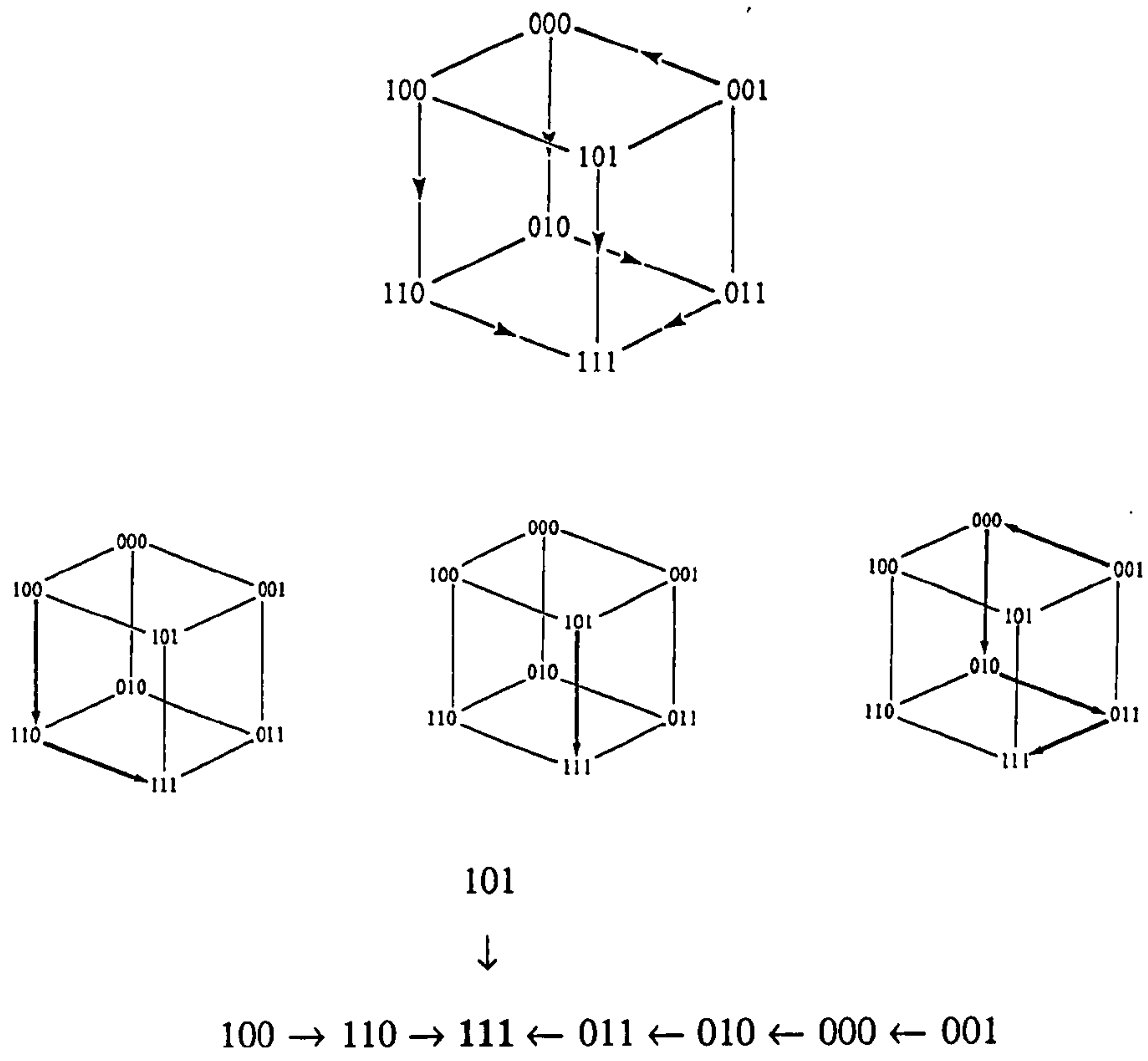


Text Figure 5.4 A five place holder binary 'hypercube'—a state space of 32 different 'locations'.

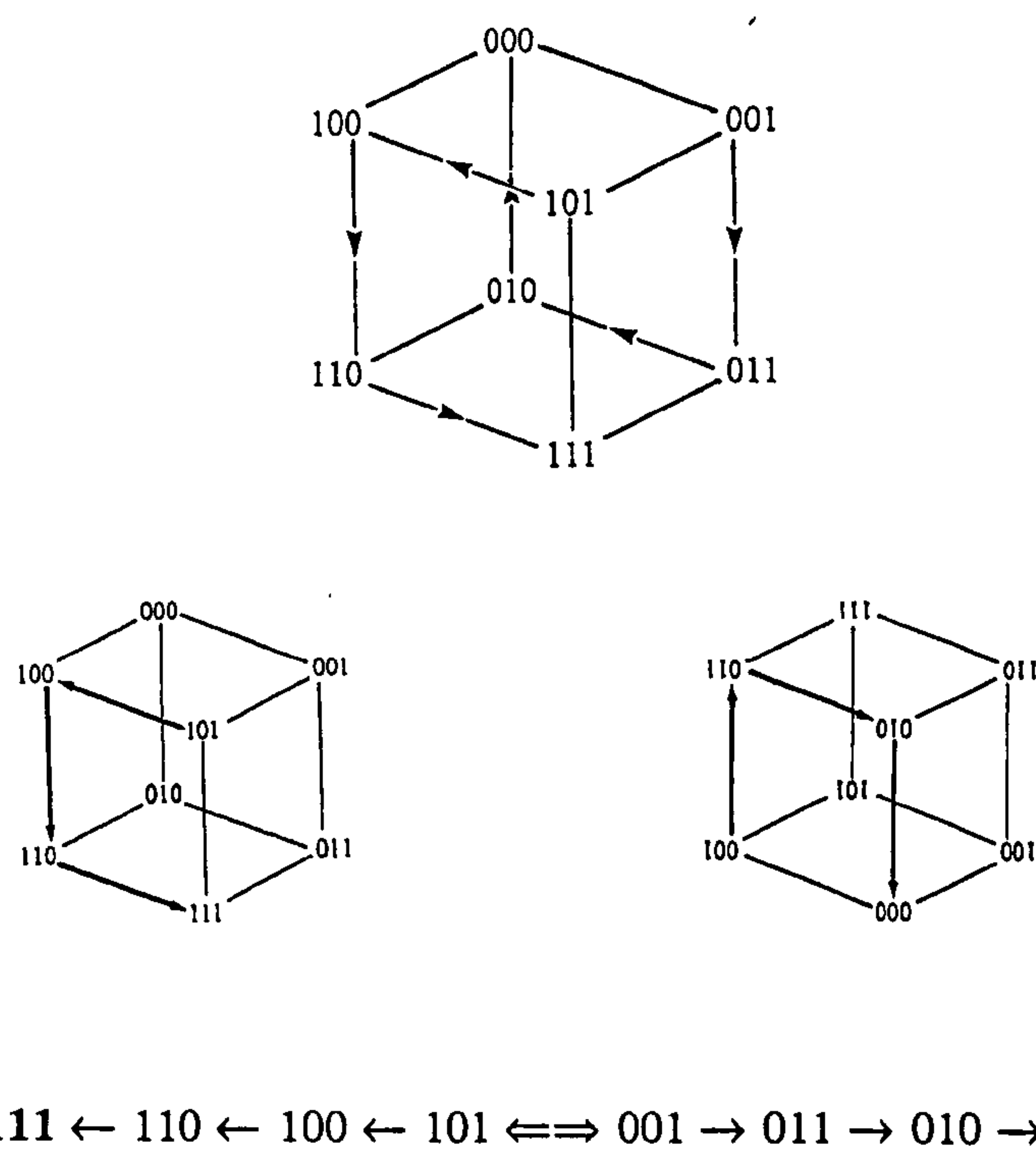
The value of this conception is that it allows us to *quantify* the possible and the actual relative to one another. With respect to Text Figure 5.3, if what we have is an *actual* string or state of affairs, representable as, say, 110, then we know it comprises 1/8 of the *total range of possibilities*. All statistical reasoning works on similar premises. The method also allows us to keep track of changes from one state to another, and to know how close together pairs of such states are.

Evolutionary thinkers have made much of conceptual spaces like these. Dawkins (1986), for example, talks about 'tracks through animal space'. For Dennett (1995), it is the 'Library of Mendel', a vast collection of tomes listing all possible 3 billion placeholder sequences of the 4 nucleotide bases ("enough to serve any serious theoretical purpose"). There are also more subtly designed conceptual spaces like Raup's (1966) molluscan morphospace, which employs continuous elements to represent descriptive parameters like rates of shell expansion and translation along the coiling axis. All of them cast actual biological designs against a backdrop of broader possibility; and all invoke some sense of proximity between the multitude of different designs, genomes, or morphologies.

Whether over the course of development or the course of evolution, change in an organism can be modelled as *motion* through state space. From this perspective there are two important types of motion to address: convergence and divergence. Text Figures 5.5 & 5.6 show these situations mapped onto the three dimensional state space used earlier. In the first (Text Fig. 5.5), it really does not matter what state the system begins from, the sequence of changes 'drains' inexorably into a single destination, which thus corresponds to a point

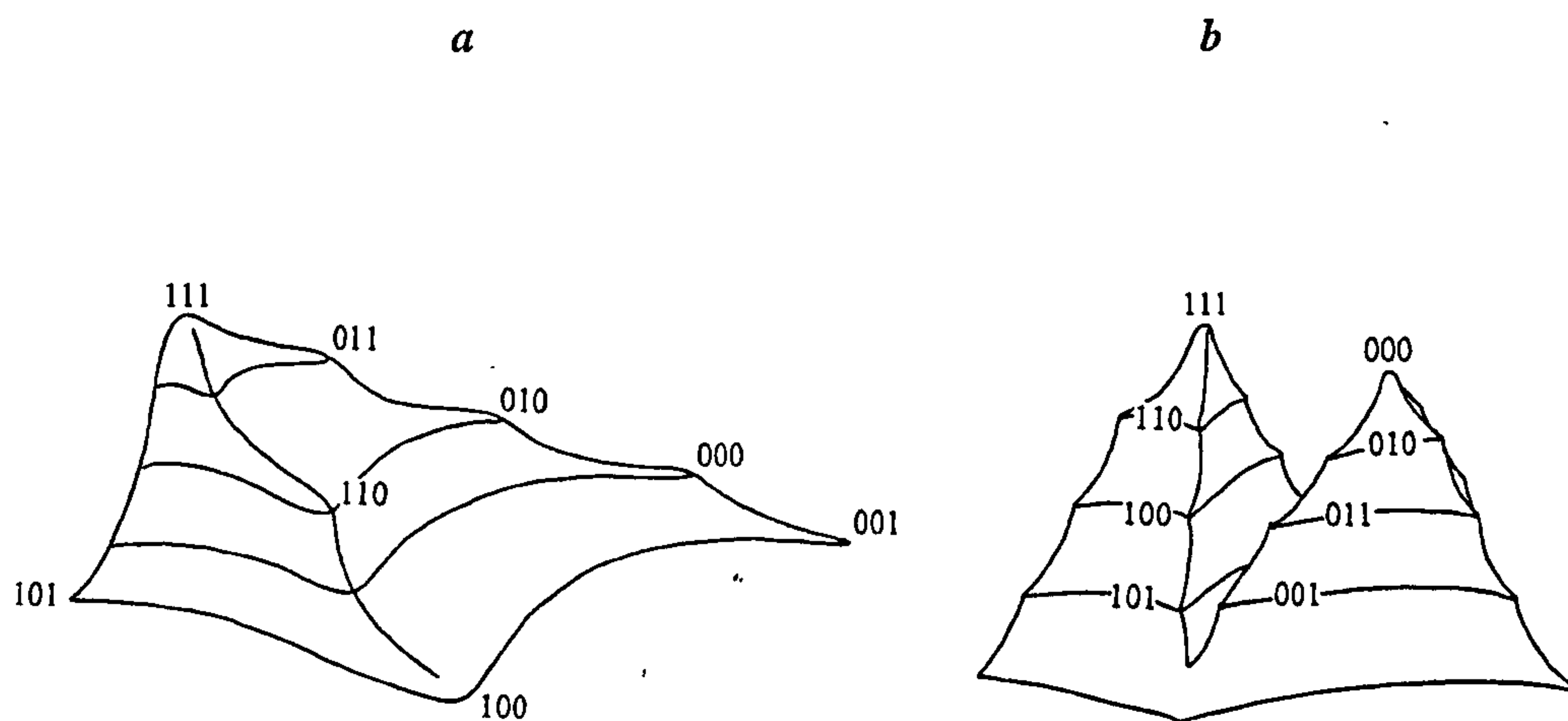


Text Figure 5.5 Causal arrows marked on a state space. Convergence occurs as the system 'drains' onto a single causal attractor (111) irrespective of starting location. Shown both as paths through state space (middle) and as transitions between string sequences (bottom).



Text Figure 5.6 Causal arrows marked on a state space. Divergence occurs across a 'watershed' (⇌⇌) between two attractors (111 & 000) shown both as paths through state space (top) and as transitions between string sequences (bottom).

attractor (see also Sections 2.2.1 & 4.2.3). In the second (Text Fig 5.6), starting from state 101, the system tips into a point attractor at 111, and two out of three single-step changes to this starting location make no difference whatsoever to the eventual destination. The third single-step change, however, a shift to state 001, is enough to cross a ‘watershed’ and tip the system into an alternative ‘drainage basin’ instead. Note the confidence-inspiring familiarity of landscape metaphor in what would otherwise be a completely dry discussion. Text Figure 5.7 takes the landscape metaphor more literally as a description for each of these cases.



Text Figure 5.7 *The two state space situations from the figures above transformed to a landscape: a. convergence; b. divergence.*

5.3.2 Fitness Landscapes

The most familiar use of terrain metaphor in evolutionary theory is Sewal Wright’s fitness landscape (1931; and many secondary sources). Here, the attractor is a ‘fitness peak’, conceptually equivalent to point A on Ronald Fisher’s adaptive sphere (Text Fig. 1.1). The causal sequence leading to this peak is selective in nature—an evolutionary ratchet: steps in the right direction happen through chance alone, but when they do occur they are amply rewarded, while backsliding is selectively penalised. Fisher and Wright had a

famous disagreement on the topography of such landscapes with Wright arguing for rugged versions and Fisher arguing for smooth ones (see Ridley, 1993, for an account).

In a rugged landscape a change in one placeholder can alter the fitness of other placeholders too. At issue is how interconnected and *internally* interdependent the system is. In extreme cases of internal connection the entire array becomes a single unit of selection.

Let us imagine that the three dimensional binary space above represents the phenotypic characteristics of an organism: 111 stands for 'herbivore teeth', 'herbivore gut', 'hoofed feet'; 000 stands for 'carnivore teeth', 'carnivore gut', 'clawed feet'. Clearly these form *complementary sets* of characteristics, and mixtures such as 101 would be maladaptive and thus selected against. The groupings 111 and 000, by contrast, are peaks of fitness to which the system will be pushed by selective forces. Note, however, that the criteria for fitness are imposed from 'outside' by the dependable (i.e. highly correlated and thus redundant) properties of diets and lifestyles: it is the toughness of grass which demands grinding teeth, compost-heap guts and thick-nailed toes.

Wright's argument involved a subtle embellishment on the scenario outlined above, and rather than environmental specification depended instead on interconnectedness during the course of development. What if, for some unknown embryological reason, it was only possible to have *either* sharp teeth and hooves *or* grinding teeth and claws? The fitness peaks of both carnivores and herbivores would be much lower for a start; but it also turns out—and sadly the three dimensional model is too simple to depict this—that there would be many more valleys between the peaks, and that the transitions between valleys and peaks would tend to be very steep (Kauffman, 1993).

This terrain, with its low peaks, sharp cliffs and a multitude of intersecting valleys is considered 'rugged' for good reason. In rugged terrains movement is difficult. There is often no global evolutionary peak to aim for, but rather a range of similar-sized summits separated by deep ravines; moving just a little higher often takes a great amount of effort. Furthermore, because selection can only take an evolving organism upwards, there is a constant danger of getting trapped on a low peak somewhere down in the foothills from which it is later impossible to escape.

Smooth landscapes follow a different line of argument, in essence the one suggested above in which complementary sets of traits (herbivore teeth, gut and toes) arise through the

shuffling of *independent* elements. In sexually reproducing organisms, the genotype is constantly being split up during meiosis with the consequence that fragments of DNA each enjoy independent evolutionary trajectories; they are therefore able to ditch those associated fragments with whom they are most incompatible, eventually being juggled into optimally complementary sets. More generally, *in a smooth landscape a change in one placeholder does not affect the fitness of other placeholders*, and since each piece of DNA is an individually selectable unit, selection itself can occur piecemeal.

In this scenario there is always a smooth, low-gradient path to the peak of 'Mount Improbable' (Dawkins, 1996). To see why, consider motion through the vast state space of Dennett's three billion placeholder string of DNA. No matter where we start from, so long as we are not already at the summit, there will always be at least one nucleotide which can be substituted for a better one; all we have to do is wait for an appropriate mutation to occur, and we can take another shuffling step in the right direction. The system shifts inexorably from state to better state, if necessary starting at the very bottom and overcoming the slight gradient with three billion miniscule adjustments.

The relevance of these two different models to *Plus ça change* and the evolutionary debate in general is straightforward: the rugged version predicts long periods of stasis, hedged in by fitness ravines that are only crossable with fortuitous quantum leaps (arising through lucky *combinations* of mutation); the other predicts continuous change along a steady path to the global summit (with frequent, small, high-probability mutations). They should be thought of as end points on a continuum. Real organisms almost certainly have a mixture of properties, ranging from some smoothly evolvable features to others so developmentally interlocking that they are best considered as a single complex character. We will see more of this reasoning below.

5.3.3 Epigenetic Landscapes

The difference between these two end-point fitness landscapes hinges on the nature of development. If there is a high density of 'epistatic' interactions between the various genetic and phenotypic components, then evolution can be expected to be rugged and episodic because it will be hard to change anything in a modular fashion (i.e. without it

having a large number of knock-on effects). If, on the other hand, there is very little interaction and the system is very modular, then evolution will tend to be smooth and continuous. The landscape model of choice for depicting these alternatives is Waddington's (1957) *epigenetic landscape*.

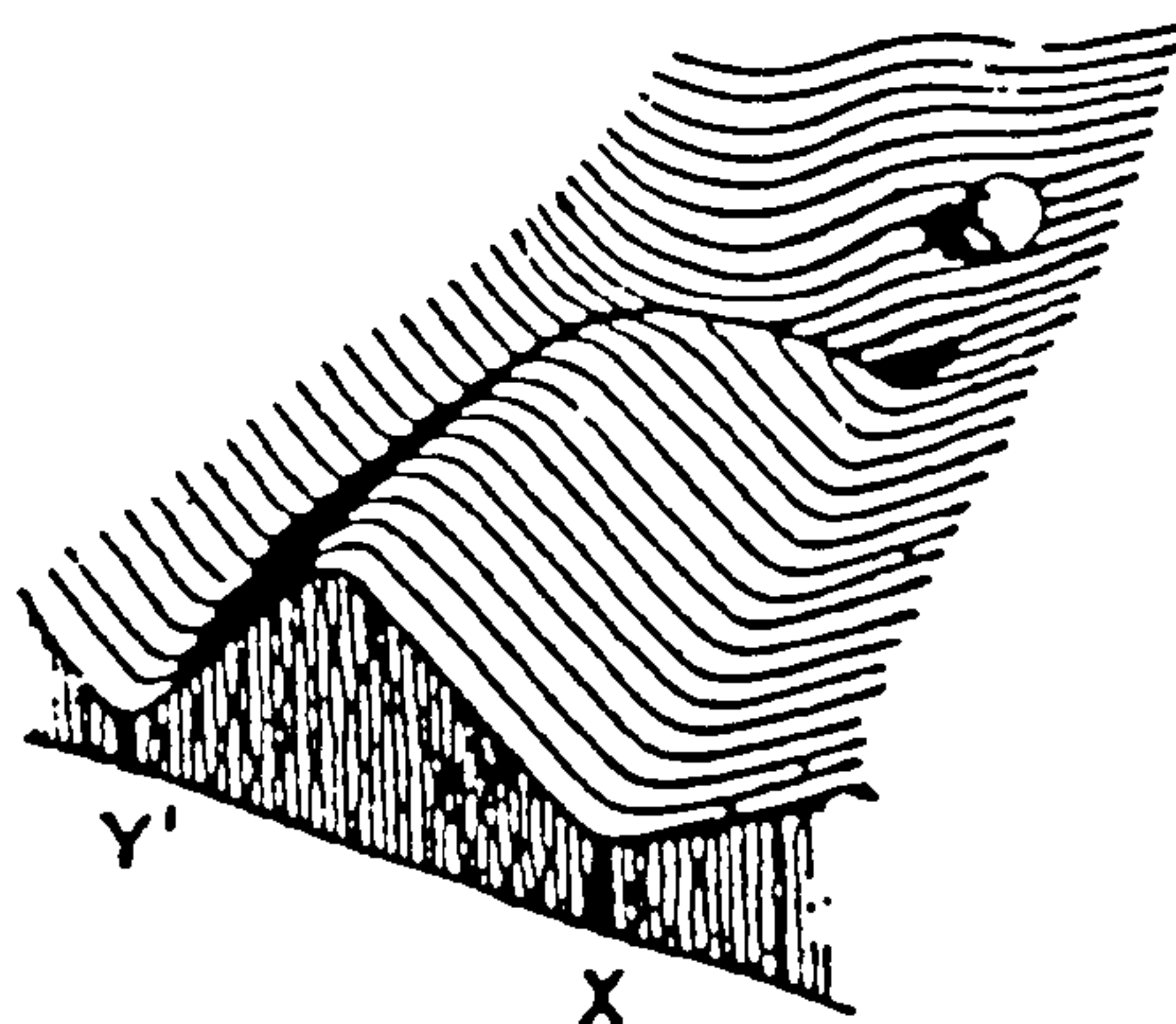
Unlike the slopes of a fitness landscape which are defined by selection, the gradients on an epigenetic landscape are all thermodynamic. Waddington's metaphor for the course of development—a *developmental trajectory*—is a ball rolling down a low, sloping plane; the plane itself is rumpled into valleys and ridges that correspond to local thermodynamic variations. Organisms are thermodynamic curiosities, as we shall see below. In the functional sense they are extremely orderly systems, but they are also thermodynamically open *dissipative structures*, requiring a constant throughput of energy and materials. Each and every chemical reaction during the course of an organic lifecycle can be understood as responding to a local thermodynamic gradient, moving the system from a high to low energy state; and globally, too, an organism's death leaves the world a more disordered place than it was before. But the local build up of energy and organisation that characterises living matter seems, superficially at least, to flout the second law of thermodynamics.

The best analogy I have come across to elucidate this thermodynamic paradox likens living systems to the eddies and whirlpools of a turbulent river (Prigogine, 1980). Overall, the water gets to its destination faster than would be achieved with a simple laminar flow, but in the process some of it ends up going in the 'wrong direction' for some of the time. Like a river full of turbulence, a universe full of living matter reaches heat death faster than it might otherwise do, but instead of creating eddies as it goes along, it generates those local concentrations of energy and order we know as organisms.

This turns out to be an important complement to the definition of an organism as a case of compression because the algorithmic definition of order (Chaitin, 1975), the classical definition of information (Shannon, 1948) and the classical definition of entropy, all share a common core (see, for example, Von Bayer, 2003, and Johnson, 1995). Another motivation for choosing information as the guiding philosophy in this work was because it seems to underpin a physical principle as fundamental as that of the second law.

So the slope of Waddington's landscape is a global thermodynamic gradient, and the rumples and folds are local perturbations which serve to push the rolling ball down one

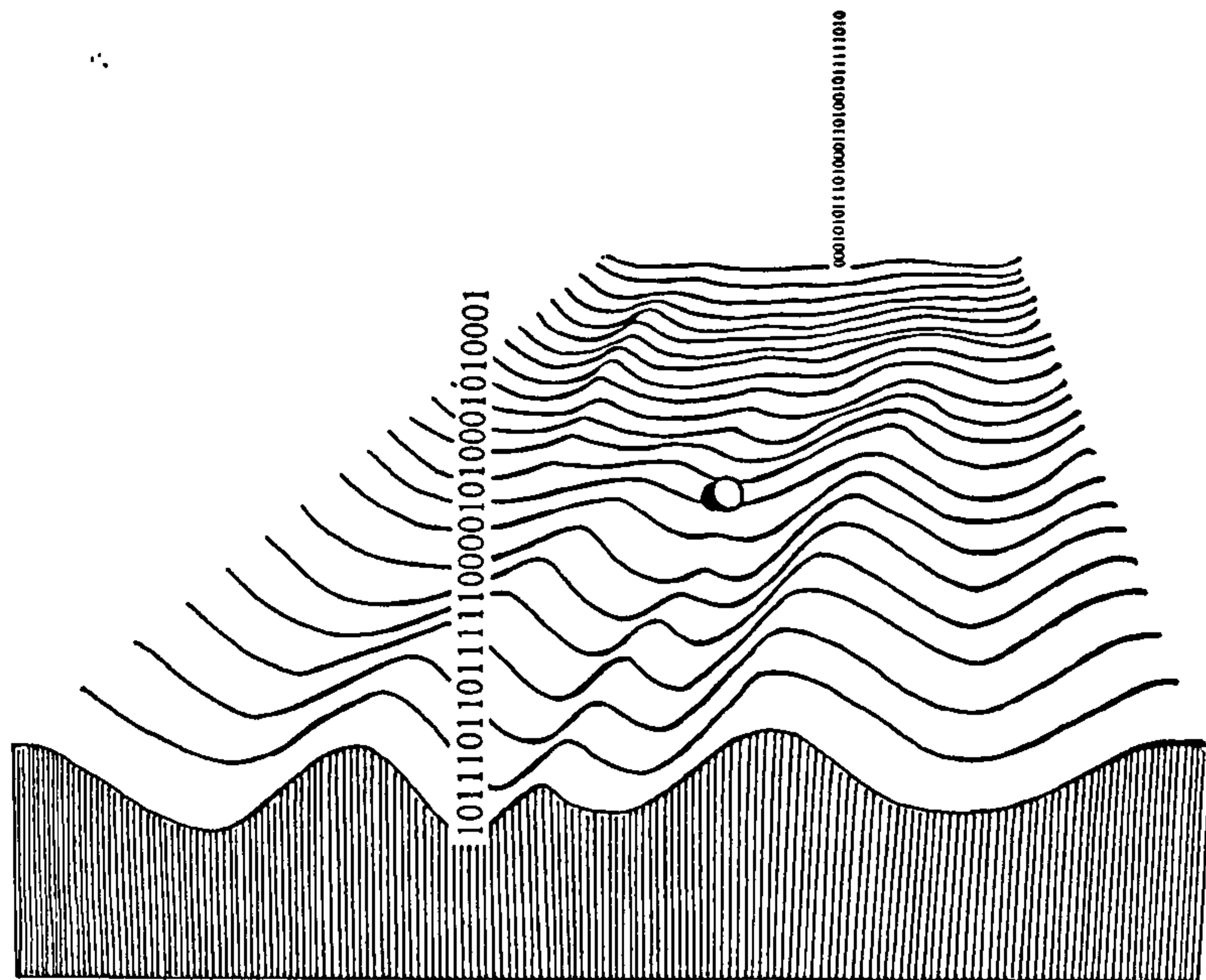
developmental channel rather than another. The system starts off (as an egg or a seed) in one portion of state space, somewhere along the top margin of the plane, and, if it can orchestrate the desired manipulation of matter and energy, will cascade down a more or less well organised thermodynamic pathway to some other portion of state space which characterises the adult form. At that point the mature organism will produce another egg or seed with a similar state space configuration to the one from which it began, and the process will repeat itself all over again.



Text Figure 5.8 *Waddington's notion of an 'epigenetic landscape' to describe a developmental trajectory. The developing organism is cast as a ball rolling down a slope. In this example, which shows only a small portion of such a vast landscape, the ball is about to hit a branch point that could lead on to two different phenotypic expressions, Y or X, depending on which side it actually travels down. From Waddington (1957).*

It is important to realise, I think, that while the depiction of development as a single vector—what Rose (1997) calls a 'lifeline'—is intuitively appealing, it does considerable injustice to the complex and massively parallel process of development itself. The image of a single, unified lifeline is appealing partly because of its simplicity, and perhaps also because we tend to think of individuals (people for example, and species too) as following a single narrative trajectory throughout their own life-history. But even the workings of a single cell are in reality more like a well conducted metabolic orchestra: thousands of 'instruments' (biochemical pathways and the like) are playing all at once but to a single unified theme. This is a metaphor worth a moment of indulgence. Just as it is possible to focus in on an orchestra and pick out the flute or the cello above all the rest, so it is possible to focus on a living system and pick out a single functional (behavioural, metabolic or developmental) component. But, equally, one can just as well talk about the symphony as a whole; and indeed, it is this bounding context that we require to give full meaning to the

tune played by any single part. Trajectories through Waddington's epigenetic landscape are more like symphonies than simple tunes, a fact which becomes particularly obvious when we think about evolution, because it forces us to understand any change in the symphony as a change in the onset, offset, or tempo of the component 'melodies' (McKinney and McNamara, 1991).

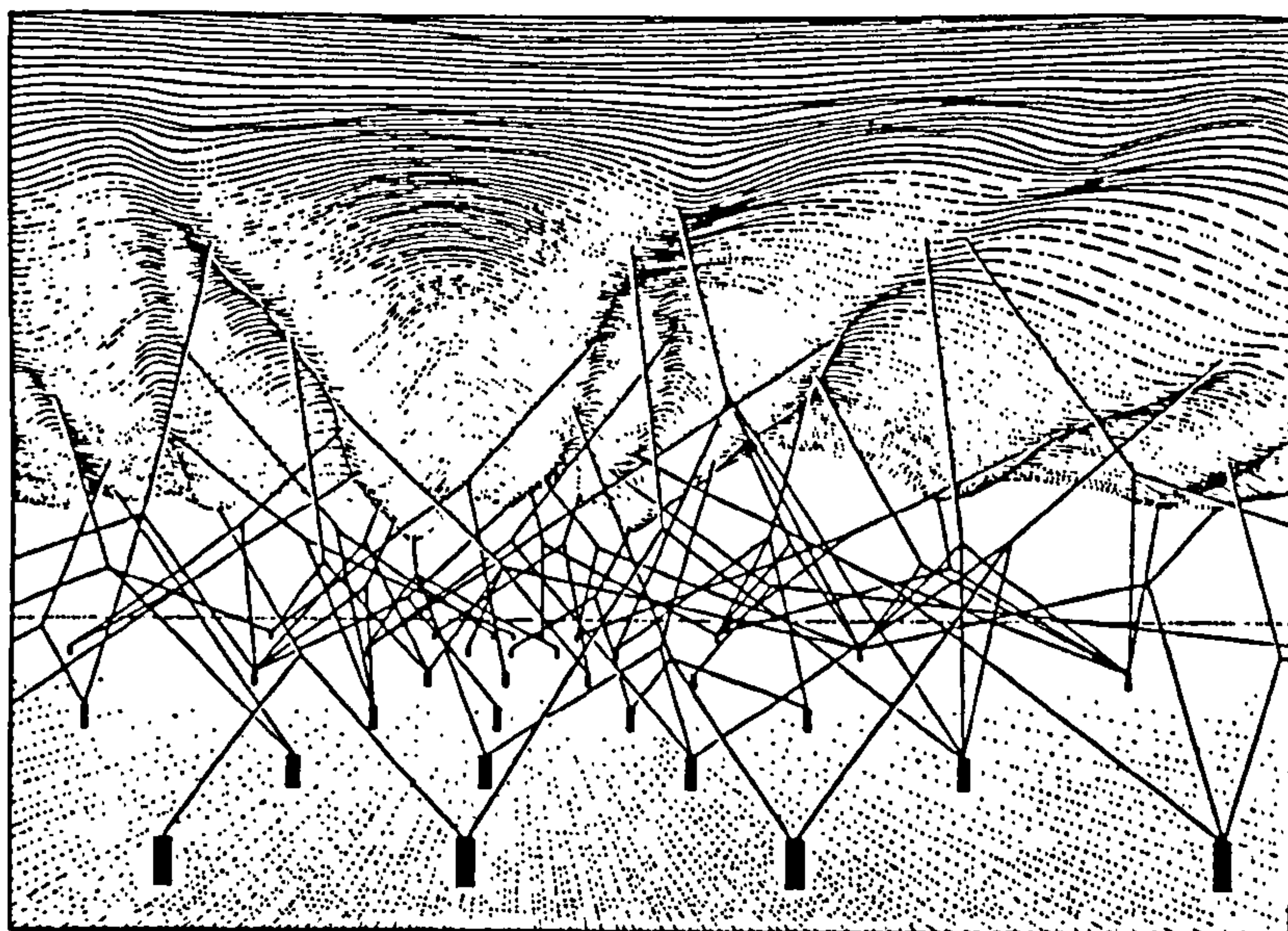


Text Figure 5.9 *An epigenetic landscape between two points in state space (shown by their binary string descriptions). Given the starting point, the contours of the intervening landscape will guide the ball (the developing organism) to its eventual destination. Changes in starting location, or changes in the landscape itself, could both lead to different destinations, as suggested by the alternative adjacent channels.*

Enlightening though the orchestra metaphor is, I shall stick with a spatial conception for now. Text Figure 5.9 shows the starting point and final destination on an epigenetic landscape as a pair of binary strings. The transition between these points runs over an essentially two dimensional sheet, despite the fact that we know the whole business must be massively multidimensional, and massively parallel, too. Subtle shifts in starting point provide the grist for selection. In terms of a fitness landscape, they are either steps in the 'right' direction (uphill), or steps in the 'wrong' one (downhill). But the real utility of Waddington's conception appears only when we ask what effects those differences in starting location will have in terms of their destination, because then we instantly see—contrary to the argument from Fisher's microscope (Section 1.1.3)—that there need be nothing like a linear, one-to-one relationship between the two locations. Small

differences in starting point can sometimes amplify to huge differences in end-product: if the change straddles a ‘watershed’, for example, it can switch the course of the ball between two divergent valleys. At other times, large differences in starting point are soaked up by the buffering effects of the system, which is capable of collecting inputs from a wide ‘drainage’ and funnelling them down through a narrow developmental channel (indeed, for reasons of stability this is often engineered by selection; it is known as ‘canalization’).

But by far the most revealing insight comes when we get a glimpse underneath Waddington’s landscape to see the scaffolding of genetic pegs and epigenetic guy ropes that hold it all in place (Text Figure 5.10). This illustrates the real difference between a rugged Wrightian fitness landscape and a smooth Fisherian one. Waddington evidently leaned towards the Wrightian conception if this figure is anything to go by. The pegs are genes. A one-gene-one-effect system would require each genetic peg to have a single guy rope of its own, mediating its influence on the overlying developmental topography. In such a system it would be possible to pull individual pegs out, changing only local parts of the landscape, and thus to patiently and smoothly sculpt its contours to those demanded by a residence at the global fitness peak. Instead, what we see is an unruly tangle of interactions, where pulling one peg could result in the landscape tightening or deflating a considerable distance away. Text Figure 5.10, Waddington’s own characterisation, depicts a recipe for ruggedness.



Text Figure 5.10 *“The complex system of interactions underlying the epigenetic landscape. The pegs in the ground represent genes; the strings leading from them the chemical tendencies which the genes produce. The modelling of the epigenetic landscape, which slopes down from above one’s head towards the distance, is controlled by the pull of these numerous guy-ropes which are ultimately anchored to the genes.” (Caption and figure from Waddington, 1957).*

5.3.4 Zeroing In

The state space concept will now permit us to see, with glorious clarity, how the main component still missing from an informational account can be slotted into its rightful place. Information, as we have seen, is a kind of causal sequence with an agent-like perspective on the receiving end. More generally, it is said to pass from a *source* to a *receiver*. The source is the controlling party in this interaction; the receiver is malleable in the face of causal influence *from* the source, reconfiguring itself in the light of the information it has received (and, of course, things start to get really interesting when the source is an agent in its own right, like the stick insect mentioned in Section 5.2.1, because then there is scope for deceit by ‘misrepresentation’). In Shannon’s (1948) original definition, information serves to *narrow down the number of states the source can be in from the perspective of the receiver*. With our concept of state space it is easy to demonstrate how this process can be quantified.

Let us use a contrived case dreamt up by Dretske (1981) to demonstrate exactly this point. He imagines an employer who requires one of her eight employees to perform some task. The boss is happy to let the underlings draw straws, but insists that when they have done so, they should inform her by writing the volunteer’s name on a piece of paper and sending it along to the head office. From the boss’s receiving perspective, that piece of paper is a source of information (with an arrow of intentionality, an ‘aboutness’, pointing back to the reference frame of the employees’ original decision), which *reduces* the uncertainty of who has volunteered from eight possibilities to just one. As such the message carries three *bits* of information. The reason it carries three bits is that it would require three binary decisions, or three successive halvings of the state space, to zero-in on the person who was chosen. We can see this by imagining that the list of binary strings in Text Figure 5.3 correspond to properties of the employees themselves: column *x* stands for old or young (0 or 1); column *y* for male or female (0 or 1); column *z* for fair or dark (0 or 1). If the volunteer is employee 100, who is thus young, male and fair, it would take three successive reductions of the range of possibilities to arrive at that point. Note also that *the amount of information depends crucially on the state of the receiver*; if the boss had already heard gossip that the volunteer was a male, the very same piece of paper would carry only 2 bits instead!

The relevance of this account to our two landscape concepts is as follows. Natural selection is a case in which an evolving lineage zeroes-in on an adaptive peak. The environment is the source, providing information to the lineage, the receiver, which is malleable in the face of that information. The organism 'learns' what the environment is like as it adapts itself to an optimized configuration. In the case of development, the major source of information is the genotype, which provides information to the developmental system by coaxing it to zero-in on a particular adult phenotype. We might say that the number of adult forms the phenotype could be in is successively narrowed down by information received from its genetic source during the process of development.

One brief digression. There is a school of thought called 'Developmental Systems Theory' which claims that the genes do not 'provide information' any more than the developing phenotype itself does (Griffiths and Grey, 1994; Oyama, 1985; Griffiths, 2001). We have already seen part of the reasoning behind this line of argument in the explanation given above: whether or not a signal 'contains information', and, if so, *how much* information it contains, depends on the configuration of the receiver as much as it does on the configuration of the source. Information passes through a causal channel, and if the receiver is to vary in accordance with changes at the source, then that channel has to be stable (I sometimes think of it as the fulcrum of a lever which has to be anchored in order to translate motion from one end to the other). The channel is contributing just as much 'information' in virtue of its stability as is the more variable source. Indeed, what constitutes a source and a channel are interchangeable, as Griffiths (2001) makes translucently clear with his excellent example of the TV testcard. Testcards were designed specifically to provide a stable signal, allowing the channel conditions to be finely tuned so that they later provide the right interpretation for a variable source once normal viewing is resumed.

I agree with the general point, but I do not think it affects the argument in the slightest. Organisms are differentiated into a source (genes), a channel (genetic code-transcription reading system) and a receiver (developing phenotype) precisely *in order* to incorporate these three informational components. The channel needs to be more stable than the message, and so the genes are the variable element in this relationship with the transcription code providing a stable channel. The fact that genes play a dominant role in encoding information is undeniable; we can say that genes are a *source* of hereditary

developmental information because that is their *function*: they have been selected for their capacity to play exactly that role in the developing system. Erwin Schrödinger, as long ago as 1944, saw that if organic information was to be kept stable between the generations it would have to be encoded in a solid; he guessed that the solid would turn out to be an aperiodic crystal of some sort, and a decade later he was proved right. No other part of the developmental system has been selected *specifically* to play that role, whatever causal influence it may have in practice.

In terms of development, the genes are a source; but it is important to appreciate that the source grades imperceptibly into the receiver in biological information encoding systems, just as we saw in the example above where the worker's gossip about the gender of the volunteer had already passed part of the source configuration on to the receiver (the boss). In the same way, we can say that the fact that the written message could be read at all was due to the boss's *capacity to read* (a channel condition), and that this in turn existed because of information already accreted at some earlier time (in school, say, when she was first being taught that skill).

In Section 5.2.3, I sidestepped the issue of a reading system, stating simply that even for digitally encoded information where the relationship is not readily apparent, there simply *must* be a functional correlation between the words on a page and the things those words represent. All function is highly context dependent, and word functions are no different; but much of the relevant context is historical. Books are meaningful only to those who have learned how to read them; learning to read is possible only in social contexts where the skill can be taught, and for organisms with the requisite faculties to perceive and act on the information received. Such organisms themselves exist as a result of the encoded information in their own developmental systems and within the ecological circumstances that crafted them, and so on. Functional context is smeared throughout the whole evolutionary history of an information processing system; for a defence of this position, see Dennett (1995; 1998).

Developmental Systems Theory is in part a reaction to the (mythical) bogeyman of 'genetic determinism'. Many people seem to have been scared witless by Dawkins's famous defamiliarising device (1976) of rendering genes as agents and organisms as mere vehicles. I don't really share that alarm, but I do think the debate would benefit from some new terminology. My preference is that we call Dawkins's replicators 'encoders' and his vehicles (after Hull, 1980) 'interactors'. The word 'replicator' should be a holistic term

reserved for a complete *encoder*—>*interactor*—>*encoder* cycle. Dawkins insists that only encoders (his replicators) truly replicate because only these pass on accumulated change (changes to the interactor, scars etc., are not passed on to the next generation: that would be a Lamarckian system, not a Darwinian one). I agree with his general point: encoders are not interactors: they are maximal compressions of self-replicating systems and do indeed constitute informational bottlenecks in just that sense (in fact homozygous gene assemblages might be thought of as the channel conditions for expressing environmental structure through changes in the frequency of their heterozygous comrades!). But both encoders and interactors (genes and phenotypes) owe their continuing (and otherwise highly improbable) existence in the world to their participation in a complete replication cycle. In this sense they are both replicators and I think our terminology should acknowledge that fact. Entities whose function it is to stabilise an information system are better thought of as encoders. Genes (and words) are the encoding elements in a complex, cyclic replication system. This is in close agreement with Developmental Systems Theory, but manages to fish the baby out before pulling the plug on all that unwanted bathwater.

Section 5.4 Information and Economy

5.4.1 The Cost of Information

With our two landscape concepts now firmly in place we have all the tools required to pursue several important arguments about living systems, and to see what insight they can give us into the process of evolution. The first argument expands on some comments made above concerning the status of life in thermodynamic terms. Living systems are *orderly* systems, despite their being thermodynamically open, and there are at least two ways of discerning this orderliness. One hinges on an appreciation that organisms are far-from-equilibrium configurations, maintaining osmotic gradients, engaging in highly non-random behaviour patterns and so forth; we shall return to this idea in a moment. The other, a kind of shortcut, is that living systems are massively compressible. The ecological data base (Appdx. Tab. 1.1) records more than 36 000 benthic foraminifera, but they can all be classified into just 45 taxonomic groups. Clearly, there is a vast amount of repetition in

there somewhere. Species cluster in state space, occupying only small islands within the vast oceans of adjacent possibility.

A major reason for this, and a significant aspect of the far-from-equilibrium argument, is selection. The struggle for survival keeps organic types clustered around the summits of fitness peaks. One can imagine them tending to diffuse down the slopes due to mutation, only to be mopped up again by selection faster than they can spread. In terms of information this is actually an incredibly important argument: it means that *information is expensive*. Let us put it in more formal terms with an argument first made (so far as I know) by Eigen and Schuster in 1979 (but see also Kauffman, 1993).

Imagine a 'genome' (a state space string) one hundred characters long in which each placeholder makes the same contribution to fitness: the fitness of each is thus 1/100th of the total. In addition, each placeholder has a constant probability of mutating during the course of any reproductive cycle. It actually does not matter what that probability is so long as it is constant, but let us say that it is one in a thousand. Every ten generations one of the 100 elements mutates and is (almost always) selected against. Next, imagine a similar situation except with a genome ten thousand characters long. Each placeholder now has a fitness of just 1/10000th but the mutation rate, being a constant, is *still the same*; consequently, this time there are ten mutations in *every* generation. Pursuing this logic, we see that as the string grows there must eventually come a point where the power of selection is overwhelmed by mutation pressure; it can no longer keep the prolifically mutating string in check. This 'event horizon' is called the *error catastrophe threshold*.

There must, of course, be ways to hold the mutation rate down, but these in turn will need to be genetically specified, and so on. Eventually physics will win over design. The argument is conceptually identical to the class of thermodynamic models describing gases that diffuse into empty jars and allows us to understand that information is a resource in itself; it hinges critically on the relative volumes of state space occupied by the string versus that which is adjacent but unoccupied. This is one useful way to interpret the phrase 'far-from-equilibrium'. The system will be at 'equilibrium' only when it is spread evenly throughout state space and thus maximally disordered (i.e. incompressible); at that point it should have no more elements showing the type of environmental correlations that could be described as adaptive than would be expected by chance alone.

Obviously, the point at which an error threshold occurs will depend not only on the volume of state space involved (which depends in turn on the dimensionality of the genome,

the number of placeholders), but also on the strength of selection. Strong selection, causing steep gradients on a fitness landscape, will tend to corral the mutating system into a smaller portion of state space than would weak selection. So once again we note that information encoding systems are highly orderly because firstly all individuals are effectively *the same* individual (they all occupy the same portion of morphospace or 'behaviour space'), and secondly because by being highly adapted they are also functionally correlated with their environment—a kind of second order redundancy.

When genes mutate, selection only ever mops up the dysfunctional mutations: 'adaptive' mutation is fostered by the evolutionary ratchet and is shuffled into the 'orderly' category, so that being orderly in the sense of being unlikely or occupying a small portion of state space becomes equivalent to 'containing information' in the intentional sense of Section 5.2.3. This information packing occurs through what Brian Goodwin (1972) once referred to as a process of 'naturalistic induction'—knowledge gathering on the basis of past experience. By viewing this inductive process from a thermodynamic perspective we can see that selection constantly has to 'work' against a mutational slide into chaos—not work in the immediate sense of expending energy (although that too), but rather in terms of constraining possibilities. We might, for example, view selection as a process of 'shovelling' information about the environment into a genome, against a steady tendency for it to 'trickle back out again'. Metaphors indeed, but what else did we ever expect from talking about the 'pressure' of selection?

5.4.2 Information Hierarchy

The fact that information is expensive has important consequences for how we think living systems should cope with their information allocation. For a start, we should expect them to treat information as economically as possible, in much the same way as any other resource. Whenever their information burden becomes too great they should prioritise, keeping the 'bits' they need and letting go of the ones they don't. They should also look for ways to reduce their overall costs, by sharing the financial burden with their allies, and, if possible, by getting what they need for free.

I said in Section 5.2.2 that the fundamental problem faced by all living systems is in deciding what next to do. Information is the difference making a crucial difference between getting those decisions right and getting them wrong. A fitness landscape is the

ultimate theatre in which such judgements are made, and by the time the procedure has reached that stage it is effectively out of the organism's control: either the right decisions have already been made or it is too late. We can imagine that the organism has 'first dibs' on each decision and then selection intervenes, often in the harshest possible way, to provide corrective feedback on whether the lineage is 'getting it right' or 'getting it wrong' (this is more clear for development than behaviour, as we shall see below). Well designed organisms are those which have already endured a lot of environmental correction, and are thus wise enough to make many right decisions all on their own during the course of development. These decisions can be modelled on an epigenetic landscape.

Decision points along the course of a developmental trajectory most clearly come in the form of nodes or watersheds on the landscape—points where the rolling ball can go *either* one way *or* go another. They are loci of control precisely because they are the points at which small changes can have large effects. The valleys, by contrast, are relatively robust and are perhaps best considered to be 'self-organizing' in some sense (I shall expand on this below). Since it is the nodes and watersheds, rather than the drainage basins and valleys, which have the most acute effect on development, these are the points at which selection should preferentially act. And we should expect gene influence to align itself with the sequence of decisions on an epigenetic landscape in such a way as to guide the system through state space most efficiently. Under the idealised circumstances of a totally smooth fitness landscape, for instance, we can imagine a single genetic peg and guy rope assigned to the control of each watershed point, tugging the epigenetic landscape so as to constitute that crucial, information-endowing difference. Alternative alleles will manifest themselves either as the *absence* of an appropriate peg, in circumstances where the alternative allele simply has no effect and thus leaves the landscape to sort itself out, or to a pair of pegs attached at different points and thus deforming the surface in slightly different ways. The fitness landscape would then sort between these alternatives. But the perfectly smooth landscape is something of an idealised extreme, and in all likelihood the genetic underpinnings of most epigenetic landscapes will be much more entangled than that. The next issue on our agenda, therefore, is whether or not we can expect to find order even in a developmentally tangled network. I think the answer is yes.

It is quite clear from the reasoning so far that some nodes will be more important than others. Those near the bottom of the ball's trajectory will have only a small influence on where the system finally ends up, but those at the top will play a large and important

role. Consequently, and this time in accordance with Fisher's Microscope, selection should work more strongly at the top of a developmental trajectory than it does at the base. Or, as Maynard Smith (1998) observed with his usual pithy style, "...if you have a cascade of regulatory genes, with A switching on (or off) genes B, C and D, which then switch on E, F, G and H, and so on, the one gene you don't muck about with is gene A."

Once an early developmental node becomes so important that changes to it are lethal, it effectively constitutes part of the 'environment' from the perspective of later acting nodes. As they see it, by the time their contribution to decision making comes around, they can depend utterly on the fact that the influence of such earlier acting nodes is already manifest somewhere within the system. Early acting genes thus become constant environmental factors to which the rest of the array can adapt itself. In effect, they form an aspect of the *reading system* for later parts of the genetic message. Deep rooted, pan-phyletic, homologous genes, like the *Hox* cluster or *Pax-6* (*eyeless*), seem to play exactly this role. They are regulatory genes which serve to 'turn on' cascades of other genes; and, because they are so dependable, they form a ubiquitous component in a multitude of different switching sequences (Levinton 2001). This multifunctional encoding constitutes a substantial information economy; but the corollary is that such genes cannot be specialist encoders of information, and that fact can be illustrated in informational terms, too. Rather than being proximally functional, like the analogue information carriers we know as structural genes (whose 'message' is straightforwardly read into the shape of the proteins they produce), regulatory genes are digital, both in the 'iconic' sense that their main function is distal to their immediate effects, and also in the 'frozen accident' sense that their full 'meaning' is provided only by the broader context in which they operate. Furthermore, the function of regulatory genes is discrete; they tend to act simply as 'on-off' switches—or in other words, they carry exactly *one bit* of information, the smallest possible amount.

This is one kind of economy we should expect living systems to adopt, and, although in its infancy, developmental genetics so far supports the model (Levinton 2001, Gould 2002). But there are other types of economy that an information encoding system can avail itself of, and these we shall call cases of 'offloading'. Offloading occurs when the system *passes the organisational buck*, either to the environment, or to the self-organizing properties of the materials it is working with.

5.4.3 External Offloading

External offloading is ubiquitous and well known. Whenever human engineers design a machine they wish to run unattended, they incorporate within it cybernetic systems. These are features which work on the basis of feedback, sometimes positive, mostly negative. The term ‘cybernetic’ itself comes from κυβερνέτεσ, the Greek for steersman—the man who controls the boat—and when feedback mechanisms are linked together in hierarchies of control and meta-control, it is indeed hard to avoid the eerie conclusion that someone is steering the system. But avoid it we should, quite obviously so for single-celled cases like foraminifera: as Dennett (1997) muses, “all that purposive hustle and bustle, *but there’s nobody home!*”

Cybernetic systems are designed to take their orders not from their creators but from their environment: they are *self-steering*. What a boon such devices are to an organisational economy! They are such an obvious innovation, in fact, that they were discovered early on in life’s grand odyssey; indeed, it is a moot point where they begin and end.

Genes do not always ‘micromanage’ either development or behaviour. Instead, they routinely code for the construction of a cybernetic system to deftly pass the organisational buck to what it considers to be an environment, and then act only in accordance with the instructions received. What constitutes ‘the environment’, however, is quite a subtle issue, and there is an important sense in which *any* gene that is switched on by other genes, constitutes a cybernetic system that ‘perceives’ its instructions as coming from ‘outside itself’. This is the sense in which genes collectively share the organisational burden of the entire life-cycle. Genes, of course, are not autonomous agents in any strong sense; developmentally, they are more like the flippers on a pinball machine, simply passing the epigenetic ball back and forth between themselves. In this manner we can imagine a genetic regulatory system as a huge mass of offloaded instructions, where each gene relies on other genes to tell it what to do. Fortunately, the list of options is gratifyingly small, normally limited to the gene being ‘on’ or ‘off’ (this being the only sense in which it is meaningful to attribute decision-making skills to a molecular assemblage in the first place). The ultimate model for this reasoning is none other than the 20th Century’s favourite source of enlightening metaphor, the computer. This is the ‘genetic program’ conception of development where the regulatory network is likened to a computer algorithm full of

logical switches, each telling the others what to do. It carves the smooth contours of an epigenetic landscape into a maze of logical propositions—a Turing machine in extreme cases—and, again, can be thought of as an information packing device *par excellence*, in which any amount of analogue structure is reduced to a mass of maximally economical binary digits.

A more common version of environmental offloading is seen in the suite of traits known as *developmental plasticity*, *ecophenotypy*, or *reaction norms*. Examples of these phenomena range from trivial to striking. As a trivial example, the presence of appropriate food items in an organism's environment constitutes an external input necessary for the achievement of most developmental goals. For the most part, food is not internally supplied—it is depended upon as an external resource, and in its absence the system fails. Claiming food as a kind of informational input seems to be stretching the definition somewhat; but it is important to see that the example merely lies at one end of a spectrum: when the *type* of foodstuff regulates the colour of camouflage pigmentation, as it does in certain leafhoppers (Otte and Williams, 1972), a label of environmental instruction is more clearly justified.

As with 'internal' elements, the effect of any external information is entangled with, and strongly dependent upon, many other internal and external developmental factors. The developmental landscape should always be viewed as a network of co-dependencies as suggested by Waddington's diagram (Text Fig. 5.10). This means that although 'external' offloading is cheaper than 'internal' coding, it is still reliant upon the internal context of an appropriate receiver for its functional meaning, and thus on the power of selection to *preserve* that internal context as a reading system capable of interpreting the message from an external source correctly. In other words, a source is only as informationally rich as the receiver that responds to it, and even cybernetic systems still require a great deal of selective engineering to perform their task.

Another point best raised here is that cybernetic plasticity is forced upon a system when the changes it is required to keep track of approach or exceed the rapidity of the system's own lifecycle. In this sense, ecophenotypic developmental systems fade imperceptibly into the real-time-decision-making of an autonomous or quasi-autonomous behavioural system. As mentioned above, the boundary between innate and environmental control is, and always has been, hazy. Bacteria evolve so quickly to antibiotics that the medical establishment has difficulty keeping up. But even bacteria rely on environmental prompts to inform them when they should be firing up the relevant genetic

engines (Monod, 1971). For a glorious account of the evolution and hierarchy of smart systems, ranging from lowly Darwinian creatures destined to find out the hard way, to culturally enhanced ‘Popperian future producers’ like ourselves who ‘let our hypotheses die in our stead’, see Dennett (1992, 1995, 1997).

5.4.4 Internal Offloading

The other great cost-saving technique available to living systems is to dispense with naturally selected information entirely and fall back on ‘order for free’. Structural biology enjoyed a resurgence in the last decades of the 20th Century, largely through the campaigns of thinkers like Kauffman (1993, 1995) and Goodwin (1994). The best analogy I can devise to illustrate what they were trying to tell us is to compare the organism to a Lego model. Once upon a time, Lego came in about a dozen different types of brick, and whatever was built from it was clunky and coarse, requiring a good deal of imagination before it looked like anything at all. These days there are so many different types of component that it is hard to see what role a child’s imagination has left (you can now buy Harry Potter Lego, complete with individual characters, spell books, wands etc.). Structural biologists were basically saying, “Look, you know how we once thought evolution was really imaginative: well it turns out that a lot of that imagination actually belonged to the manufacturer, and it simply came with the kit.” They ‘offloaded’ much of the creativity in organic design by passing it to the structural properties of the building components; and organisms themselves, I suggest, do exactly the same thing, but for reasons of informational economy.

Modern structural biology is part of the long and distinguished tradition of Continental philosophy. Wentworth D’Arcy Thompson (1917) is widely regarded as the immediate forefather of the modern branch, but the tradition goes much further back, to St Hillaire and Cuvier (see Goodwin, 1994; Gould 2002), and probably ultimately to Plato. Natural selection has to be the natural selection *of something*; and no matter how precisely sifted and selected they are, genes have to have *something* to organise during the course of development. Those somethings are ‘order for free’. The natural world abounds with it. Fluids immersed in other fluids spontaneously form

form spherical interfaces; no-one tells them how to do it. Crystals grow according to molecular packing rules and three dimensional symmetries. Waves form spontaneously in dynamic media under the influence of opposing forces. More recently we have discovered that all manner of complex dynamical systems self-organize themselves around strange attractors and fractal patterns. Nature is a wonderful thing. But not *that* wonderful:

“You may throw cells together at random, over and over again for a billion years, and not once will you get a conglomeration that flies or swims or burrows or runs, or does anything, even badly, that could remotely be construed as working to keep itself alive” (Dawkins, 1986).

Clearly the role of self-organization in nature has to be tempered somewhat with a selective influence; I think even the structural hardcore recognise that fact. The issue, therefore, concerns the precise mix of selective and self-organizing influences.

Self-organization is actually so ubiquitous that it is easy to overlook. Nor is it always obvious what should count. Consider the newly formed amino acid sequence trailing from a ribosome: first, it spontaneously twists into an alpha helix, then it scrunches up into a tertiary protein structure. It does these things because of electrical imbalances along the length of the molecule: the tertiary structure, for instance, is normally formed by minimising the interface between hydrophobic, non-polar R-groups and the surrounding aqueous medium. It is self-organizing in exactly the same way, and for exactly the same reason, that D’Arcy Thompson’s fluid droplets are.

A protein’s design is in its three dimensional shape, but the important organisational aspect of that shape was all implicit in the primary amino acid sequence. Like an entire organism on an epigenetic landscape, the trick is to get the protein precursor to the right starting point in the first place. Indeed, we can imagine a mini-epigenetic landscape underlying each and every instance of protein formation, with different state-space starting points determining which valleys will guide the process to completion—substitute valine for glutamic acid at the wrong location and your haemoglobin molecule will be catapulted down a different valley to become the sickle-cell type, with potentially disastrous or life-preserving consequences depending on the setting.

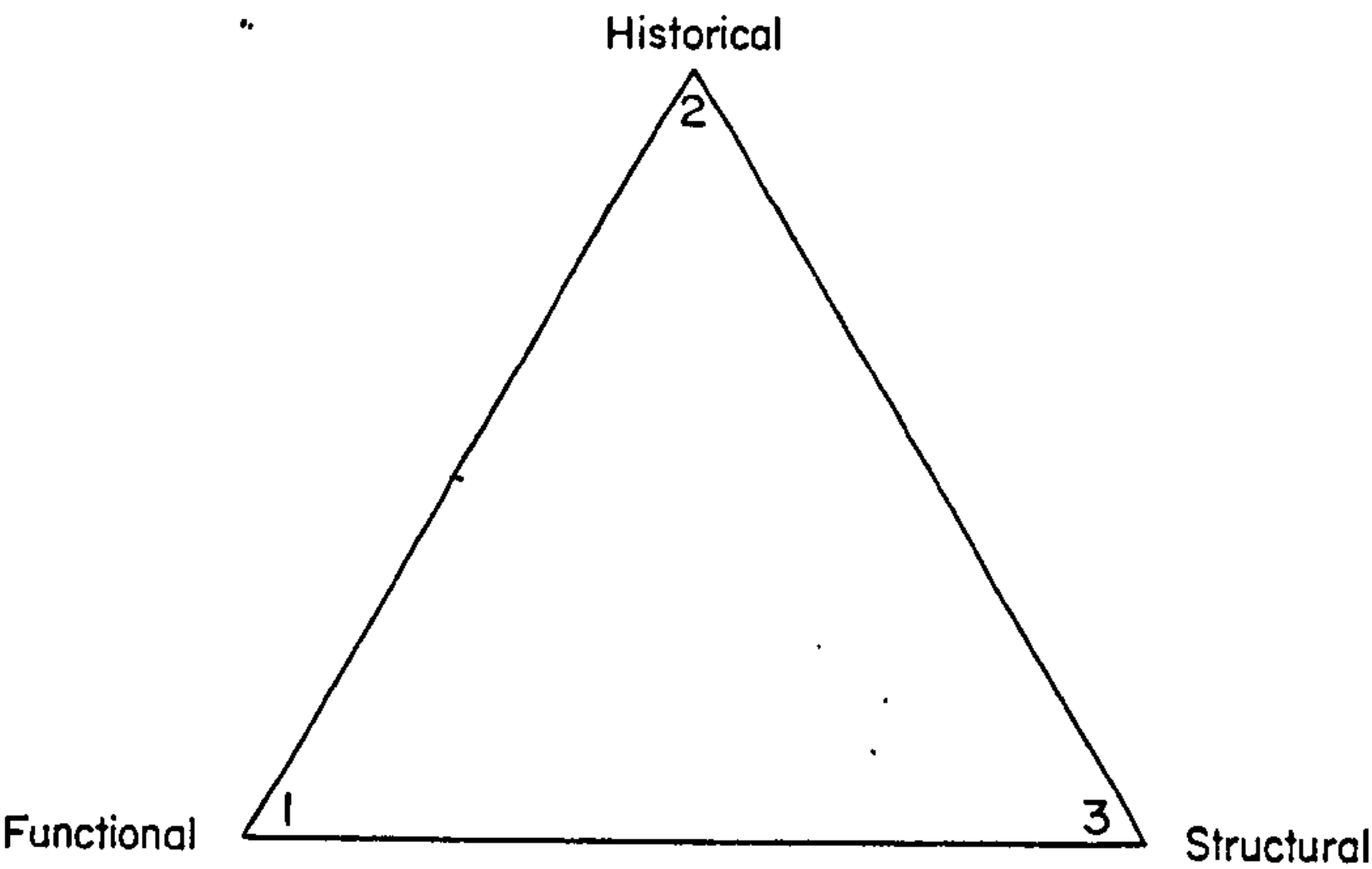
This is what I meant in the paragraphs above when I said that the valleys on a landscape could be thought of as self-organizing, and, in the case of a non-interactive allele, that it leaves the system ‘to sort itself out’. The whole point of information is that it is there to *stop* the system doing what it is naturally inclined to do. That is why Kauffman (1993)

talks about self-organization “in spite of selection”. The transition between *any* pair of contours on an epigenetic landscape (Text Figure 5.9) can be thought of as a case of self-organization; really, it is only the nodes which play an organisational role. So the maximally economical organism should have the smallest number of nodes, and the longest stretches of valley that it can get away with. And the corollary is that when adaptation to a specialized niche forces an organism to refine its organisational parameters, the process should be equivalent to packing its developmental trajectory with information encoding nodes, and upsetting the natural self-organizing tendency of the building materials in favour of functional optimization.

Section 5.5 The Shape of Life

5.5.1 Progress and Directionality

I next want to use the information-theoretic perspective to sketch out a general framework for evolution, demonstrating that it can be firmly rooted in one of the conceptual tools most dear to palaeontology: Seilacher’s Triangle (1970). Seilacher’s analysis of the three influences on form (structure, function and history) is a masterpiece of simplicity, and it captures something absolutely fundamental about the nature of living systems.



Text Figure 5.11 *Seilacher’s Triangle showing the three universal influences on organic form (after Seilacher, 1970; from Gould 2002).*

Evolution is life's functional transcendence of the inanimate realm via natural selection; that is the position I am defending. Information concerns only history and function; it is agnostic about the substrate. But a material substrate is always required, so there can never be complete freedom from structural interference. Information is gathered inductively: in addition to being 'about' its current environment, it is also intrinsically genealogical in nature, and therefore autobiographical as well. A closer intersection with Seilacher's Triangle is hard to imagine, and, with this in mind, it is possible to hope that everyone at the High Table can be friends.

Life started from a state of almost total simplicity, jammed into the lower righthand corner of Seilacher's ternary plot—all fabric, you might say, with no history and with only a basic self-replicative function. Since then it has been drawn inexorably toward the functional corner, carving itself a history in the process. It is important to appreciate that what we call 'function' is simply an explanatory shortcut allowing us to 'black box' (i.e. compress) long chains of history and causality. It happens when we shift from analogue to symbolic descriptions of information, and when we shift from case-specific causal/historical accounts to all-encompassing equilibrium ones. Take the evolution of land plants by way of illustration. Early forms are packed with fabricational influences and geometric constraints, manifested as simple bifurcations and Fibonacci spirals. Who knows what those early features were 'for', although it is easy enough to say how they arose (Mitcheson, 1977). By contrast, it is easy to say what the flowers of a modern bee-orchid are 'for', but far more of a challenge to explain how such complex structures are made. Indeed, as with any equilibrium account, it really doesn't matter *how* the bee-orchid flower is made because structural influences clearly play second fiddle to functional ones; we can readily appreciate that for the niche it inhabits, a bee shaped floral organ would need to be the output product of any number of possible developmental routines. The difference between these examples rests entirely on the fact that functionality has 'floated to the surface' to such an extent in the bee-orchid that a structural explanation becomes irrelevant.

We are talking about a shift from coarse-grained, 'blocky' structural influences with generalised and ill-defined functions to structurally 'fine-grained' and exquisitely sculpted ones, the functions of which are specialized and highly apparent. I shall argue that transitions of this type define, or at least depend upon, a particular axis of directionality to evolution. There is nothing new in this idea; it was around well before Darwin and has the

kind of intuitive appeal that ensures it is resurrected by generation after generation of evolutionary thinkers.

Normally this directionality is couched as 'progress' and not everybody likes that idea. Gould (1988) denigrates the notion of evolutionary progress as "a noxious, culturally embedded, untestable, non-operational, intractable idea that must be replaced if we wish to understand the patterns of history"; it wouldn't be too much of an exaggeration to say that he dedicated his career to demolishing it. My own position is that as with the distinction between bottom-up and top-down explanation given in Section 5.2.1, the 'patterns of history', if they are merely causal/historical accounts, might well be missing the point. It is possible to imagine global solutions to the problems of existence that will be found time and time again, regardless of the particular historical path that leads to their discovery. Admittedly, it can often be fiendishly difficult to demonstrate that the patterns of history *are* anything other than chance events writ large—three decades of stochastic thinking have amply demonstrated that (e.g. Raup et al., 1973; Stanley, 1973; Van Valen, 1973; Gould et al., 1977; Raup and Crick, 1981; Gould, 1988, 1989, 1996). But, equally, there can be little doubt that at least some types of directional process do exist, and these certainly merit an explanation.

Consider, for instance, the exponential increase in diversity over the Phanerozoic, at various taxonomic levels (Sepkoski, 1978, 1981, 1984). Or the preponderance of bottom-heavy clades early in the fossil record and top heavy ones later on, suggesting that most groups produce a maximum of diversity early in their evolutionary history, thereafter tailing off as they are displaced (or at least replaced) by later evolving groups (Gould et al., 1987). Or the bias in extinction and speciation rate between ancestors and their descendants, with descendant species more likely to speciate, and less likely to go extinct than their ancestors (Pearson, 1998). Or the various studies of increasing organisational complexity through time, either in body parts (e.g. Cisne, 1974), cell types (Bonner, 1988) or volume of coding material (Maynard Smith, 1988).

The most common objection to there being a directional component to any of these cases, much less one that could be described as 'progressive', is that instead they merely represent some sort of 'diffusion' away from 'a wall of minimal complexity' (Gould, 1988, 1996). This line of argument draws an implicit comparison between organisms spreading out through morphospace and a gas spreading out through an empty vessel once it has been released from confinement. But while it has a certain intuitive appeal, the analogy does not

stand up to scrutiny. Organisms are hugely non-random; any 'diffusion' through morphospace that also involves an increase in complexity must actually be working locally against the inexorable slide to entropy. If 'more complex' is the only direction in which to go, there still has to be a 'driving force' to get there.

A second component of the diffusion argument, therefore, involves the 'decoupling' of different levels of evolution (Stanley, 1975; Gould and Eldredge, 1977; Arnold and Fristrup, 1982; Vrba and Eldredge, 1984; Vrba and Gould, 1986). McShea (1991, 1993), for instance, looked for increasing complexity in mammalian vertebrae; he found that there was no 'intrinsic tendency' towards increasing complexity, but rather that lineages went equally in either direction. Significantly, those that simplified tended to be mammal lineages returning to an aquatic life after residence on land: in an obvious case of analogue correspondence, their backbones morphed to match the bland, isotropic homogeneity of their new watery home. Evolution is thus acknowledged to be directed locally, but not globally; and while it may be acceptable to talk about individual lineages becoming more perfectly adapted to their particular niches, there is no sense in which the whole ensemble can be said to be 'going somewhere' or 'getting better'.

And yet there are numerous quite obvious candidates for universal 'attractors' to any evolving system. Dawkins's (1976) holy trinity, *fidelity*, *fecundity* and *longevity* are cases in point. If two otherwise identical replicating systems differ in any of these qualities, the one which replicates most faithfully, most prolifically or shows the least tendency toward degradation, will normally survive at the other's expense. To these I would add *economy*, meaning any system which can do the same as another but using a reduced budget of energy or materials; and *universality*, meaning any system that copes equally well in all circumstances. Indeed, there must be a whole host of similar dimensions (often, admittedly, pulling in contradictory directions) that do not correspond to any particular environmental circumstance, but which can nevertheless be used to objectively sort between the various competencies of living systems.

Among the candidate universal functional attractors, one in particular stands out as relevant to the *Plus ça change* model: *evolvability*. The general consensus among those who have taken the notion seriously (e.g. Dawkins, 1989; Wagner and Altenberg, 1996; Kirschner and Gerhart, 1998) is that it has a lot to do with modularity. The reasoning is basically the same as that given above in Section 5.3.2: in order to maximise an adaptive organism-environment correlation, the fitness landscape needs to be as smooth as possible.

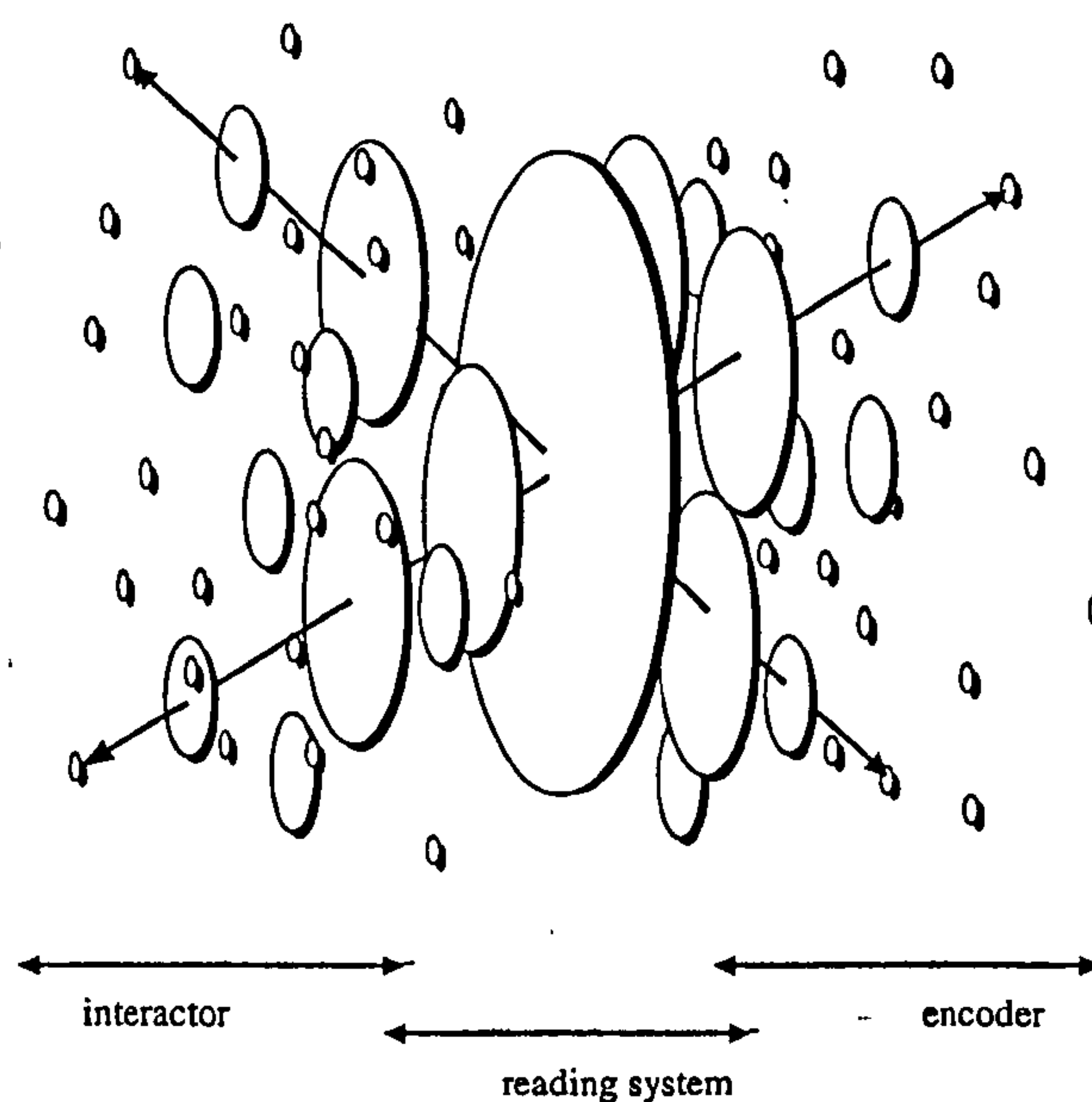
That this flies in the face of informational economy is an obvious restriction and counterbalance.

Another idea that I find particularly intriguing, therefore, is that maximum *compression* itself might be an evolutionary attractor. What I envisage in this case is a situation where one organism functions as well if not better than another, but is more economically organised in terms of development, and is thus able to encode its information in a slimmer format. Since it is not immediately apparent what this might mean in organic terms, a human analogy will help. When the old Victorian theories of 'electricity' and 'magnetism' were combined to form Maxwell's theory of 'electromagnetism', the new equations could do everything the old ones did, but more powerfully. Two separate theories had been compressed into a single unified model, which was thus more economical, more universal, and, if we take the idea of cultural information spread seriously, has proved to be more prolific and long-lived than either of its predecessors. Could it possibly be, contra Gould (1989), that a typical modern organism, replete with its sophisticated array of perceptual, behavioural and metabolic technology, would fairly wipe the Burgess Shale fauna off the Cambrian sea floor if transported back in time?

5.5.2 The 'Open End' of Life

Let us start at the very beginning with Dawkins's (1976) primordial Replicator molecule. We can imagine it floating around in a series of intertidal rock-pools, little more than a self-sustaining chemical reaction, until, one day, a slightly different version mutated into existence. This new form replicated faster than the original wherever the ambient temperature was above a certain point, but slower where it was below. The two lineages, old and new, could thus be said to have their own ecologies, with each 'species' out-competing the other at opposite ends of a shared thermal niche-dimension (the same argument would hold if we had started out with a Kauffman-style self-organizing autocatalytic network). Once they had been in competition for a while, the two forms could also be said to be storing information *about* their environment: given the different ecological preferences, sampling the chemistry of a rockpool would also provide an insight into its temperature! That branch point in the history of life would have marked the birth of representation in all its multifarious later forms.

Systems in which at least some mutations are heritable (rather than systems in which any mutation simply causes replication to cease) are known as *open-ended* replicators (Maynard Smith and Szathmary, 1995). Clearly, all extant life is descended from replicators of the open-ended variety, with new structures and functions constantly being built on top of earlier ones, apparently indefinitely. In complex, massively parallel systems, the structural components of the replication cycle can be shuffled in and out of step with one another to produce the shifting developmental mosaic we know as heterochrony (McKinney and McNamarra, 1991). But even in very primitive systems, novelty, in the form of symmetry breaking and the discovery of hitherto unexploited structural interactions, would define the 'open end' of an evolving lifecycle. As I argued in Section 5.3.4, information naturally tends to segregate into static and dynamic forms, and once the system had, for reasons of stability, crystallised into a set of encoders to organise the behaviour of the other elements (which would thus become the interacting part), there really would be a sensible way to talk about 'ends' of a replication cycle.



Text Figure 5.12 *Conceptual architecture of a replicator based on the form of Text Figure 5.9 and following from the arguments proposed in this chapter. The disc diameter represents 'niche size', generalist function being broader; the whole array is arranged hierarchically and centred on the generalised and thus stable reading system in the middle. Specific encoders are linked to their interactors (by arrows in the figure) through the mediating presence of the reading system.*

I generally envisage the whole configuration as shown in Text Figure 5.12, above. The array grows out in two directions from a historically embedded bottleneck of invariant structure that constitutes the reading system: the encoders get more complex, adding new layers to their command hierarchy and preserving ancient, deeply entrenched control parameters (*Hox* gene clusters and the like) which thus blend into the reading system; while at the other end, any changes in the encoders are translated to morphological shifts and novel discoveries among the numerous developmental or behavioural ‘modules’ of the interactor.

I cannot stress firmly enough that the hierarchy of the encoder is a *control hierarchy*: in terms of any kind of material structure it is ‘flat’. Superorganisms like ant colonies contain metazoan individuals; metazoan individuals contain eukaryotic cells; eukaryotic cells contain organelles; and within certain organelles is found DNA, much of it in the form of virus-like molecular replicators. This is a somatic hierarchy. It represents both a nested history of earlier free-living life forms, and a nested hierarchy of variously differentiated functional components. But it is *all interactor* (yes, strictly speaking, even the DNA!). The hierarchy of the encoder, by contrast, is informational; it is to do with sequential levels of control and functional relationships—with pattern, not with outright structure. There has been a persistent failure to grasp this fact (e.g. Gould, 2002), despite some extremely competent attempts to be crystal clear about the distinction (e.g. Dawkins, 1982a, 1982b).

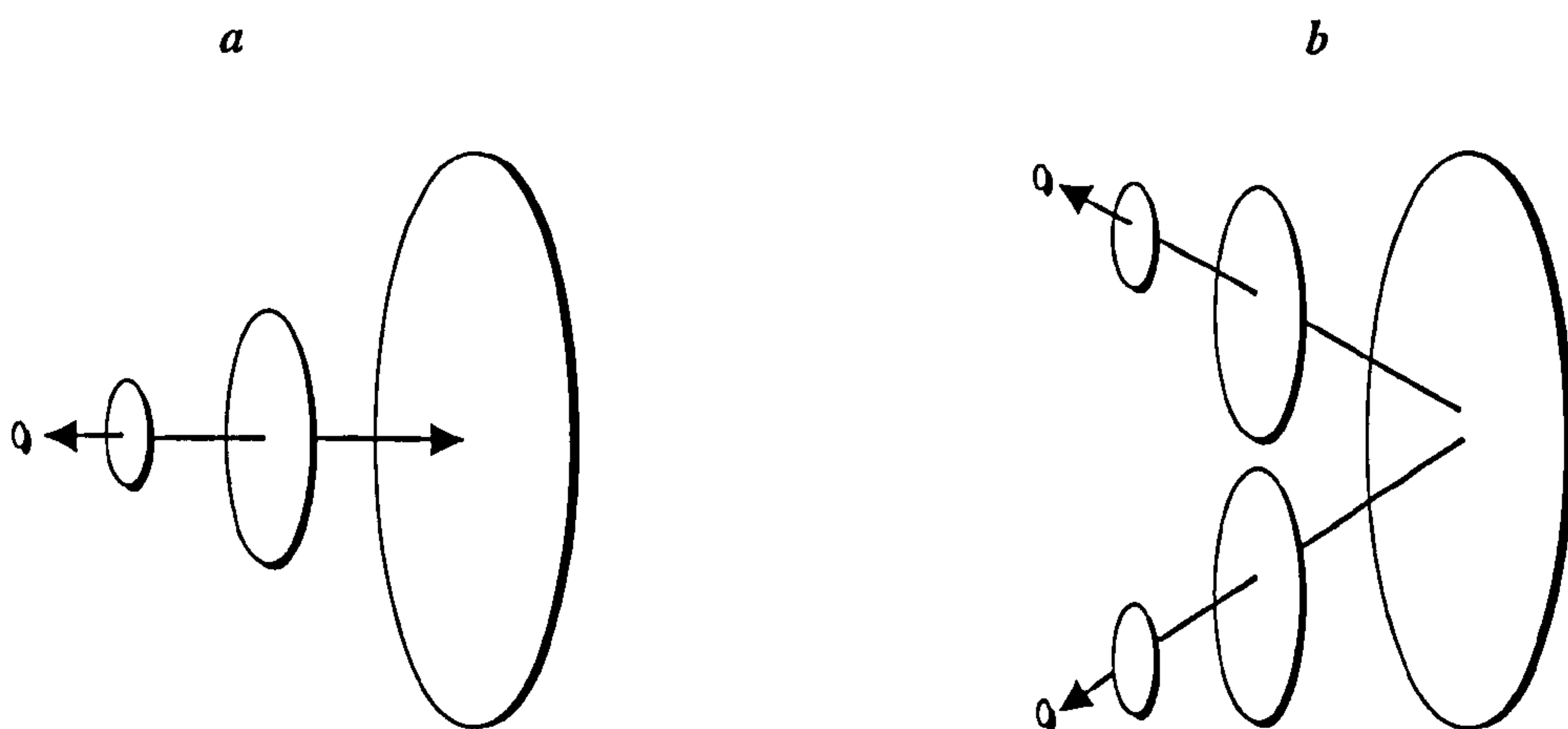
The configuration of the interactor plays a proximal causal role in *selection*, ‘screening-off’ the genes from direct environmental contact (Brandon, 1988). The configuration of the encoder plays a proximal role in *development*, by limiting alternative developmental expressions. Each half of the system therefore also plays a complementary *distal* role in the other’s domain: the encoder limits later rounds of selection since it records only a small sub-set of possible developmental parameters, and the interactor limits later rounds of development when selection filters the products of sub-optimal encoding.

Having defined a life cycle in terms of its ‘open ends’ it is now necessary to connect the structure to the process of evolution itself, a process that can be cast as exploration *at* those open ends. Niles Eldredge (1984, 1985) came very close to the model I envisage when he suggested evolution was an interaction between the twin hierarchies of

genealogy and ecology (although I have to say I disagree with much of the other classification in his scheme).

Genealogies form hierarchies when lineages split. When a split first occurs, the two daughters are very similar to one another in most respects; they should thus fall foul of the law of competitive exclusion (Hardin, 1960) and show a tendency to 'repel' one another. The law of competitive exclusion can usefully be compared to the physical restriction that two objects cannot be in the same place at the same time, except that here it refers to a location within a niche space—an information space—rather than a physical space *per se*. Obviously some kind of physical interaction is also required: information is just a shorthand description of complex causality, so information spaces are fundamentally ecological in character and thus they are concerned with strategies of competition for physical resources, of which real space is an important component. If speciation occurs via the allopatric mode, for instance, evolutionary repulsion will not occur until the two sundered strands of the lineage meet up again.

To simplify things, let me suggest that the budding branches of a genealogical tree can avoid competitive overlap by evolving in one of two conceptually distinct directions. They can evolve either *along* the universal niche axis, with one branch specializing and the other generalizing, or they can evolve *orthogonally*, both specializing but with each discovering a different suite of environmental regularities to exploit. These alternatives are depicted in Text Figure 5.13.



Text Figure 5.13 Two ways of avoiding ecological overlap. *a.* Species can evolve away from one another along the same niche axis, one specializing, the other generalizing; *b.* or they can switch niche dimensions entirely. The diameter of the discs once again representing 'niche size', generalism being broader than specialism.

5.5.3 Melting Metaphors

The diverging and differentiating effect of joint specialization evidently defines a direction of expansion, an 'open end' to evolution. This open end to evolution is not the same as the open end of an individual lifecycle, although I shall argue that we should expect the two to be correlated. Increasing ecological differentiation as a default direction for evolution is basically a packing problem: as pointed out in Chapter 4, there are simply more ways to be a specialist than there are to be a generalist.

But it is not *just* a packing problem: there are also structural and historical components at play. Very often a radiation into new niche space will occur only because of a structural innovation, of which the jaw bone dislocation in chichlid fish provides a striking example. And innovations of any type, whether we understand them in ecological or structural terms, will depend for their effectiveness on fortuitously occurring in the right place at the right time. This latter is a major source of historical contingency (Eble, 1999); indeed, it is the element of contingency that makes evolution superficially describable as a form of 'diffusion'.

There are important issues here that deserve to be pressed home. Most celebrated examples of evolutionary convergence—marsupial and placental mammals in particular—whilst often cited as evidence for equivalent ecological constraints, tend to be relatively phylogenetically similar, thereby overlooking the closely related structural and historical material with which selection was forced to work. In other circumstances, especially those in which the lineages concerned are very distant in type (and here I am thinking of the morphological convergence between, say, hummingbirds and moths), the influence of an overwhelming ecological component is more convincing. But even in these cases, or in ones as striking as the match between bugs and the leaves they live on, or sea horses disguised as seaweed, it pays to pause for a moment and consider the alternatives. Dennett (1995) backhandedly illustrates this very obligation when he points out how tempting (and mistaken) it is to assume that a butterfly camouflaged against one forest floor represents a species that would have been differently camouflaged had it evolved in a different woodland setting (and I refer back to my own sentiments about the bee-orchid in a similar vein!).

The fact is that Seilacher's Triangle has three corners—not just one or two—all of which will be active to a greater or lesser extent in any individual case. That is why when Dobzhansky (1937) characterised the Carnivora in ecological terms as a landscape of mountains, with the Felines and Canines as sub-chains representing separate broad niches, Eldredge (1995) was able to redefine it as a mountain chain of homologous phylogenetic patterns. Neither, I should add, was more 'right' than the other.

Nevertheless, a case can be made for selection imposing a constant pressure towards the functional corner of Seilacher's plot. The argument for this influence has, I think, to be made on the *a-priori* grounds that if selection *could* optimize an organism any further, it *would*. This casts the relentless pressure to optimize as akin to the force of gravity: that is, whenever we find an organism 'at rest', we assume it is being acted upon by a force of equal and opposite magnitude. This is not to unquestioningly swallow A. J. Cain's belief in the 'perfection of animals' (Cain 1964, in Ridley, 1997), which cannot even be specified without knowing the total space of possibilities. Rather, it is to use optimization as a *default expectation* (Maynard Smith, 1978; Dennett, 1983) and as a rationale for asking further questions (like whether there are pay-offs or historical or structural constraints at play) whenever the optimum condition is demonstrably not met. The strategy is thus equivalent to maxims like Occam's Razor; and nobody ever proclaimed that 'falsified' because something turned out to be more complex than expected!

Sometimes optimization means generalization. As I argued above, specialization normally involves packing an organism with costly organizational devices. All things being equal, the more specialized the function, the more complex the tools required; complex tools do not come free but have instead to be assembled at a substantial organizational cost from a multitude of individually variable structural components. In terms of Lego, it means building something from thousands of different pieces according to a long list of instructions. Ever the economist, we can expect Nature to take short-cuts where it pays her to do so. Sometimes her strategy is to generalize and cut back on functional specificity in favour of a cruder and cheaper model.

Much of the time, however, optimization *will* mean specialization, if for no other reason than that there is a larger available space of possible applications. This is movement along the universal niche axis, and for an individual lineage it clearly corresponds to the phenomenon of 'zeroing-in' (Section 5.3.4). When organisms specialize, they zero-in on

the useful but hitherto unexploited redundancies in their environment, ‘representing’ all that fine-grained structure in analogue (interactor) and digital (encoder) form.

Think for a moment about the logic behind allopatric speciation. The world is heterogeneous; it differs from place to place at a variety of scales. Rock pools are very different from the exposed rock surfaces surrounding them, but even shallow dips in vast prairies are subtly different from the adjacent high ground. Different conditions in different locations impose subtly or drastically different selection pressures on the organisms inhabiting them. We expect such local selection pressures to act differentially on a widely dispersed lineage, teasing it apart into a series of local ecotypes; interbreeding *between* those local populations then acts to reverse the effect (which is why Sterelny (2001) refers to it as ‘Mayr’s Brake’—the brake being *off* during allopatric separation). Indeed, a good way to view a species in representational terms is as a kind of multilevel focusing device akin to Fisher’s microscope, with the concentration of adaptation in small demes focusing on fine detail, and gene flow across the species as a whole ‘panning back’ by blurring the local picture and focusing instead on a regional average.

How do we link all of this reasoning together? I suggest the following scheme: functional modules (behaviours or organs) designed to cope with general or average or truly persistent features of the environment get shuffled up the information hierarchy, inward towards the reading system where they lodge at the organism’s ‘crystalline core’; they become ‘general’ representations of ‘universal’ fixtures in the ecology of the organism. Those designed to cope with specific or idiosyncratic or transient environmental elements accumulate around the organism’s ‘fluid periphery’, where they can react quickly to changing conditions. If this argument seems familiar, it is: it is none other than the ecological ‘hub model’ outlined in Chapter 5 and transposed to the organism itself. Perennial environmental features should end up matched by ‘locked-in’ developmental parameters, while transient ones are captured instead by a sea of ever shifting specialist modules. I think it is no coincidence, for example, that in animals the *Hox* gene cluster codes for features like anterior-posterior patterning, since the functional benefits of ‘going forward’ and ‘having your sense organs at the front end’ were discovered long ago in the early rounds of Precambrian symmetry breaking, and the rationale behind encephalisation has not changed substantially since then. This kind of hierarchical structure permits maximum economy, and thus maximum compression, by distributing the smooth fitness

landscape of highly evolvable but expensive elements where it counts the most—on the ‘outside’.

At this point the argument becomes extremely relevant to *Plus ça change*. Using a ‘states of matter’ metaphor to grapple with organic complexity, let me suggest that under perfectly stable environmental conditions, organisms exhibit a constant tendency to ‘melt’, with ever increasing fidelity, into the shape dictated by their environment (like hot wax poured into a mould). This tendency depends partially on the environment providing a *static target* for the organism to ‘find’. It also depends on the organism (and here I really mean a species or ‘codex’—a genealogy with a perspective on the world) being able to branch and diversify indefinitely so as to track small idiosyncracies without contradicting itself (i.e. without one point of optimization detracting from another).

If, on the other hand, the environment has many elements that keep shifting around and thus do *not* present a static target, then the organism will be restricted to its crystalline core—a brittle and functionally generalized description of the world, recording only its most stable parameters. (I should also add that when the environment starts shifting faster than the resolution of a single lifecycle, the organism should opt for a cybernetic solution—see Section 5.4.3 for discussion). We should therefore expect stable environments to collect fluid, specialized organisms, and unstable ones to collect crystalline, generalized ones. So far so good. But in terms of the microevolutionary version of *Plus ça change*, this metaphor can be pushed further: it suggests that organisms should be *thixotropic*, like wet sand or cornflour—they should ‘melt’ when the environment changes slowly enough for them to track, and ‘solidify’, by falling back on a generalist ecology, when it speeds up too fast for them to deal with.

This is my answer to the *Plus ça change* model’s missing mechanism, and although it deploys a phenomenal range of linguistic tricks to get the message home, I hope I have at least been consistent in showing how and why I think these work.

5.5.4 A Theory in Search of A Metaphor?

All this theory may seem a far cry from the practical realities of working palaeontology; but evidence and theory go hand in hand, for without evidence theory is

empty, and without theory evidence is formless. The need to provide a general theoretical framework through which palaeontological data can be interpreted is acute, especially given the difficulties of straightforward extrapolation from observational biology (Chapter 1). My desire was to find a theory sufficiently abstract that it could be readily scaled to different timeframes.

I chose information as a founding principle partly because *Plus ça change* seemed to be a model about signal reception in settings with various degrees of background noise, but also because I have long been fascinated by the problem of human consciousness, and information seems to be the answer to that, too (see Dennett, 1991; Chalmers, 1995; Edelman and Tuoni, 2000). In my estimation, an information-based account makes biology more complete by providing a role for subjectivity, along with many of the attributes we are encouraged (erroneously) to think of as ‘nurture’ rather than ‘nature’.

I always found the subjective element to *Plus ça change* quite intriguing—the fact that the model was designed to work ‘from the perspective of an evolving lineage.’ I was particularly keen to flesh out an image I had early on, of *Tritaxia* ‘reading’ the Milankovitch cycles of the Lower Chalk, like a laser scanner reading a bar code. It was clear from the outset, however, that anything specific about the information *Tritaxia* was picking up from its environment was going to be off-limits, and that instead whatever mechanism I found would simply have to make general predictions about how evolvable the lineage might be under certain circumstances, thus complementing Sheldon’s original approach.

In retrospect, I think I made a lucky guess: ‘information’ seems to be maturing into a major founding principle in physics (see Johnson, 1995; Von Bayer, 2003) and also in the biological sciences as well. In what must have been one of the last papers he wrote, John Maynard Smith (2000) defended the use of information-theoretic language in biology. His article was rapidly met by responses from Peter Godfrey Smith (2000), Kim Sterelny (2000) and Paul Griffiths (2001), three of the key players in contemporary philosophy of biology. They had all been thinking about the same thing.

Maynard Smith had a remarkable talent for guessing where the action would be, as shown by the fact that he wrote a paper defending adaptationist strategies a year before Lewontin and Gould published ‘The Spandrels of San Marco’ (Maynard Smith, 1978), and by the fact that he was first name on the eight-authored constraints paper that is now regarded as a definitive declaration on the subject (Maynard Smith et al., 1985). I think he

was right again, and that the information-theoretic paradigm will result in a substantial cross-disciplinary attitude-shift in the decades to come.

The concluding paragraph of a review article published in *Nature* to summarise ‘*The Major Transitions in Evolution*’ (Maynard Smith and Szathmary, 1995; Szathmary and Maynard Smith, 1995), reads:

A central idea in contemporary biology is that of information. Developmental biology can be seen as the study of how information in the genome is translated into adult structure, and evolutionary biology of how the information came to be there in the first place. Our excuse for writing an article concerning topics as diverse as the origins of genes, of cells and of language is that all are concerned with the storage and transmission of information. The article is more an agenda for future research than a summary of what is known. But there is sufficient formal similarity between the various transitions to hold out the hope that progress in understanding any one of them will help illuminate others.

I hope that with all the context they were given, the metaphors I chose did their job properly. We need some way to structure our thoughts, and metaphors are perfect tools for the advocate’s trade. In the background all along was an understanding that the human mind is a kind of information space—a ‘virtual epigenetic landscape’—implemented in analogue form on a purpose built cybernetic machine, and supplemented by the cultural (memetic) encoding system we call language. In one of the most claustrophobia-inducing insights I ever came across, a philosophically gifted friend of mine described language as “like telepathy, but with words”. So it is. Language can be used by an author or speaker to ‘reach inside’ the mind of their audience, and thus to ‘guide’ the thoughts of others, to ‘zero them in’ on a particular conclusion. Metaphor is a principal tool in such guidance, as a critical analysis of any newspaper or politician’s speech will quickly show.

But on closer inspection, even ordinary language turns out to be *made* from metaphors and other analogy-based descriptive devices: the word ‘language’ itself, for instance, comes from a Latin ‘root’ meaning ‘tongue work’. Even apparently abstract nouns for first person experiences have a basis in comparison, as revealed by their etymology: ‘green’, for instance, derives from the Old High German *gruoni*—to grow. Once you start ‘seeing’ metaphors ‘in’ language, you soon ‘find’ them ‘inescapable’ (see Lakoff and Johnson, 1980); it thus seems sensible to simply acknowledge the role they play and add them self-consciously to the toolbox of techniques for communication.

But is misleading to think of this model (or indeed any model) as *just* a metaphor, because metaphors work for a reason. As Szathmary and Maynard Smith suggested in their concluding paragraph, the key idea is ‘formal similarity’—isomorphism. Metaphors tease novelty from the everyday via small structural adjustments. As such their use compares favourably with the process of natural selection itself, for that also—albeit in analogue form—crafts something new from something already made, in a series of shape-preserving, novelty-introducing, rule-bending steps.

Peter Sheldon once complemented me on a ‘fine analogy’ when I suggested we should consider the genomes of aphids and dandelions as biological ‘text messages’—brittle and short, highly compressed, with no internal redundancy. Thank you, Peter, but to call it an analogy misses the mark. The argument is about information, and at some abstract level both text messages and aphids simply *are* massively *r*-selected encoders of very generalized information. There is no analogy about it. The substrates are different but the ecological constraints are the same. Like the spiral shape of the galaxy, the hurricane and the mollusc shell in Section 5.2.1, this is an identification of pattern, not stuff.

In complete contrast to the way it is understood by some (e.g. Chalmers, 1995; Johnson, 1996), almost the defining property of information is that it has no ‘essence’. It can never be ‘touched’ or ‘pinned down’, but merely alluded to. Metaphors are a means of approach precisely because they are already grounded in something more solid, historical and familiar, and thus do not need to land squarely and safely on their target. They can, if necessary, reach out indefinitely. But reach out for what?

What is ‘information’? Nothing but an eleven letter word with a difference-making effect on certain reading systems; reading systems that will hopefully now, in virtue of their own history, endow it with an enhanced functionality (presuming they have read this far in sequence). ‘Information’ is a compression about the fact of compression itself. It is an exploitation of a redundancy inherent in all living systems, including the one of which it is part. All the ‘aboutness’ of information is aboutness about ‘aboutness’ itself. We have zeroed-in on the idea of zeroing in. When Paul Griffiths (2001) was pondering his ‘metaphor in search of a theory’, he had the problem upside down. The theory already exists: it is the physicist’s information theory. What it needs to give it ‘body’ and to ‘bring it to life’ is an acknowledgement of the role metaphor plays. Wittgenstein, by contrast, had it dead right. In one attempt to answer his critics he drew a kettle spouting steam and said, “Asking about the content of language is like asking about the content of this kettle: it

hasn't any, it is just a picture of a real thing." At another point he says, "He who has understood me, must, so to speak, use my words as a ladder to climb up, which, after the climb, he must cast aside." Another bull's-eye. And finally (and somewhat mystically), "The solution to the problem of life is seen in the vanishing of the problem." But that, I would say, is the epitome of evolution.

As for the proposal of a fundamental architecture for living systems: it is essentially an ecological model, which is to say that it is about functional fit within a universal environmental framework. It is caused by the intersection of genealogical hierarchies with an axis universal organisation; but it is also underpinned by a mechanism for connecting development to ecology through the notions of modularity and evolvability. I believe it is a pattern that will be discovered by information encoding and utilising entities anywhere in the universe, at any time in its history, regardless of the substrate on which it is expressed (I suspect it manifests itself in language as Zipf's Law, for instance). It should be thought of as an environmentally induced, lowest-energy configuration, and be placed alongside sand dunes and water droplets in our conceptual taxonomy. It is a major aspect of the shape of life, and throughout the chapters to come it will form the foundation for my discussion and interpretation of the evolving relationship between *Tritaxia*'s development and its ecology.

Summary

The information theoretic perspective has given us a novel shortcut for thinking about the relationship between living systems and the environments they inhabit: in virtue of their representational capacity, organisms contain 'a picture' of their niche. The picture is expensive, however, and so generalists make do with blurry images because that is all they can afford, while specialists need sharply focussed but correspondingly expensive ones. Such pictures take time to develop and can only be used to capture environmental features of an adequate level of stability. Furthermore, the picture forming attributes of the organisms themselves are variable. Switching to a substance metaphor, organisms have an inherent tendency to 'melt' under conditions of environmental stability, trickling into an ever more perfect fit with their environmental mould. When the environment cannot be tracked, however, the organisms 'freeze hard' and go 'brittle', losing the shape of their template. With time, the malleable aspects of a living system are juggled to line up with the malleable aspects of their environment, to produce the information hierarchy.

Chapter 6 *Tritaxia pyramidata*

Introduction

To test the *Plus ça change* model we need to track a single lineage through the environmental circumstances described in Part II. *Tritaxia pyramidata* is the lineage most central to this research programme, and because evolution is the control of *development* by ecology, a major aim of Part III is to generate a model of *Tritaxia* in four dimensions, and eventually as a developmental trajectory across a well-defined epigenetic landscape. The first step must be to assess the material traces at our disposal, so this chapter introduces and summarises the entire morphological database for the focus lineage, as a precursor to understanding the developmental sequence itself.

Section 6.1 Morphology in 3 Dimensions

6.1.1 *Tritaxia* in the Literature

Order	Foraminiferida
Suborder	Textulariina
Superfamily	Lituolacea
Family	Ataxophragmidae
Subfamily	Verneulininae
Genus	<i>Tritaxia</i>
Species	<i>pyramidata</i>

(Carter and Hart, 1977)

The structure known as *Tritaxia* has a long history of recognition, being primarily identified by Reuss in 1844 as *Textularia tricarinata* (in Loeblich and Tappan, 1964). Thereafter, it was designated as various genera including *Verneuilina* (by Reuss), and *Gaudryinella* and *Clavulina* (by Cushman), before being called *Tritaxia* by Franke in 1925 and sticking to that name ever since (details in Carter and Hart, 1977). As far as I can tell, it

fits Loeblich and Tappan's (1964) description of *Verneuilina* quite as well as any other, but they regard *Tritaxia* as distinct on the basis of 'adventitious final chambers'. Most authorities on the Lower Chalk seem content with this designation, so *Tritaxia* is the name we shall use.

There is, however, some disagreement concerning its status as a single species. Carter and Hart treat all forms of *Tritaxia* from the beds below the Plenus Marls as a single species: *pyramidata*. But in 1962, Jefferies, working exclusively on the Plenus Marls, distinguished three discrete forms, one of which he also called *pyramidata*, the two others being *plummerae* and *macfadyeni*. In Jefferies' scheme these forms had the status of subspecies so that there was a *Tritaxia tricarinata* var. *pyramidata* etc., although he lumped them all together for the purposes of his discussion and did not distinguish between any of them on his plots. More recently, Paul et al. (1994) listed two separate species of *Tritaxia*, *T. pyramidata* and *T. plummerae*, and even considered the absence of *T. plummerae* in certain horizons as an event significant enough to mention. It is my opinion that all of these forms belong to the same species, and even the same variety, and that the morphological divergence among them represents a gradation of stages which have an entirely separate explanation. I shall make a case for this below in Chapter 7.

The genus apparently spans from the Lower Cretaceous to Recent (Loeblich and Tappan, 1964; Murray, 1991), although I have been unable to find any studies of extant species that do more than list them as a component of one assemblage or another, suggesting that *Tritaxia*'s abundance in modern environments may be far lower than it was in the Cenomanian Chalk Sea. Carter and Hart (1977) suggest the species *T. pyramidata* ranges from their Zone 3 in the Middle Albian up to Zone 14(ia) (Jefferies' Bed 3 of the Plenus Marls), although their analysis of this appears to be based on the work of Jefferies rather than their own observation. Cottle (1990) lists *Tritaxia tricarinata* as one of his Turonian specimens and from the photograph he includes it seems to be a very similar form to the Cenomanian lineage, so it is probable that the lineage of *Tritaxia pyramidata/tricarinata* survived well into the Middle Chalk, if not higher.

As we have seen, *Tritaxia* dominates the benthic portion of most samples taken from the Lower Chalk; indeed, Carter and Hart describe it as being in 'flood abundance' in the early beds.

6.1.2 Choice of Characters

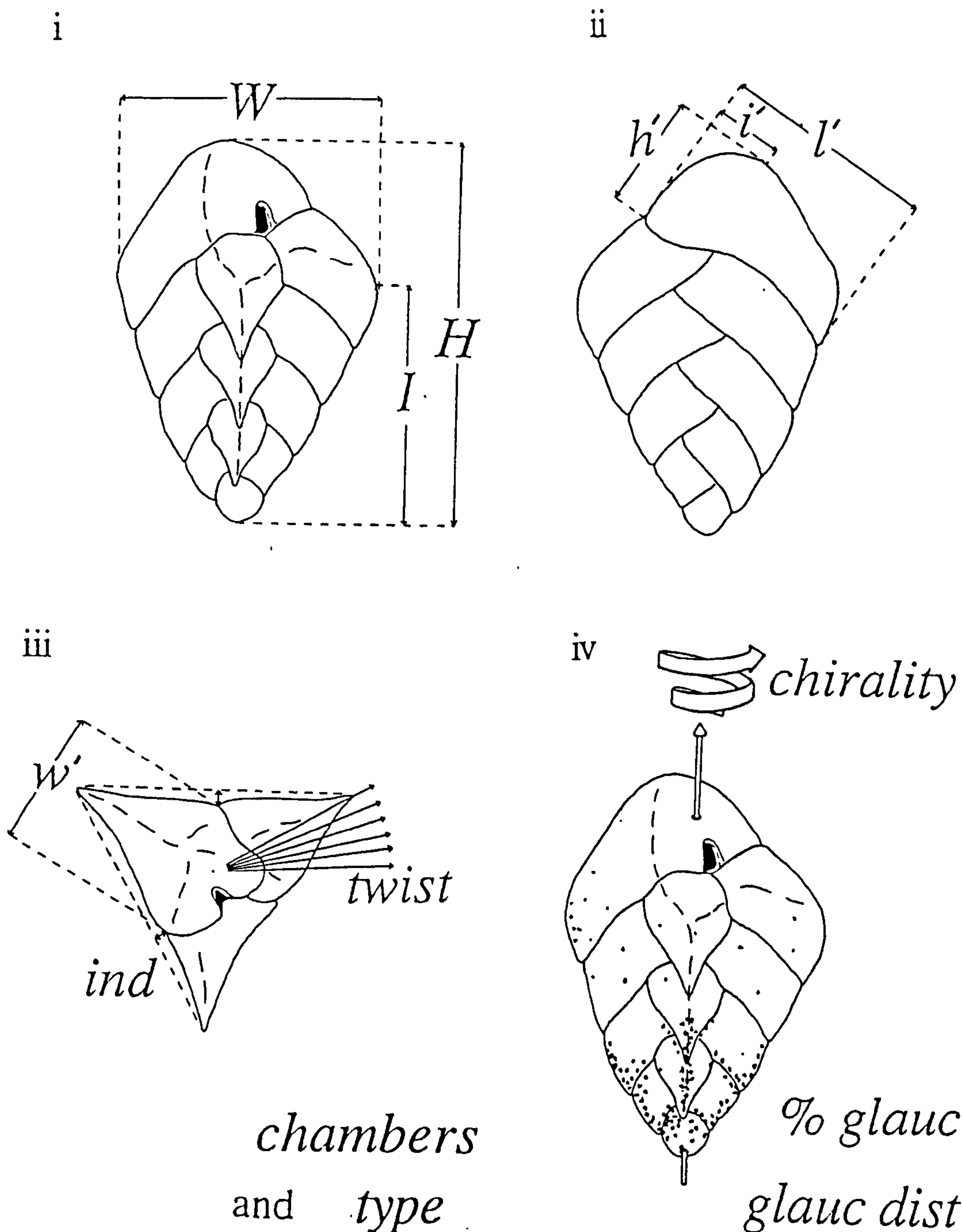
Tritaxia pyramidata has a triserial test, triangular in cross-section, which sometimes becomes uniserial or biserial for the last few chambers. It is unilocular with a terminal aperture in the uniserial stage, or an arched interiomarginal one when growing triserially. According to a diagram in Loeblich and Tappan (1964), this aperture leads directly into a thick tube which spirals around the axis, connecting foraminae and effectively bypassing the final few chambers, although I have (admittedly rather clumsily) dissolved the final chambers of several specimens and never succeeded in seeing such a thing. Each chamber in the triserial stage is normally stacked directly above the third one back, and this sequence completes one full whorl, though there may sometimes be a slight offset so that the whole test is twisted.

The test itself is composed of various sizes of mostly calcitic grains, coarser towards the middle of each wall and covered in finer grade material on the outside. In well preserved specimens a translucent calcite glaze is present, which imparts a smooth and seamless appearance to the test. In some specimens, tiny grains of a green mineral can also be seen beneath the surface glaze. This is probably glauconite and is evidently of a sedimentary origin, being incorporated into the test during construction. Sometimes this glauconite is randomly scattered throughout, but more commonly it is concentrated around the outer, carinate corners of each chamber, or in the early chambers only. The percentage of glauconite also varies, being generally less than a percentage or two, if any at all, but sometimes rising to 50% or more of the total agglutinating surface material, and giving the test a striking green speckled appearance.

The following set of fourteen 'characters' were eventually chosen to represent the form of this species (Text Fig. 6.1).

- 1) H - maximum height of whole test along the growth axis
- 2) W - maximum width of whole test
- 3) I - intersection of H and W , measured up from the proloculus and parallel to H
- 4) l' - maximum length of the long axis of the final chamber
- 5) h' - maximum height of the final chamber, orthogonal to l'
- 6) i' - point of intersection of h' on l' , measured from the apertural end
- 7) w' - maximum width of final chamber, parallel to the long axis of the aperture

- 8) *Ch* - total number of chambers
- 9) *ind* - average depth of indentation between adjacent carinate corners
- 10) *tw* - twist: deviation from 120° rotation for successive chambers
- 11) *chir* - chirality: direction of rotation along coiling axis
- 12) *g%* - percentage of glauconite in test materials
- 13) *g.dist* - distribution of glauconite in test
- 14) *type* - growth type: the configuration of the final few chambers



Text Figure 6.1 Schematic drawings of *Tritaxia* and the characters chosen to represent it: i. *H*, *W*, *I*—longitudinal view, 'front'; ii. *l'*, *h'*, *i'*—longitudinal view, 'back'; iii. *w'*, *ind.*, *twist*—section view back along the growth axis; iv. *chir*, *g%*, *g.dist* and also number of chambers (*Ch*) and final chamber type (type not shown, see Section 6.1.3.i)—longitudinal view, 'front' again.

6.1.3 Character Measurements

Character values were measured in a number of ways. All specimens were examined under a Wilde binocular microscope which could be racked up to the maximum magnifying capacity available from the variety of lenses it possessed. This happened to be $\times 625$ resulting from the combination of a $\times 50$ objective lens, a $\times 10$ eyepiece and a $\times 1.25$ camera turret that could be fitted part way along.

Continuously varying characters amenable to metric evaluation (H , W , I , l' , h' , w' and i') were measured with a graticule and then converted into microns. The graticule had 40 cross-bars, providing a measurement every $15.6\ \mu\text{m}$, or every $7.8\ \mu\text{m}$ to the nearest half-interval estimate.

ind (indentation) was also measured with the graticule but not translated into microns. For reasons which will be explained below, this character is better treated as a discretely varying trait in which low graticule categories such as 0.5, 1, 1.5 etc. make more sense than odd and sometimes fractional numbers of microns.

For whole test characters (H , W , I), the specimen was simply laid flat on the side shared by the final two chambers with the third chamber back pointing vertically away from the slide (Text Fig. 6.1.i). For three of the final chamber characters, h' , l' , and i' , the measurements were taken from the opposite side of the test. This side normally had the straightest sutures and most easily identifiable homologous points, but it meant that the fossils had to be flipped over and balanced on their opposite carinate edge (i.e. the edge three chambers back from the final chamber: Text Fig. 6.1.ii). Similarly, measuring the width of the final chamber, w' , along with the *ind* and *twist*, required that the test be balanced on its prolocular apex (Text Fig. 6.1.iii). In order to get at these awkward features it was necessary to prop specimens up against something, and the most convenient object turned out to be a particularly large and unusually deformed specimen with a dramatic twist imposed upon the normal prismatic shape. This effectively provided a smooth, curved surface along which another test could be arranged and stuck by the surface tension of a thin film of water. In this way it was possible to organise any other specimen so that it would balance on a carinate edge or vertically on the prolocular apex and allow accurate, leisurely measurements to be taken. Admittedly this was all very fiddly, and it sounds positively primitive, but it worked well enough and resulted in a good three dimensional representation of the fossils.

Measurement always took place relative to easily identifiable points that seemed to be homologous between specimens. H was simply the maximum dimension of the test along the coiling axis, and W an equivalent measurement at 90° . Final chamber length, l' , was taken from the point of intersection between the apertural end of the final chamber and the next chamber back, to the point at which the same suture met the carinate edge. This suture could always be fairly clearly traced, and, as mentioned above, was normally at its most straight and regular on this side of the final chamber. Where it curved the length was still taken as a straight line between the specified points. In cases where the aperture was apical or obscured, the measurement was taken from the location that would correspond to a normal aperture; that is, at more or less the surface point of conjunction between all three chambers in the final whorl.

h' was taken to be the maximum extent of the final chamber in a direction at 90° to the length. i' was the point of intersection between this pair, and was measured from the apertural end of the length axis.

w' , too, was defined relative to the aperture. In normal triserial growth the aperture is an elongate arch which interrupts the suture between the final chamber and the chambers below it, at a point somewhere close the coiling axis. In these triserial cases, therefore, the axis of the apertural arch runs in more or less the same direction as the length measurement—from the coiling axis curving back along the final chamber towards the carinate edge of the test. Thus, in triserial cases w' was taken to be perpendicular to l' . There are, however, exceptions to this relationship between the aperture and w' .

For reasons which will shortly be explained (Section 6.2.2.ii), certain specimens had oddly arranged final chambers (catalogued as *type*) in which the aperture stretched in a direction off-set from the usual alignment with the carinate edge, being oriented instead somewhat towards the flat wall of the test. In all such specimens, l' , as always, ran between the aperture and the carinate edge, but w' was taken to be at 90° to the long axis of the *aperture*, even though that direction was no longer perfectly perpendicular to l' ! There are good reasons for choosing this definition, which will become more apparent when we consider the mechanisms of *Tritaxia*'s growth; for now, suffice it to say that the motivation was to identify homologous points from which measurement could proceed.

There was no measurement made of the intersection of l' and w' because for the most part such a point would have been the identical to i' . The unfortunate exception concerns those very same specimens having an unusual final chamber in which a measurement of the l' - w' intersection would have been useful; but by the time I came to appreciate why, the majority of the specimens had already been examined.

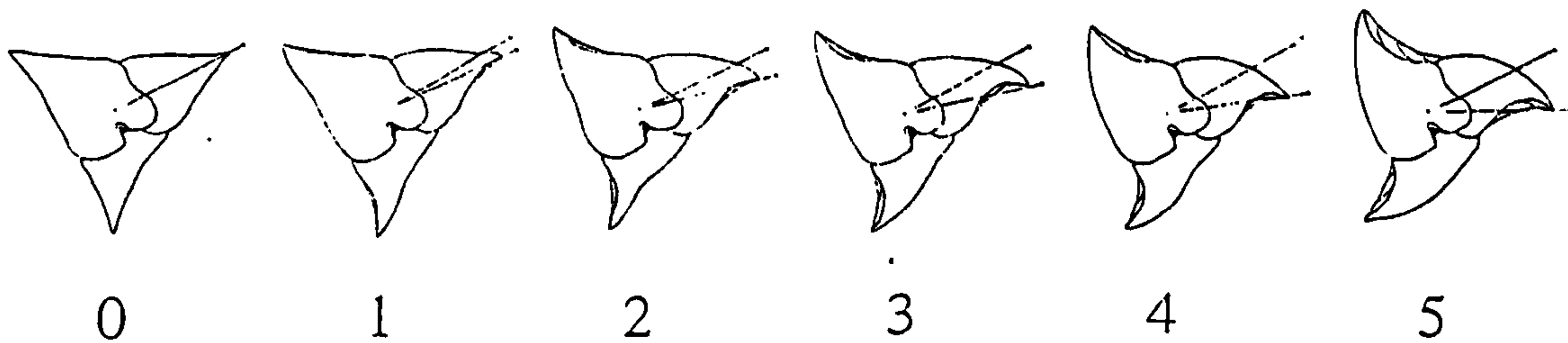
For most metric characters it was possible to measure each test to the nearest half graticule spacing (7.8 μm); however, two characters demanded a lesser degree of accuracy. The H - W intersect, I , was supposed to be the point of intersection between maximum height (H) and width (W), but because the test is a spiral structure, the widest point on one column of chambers is not the same height as the widest point on the others. As a result, the measure of I , which was intended to suggest a kind of 'centre of gravity', fell midway between the two. Similarly, i' , the intersection of maximum height (h') and length (l') of the final chamber, was often located on such a gently curving slope that to imply any great precision would be misleading. Consequently, both of these characters are measured only to the nearest whole graticule spacing instead of to the nearest half.

Like the metric variables described above, *ind* (indentation) was also measured with the graticule, but this time the measurements were not translated into microns. For reasons which will be explained below, this character is better treated as a discretely varying trait in which low graticule categories such as 0.5, 1, 1.5 etc. make more sense than odd and sometimes fractional numbers of microns. Indentation (*ind*) was a divergence of the middle concave face of the test from an imaginary line joining any two carinate corners, when looking down the growth axis (see Text Fig. 6.1.iii). For asymmetric specimens it was roughly the average such measure of each side. For example, if two sides were indented by 1 graticule spacing each and the remaining one by only 0.5, then the mean being $2.5/3 = 0.833...$ the value recorded would be 1.

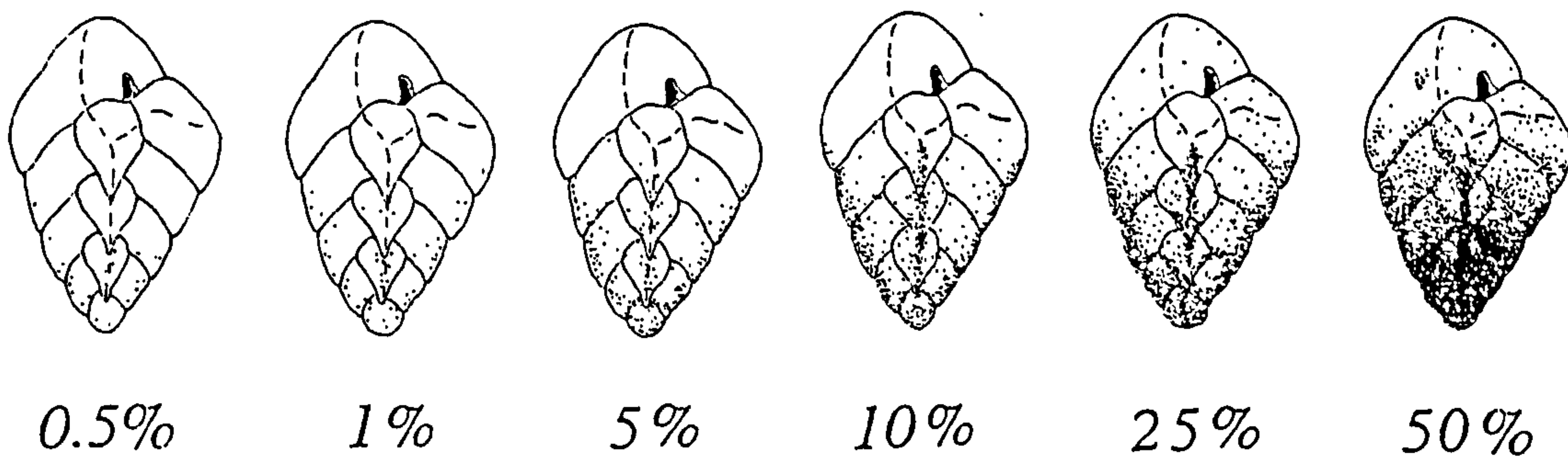
All other characters (Text Fig. 6.1.iv) — *Ch*, *g%*, *g.dist*, *chir*, *tw* and *type* — were counted, estimated or otherwise classified by turning the specimen over and generally rolling it around until enough had been seen to satisfy my judgement.

These other values were easier to come by since they simply involved either counting (*Ch*), a visual estimation which rendered continuous variation as categorical (*tw*,

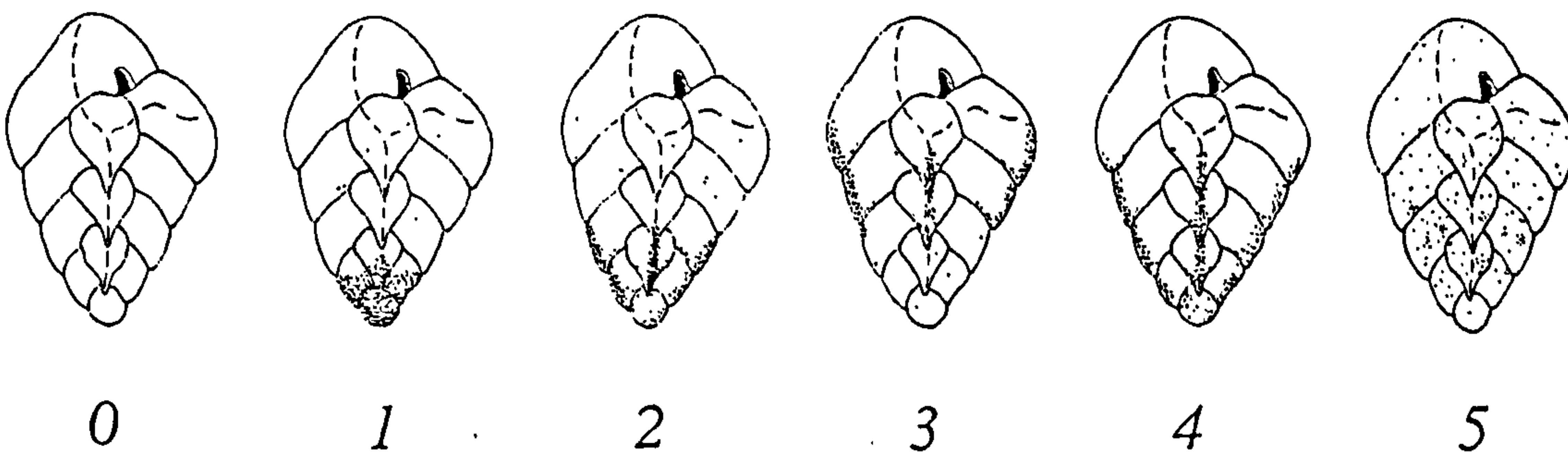
i



ii



iii



Text Figure 6.2 Categories for non-metric variables: i. degree of twist (tw); ii. percentage of glauconite (g%); iii. distribution of glauconite (g.dist.).

g%), or simply by noting from a range of predetermined possibilities those categories applicable to each specimen (*g.dist*, *chir*, *tw*, *type*).

Twist (*tw*) was judged from the divergence between the carinate edge and the concave side of the test (Text Fig. 6.1.iii & Text Fig. 6.2.i). Assessment would have been a great deal more accurate had I had access to a graticule measuring angular deviation directly, but that was not to be; so instead I selected examples from what I thought was the range of *twist* expressions, drew them, and used the sketches as a template to categorise individual specimens (Text Fig. 6.2.i, below). This measure of torsion was designed to increase in roughly equal increments (five degree chunks) from category to category and by and large the scheme worked very well, producing results in accordance with a cursory and more intuitive assessment of the sample populations.

Counts of the glauconite content per specimen were based on the standard geologist's percentage estimation charts with the range of values shown in Text Fig. 6.2.ii. Categories of glauconite distribution (*g.dist*) can be found in Text Figure 6.2.iii. An explanation of the *type* categories can be found in Section 6.1.3.i (below).

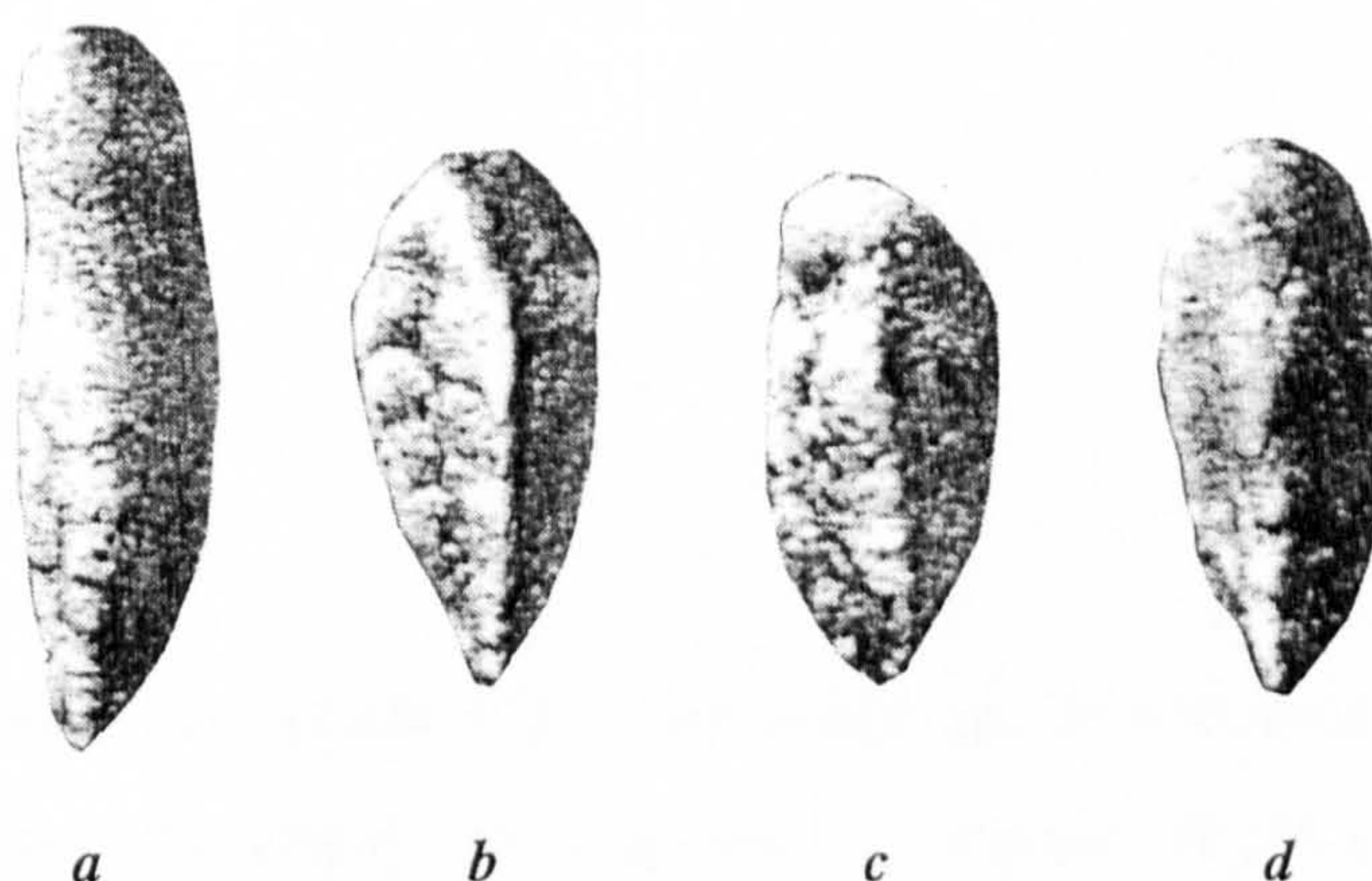
The full range of characters was only arrived at through experience. *H*, *W*, *I*, plus some of the final chamber measurements, were obvious places to start; other elements of the test were added to the list of characters as it became apparent that there was variation to be found among them. The majority of the Folkestone 100 kyr data set was measured at least twice, once in an exploratory way using only 30 specimens per horizon, then again after adding to and refining the initial measuring scheme, and with another 15 specimens included in each sample population.

For some characters, particularly those estimates demanding the most qualitative input (e.g. *g%*, *tw*), my practice was refined by experience so that by the time I had finished the whole data set I was routinely recording larger or smaller average values per population than I had at the beginning. Consequently, the very last thing I did was to go back over all the specimens during the course of a fortnight or so and very quickly re-assess these two characters (and conduct for the first time some *chirality* assignments and certain of the *type* ones which only occurred to me late in the day). Fortunately, these are all easy measurements, quick to make, and the comforting results were that even though the *absolute magnitude* of my estimations had indeed drifted (becoming more conservative and less liable to be swayed by what must initially have appeared to be unusual examples), the

drift had been sufficiently uniform to preserve the same sequence of positive and negative steps, and even the relative magnitude of changes for samples from the same site. In short, the general results seem to be highly reproducible, especially if done in fast succession so as to avoid unconscious change of practice.

6.1.3.i Exotic Growth Types

Each of the forms discerned by Jefferies in 1962 (see Text Figure 6.3) and designated as a separate variety, is distinct because of differences which hinge on the arrangement of the final few chambers. The first, dubbed *plummerae*, bears a uniserial stack and is clearly a considerable departure from the basic triserial pattern. The second is *pyramidata*, so called because of a pyramid-shaped final chamber, centrally placed so that it spreads across most of the three triserial columns. The third form is *macfadyeni* of which he gives two instances—one with a slightly domed final chamber, somewhat similar to that of *plummerae* but nowhere near as well developed; and the other with an oddly pinched-in style that renders the overall test high for its width but without the regularity of *pyramidata*. None of his pictures shows a fully triserial specimen.



Text Figure 6.3 Figures of foraminifera reproduced from Jefferies, 1962. *a*, *Tritaxia tricarinata* var. *plummerae*; *b*, *Tritaxia tricarinata* var. *pyramidata*; *c* & *d*, *Tritaxia tricarinata* var. *macfadyeni*.

Clearly, the occurrence of these features is of considerable interest, for several reasons. Firstly, because of what they have to say about the overall functional significance of tritaxiid form and its occupancy of a particular ecological pocket. Secondly, because of what they have to tell us about the underlying developmental processes that went into constructing the test. But also, as Jefferies and some others believe (Section 6.1.1), because such diversity suggests different lineages; and if we are dealing with two or more genetically distinct groups we most certainly want to know about it.

The scheme developed here for categorising the incidence of different final chamber types reflects many of the same distinctions made by Jefferies, but my scheme is more detailed, being hierarchically subdivided along various character dimensions. The major subdivisions are called 'phases' of growth; phases can be split into 'character groups' defining variability along different measurement dimensions; and, finally, character groups are split into specific developmental *types*.

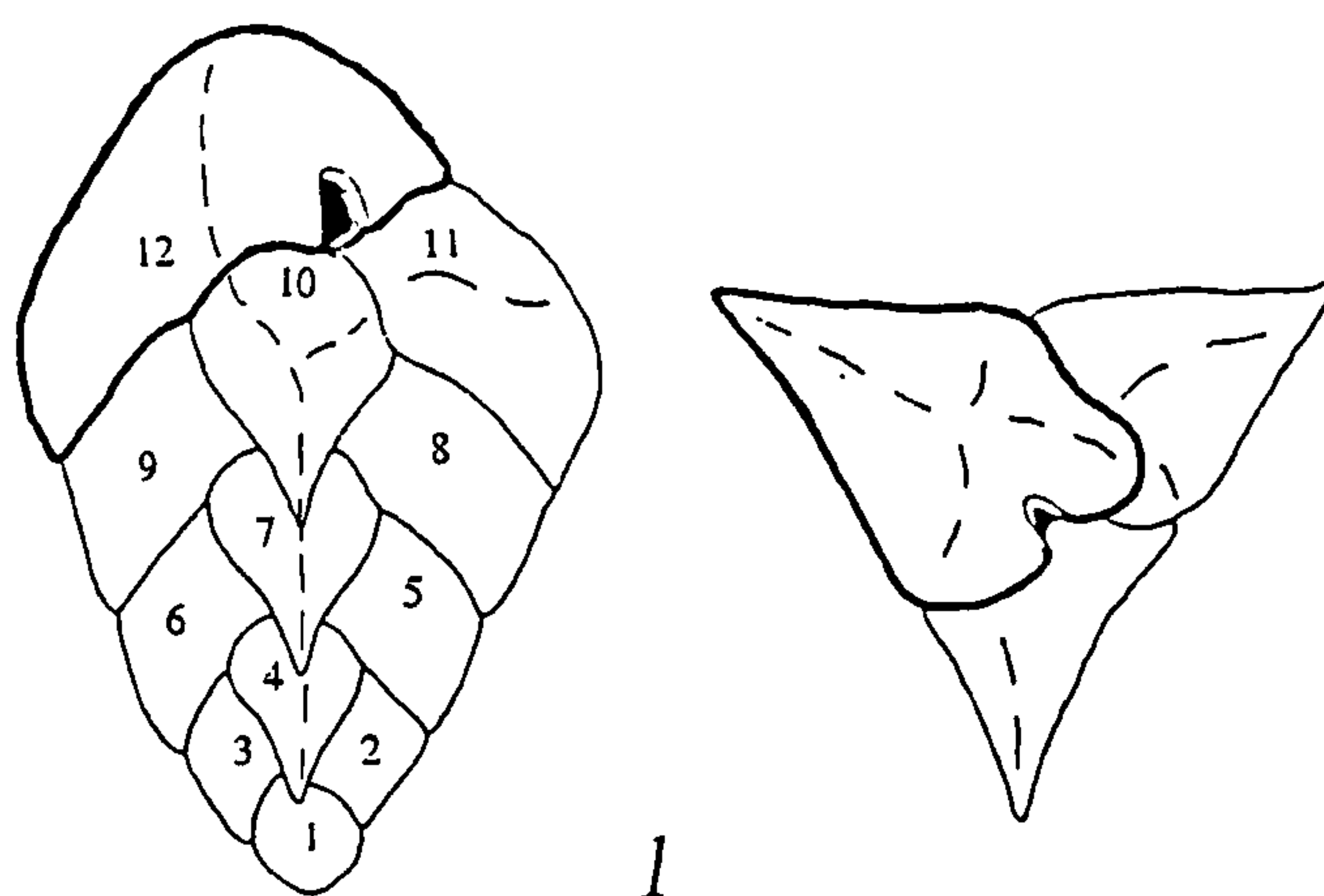
Please note that although the chambers are numbered on one of the figures, this is for reference purposes only and does *not* specify which chamber in the sequence the various categories apply to. Exotic growth types sometimes occur quite early on in development at around 9 or 10 chambers, while in other cases an individual can have more than 20 chambers without there being any break in the triserial pattern. Some of the exotic forms are also successfully captured as the SEM images shown in Appendix Figures 2.3.

Phase I

type 1

All specimens have a portion of their test which grows in triserial fashion, and most display no other form; the entire sample population contains 79.3% exclusively triserial specimens. Simple triseriality is therefore the first category.

In triserial specimens, the arch of the aperture runs parallel with *l'*, and *w'* is measured perpendicular to both. Phase I is not subdivided, so all Phase I individuals are also *type 1* (Text Figure 6.4, below).



Text Figure 6.4 Phase I, type 1: normal triserial growth. Chambers are arranged triserially, one chamber per column along the coiling axis, three chambers per complete whorl. Each chamber is positioned directly above an earlier chamber three chambers back in the sequence (e.g. Ch 12 is situated directly above Ch 9; Ch 9 above Ch 6; Ch 6 above Ch 3 etc.). Two of the final chamber dimensions, w' and l' , are thus defined by the cross-sectional shape of the test: l' extends from the coiling axis to the outer, carinate edge; and w' must be narrow enough to permit three chambers per whorl without interference. These restrictions on triserial growth are important to note because they are violated in the non-triserial phases (see below). The figure shows a tritaxiid test in lateral (left) and apical (right) perspectives; the chambers are numbered and the final chamber is marked in bold. Note that the chamber numbering is for reference purposes only and does not specify the only chambers exhibiting this triserial growth pattern.

Phase II

types 2, 3 & 4; types 1.5, 2.5 & 3.5

Phase II individuals have broken their triserial form *but for a single chamber only*. After a single, non-standard expression of growth, further chamber addition has ceased. Phase II individuals comprise 17.4% of the total sample population and are subdivided into two main character groups, each of which is divided in turn into three *types*.

First, the two main groups. These are distinguished by which character axes the final chamber deviates along. Most individuals deviate along w' only; other individuals deviate along l' only; some individuals deviate along *both* w' and l' . The range of *type* categories was designed to reflect the relationships between these different growth styles, and the labelling scheme to reflect the fact that deviations along w' are far more common than deviations along l' .

Character Group 1 - Deviation along w' :

types 2, 3 & 4

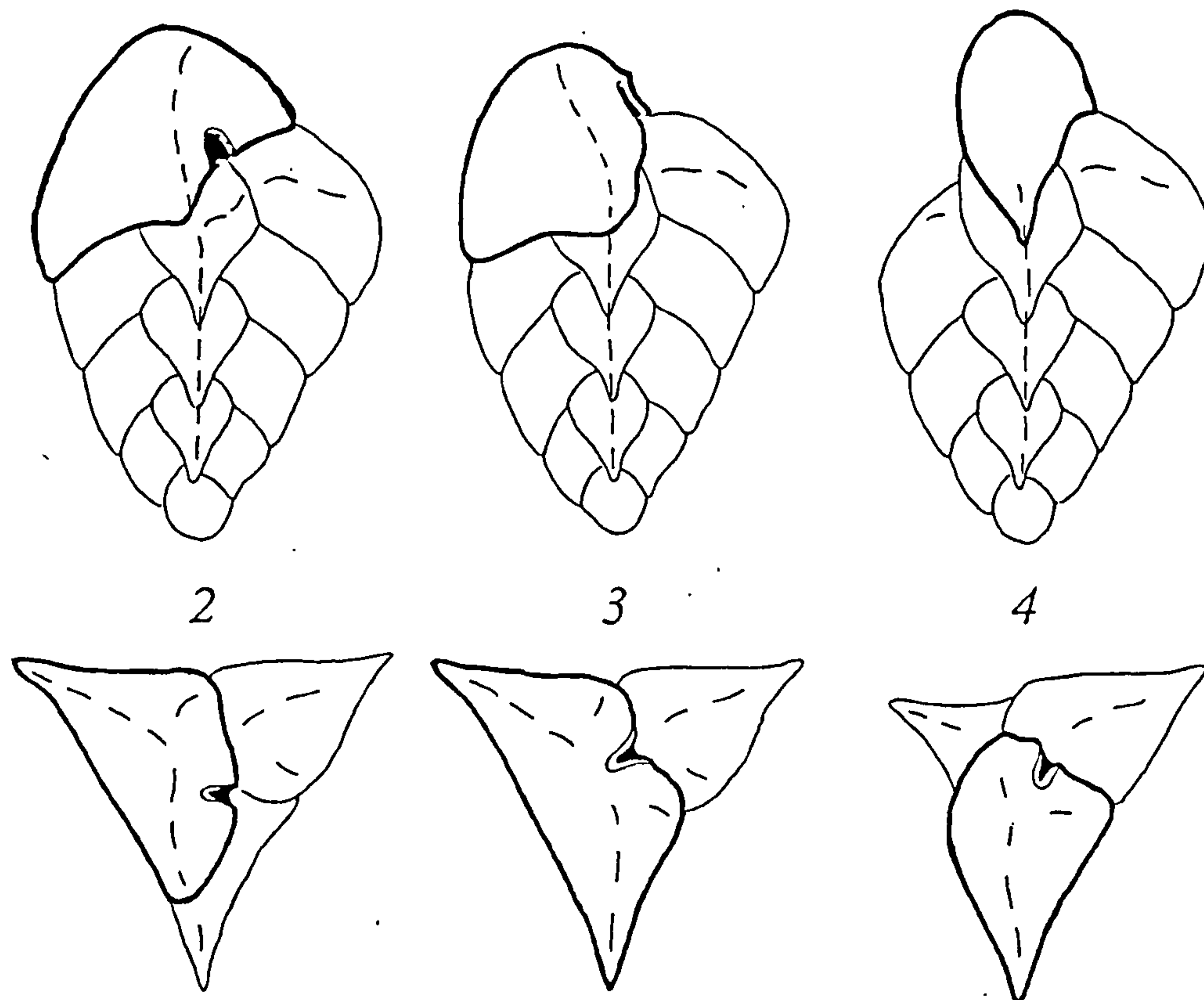
Individuals which deviate along w' have final chambers that are somewhat *wider* than those permitted by normal (*type 1*) triserial growth. For the purposes of defining such deviations we can split the triserial form into three *columns* in which each chamber overlies another chamber lying three chambers back in the sequence (three chambers comprising one whole *whorl*). Each new chamber, therefore, has an allotted column on which it must reside if triserial growth is to be maintained.

In the case of Group 1 width (w') deviations, the final chamber has spilled from its designated column onto an adjacent column further along in the coiling direction, thus occupying a portion of the test which would ordinarily be reserved for the next chamber to come. The next chamber to come never actually arrives in Phase II individuals because growth ceases with a single deviant final chamber; but if growth *had* continued (thereby passing the individual from Phase II to Phase III), the new chamber would have to have been added at a location dictated by its wider-than-usual precursor.

type 2 - individuals show final chambers with a moderate amount of extension along w' , thereby occupying about half of the adjacent space on the next column along.

type 3 - individuals show final chambers with a large extension of w' , typically doubling its magnitude. The final chamber therefore occupies space on both its own allotted column and entirely covers the next one along. In some cases such chambers occupy all three columns and are therefore apical (like Jefferies' *pyramidata*); this situation will be discussed below.

type - 4 individuals do not show any actual extension along w' , but there is a different style of displacement on the w' axis. In this case, the final chamber has come to occupy a position one column further along in the coiling direction than it would otherwise have done, skipping a column entirely.



Text Figure 6.5 *Phase II, Group 1, types 2, 3 & 4: deviations from triserial growth occur when the final chamber shifts along its w' dimension. In type 2, Ch 12 covers Ch 9 and also part of Ch 10. In type 3, Ch 12 covers Ch 9 and all of Ch 10. In type 4, Ch 12 skips Ch 9 and covers Ch 10 instead. The figures show both lateral and apical perspectives, chambers are numbered as for Text Figure 6.4, and the final chamber (12) is marked in bold. Note that the chamber numbering is for reference purposes only and does not specify the actual or only chambers exhibiting this growth pattern.*

Character Group 2 - Deviation along l' :

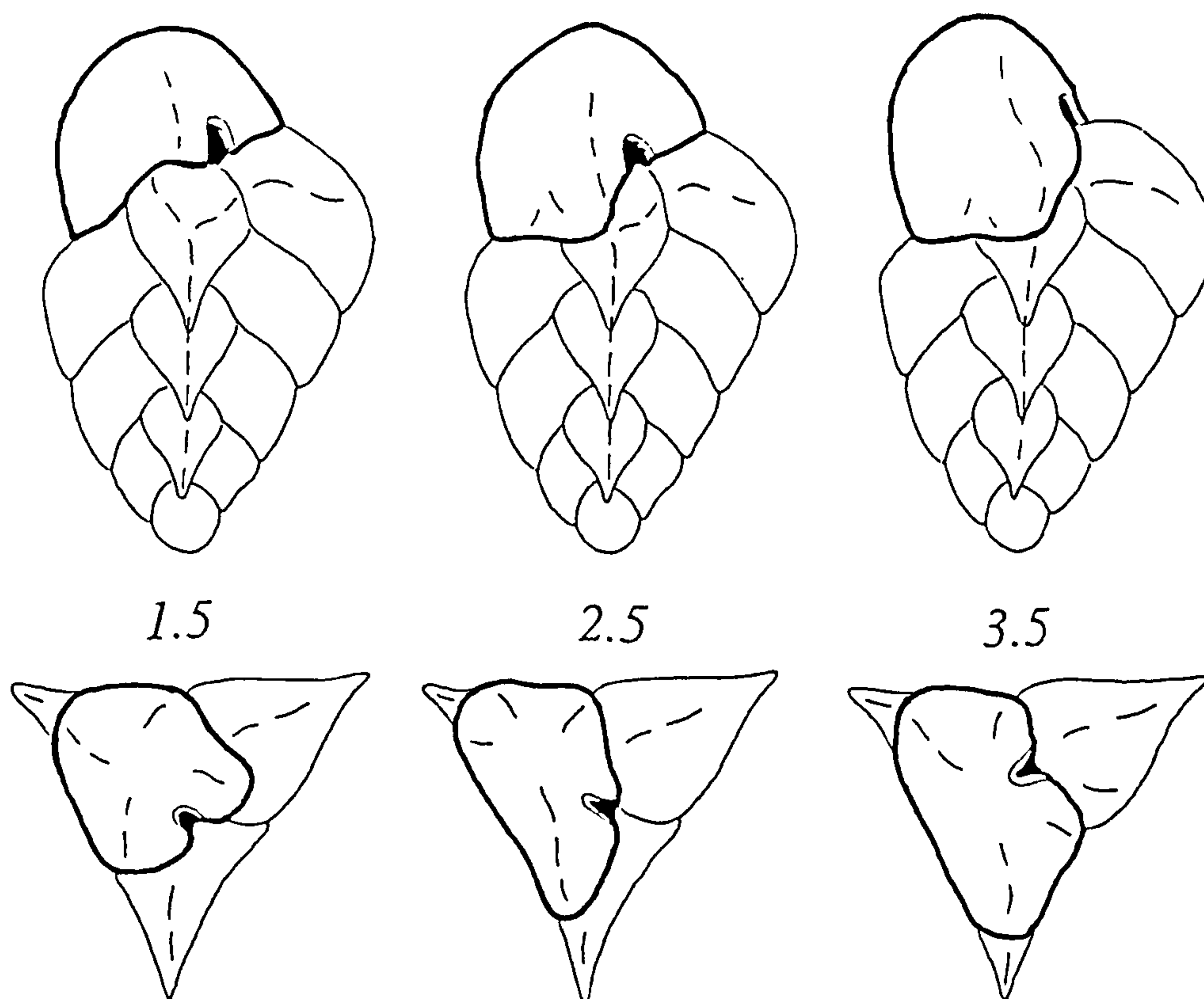
types 1.5, 2.5 & 3.5

Individuals which deviate along l' have stubby final chambers which are shorter than they should be because they do not extend all the way to the carinate edge. Sometimes this shortening of l' appears to be the only deviation from normal growth, but more often it is combined with an extension along w' .

type 1.5 - individuals have short, stubby final chambers capping standard triserial growth; the final chamber is of roughly normal width.

type 2.5 - individuals have short, stubby final chambers but they are also wider than they should be and thus cover a portion of the adjacent column too.

type 3.5 - individuals have short, stubby final chambers which are also considerably wider than they would normally be, extending right across the adjacent column.



Text Figure 6.6 Phase II, Group 2, types 1.5, 2.5 & 3.5: deviations from normal triserial growth occur when the final chamber shifts along its l' dimension. In type 1.5, Ch 12 is positioned squarely above Ch 9 in the normal triserial location but does not extend to the carinate edge and is thus shorter than it should be. In type 2.5, Ch 12 covers Ch 9 and also part of Ch 10, but is also drawn back from the carinate edges and is thus shorter than it should be. In type 3.5, Ch 12 covers Ch 9 plus Ch 10, and is also drawn back from the carinate edges. As with the other figures in this series, both lateral and apical perspectives are shown with chambers numbered as in Text Figure 6.4 and the final chamber (12) is marked in bold. Once again, the chamber numbering is for reference purposes only and does not specify the actual or only chambers exhibiting this growth pattern.

Note that the numbering system for Phase II Group 2 categories (i.e. the addition of '.5' to Group 1 category labels) reflects the fact that l' type deviation is relatively rare (see Appdx. Fig. 4.1.3.v), and also the fact that in terms of effect it is often indistinguishable from, and dwarfed by, Group 1 w' type deviation. For types 2.5 and 3.5, for instance, it is generally not possible to separate the influence of deviation in l' from that in w' ; indeed, it actually often looks very much as though a reduction in the l' axis has *caused* an extension along w' as an attempt to accommodate the same chamber volume within a different shape. A mechanism for test construction based on this hypothesis will be advanced in Chapter 7. It is the usefulness of l' type deviations to validating this mechanism which makes them worth specifying in the first place.

More importantly, from the perspective of presentation, is the fact that although Group 2 deviations are mentioned here and also appear in the raw data, charts showing *type* distinctions (e.g. Appdx. Figs. 4.2.1, 4.3.1) often do not distinguish *l'* type deviations at all. Where figures do show the population split into different categories, only *types* 1, 2 and 3 will normally be presented, and these will each contain the sub-sets of 1.5, 2.5 and 3.5, respectively. The motivation for this is simply clarity of presentation; it does not affect the interpretation.

Phase III

Phase III specimens comprise those individuals which have *continued growing even after they have broken their basic triserial form*. They may have added just a single chamber to their first deviant type, or they may have added several more. It would have been possible to classify specimens on the basis of how many more deviant chambers were added, but it seems unnecessary to do so. Phase III individuals are rare, constituting just 3.3% of the total population, and only three types are included under the Phase III heading:

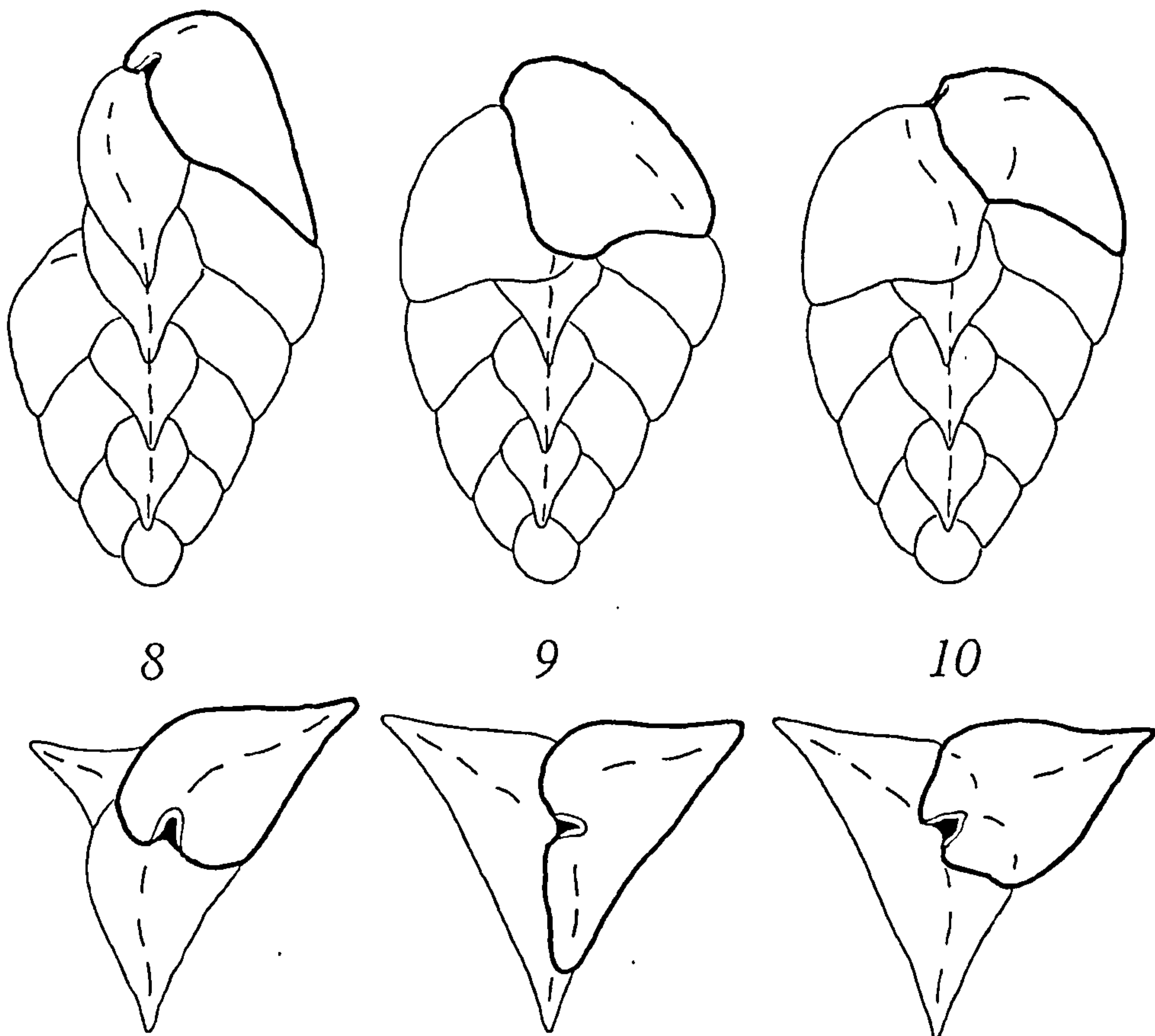
type 8 - is a biserial development arising from *type* 4: after the first deviant chamber has skipped a column, growth continues on a biserial form by adding chambers that are of roughly normal dimensions.

type 9 - following an initial transition to *type* 2 or 3, growth continues on a roughly biserial form by adding chambers that are generally *wider* than usual.

type 10 - following an initial transition to *type* 2 or 3, growth continues on a biserial form, as an alternating series of normal and wider than normal chambers.

Notice that there is a gap in the labelling system between *type* 4 and *type* 8. This reflects the fact that as with all the character designations, *type* categories were recognised and defined only through extensive practice. *types* 5, 6 and 7 refer to distinct growth styles and still remain on the database (Appdx. Table 2.1 - 2.3); but they were very rare categories and only ever consisted of a handful of cases. *type* 5 was true uniseriality, like Jefferies' var. *plummerae*, while *type* 7 was somewhere between uniserial and biserial. In each case,

there were only a couple of specimens and these have now been condensed into *type 8* for the purposes of adding them to the plots. *type 6* designated the apical forms that Jefferies called *pyramidata*; these generally occur only on very large specimens and are probably best thought of as an angular version of *type 3*, the category into which they have been condensed for the purposes of inclusion in the plots.



Text Figure 6.7 Phase III, types 8, 9 & 10: deviations from normal triserial growth occurring for more than a single deviant chamber. In type 8, growth continues biserially from a type 4 initial state, skipping a column entirely and adding chambers that are of roughly normal width (or sometimes narrower): e.g. Ch 13 is of normal width and is positioned above C11. In type 9, growth continues in a roughly biserial fashion, adding a series of wider than usual chambers: e.g. Ch 13 covers all of Ch 11 plus some of Ch 12. In type 10, growth continues in a roughly biserial fashion by alternating between normal and wider than normal chambers: e.g. Ch 13 covers Ch 11 but is of normal width. As with the other figures in this series, both lateral and apical perspectives are shown with chambers numbered as in Text Figure 6.4 and the final chambers are marked in bold. Once again, the chamber numbering is for reference purposes only and does not specify the only or actual chambers exhibiting this growth pattern.

For the record, of the two illustrations referred to by Jefferies as var. *macfadyeni* (Text Fig. 6.3), *c* looks as though it should be classified as a *type 9* (i.e. a *type 2* or *3* final chamber added onto a *type 2* or *3* initial deviant), while *d* appears to be a rather rounded *type 3* (compare it to *b*, his var. *pyramidata*, which is basically a *type 6* apical, angular version of the same growth pattern). Of course, that is only a visual impression from blurry

pictures; good classification really requires the ability to move fossils around and examine them from various angles to see how the chambers relate to one another. My own attempts to capture the exotic growth styles as SEM images were not entirely successful either, which is why only a selection appear in Appendix Figures 2.3.

6.1.4 The Platonic Foram

The purpose of this chapter is to construct a *general* understanding of *Tritaxia*'s morphology and to that end the entire morphometric data set will be deployed. The resulting model will not be relevant to any specific sample population but should instead apply, to some extent, to all of them. The disadvantage of constructing such a broad model, especially if there has been extensive evolution, is that it may constitute a rather blurry picture. But we have to start from somewhere. Any investigation of evolutionary change requires us to have an idea of what was changed into what else, and that means we must have a reasonable idea of what we are looking at. However, in order to avoid pre-empting any particular conclusion, the more general the starting point the better. The fairest way to ensure an unbiased perspective is to include as many specimens as possible in the initial model, and only at a later stage (Part IV) to partition this material into data from individual sampling horizons.

Let us first inspect the distributions of the character variables themselves since these will determine a great deal of the subsequent treatment. Of the simple metric features, H , W , I , l' , h' , w' , i' , and also Ch , all have a more or less normal, unimodal spread (Appdx. Figs. 4.1.1), albeit with a slight positive skew. The final chamber characters (l' , h' , w' and i') are also approximately normal with a slight skew, but in addition seem to possess a somewhat multimodal quality. This is an artefact. For a while I thought it might represent sub-populations of various ages or growth stage, but on closer investigation it turns out to be interference between the 15 μm categories on the histograms and the 15.6 μm measurement interval of the graticule spacings.

There are three good reasons to expect a positive skew from this data set. The first is that since organic development starts off from a tiny single cell there is always a sharp lower boundary to size, whereas there is often a rather hazy upper boundary because many

creatures never stop growing so long as they are still alive. Foraminifera exhibit this mode of continuing growth, so we should occasionally expect very large individuals of any given species to turn up in the samples: they do. The second reason is that even in cases where there is a fixed maximum size for adults, data from natural populations tends to show a positive skew because juvenile mortality rate is generally higher than for established individuals; the majority of any cohort never make it to old age.

The third reason is one of sampling artefact. Even if the fossil distribution was initially perfectly symmetrical, the fact that the specimens were passed through a sieve with a cut-off point part way along the size range guarantees the population a positive skew. The marked truncation to the lower end of *W* (maximum width) is the most obvious example of this kind (App. Fig. 4.1.1.ii) and it seems likely that this character, rather than the alternative test-bounding dimension, *H*, was the main parameter controlling which specimens were caught by the 250µm sieve.

For perfectly symmetrical data, the median and the mean are equal. The extent of any asymmetry can be rendered as a dimensionless metric using the following method:

$$\frac{3 \times (\text{sample mean} - \text{sample median})}{\text{sample standard deviation}}$$

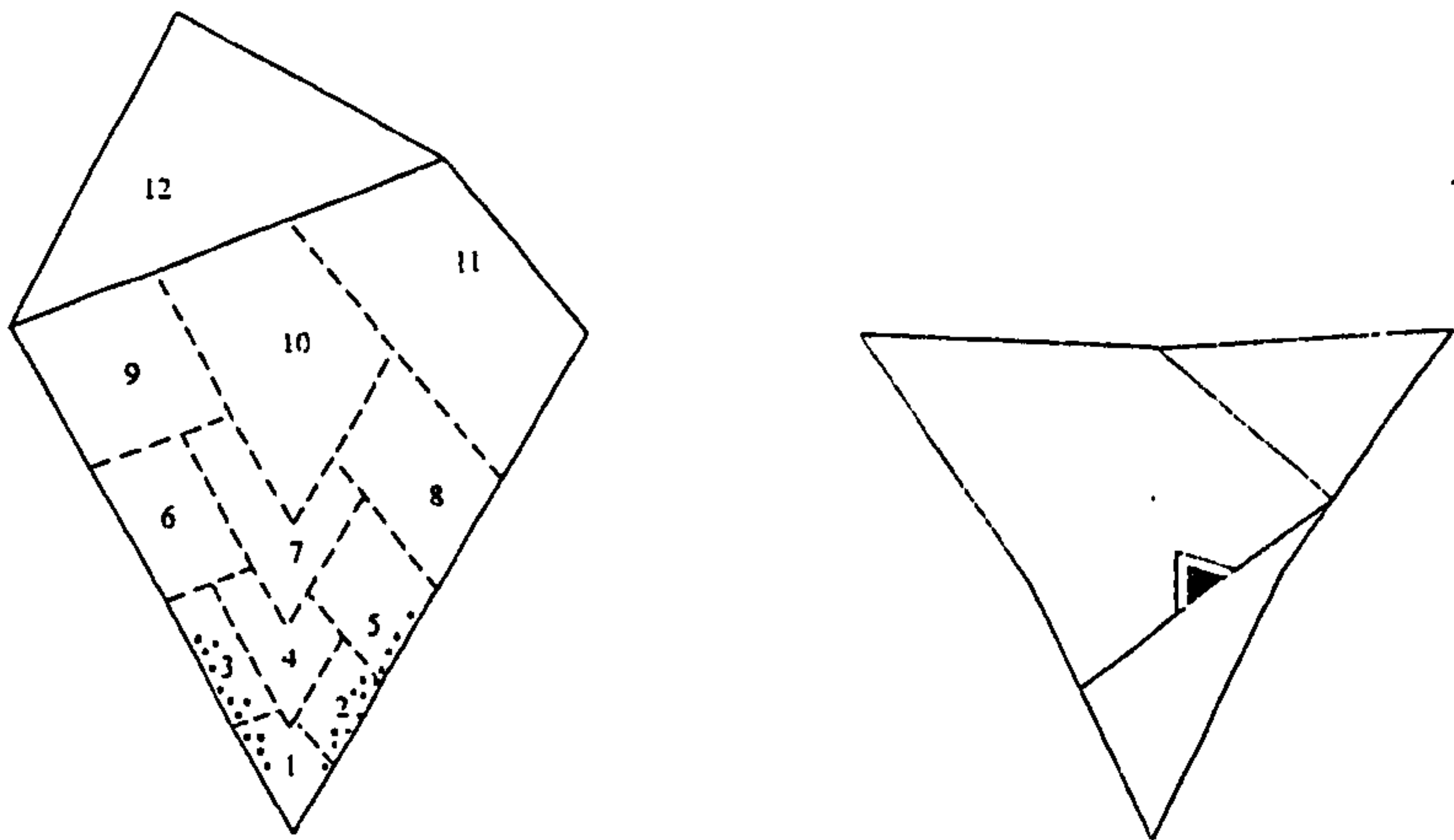
If the result is >1, the data are considered to be significantly positively skewed; if <-1, significantly negatively skewed. Considered as a bulk set and using this measurement, none of the metric characters has a significant skew; thus, they can all be adequately summarised by their mean and standard deviation. Strictly speaking, *Ch* (number of chambers) is a discrete measurement and the fractional chamber numbers generated by a calculation of the mean have no correspondence with the real world; but there is a wide enough range of expression for the character to imitate a continuous variable, and so for the purposes of summary it can be represented by either the mean or the median depending upon circumstances.

Of the remaining characters, indentation (*ind*), twist (*tw*) and percentage of glauconite (*g%*) are also continuous variables but do not have anything like normal distributions (Appdx. Figs. 4.1.3.i, ii & iii). *tw* and *g%* have a highly skewed 'decay curve' distribution, while indentation has a unimodal uneven hump, consisting in the main of just five size categories. For many purposes throughout the thesis these three will be regarded as though they were comprised of a number of discrete categories (which in terms of

measurement they are) and be treated the same as the truly categorical data. In this chapter, where appropriate, they will be summarised by their median values. The more truly categorical characters, *chir*, *g.dist* and *type* (shown in Appdx. Figs. 4.1.3.iv, v & vi, respectively) are summarised by their modal values.

Using the continuous metric variables as a foundation, it is possible to construct a totally generalised model *Tritaxia* based on the chosen characters (Text Fig. 6.9). It has an overall height (*H*), width (*W*) and *H-W* intersection (*I*) in accordance with the means for these characters, and likewise with the mean values of final chamber parameters (Text Table 6.1). We can fill in this idealised shape with details such as the median number of chambers, indentation, degree of twist and proportion of glauconite, plus the modal values for chirality, glauconite distribution and final chamber type. What we then have is a 'joe average' tritaxiid, which I cannot resist calling the 'Platonic Foram'. This abstract creature is rendered in pictorial style in Text Figure 6.8 to demonstrate just how well the chosen measurements capture these fossils.

surely it
one of
the others?

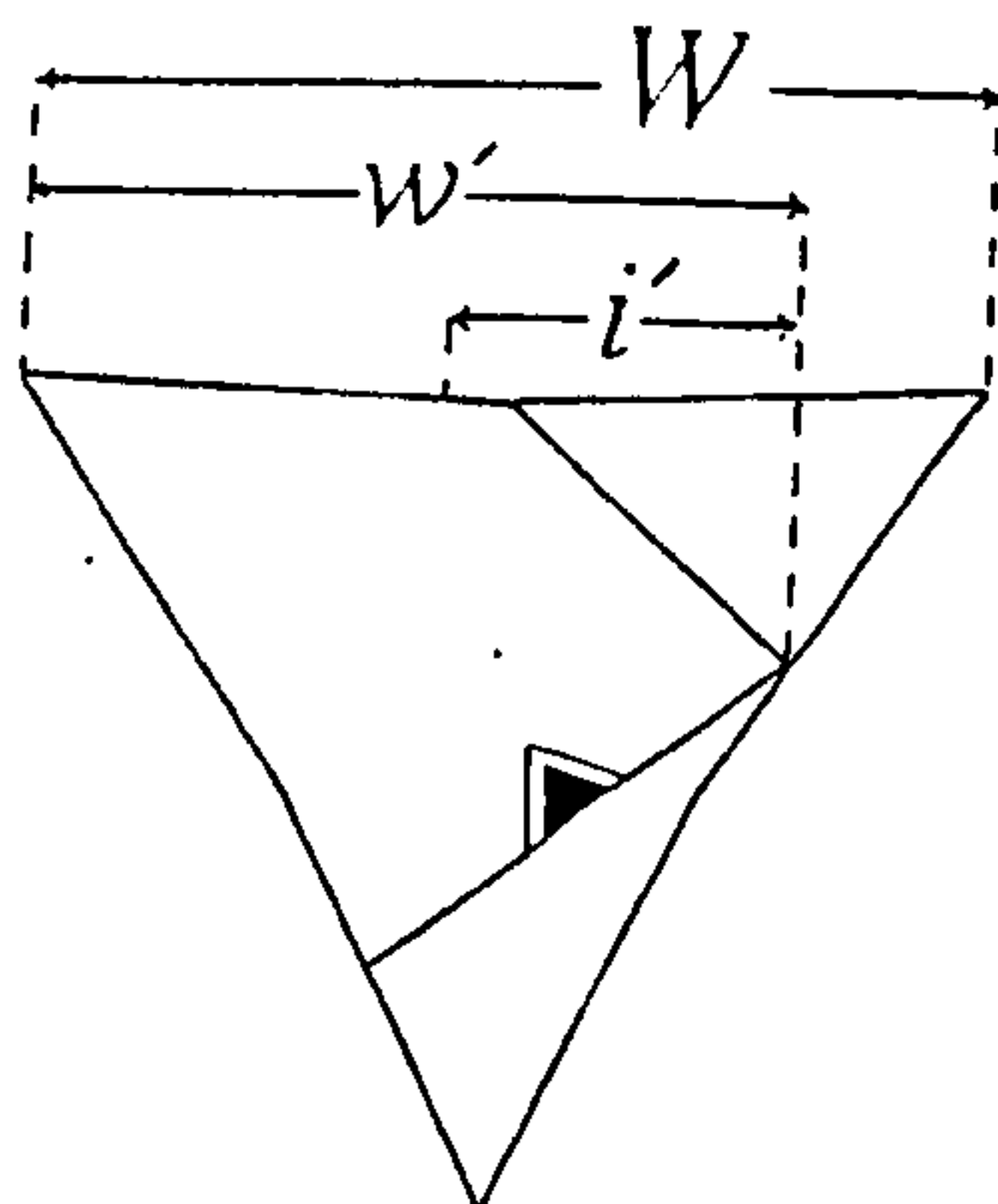


Text Figure 6.8 The 'Platonic Foram', a totally generalised model tritaxiid using the average values for each character (see Text Table 6.1).

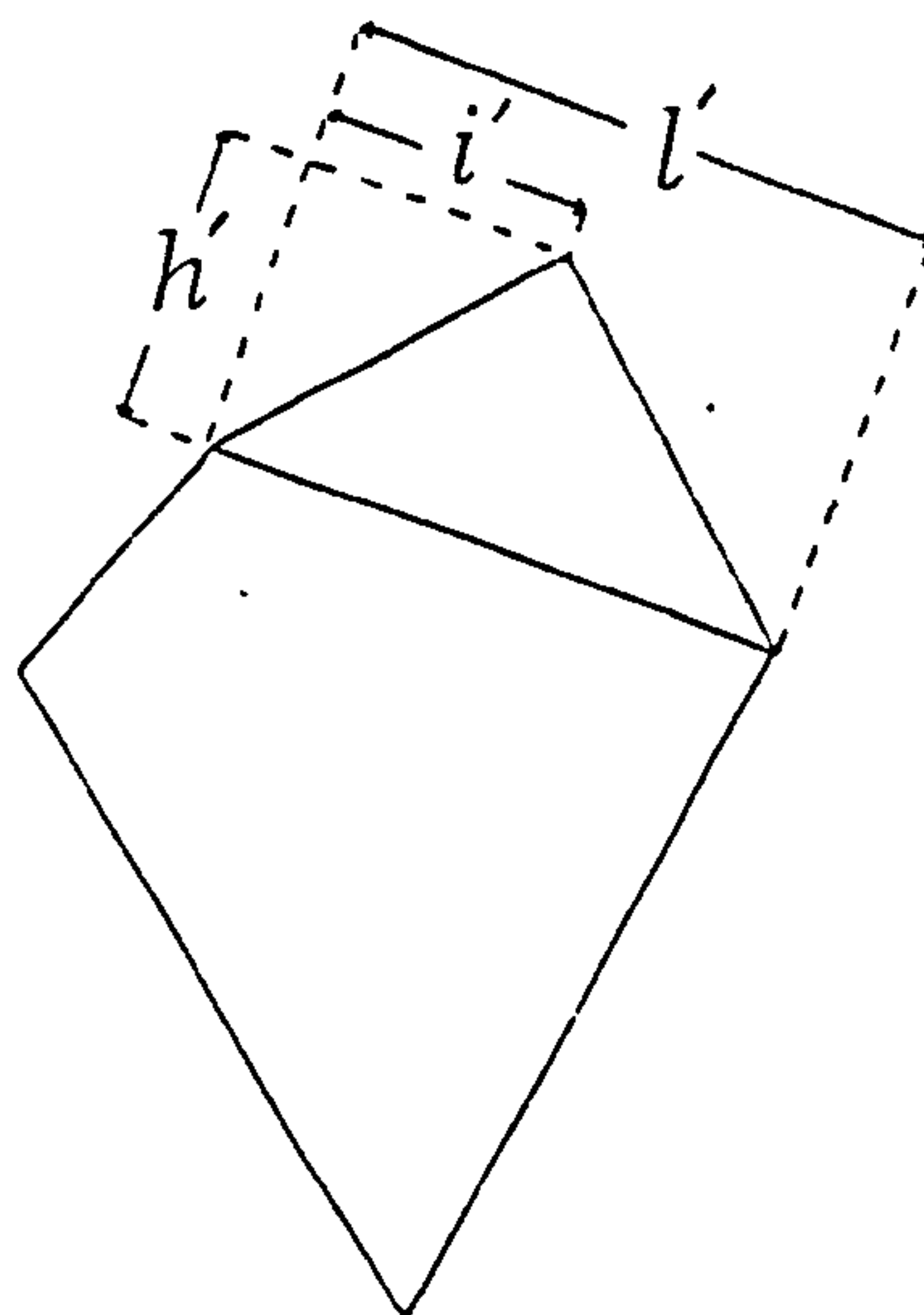
<i>H</i>	<i>W</i>	<i>I</i>	<i>l'</i>	<i>i'</i>	<i>h'</i>	<i>w'</i>
576.7	407.6	352.3	326.3	143.7	163.5	246.1
<i>Ch</i>	<i>ind</i>	<i>tw</i>	<i>g%</i>	<i>g.dist</i>	<i>chir</i>	<i>type</i>
12	1	0	0.5%	2	dextral	1

Text Table 6.1 Average values for characters from the entire data set (*n* = 2357). Mean values in microns for *H*, *W*, *I*, *l'*, *i'*, *h'*, *w'*; median values in graticule spacings for *ind* and other appropriate categories for *Ch*, *tw* and *g%*; modal category values for *g.dist*, *chir* and *type*.

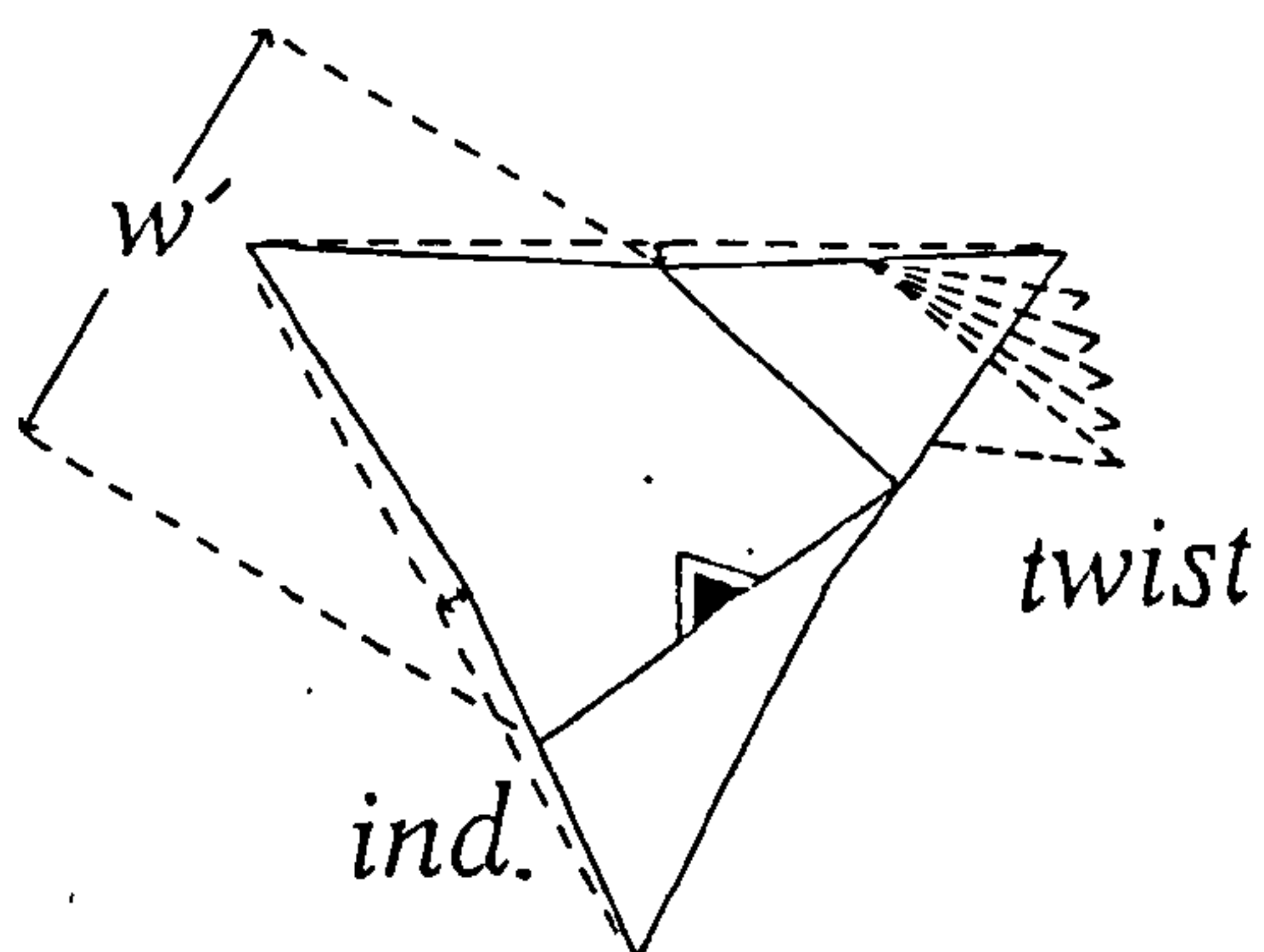
i



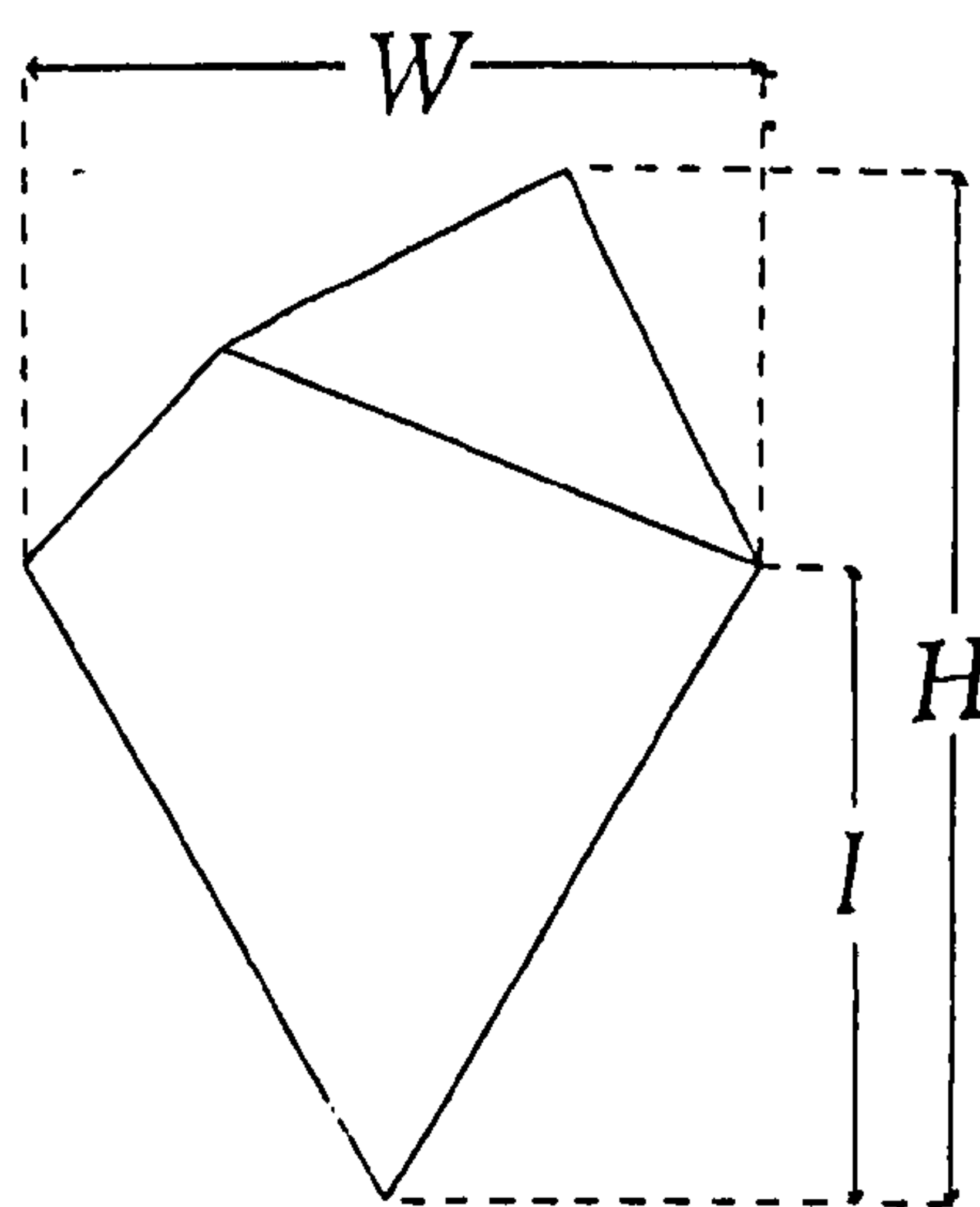
ii



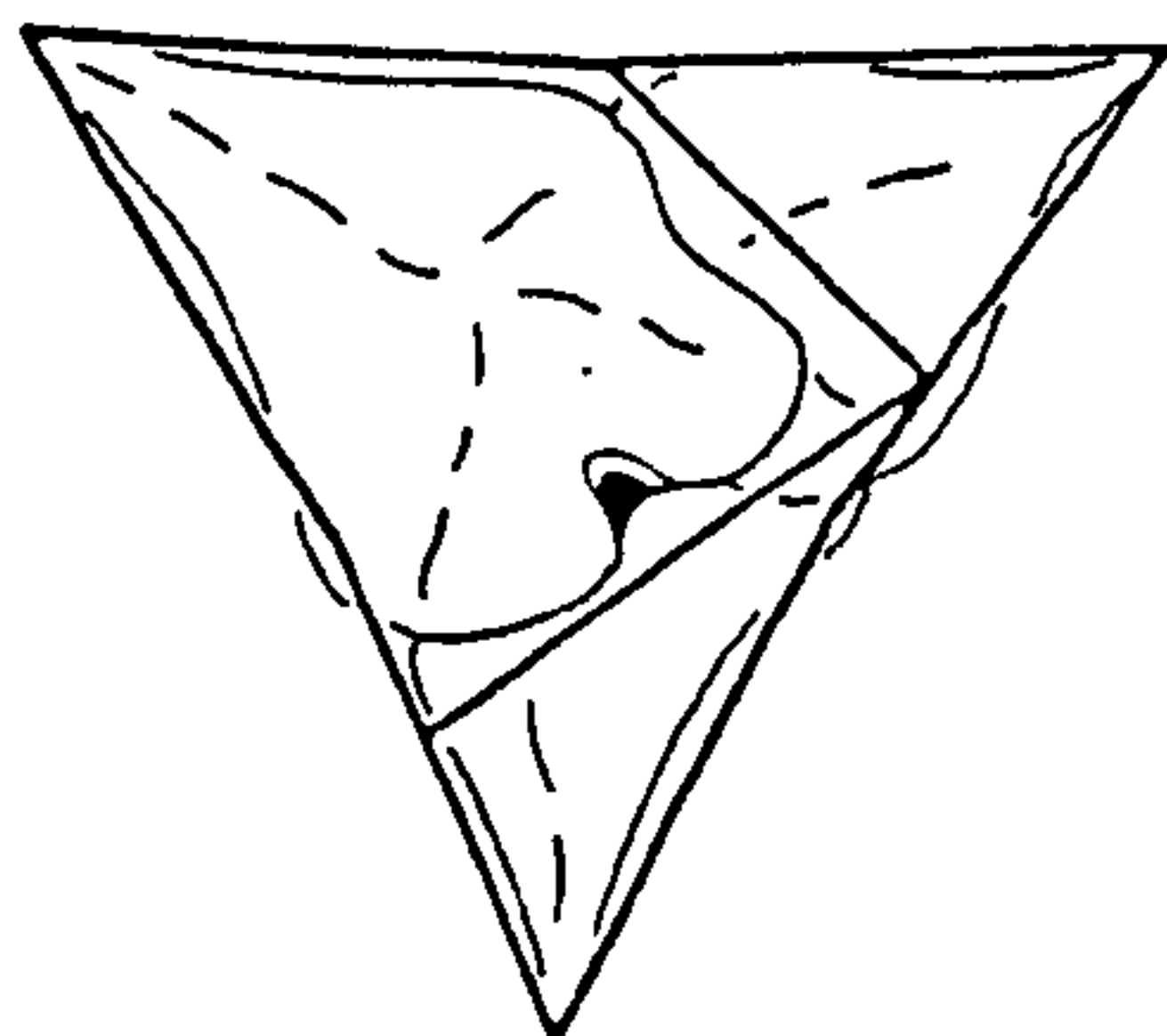
iii



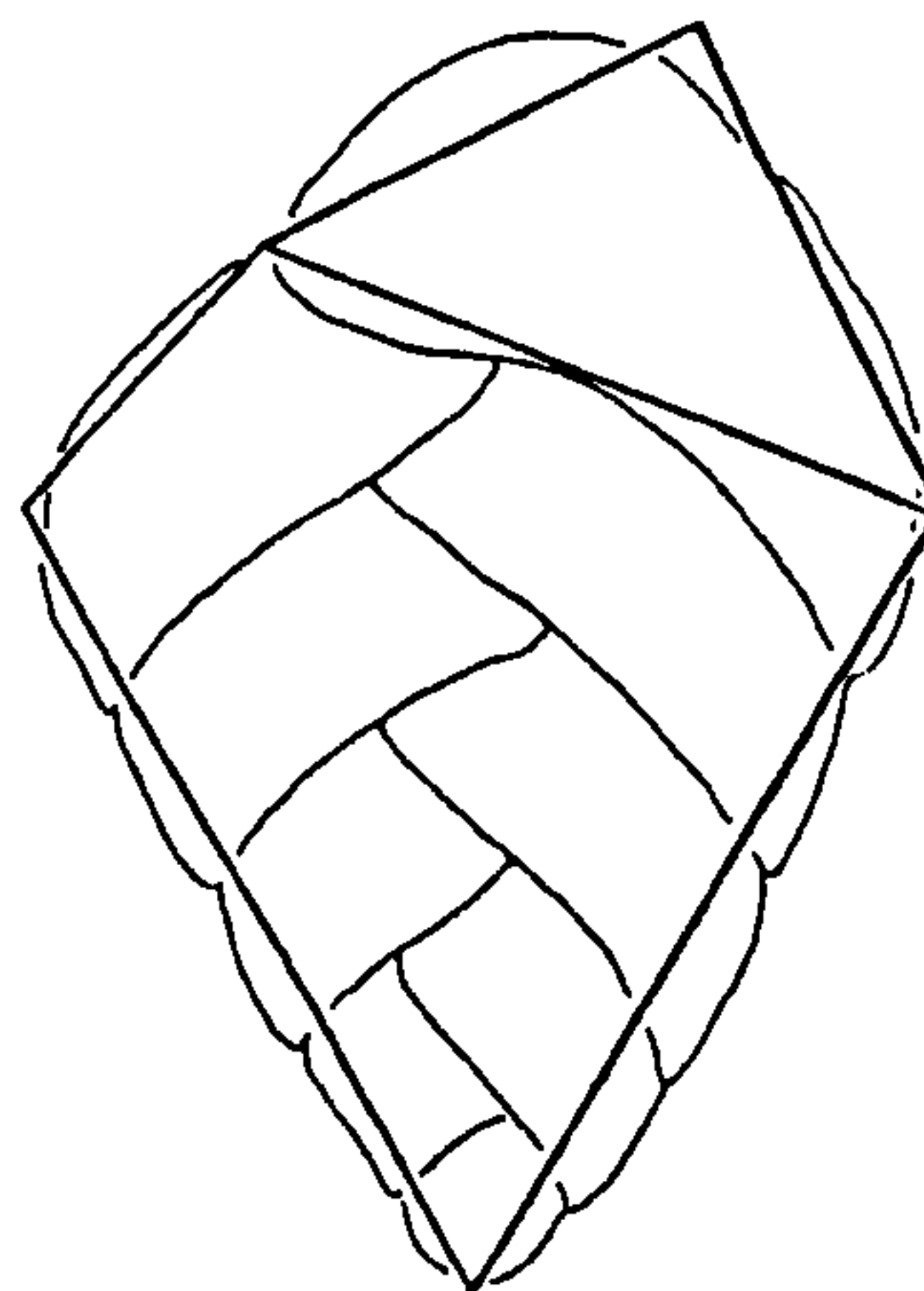
iv



v



vi



Text Figure 6.9 Derivation of model Tritaxia composed of measurements alone: i. W , l' , i' , section view; ii. l' , i' , h' , longitudinal view; iii. w' , ind , tw , sectional view; iv. H , W , I , longitudinal view. Geometric models overlaying schematic diagrams for comparison: v. section view; vi. longitudinal view.

Section 6.2 *Tritaxia* in 4 Dimensions

6.2.1 Growth and the Problem of Age Dependency

The Platonic Foram is a creature carved out of morphospace and frozen in time. It has no developmental trajectory, no 'lifeline'. Instead it represents the average fate and destination of all growth trajectories in the entire sample population. To gain some idea of how the real *Tritaxia* grew, therefore, we need to introduce a temporal dimension to this otherwise static entity.

Few of the basic character measurements are obviously independent of age. Coiling direction (*chir*) most definitely is, but the continuous variables (*H*, *W*, *I* etc.) would all have increased in magnitude as an individual grew, as would the number of chambers (*Ch*). It is an open question as to whether or not any of the other characters changed throughout an individual's lifespan, but the fact that they might have done is enough to warrant some consideration.

Since all the data presumably come from populations incorporating individuals from a wide variety of ages, differences in the average value of any age-dependent variable, from any sub-set of the database, can be attributed to two distinct classes of explanation: either the values differ *per unit of age* such that two individuals of equivalent age, or two populations of equivalent age-structure, nonetheless show different values; or, the *age-structure itself* has changed such that one individual is older than another, or one population has a higher proportion of older individuals. Without some measure of age in the individual and in the age-structure of the populations, it is impossible to test which of these (if not both) is applicable in any particular situation. This is the problem of age dependency in morphological parameters.

In the case of *Tritaxia*, there is no certain method for determining the age of an individual because the test does not incorporate features securely linked to changing time, as, for example, do the seasonal growth bands in brachiopods or the rings of trees. Fortunately, the discrete addition of chambers provides us with an alternative. If we say that the number of chambers in an individual test is an indication of the *stage* it has reached in a

growth sequence, then it becomes meaningful to compare individuals with an equal number of chambers. There is still no certainty that chambers were created at an equal temporal rate, but in a sense that no longer matters because we are now treating the organism's development as a sequence of discrete steps which have alternative markers than just their distance in time from the starting point.

If we think about the accumulation of 12 chambers as 'morphology at stage 12' then we can talk about the overall height of the test at stage 12 irrespective of whether that stage was attained in six weeks or six months. This is not to suggest that the actual time it took for an individual to reach stage 12 is of no interest to us, since any differences probably reflect important variations in the developmental process, and will thus depend upon a range of genetic or environmental factors. Rather, the issue of whether elements of a developmental sequence are unfolding in step *with one another* is a separate consideration from whether any of them is unfolding in step with an external physical variable such as time (or, for that matter, with other physical variables such as temperature or nutrient availability).

Age (or stage) dependency is not really an issue at all for the Platonic Foram. It is firmly fixed at stage 12 without ever having had to get there. More importantly, it is a transcendent creature and not confined to any particular sample population: there is nothing, age-structured or otherwise, to compare it with. That is precisely the reason it has been chosen to form the reference point for everything else. When we come to look at populations from different sampling horizons, however, the problems of age-dependency could be considerable.

Given the nature of this situation it may have been better if the sample populations had originally been assembled by selecting a standard, comparable set of specimens, each having, for instance, ten individuals with 11 chambers, ten with 12, 13, 14, etc. If this had been done, it would have introduced uniformity at the expense of any information on population age structure itself, along with raising the practical difficulty of whether or not a sample population could always be made to yield ten 11-chambered individuals and so forth. But in any case, that is not how the data were gathered, and so some other strategy is now required.

One possibility would be to couch the value of every character measurement in relation to the number of chambers borne by the individual it was taken from, as a ratio.

The age/stage dependency problem would then disappear because the data would effectively be standardised to a common chamber-number calibration point. A big disadvantage with this course of action is that it would tend to obscure the original measurements themselves. It is perfectly straightforward to say that the test height of an average tritaxiid is $H = 576.7$ microns, but less obvious what it means to say that the chamber to height ratio of the average test is 48.1 microns, especially when we pause to appreciate that the original height has been spread equally between the 12 chambers rather than being doled out in size fractions depending on each chamber's place within the expanding spiral.

I have thus chosen to deal with the age-dependency problem on a piecemeal basis. There are times (e.g. Section 9.5.1, Part IV) when it will be useful to consider changes of size and shape as a ratio of the chamber number, but, in general, the technique has been applied sparingly. The notion of using chamber number as an index of growth stage, however, is still extremely useful, and will be employed extensively in the chapters to come. But wherever possible, the basic data, summarised by the simplest statistical techniques, will be close at hand to provide a foundation for any subsequent and more complicated analysis.

6.2.2 Character Correlations in General

The connection between a particular morphological character and other features representing growth is only a special case of using *correlated* variables in general. When the relationship between any pair of spatial character measurements is well correlated, it can be rendered as a dimensionless ratio and used as an indicator of *shape* rather than size; again, this has the advantage of unravelling two entangled pieces of information in one sense and the disadvantage, in a different sense, of obscuring each of them entirely. The situation is amply illustrated by the problem posed above in which it was (at least potentially) useful to separate the *magnitude* of the dimensions involved, in that case the dimension of time (or 'stage') plus a spatial character measurement, from the *relationship* between the two, the ratio, in order to use the latter as a standardised, dimensionless metric. In actuality, this ratio is only one of two relationships we might be able to isolate for processes of morphological change in development (the second being an exponential

function governing the rate of change of the first); but in any case a well behaved correlation is required before we can get at either.

Correlations are significant to the study of form for two rather different reasons. One is the situation just mentioned: they give us a way to summarise complex situations; the other is that good correlations also suggest a causal relationship between pairs of characters. Statisticians routinely surround proofs of association with warnings that simple causal relationships cannot be assumed to follow; specifically, that if x and y happen to be correlated we must not claim that x causes y or that y causes x (and David Hume notoriously argued that the existence of 'causality' itself cannot be justified for largely the same reason). However, the structure of probabilistic argument and the principle of parsimony provide us with good reason (Hume aside) to postulate causal linkage at some level—it is highly unlikely that two features would be in constant association for purely random reasons, and of course the validity of statistical tests for correlation depend wholly upon such reasoning.

Determining the nature of the underlying causes, however, is an entirely different enterprise, and one which will occupy much of the forthcoming discussion; but it is worth recognising, even at this early stage, that the use of correlations rather than single measurements as data lies at the crux of an important evolutionary consideration. The issue at stake is whether the correlations exist because selection imposes them on a system, or whether it is because the system itself is defined by such correlations in the first place. In other words, whether the correlations are 'externally' imposed functional constraints on the range of possibilities, or 'internally' generated structural features (Sections 1.1, 5.5). In a sense, such character associations are important for exactly the opposite reason that age dependency was: whereas the age example involved two pieces of information (growth stage and character dimension) concealed as a single piece (the size of a character), apparently separate but synchronous signals from two characters, if they are somehow *forced* to be in synchrony, effectively constitutes only one such datum. Good correlation is therefore a flag for identifying those relationships to which a more considered exploration might be aimed.

As long as we are only interested in summarising a single character dimension at a time, the appropriate standard metrics for variation and central tendency (e.g. standard deviation and the mean) will tell us all we need to know. But real organisms have as many

character ‘dimensions’ as we care to measure on them; and, in addition to understanding each one separately, it is also useful to know how they all slot together. This raises the practical problem of how we are to represent multiple character relationships simultaneously.

As mentioned in the last chapter, spatial metaphors are some of the most powerful and ubiquitous conceptual tools we possess, so an ideal method for representing multiple character relationships ought to be to plot them in an n -dimensional ‘space’. Sadly, with only three genuine spatial dimensions at our disposal (or two once a plot has been squashed flat onto a sheet of paper), n -dimensional arrays have a nasty habit of producing a rash of barely comprehensible dots that often leave their audience confused rather than enlightened. As part of my commitment to translucency in scientific practice, I have shied away from multi-dimensional analysis and opted instead for the long-hand version: we shall mainly address the character relationships two by two, on simple bivariate plots, working steadily from there into multi-dimensional spaces where we can do so without losing track of the original data.

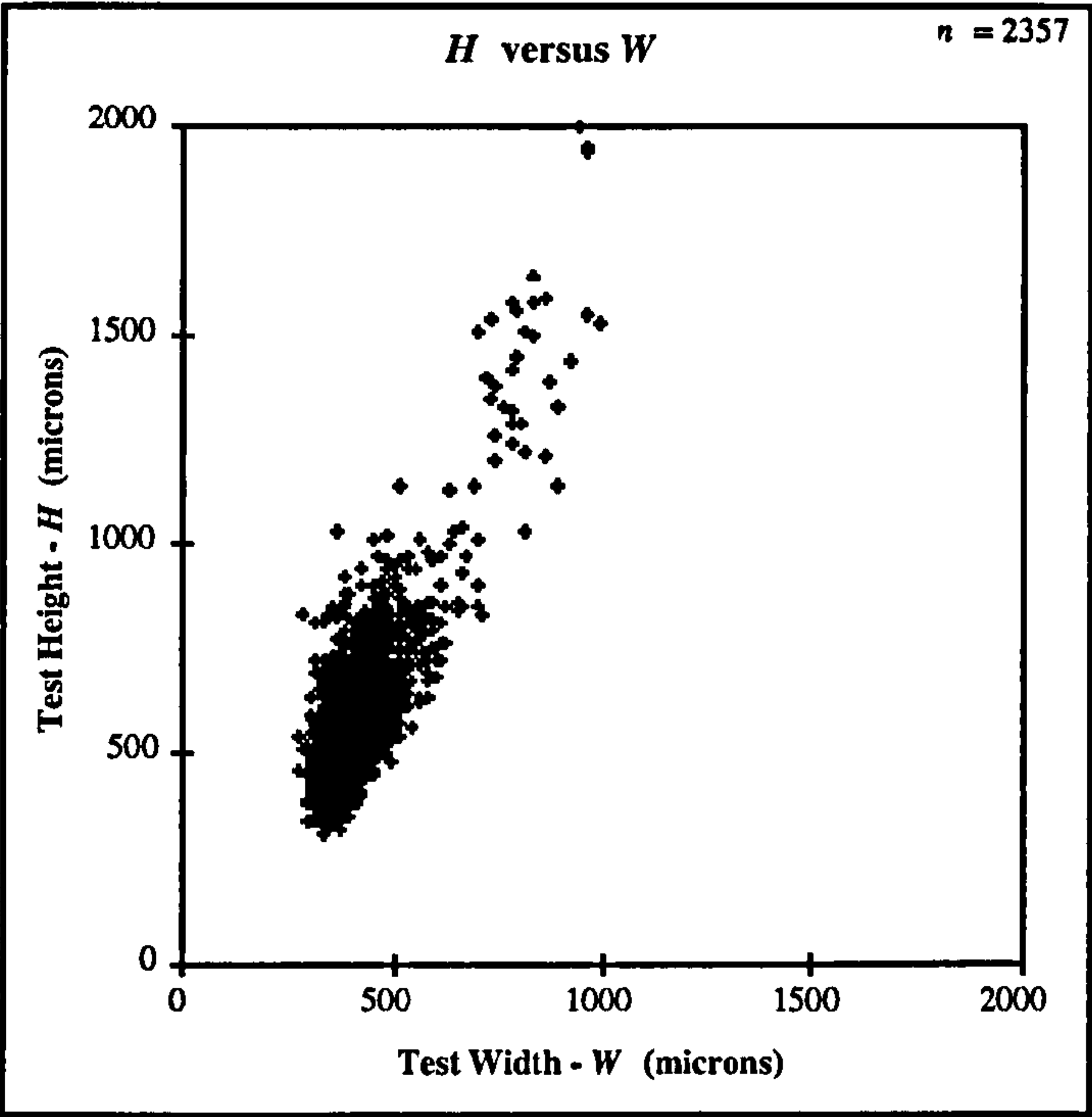
6.2.2.i Association of Continuous Variables: The Correlation Coefficient

For normally distributed continuous variables such as H , W , I , l' , h' , w' and i' , and also for Ch , which will be treated here as a continuous variable for the purposes of establishing a common link between the other characters and growth stage, the appropriate test to use is the Pearson correlation coefficient (e.g. Campbell, 1990; Rees, 1995).

$$r = \frac{\Sigma xy - \frac{\Sigma x \Sigma y}{n}}{\sqrt{\left[\Sigma x^2 - \frac{(\Sigma x)^2}{n} \right] \left[\Sigma y^2 - \frac{(\Sigma y)^2}{n} \right]}}$$

where r is the value of the correlation coefficient, x and y are the character variables, and n is the number of specimens. r can vary from 0 for cases of exactly no correlation to +1 for perfect positive correlations, and -1 for perfect negative ones; normally it falls somewhere in between.

As an example, in the case of H versus W for the entire data set, the value of r is 0.783, so they are apparently very strongly positively correlated (Text Figure 6.10).



Text Figure 6.10 *A positive correlation: H versus W for the entire data set.*

The significance of such apparent correlations can in fact be quantified by calculating a test statistic, t :

$$t = r\sqrt{n-2}/\sqrt{1-r^2}$$

where t is the test statistic, r is the correlation coefficient and n the number of specimens.

A t -test allows us to estimate how likely it is that the observed correlation has arisen through random sampling of a genuinely uncorrelated parent population. The significance of the t value depends on both the degrees of freedom within the sample (ν) and the confidence level we require (α). For a two variable situation, ν is $n-2$ (in this case 2355); and $\alpha = 0.025$ (95%, two tailed) is normally considered to be a sufficiently reassuring level of confidence.

Having calculated a value for the *t*-statistic we next need to run it through a hypothesis testing procedure, thus:

- i) Assume as a default position (null hypothesis) that the parent population has no pattern (zero correlation), and that any apparent correlation is therefore a misleading quirk of the sampling procedure.
- ii) Calculate the appropriate test statistic and compare with tables of values (prepared on *a priori* grounds and depending upon degrees of freedom and confidence level) which state the necessary size of a test statistic if it is to be considered significant.
- iii) Abandon the null hypothesis if, and only if, the test statistic falls outside the bounds of the relevant given value.

The relevant value for two-tailed *t* tests at 95% confidence level and infinite degrees of freedom (i.e. an infinite number of specimens) is ± 1.960 , being only slightly higher for sample numbers in the thousands. For the same situation at 99% and 99.9% confidence the values are ± 2.576 and ± 3.291 , respectively. Meanwhile, the calculated test statistic for the *H-W* correlation of the entire data set is $t = 61.134$! —so the chances of sampling an uncorrelated parent population and randomly generating the pattern we see is exceptionally unlikely. Correlation coefficients and *t* statistics for all the other correlations are given in Text Table 6.2 (below). Note that everything correlates spectacularly well with everything else (i.e. with far less than a one-in-a-thousand chance of error).

-----	<i>r</i>	<i>r</i>	<i>r</i>	<i>r</i>	<i>r</i>	<i>r</i>	<i>r</i>	<i>r</i>	<i>r</i>
<i>t</i> -stat	-----	<i>H</i>	<i>W</i>	<i>I</i>	<i>Ch</i>	<i>l'</i>	<i>i'</i>	<i>h'</i>	<i>w'</i>
<i>t</i> -stat	<i>H</i>	-----	0.783	0.889	0.838	0.764	0.436	0.719	0.772
<i>t</i> -stat	<i>W</i>	61.1	-----	0.776	0.606	0.863	0.670	0.681	0.730
<i>t</i> -stat	<i>I</i>	94.4	59.8	-----	0.777	0.758	0.540	0.661	0.688
<i>t</i> -stat	<i>Ch</i>	74.4	36.9	59.9	-----	0.584	0.324	0.524	0.589
<i>t</i> -stat	<i>l'</i>	57.4	83.0	56.4	35.0	-----	0.651	0.783	0.705
<i>t</i> -stat	<i>i'</i>	23.5	43.8	31.1	16.6	41.6	-----	0.472	0.405
<i>t</i> -stat	<i>h'</i>	50.2	45.2	42.8	29.9	61.1	26.0	-----	0.656
<i>t</i> -stat	<i>w'</i>	58.9	51.8	46.0	35.3	48.3	21.5	42.2	-----

Text Table 6.2 Correlation coefficients (upper right half) and *t*-statistics (lower left half) for all combinations of metric variables and chambers for the entire data set. Note that everything is extremely well correlated with everything else.

6.2.2.ii Association of Categorical Variables: The χ^2 Test

For cases in which the data are taken to be categorical—*g.dist*, *chir*, *type* and *Ch* as genuine cases, plus, for the present purposes, *tw*, *ind* and *g%* —a different statistical test is appropriate: the χ^2 test. χ^2 works from a two way contingency table in which one category of variables is pitted against the other to produce an array of pigeonholes (see Text Table 6.3). Each of these cells shows the number of instances in which an individual specimen has both of the relevant characteristics. χ^2 works by comparing these observations with the values that would be expected if none of the categories was correlated with any of the others. Expected values are calculated from the contingency table row and column totals:

$$E = (nr \times nc)/n$$

where E is the expected value per pigeonhole, nr is the number of individuals in the pigeonhole's row, nc is the number of individuals in the pigeonhole's column and n is the total number of individuals in the entire sample population.

For the test itself, each expected value is subtracted from the corresponding observed value, the result squared to return positive figures only so as to not cancel one another out, and then divided by the expected number again to give a proportion. χ^2 is then simply the sum of all such calculations throughout the table:

$$\chi^2 = \sum (O - E)^2/E$$

Two important limitations should be mentioned. In order for the test to be robust, none of the expected values should be lower than 5; and there should always be more than one degree of freedom. In practice, expected values are frequently smaller than 5 and the standard procedure is to collapse rows or columns into one another, where it is meaningful to do so, until the figure reaches the desired proportions. The number of degrees of freedom (ν) depend on the total number of rows and columns that are not constrained by others; ν can be calculated by multiplying the number of rows minus one by the number of columns minus one: $(r - 1) \times (c - 1)$. For cases in which ν is one (i.e. a 2×2 grid) the Yates's continuity correction should be added, but there was never any need for the *Tritaxia*

data. Text Table 6.3 (below) shows the case of twist versus indentation as a worked example.

Observed	<i>tw</i>	0	1	2	>3	-----	<i>nr</i>
<i>ind</i>	-----	-----	-----	-----	-----	-----	-----
0	-----	344	93	25	7	-----	469
0.5	-----	399	142	32	10	-----	583
1	-----	482	253	69	49	-----	853
1.5	-----	170	84	30	23	-----	307
>2	-----	89	29	15	12	-----	145
	-----	-----	-----	-----	-----	-----	<i>n</i>
<i>nc</i>	-----	1484	601	171	101	<i>n</i>	2357

Text Table 6.3.i *Observed instances of *tw* and *ind* for the whole data set. Note that many of the higher categories have been collapsed into a single grouping e.g. >3.*

Expected	<i>tw</i>	0	1	2	>3	-----	<i>nr—obs.</i>
<i>ind</i>	-----	-----	-----	-----	-----	-----	
0	-----	295.3	119.6	34.0	20.1	-----	469
0.5	-----	367.1	148.7	42.3	24.9	-----	583
1	-----	537.1	217.5	61.9	36.6	-----	853
1.5	-----	193.3	78.3	22.3	13.2	-----	307
>2	-----	91.3	36.9	10.5	6.2	-----	145
	-----	-----	-----	-----	-----	-----	<i>n</i>
<i>nc—obs.</i>	-----	1484	601	171	101	<i>n</i>	2357

Text Table 6.3.ii *Expected values given the observed column and row totals (see text for details). Note that all the category values exceed 5.*

χ^2	<i>tw</i>	0	1	2	>3	-----	<i>nr.</i>
<i>ind</i>	-----	-----	-----	-----	-----	-----	
0	-----	8.04	5.91	2.39	8.54	-----	24.88
0.5	-----	2.78	0.30	2.51	8.99	-----	14.57
1	-----	5.64	5.79	0.82	4.24	-----	16.50
1.5	-----	2.81	0.42	2.68	7.37	-----	13.27
>2	-----	0.06	1.72	1.91	5.39	-----	9.07
	-----	-----	-----	-----	-----	-----	<i>n</i>
<i>nc</i>	-----	19.32	14.14	10.31	34.52	<i>n</i>	78.29

Text Table 6.3.iii *χ values drawn from differences in the two tables above and rendered as positive (χ^2) to avoid a zero sum.*

The standard round of hypothesis testing should next be followed. Once again, our null assumption is that there is actually no association between the categorical variables at all and that where an association is apparent it is simply due to chance. The level of significance (α) is a matter of choice, but is necessarily one tailed since χ^2 must always be positive, and the values to be exceeded are drawn from a standard χ^2 distribution table according to the relevant υ . For our example which had $\upsilon = 12$ i.e. $(5 - 1) \times (4 - 1)$, if $\alpha = 0.05\%$, 0.01% or 0.001% , χ^2 needs to be 21.0, 26.2, or 32.9 respectively. At $\chi^2 = 78.3(!)$, *tw* and *ind* are very definitely non-randomly associated.

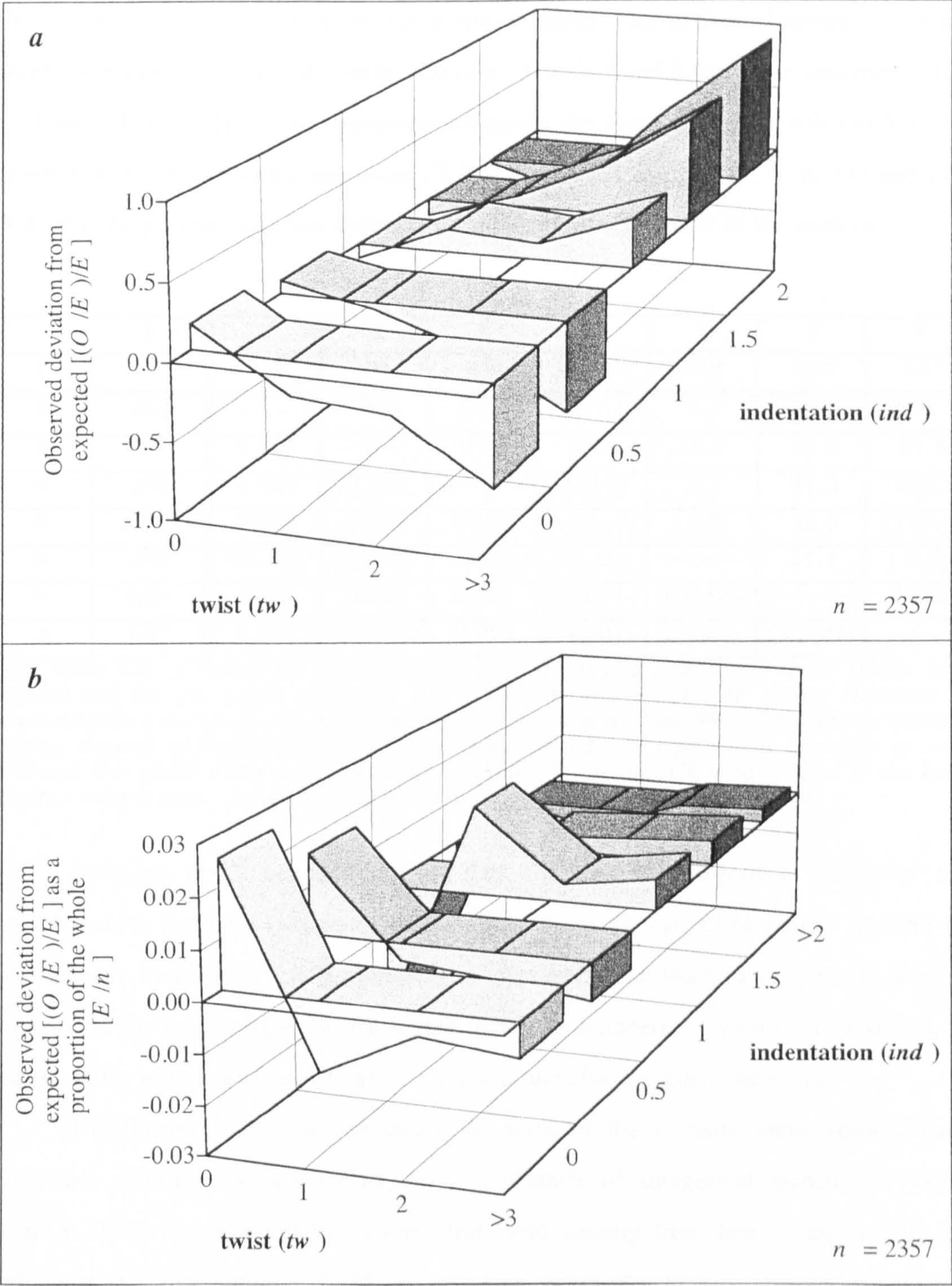
The question that immediately arises is, ‘What *kind* of non random association do we have?’ For the continuous variables, correlations could be either positive or negative; to visualise them we simply needed to draw up a bivariate scatter. But a contingency table is a much more difficult item to wring the relevant information from. With categorical material there need be no trend or rank ordering, and so in theory any category could be non-contingently associated with any other.

To assist in this matter, I found it worthwhile to use a graphical method of my own invention, which takes a version of what I shall call the ‘ χ ’ distribution and plots it in three dimensions. χ alone was used, rather than the χ^2 of the tests themselves, because χ^2 conceals half of the relevant data: it measures how far the observed values deviate from those expected, but, with all the values rendered positive, it does not tell us in which *direction* a deviation occurs. In addition to positive values, χ also provides negative ones wherever there are fewer members than one would expect for a given category pairing. Text Figure 6.11.a is a χ plot for the worked example of indentation versus twist.

We need to be careful about exactly what this plot is showing us. Without squaring the calculation, each cell of the contingency table contains just $(O - E)/E$ (panel a). The problem with this otherwise wonderfully simple formula is that it can generate some rather misleading scaling effects which arise because we are measuring how far away any observed values are from those expected *as a proportion of the expected value only*. This means that for cells with small expected values the probability of a large deviation arising for purely random reasons is much higher than for cells with larger expected values; that is why the statistical test itself requires the expected category to house at least five representatives, and why the plots are likewise limited to the same, often collated, category ranges.

On a plot showing just $(O - E)/E$, any deviations in rarely expected categories appear as anomalously high peaks or troughs. To avoid them dominating and distorting the analysis, I chose to supplement the basic χ charts with a version that takes the size of the expected categories into account as well. Text Figure 6.11.b shows deviations from expectation calculated as $(O - E)/(E \times E/n)$. The units of deviation in these charts, therefore, are as follows: whereas with $(O - E)/E$, an observed value twice that of the expected would come to 1 (and a zero observed count would be -1), in the formulation used in the $(O - E)/(E \times E/n)$ plots, that value becomes $1/E/n^{\text{th}}$ of the total number of specimens. Deviations in rare categories are thus damped in accordance with the expected size of category membership, and where there are substantial peaks and troughs on these plots they are less

in rare categories are thus damped in accordance with the expected size of category membership, and where there are substantial peaks and troughs on these plots they are less likely to record sampling error and more likely to reveal genuine associations between the characters.



Text Figure 6.11 *a* Reproduced from the Appendix, a χ plot of $(O - E)/E$ for the character variables *ind* vs. *tw*; *b* χ plot of $(O - E)/(E \times E/n)$ for the same character variables. See text for discussion.

The results of χ^2 tests for all the categorical data can be found in Text Table 6.4 (below); the corresponding χ diagrams are in Appdx. Figs. 4.2.2 & 4.2.3. The six pairings of coiling direction (*chir*) are not presented in the series because they do not show any significant association, but every other character does: each of them is non-randomly associated with each of the others. Note that to make its categories tractable, the character *Ch* is resolved only to the level of entire whorls rather than individual chambers. Each whorl comprises a full layer of triserial structure. Whorls 1 and 2 (chamber sequences {1, 2 & 3} and {4, 5 & 6}) are not represented because the specimen count was too low, but whorls 3, 4, 5 and 6 (chamber sequences {7, 8 & 9}, {10, 11 & 12}, {13, 14 & 15} and {16, 17 & 18}) do possess sufficient membership and thus form the basis of the analysis.

	χ^2	χ^2	χ^2	χ^2	χ^2	χ^2	χ^2	χ^2
α		<i>ind</i>	<i>tw</i>	<i>g%</i>	<i>g.dist</i>	<i>chir</i>	<i>type</i>	<i>Ch*</i>
α	<i>ind</i>	-----	78.3	61.1	107.1	4.3	29.8	196.2
α	<i>tw</i>	0.001	-----	37.5	45.3	1.7	83.0	91.8
α	<i>g%</i>	0.001	0.001	-----	821.8	6.2	41.5	105.3
α	<i>g.dist</i>	0.001	0.001	0.001	-----	8.5	52.5	114.3
α	<i>chir</i>	not sig.	not sig.	not sig.	not sig.	-----	11.1	5.8
α	<i>type</i>	0.01	0.001	0.001	0.001	not sig.	-----	318.3
α	<i>Ch*</i>	0.001	0.001	0.001	0.001	not sig.	0.001	-----

Text Table 6.4 χ^2 values for associations (upper right) and confidence levels (lower left) between *ind*, *tw*, *g%*, *g.dist*, *chir*, *type*, and *Ch* for the entire data set. Every character is non-randomly associated with every other character to more than 99.9% confidence (taking varying degrees of freedom into account) except for *ind* and *type* which correlate at only 99% and *chir* which never correlates with anything. *Note that *Ch* is calculated to the level of entire whorls only. See text for discussion.

Although the χ^2 test demands we treat the data as categorical, several of the characters do in fact have linear components. *ind*, *tw* and *g%* can all be ranked in terms of measurement magnitude, *Ch* is obviously a cumulative measure, and there is even a sequence to the *type* category which is reflected in its numbering system (i.e. Phases I, II and III reflect progressive uncoiling). Only *g.dist* and *chir* are truly categorical.

This linearity shows up very clearly on some of the χ charts, demonstrating their utility and adequacy as tools for exploring the nature of categorical association. Text Figure 6.11, for instance, exhibits a very clear trend passing from low values to high for both twist and indentation. Recalling that both characters have a skewed distribution whereby the higher categories also tend to be the rarer ones, the upper version, (*O* - *E*)/*E*,

emphasises the far end of the range (the rare categories) and the lower version, $(O - E)/(E \times E/n)$, the nearer end (the common ones). In both depictions the trend is impressively clear.

Text Table 6.5 sorts the categorical associations into those which appear to have *linear* trending features of some sort (L) from those which are *disordered* (D). For the most part, these designations occur where we might expect them to: associations in which both characters have a rank order tend to be linear, and where there is no rank order (e.g. the pairings with *g.dist*) the pattern is disordered. There are some deviations from this general rule (e.g. *g%* vs. *ind* and *type* vs. *ind* are both disordered; *g.dist* vs. *tw* might, perhaps, be linear), but since it is easy to see both why the rule should apply and that it very often does, there seems little point in testing the data further (there is a technique called a ‘chi trend test’, for instance, which measures linearity, but it is difficult to calculate for large amounts of data so I shall not be using it here). It is fortunate that this linear component should be so obvious where it does occur because it plays an important role in the next phase of our analysis.

	<i>ind</i>	<i>tw</i>	<i>g%</i>	<i>g.dist</i>	<i>chir</i>	<i>type</i>	<i>Ch*</i>
<i>ind</i>	-----	L	<i>D</i>	D		<i>D</i>	L
<i>tw</i>		-----	L	<i>L</i>		L	L
<i>g%</i>			-----	D		L	L
<i>g.dist</i>				-----		D	D
<i>chir</i>					-----		
<i>type</i>						-----	L
<i>Ch*</i>							-----

Text Table 6.5 Significant associations between the categorical characters can be usefully split into those which appear to have a linear component (L) and those which are simply disordered (D). Italicised entries mark cases where a pairing does not have the pattern we might expect from the style of the data (see text for discussion).

6.2.2.iii Associations Between Both Continuous and Categorical Variables

Aside from splitting the continuous data into categories and trudging long-windedly through χ^2 tests, there is no ready method, so far as I know, for analysing associations between categorical and continuous forms of measurement. That is why the chamber number (*Ch*) has been pressed into service twice, once as an honorary continuous variable and once as a genuinely categorical one. *Ch* breaks readily into discrete groupings at the level of individual chambers and entire whorls alike, but the chambers themselves are

sufficiently numerous to approximate a continuous variable; we can thus use this character as a bridge between the two data series. Since all the continuous variables are correlated with *Ch* (to an extravagant level of significance), and all the categorical ones likewise show some non-random association (again, to a very high level of significance), we can fairly safely conclude that the continuous characters and the categorical ones, in general, share a common association.

That this association evidently has a linear component, especially in the case of *Ch*, is even better news because it suggests that the whole array of characters is linked throughout development in the most straightforward way—as an individual grows, everything gets bigger. Not only do characters like *H* and *W* increase in a correlated fashion, but there is also a shift along the ordered ranks of categorical measurements like *tw*, *ind* and *g%*. (In the case of *type* (Section 6.1.3.i), the category ranking is less obviously a natural feature and more clearly an artificial one; but even here the categories were chosen long before the correlations were ever tested, on the basis that they reflect a sequence of shifts spanning from triserial towards biserial forms of growth.)

To conclude: the measured characters of *Tritaxia pyramidata* are almost all correlated or otherwise non-randomly associated with one another (the only exception being coiling direction which has no significant connections at all). These non-random associations already serve to *narrow down the space of possible morphological forms* that the measurements would otherwise define. The fact that a major component of this narrowed range of expression is also correlated with chamber number (or growth stage) is particularly important because it tells us not only about *Tritaxia*'s location *in* morphospace but also about its developmental trajectory *through* that space. This argument will be developed further in the next chapter, but before we get to it we need to use the correlations we already have to define two other, important types of 'space'.

6.2.3 Allometry: Separating Constants from Magnitudes

By their very nature, continuous variables have a linear component—the dimension of variability along which they are measured. This is essentially what is captured by the correlation coefficient which defines linearity in relation to spread for any pair of characters

to which we apply the calculation. One of the reasons we were interested in joint linearity is that it holds the promise of yielding a constant value with which to summarise the relationship between a character pair. In the case of the categorical characters, even the logically ordered ones, it is not possible to quantify the situation any further; but with continuous data there are well accepted methods of separating the desired parameters from one another.

Thus far we have been implicitly assuming that the association between continuous variables is a straightforward linear one, in which case the constant we seek is equivalent to the slope of a straight best-fit line (a reduced major axis) that runs along the length of the cloud of data and passes through the point corresponding to the intersection of the two means. The constant is a ratio relating the average x component of a line to its equivalent y component, and can be found simply by dividing the standard deviation of variable y by the standard deviation of x .

Such an occurrence is known as *isometry* because it corresponds to situations where shapes are preserved regardless of size. But the living realm is full of circumstances in which shape is *not* preserved throughout the growth of an organism, a situation known as *allometry*. When *shape* is transformed along with magnitude, there can no longer be a straight line through the spread of different sized data points; rather, the best fit is a curve. In such cases, the relationship between two variables cannot be summarised by a single value, a ratio, but also requires a further constant, a power function, to account for the curvature of the growth trajectory and to represent the *rate of change of shape*.

More formally, the equation for isometry is:

$$y = bx + c$$

where x and y are any values on the abscissa and ordinate, respectively, b is the constant of proportionality (the ratio) linking the two, and c is the intercept of $x = 0$ on the y axis, which takes into consideration the likelihood that even the initial starting configuration is not equidimensional (c can be positive or negative). In most biological cases the value of c is set by the form of the larva or seed (in foraminifera it would be the proloculus), and the extent of the inequality is typically sufficiently small that it is trivial in comparison to subsequent size increases. Consequently, the initial heterogeneity can often be ignored.

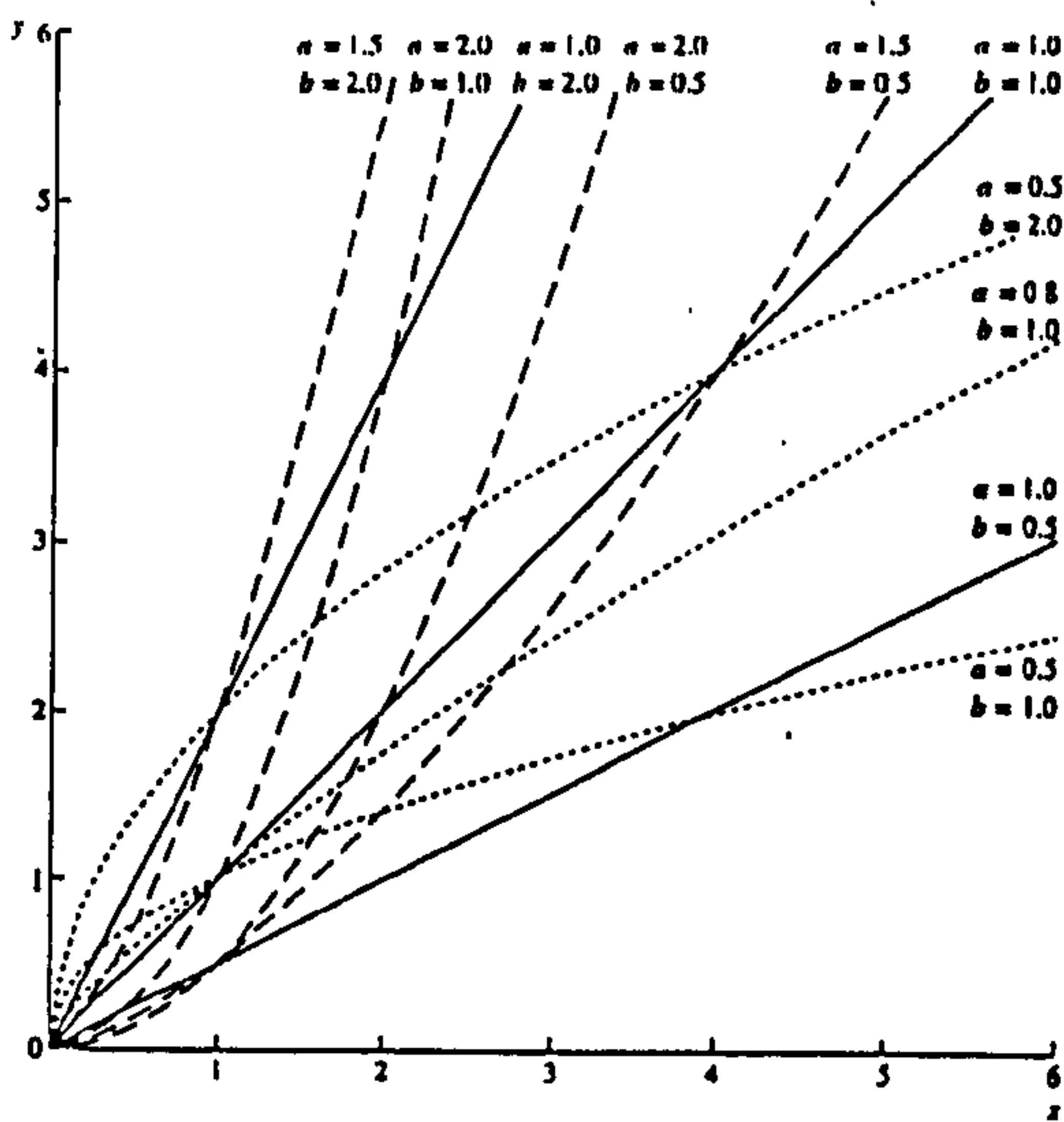
By comparison, the equation for allometry is:

$$y = bx^a + c$$

where the added value, a , is the allometric exponent responsible for defining the curvature of the growth trajectory. But we should also note that the two equations are essentially identical since the isometric case is none other than the allometric case for situations in which the exponent is exactly 1.

In allometric cases it is the constants a and b we are most interested in because these define the relationship between the variables for every phase after the initial one. By contrast, c is of comparatively small importance, a fortunate detail because its calculation is problematic. Whereas in isometric situations c can be estimated by falsely extrapolating the best fit line back to $x = 0$, the operation for revealing the allometric exponent effectively loses all information about c because it assumes the curve to begin at the origin.

A further point to be made concerning the exponential factor is that its value depends upon the way we distribute the variables. If we place the faster increasing character on the y axis, the resultant a is greater than 1 and is said to be positive; if we put it on the x axis a will be less than 1 and therefore negative. This issue will become important in Part IV when we consider the ‘direction’ of shifts in shape and trajectory parameters. Text Figure 6.12 shows the effect of different combinations of a and b on how growth lines relate to the axes.



Text Figure 6.12 *The effects of different values of a and b on how growth trajectories relate to the axes.*

By way of a concrete demonstration, let us take H and W once again (Text Fig. 6.10), with H on y and W on x , and use values from the entire data set. Let us assume for the time being that although the correlation is good, the relationship between the variables is likely to be allometric; if an a value not significantly different from 1 subsequently emerges we can take things from there.

The standard method for dealing with such curves (e.g. Skelton, 1993, p 480) is to map them onto a logarithmic scale, in this case common logarithms. This straightens the curve out (in effect by bending the axes) and from there on the process is simple. The data can now be dealt with in a manner analogous to the isometric case with the exponent (a) being the ratio between the two log standard deviations, and the constant of proportionality (b) associated with the new intercept of $x = 0$ on the y axis. That is:

$$a = s_{\log y} / s_{\log x}$$

where s_{\log} is the standard deviation of the logarithmic values (rather than the logarithmic values of the arithmetic standard deviations), and

$$b = 10^{\log b}$$

i.e. the antilog of $\log b$ where

$$\log b = \text{mean log } y - a(\text{mean log } x)$$

and corresponds to the point at which a reduced major axis running from the conjunction of both mean $\log x$ and mean $\log y$, and having a slope of a , intersects the ordinate (y) at $x = 0$.

In our example,

$$\text{mean log } H = 2.747 \text{ and mean log } W = 2.604$$

and

$${}^{\circ}\log H = 0.104 \text{ and } {}^{\circ}\log W = 0.070$$

so that

$$a = 1.50$$

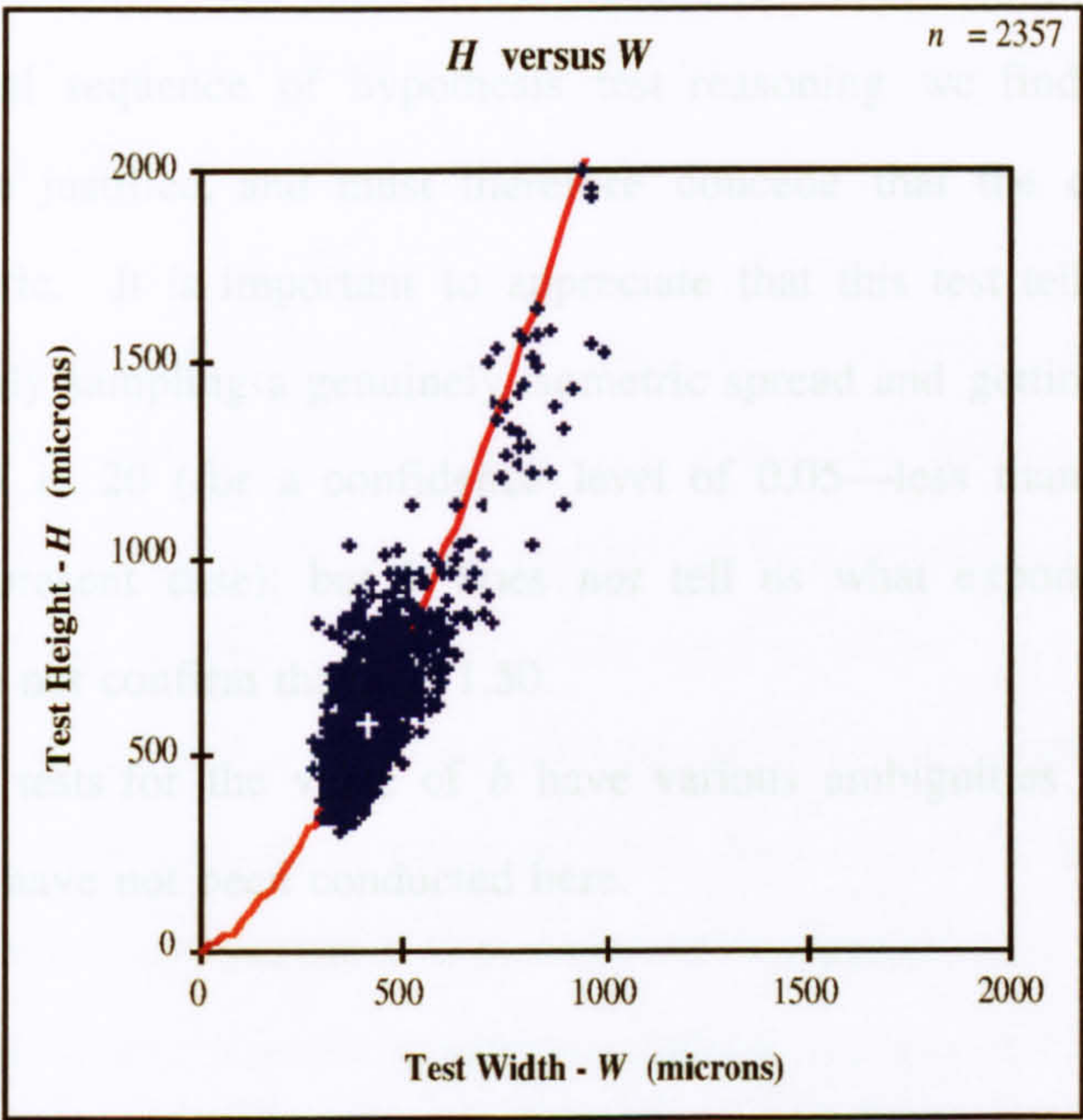
and (since $\log b = -1.148$),

$$b = 0.07$$

The equation describing the H/W trajectory in *Tritaxia*, therefore, is:

$$576.7(\mu\text{m}) = 0.07 \times 407.6(\mu\text{m})^{1.50}$$

Note that the factor c has disappeared entirely. It must still have some impact but the contribution is now lost as ‘noise’ (so hopefully its value was as small as we assumed it to be).



6.2.4 Visualising Morphological Spaces

Text Figure 6.13 H and W are indeed allometrically related. The central white cross marks the mean and the red curve a trajectory with a positive allometry of 1.50.

Now that we have tools with which to effectively manage the data, the way is open to developing a useful application of them and a very simple one is possible for *Tritaxia*. Since the value of the exponent, a , was not 1 for H/W , the relationship between these characters does indeed appear to be allometric (Text Fig. 6.13). But, given the variance in the data, it is once again entirely possible that we have revealed a spurious curve for no other reason than chance alone. Again, there is a statistical test to help firm up our intuitions, but first we need to assess exactly how much spread there was on that data, and to do this we must determine the standard error, s_e :

$$s_e = a \sqrt{(1 - r^2) / n}$$

The significance of a correlation is that a great deal of the existing space, defined by where n and r have their usual identities, although note that r here is the coefficient for the logarithmic values. The s_e for the H - W scatter is 0.0216.

Once we have the standard error we are in a position to calculate another test statistic, this time called Z :

$$Z = (a - 1) / S_e$$

As with the t test, the value of Z must be outside the relevant limits imposed by a pre-calculated statistical distribution in order to qualify as significant; specifically, it must be ± 1.96 for 95% confidence. The calculated Z statistic for the H - W exponent, a , is 22.93!; by following the usual sequence of hypothesis test reasoning we find again that the null position cannot be justified, and must therefore concede that the curve is likely to be genuinely allometric. It is important to appreciate that this test tells us merely that the chances of randomly sampling a genuinely isometric spread and getting an a value of 1.50 are far less than 1 in 20 (for a confidence level of 0.05—less than 1 chance in several thousand in the present case); but it does *not* tell us what exponent a *really* is, and specifically it does not confirm that a is 1.50.

Equivalent tests for the value of b have various ambiguities associated with them (Jones, 1987) and have not been conducted here.

6.2.4 Visualising Morphological Spaces

Now that we have tools with which to effectively manage the data, the way is open to developing a better appreciation of form and developmental sequence in *Tritaxia pyramidata*.

Every one of our character variables has a range of expression; for the truly categorical features it is more a number of 'states' than a range *per se*, but for any other feature, including those categorical characters with a logical ordering, a one dimensional *range* of values is clearly what we have in mind. For pairs of characters the equivalent is a *space*, and so on up to n -dimensional hyper-volumes.

The significance of a correlation is that a great deal of the existing space, defined by the end points of the character ranges, is empty. The point of talking about abstract, non-existent specimens is that by doing so we are striking at the very core of what a physical expression of morphological form is all about: in order to talk about what something *is* we

are also implicitly discussing what it is *not*; what it might be instead. Furthermore, this idea allows us to *quantify* those possibilities, in microns for foraminifera, and to gauge the actualities relative to them. It is an analogue version of the bit by bit measurement of an information space as outlined in Section 5.3.1. Harking back to earlier theoretical considerations, the form of *Tritaxia* supposedly results from an interplay between genetic instruction, cellular machinery and environmental input; and although we do not yet know how any of these factors contributed to the finished product, at least we now have a solid foundation, in the form of a restricted space of actual finished-product outputs, from which we can to begin work back.

Given the operations described above, there are three different types of ‘space’ we might consider. The first is straightforward *size space*, the normal volumetric stuff we routinely inhabit. Variables in this region possess all their usual physical characteristics of being x microns long or high or wide. The next is *shape space* in which the real magnitudes are lost completely and are replaced by the values of a derived feature, the ratio, which is calculated from the original measurements. And, if we broaden the definition from characteristics of individual specimens to those of whole populations, we can talk about the space of expression of the allometric exponent, a , which might be cast as ‘*change of shape*’ space, or, with epigenetic landscapes in mind, *trajectory space*.

This arrangement evidently constitutes a kind of hierarchy of morphological regions related to the sequence of methods we have used to transform the original data. Shape space is derived from, and was thus somehow ‘lodged within’, size space; trajectory space concerns the range of possible pathways through chunks of size *and* shape space. If it is a ‘developmental program’ we are searching for then trajectory space is probably a good place to look; but it is wise to proceed slowly and to carefully examine the terra firma of more familiar, and thus more comprehensible, ‘lower’ spaces, too.

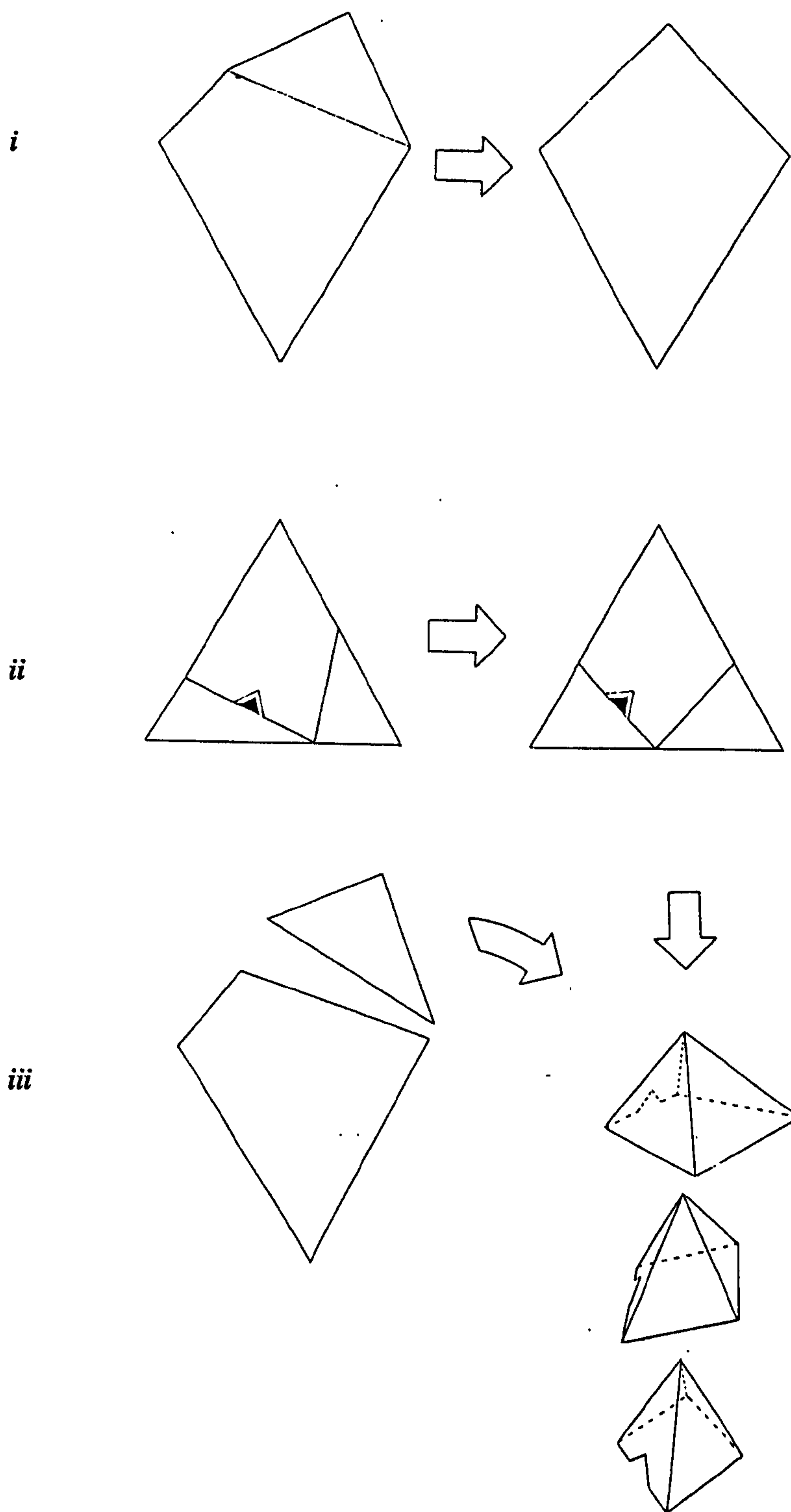
Having already reviewed the single character dimensions (Appdx. Figs. 4.1.1, 4.1.3) we are in a position to begin building a multidimensional lifeline for the Platonic Foram. Starting with the continuous variables, bivariate scatters allow us to examine the relationship between size, shape and trajectory parameters, all at a single glance (e.g. Appdx. Figs. 4.2.1). To do the job properly, pitting every continuous variable against every other one, would require us to examine 28 different pairings. This is clearly a tall order, so I have

opted instead to examine a representative selection of six of these in order to sample *Tritaxia*'s lifeline without getting tangled up in it. The pairings chosen are H/W , H/I , l'/h' , l'/w' , l'/i' , and w'/h' , which provide a meaningful and informative sample drawn from both the whole-test bounding characters (H , W , I) and those of the final chamber (l' , w' , h' , i'). Appendix Figures 4.1.2 show that like the sizes, these shapes also have non-significantly skewed, more or less normal distributions.

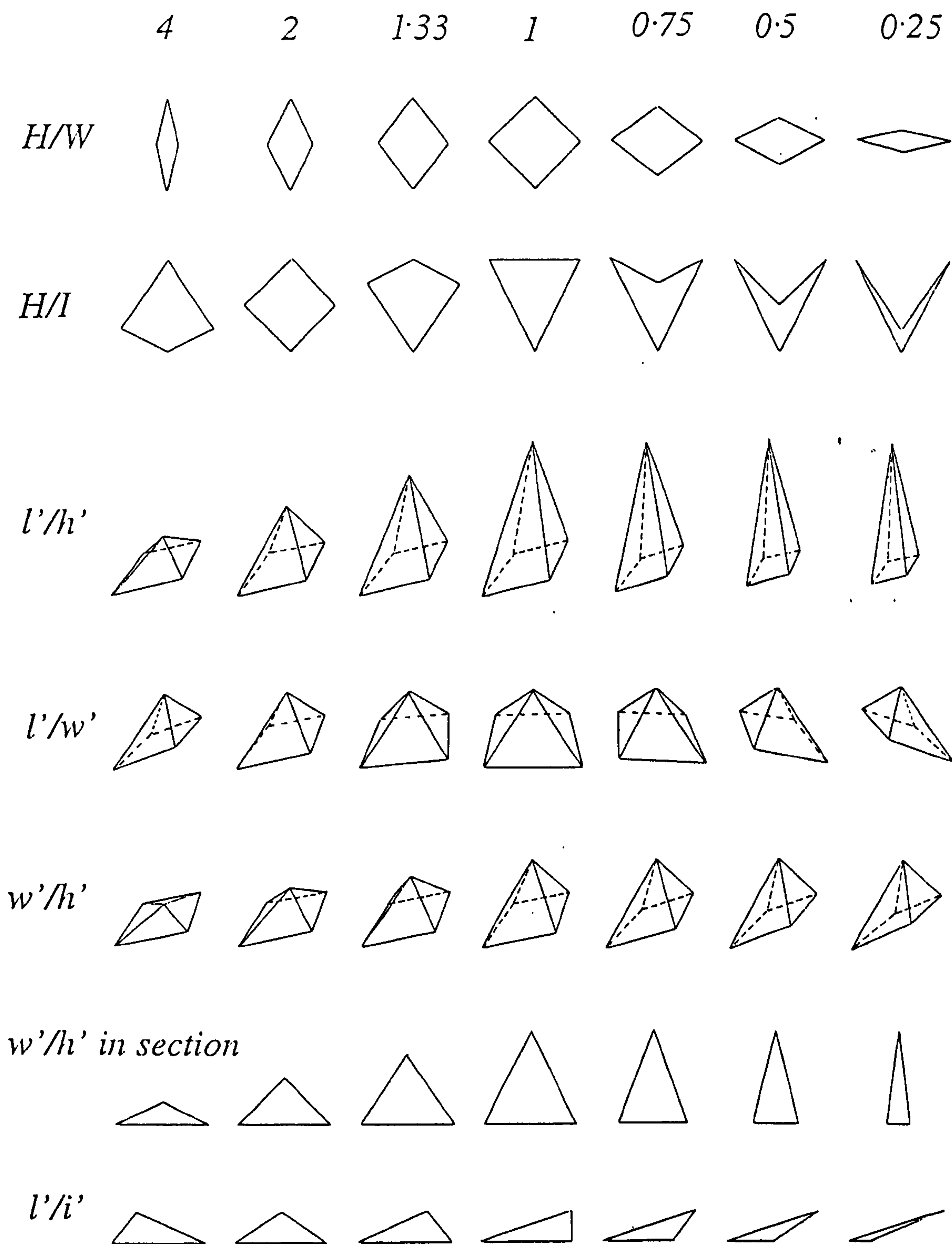
Relationships with Ch are not considered at this point. They would swell the number of 'shape' ratios considerably, adding another 7 pairings to the list above if each metric character was related to its chamber number ratio. Also, Ch plays a prominent role in the next chapter where its discrete nature is exploited to provide a step by step characterisation of the developmental sequence.

Basic character sizes, along with the shape and trajectory ratios, can be clumped into two distinct groups, one reflecting the broad outlines of the *whole test* (H/W , H/I) and the other those of the *final chamber only* (w'/h' , l'/h' , l'/w' , l'/i'). Although several relationships *between* these two groupings were explored at some length in preliminary investigations (H/h' , W/l' , H/Ch), nothing noteworthy was revealed; and so, for reasons of economy, clarity and taste (i.e. they were awkwardly hard to visualise), they have been omitted from the presentation, and the relationships involved are considered in the sections to come only through the more accessible medium of those ratios listed above.

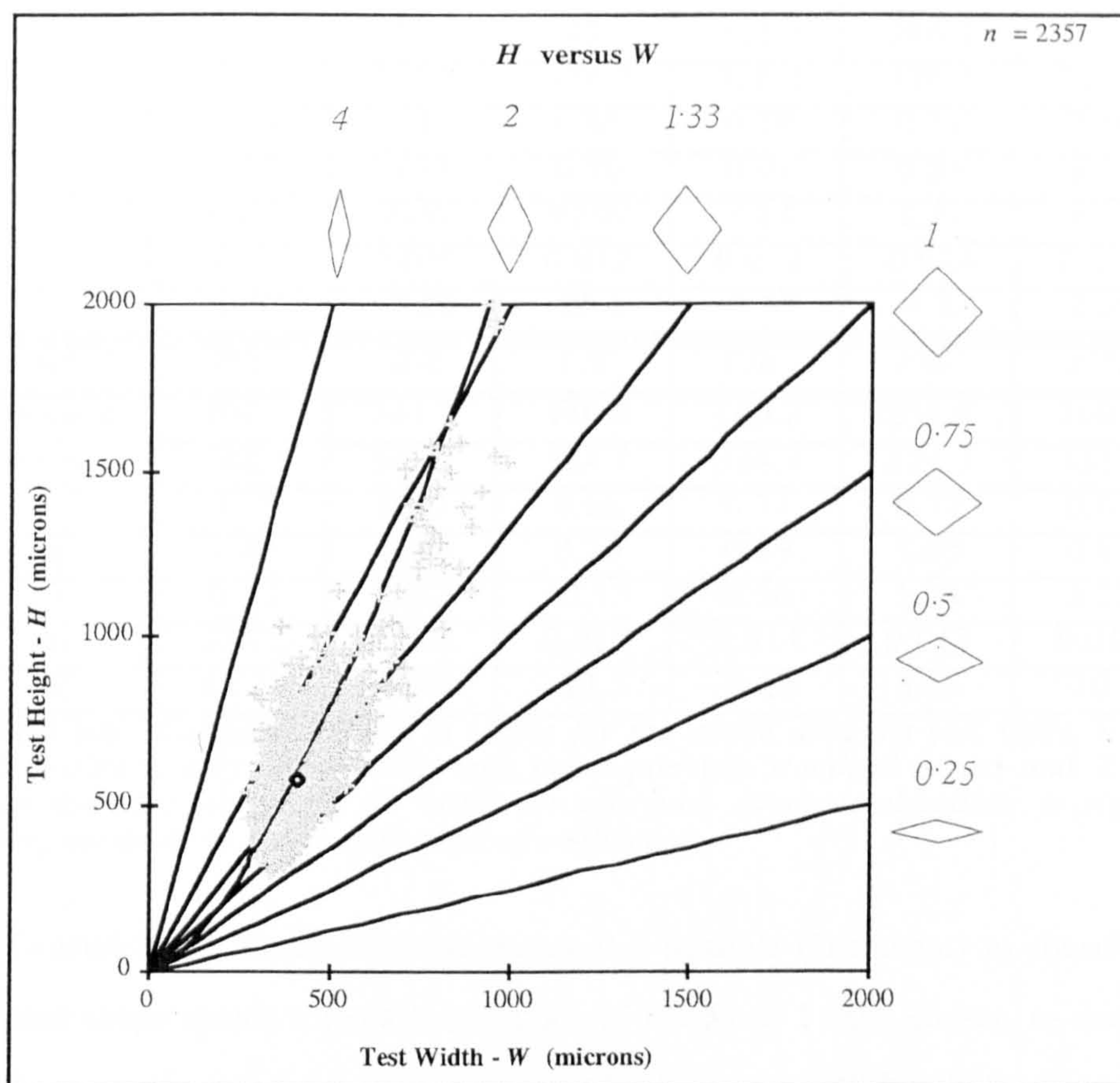
The key to interpreting such multidimensional morphometric plots lies in being able to visualise the relationships they represent; to this end, all the pairings chosen have the advantage of being easy to depict as two or three dimensional sketches. Text Figure 6.14 shows how the Platonic Foram can be broken up into simpler geometric figures—kites, rhombi, triangles, pyramids etc.—reflecting idealised relationships between the character measurements. These are easy to understand and should help us keep track of any changes in shape. As an orienting device, Text Figure 6.15 shows these geometric ideals combined into different shapes according to a standard set of ratios, which in turn correspond to radial lines marked out on the Appendix Figure bivariate plots. Text Figure 6.16 provides a graphic explanation of how these features relate to one another for the H/W bivariate spread.



Text Figure 6.14 The idealised tritaxiid can be converted into even simpler geometric approximations. *i*, instead of a lop-sided form, the characters H , W and I can be used to create a symmetrical kite shape which is easier to sketch; *ii*, a similar operation to the w' and l' dimensions of the final chamber renders it equally easy to depict in plan view; *iii*, with the asymmetric base-plan of the final chamber turned into a regular diamond, it becomes possible, by adding the character variable, h' , to sketch the final chamber as a pyramid-shaped 'tent'. Various shape ratios of these idealised figures are shown in Text Figure 6.15, overleaf.



Text Figure 6.15 Idealised shapes of the six basic bivariate character pairings as relating to the ratio guide lines on Appendix Figures 4.2.1 (i.e. $y:x = 4:1, 2:1, 1.33\dots:1, 1:1, 1:1.33\dots, 1:2$ and $1:4$). See also Text Figure 6.16 overleaf.



Text Figure 6.16 *H/W with ratio lines labelled to show the shape of specimens at various points on the field.*

Appendix Figures 4.2.1 and 4.2.3 are also split into two panels, the upper one showing just triserial specimens, the lower showing all growth types (*type*) superimposed. This is because the same figures are also used in Chapter 7 where we shall be considering non-triserial growth phases in more depth. The triserial/non-triserial division does not concern us much here. All specimens have a triserial stage, no matter what form they take in later growth, and so the triserial panel is of general interest: at the very least we should try to understand basic triserial growth before considering the more exotic cases. The all-growth-types panel demonstrates the full extent of each given bivariate morphospace occupied by the entire sample population, so these, too, are equally relevant to an understanding of the Platonic Foram.

Values for the parameters used in constructing the Appendix Figures can be found in Text Table 6.6, below. Note that virtually all the metric pairings have a significant allometric relationship (the exception is w'/h' for all *types*), meaning that growth sequence in *Tritaxia* involves movement through shape space as well as through size space.

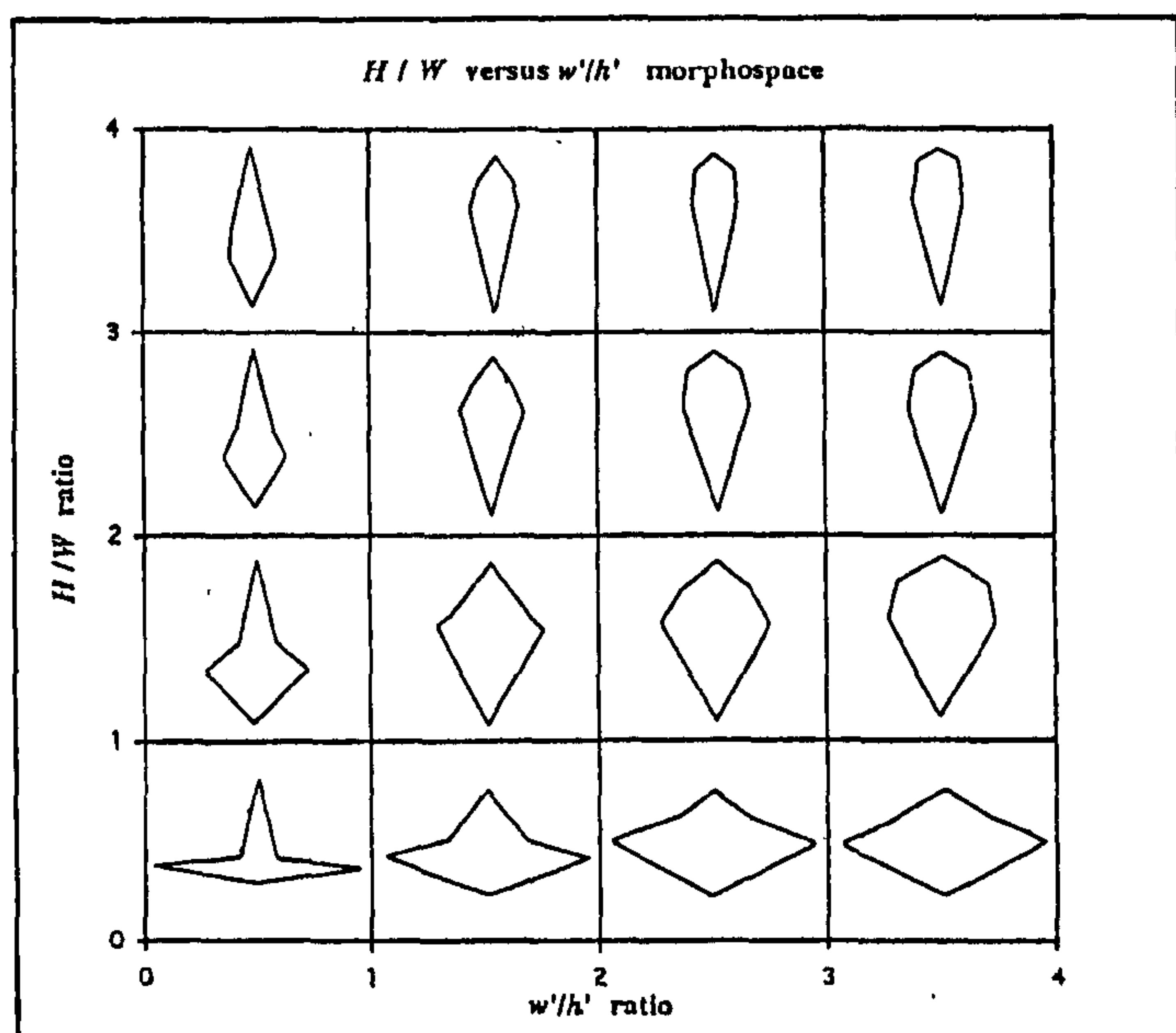
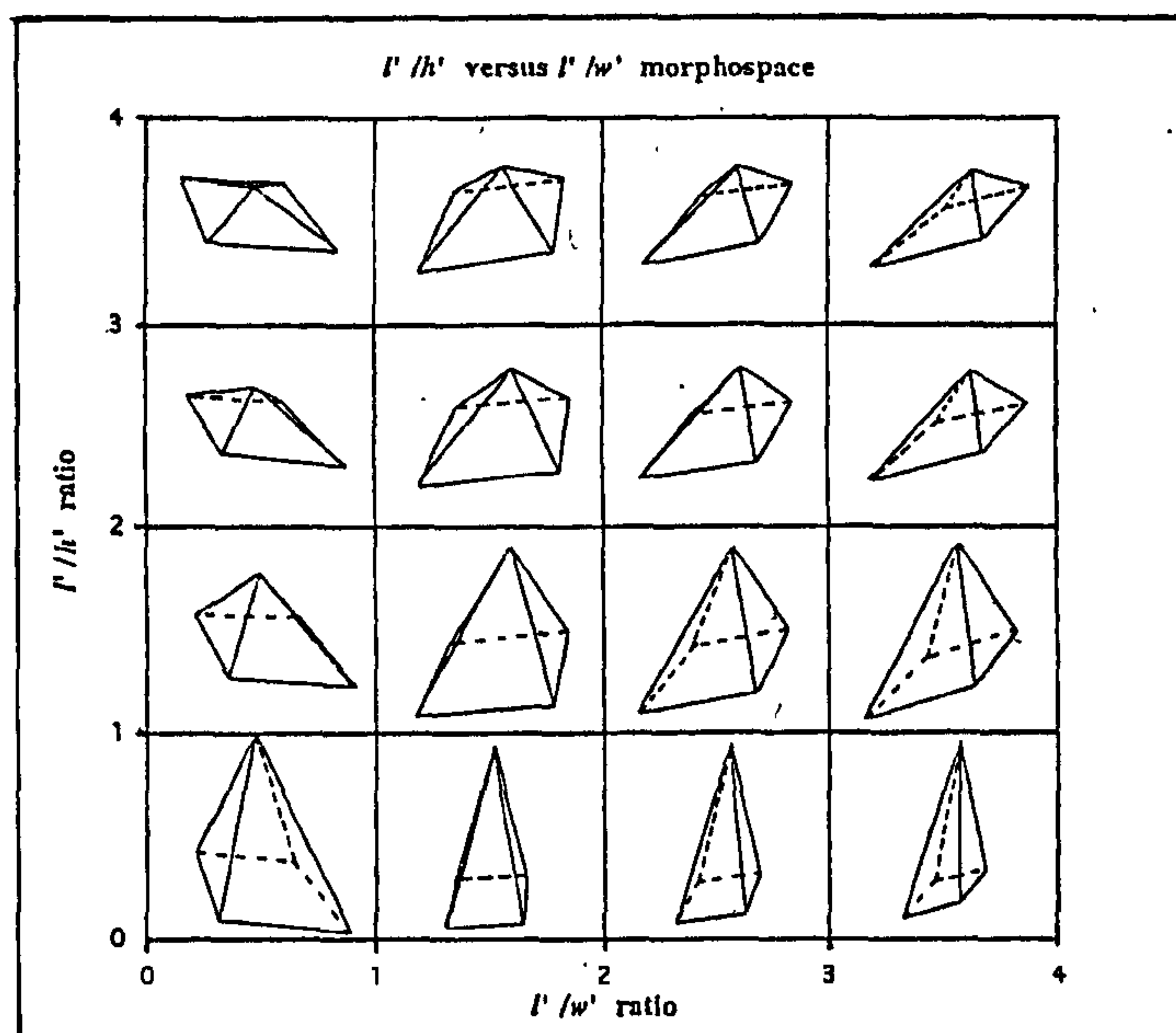
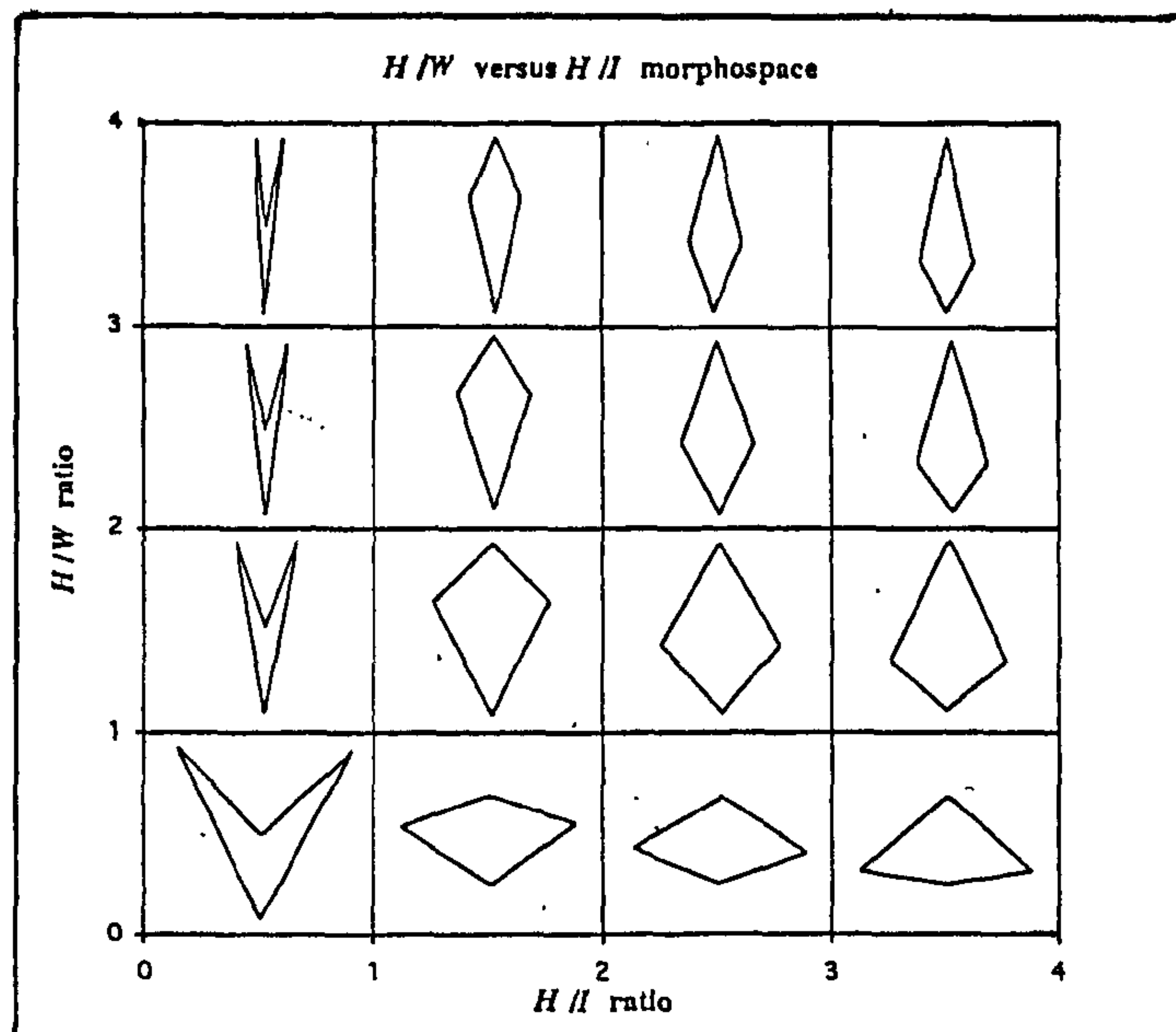
all types	H/W	H/I	l'/i'	l'/h'	l'/w'	w'/h'
mean x	407.6	352.3	143.7	163.5	246.1	163.5
mean y	576.7	576.7	326.3	326.3	326.3	246.1
r	0.78	0.87	0.65	0.78	0.71	0.66
a	1.50	0.93	0.70	0.91	0.88	1.02
b	0.07	2.46	10.07	3.24	2.51	1.33
Se	0.022	0.010	0.012	0.012	0.014	0.017
Z	22.93	-7.23	-25.5	-7.67	-8.33	1.39
triserial	H/W	H/I	l'/i'	l'/h'	l'/w'	w'/h'
mean x	404.1	341.5	146.6	160.2	235.9	160.2
mean y	542.1	542.1	324.7	324.7	324.7	235.9
r	0.79	0.92	0.66	0.77	0.77	0.63
a	1.41	0.86	0.70	0.89	1.05	0.85
b	0.11	3.52	10.15	3.56	1.04	3.23
Se	0.022	0.008	0.012	0.014	0.017	0.015
Z	18.74	-16.3	-23.5	-8.15	3.14	-10.1

Text Table 6.6. Calculated a and b values for the entire data set (all types, $n = 2357$; triserial specimens only, $n = 1867$), with accompanying standard errors and Z statistics. Note that with the exception of w'/h' for all-types, every combination is significantly allometric, normally to a very high level of confidence.

Expanding on simple bivariate spaces, it is possible (just about) to consider 3 or 4 dimensional shape spaces without losing track of the data. I have chosen to examine the higher dimensional groupings $(H/W)/(H/I)$, $(l'/h')/(l'/w')$, and $(H/W)/(w'/h')$ as representative cases, where both axes of the new bivariate plot display character ratios freed entirely from their magnitudes (Appdx. Figs. 4.3.1).

For clarity, these plots are also supported by a grid of shapes (Text Figure 6.17, overleaf), again derived from standard geometric approximations of the Platonic Foram (Text Figure 6.15), and with each one corresponding to the mean form specified by the cell on the grid it appears in.

It is important to recognise that such shape spaces are only possible by seriously contorting the original bivariate plots: the horizontal and vertical grid lines, which appear as parallel frames of reference here, actually correspond to the converging ratio lines on the bivariate originals! Also, in terms of growth trajectory, these plots are distorted by the curvature of the allometric relationship; by concealing absolute size, the effects of the exponent are blurred (and I shall not pursue the issue further at this point except to suggest the reader might try to imagine a growth trajectory running vertically up and out of the page—this technique is fleshed out in Chapter 7, Section 7.5). These charts provide our n -dimensional morphological model of *Tritaxia*.



Text Figure 6.17 Higher dimensional idealised shapes in their appropriate regions of morphospace.

Summary

The agglutinated structure known as *Tritaxia* has a long history of recognition, dating back to the mid-19th Century. It is triserial, triangular in cross-section, sometimes exhibiting non-triserial growth in the final few chambers, and we have every reason to believe it is a foraminiferal test related to an extant genus of the same name.

A mix of 14 continuous and categorical character measurements were taken on a population of 2357 specimens, collectively providing an excellent three dimensional representation of *Tritaxia*'s morphology. The average foraminiferal configuration drawn from the entire data set was dubbed the Platonic Foram.

The number of chambers (*Ch*) is a discrete categorical character but can be treated as a continuous variable for certain statistical purposes; it thus provides a bridge between the continuous and categorical data sets. Because foraminifera grow by discrete chamber addition, and in order to combat the issue of age dependent differences in character expression, *Ch* is also used as an indicator of 'developmental stage'.

Using statistical tests appropriate to the type of data, correlations were established as existing between virtually every character and every other character. It seems likely that most characters change with age, and that age, or stage of development, is thus the predominant dimension of association between the morphometric variables. For the mathematically versatile continuous variables it is possible to plot locations in size, shape and trajectory space, the latter providing a proxy for the temporal passage across an epigenetic landscape.

Chapter 7 A Lifeline

Introduction

Chapter 6 defined *Tritaxia*'s location in n -dimensional morphospace and went a considerable way towards exploring the zones through which it moves during the course of an average lifecycle. But growth in a foraminiferan is not really as smooth and continuous as an allometric trajectory suggests: rather, it is episodic and discrete — foraminifera grow via the sequential addition of new chambers. Growth by discrete chamber addition, and the processes involved in chamber formation itself, are thus the major themes of this next chapter. The overall goal is to imagine, in as much detail as possible, the construction of *Tritaxia*'s test from the perspective of the tiny blob of cytoplasm which created it. The aim is to 'get inside' the organism, to see how it gets things done, and, ultimately, to assess the prospects for evolutionary change from *its own* perspective.

Section 7.1 Growth Sequence in *Tritaxia*

From the image of an elegant, allometric growth curve, we must next shift our focus to a version based on discrete chamber formation. Our first task, therefore, is to see how closely this discrete model compares with the trajectory version we already have. As in Chapter 6, we will be using as much of the entire data set as possible, but this time it will be split into populations according to growth stage; that is, according to the number of chambers an individual possesses. The populations chosen are complementary to those comprising the four whorls used in the categorical associations of Section 6.2.2.iii; they range from specimens with 7 chambers (where $n = 14$) to specimens with 18 (where $n = 22$); see Text Table 7.1, below, for details. Individuals with fewer or more chambers are not included in this analysis because their numbers are too low to provide anything approaching a trustworthy average; but it is important to appreciate that individuals with lower numbers of chambers are excluded primarily by the sieve size, rather than any genuine absence from the lifecycle.

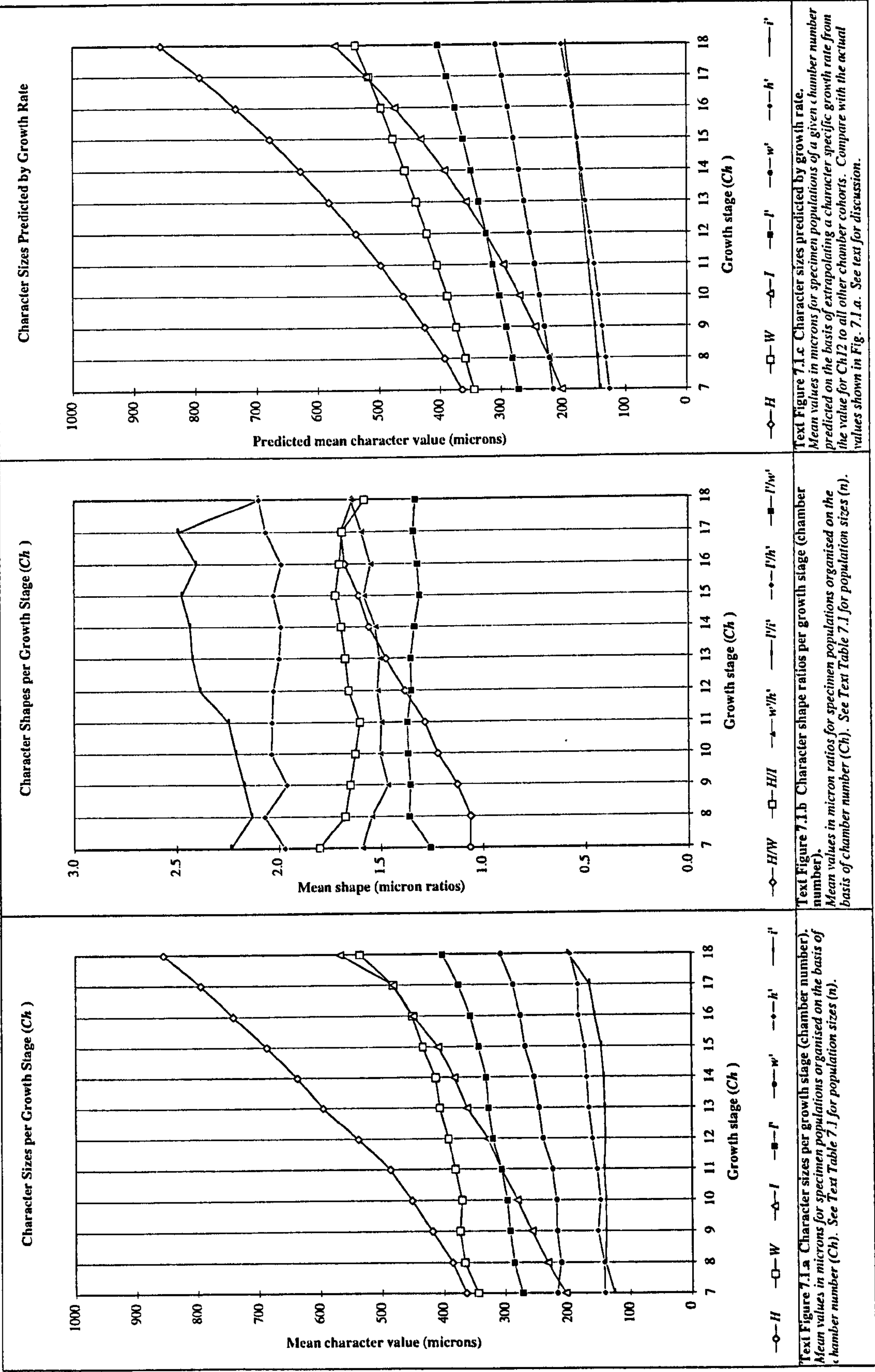
<i>Ch</i>	<i>n</i>	<i>H</i>	<i>W</i>	<i>I</i>	<i>l'</i>	<i>i'</i>	<i>h'</i>	<i>w'</i>	<i>H/W</i>	<i>H/I</i>	<i>l'/w'</i>	<i>l'/h'</i>	<i>l'/i'</i>	<i>w'/h'</i>
7	14	364	345	204	272	126	140	217	1.06	1.80	1.26	1.97	2.23	1.59
8	71	386	366	233	286	139	142	212	1.06	1.67	1.36	2.07	2.13	1.54
9	150	418	373	257	293	138	151	218	1.12	1.65	1.35	1.96	2.17	1.46
10	189	451	371	280	297	138	147	218	1.22	1.62	1.37	2.04	2.21	1.50
11	324	486	381	306	306	140	152	225	1.28	1.60	1.37	2.03	2.24	1.50
12	428	538	393	328	320	139	160	240	1.38	1.66	1.35	2.02	2.38	1.52
13	479	596	407	362	327	140	166	246	1.47	1.67	1.35	2.00	2.42	1.51
14	332	638	413	382	331	141	168	254	1.56	1.69	1.34	1.99	2.43	1.53
15	180	688	434	409	344	146	172	268	1.61	1.72	1.31	2.02	2.47	1.58
16	85	742	451	449	357	156	182	275	1.68	1.70	1.32	1.99	2.40	1.55
17	37	795	482	481	376	164	184	288	1.69	1.69	1.34	2.06	2.49	1.59
18	22	856	535	568	403	199	196	307	1.64	1.58	1.33	2.10	2.10	1.64

Text Table 7.1 *Mean values in microns and micron ratios for size and shape parameters during growth through stages Ch 7 - 18. Note the variation in sample size (n).*

Text Figure 7.1.a shows changes in mean size for the seven metric variables in populations sorted by *Ch*. In every case the character size appears to increase quite steadily with progressing growth stage. Text Figure 7.1.b shows an equivalent graph for changes in mean shape. Sometimes these, too, show increases or decreases during growth, as, for example, with *H/W* (although we should be cautious about what it means for a ratio to ‘increase’—see Section 8.1.5.i for a discussion); in other cases a ratio remains roughly constant throughout, for instance with *l'/w'* and *l'/h'*. Several ratio profiles exhibit a markedly S-shaped, logistic curve, most notably *H/W* and *H/I*, and also *l'/i'*, albeit rather jaggedly.

Statistical tests (*t* tests) can be performed to establish whether these shifts in size and shape are significant or not. The methodology can be found in Chapter 8 (Section 8.1.3.i) where such tests are used extensively; the results appear in Appendix Tables 3.1.1 & 3.1.2. They confirm most of our intuitions about the charts. Character *sizes* do indeed mostly involve significant shifts between successive chamber number cohorts (*i'* is the main exception, showing least of all), whereas most of the *shape* changes do not (with *H/W* as the exception in this case).

On average, size increases apparently occur at a slightly exponential rate for each character (Text Table 7.2). Here, the rates were calculated simply by dividing the mean character value for each chamber cohort by that of its predecessor, and then taking the series mean as an index of the whole. If growth had occurred by adding a sequence of



equal-sized chambers, this procedure would have yielded a steadily declining series of ratios, whereas, in fact, the ratios always turn out to be slightly positive.

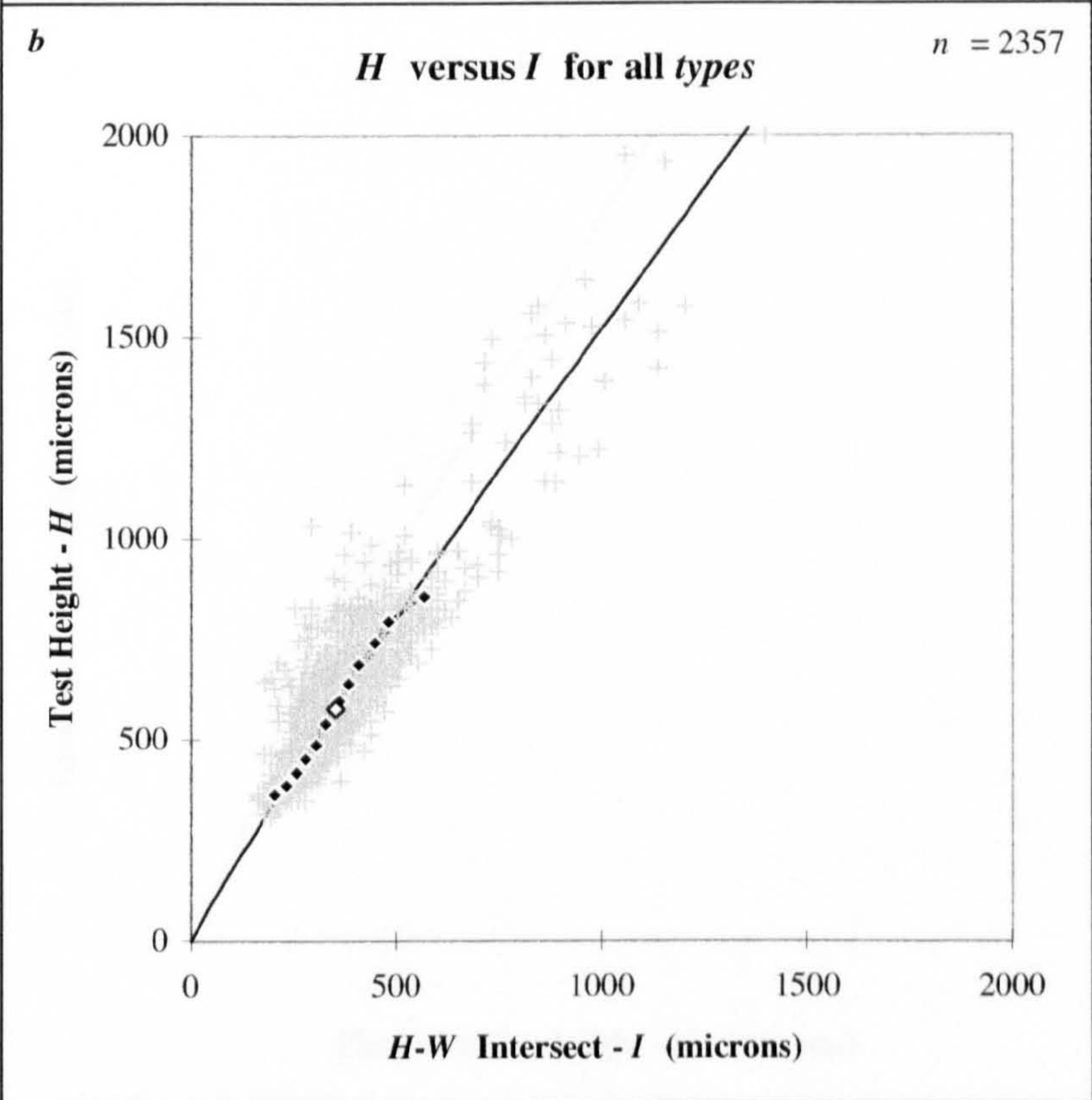
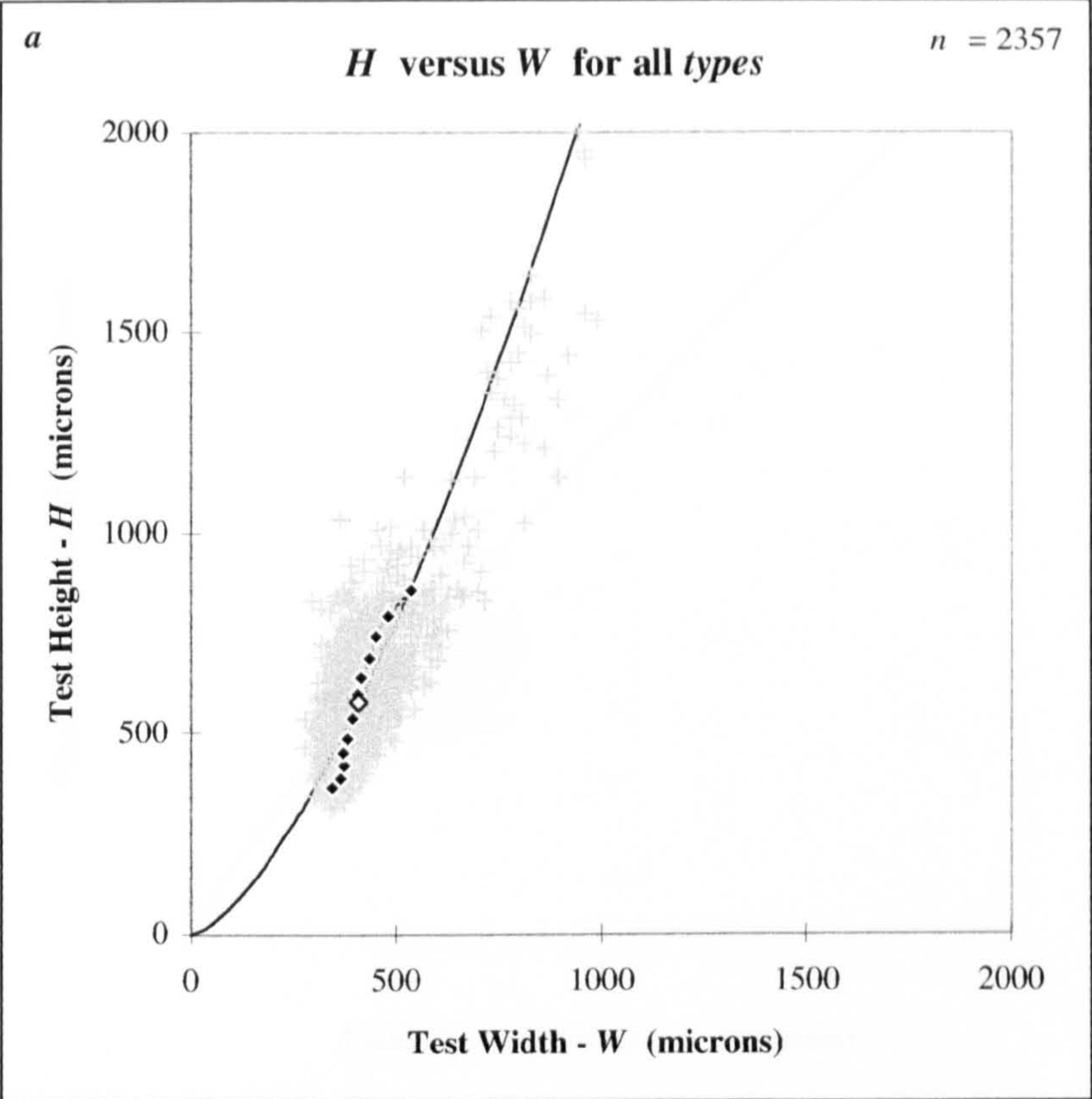
Character	<i>H</i>	<i>W</i>	<i>I</i>	<i>l'</i>	<i>w'</i>	<i>h'</i>	<i>i'</i>
Growth rate	1.081	1.041	1.098	1.037	1.032	1.031	1.044

Text Table 7.2 *Average calculated rates for size increase per chamber during growth.*

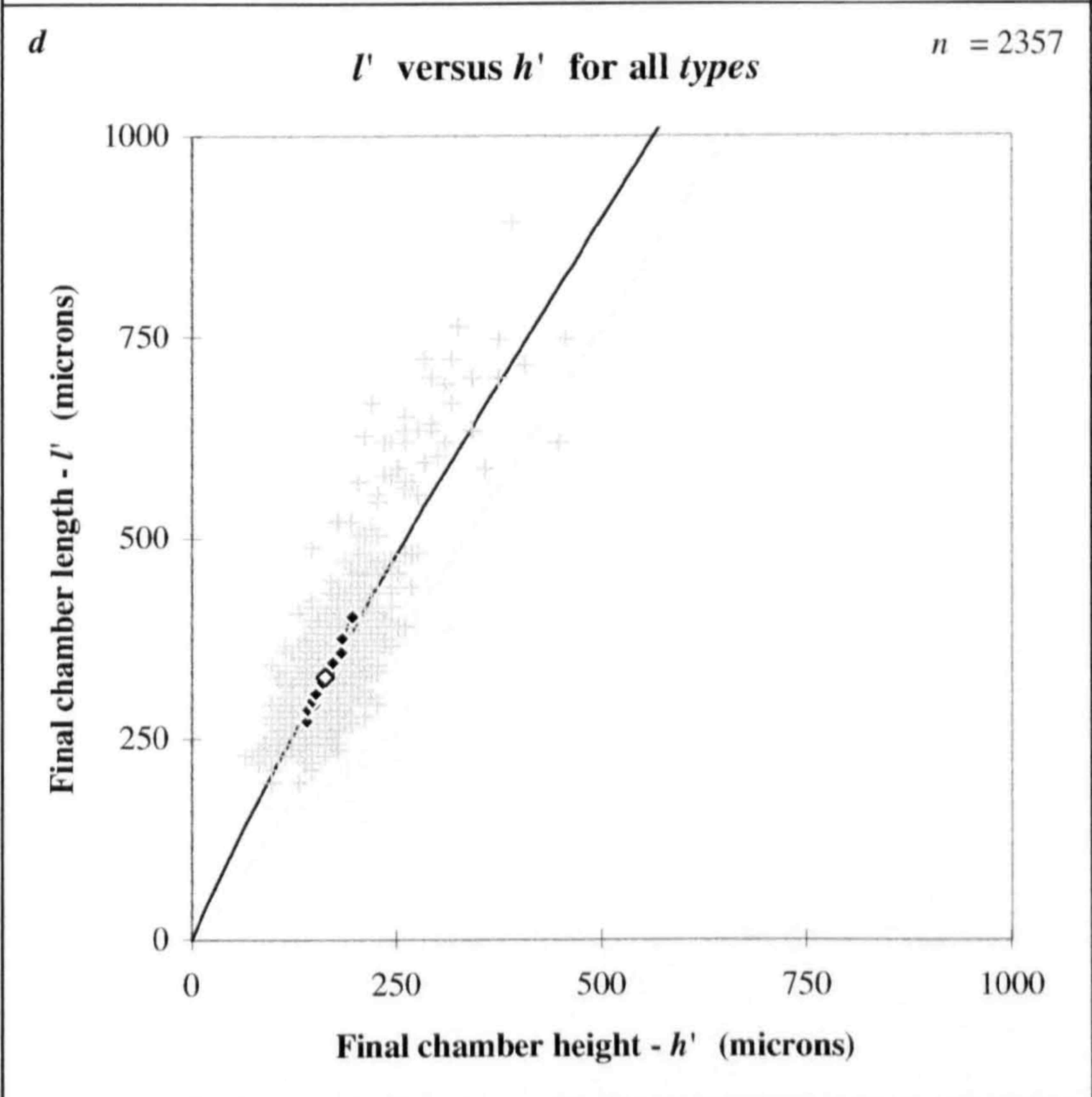
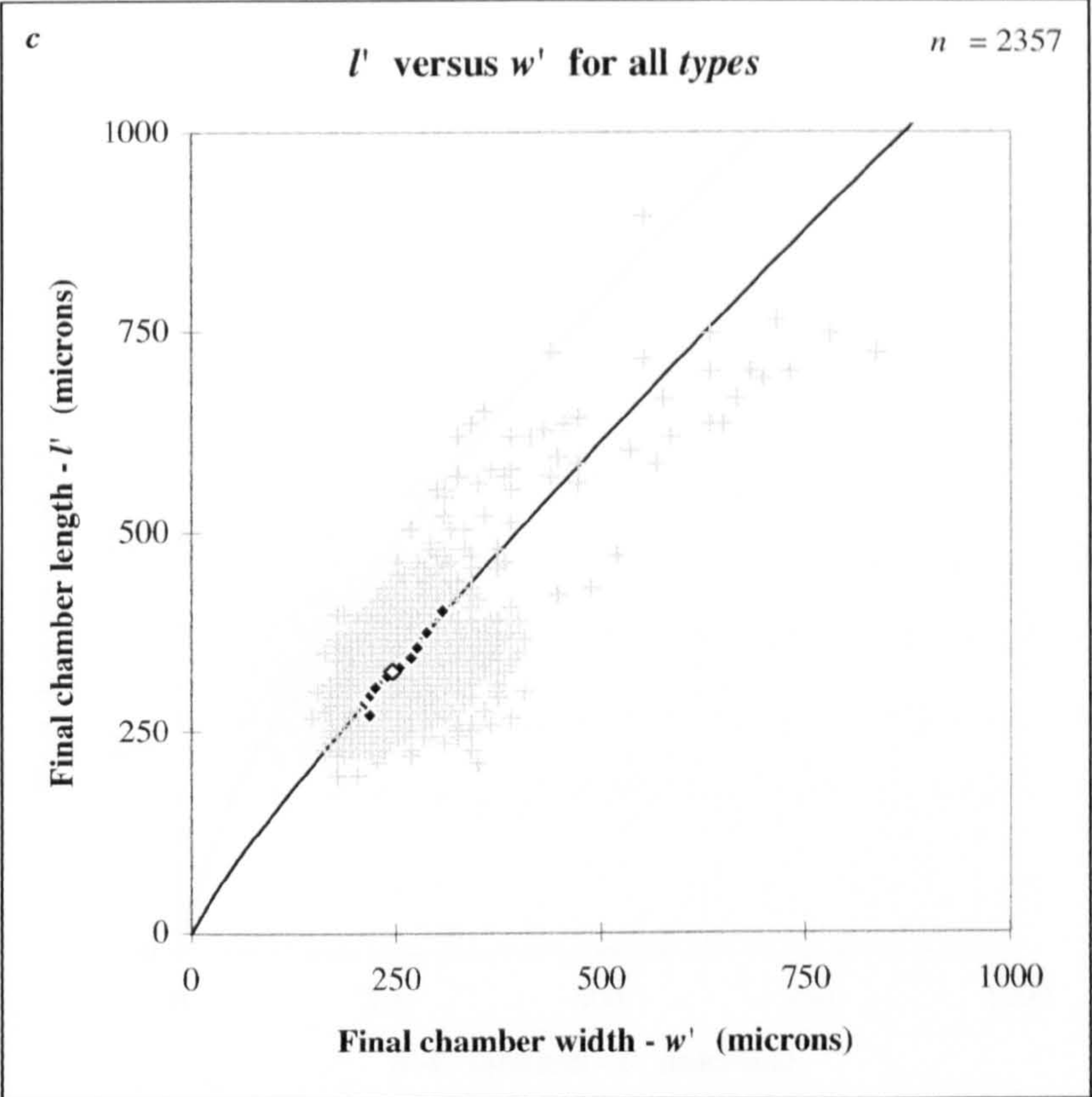
The method conflates the exponential and proportional (*a* and *b*) components of the growth trajectory (see Section 6.2.3), and is only possible because of the discrete nature of the chamber number cohorts; nevertheless, it serves to demonstrate that the growth lines are somewhat curved, whether they look it or not. When average growth rates so calculated are extrapolated from the mean character values for middle-sequence cohort, *Ch* 12, they predict the rest of the profiles very well indeed (Text Figure 7.1.c), a result which would have been impossible had the size shifts varied greatly about the mean or between different stages of growth. There is thus a very regular component to the development of *Tritaxia*.

While different for each character, all the calculated rates are slightly greater than, but very close to, 1. Rates for the three principal final chamber axes, *l'*, *w'* and *h'*, are particularly similar in value, and this is reflected in the developmental stability of their shape ratios (*w'/h'*, *l'/w'* & *l'/h'* in Text Fig. 7.1.b). The positive growth rate suggests that each new chamber, once filled with cytoplasm, must have constituted not only a unit of higher *absolute* economic value than any of its predecessors, but also a slightly higher *relative* value, too. The positive edge, however, is very small, but it is consistent and might conceivably reflect a capitalisation on increasing economies of scale as growth progressed; alternatively it might reflect some reliance on a mathematical principle of the type suggested by Thompson (1917).

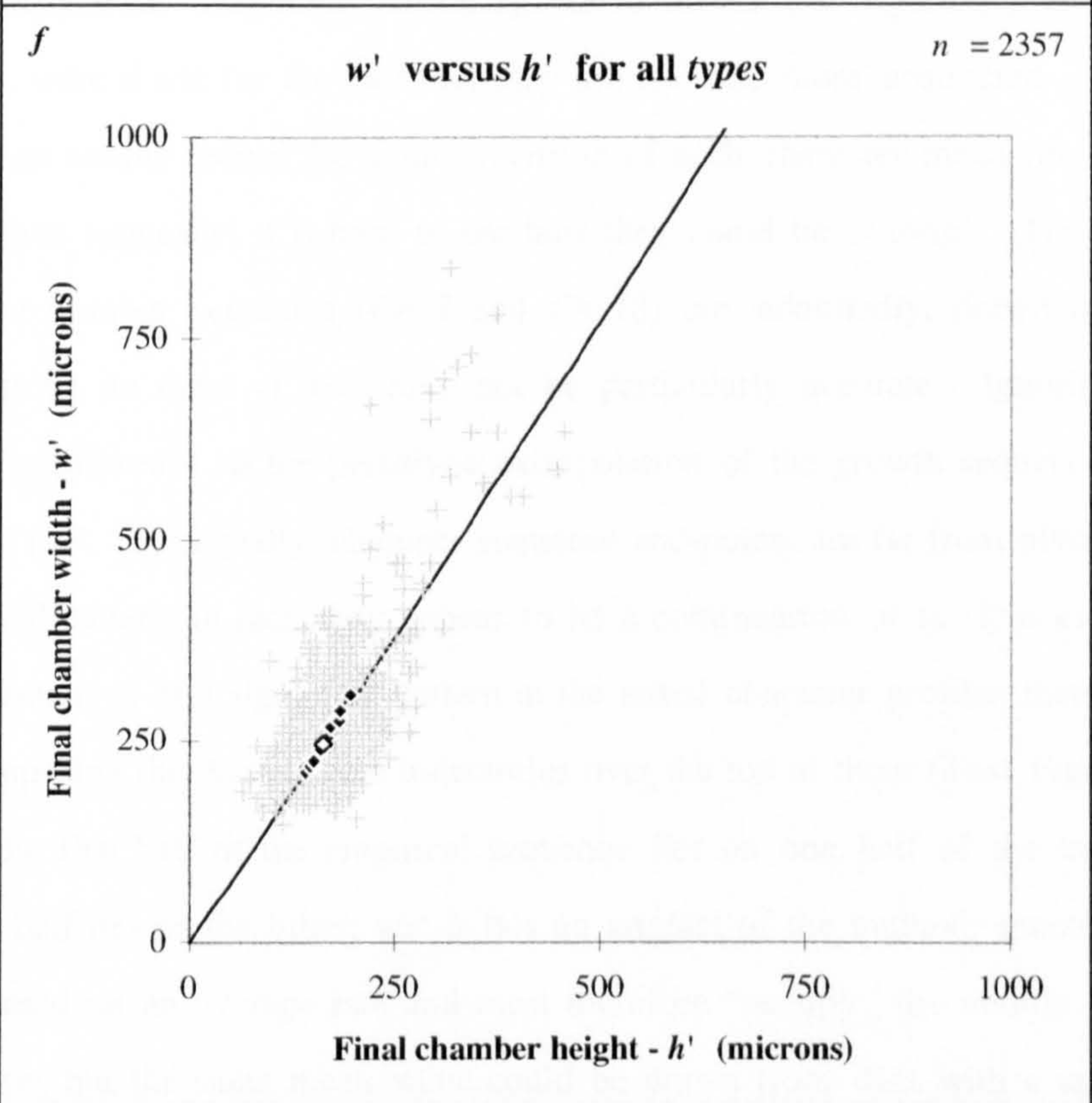
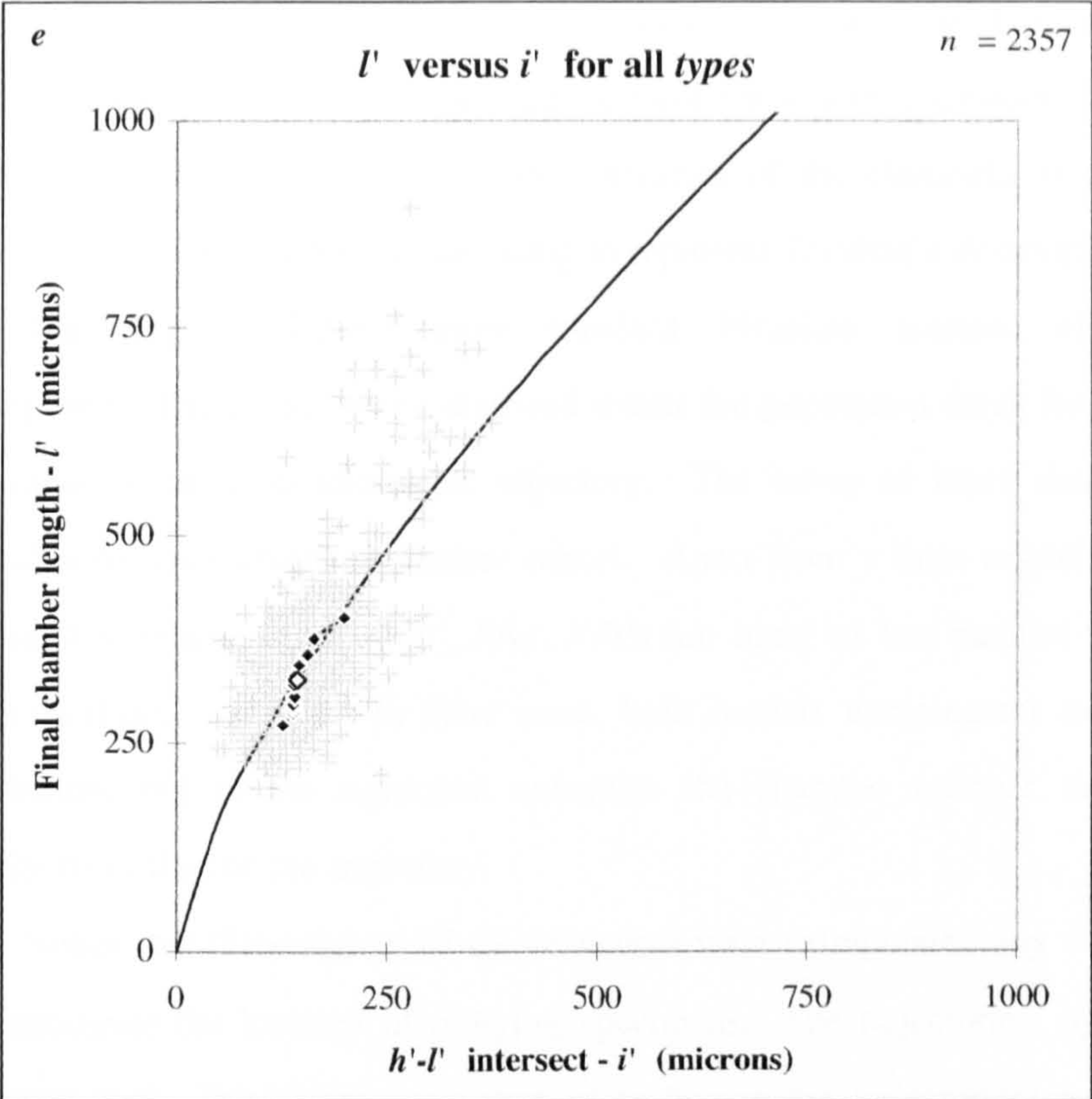
The sigmoidal ratio curves are deeply intriguing. To me they suggest some form of negative feedback or compensation, similar in kind to the ever declining portion of unexploited environment in the case of population growth curves, or the declining density of susceptible hosts in the case of pathogens. According to McKinney and McNamara (1991), such curves are typical of growth relationships between pairs of character variables. The fact that the relationship involves pairs of characters seems to indicate that growth along one morphological dimension is inhibiting growth along the other. The most plausible



Text Figure 7.2 a & b Alternative versions of a lifeline. **a**) *H*/*W*. **b**) *H*/*I*. The curve is a developmental trajectory calculated from the allometric equation; the central white diamond marks the mean of the entire sample population. The string of black diamonds marks the mean values for populations split on the basis of chamber number. The lowermost is for 7 chambers, the uppermost for 18. Individuals with fewer or more chambers are present in the specimen population but are not marked by a diamond because their numbers are too low to provide a robust mean. See text for discussion.



Text Figure 7.2 c & d Alternative versions of a lifeline. **c**) l'/w' . **d**) l'/h' . The curve is a developmental trajectory calculated from the allometric equation; the central white diamond marks the mean of the entire sample population. The string of black diamonds marks the mean values for populations split on the basis of chamber number. The lowermost is for 7 chambers, the uppermost for 18. Individuals with fewer or more chambers are present in the specimen population but are not marked by a diamond because their numbers are too low to provide a robust mean. See text for discussion.

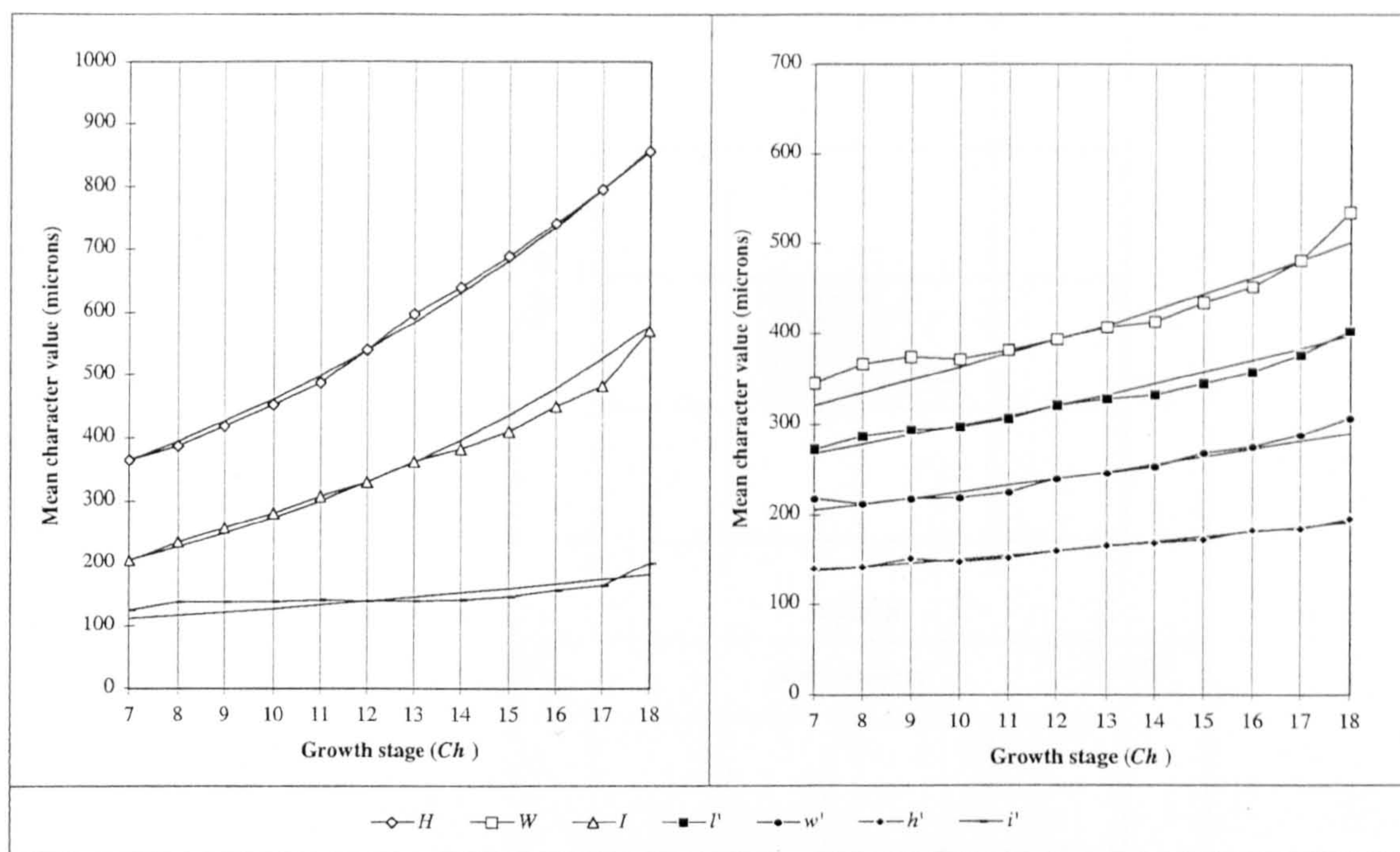


Text Figure 7.2 e & f Alternative versions of a lifeline. *e*) l'/i' . *f*) w'/h' . The curve is a developmental trajectory calculated from the allometric equation; the central white diamond marks the mean of the entire sample population. The string of black diamonds marks the mean values for populations split on the basis of chamber number. The lowermost is for 7 chambers, the uppermost for 18. Individuals with fewer or more chambers are present in the specimen population but are not marked by a diamond because their numbers are too low to provide a robust mean. See text for discussion.

reason I can think of in the case of *Tritaxia* is that there is some kind of elastic effect in the foraminiferal cytoplasm; this will provide the topic for a later discussion (Section 7.4). For now, the important thing is that the extra curvature of the sigmoidal trace marks a major divergence in the two models we are using to represent *Tritaxia*'s development.

Text Figures 7.2.a-f show standard bivariate scatters with both models superimposed. The central white diamond marks the population mean for each pairing, and the continuous curve its allometric trajectory. The string of black diamonds marks the mean value for each chamber number cohort. Apart from a little wobbliness, the principal final chamber relationships (w'/h' , l'/w' , l'/h') run more or less parallel to their allometric trajectories (Figs. c, d & f). In these cases, both models complement each other with no contradiction; but in the sigmoidal examples the chamber number description departs markedly from that of the trajectory.

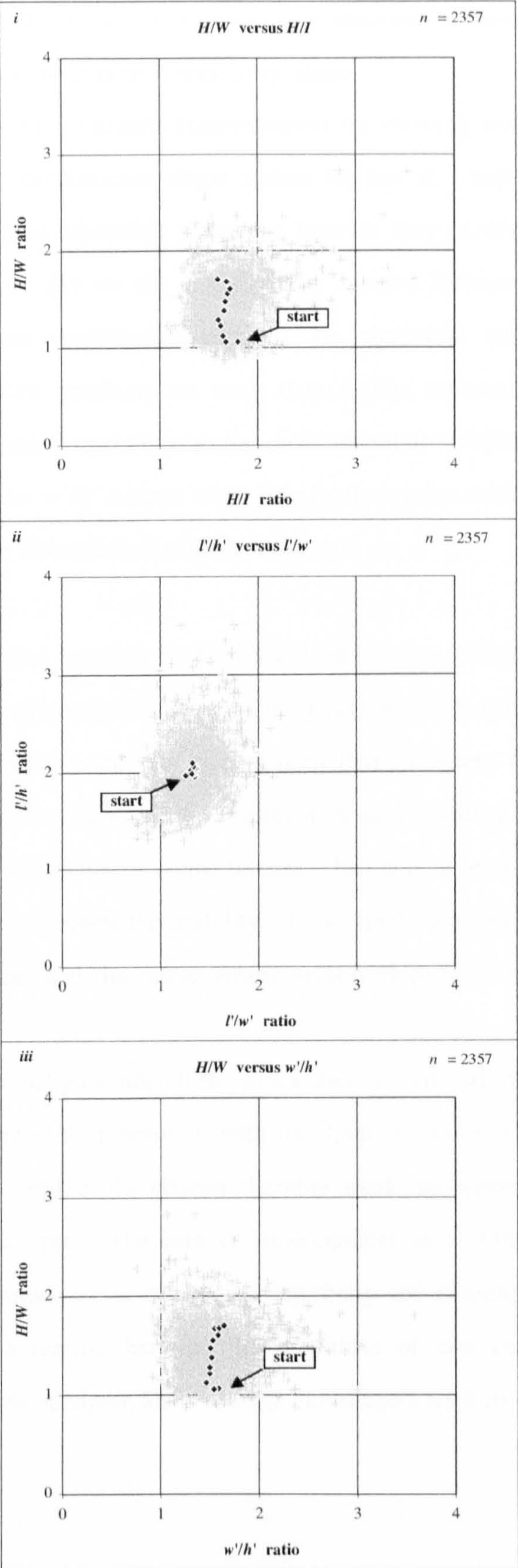
Notice that if the sigmoidal *Ch* sequences were extrapolated any further, they would fail to anticipate the location of outlying specimens. The trajectories, by contrast, predict these fairly well. This might encourage us to favour the trajectories as the more faithful models, were it not for the fact that they are also the more abstracted. Chamber number groupings simply record the *actual location* of each character mean for different stages in the growth sequence; it is hard to see how they could be 'wrong'. The end-points of the chamber number sequence (*Ch* 7 and *Ch* 18) are, admittedly, drawn from small sample populations, so these at least may not be particularly accurate. Ignoring them certainly makes a difference to the perceived extrapolation of the growth sequence, particularly for *H/I* and *l'/i'*. But equally, chamber sequence end-points are far from pivotal in creating the sigmoidal pattern; in fact, they appear to be a continuation of it. It is even possible to see the foundations of a sigmoidal pattern in the initial character profiles themselves, simply by superimposing the derived rate trajectories over the top of them (Text Figure 7.3). In most cases, the first half of the empirical sequence lies on one half of the trajectory while the second half lies on the other; nor is this an artefact of the method: granted, the trajectories were based on an average rate and must therefore 'occupy' the middle of the data series somehow, but the same mean value could be drawn from data with a saw-toothed pattern (indeed, for one character, *h'*, that's how it seems to be). So, although the sigmoidal component is sometimes a little clumsy for individual characters, the fact that it is present at all, and that it is amplified and refined by character combinations instead of simply being stifled, implies that it reflects a genuine regularity in the data set.



Text Figures 7.3 Comparison of empirical data with derived growth rate extrapolation (see Text Figure 7.1 for original versions) in order to highlight the weakly sigmoidal signature present in the basic character profiles. Character profiles have been split into two, non-overlapping groups for clarity. Note the difference in scales.

Should we be worried that despite being a fairly ‘literal’ and underived representation of the growth sequence, the sigmoidal pattern fails to anticipate the outlying specimens, and flat contradicts the allometric trajectory? I hope the answer is no. The *Ch* sequence model was drawn from a limited sample range and simply ignores specimens with more than 18 chambers. By comparison, the trajectories were drawn from the entire population so they are guaranteed to take the outliers into account. But most importantly, the acid-test of prediction is only problematic if we stick rigidly to the idea of continuity. If the mode of growth changes radically and discontinuously at some point between the main bulk of the population and its outer reaches, then any model based solely on the former will fail to anticipate the latter. That wouldn’t make it wrong: it would simply make it inapplicable beyond a certain point.

In any case, this disparity between the two models does not need to be sorted out here and now. The motive for discussing it is mainly to draw attention to the fact that there are two very different ways of organising the data on *Tritaxia*’s developmental sequence. Whether they are more accurate or less, the trajectories will be used in Part IV simply because there are not enough specimens in an individual (horizon-specific) sample population to produce a chamber sequence version. Likewise, whether it is more accurate



Text Figure 7.4 Growth sequence through shape space. Multivariate plots showing mean values for cohorts of equivalent growth stage (Ch) against a background of specimens in the total population. Starts at Ch 7. See text for discussion. Panels *i*) H/W vs H/I ; *ii*) l'/h' vs l'/w' ; *iii*) H/W vs w'/h' .

or less, the chamber sequence model allows us to investigate volumes of morphospace we cannot easily comprehend with a developmental trajectory alone.

Text Figure 7.4 provides an admirable demonstration by showing chamber cohort sequences overlaying the higher dimensional shape spaces we met in Chapter 6. These spaces could not be tackled using an allometric trajectory because they involved too many character dimensions. In H/W vs. H/I we see a spectacular inverse S-shape meandering across the region, evidently some combination between the sigmoidal curves of both bivariate components. l'/h' vs. l'/w' produces no more than a tiny, randomly distributed cluster in the centre of the zone, and is testimony to the developmental stability of the final chamber components. And H/W vs. w'/h' smears what little final chamber malleability there is, out across the whole-test shape dimension in a long, loose coil.

Given that in each case the location of individual specimens defines a roughly circular patch, it is interesting to discover that the growth sequences were sometimes quite linear. This observation will not really come into its own until Part IV where we discuss the difference between changes over the course of development in an individual, and changes over the course of evolutionary history for an entire lineage. But it is at least instructive to note the difference in behaviour between the stability of the final chamber, the twisting convulsion of the whole test shape, and the rather erratic relationship between the pair of them.

This latter, the H/W vs. w'/h' plot, has all the grace and co-ordination of a drunk. Growth lurches forward along the H/W dimension, with the final chamber wobbling back and forth on its own shape axis, until, at the sixteen chamber mark, the system can go no further and appears to simply collapse. The idea of development as a subtle and finely balanced mix of elegance and clumsiness; or of ordered simplicity and complex, disordered catastrophe; or maybe just as a tension between the equilibria of two complementary structural and functional influences (Chapter 5), is exactly the image I wish to encourage.

Section 7.2 Some Bones of Contention

So far we have been working under an implicit assumption that the calcareous structure called *Tritaxia* is all one species, and all one indivisible portion of that species, too. Since I mentioned in Sections 6.1.1 & 6.1.3.i that there is, in the literature at least, a divergence of opinion on this matter, the assumption may seem to be something of a liberty. But in order to answer the question of whether or not these fossils are all of one kind, it was necessary to construct some sort of framework around them; that was the purpose of the Platonic Foram. With the understanding we now have, we are better placed to tackle this issue than anyone has ever been before (and certainly I have never seen anything remotely like a stringent multivariate analysis of *Tritaxia* in the literature).

It is important that we establish whether or not the fossils all (plausibly) belong to a single interbreeding and ecologically moulded lineage, because if not then they might have courted very different selective regimes. There is no point in advancing evolutionary hypotheses to account for 'shifts in morphology' if what we're *really* observing are shifts in the relative abundance of two different species: that would compromise our evolutionary analysis from the very outset.

For an organism like a foraminiferan, there are two ways in which an important biological division might occur: the fossils might actually come from two or more different species, or from two different phases in the lifecycle of a single, unified species.

7.2.i One or More Species?

Contrary to Williams (1992), species *are* units of fundamental biological importance. Like the Platonic Foram, species were originally considered to be fixed types and were therefore defined phenetically, through measurement, for the purposes of classification. Once Darwin had demolished the notion of fixed types, a different and more meaningful identity for species was gradually developed, culminating in Mayr's (1969) seminal definition of them as actively or potentially interbreeding populations, *reproductively isolated* from other such populations.

The benchmark of reproductive isolation applies only to sexual organisms; for an asexual pedigree, each replication (or perhaps each point mutation) is also a kind of speciation event, producing a daughter lineage that will never re-converge with any of its descendent stock. Within the reproductive envelope of a sexual species, genes or gene clusters are the units equivalent to an 'asexual' lineage, so that the species itself forms a kind of higher-order genealogical entity. The important point (and Williams is right this time) is that all such entities can be modelled by a dendrogram; they therefore constitute historically grounded reference points, or agent-centred perspectives, from which changes in the relationship between the lineage and its environment can be judged to be good or bad (Section 5.2.2).

The best evidence that species really do constitute a kind of higher-order genealogical *individual* (Ghiselin, 1974) comes from the fact that sexual species themselves actively maintain their own boundaries, often policing them with a host of finely tuned 'specific mate recognition systems' (Paterson, 1985). The motivation for squandering organisational resources on keyholder-specific security devices is to stem the flow of non-neutral alleles between ecologically specialised populations (Mayr, 1988). Gene sharing with other ecological units is a two way diffusion system and is therefore costly both when 'bad' genes diffuse in, and when 'good' ones diffuse out. The drive to speciation can thus be seen as an attempt to sort all the genes in a gene pool into complementary sets by matching 'common fates' to 'common interests': eventually, genealogies end up split along the lines their ecologies dictate (and see Sections 2.2.2 & 5.2.4 for the role played by resource 'granularity').

This conceptual framework leads us to certain expectations about how species behave over time which are useful to note in the present context. For instance, biologists working with Mayr's biological species definition have discovered so-called 'sibling species', such as the fruit flies *Drosophila pseudoobscura* and *D. persimilis*. Although these taxa are virtually identical morphologically they do not interbreed (and I presume they must be ecologically overlapping — although I've not yet been able to find a source to confirm this — or the discovery would be trivial). But, if they are competing in the same manner for the same resources in the same environment, we expect such individually bounded lineages to eventually diverge ecologically, and thus morphologically (Section 5.5.2), because every environmental resource going into making a *D. pseudoobscura* is (presumably) being poached from a *D. persimilis*, and vice versa.

Our default expectation, therefore, is this: If *any* two lineages are both genealogically separated *and* in ecological competition, we expect them to be unstable in the long term, and destined to either diverge or to drive one another extinct (the same argument holds for the multiple strands of asexual lineages). This was the argument advanced in Section 5.5.2 as the ‘law of competitive exclusion’. And the significance of this way of thinking for fossil morphologies spanning hundreds of millennia is that it leads us to expect them to be morphologically continuous if, and only if, they are also genealogically continuous. Equivalently, if a morphological discontinuity is found, it is taken as evidence of multiple ecological strategy and thus of multiple genealogical identity, unless, as we shall see below, there is some evidence for a life history segregation, such as a larval stage, an alternation of generations, or a sex-specific ecological specialization.

Given the lengthy periods encompassed by palaeontological observation, the non-fixedness of genealogical individuals presents problems of its own. Species (and genes) are, as Hull (1988) concisely put it, ‘genealogical actors playing ecological roles’. But just as the same role can be played by different actors, so, too, the same actor can play different roles at different times. If a genealogical individual is tracking a changing environment, or switching its ecological role, we can expect its morphology to change as well, either fairly continuously in the gradualistic mode, or relatively suddenly and discretely in the saltational one.

For the purposes of statistically bolstering the data-set, and of avoiding any temporal bias in the initial species description, I have deliberately squashed a million year history of *Tritaxia pyramidata* into the timeless morphospace of the Platonic Foram. If there are any evolutionary changes in the lineage they will thus appear in this representation as cases of ‘blurred vision’ if the changes were gradual, or as ‘double vision’ if they were discrete.

There is very little we can do about such issues at this stage. The best we can hope for is a good general picture of *Tritaxia*, and an opportunity to see how much variation there was overall. The evolutionary analysis of Part IV will be the place to sort out long term temporal changes; what we are looking for at this stage is simply dead-giveaway evidence that *Tritaxia* was of more than one type. And the standard method for palaeontologists embarking on this kind of quest is to look for morphological clumping — in one morphological dimension, then in two, then in as many as we can handle.

7.2.ii One or More Generations?

Although foraminiferal lifecycles can be very diverse in character (Section 5.1), there is a ‘classical’ version in which haploid, sexually reproducing ‘A’ stages alternate with diploid, asexual ‘B’ stages. The hallmark of this lifecycle is the division of test morphologies into micro- and megalospheric forms; and, with this in mind, it is not immediately obvious whether *Tritaxia* exhibits an alternation of generations, or not.

Chambers can normally be discerned in well preserved specimens because either the chamber sutures are visible on the outer surface of the test, or because the cavities themselves appear darker due to infilling minerals. There certainly *are* differences in the sizes of initial chambers, but it is not at all evident that these fall into two distinct micro- and megalospheric categories; there are, after all, differences in the sizes of all equivalent-staged chambers. Nor is it possible to apply measurement, as it was for the final chambers, partly because later chambers overlap earlier ones so that the location of suitable measuring points can normally only be guessed at, but also because the entire volume of an initial chamber is close to the finest measuring resolution on the available equipment. In any case, if there is more than one component to the lifecycle, it will have to generate a greater divergence of form than just the size of the proloculus if we are to worry about it having a different ecology. We therefore need to examine disparity among the other characters.

First, let us review the options. A number of explanations could account for the fact that there is no *obvious* alternation of generations appearing in *Tritaxia*. The first is that there really *was* no alternation of generations, as is the case in other foraminiferal species (Lee, 1990). Or it may be that while there *was* an alternation of generations it simply did not manifest itself in any strikingly divergent patterns of test morphology. If either of these is the case, then we are safe to treat the fossil populations as a single kind because neither instance challenges the assumptions of our evolutionary analysis (which are that we are dealing with a single genealogical actor occupying, over biological time spans at least, and no matter how broad, a single, unitary ecological role).

Alternatively, the micro- and megalospheric generations might really be present, but might have developed in such radically different ways that one of them was either small enough to pass through the sieves — in which case it is out of the way and can safely be

ignored — or weird enough to be wrongly classified as another species. Regarding this latter possibility, we have already reviewed the ecological data and know that there is no other form which tracks the patterns of abundance, or occurs in sufficient numbers, to be the counterpart of *Tritaxia* (I noted in Section 4.2.3 that there are other species which basically mirror *Tritaxia*'s patterns of abundance—*Dorothia gradata*, for instance—but this is exactly the opposite of what a counterpart to the observed lifecycle would do, and there is a better ecological explanation for it).

We now have only one option to worry about: that there are non-obvious, but still very real, alternating generations hidden within the data set, and that they will show up as subtle clusterings in morphospace.

Section 7.3 Distribution Through Morphospace

Everyone who partitions *Tritaxia* into different species or sub-species seems to do so on the basis of variations in the growth form of the final chambers (Section 6.1.1). These are the most tangible signs of significant departure from a common morphology. The varieties of late chamber growth *type* were described in Section 6.1.3.i, and they are the features we shall be focusing on next. But regardless of the style of growth exhibited by the final few chambers, all individuals have a triserial portion, so it is sensible to examine *both* the triserial *and* later phases, separately and together, to observe how they relate to one another. To this end, the various morphospaces used to define the Platonic Foram's lifeline were partitioned into paired charts, one showing triserial specimens only and the other showing all *types* together (Appdx. Figs 4.2.1 & 4.3.1).

Note that for the purposes of demonstration, Phase II Character Group 2 individuals (i.e. those which deviate along *l'*) have been collapsed into their complementary categories (i.e. 1.5 has been placed in with *type* 1; 2.5 with *type* 2; and 3.5 with *type* 3). This is purely to simplify the charts and highlight certain patterns; it does not affect any of the conclusions which would be exactly the same if the data were differentiated in maximum detail.

7.3.i Continuity: The Case for A Single Species

Concentrating first on the *triseri*al charts *only*, there are no obvious tendencies towards clumping that would lead us to think that we are dealing with two separate morphological forms. For basic character pairings (Appdx. Figs 4.2.1.i-vi – panel *a* only), the only hint of discontinuity lies *along* the growth trajectory, where it is possible to perceive a main bulk of the population low down, separated by a slight thinning of specimens from a second cluster a little further along. It is even possible to imagine that there is a third series at the very limits of the population, represented only by an outlying specimen or two (e.g. Appdx. Fig. 4.2.1.i.a/Text Figure 6.10). If these are real features — and it is not terribly clear that they are — then they almost certainly reflect a partitioning into specimens from a single summer's growth season versus a few members from the year before. The absolute outliers would then represent a handful of very rare three year old individuals that successfully overwintered twice and made it through to a third summer of growth. Under no circumstances, however, should we regard these clusters as evidence of separate genealogies or ecologies.

Turning next to the higher dimensional shape spaces (Appdx. Figs. 4.3.1), we find here, too, that there is no suspicious clumping among the triserial specimens. Individuals are smeared out over various regions of morphospace, tending to feather further in some directions than in others, but with no striking discontinuities to suggest a separate species. The feathering is intriguing, however. While some regions are densely packed with specimens and quite sharply bounded, others have a more dispersed and ragged look about them. These zones appear to be 'exploratory', hinting that morphospace might not be 'isotropic' but rather has some underlying influence that renders certain directions of shape change more accessible than others. This is a line of argument I shall be pursuing below (Section 7.5).

When we examine the overlay of non-triserial growth types on the companion charts (Appdx. Figs. 4.2.1.i-vi. panel *b*), we find that they *do* exhibit some clumping, but that it always overlaps with the triserial phase beneath. The most clearly developed instances of clumping on the bivariate plots occur along the w' dimension for the pairings l' versus w' and w' versus h' (Appdx. Figs. 4.2.1.iii.b & 4.2.1.vi.b). Given the nature of the *type* categories (Section 6.1.3.i), this is hardly surprising. It is possible to follow the series from

type 1 triserial growth to *type 2* and *3* increases in final chamber width (but not *type 4*, in red, which has a normal final chamber width), and then back into the central triserial zone again for those Phase III additions involving standard chamber widths (i.e. *types 8* and *10*, but not *type 9* which is wider than it should be). In other words, the measurements reflect the *type* categories very clearly indeed (which should give us confidence in the validity of the category designations), but they do so in a way that makes it quite evident that while exotic growth styles shift individuals around in morphospace, they do not separate them entirely from the main triserial stock.

The same pattern of expression can be seen in the higher dimensional shape spaces of l'/h' versus l'/w' and H/W versus w'/h' (Appdx. Figs. 4.3.1.ii.b & 4.3.1.iii.b). As with the bivariate examples, differentiation along with w' axis can clearly be picked out; the specimens are clumped and some of the exotic individuals are exploring portions of shape space that triserial specimens do not reach—but *there is always an overlap*. Despite the element of exploration, many of the growth types classified as exotic still occupy the same regions of shape space that characterise their purely triserial counterparts.

Finally, the whole test parameters (H/W vs. H/I) demonstrate the relationship between triserial and exotic growth phases even more clearly: it is one of continuation, not separation. The H versus W *bivariate* plot (Appdx. Fig. 4.2.1.i.b) reveals a sequence of transformations in which triserial Phase I gives way to Phase II, which in turn is capped by Phase III, as growth proceeds from shape ratios of 1:1 to 1:1.3 then 1:2. H versus I provides a similar, if messier, picture (Appdx. Fig. 4.2.1.ii.b); and the combined input of all three whole test parameters (H , W & I) gives us a diagonally expanding sequence of zones in the H/W versus H/I plot (Appdx. Fig. 4.3.1.i.b). (Note, incidentally, that in H/W vs. H/I and H/W vs. w'/h' the exotic growth types are chiefly responsible for spilling specimens into those zones of whole-test morphospace characterised by feathered edging of the triserial portion; but also note that this is not the case for the final chamber parameters, l'/h' vs. l'/w').

Given the continuity in morphological expression we find both within and between the triserial and non-triserial growth types, I find it hard to justify splitting the data set into fundamentally separate units. It may well be that there are hidden clusters in more inclusive regions of morphospace, but it seems insufficiently likely to merit further investigation (it

would involve us trying to understand multidimensional plots like $((H/W)/(H/I))/((l'/h')/(l'/w'))$; or, worse, a version that included *all* the characters at once).

Despite the intuitions of various authors (Section 6.1.1), therefore, it seems that exotic growth types do not partition the population into discrete, species-like clumps after all. So what about the other categorical variables? Here the situation is less clear-cut because categorical data are clumpy by their very nature. To illustrate the point, consider coiling direction (*chir*). We have two complementary morphological clusters splitting the population clean in two: might we be dealing with a pair of equally abundant species, or could this be the long anticipated alternation of generations? To be fair, it *could* be either; but to be honest, it's more likely to be neither. There is no reason whatever to suppose that these twin categories represent anything other than a geometric constraint (i.e. the fact that there only *are* two alternative coiling directions) with no selective advantage to either side: *Tritaxia* has to coil in one direction or another, it simply isn't fussy about which it is. (In fact, this simplifies the situation somewhat; I suspect that coiling direction might involve a certain selective component, but this will be explained in Section 7.5 below).

Next, consider glauconite distribution (*g.dist*). We already know from Section 6.2.2.iii that most of the categorical features are associated with *Ch* and are therefore likely to form clusters simply because of co-ordinated category transitions during the course of development; we also know that the main exception to this rule is *g.dist*. *g.dist* does not correlate well with *Ch*, nor does it have a linear relationship with any of the other characters, apart (apparently and mysteriously) from twist (*tw*). There are at least two good reasons for its lack of correlation with growth. Firstly, *g.dist* does not have any kind of ranking to its categories (i.e. there is no sense in which *g.dist* 1 is 'less' than *g.dist* 2, 3, 4 or 5); and, also, since the glauconite appears to be woven right into the agglutinated fabric of the test, it is hard to see how that distribution could be modified throughout growth.

Now, this latter reason is clearly an argument for discrete developmental form: tritaxiid specimens can be *either g.dist* 1, *or g.dist* 5 etc., but not more than one at a time, or more than one over the course of a single lifecycle. Could it also be an argument for multiple species? Well, as with the coiling direction, I suppose it *could*: each category *might* conceivably represent a separate lineage. But since the categories appear to cross-cut every other character designation, from *Ch* through to *type*, and since the metric data exhibits no discrete clumping at all, I remain totally unconvinced. It might possibly be that each *g.dist*

category reflects an individual gene lineage, so that glauconite distribution is a kind of foraminiferal equivalent to eye-colour; but that is not grounds for a species level designation. I think the case for splitting the data base along *g.dist* categorical boundaries is totally uninspiring.

Since all the other categorical features are linked to growth (*Ch*), and thus appear to change during the course of development, they are not likely to reflect multi-species clumping either. As with the continuous variables, therefore, the categorical characters also point to a single unified form for *Tritaxia*.

The only really outstanding issue is whether or not there was an element of gradualistic change present in the lineage, one that would smear the form of *Tritaxia* into anagenetically segregated chronospecies. Since we cannot answer that question without dividing the data set into a temporal sequence, and since that is exactly what we shall be doing in Part IV, our task here is done. At the very least, we know from the outset that there is no obvious case of multiple clades, and that we therefore appear to be dealing with a single coherent lineage — a unified ‘genealogical perspective’ — just as the *Plus ça change* model demands.

7.3.ii Discontinuity: The Case for Teratism

If exotic chamber formation is not the hallmark of a separate lineage, then what is it? It is remarkable enough to deserve a mention in the *Treatise* (as *Tritaxia*’s diagnostic ‘adventitious final chambers’; see Section 6.1.1), and various workers have used it to support their favoured level of taxonomic designation. Exotic development must surely have occurred for a reason.

According to the morphospace plots, we appear to be dealing with something that is more a continuation of the standard triserial mode than a fundamentally novel phenomenon. Perhaps exotic growth is a perfectly normal facet of *Tritaxia*’s developmental sequence: just another phase in the unfolding plan. But, if so, why don’t *all* individuals past a certain growth stage exhibit non-triserial development? Why do so many of them continue to grow triserially until they are several times the size of an average exotic specimen?

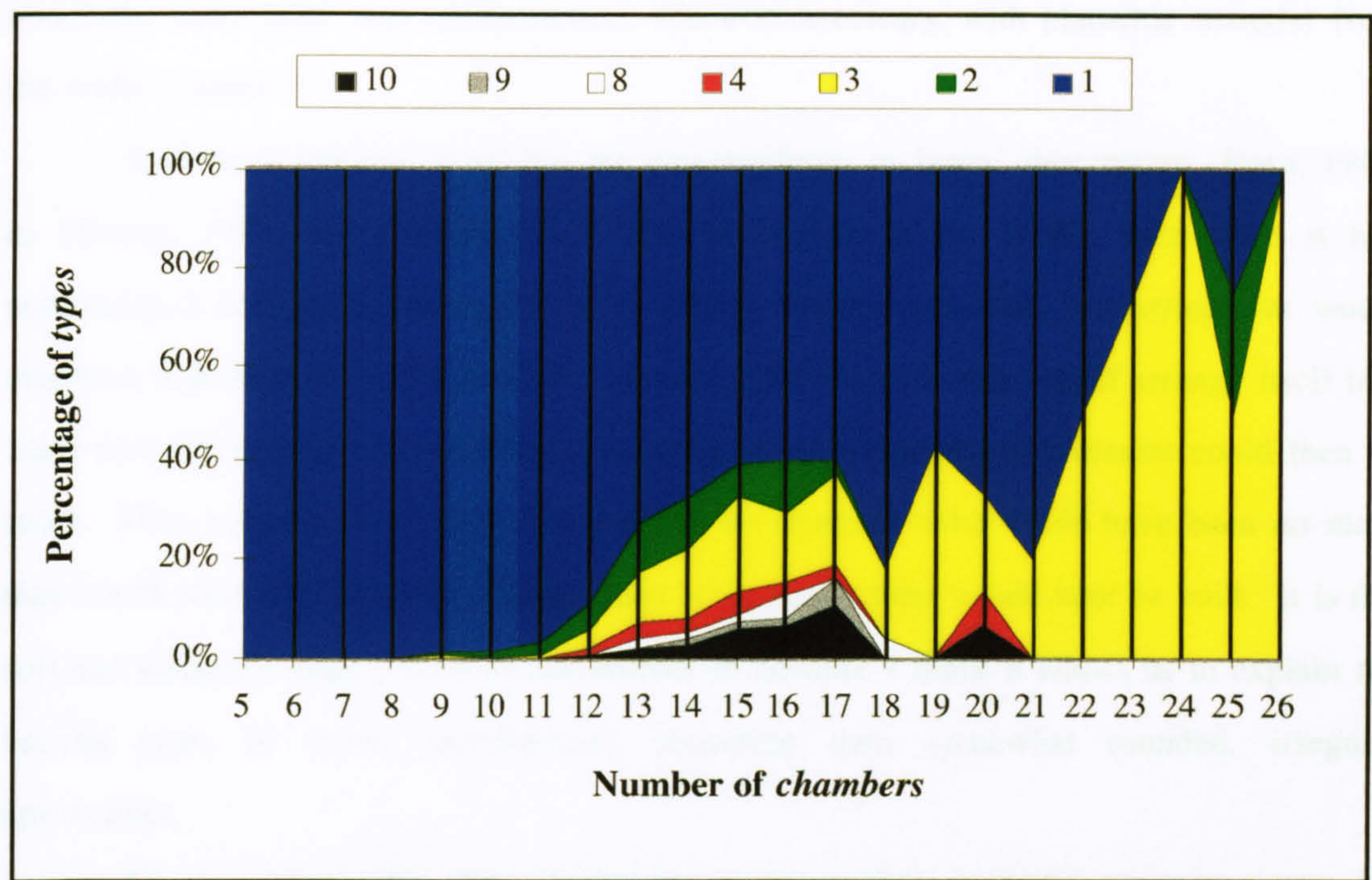
Perhaps the switch in developmental styles is a response to some novel situation or stimulus, the realisation of perfect breeding conditions, for example, rather than an expression of internally calibrated developmental control. Did a particular environmental prompt induce *Tritaxia* to enter a phase of non-triserial growth? If so, what was its purpose? And why did growth terminate after producing a single deviant chamber in some individuals but continue on for a small proportion of others?

One peculiar and striking feature of the exotic specimens is how shoddy they look. Whereas triserial individuals are generally well-proportioned and straight, those which terminate in exotic chambers are often bent and twisted. Apart from the pyramid-shaped *type 3* specimens (Jefferies' *pyramidata*, or *type 6* in Appdx. Tabs. 2.1 – 2.3), which are unusual in having neat, angular edges to their terminal cap, most of the chambers formed by exotic growth have a strangely irregular appearance, generally being humped or rounded or at odd angles to the rest of the structure. The sense of aesthetic discord associated with these exotic growth phases prompts me to think of them as poorly designed — and certainly they are far less regular than the normal triserial phase, as their broader occupancy of morphospace demonstrates (Appdx. Figs. 4.2.1 & 4.3.1).

However, the most enlightening piece of evidence concerning non-triserial growth comes from examining its relationship to growth stage. Deviation from the triserial path rarely arises in early development, but becomes ever more common as growth proceeds (Text Fig. 7.5 - overleaf). Nor does the switch come suddenly upon reaching a particular growth stage, as one might expect of a pre-set sequence; rather it appears to become increasingly likely, but by no means guaranteed, past a certain point. That point happens to be close to the average number of chambers. At stage 11 just 3.4% of specimens show some exotic development; by stage 12 the number has more than tripled to 11.7%, and by stage 13 it has doubled again to 27.6%! If we take the average chamber number (median 12, mean 12.5) to reflect the growth stage an individual expects to achieve, and suppose that it was in an individual's interests to reproduce at or before that stage, then we have an interesting reference point: we find that there is very little incidence of exotic development *before* the average reproductive age, but an ever increasing amount thereafter.

Now it is entirely possible that such a change in growth styles was associated with reproduction itself, in which case we have a tag on the proportion of any population reaching reproductive maturity, and the stage at which they did so. But it is also possible that the association of non-triserial growth with increasing age represents something very

different. The classic explanation for progressive degeneration and death by age-related disorders is that genes with an early deleterious effect are cleared from the gene pool by selection, whereas those with expressions later than the onset of maturity tend to accumulate behind a *reproductive barrier* (Medawar, 1952, in Ridley, 1997); such genes are invisible to



Text Figure 7.5 *The relationship between growth type and chamber number. Sample sizes are low after 18 chambers but the trend is clear enough, despite an erratic signal later on.*

selection because they are normally passed on before having an opportunity to be expressed. Cancers are the exemplar for us metazoans and clearly do not apply to a single-celled foraminiferan; but other variations in the developmental sequence may well do. And this casts exotic growth patterns in a new light: as construction mistakes — teratisms — rather than the ultimate products of an unfolding plan.

Section 7.4 A Mechanism For Chamber Formation

In fact, viewing non-triserial development as error rather than design helps tie together a whole range of observations, including the ‘shoddy’ appearance of the (now aptly termed) ‘adventitious’ chambers. We expect the form of *Tritaxia* to be a developmental product of genetic and environmentally encoded information, working

through the fabricational constraints of the medium in which it is expressed. What I am ideally trying to do in this part of the thesis is to tease apart these various influences.

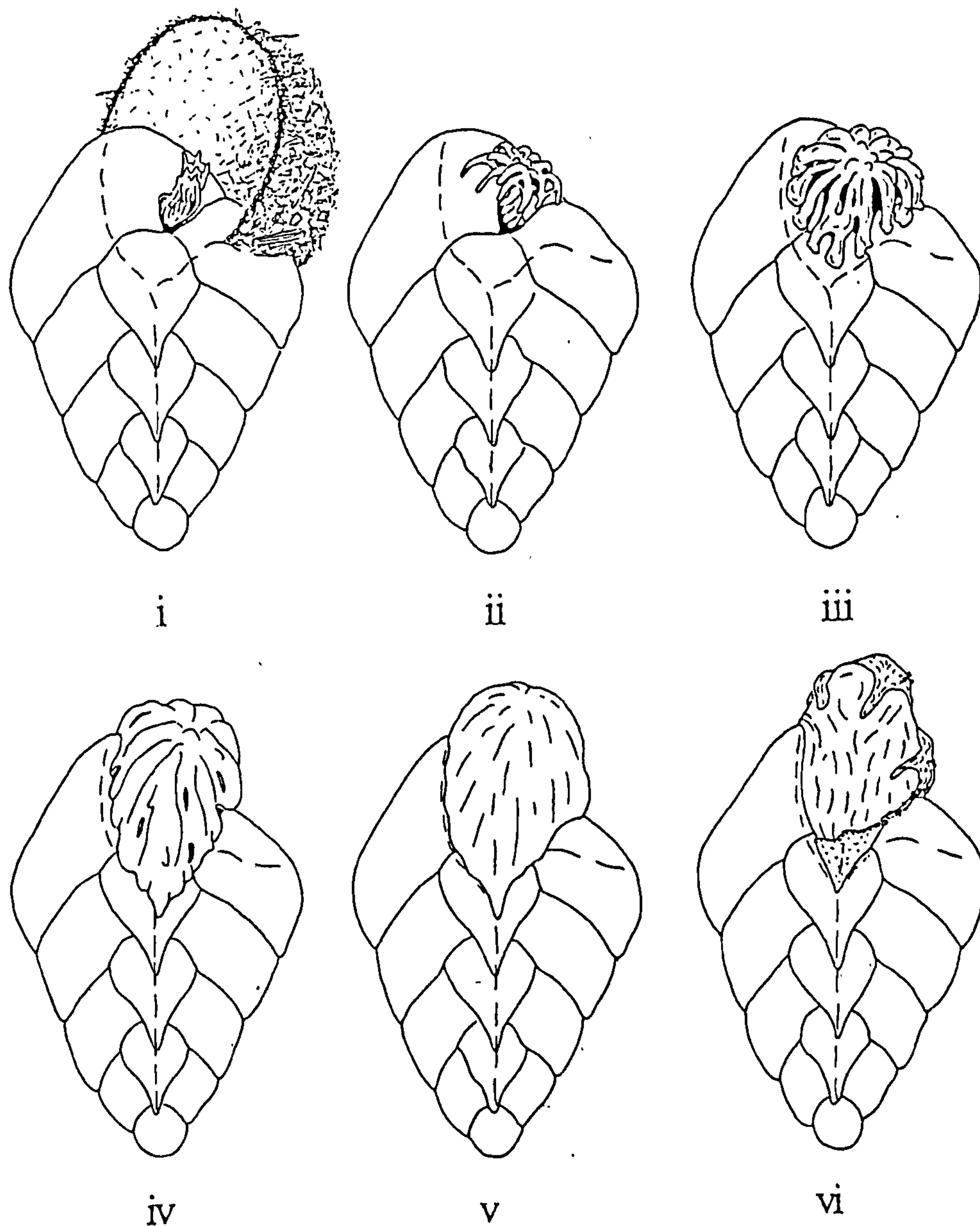
The only way to proceed from here is boldly. Let us consider a constructional '*Just So* story' about *Tritaxia*'s developmental process, cobbled together from what we know about the fossil itself, and supplemented, wherever necessary, with plausible material from the wider literature.

If *Tritaxia* behaved at all like the foraminiferan in Jepps' description (Jepps, 1942, in Murray, 1981; see Section 5.1.4; also Hemleben et al., 1989), then once it had accumulated enough resources to justify adding another chamber, the cytoplasm would construct a protective cyst around the aperture, and inside of this would arrange itself into some sort of template with a suitable configuration, on which bits of sediment could then be stuck. Thus, early in the construction process, the chamber-to-be would have been no more than a soft mass of cytoplasm around which something harder would later be built. It is this soft and malleable stage I want to concentrate on because I think it allows us to explain the various types of exotic development, including their somewhat rounded, irregular appearance.

Let us imagine that this cytoplasmic mould initially had the properties typically found in animal cells (Gilbert, 1997; Ingber, 1998*a*, 1998*b*), being dominated by the cytoplasmic skeleton's quasi-rigid internal structure and balanced by the tension of a stretched cell membrane, this latter being partly caused by adhesive contact between the membrane and its surroundings. Now *Tritaxia* must have had *some* way of 'knowing' what shape to build its next chamber, and my suggestion is that the cytoplasmic template took its cues from what it considered to be 'the environment' inasmuch as the shape of previous chambers provided crucial input on how to build the next.

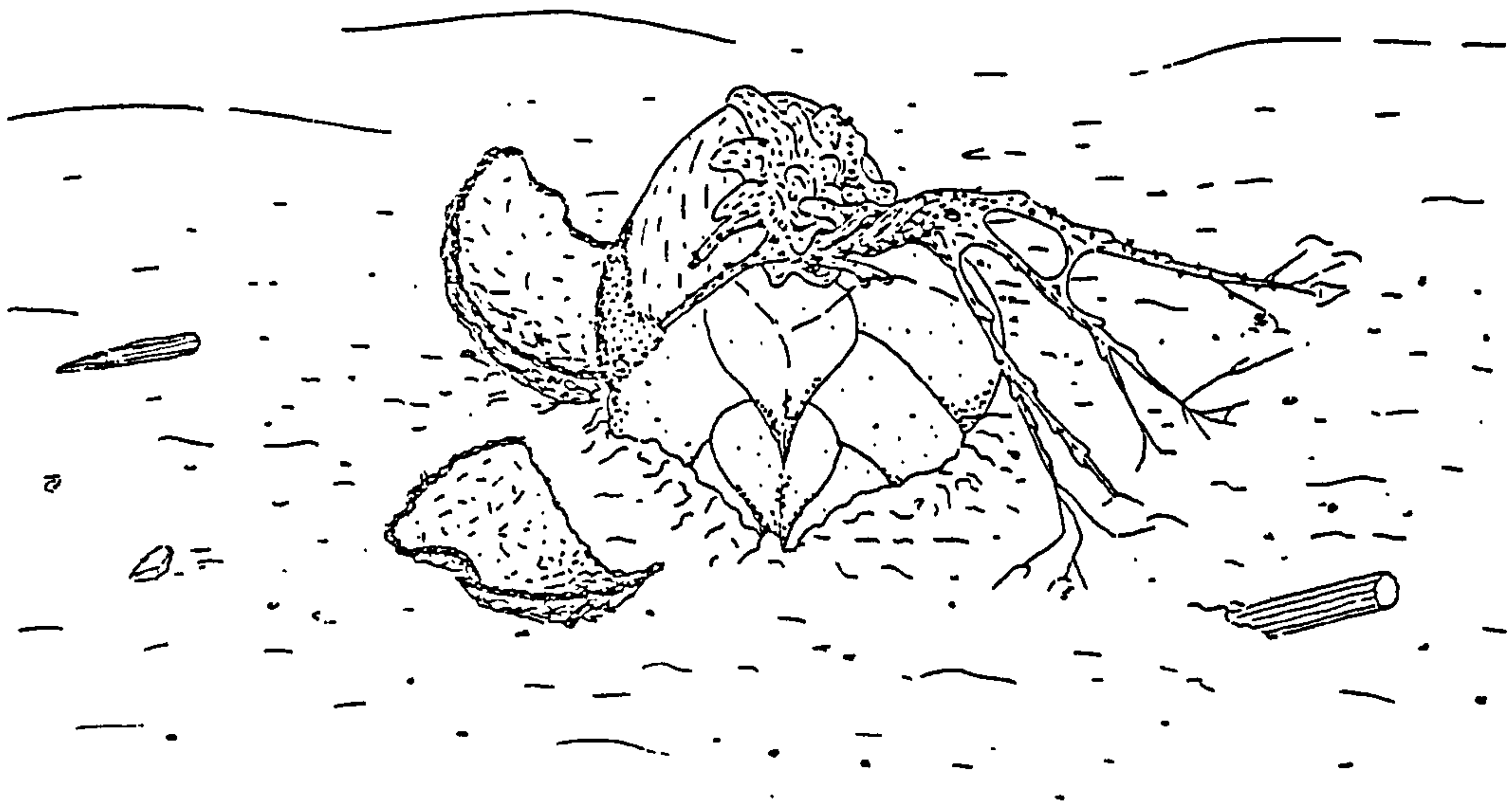
I envisage this process proceeding somewhat like the erection of a tent (Text Figure 7.6) but with a cytoskeleton of growing microtubules instead of poles. First, cytoplasm extrudes from the aperture to form a hemispherical blob, supported internally by a radiating mass of growing microtubules. Adhesive properties glue the membrane to the pre-existing test surfaces, aligning it to the sutures of adjacent chambers; this produces sufficient counter-pressure to stop the tubules growing and extending in certain directions, specifically, limiting expansion in the *w*' direction. Next, the long (*l*') axis of the template is extended and glued as far down the carinate edge of the test as it can reach, stretching the

basal surface and leaving the only remaining direction of tubule growth along the h' axis. Extension along h' then pulls the membrane taut and gives it some sharper edges (Text Fig. 7.6). Hey presto! The cytoplasm of the new template takes on the asymmetric pyramid



Text Figure 7.6 Chamber formation in *Tritaxia*:

- i) within the confines of a protective cyst (shown only in the first figure);
 - ii) "...an unusually dense, fan-shaped mass of anastomosing pseudopodia make their appearance..."
 - iii) "...which arch into a reticulum, outlining the cavity of the future chamber..."
 - iv) "...gradually swell at their bases and merge..."
 - v) "...whilst a fluid wells out amongst them and comes to fill up the space..."
 - vi) "...as soon as the surface is available a collection of shining granules [calcuim carbonate crystals] appear..." (in *Tritaxia* sediment grains would be imported by the ectoplasm, shown here as the different textured material carrying grains, and arranged on this new template to form an agglutinated wall). See also Text Figure 7.7.
- Quoted from Jepps (1942 – in Haynes, 1981).



Text Figure 7.7 *Reconstruction of Tritaxia pyramidata, half buried and amid the fragments of a prematurely removed cyst, its ectoplasm groping for sediment grains to arrange on the template of a new chamber. Note that in this species the choice of grains was not arbitrary but involved a capacity to select both within a certain range of sizes and compositions, and also to arrange these selectively on specific parts of the test. Despite the hypothesised economy of organisation in forming the final chamber template, the cell was clearly capable of processing an impressive amount of environmental information.*

shape of previous chambers, and its basal area, being set by the adjacent chamber sutures themselves, fits snugly into place with the minimum amount of 'internal' genetic specification. Once the membrane is stiff enough to support sediment grains the chamber wall can be built, and later glazed over to smooth it in with the rest of the test (Text Figure 7.7).

If the reasons for proposing this model seem obscure then consider how *you* would put up a pyramid-shaped tent if you had to do it all from the inside, by touch alone. The rules of this game are that there is no 'overview', so you are effectively blind and have to do everything using only environmental feedback. You begin, draped in your flysheet, from a position situated in the V-shaped space between two already erected neighbouring tents (the most recently erected one of which you've just come out of). You know there's an allotted space for you, you just don't know where it is yet. So you begin by pegging a corner of your own flysheet to the most obvious reference point you can find, the inner angle of the V at the intersection of the two adjacent tents (for *Tritaxia* this is the central pivot of the coiling axis). After that, you crawl around in the dark, pushing out the edges of your groundsheet until they meet resistance from the tents to either side. Only having pegged out all the available edges of the V are you then safe to pull the groundsheet as far

as possible down the diagonal axis, away from the initial peg, and to erect the central pole until the flysheet is taut.

I should make it very clear that there is no direct observational evidence to link *Tritaxia* with the chamber template forming process exactly as described, but it is well in keeping with both Jepps' description of *Elphidium* plus Ingber's architectural 'tensegrity' models, and it accounts for the non-triserial growth patterns very well. By using it we can explain Phase II Group 1 individuals as having failed to find the right environmental cues for how far to press their lateral extent, w' (i.e. having failed to identify the edge of an adjacent tent), thus spreading too far, sometimes by a little (*type 2*), sometimes by a lot (*type 3*) (Text Fig. 6.5). Exploiting the elastic nature of the cytoplasm-membrane relationship (the flysheet and pegs), we also have an explanation for Phase II Group 2 development by concluding that adhesion has been overwhelmed by tension so that the cytoplasm has sprung back from the leading edge of the long chamber axis, l' , which should be glued to the carinate corner instead (i.e. the furthestmost diagonal peg came out when the central pole went up), either early enough to allow more lateral spread than there should be (*types 2.5 & 3.5*), or, later, once lateral expansion had halted and the only way to take up the slack was vertically (*type 1.5*) (Text Fig. 6.6). Phase III individuals are explained by appealing to the ongoing reliance on local markers: having lost its way once, the building process is poorly placed to find the right cues thereafter and just continues to heap error upon error (Text Fig. 6.7).

These are only suggestions and are not intended to be conclusive; but they do at least engage the data at what seems to be a useful level of explanation. If we are looking for some way of understanding the processes which give rise to a range of protozoan test shapes, then a mechanistic account, based on the execution of locally generated rules and involving the ubiquitous biochemicals of cytoskeleton and membrane, is just the ticket. If it seemed surprising that a single cell could 'know' how to build a delicately tuned structure like a test, then this account is satisfying precisely *because* it requires a minimum of knowledge. All the cell needs to know is how much cytoplasm to extrude, how thick a bundle of microtubules to erect, how much adhesive to use; all the rest is relegated to the pre-formed structure of the test itself. The test, if you like, becomes its own encoding structure; the DNA 'knows' very little about it, or very little in any explicit form.

Of course, all this is reliant on the DNA orchestrating a system that starts off on the right foot in the first place, and which thus 'knows' how to exploit the information already

encoded in a partially built test. But it gives some ground to a structural account without falling back on the all-too-frequent hand-waving rhetoric of ‘emergence’ and ‘order for free’. More importantly, it allows us to see how evolution might be ‘channelled’ through biases in these developmental tendencies.

Section 7.5 The Fabric of Morphospace

To tie together all that has been discussed in Part III, I want to sketch a vision of *Tritaxia*’s developmental trajectory through morphospace, including not only what happens when things go right, but also what happens when things go wrong. As with the account above, it will be something of a *Just So* story because short of direct experimentation with modern specimens there really is no way to be sure about all the factors involved. Even so, we have enough material to tell a good tale without resorting to wholesale Kiplingesque fantasy.

First, let us start at the speculative end with some more biochemical fancies, just to demonstrate that there are plausible low-level mechanisms available to account for the kinds of larger scale pattern we are really interested in.

Consider, for instance, the following potential connection between the process of chamber formation as described, the exotic growth patterns, and two other categorical features, *twist* and *chirality*. In most triserial specimens, each chamber sits directly above a chamber three chambers back, such that the test is arranged in layers (whorls) of three vertical columns. In twisted specimens, however, there is an offset so that vertically aligned chambers are roughly in place but do not sit quite so perfectly above one another as they should. With regards to chirality, *Tritaxia* is split fairly evenly into sinistral and dextrally coiling forms. Regrettably, I do not know what the relationship between twist and coiling direction is; specifically, I took no measurements of whether or not when a twist occurred, it occurred in the *same direction* as the coiling direction, although it would be very useful if I had.

We do know, however, from the χ^2 tests, that there is a non-random association between final chamber *type* and *twist*. It strikes me that according to the kind of reasoning used above, highly twisted specimens might be *much more likely* to lose their way during

development, and thus to extend a chamber too far (or not far enough) in the direction they are coiling. If so, twist, coiling direction and exotic chamber formation may be very closely linked.

The tent analogy used above is fine as far as it goes, but the components of a cell are not rigid poles and tough sheets; rather, they are unwieldy, bendy cytoskeletons, stretchy, sticky membranes and viscous cytoplasmic jelly: in other words, the kinds of unruly materials which could easily misbehave. As it happens, the microtubules of cytoskeletons are themselves composed of spiralling protein sub-units and so, like the helix of *Tritaxia*'s test itself, they also come in sinistral and dextral forms. It is therefore possible to imagine that what keeps an unruly tritaxiid developmental sequence in regular spiral form is an almost perfect mixture of sinistral and dextral microtubules in its cytoskeleton scaffolding. Slight initial imbalances may be responsible for setting the spiral off in one direction or another; but, because of the evenness of the mix, overall growth is generally straight, so that successive chamber columns more or less line up. Larger imbalances, however, might skew successive chambers somewhat and be amplified by the process of cumulative stacking, tainting the form of the entire test and eventually leading to exotic chamber formation of a Phase II Group 1 type (i.e. *types* 2, 3 or 4). (And, since I don't have much relevant evidence at this stage, let me pay my dues to the scientific method by turning this *Just So* story into an empirical hypothesis: if the model is correct, it *predicts* a correspondence between the coiling direction and the direction of twist.)

The point of indulging in this much imagination is not to speculate about *what really was* the case for *Tritaxia*, but simply to illustrate *how something could be*. The broad point is that it explains triserial growth as a 'boxed-in' phenomenon. An almost (but never quite) perfect 50:50 mix of sinistral and dextral microtubules ensures good triserial growth. But more substantial deviation in either of *only two possible directions* (i.e. more sinistral or more dextral) leads inevitably to the same result: the test begins to twist, and before long it is out of kilter and has flipped from triserial to non-triserial growth patterns (see Text Figure 7.8 below for a graphic explanation). Because the initial error amplifies with each new chamber addition, this is precisely the kind of 'sensitive dependence on initial conditions' that chaos and complexity theorists, and structural biologists alike, generally welcome.

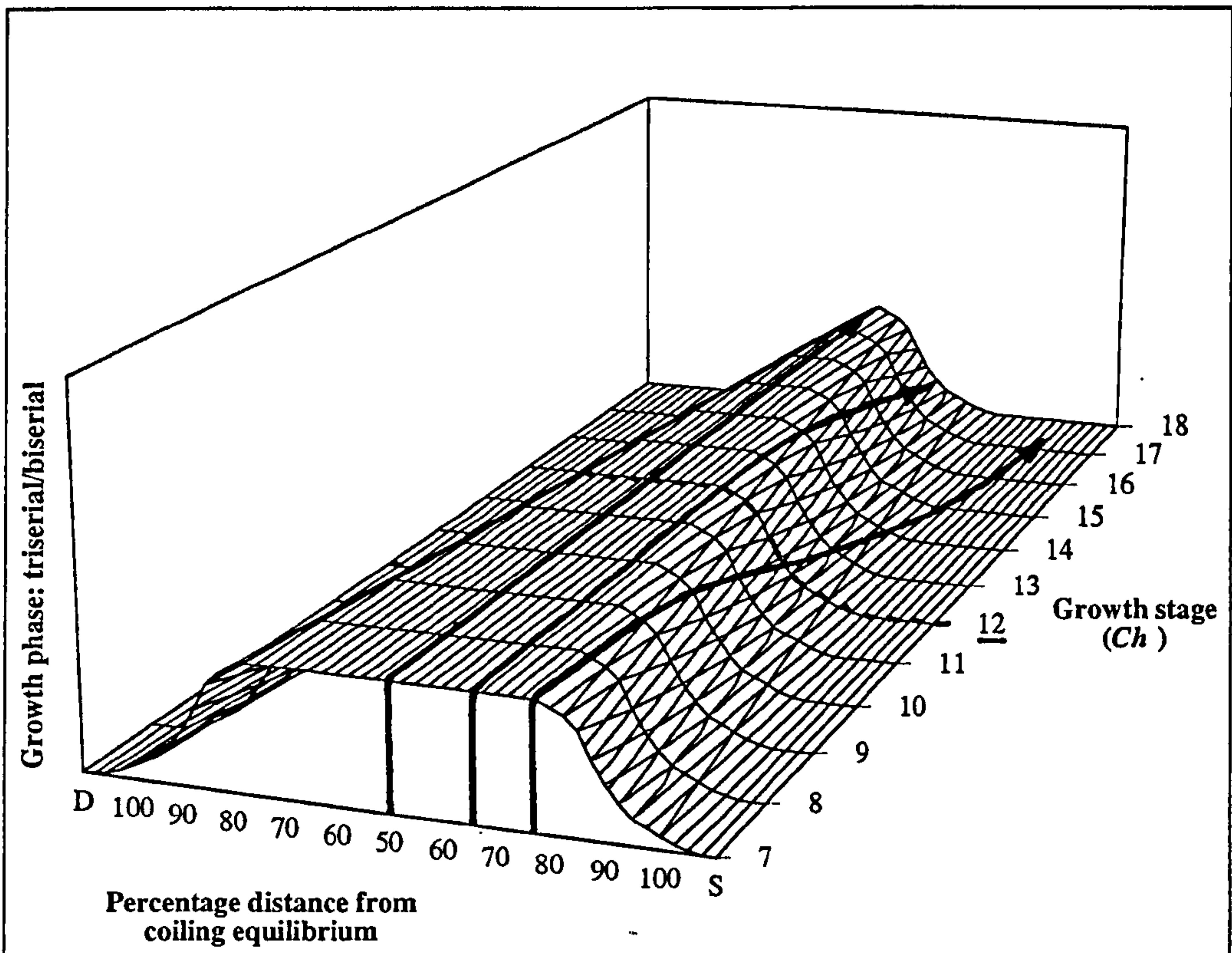
Turning next to the Phase II Group 2 growth types, we find we can tell a similar story. In this case it is not an imbalance in cytoskeletal chirality that causes development to go wrong, but an imbalance in the cytoplasmic tension instead. Either the cytoplasm was too viscous and springy, or the membrane adhesion was too weak; but whatever it was, it caused the long axis (l') of the final chamber to spring back in the way described above, and to spill from there onto adjacent chambers. Once again, beyond that point the process was all downhill. We have come to roughly the same conclusion via a slightly different route: *Tritaxia*'s developmental system appears equally 'boxed in', since no matter what went wrong, it always produced the same result.

Now, there is a sense in which all these arguments are highly contrived because the arguments themselves are 'boxed in' by the available evidence: having decided that exotic chamber growth was a developmental error of some sort, all subsequent scenarios are rigged, like a Greek tragedy, to lead inexorably to the same disastrous conclusion. This is the unacceptable face of *Just So* storytelling, rightly lampooned by Lewontin and Gould (1979). But note that the evidence itself *does* exist: 20.7% of all specimens in the data set exhibit some form of non-triserial development, and 87.5% of those occur only after the average growth stage has been exceeded. This is not the implausible claim that *Tritaxia* must commit a developmental error because it is doing what we have already defined as an error; rather, it is to say, 'Look how many different ways there are to imagine *Tritaxia* embarking on what we think is an erroneous course; and for that course, despite its multiple underlying reasons, to effectively end up always being the *same* course, so that such a large proportion of the population past the average expected growth stage *could* have made it.'

All clichés hold a grain of truth, and this one is no exception: having reached the top, the only way to go is down. The image of *Tritaxia* that I am trying to foster is one in which triserial growth was precariously balanced on a narrow 'developmental plinth', such that almost any degradation in the coding pushes it off and onto the next stable developmental trackway. That this plinth is itself atop a fitness peak completes the image I am arguing for (and see Sections 5.3 and 5.4 for some helpful conceptual tools).

Text Figure 7.8 shows the argument in graphic form for the chiral instability version given above. In the chirality version there are only two possible directions for development to go: too dextral or too sinistral. Like Goldilocks, *Tritaxia* is happiest somewhere in the middle, where a 50:50 mix of developmental influences renders its

trajectory just right. But the argument can easily be imagined scaled up to multiple developmental dimensions without having to swallow any of the specifics I have discussed here. All that is required is *any* situation where the vast majority of possible genetic mutations turn out, once they are expressed, to result in roughly the same phenotypic shift. And this, in turn, implies that there is a major element of channelling in the morphospace surrounding *Tritaxia*'s normal, triserial developmental pathway.



Text Figure 7.8 Growth form as a product of developmental instability arising from an imbalance of chiral elements in the cytoplasm.

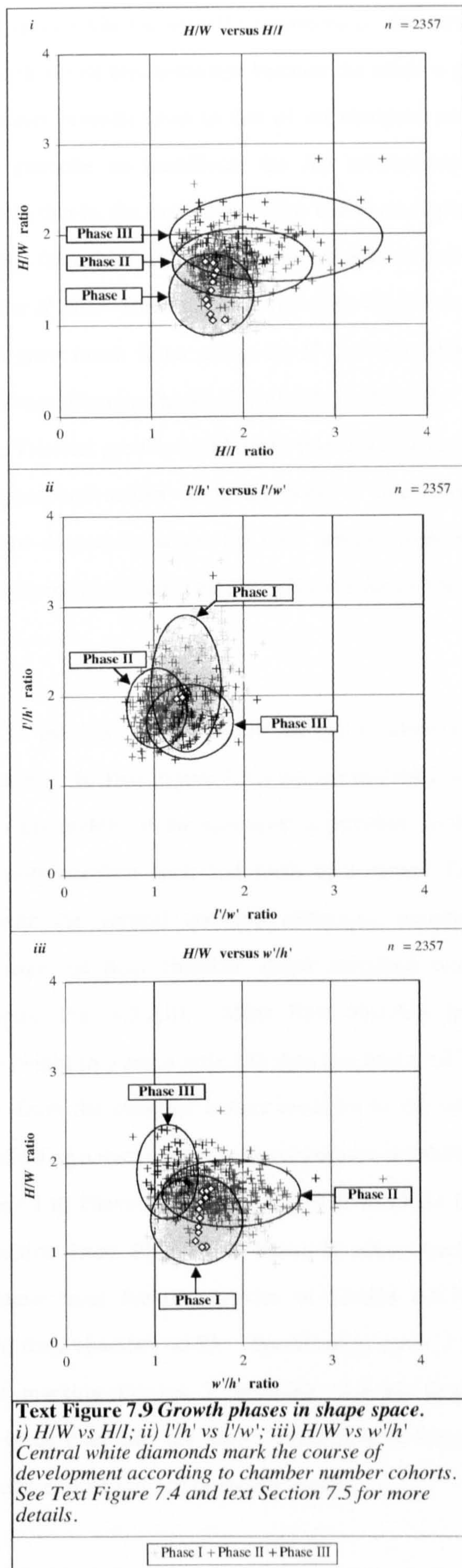
The raised central zone of this landscape represents the triserial growth phase which is relatively unstable and can decay into biserial or uniserial phases once thresholds have been exceeded. Various trajectories are shown by the solid arrows. Growth proceeds from the foreground in a discrete chamber addition sequence, and is stable for a certain number of steps depending on the balance of chiral elements in the starting configuration. For individuals with an equal mixture of sinistral (S) and dextral (D) elements, triserial growth is indefinitely stable and in this case continues for a whole 18 chambers, as shown by the middle trajectory. For individuals with more of an imbalance, in this case a small predominance of sinistral elements, growth proceeds for 15 chambers before the instability takes over and shunts the trajectory away from the triserial phase and into a biserial sequence. Individuals with this amount of chiral imbalance only reach instability after the average reproductive age of 12 chambers (shown by a contour in bold) and therefore cannot be entirely eliminated by selection, even if non-triserial growth is highly maladaptive. In the third case, individuals have an even larger proportion of sinistral elements and therefore much more imbalance, so much so that the instability manifests itself very early on, shifting the individual into a non-triserial phase after just 9 chambers. If they are maladaptive, non-triserial growth phases manifesting themselves this early in the sequence can be mopped up by selection because they generally occur prior to the average reproductive stage of 12 chambers.

Returning to the fossil data where we can pursue the line of argument with more substance, we see that the chirality model of Text Figure 7.8 maps neatly onto Text Figure 7.5 (as a folded-out mirror-image version—imagine the blue triserial Phase I as the plateau, the Phase II trio of *types* 2, 3 & 4 as the slope, and the Phase III cluster as the floor). Again, I am not suggesting that an imbalance in chiral elements is *actually* responsible for causing this pattern, just that something of an equivalent nature seems to be.

From here we have a easy way to translate between the ever-narrowing-plinth model and the growth sequence as we mapped it out in the earlier parts of this chapter. Specifically, by splitting morphospace scatters into discrete chamber by chamber sequences, we can watch *Tritaxia* uncoiling in the multidimensional regions of H/W vs. H/I , l'/h' vs. l'/w' and H/W vs. w'/h' , observing both when the exotic transitions take place and where in shape space they pitch the population. I suggested in Section 6.2.4 that some sense can be made of these higher dimensional shape spaces by visualising a developmental trajectory running up and out of the page, and it is now time to put flesh on that idea. Appendix Figures 4.3.2.i-iii show the data split into individual chamber cohorts which can readily be imagined as stacked on top of one another in a vertical sequence.

In the case of H/W vs. H/I , we already know that the population begins at the lowermost margin of the 1:1 grid and moves steadily up-field. Text Figure 7.4.i showed us that the mean values trace a long, inverse S-shaped course across this zone. Appendix Figure 4.3.2.i confirms that a few exotic specimens appear as early as *Ch* 9, but they do not become significant until *Ch* 12, after which point they effectively take over in terms of the proportion of shape space explored. Text Figure 7.9.i, below, shows (roughly) the sequence of regions colonised, first by Phase I, then Phase II, followed by Phase III development. We find an ever expanding zone of morphospace occupied by each new wave of development, heading from the triserial heartland in many different directions—vertically, diagonally but mostly laterally—and into those spaces characterised by a feathering of the triserial portion itself.

The area below the 1:1 ratio on each axis remains relatively untouched, and we can easily work out why if we bear the uncoiling model in mind. Looking back at the illustrated shape space (Text Figure 6.17) we see that regions south of the 1:1 border where $H/W < 1$ are characterised by roughly lenticular forms, somewhat similar to *Lenticulina rotulata*, which we met in Part II. By contrast, forms in the region west of the $H/I = 1$ boundary seem to be open trochospire, having an umbilicus within their outermost



chambers reminiscent of species like *Gavelinella cenomanica*. The triserial path of *Tritaxia* pushes almost straight north across this landscape because the relative growth rates of H and W shift the test from a squat juvenile form to that of an elongate adult without the spiral opening far enough to generate an umbilicus; the H/I relationship thus remains fairly constant throughout. Until, that is, the first adventitious chambers appear, at which point the character I is left flagging far behind in exotic forms because it marks the intersection of maximum width, W , on the H axis. Since the new chambers fit two or one instead of three to a whorl, exotic forms grow much faster along the H axis than along W , and the scatter spills northward and eastward through Phases II and III, in the only direction open to an uncoiling triserial stack. Triserial growth could never take *Tritaxia* into $H/W < 1$ or $H/I < 1$ portions of this shape space, and neither could a process of uncoiling. Instead, uncoiling tends to push the test shape diagonally across the field towards regions in the upper north-east quadrant which host forms reminiscent of *Dorothia gradata* (Text Figure 6.17; Appdx. Figs. 2.3.10 & 2.2.1.x).

If we next turn to the l'/h' vs. l'/w' plots we get to observe the final chamber's behaviour during this process. In Text Figure 7.9.ii we see that the average values occupy a roughly circular zone in the middle of the specimen population so that the developmental sequence appears to simply oscillate back and forth in a narrow field. Combining this notion of oscillation with the vertical stacking technique mentioned above, we can appreciate that *on average* the final chamber shape remained remarkably constant as growth progressed (Appdx. Fig. 4.3.2.ii). Mean final chamber length (l') was always almost exactly twice the height (h') and a little less than one and a half times the width (w'). But when we shift focus from the chamber cohort averages to the sample population itself we see that many individual specimens must have undergone a substantial shift in location as they passed from Phase I to Phase II and from Phase II to Phase III. While not exactly discontinuous, the transition from Phase I to Phase II often marks a sharp break in behaviour, which we know from the descriptions in Section 6.1.3.i was because of a characteristic increase in final chamber width. Specifically, *types 2 and 3* are frequently found west of the line marking $l'/w' = 1$, meaning that the final chambers of these specimens are actually wider than they are long. Transition to Phase III often places the exotic final chambers back east of the 1:1 boundary again.

Note also that there is a long axis to the l'/h' vs. l'/w' scatter running roughly north-south and feathering out at the northern end. Despite the relative stability of the chamber cohort means (and even these have a slightly preferential north-south spread), it seems that there was quite a lot of free play on the l'/h' axis, even for normal triserial types. In terms of the tent-pegging model, this axis corresponds to how far the last corner of the groundsheet (the end attached to the carinate edge of the tent) could be dragged away from the anchor pin (the coiling axis) relative to the height of the flysheet propped up by the central tent pole. According to the model, an increase in one of these factors is likely to cause a decrease in the other (there being only so much tent to go around), so an element of free play due to compensation is predicted. It is therefore confidence inspiring to find that the specimens themselves seem to record the same pattern.

Finally, the H/W vs. w'/h' plot provides the most graphic example of what happens when *Tritaxia* falls off its narrow triserial path. In this example we start with the wholly triserial population centred around $w'/h' = 1.5$. Text Figure 7.9.iii shows the chamber cohort averages making their slightly wobbly way due north, and we can watch the same event playing out in the sample population itself (Appdx. Fig. 4.3.2.iii) until it reaches a location around $H/W = 1.5$. At that point the structure has reached stage 12 of its growth sequence and is starting to spit out individuals that have fallen off their triserial pedestal. Those passing from Phase I to Phase II are normally shunted to the east of $w'/h' = 1.5$ (the exceptions being chiefly *type 4*); then those passing from Phase II to Phase III are shunted back over the line to occupy the north-west corner of the field. And remember that this all needs to be squared with the plinth model itself (Text Fig. 7.8) in which the slope is Phase II and the ground Phase III: in other words, simple though the model is, when we translate it into morphospace we find that it involves quite sharp and substantial transitions from zone to zone as the phases of exotic growth unfold.

This developmental model for *Tritaxia*, and the data that support it, are highly reminiscent of the models proposed by soft structuralists (like Oster and Alberch, 1982) who cast developmental variation as a series of discrete hops between bounded zones of phenotypic expression. What we have here, therefore, is a classic description of structural influences on form resulting in an anisotropic morphospace with clumpy phenotypic distribution. This teratological aspect plays a substantial role in the model we must take to our examination of *Tritaxia*'s evolution in Part IV.

Summary

The simple, elegant, allometric accounts of developmental motion through morphospace put forward in Chapter 6 have now been supplemented with a description of growth via discrete chamber addition. The chamber-based version is able to elucidate multidimensional changes in development (e.g. H/W vs. H/D), and also casts new light on the simple bivariate relationships themselves, revealing many of these to be logistic in form and suggesting that growth often involves a tension between different character dimensions.

There is no evidence from *Tritaxia*'s distribution through morphospace that we are dealing with more than one lineage or morphotype. Although specimens exhibiting some form of exotic growth do tend to explore different regions of morphospace, they are relatively continuous rather than radically discontinuous with respect to those specimens showing only the normal triserial mode, and what discontinuity they have is manifested along a temporal/developmental dimension. Since the degree of morphological separation characteristic of functional or phylogenetic disparity seems to be absent, a structural explanation for exotic growth is proposed.

Although quite common, the fact that exotic growth is manifest primarily after the average life expectancy (in chamber numbers) for the overall population seems to suggest that it is a construction mistake—a teratism. Evidence of things going wrong is often enlightening when trying to work out how things go right, so the patterns of teratism have been used to suggest a model of chamber formation in *Tritaxia*. The model assumes that construction was accomplished with no overview and by using a maximum amount of self-organisation, thus ensuring that informational control was as economical as possible.

Finally, this model of chamber formation is used to sketch a holistic description of *Tritaxia*'s developmental sequence through morphospace, including both normal triserial development and also the construction mistakes. It is clear from this model that morphospace is anisotropic, rendering wholesale movement in some directions easier than in others.

Part IV Evolution

General Introduction

Down in the dark and silent mud of the Cenomanian Chalk Sea, a pattern of organization trickled through millions of repetitions and countless billions of individual manifestations to leave behind it the fossils we know as *Tritaxia pyramidata*. *Tritaxia*'s agglutinated test was constructed from the surrounding sediment by a single cell, a piece of living nanotechnology whose mechanics can be conceptually partitioned into a portion concerned with encoding and a portion whose job it was to interact both with its surroundings and with other parts of itself.

Natural selection crafted that pattern from the raw materials it had to hand. An indifferent physical environment and an artful biotic one collectively conspired to filter the range of candidates, sifting chance until it became design. In doing so, the patterns of the environment were transferred to the patterns we see in the fossil record, albeit in an indirect and rather cryptic manner. Somehow *Tritaxia* must be stamped with the mark of its history and setting; that is the fundamental reasoning behind *Plus ça change*, and indeed behind any model of evolution by natural selection.

At this point we have seen enough of both *Tritaxia*'s ecological setting and its developmental parameters to have some idea of the external and internal tensions selection had to negotiate between. In Part IV we pick up *Tritaxia*'s genealogy at B31, the lowermost sample point of the 100 kyr timeseries, and travel with it for a million years, watching to see how the fossil lineage responded to changes in its environment. Once the huge wealth of morphological data, split into different sites and timeframes, has been fully digested, we can move on to address the issues set out in Part I with more confidence. In the final chapter, the full weight of empirical and theoretical material developed throughout the thesis will be brought to bear on the *Plus ça change* model.

Chapter 8 Changes Through Time

Introduction

Chapter 8 examines the evolutionary data set. Like the ecological material presented in Chapter 3, it is distributed between three different sites and three different sample scales; like the morphological material presented in Chapter 6 it is also distributed between fourteen basic characters, half of which are further combined to form shape ratios and allometric trajectories. The challenge will be to present this voluminous data set in such a way as to keep the parameters separate, well-organised, and to avoid repetition. To that end, the first half of the chapter is dedicated to explaining the various tests, summary methods and conceptual schema that have contributed to the final product. The second half then presents the data itself, and is sub-divided into appropriate nested sections to lighten the organisational load. (The contents listing for both text and appendix will provide a helpful overview.)

Section 8.1 Method and Analysis

8.1.1 Sample Populations

The measurements of *Tritaxia* described in chapter 6, were performed on 2357 individuals drawn from throughout the sampling points documented in Part II. Most horizons provided at least 45 measurable specimens but there were certain exceptions (Text Table 8.1). The mid-chalk sample, C13-9 [16], is represented by only 15 individuals because it took a week to pick through the mass of highly congealed debris, and even then yielded only 66 specimens of *Tritaxia* in total, most of them encrusted and obscured by bits of chalk. Also, as the palaeoecological data revealed, *Tritaxia* was very rare during the formation of couplet B41, so at this level the morphological data from every site is represented by fewer than the sought after 45 specimens. Southerham provided 40 measurable individuals on the first pass, which was deemed close enough, but the marginal

sites took more work. In the first round of picking, Folkestone and Escalles gave only a handful of tritaxiids (Escalles yielded just three, two of them broken!), so larger quantities of material then had to be processed and scanned for *Tritaxia* alone. B41 at Folkestone is now represented by 40 individuals, and at Escalles by 20.

Horizon	B31	B37	B41	C5	C10	C15	C21	C29	C35	C40	C45		
S 100 kyr	45	45	40	45	46	45	46	46	46	46	46		
F 100 kyr	46	46	40	46	46	45	46	46	46	45	46		
E 100 kyr	-	46	20	46	46	46	46	45	46	46	46		
Horizon	C10	C11	C12	C13	C14	C15	C16	C17	C18	C19	C20	C21	
F 20 kyr	46	46	46	46	46	45	46	46	46	46	46	46	
Horizon C13	-0	-1	-2	-3	-4	-5	-6	-7	-8	-9	-10	-11	-12
F 2 kyr	45	46	46	46	45	46	46	46	45	15	45	45	46

Text Table 8.1 *Specimen numbers per sampling horizon. Those with 46 specimens contain a single large outlier, all others contain only specimens within the normal range.*

The specimens were drawn from those with the best preservation. There is no reason to suppose that taphonomy was correlated with any morphological feature (and no way to find out other than by extensive measurement), so the best specimens were taken to be an essentially random mix, and thus suitable for statistical purposes. Where the pool of adequate specimens was much larger than the 45 required, I tried to choose randomly wherever it was possible to do so. Some individuals, however, were impossible to treat indifferently. As discussed in Section 6.1.4, the size range of *Tritaxia*, and probably of all foraminifera, is somewhat skewed: these organisms grow until they either reproduce or die, and if they do neither for a long time then they get very big indeed. Consequently, sample populations often had a fairly indistinguishable mixture of ‘normal’ sized specimens, plus a small number of absolutely huge ones. It was impossible to choose a huge specimen ‘at random’ (i.e., without being dreadfully aware of it), and so I *deliberately* selected a single large individual whenever there was a well preserved one available. However, the inclusion of such large specimens in a sample population has a substantial effect on the mean; this might have been acceptable if every population had had one, but unfortunately only about half them did (a result which probably is genuinely random), making these incomparable with the rest.

Since the large specimens were impossible to ignore and equally misleading to include, my solution has been to leave them out of the measured populations for most

purposes, but to include them on charts such as the bivariate scatters and histograms displayed in association with Chapters 6 and 7 because they provide legitimate data on the end points of growth curves. The continuous variables can thus be considered as having roughly normal distributions, so that sample means adequately sum up their general properties without too much information being lost by neglecting the outliers; and although the outliers have a negligible effect on the calculation of growth trajectories for individual horizons, for consistency they were left out of the calculations of these, too.

Sometimes the sample populations from individual horizons are skewed (see Section 6.1.4 for the measure of skew and Appdx. Tables 2.1 - 2.3 for the results), but since the incidence is fairly rare (normally less than 5%), and since none of the continuous variables has a skewed distribution overall (Section 6.1.4), I decided to treat them all as normal for the purposes of statistical tests. Strictly speaking, this means that a small proportion of such tests will have their basic requirements violated; but there are so many tests performed, and the conclusions drawn from them are so broad, that I considered it more important to apply standardised techniques than to deal with an irregular hotch potch of methods, each rigorously tailored to exact statistical standards, but too confusing or heterogeneous overall to give us the kind of broad-brush picture required by the project.

As with the palaeoecological material, the inclusion of C13 within the 20 kyr resolution series is provided by an amalgamation of data from horizons C13-3, C13-4 and C13-5 [4-8]. In this case the specimens were drawn from the first 15 of horizon C13-3 [4], the second 15 from horizon C13-4 [6] and the final 15 plus the outlier from horizon C13-5 [8].

8.1.2 Summarising Data

8.1.2.i Sizes

As shown in Chapter 6, the continuous metric variables, H , W , I , l' , h' , w' and i' , have roughly normal distributions and can be summarised by using their mean and standard deviation. The number of *chambers* can also be represented in this manner because

although discrete, the range of measurement categories is broad enough to approximate continuous, at least for the purposes required by this study.

8.1.2.ii Shapes

Simple linear measurements can only tell us about sizes, but changes in shape are just as much a matter of interest. The same combinations of character pairings used in Chapter 6 are once again considered (H/W , H/I , w'/h' , l'/i' , l'/h' , & l'/w'), and because the distribution of these ratios is also approximately normal, their means and standard deviations are once again used to summarize them.

8.1.2.iii Trajectories

All the combinations of characters exhibit significantly allometric relationships during growth (Section 6.2.2), and it is hard to tell from ratios alone whether any differences in shape are true differences, or just an allometric fallout of changes in size. The two factors of the allometric equation, the exponent, a , and the constant of proportionality, b , are used to represent growth curves for the same set of standard character combinations as used in Part III (i.e. H/W , H/I , w'/h' , l'/i' , l'/h' , & l'/w').

I have found no generally recognised method of summarising variation in an allometric scatter (although I guess one might be developed via the standard error) and so there is no attempt here to address the issue of spread in different developmental trajectories.

8.1.2.iv Categories

The categorical characters require a little more imagination if their properties are to be condensed into something useful without obscuring too much useful data. For continuously varying characters with non-normal distributions (e.g. *ind* and *tw*), or non-equal measurement categories (e.g. *g%*), the median is traditionally the best method for summary purposes. But in terms of change this average provides almost no information, because *tw* is so skewed that the median of any sample will always be the lowest category

(zero), whereas the unequal categories of *g%* suggest large and sudden shifts in central tendency which do not reflect the gentle nature of many sample differences. The central tendency for *ind* is more appropriately represented by a median value, but even in this case the number of categories is so small that most sample medians record an oscillation between just two values (0.5 and 1), thus concealing more than they express. For the truly categorical, non-ranked characters (*g.dist*, *chir* and *type*) there is absolutely no meaning to averages other than the mode, which again tells us very little and simply jumps between values once a threshold has been passed.

In fact, by far the best summary method for any of the categorical characters is as a histogram for a visual appraisal, or as a series of percentages for numerical purposes, both of which are too bulky to act the way a single summary value would. Nevertheless, percentages can be used to compare between pairs of samples, and a method along those lines will be introduced shortly. More usefully, in terms of a single value, the proportionality approach can be extended to give us a metric of variation: the Shannon index used in Part II provides a good measure of how evenly category membership is spread throughout a population, so long as we do not need to know a 'direction' for the variation to occur in (categorical features have a dimensionality as high as the number of categories, so that the population can be equally 'variable' in numerous different ways). But in fact, the best results for assessing these characters will come from a combination approach, employing an initial visual assessment of the data to see what has shifted to where, backed up by a more general numerical one based on percentage similarity or diversity scores.

8.1.3 Measuring Difference

8.1.3.i Size and Shape: *t* tests, *F* tests and *haldanes*

A number of calculations have been used to evaluate the intuitive impression of change both in central tendency and in variation of size and shape. Because these parameters both have roughly normal distributions (Appdx. Figs. 4.1.1 & 4.1.2), robust and traditional statistical tests can be used to establish the *likelihood* of genuine differences

between the means and standard deviations of pairs of samples. These are supplemented by a calculation of rates of change which assess *how much* difference exists between particular pairs.

8.1.3.i.a t tests

A t test for assessing the probability of drawing random correlations was introduced in Chapter 6; there is also a t test for comparing the means of pairs of samples. This time the t statistic is calculated thus:

$$t = \frac{\bar{x}_1 - \bar{x}_2}{s_e}$$

where \bar{x}_1 and \bar{x}_2 are the means of the two samples, and s_e is the standard error for the difference of the means.

The standard error is calculated from the variance of the two samples:

$$s_e = s_p \sqrt{\frac{1}{n_1} + \frac{1}{n_2}}$$

where s_p is the pooled estimate of the standard deviation for both samples, and n_1 and n_2 are the sample sizes.

s_p , itself, is calculated by combining the standard deviations of the two samples:

$$s_p = \sqrt{\frac{(n_1 - 1) s_1^2 + (n_2 - 1) s_2^2}{n_1 + n_2 - 2}}$$

where s_1 and s_2 are the standard deviations of the two samples. The t test calculates the probability of drawing two means with the given values at random, from populations with the given distributions, as estimated from their standard deviations.

A related measurement, this time concerning only a single mean, is the confidence interval used to set limits to the 'error bars' which customarily accompany the average values on a time-series chart. A confidence interval gives us a range of values within which the parent population mean (rather than the sample mean) should lie, given the information present in the standard deviation of the sample. The formula for its calculation is:

$$\bar{x} \pm 1.96s/\sqrt{n}$$

where \bar{x} is the sample mean, s the sample standard deviation, 1.96 the range within which 95% of the population should lie, and n the number of individuals in the sample population.

8.1.3.i.b *F* tests

Another test, this time for comparing the variation in two normally distributed populations, exists in virtue of the *F* statistic. *F* is generated by squaring the standard deviations of two populations and dividing the larger one by the smaller.

$$F = \frac{s_1^2}{s_2^2}$$

where s_1^2 and s_2^2 are the larger and smaller values, respectively.

For data drawn from identical populations, the ratio of pairs of means and standard deviations is unlikely to stray far from 1, depending upon the degrees of freedom. Statistical tables provide the information on exactly how unlikely, and allow us to assign a judgement depending upon the level of significance we wish to employ. In this study, all *F* tests were evaluated at the 0.05 level.

8.1.3.i.c *haldanes*

Statistical tests show us roughly *how often* we can bet that an apparent change in central tendency or variance is a real feature, but, beyond specifying a threshold for

significance, they provide no measure of *how much* of a change has occurred. Measures of morphological change must overcome several obstacles if they are to be comparable between characters, organisms and timescales of observation. The metric of choice here is the *haldane* (Gingerich, 1993). A haldane is defined as a change by a factor of one standard deviation per generation, and the formula for its calculation is:

$$\text{rate (h)} = \frac{\left(\frac{\ln x_2}{s_{\ln x}}\right) - \left(\frac{\ln x_1}{s_{\ln x}}\right)}{t_2 - t_1} = \frac{\bar{z}_2 - \bar{z}_1}{t_2 - t_1}$$

where $\ln x_1$ and $\ln x_2$ are representative natural log measurements, or sample means of \ln measurements, at times t_1 and t_2 , respectively, these times being measured in numbers of generations, and where $s_{\ln x}$ is the pooled standard deviation of $\ln x_1$ s and $\ln x_2$ s.

Haldanes thus avoid most of the limitations incurred by more conventional metrics such as the *darwin* (see Gingerich, 1993, for a detailed discussion). By converting the initial data to natural logarithms, haldanes become comparable between characters of vastly differing magnitudes; by rendering them as a proportion of the sample standard deviation it is possible to compare values between characters of different dimensionality—between sizes and shapes or volumes, for example—even when the relationships are allometric; finally, by expressing the timescale in terms of reproductive cycles, the natural unit of evolutionary change, the metric becomes comparable between different organisms.

For the present purposes of comparison within a single study, foraminiferal generations have been set at 1 per year, although they could easily have been at least an order of magnitude higher. The important thing is to have everything standardised within the confines of the study itself; should it become necessary to extend the comparison further afield, an appropriate adjustment of generation times will be easy enough.

Reversals of direction within a coarsely sampled transect will inevitably lower the measured rate of overall change. Time averaged values are just as valid as pure directional trends, so long as we recognise them for what they are; as with all rate metrics, therefore, haldanes need to be indexed with the magnitude of the measurement interval. Conventionally, sample spacings are registered as \log_{10} values, such that rates measured across 2 000, 20 000 and 100 000 year intervals are denoted $h_{3,3}$, $h_{4,3}$ and h_5 , respectively.

8.1.3.ii Trajectories

8.1.3.ii.a Z tests

When the relationship between two different metric characters is summarised by the a and b values of an allometric growth trajectory, the likelihood that a pair of apparently different a values were in fact drawn from identical parent populations can be evaluated with a Z test:

$$Z = \frac{a_1 - a_2}{\sqrt{s_{ea1}^2 + s_{ea2}^2}}$$

where a_1 and a_2 are the two slopes being compared, and s_{ea1} and s_{ea2} are the standard errors for each slope (the method for determining standard errors for potentially allometric bivariate scatters was given in Section 6.2.3). The magnitude of Z must then exceed an appropriate test value (± 1.96 for $\alpha = 0.05$ in infinite populations, ± 2 for sample sizes where $v = \sim 40$) in order to be considered significant.

There are also versions of a Z test to compare pairs of b values, but they require some rather arbitrary assumptions to be made, and many statisticians are not entirely happy with them (Campbell, 1990); for that reason they have not been included in this study.

8.1.3.iii Categorical Variables

8.1.3.iii.a Statistical Tests

Because the categorical characters have not been summarised using standard metrics like the median, statistical tests which employ those measures are obviously inapplicable. It is worth noting, however, that such tests would still have been inapplicable even if medians *had* been selected to summarise central tendency. Methods like the Mann-Whitney U test, for instance, require values to be ranked, and the rather coarse and unevenly distributed

categories of the present data set inevitably generate an overwhelming preponderance of tied ranks. Under these circumstances statistical tests fail due to poor resolution (Campbell, 1990).

For the purposes of comparing pairs of samples, then, the non-metric characters have to be treated as though they are truly categorical. χ^2 tests might have been used to assess whether pairs of samples are likely to be truly different, but those analyses are very time consuming to calculate. Individual cases need to be checked to see whether membership of the rare categories is sufficient for them to be valid, and rows or columns of the grid collapsed together where necessary (Section 6.2.2.ii). Since this is a factor which varies from case to case, checking the whole data set would require hundreds of individually tailored calculations, and many of them would be valid only at very low resolution (i.e. with many coalesced categories).

In the end, I decided to evaluate the categorical characters free from statistical support. The strategy pursued here, therefore, will *not* yield statistically defensible results for the categorical variables. Instead, I have chosen to rely on the continuous variables to provide the more robust characterisation of morphological change across the Lower Chalk, and simply used the categorical features to 'fill in' this metric framework with more intuitively evaluated findings.

8.1.3.iii.b Percentage Similarity

Without aspiring to statistical authority, we can still improve on simple intuition alone. Percentage similarity scores provide an objective assessment of how different pairs of specimen populations are in the distribution of their categorical characters. The formula for calculating similarity is:

$$1 - \sum (x_1/n_1 - x_2/n_2)$$

where x_1 and x_2 are, respectively, the larger and smaller number of representatives in a particular category, and n_1 and n_2 are the total number of representatives in all categories from those samples. Percentages are obtained by multiplying the result by 100.

Percentage similarity measures were performed for vertically *adjacent* pairs of horizons *only*; they tell us how similar the composition of a population is to the one below it. More extensive comparisons were considered neither necessary nor useful.

8.1.4 Statistical Summaries

With such a large number of variables, plus the calculations to perform on them (8 sizes, 6 shapes, 6 trajectories and 6 categories, with *t* tests, *F* tests, *Z* tests and *haldanes* for the metrics, and similarity and diversity indices for the categoricals, each spread between three different sampling sites and three timescales—360 potential combinations in all!) the mass of material and options for comparison can be extremely unwieldy. Consequently, not all of the possible cross-comparisons were drawn, and, for those that were, the only way to get much of a grip on the data has been to summarise them, and then to summarise the summaries. The aim of this section and the next is to explain how all of these findings have been organised and condensed into a manageable form, and to prepare the reader for their presentation so that patterns will emerge more readily.

8.1.4.i *t*, *F* and *Z* tests: Appendix Tables

The statistics for *t*, *F* and *Z* tests were calculated for pairs of sample populations in two types of comparison. In one, samples from each of the three 100 kyr resolution transects were compared, both *within* each site (e.g. all Southerham samples with one another), and *between* sites (e.g. all Southerham samples with all those from Folkestone and Escalles). In the second block of tests, samples in the 100 kyr, 20 kyr and 2 kyr transects from Folkestone were compared, both within each scale (e.g. all 2 kyr samples with one another) and between scales (e.g. all 2 kyr samples with all 20 kyr and 100 kyr ones). These comparisons were made for each type of parameter variable (size, shape, trajectory) and for each type of test (*t*, *F* and *Z*); the results appear as Appendix Tables 3.2 & 3.3. Tests were *not* performed for pairings between the finer resolution transects at Folkestone and the coarse resolution transects at Southerham and Escalles, partly because this would

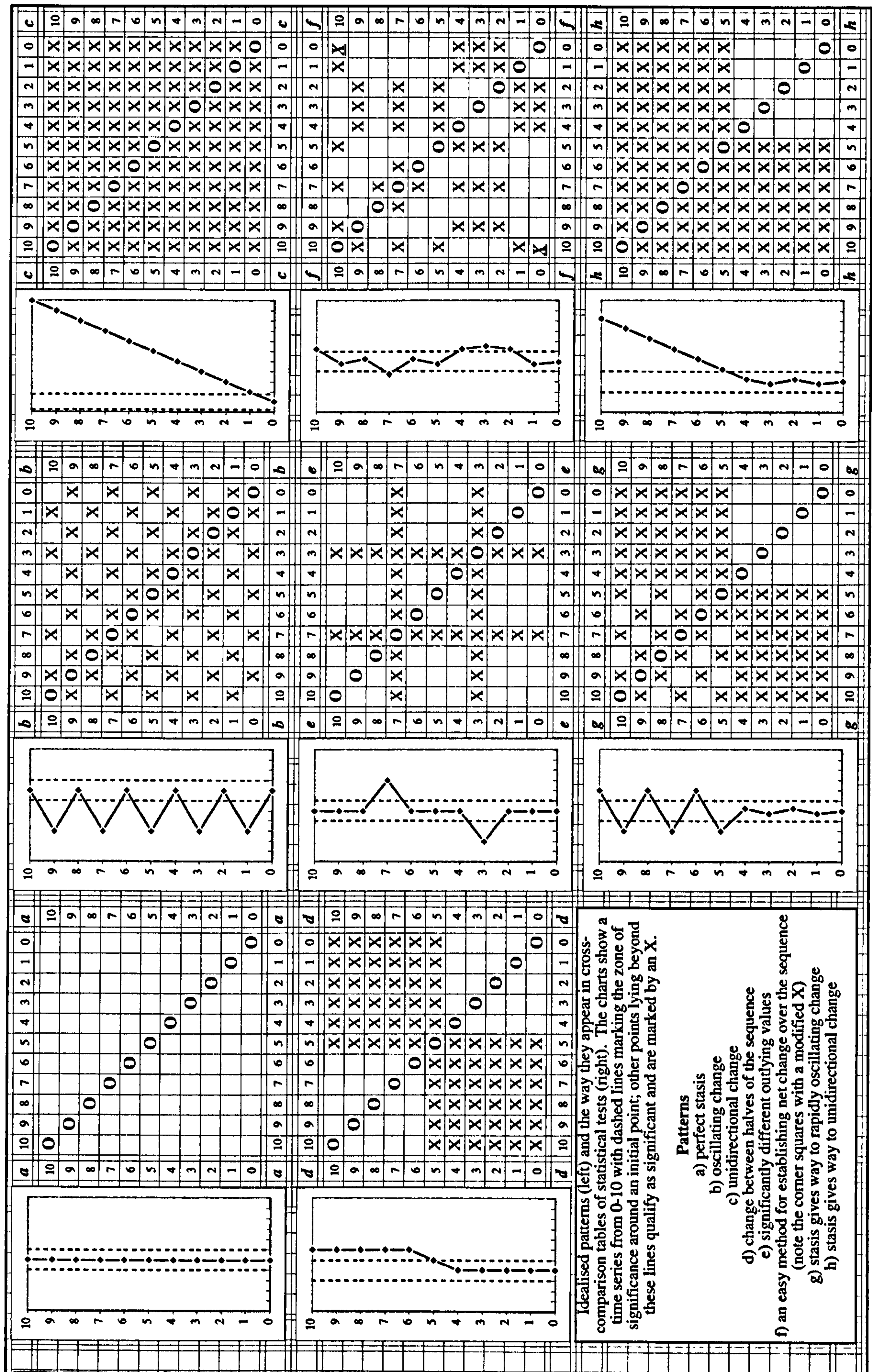
have doubled the amount of analysis, but mostly because it was simply unclear as to what it might add to the project.

The results of these statistical tests are arranged in cross-comparison grids (Appdx. Tabs. 3; Text Figure 8.1, below). Grid locations marked with an X show a statistically significant difference between pairs of samples at the 0.05 confidence level for whatever test is under consideration; grid locations left blank show that a null hypothesis of no significant difference remains in place; grid locations marked with a O cover the meaningless comparison of a sample with itself.

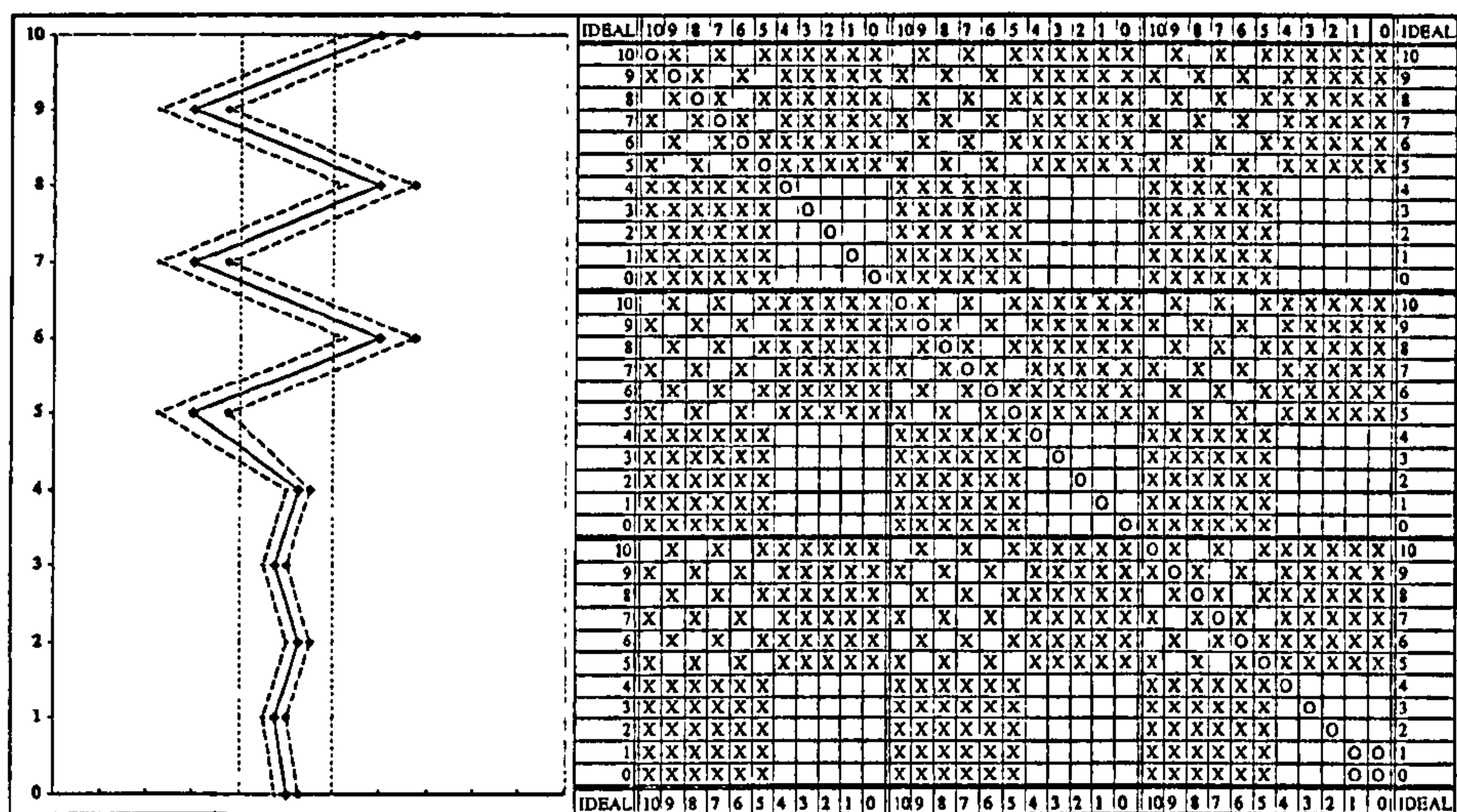
Because the grids are rather hard to take in on first impression, I present here a number of well defined patterns for demonstration purposes. Text Figure 8.1 (a) shows stasis, (c) unidirectional anagenesis and (b) is regularly oscillating anagenesis or, equally, wobbly stasis. Below these are patterns which frequently occur: (d) depicts a general change between upper and lower halves of a transect, here shown as instantaneous; (e) a single outlying value which registers as significantly different from all the other points in a transect (there are lots of these); (f) is a quick method for checking net change across a section by looking for the presence or absence of an 'X' at the top right hand corner.

The lower layer contains two idealised versions of how the *Plus ça change* model might look given the background environmental conditions in the 100 kyr transects. In the first version, (g), stasis throughout the environmentally unstable lower half gives way to regularly oscillating anagenesis in the more stable upper half; in the second version, (h), stasis in the lower half gives way to unidirectional change.

All these examples represent only those relationships in the blocks running *diagonally* across the middle of the grids from top left to lower right (i.e. those marked by a string of 'O's), which is to say they show patterns occurring *within* a single transect at a single site. Patterns *between* transects (between sites or scales) are more difficult to depict because of the numerous possible combinations, but an absolutely idealised situation for a three site case based on a *Plus ça change*-style pattern like that shown in panel (g) of Text Figure 8.1 is presented in Text Figure 8.2, below. Note that if the morphological behaviour differed much from site to site, this kind of regularity in the grid would be severely impaired; nevertheless, it is possible to see that a 6 x 6 chequered arrangement is a hallmark motif of *Plus ça change*.



Text Figure 8.1 Idealised timeseries patterns as they appear in the statistical grids of Appendix Tables 3.1 - 3.4. See adjacent text for discussion.



Text Figure 8.2 An idealised pattern for the three-site version of *Plus ça change*, as depicted in Text Figure 8.1, panel g.

8.1.4.ii Fields of Possible Combination

To further summarise the statistical results arranged on these Appendix Table grids, much use has been made of the *space of possible combinations* of sampling horizons. For example, we can meaningfully ask whether there are more significant values generated within the 100 kyr transect at Folkestone than there are from within the 100 kyr transect at Southerham. Since there are eleven sampling points at each site, the combination of every value with every other one must be $11 \times 11 = 121$, minus 11 because of the meaningless comparison of any horizon with itself (marked by 'O'), to give 110, which is then divided by 2 because horizon 6 versus 5, say, is the same comparison as 5 versus 6—leaving us with 55 possible combinations for each site.

In cases of perfect unidirectional anagenesis, with significant shifts between each sampling horizon, it is possible to find 55 significant values from such an array; it is also possible to find none at all (Text Figs. 8.1.a & b). If we discover for one particular test or character that Folkestone has 33 significant values whereas Southerham has only 3, then we can reasonably conclude that there were more significant changes taking place at Folkestone.

Converting these numbers to percentage scores then allows us to compare between fields with *different* areas. For example, the percentages in the example used above would

have been 33 out of 55 = 60% for Folkestone and 3 out of 55 = 5.5% for Southerham. But if the fields under consideration had had different areas, 55 possible pairings at Folkestone, and, for the sake of argument, only 5 possible pairings at Southerham, then both would have scored 60%.

By using this method we can ask not only whether there were more significant differences between different sites, but also whether there are differences between scales, between types of test, between sizes, shapes and trajectories, or between different individual characters. In addition, splitting the field from a given transect into zones, such as the upper and lower halves, also allows us to ask whether one of these zones shows a higher proportion of significant values than the other. In the case of the 100 kyr resolution transects, a division into upper versus lower halves usefully translates into a comparison between a stable environment and an unstable one, which is of course why these sections were chosen in the first place. Because of the differences in cycle strength, the upper and lower halves of the 20 kyr transect can also be argued to constitute more and less stable zones, respectively.

Note that for the 100 kyr transects there are an odd number of sampling points (ignoring the missing level at Escalles). The middle horizon, C15 [500], thus bridges a transition between the unstable lower and more stable upper halves, and for this reason it was included as a sample in both. A justification for inclusion rather than exclusion will be advanced shortly. Because C15 was taken to be the bridge between upper and lower zones at the 100 kyr scale, it was also taken to be the bridge and therefore the point of overlap at 20 kyr resolution, too, even though it does not split that section into two perfectly symmetrical halves.

With the 2 kyr scale, the lower half is probably the most stable in both a geological and an ecological sense since it incorporates only the steady setting of the marl, in contrast to the upper half which houses two sediment transition zones plus the chalk itself (Section 3.3.1). In terms of sediment type, the single couplet can more meaningfully be split into a zone of chalk (horizons C13-8, 9, 10 & 11, [14, 16, 18 & 20]), a zone of marl (C13-1, 2, 3, 4, 5 & 6 [0, 2, 4, 6, 8 & 10]) and a transitional or 'boundary' zone (C13-0, 6, 7, 8 & 12 [-2, 10, 12, 14 & 22]). Note that some horizons (C13-6 and C13-8) once again appear in more than one category.

The disadvantage of splitting fields of possible pairings into small zones of different character is that as the regions under consideration are ever more restricted they become increasingly prey to randomising effects; we should thus be wary of drawing too firm a conclusion in any particular case. At only 95% confidence we must always expect one in twenty pairings to seem significantly different when in fact they are not (a Type I error), or not significantly different when in fact they are (a Type II). If either of these crops up in a small field it can substantially affect the results. Consequently, whenever a sample could fit equally well into either of a pair of categories, and whenever there was equal justification for lumping it with either or for leaving it out of both, inclusion was the option of choice.

Inclusion serves to lower the impact that either Type I or Type II errors will make by averaging the effect across a larger sample number. The price paid for this strategy is that it consequently tends to conceal legitimate differences between a pair of sample zones by blurring or ‘smoothing’ the data between them. In other words, inclusion *decreases* the chance of spuriously concluding that upper and lower categories are different due to a Type I or Type II in either of them by *increasing* the likelihood that we will miss a genuine difference because we smoothed it out; it thus creates a kind of higher-order Type II effect. The point is, that with regards to the null hypothesis of the *Plus ça change* model, we will be erring on the cautious side and rejecting the model unless the evidence is good enough to overcome our slight methodological bias. Given the purpose of the project, this seemed to me to be the fairest strategy.

8.1.4.iii Rates of Change

Haldane values were calculated for each of the possible pairings in grids of the type used for the statistical tests (i.e. 100 kyr sections for Southerham, Folkestone and Escalles, and Folkestone sections at 2 kyr, 20 kyr and 100 kyr resolution), but such comprehensive processing was largely a matter of convenience since the data were already arranged in grids of those configurations. Most of the values calculated are not discussed in the text, and, once again, this is mostly a matter of convenience: there is already a vast amount of material to examine, much of it attempting to confirm conclusions which are partially established by other means; the less overlap the better. The forthcoming discussion of rates, therefore, is limited to just two types of relationship: *vertically adjacent* sample pairings for all scales and sites, and also *laterally adjacent* sample pairings between the three 100 kyr transects.

Vertically adjacent values show *how rapidly* a character was changing between successive sampling horizons. And, because the sample points within a given transect are separated by (roughly) equal-sized temporal gaps, the values therefore also show *how much* the character has changed. This is information that cannot be gleaned from statistical tests, which merely evaluate how confident we should be that a change of some sort has or has not occurred. Translation of *haldane* values into a ‘quantity’ of change, however, is limited by the terms of the calculation itself; it is important to recall that shifts in the mean are normalised relative to the pooled variance of the sample populations so that differences in magnitude reflect *not only the shifting magnitude of the mean, but also the variance* of the sample pairs themselves.

Finally, straightforward comparison between vertically adjacent samples is valid only in those cases where the temporal separation *is* equal; it does not extend to a comparison between transects sampled at different resolutions. In some cases the separation between vertically adjacent sampling points is not equal even within the same sampling scale: the different rates of sedimentation across C13 would be a case in point; and there are several examples to be found in the 100 kyr sections, which are not always perfectly evenly separated, either.

In the case of C13, the differences seem trivial and have been overlooked: the separation is taken to be a uniform 2 kyrs. In the case of the 100 kyr sections the differences in temporal spacing are more serious. Specifically, the separation between B41 and C5 is actually 140 kyrs because of two eroded cycles at the top of Gale’s B series rhythms (see Section 2.1.4 for a discussion); the separation between C15 and C21 is 120 kyrs; the separation between C21 and C29 is 160 kyrs. These latter two discrepancies arose in the field because of a greater need for confidence in sampling the same bed at different sites rather than simply ensuring an equal temporal separation between samples. The consequent inequality in separation is registered in the rate calculations themselves, which are thus equivalent as they appear on the charts and tables. It is normally glossed over in the text, however, by using the term ‘100 kyr scale’ ubiquitously to refer to the general temporal spacing of the three main sections. This matter is covered in Sections 3.1.1 & 3.2.6; the graphic logs themselves (Appdx. Fig. 1.1) depict the sample separations true to form and in the most literal possible way.

In the laterally adjacent 100 kyr transects, it is possible to measure the amount of morphologic difference *between* sites by setting the temporal denominator of the *haldane* equation to 1 (i.e. differences were taken at face value without dividing them out through time). Gingerich (1993) calls this metric the ‘intrinsic rate’ because, when it does refer to changes through time, it corresponds to those differences accumulated over the course of a single generation. My usage here corresponds to differences through space: equivalent horizons are taken as being ‘contemporary’ (which they can only really be on a geological resolution!). Lateral comparisons using the intrinsic rate are just a handy way of judging the differences spread over space via the same variance normalised, dimensionless method which the *haldane* formula normally smears across time. If the method were to be used in a more formal context then some method of calculating these values according to the magnitude of distance might be appropriate (e.g. dividing them by their separation in kilometres), but for now I have overlooked that kind of detail.

8.1.4.iv Similarity Scores

Similarity scores presented a problem in terms of their large-scale calculation. An array of categories rendered as percentage scores of the total population is not an easy a thing to manipulate—certainly not as easy as a single value like a mean—and they do not lend themselves to the construction of large cross-tabulated databases. Percentage similarity values need to be tackled on a piecemeal, pair by pair basis and have thus only been calculated for a small set of the possible combinations. Like the rates, they are available for vertically adjacent samples in both the 2 kyr and 20 kyr transects, and for both vertically and laterally adjacent samples in the three 100 kyr resolution transects.

The options for quantitatively summarising rates and similarity scores to assess their behaviour in different zones of interest are somewhat more restricted than they are for the statistical tests, but it is still possible to separate them into upper and lower halves of a given transect (or into chalk, boundary and marl for C13). Recalling that rates and percentage similarities represent *magnitudes* rather than the simple yes/no categories of a statistical test, the upper and lower-half values for these measurements thus constitute *average* magnitudes for a vertical run, rather than proportions of a space of possibility, as was used for the statistics.

8.1.5 Presentation of Results

8.1.5.i Evolutionary Timeseries

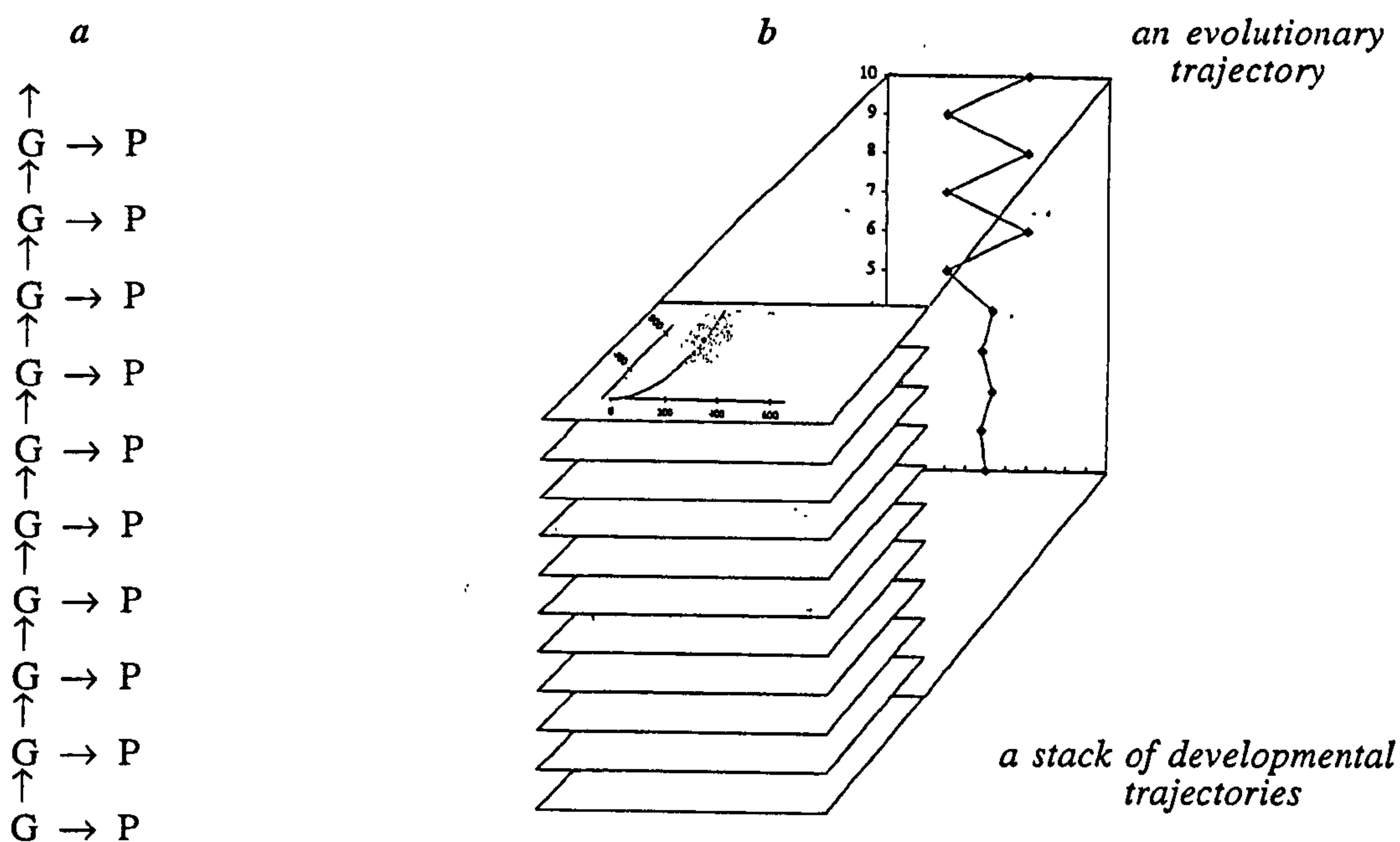
From an evolutionary perspective, we are interested in change (or lack of it) in groups of morphological characters through time, and the only really sensible way to arrange this kind of material for visual appraisal is as a linear time-series. In line with longstanding palaeontological tradition, bivariate graphs with time on the y axis and character values on the x axis have been employed to demonstrate both continuous and categorical data. However, by following this convention, one of the spatial dimensions we might otherwise use to represent character variation is already assigned to the portrayal of time. Thus, the already cramped work-space of a two dimensional page is limited even further, and certain complications concerning the apparent direction of evolutionary change arise as a consequence (these will be discussed shortly). Nevertheless, timeseries charts are extremely valuable and have been adopted throughout.

In order to emphasise their potential as an aid to evolutionary inquiry, I wish to suggest a particular way of thinking about such diagrams right from the outset. A well known way of depicting the relationship between genotype and phenotype is shown in Text Figure 8.3 (below). Note that the arrows in each case represent causality (and therefore also time), but that the line of genotypes persists indefinitely while each phenotype is an evolutionary dead-end and is thus shown running orthogonal to the germ-line.

The arrows from each genotype to its phenotype can be thought of as multiple individual *developmental* trajectories, and the arrows between successive pairs of genotypes as a single *evolutionary* trajectory. Translated back to the more familiar format used in Part III to depict development, the arrow $G \rightarrow P$ can be thought of as running *along* the developmental trajectory from the origin to the population mean (or in terms of an epigenetic landscape, as running from the average egg to the average adult). And with the forthcoming sections in mind, the arrow $G \rightarrow G$ can be thought of as running along the temporal axis of an evolutionary timeseries.

Consequently, we can usefully imagine that an evolutionary timeseries is basically a stack of developmental trajectories squashed flat so it will fit on a chart. Shifts along the

abscissa on an evolutionary timeseries will correspond to shifts along the developmental trajectory if size is changing, or shifts roughly at right angles to the developmental trajectory if shape is changing, or shifts in the curvature of the trajectory itself if the values of the allometric parameters themselves are changing. Clearly, this kind of interpretation bends the rules a bit and is not meant to be taken too literally, but as a method of conceptualising the relationship between evolutionary and developmental trajectories it is quite useful, and should facilitate an easy translation between the charts used in Parts II and III, and the charts to come in Part IV.



Text Figure 8.3.a A common depiction of the relationship between genotype and phenotype, helping to illustrate *b*, the relationship between an evolutionary trajectory and a developmental one.

8.1.5.ii Presentation Format

For both sizes and shapes, a panel of three timeseries charts is employed to present the data (e.g., Appdx Figs. 5.1.1 & 5.1.2). The left-most chart in each series shows sample populations summarised by their mean value. Error bars indicating a 95% confidence interval for the location of the mean are also included, although the reader is warned that these tend to dampen the signal and make a sequence look less dynamic than it would otherwise appear.

Because specimen numbers are generally the same from sample to sample, error bars alone might have sufficed to depict the variance of the populations; in practice, however, they turn out to be hard to compare with one another. Since the *Plus ça change* model is so explicitly concerned with changes in variance, time-series charts of standard deviation are presented in the middle position.

The final, far-right chart in each series shows the rate of change in *haldanes*. These are measurements summarising the relationship between vertically adjacent *pairs* of sample populations, and are thus situated at the mid-point between sampling horizons. Remember that haldane values are indexed with the scale at which sampling occurred (i.e. $h_{3,3}$, $h_{4,3}$ and h_5 , for 2 kyr, 20 kyr and 100 kyr scales, respectively).

For developmental trajectories, two panels showing the values of parameters *a* and *b* are used, appearing side by side to emphasise relationships between them (e.g. Appdx. Figs. 5.1.3).

For categorical characters, proportional area plots with a timeseries component are used, just as they were for the community structure display in Chapter 4. These charts show the *relative abundance* of each category and thus give us all the available information apart from sample size. Unfortunately, working out the magnitude of each category's proportional chunk is not a particularly straightforward task—an awkward quirk of the chart display which cannot easily be remedied—so an attempt has been made to offset this deficit by accompanying each proportional area chart with a percentage similarity plot that provides a numerical measure of the changes occurring between adjacent sample populations, and also with a diversity chart giving a Shannon index value for the whole array at each time slice. These quantitative summaries show how different two populations are, but, as I shall discuss in a moment, because there are numerous axes along which a multidimensional (multi-categorical) population might vary, they do *not* tell us in which direction a change has occurred. By far the best insights, therefore, come from using the proportional area plot in conjunction with the diversity and similarity metrics, and to this end all three appear on the same page wherever possible (e.g. Appdx. Figs. 5.1.4).

9.1.5.iii. 'Scalar' and 'Vector' Values

This brings us to a general point worth bearing in mind when examining any of these graphs—the distinction between what I shall call 'scalar' and 'vector' quantities. As a physicist would use the terms, *scalar* refers to those quantities such as time or temperature that have a magnitude which does not require any further specification of a direction; *vector* refers to those such as force or acceleration that do require a direction to be specified in addition to any magnitude. Here, I am using the same terms to refer to something similar but specific to the morphometric data. Scalars are straightforwardly dimensional: they are those quantities in which a magnitude alone is sufficient to exhaustively constrain the measurement; vectors are dimensionless: they are underlain by additional elements of free play which need to be acknowledged if we are to make a truly valid comparison between cases.

By way of example, if one examines a timeseries chart showing changes in mean size, then the abscissa bears an axis with a well-defined direction; there is no need to specify the meaning of 'increase' any further because that term is part and parcel of what we mean by the measurement itself. Like an increase in temperature, an increase in size is a scalar property: it can occur in only one possible direction. Contrast this with a timeseries chart showing changes in mean shape. The 'magnitude' of that mean is given by a dimensionless ratio, and all the 'directionality' of the ratio is dependent on which of the two variables was chosen to play the role of denominator. There is no such thing as a simple and unambiguous 'increase' in mean shape.

Just as two vector quantities in the physicist's sense are equal only if they have the same magnitude *and* direction, so two shifts in shape are equal only if they involve equivalent changes in both scalar components. From the shape charts alone there is no way to determine what a change in shape actually consists of. A shift in the ratio could equally have been a case of the denominator increasing or the numerator decreasing; if the operands had been reversed, the shift itself would have been in the opposite direction. In order to settle exactly what is entailed by a change of shape, we need to know something about the way the ratio was set up in the first place, and then go on to consider the magnitudes of whatever scalar variables were involved.

I raise this issue not because it poses any serious problem to interpretation, but simply because it demands we proceed with caution. The stark format of the timeseries

mode of presentation has a tendency to make different types of data look more similar and readily comparable than they really are. Of particular concern is the reflexive tendency to imagine that a shift rightwards along the abscissa denotes an 'increase' of some sort. In the case of mean size, standard deviation, rate of change, diversity, or percentage similarity, that is exactly what a shift to the right entails; but it implies no such equivalent thing for mean shape or the trajectory parameters. Furthermore, even though measurements like rate of change or diversity *are* scalar as they appear on the graphs, the measurements themselves still contain additional hidden, vector-like components such that we cannot discern from the magnitude of the value alone in which 'direction' an increase or decrease has occurred—there might, for instance, be any number of ways for a population to increase in morphological diversity.

8.1.5.iv Correlations

As we saw in Part II, the traditional timeseries format is a wonderful medium for accentuating patterns; indeed, it is a style of presentation that positively invites us to their discovery. By spreading sample values out along a temporal axis, trends become particularly easy to spot, while correlated behaviour simply leaps from the page whenever multiple data sets are arranged side by side. To this end, abscissa scales of the appendix charts are tailored to emphasise patterns rather than absolute magnitudes.

But, this mode of analysis also merits caution. Raup (1973) drew attention to the unfortunate habit of misidentifying trends by discovering a simple statistical correlation between timeseries patterns and the time over which they occur. In the case of trends, the problem is that timeseries patterns are Markovian in nature (history dependent), so that when comparing the sequence with time itself we are not comparing the two independent variables demanded by statistical reasoning; consequently, even random walks throw up spuriously 'significant' correlations with alarming frequency. For this reason, I have not attempted to rigorously identify trends beyond pointing out significant differences between the lowest and highest members of a sequence. But correlations between *pairs of timeseries patterns* are a different matter, and in this chapter I have made extensive use of statistical correlation as a method of identifying systematic, non-random relationships.

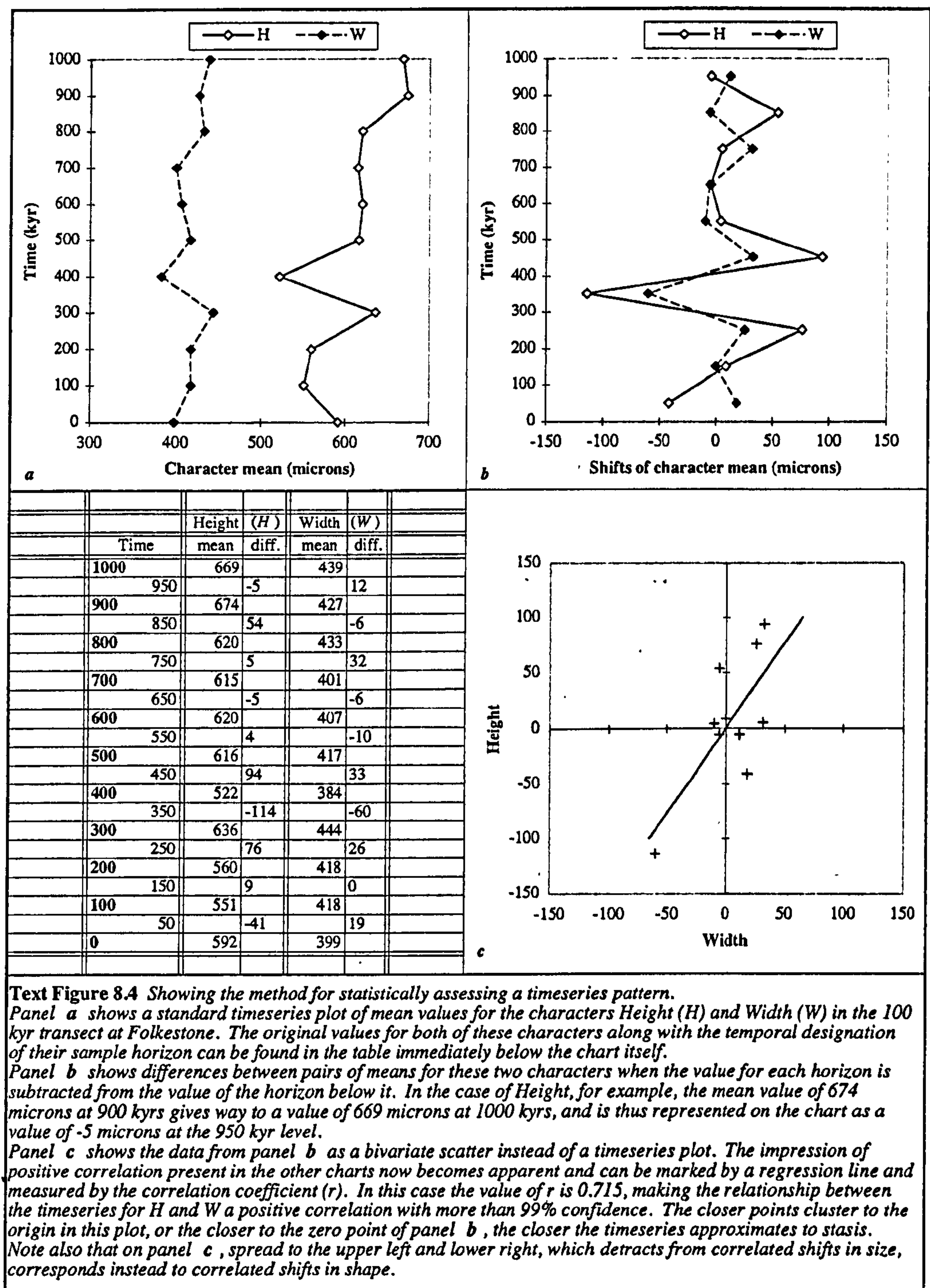
Apart from time itself, timeseries data consist of two components: the sign of a shift and its magnitude. These jointly contribute to an impression of correlated pattern. In an

earlier draft of this chapter, I analysed the Appendix Figure charts simply via sign shift, which effectively involved treating each pattern as a coin tossing run of positive and negative steps, then using binomial probability to make a statistical argument. But a more effective and sensitive technique takes the magnitude of each shift into account as well, and I have since adopted this test wholesale.

Ideally, we want to know not just where a population parameter lies in morphospace, but how it has shifted between observations. The method is to take each point in the sequence and subtract from it the value of the point which came immediately before. If a given value has a magnitude of 105, say (in whatever units), and the one before it had a value of 96, then the relationship between the two is +9; if the value before happened to be 110 then the relationship would be -5, and so on. The method is roughly equivalent to that used by McShea (1994) to generate his polarity values (see Section 3.2.4) and the result is a new timeseries with one fewer members than the original. Once this has been accomplished for a pair of timeseries, the correlation between them can be measured with a standard correlation coefficient (r) and then tested with a two tailed t -test (see Section 6.2.2.i). Text Figure 8.4 (below) provides a graphic description of the process.

It is important to understand that the correlation calculation is a measure of linearity that effectively works by quantifying the area of an actual set of values as a proportion of those alternatively possible, where the space of those other possibilities is itself defined in terms of the data sets actually given. This means that the calculation is insensitive to absolute magnitude and will give equivalent results even when the axes are very different. If the magnitude of the points on one axis are uniformly raised by several orders of magnitude relative to the other, it will not alter the r value at all. Or, to put it another way, if we have a pair of correlating series which run $x = 1, 2, 3, 4...$ versus $y = 1, 2, 3, 4...$ we can raise one of them up to 1000, 2000, 3000, 4000..., or to 1001, 1002, 1003, 1004... etc, without changing the value of r , which will always be exactly 1. I mention this point because it was raised in discussion, but having run the technique by a statistician I am now confident that it is sound.

There are, however, two caveats worth noting. The first is that the t -test for correlation assumes each of the variables to have a normal distribution, and the second is that it also assumes the variables to be independent. The first assumption appears safe for every situation but the trajectory b values, which are centred on the isometric value of 1 and



asymptote to zero or infinity in opposite directions. Nevertheless, even in this case, the available data are put to better use than they would be under the simpler binomial alternative, and the method still gives good quantifiable results, well in keeping with intuition.

The second assumption is safe for all the simple magnitudes but not necessarily for the shape ratios. Correlations such as H/W versus w'/h' are clearly independent in a way that ratios like H/W vs. H/I or w'/h' vs. l'/w' are not. In these latter cases a change in the

common factors, H or w' , is likely to change both sides of the pairing and thus to generate a correlation because of a lack of true independence. However, in order to keep the calculation procedure as straightforward as possible I have simply treated all ratios the same way and dealt with the fall-out from lack of independence in a piecemeal fashion when discussing the results (see Section 9.2.2).

Note that this procedure is *not* simply a case of re-measuring the same features we explored with correlations in Part III. There, we were interested in developmental relationships occurring over the lifecycle of a typical individual, and we clumped all the sampling horizons together to find them. Here, the correlations we are interested in occur over evolutionary timescales: we are looking for correlated shifts in the developmental relationships themselves. We already know *that* the characters are linked to one another over the course of development, and for the generalised case we know *how*. What we are looking for at this stage is evidence of heterochrony and heterotopy (what McKinney and McNamarra (1991) call *allometric heterochrony*)—we want to know *how firmly* those general developmental relationships are linked across evolutionary timescales; and, should they prove to be at all loose, *in what way they vary* through time and space.

In this situation it is an open question as to which null hypothesis we should choose when examining the statistical data for timeseries correlations. If we take the findings from Part III at face value and apply them to the timeseries model presented above (in Section 8.1.5.i), then our default expectation might be one of 100% correlation, whereby a change in one character results in lockstep change for all the others, too. On the other hand, while this model might apply to simple size parameters, almost every growth curve investigated revealed an allometric relationship between the variables, and that might lead us to postulate very little correlation between characters as they shift up and down their trajectories. We are thus free to play the null hypothesis either way, with different assumptions underlying different strategies. What is most important at this juncture is simply that we have an empirical measure of pattern to bolster our intuitions, and that is what the correlation test provides.

Text Table 8.2 (below) explains how the correlation tests from various types of character, measurement, and scale are presented.

	H	W	I	Ch	l'	h'	w'	i'	sd		H	W	I	Ch	l'	h'	w'	i'	
H	<u>x</u>	sd	sd	sd	sd	sd	sd	sd	H	H									H
W	m	<u>x</u>	sd	sd	sd	sd	sd	sd	W	W	r								W
I	m	m	<u>x</u>	sd	sd	sd	sd	sd	I	I	r	r							I
Ch	m	m	m	<u>x</u>	sd	sd	sd	sd	Ch	Ch	r	r	r						Ch
l'	m	m	m	m	<u>x</u>	sd	sd	sd	l'	l'	r	r	r	r					l'
h'	m	m	m	m	m	<u>x</u>	sd	sd	h'	h'	r	r	r	r	r				h'
w'	m	m	m	m	m	m	<u>x</u>	sd	w'	w'	r	r	r	r	r	r			w'
i'	m	m	m	m	m	m	m	<u>x</u>	i'	i'	r	r	r	r	r	r	r		i'
m	H	W	I	Ch	l'	h'	w'	i'		r	H	W	I	Ch	l'	h'	w'	i'	

a. Model example of the grid for timeseries correlations in size parameters.

	H/W	H/I	w'/h'	l'/i'	l'/h'	l'/w'	sd		H/W	H/I	w'/h'	l'/i'	l'/h'	l'/w'	
H/W	<u>x</u>	sd	sd	sd	sd	sd	H/W	H/W							H/W
H/I	m	<u>x</u>	sd	sd	sd	sd	H/I	H/I	r						H/I
w'/h'	m	m	<u>x</u>	sd	sd	sd	w'/h'	w'/h'	r	r					w'/h'
l'/i'	m	m	m	<u>x</u>	sd	sd	l'/i'	l'/i'	r	r	r				l'/i'
l'/h'	m	m	m	m	<u>x</u>	sd	l'/h'	l'/h'	r	r	r	r			l'/h'
l'/w'	m	m	m	m	m	<u>x</u>	l'/w'	l'/w'	r	r	r	r	r		l'/w'
m	H/W	H/I	w'/h'	l'/i'	l'/h'	l'/w'		r	H/W	H/I	w'/h'	l'/i'	l'/h'	l'/w'	

b. Model example of the grid for timeseries correlations in shape parameters.

	H/W	H/I	w'/h'	l'/i'	l'/h'	l'/w'	b
H/W	<u>x</u>	b	b	b	b	b	H/W
H/I	a	<u>x</u>	b	b	b	b	H/I
w'/h'	a	a	<u>x</u>	b	b	b	w'/h'
l'/i'	a	a	a	<u>x</u>	b	b	l'/i'
l'/h'	a	a	a	a	<u>x</u>	b	l'/h'
l'/w'	a	a	a	a	a	<u>x</u>	l'/w'
a	H/W	H/I	w'/h'	l'/i'	l'/h'	l'/w'	

c. Model example of the grid for timeseries correlations in trajectory parameters.

	ind	tw	g%	dist	chi	type	%
ind		%	%	%	%	%	ind
tw	H		%	%	%	%	tw
g%	H	H		%	%	%	g%
dist	H	H	H		%	%	dist
chi	H	H	H	H		%	chi
type	H	H	H	H	H		type
H	ind	tw	g%	dist	chi	type	

d. Model example of the grid for timeseries correlations in categorical parameters.

Text Table 8.2 a – d. generic formats for timeseries correlation grids. A full explanation is given in the commentary overleaf.

Text Tables 8.2 a – f.

Grids a – d. (previous page) show the general format for timeseries correlation as presented in the text of forthcoming sections. The lefthand box of grid a and grid b (sizes and shapes) display the values for means (m) and standard deviations (sd) with correlations between a mean and standard deviation for the same character appearing in the underlined diagonal position across the centre (x); the righthand part of both grids a and b give an equivalent field for rates of change (r).

Grid c shows this same array for the trajectory parameters which have no rate measurements. Again the central diagonal (x) shows the relationship between ‘a’ and ‘b’ values for each individual character ratio.

Grid d shows the same arrangement for the categorical parameters of diversity (H) and percentage similarity (%). Note that the diagonal position is left unfilled as it is impossible to seek correlations between these two parameters when ‘H’ measures a characteristic of each sample population whereas ‘%’ measures the relationship between pairs of sample populations.

100 kyr Folkestone - Size																			
<u>x</u>	H	W	I	Ch	<u>l'</u>	h'	w'	i'	sd		H	W	I	Ch	<u>l'</u>	h'	w'	i'	
H	<u>1</u>	0	1	1	0	0	1	0	H	H									H
W	1	<u>0</u>	0	0	1	0	0	0	W	W	0								W
I	1	1	<u>1</u>	1	0	0	0	0	I	I	1	0							I
Ch	1	0	0	<u>1</u>	0	1	0	0	Ch	Ch	0	0	0						Ch
l'	1	1	0	0	<u>0</u>	0	0	1	l'	l'	0	1	0	0					l'
h'	0	1	0	0	1	<u>0</u>	0	0	h'	h'	0	0	0	0	0				h'
w'	1	1	1	0	1	1	<u>0</u>	0	w'	w'	0	0	0	0	1	0			w'
i'	0	1	0	0	0	0	0	<u>0</u>	i'	i'	0	0	0	0	0	0	0		i'
m	H	W	I	Ch	l'	h'	w'	i'		r	H	W	I	Ch	l'	h'	w'	i'	

actual & possible	14	28	3	8	7	28	3	28	27	92
% significant	m	50.0	x	37.5	sd	25.0	r	10.7	all	29.3

e. A genuine example of a grid displaying statistical tests of timeseries correlations in size parameters for the 100 kyr transect at Folkestone.

100 kyr Between-Site — Size											
	H	W	I	Ch	l'	h'	w'	i'		% sig	
SF	1	0	1	1	1	1	0	0	m	62.5	m
FE	1	1	1	1	1	1	1	0	m	87.5	m
ES	1	0	1	1	1	1	0	0	m	62.5	m
SF	0	0	0	0	0	1	1	0	sd	25.0	sd
FE	1	0	0	0	0	0	0	0	sd	12.5	sd
ES	1	0	0	0	0	0	0	0	sd	12.5	sd
SF	1	0	1	1	0	0	0	0	r	37.5	r
FE	0	0	0	0	0	0	0	0	r	0.0	r
ES	0	0	0	0	0	0	0	0	r	0.0	r
	H	W	I	Ch	l'	h'	w'	i'		% sig	

f. An example of a grid displaying statistical tests of timeseries correlations in size parameters for the 100 kyr transects.

When these grids appear in the text, all the correlations significant at 95% confidence are shown in bold. Positive correlations are marked with '1' and negative correlations are marked with '-1'. Cases of no significant correlation are marked with '0'. Grid e (last page) shows a genuine example drawn from the text: it is the table of correlations in size parameters for the 100 kyr section at Folkestone (compare it with specimen grid a from two pages back). It tells us, for example, that timeseries shifts in the mean and standard deviation for H (\underline{x}) are both correlated with one another, and that the correlation is positive (upper lefthand underlined cell in the leftmost grid). It also tells us that the timeseries for mean (m) H positively correlates with the timeseries for mean W (next cell down), but that the standard deviation (sd) timeseries for H and W do not correlate (second cell along on the upper row). These findings can be investigated further by examining Appendix Figures 5.3.1.i and 5.3.1.ii to which the correlation tests relate.

The lowermost strip of Text Table 8.2.e is a summary table showing the proportion of significant correlations as a percentage of those possible. Here we see that there are 28 possible ways for a timeseries of mean values to correlate with another such timeseries (e.g. H with W , H with I etc.) and from that field of 28 possible combinations 14 of them (50%) do in fact register as significant.

The tests are two tailed, meaning that the probability level of 95% applies to correlations of any sort, both positive and negative; consequently, any individual case of positive or negative correlation actually needs to be significant to a level of 97.5% to pass. Default expectation under a null hypothesis of zero correlation is for 5% of the cells to register as significant; default expectation under a null hypothesis of complete correlation (positive or negative) is for 95% of the cells to register as significant.

An additional type of grid, shown above as f, is used with the 100 kyr sections to summarise relationships between the three sites. SF stands for Southerham-Folkestone, FE for Folkestone-Escalles and ES for Escalles-Southerham. Each character is paired only with the same character between sites, so the space of possible combinations is 8 for the sizes and 6 for shapes, trajectories and categories; the percentage of significant correlations as a proportion of those possible is summarised in the righthand column.

Like grid e, grid f is an example drawn from genuine data and shows that the timeseries of mean values for most characters are highly positively correlated between all

three sites (up to 7/8 or 87.5% for FE) but that the standard deviations and rates are not. Again this can be investigated further by examining the graphic display of this data presented in Appendix Figures 5.3.1. The primary purpose of the grids is to draw attention to correlated pairings from among the mass of Appendix Figures, and to simultaneously act as an easy reference point for checking visual intuition when looking at the figures themselves.

8.1.6 Presentation Sequence

Like the material appearing in Parts II and III, the morphometric timeseries charts are presented in a standard sequence. Firstly, they are broken into separate scales, as they were for the environmental data in Part II. The sequence is once again: 2 kyr, 20 kyr and 100 kyr, followed by all three scales combined in a single format. Within each of these blocks, the data are then broken into character types, so that size changes are examined first, followed by shapes, then trajectory parameters, and finally the categorical characters. For the calculations, *t* tests come first, *F* tests second and *Z* tests third, with *haldanes* considered last. Within each parameter or test type block the character ordering introduced in Part III is normally preserved: *H*, *W*, *I*, *Ch*, *l'*, *h'*, *w'*, *i'*; *H/W*, *H/I*, *w'/h'*, *l'/i'*, *l'/h'*, *l'/w'*; *ind.*, *tw*, *g%*, *g.dist*, *type* and *chir*.

The presentation of appendix figures and tables both follow this sequence, with its general structure clearly visible in the contents listing. Likewise, the text discussion follows the same set pattern, split into scales and into character types. However, the text itself also has an intermediate layer of organisation. Within each section covering a specific sampling scale the discussion is separated into three distinct areas of interest:

- *Patterns of individual characters*: similarities and differences in central tendency, variation, trajectory parameters, rate of change, or categorical measurement per specific character (*H*, *h'*, *H/W* ratio, *H/W a* value, *twist* etc.); these include trends, saltations, net changes, stasis, oscillation, parallel tracks and so forth.

- *Patterns of a systematic nature:* similarities and differences in magnitude or frequency of change between general types of parameter: between sizes, shapes and trajectories; between central tendency and variance; between sites or scales and so on.
- *Patterns correlating with environmental factors:* systematic distinctions of any type between zones of interest; between zones of relative stability, or between lithological divisions in the case of the single couplet.

One other factor, mentioned here simply because there is no other suitable context, is that one of the categorical characters, glauconite distribution (*g.dist*), receives two modes of presentation. Originally, the presence of no glauconite at all was classed as category 0, alongside categories 1-5 (see Section 6.1.3). On examination, however, it soon became apparent that the zero glauconite category is rather large and tends to totally dominate any chart or measurement it features in, especially in cases of relative abundance. It seemed a little unfair to be judging glauconite distribution mostly by its absence, so the solution has been to present *g.dist* twice, once with the zero category in place and once with it removed. Since the zero-free populations then have very variable sample numbers which need to be listed somewhere, that somewhere, for the record, is in Text Table 8.3.

Horizon	B31	B37	B41	C5	C10	C15	C21	C29	C35	C40	C45		
S 100 kyr	38	42	35	40	23	38	30	33	43	44	38		
F 100 kyr	35	31	28	36	23	21	38	42	43	40	42		
E 100 kyr	—	39	15	40	30	29	24	42	44	41	43		
Horizon	C10	C11	C12	C13	C14	C15	C16	C17	C18	C19	C20	C21	
F 20 kyr	23	39	38	34	38	21	25	41	42	38	43	38	
Horizon C13	-0	-1	-2	-3	-4	-5	-6	-7	-8	-9	-10	-11	-12
F 2 kyr	41	42	45	35	33	33	39	41	37	13	44	43	34

Text Table 8.3 *Specimen numbers per sample for the non-zero category g.dist populations.*

8.1.7 Taphonomic Considerations

Having already used Section 3.2.5 to examine the range of taphonomic effects, there is not a great deal to add. Taphonomic interference can affect the morphological signal in various ways. Firstly, poor preservation can mask measuring points, the most

likely examples of which occur when chamber sutures are concealed by cemented detritus or recrystallisation, or when the carinate edges of the test are worn enough to produce a false magnitude for the *W* or *ind* measurements. Although the specimens examined were, for the most part, very well preserved (or at least the best available), there *are* differences in the quality, and as a result some measurements must be a little less precise than they would be under ideal conditions. The second and more important effect is when the general quality of preservation differs from bed to bed. Preservation blackspots have already been highlighted in earlier sections (see Text Figure 3.4), so the cautious reader might care to take these into account when evaluating the morphological patterns. I am confident, however, that they have a negligible influence on the overall conclusions.

Section 8.2 Results

8.2.1 2 kyr Resolution

The closely spaced sample points of C13 provide the highest resolution portrait we have of morphological change in *Tritaxia*; they represent the nearest interface with events observable on a neontological time frame. Text Table 8.4 shows the location of charts and tables relevant to this scale of investigation.

Charts	Contents	Location
Size	means and standard deviation	Appdx. Figs. 5.1.1.i-viii
Shape	means and standard deviation	Appdx. Figs. 5.1.2.i-vi
Trajectory	<i>a</i> and <i>b</i> values	Appdx. Figs. 5.1.3.i-vi
Categoricals	area, % similarity, diversity	Appdx. Figs. 5.1.4.i-vii
Tables	Contents	Location
Size	<i>t</i> tests	Appdx. Tabs. 3.2.1.i-viii
Size	<i>F</i> tests	Appdx. Tabs. 3.2.2.i-viii
Size	<i>haldanes</i>	Appdx. Tabs. 3.5.1.a
Shape	<i>t</i> tests	Appdx. Tabs. 3.2.3.i-vi
Shape	<i>F</i> tests	Appdx. Tabs. 3.2.4.i-vi
Shape	<i>haldanes</i>	Appdx. Tabs. 3.5.1b
Trajectory	<i>Z</i> tests	Appdx. Tabs. 3.2.5.i-vi
Categoricals	% similarity	Appdx. Tabs. 3.6.1
Categoricals	diversity	Appdx. Tabs. 3.6.2

Text Table 8.4 *Location of morphometric information for the 2 kyr scale transect.*

8.2.1.i Individual Patterns

8.2.1.i.a Size

While there are certain similarities between the timeseries patterns of individual characters, good correlations are surprisingly rare for what we know to be developmentally linked features (Section 6.2.2). Indeed, the four fields of Text Table 8.5 (*m*, *sd*, *x̄* (i.e. *m* vs. *sd*) and *r*) record just 7 examples of correlation out of 92 possible cases—only 7.6%, and thus very close to the expected 5% of a zero-correlation null hypothesis.

2 kyr Folkestone — Size																			
<u>x</u>	<i>H</i>	<i>W</i>	<i>I</i>	<i>Ch</i>	<i>l'</i>	<i>h'</i>	<i>w'</i>	<i>i'</i>	<i>sd</i>		<i>H</i>	<i>W</i>	<i>I</i>	<i>Ch</i>	<i>l'</i>	<i>h'</i>	<i>w'</i>	<i>i'</i>	
<i>H</i>	<u>0</u>	0	0	1	0	1	0	0	<i>H</i>	<i>H</i>									<i>H</i>
<i>W</i>	0	<u>0</u>	0	0	1	1	0	0	<i>W</i>	<i>W</i>	0								<i>W</i>
<i>I</i>	0	0	<u>0</u>	0	0	0	0	0	<i>I</i>	<i>I</i>	0	0							<i>I</i>
<i>Ch</i>	1	0	0	<u>0</u>	0	0	0	0	<i>Ch</i>	<i>Ch</i>	0	0	0						<i>Ch</i>
<i>l'</i>	0	0	0	0	<u>0</u>	1	0	0	<i>l'</i>	<i>l'</i>	0	0	0	0					<i>l'</i>
<i>h'</i>	0	0	0	0	0	<u>0</u>	0	0	<i>h'</i>	<i>h'</i>	0	0	0	0	0				<i>h'</i>
<i>w'</i>	0	0	0	0	0	1	<u>0</u>	0	<i>w'</i>	<i>w'</i>	0	0	0	0	0	0			<i>w'</i>
<i>i'</i>	0	0	0	0	0	0	0	<u>0</u>	<i>i'</i>	<i>i'</i>	0	0	0	0	0	0	0		<i>i'</i>
<i>m</i>	<i>H</i>	<i>W</i>	<i>I</i>	<i>Ch</i>	<i>l'</i>	<i>h'</i>	<i>w'</i>	<i>i'</i>		<i>r</i>	<i>H</i>	<i>W</i>	<i>I</i>	<i>Ch</i>	<i>l'</i>	<i>h'</i>	<i>w'</i>	<i>i'</i>	

actual & possible	2	28	0	8	5	28	0	28	7	92
% significant	<i>m</i>	7.1	<u><i>x</i></u>	0.0	<i>sd</i>	17.9	<i>r</i>	0.0	all	7.6

Text Table 8.5. Timeseries correlations for size parameters in the 2 kyr transect. Results in bold are significant at the 95% confidence level. See Text Table 8.4 (above) for the chart locations and Section 8.1.5.iv for a discussion of the correlations and correlation grid layout. The lowermost strip summarises actual significant values as a percentage of the total number possible for each of five fields: means with means (*m*), standard deviations with standard deviations (*sd*), means with standard deviations (*x*), rates with rates (*r*), and all these fields collectively (*all*).

For some character dimensions (e.g. *W*, *I*, *w'* and *i'*), the values at lower sample horizons (C13-0 – C13-3 [-2 - 4]) are often significantly larger than those of populations from higher in the transect, particularly from samples in the chalk (C13-9 – C13-11 [16 - 20]). Even in other characters where the effect is less marked, there is rarely a significant difference between chalk and marl in which a chalk value is larger than one from the marl (Appdx. Tabs 3.2.1); the only exception is chamber number (*Ch*), which shows a significant spike across the chalk. One tentative conclusion, therefore, although the effect is not striking, is that specimens from the chalk are often smaller in some way than specimens from the marl. Supporting evidence is to be found in the absence of unusually large individuals (the outliers excluded from the calculated averages) from any chalk samples (see Text Table 8.1).

W, and to a lesser extent the whole suite of final chamber characters, *l'*, *h'*, *w'* and *i'*, all show a peak of variation around the marl to chalk transition zone in the middle of the couplet (at C13-7 [12]). Standard deviation does not correlate with the patterns shown by central tendency, suggesting that variation is an independent aspect of the sampled populations. This is by no means an obvious finding since we are dealing with ‘scalar’ characters tethered to a wall of minimum size; it would be perfectly reasonable to expect

diffusion away from that wall to result in an increase of magnitude in both variation and central tendency, but in fact this seems rarely to happen. Variation does generally decrease across the cycle, however, being higher in the early half of the couplet than it is later on in the chalk, and this pattern might reflect a weak link with the changes in mean size

Rates correlate particularly poorly between characters. Spurts of change in one character dimension are offset by relative stasis in other characters, giving an impression of morphology as a patchwork of independently slipping variables. There is little indication that a particular rate of change was associated with either specific characters or zones of the couplet, and the overall impression from central tendency, variation, and rate plots alike, is one of general stability.

8.2.1.i.b Shape

2 kyr Folkestone — Shape															
<u>x</u>	H/W	H/I	w'/h'	l'/i'	l'/h'	l'/w'	sd		H/W	H/I	w'/h'	l'/i'	l'/h'	l'/w'	
H/W	<u>0</u>	0	0	0	0	0	H/W	H/W							H/W
H/I	0	<u>0</u>	0	0	0	0	H/I	H/I	0						H/I
w'/h'	0	0	<u>0</u>	0	1	0	w'/h'	w'/h'	0	1					w'/h'
l'/i'	0	0	0	<u>0</u>	0	0	l'/i'	l'/i'	0	1	1				l'/i'
l'/h'	0	0	0	0	<u>0</u>	0	l'/h'	l'/h'	0	0	0	0			l'/h'
l'/w'	0	0	0	0	1	<u>0</u>	l'/w'	l'/w'	0	0	0	0	0		l'/w'
m	H/W	H/I	w'/h'	l'/i'	l'/h'	l'/w'		r	H/W	H/I	w'/h'	l'/i'	l'/h'	l'/w'	

actual & possible	1	15	0	6	1	15	3	15	5	51
% significant	m	6.7	<u>x</u>	0.0	sd	6.7	r	20.0	all	9.8

Text Table 8.6. Timeseries correlations for shape parameters in the 2 kyr transect. Results in bold are significant at the 95% confidence level. See Text Table 8.4 (above) for the chart locations and Section 8.1.5.iv for a discussion of the correlations and correlation grid layout. The lowermost strip summarises actual significant values as a percentage of the total number possible for each of five fields: means with means (m), standard deviations with standard deviations (sd), means with standard deviations (x), rates with rates (r), and all these fields collectively (all).

The shape characters show only 5 correlations from four fields collectively comprising 51 possible instances, but at 9.8% even this modest number is roughly twice what we should expect from a null hypothesis of zero correlation.

The mean H/W ratio shows a long trough across the marl-chalk boundary and then a pronounced and significant peak in the upper reaches of the chalk, especially at horizon C13-10 [18], in which the specimens tend to be particularly narrow relative to their overall

height. H/I , by contrast, shows a low point early on at C13-3 [4], which then passes into a high jagged plateau, culminating in a peak at C13-10 [18], and representing a transition from a population with ‘high centre of gravity’ individuals early on (i.e. those in which W intersects H close to the final chamber) to low centre of gravity forms (with W closer to the mid-point of H) in the chalk horizons.

Of the final chamber combinations, w'/h' and l'/i' show long, loose oscillations over several sampling horizons, whereas l'/h' and especially l'/w' show something closer to a transition from stasis early on to sharply oscillating anagenesis in the cycle’s upper half, an intuition confirmed by a glance at their rate of change. Note that the l'/h' ratio also shows a pronounced kink at C13-10 [18] corresponding to a final chamber type which is high for its length (as is also quite clear from the size parameters).

Together, these low centre of gravity forms with final chambers high for their length suggests that the chalk tended to host exotic growth types akin to the Phase II B forms described in Section 6.1.3.i; the categorical data confirm this suspicion.

8.2.1.i.c Trajectory

2 kyr Folkestone — Trajectory							
<u>x</u>	H/W	H/I	w'/h'	l'/i'	l'/h'	l'/w'	b
H/W	-1	0	0	0	0	0	H/W
H/I	0	-1	0	0	0	0	H/I
w'/h'	0	0	-1	0	0	0	w'/h'
l'/i'	0	0	0	-1	0	1	l'/i'
l'/h'	0	0	0	0	-1	1	l'/h'
l'/w'	0	0	-1	1	0	-1	l'/w'
a	H/W	H/I	w'/h'	l'/i'	l'/h'	l'/w'	

actual & possible	2	15	6	6	2	15	10	36
% significant	a	13.3	<u>x</u>	100.0	b	13.3	all	27.8

Text Table 8.7 *Timeseries correlations for trajectory parameters in the 2 kyr transect. Results in bold are significant at the 95% confidence level. See Text Table 8.4 (above) for the chart locations and Section 8.1.5.iv for a discussion of the correlations and correlation grid layout. The lowermost strip summarises actual significant values as a percentage of the total number possible for each of four fields: a values with a values (a), b values with b values (b), a values with b values (x), and all these fields collectively (all).*

With 10 out of the 36 possible pairings significant (27.7%), Text Table 8.7 immediately tells us that there is more regularity in the trajectory data than we saw for either

sizes or shapes. As mentioned earlier in Section 8.1.5.iv, the *b* value data have a skewed distribution which renders the *t* test methodology rather suspect, but a glance at the charts themselves rapidly confirms the statistical result we see here. This striking negative correlation between the values of *a* and *b* is eerily consistent for all the character pairings, and it absolutely demands an explanation (I shall provide one in the next chapter).

Other than that, values for the *H/W* exponent (*a*) show a large and significant kink at the marl-chalk boundary (horizons C13-6, 7 & 8 [10-14]), swerving away from a jagged plateau of 1.5 - 1.75 towards isometry. None of the other pairings has a regular or easily classified nature; most of them oscillate around an average value, occasionally deviating far enough to qualify as significant, but with nothing like a trend or any other outstanding pattern to their behaviour.

8.2.1.i.d. Categorical

2 kyr Folkestone — Categorical							
	<i>ind</i>	<i>tw</i>	<i>g%</i>	<i>dist</i>	<i>chi</i>	<i>type</i>	H
<i>ind</i>		0	0	0	0	0	<i>ind</i>
<i>tw</i>	0		0	0	0	0	<i>tw</i>
<i>g%</i>	0	1		0	0	0	<i>g%</i>
<i>dist</i>	0	0	0		0	0	<i>dist</i>
<i>chi</i>	0	0	0	0		0	<i>chi</i>
<i>type</i>	0	0	0	0	0		<i>type</i>
<i>s %</i>	<i>ind</i>	<i>tw</i>	<i>g%</i>	<i>dist</i>	<i>chi</i>	<i>type</i>	

actual & possible	0	15	1	15	1	30
% significant	H	0.0	s %	6.7	all	3.3

Text Table 8.8 *Timeseries correlations for category parameters in the 2 kyr transect. Results in bold are significant at the 95% confidence level. See Text Table 8.4 (above) for the chart locations and Section 8.1.5.iv for a discussion of the correlations and correlation grid layout. The lowermost strip summarises actual significant values as a percentage of the total number possible for each of three fields: H values with H values (H), percentage similarity values with percentage similarity values (s %), and both these fields collectively (all).*

A single positive correlation in a field of 30 possible pairings cannot be distinguished from noise, so we must accept that these changes in the categorical metrics are essentially independent from one another over the 2 kyr transect.

Several of the categorical characters—*ind*, *tw*, *g%* and *g.dist*—seem to show an increase in diversity and magnitude of change around the middle of the transect, but aside from that there is little regular or pattern-like behaviour to be found. Some characters, like *tw*, *type* and *chir* maintain well-defined and relatively stable relationships between their categories, while others, such as *g.dist*, do not appear to possess stable character frequencies at all, having populations that oscillate fluidly and rapidly between adjacent samples. In anticipation of the sections to come, the most noteworthy feature appearing in the 2 kyr categorical charts is a small increase in exotic, non-triserial growth *types* towards the upper reaches of the chalk.

8.2.1.ii Systematic Patterns

Four of the size characters, *H*, *I*, *w'*, and *i'*, show a net change between the base of the transect and the top, but none of the shape or trajectory parameters do. Many other significant differences are to be found within the transect, all of them cancelling out due to reversals. Genuine saltations are fairly rare, but lurches like the change in *H/I* ratio between C13-4 and C13-5 [6-8], or spikes like the one in the *l'/h'* plot at C13-10 [18], might qualify.

Examination of a summary table for statistical tests (see Text Table 8.37 placed ahead on p 407 for a comprehensive listing or Text Table 8.9, below, for highlights) reveals that there were many more significant changes in mean shape than in size (half as many again—19.7% vs. 29.7%, shown in cells d10 and d17, respectively), and fewest changes of all in trajectory parameter *a* (12.2%, in cell d44). There is an order of magnitude difference between the highest and lowest percentages of actual-as-a-proportion-of-possible differences (47.4% for *H/I* vs. 3.8% for *h'*), but no obvious partition in this transect into, say, whole test characters versus final chamber ones.

With respect to the *F* tests identifying shifts in variance, there is far less divergence between sizes and shapes (20.5% vs. 22.9% - cells d28 vs. d35 in Txt Tab. 8.37) than there was with the *t*-tests for shifts in central tendency. Finally, rates of change also tend to be slightly higher for shapes than for sizes (Appendix Tables 3.5.1.a & b, final column).

Size	<i>H</i>	<i>W</i>	<i>I</i>	<i>Ch</i>	<i>l'</i>	<i>h'</i>	<i>w'</i>	<i>i'</i>	Mean
% sig. <i>t</i> test	10.3	21.8	39.7	11.5	11.5	3.8	30.8	28.2	19.7
% sig. <i>F</i> test	14.1	33.3	20.5	15.4	21.2	12.2	12.2	35.3	20.5
Shape		<i>H/W</i>	<i>H/I</i>	<i>w'/h'</i>	<i>l'/i'</i>	<i>l'/h'</i>	<i>l'/w'</i>		
% sig. <i>t</i> test		26.9	47.4	28.2	26.9	16.7	32.1		29.7
% sig. <i>F</i> test		14.1	37.2	15.4	23.7	35.3	11.5		22.9
Trajectory		<i>H/W</i>	<i>H/I</i>	<i>w'/h'</i>	<i>l'/i'</i>	<i>l'/h'</i>	<i>l'/w'</i>		
% sig. <i>Z</i> test		15.4	6.4	14.1	10.3	6.4	20.5		12.2

Text Table 8.9 *Significant differences as a percentage of those possible between variation and central tendency values in the 2 kyr resolution transect: size and shape, F and t tests at 95% confidence for means and standard deviation, trajectory Z tests at 95% confidence for values of the allometric exponent, ‘a’.*

8.2.1.iii Environmental Patterns

As explained in Section 8.1.4.ii, the single couplet was partitioned in two different ways. To mirror lithological changes the transect was split into a portion representing the marl (sample points C13-1 to C13-6 [0 - 10]), a portion representing the chalk (C13-8, C13-9, C13-10 & C13-11 [14 - 20]), and one representing the boundary zones (C13-0, C13-6, C13-7, C13-8 & C13-12 [-2, 10, 12, 14 & 22]); the percentage of statistical shifts in each of these fields is presented in Text Figure 8.10. In spite of the overlap between them, some of these fields are still very small and thus highly subject to sampling error; consequently, a more robust but less discriminating partition was also performed, this time into upper and lower halves, split around bed C13-6 [10], which contributes to both sides (Text Table 8.11).

The results are fairly even, but with a weak tendency for change to be concentrated in the marl (which has a sample point more than the boundary, and two more than the chalk), or in the lower half, depending on which division is used. The tendency, however, really is weak—probably weak enough to be discounted as random. Out of 34 possible factors (8 mean sizes and their variances, 6 mean shapes and their variances, and 6 trajectory *a* values), the marl had the highest proportion of significant differences in 13 cases, the boundary in 9 and the chalk in 9, with 3 ties; when split into upper and lower halves, the lower (marly) half had 19 instances in which the proportion of significant differences was highest, the upper half (chalk plus boundaries) had 14, with one tie. And when character values are averaged (rows 10, 17, 28, 35 & 44 of Text Table 8.10), the results come out

	a	b	c	d	e	f	g	h	i	j
1	<i>t tests</i>	chalk	b'dry	marl	m. int.	c-m	c-b	m-b	m. ext.	m. all
2	<i>H</i>	0.0	20.0	13.3	11.1	8.3	0.0	23.3	10.6	10.8
3	<i>W</i>	16.7	10.0	0.0	8.9	41.7	20.0	10.0	23.9	16.4
4	<i>I</i>	0.0	30.0	46.7	25.6	45.8	15.0	53.3	38.1	31.8
5	<i>Ch</i>	0.0	0.0	0.0	0.0	29.2	25.0	0.0	18.1	9.0
6	<i>l'</i>	33.3	10.0	6.7	16.7	12.5	15.0	6.7	11.4	14.0
7	<i>h'</i>	0.0	0.0	6.7	2.2	4.2	0.0	6.7	3.6	2.9
8	<i>w'</i>	0.0	40.0	26.7	22.2	41.7	25.0	30.0	32.2	27.2
9	<i>i'</i>	0.0	20.0	6.7	8.9	54.2	20.0	20.0	31.4	20.1
10	m.size	6.3	16.3	13.3	11.9	29.7	15.0	18.8	21.1	16.5
11	<i>H/W</i>	33.3	30.0	20.0	27.8	33.3	50.0	16.7	33.3	30.6
12	<i>H/I</i>	33.3	0.0	60.0	31.1	62.5	30.0	50.0	47.5	39.3
13	<i>w'/h'</i>	0.0	30.0	33.3	21.1	37.5	20.0	23.3	26.9	24.0
14	<i>l'/i'</i>	0.0	0.0	0.0	0.0	62.5	10.0	26.7	33.1	16.5
15	<i>l'/h'</i>	50.0	0.0	0.0	16.7	25.0	25.0	3.3	17.8	17.2
16	<i>l'/w'</i>	0.0	60.0	46.7	35.6	33.3	30.0	40.0	34.4	35.0
17	m. shape	19.4	20.0	26.7	22.0	42.4	27.5	26.7	32.2	27.1
18	m. c.t.	11.9	17.9	19.0	16.3	35.1	20.4	22.1	25.9	21.1
19	<i>F tests</i>	chalk	b'dry	marl	m. int.	c-m	c-b	m-b	m. ext.	m. all
20	<i>H</i>	0.0	20.0	26.7	15.6	20.8	5.0	30.0	18.6	17.1
21	<i>W</i>	41.7	40.0	0.0	27.2	33.3	45.0	20.0	32.8	30.0
22	<i>I</i>	0.0	0.0	26.7	8.9	33.3	5.0	26.7	21.7	15.3
23	<i>Ch</i>	33.3	0.0	20.0	17.8	16.7	25.0	23.3	21.7	19.7
24	<i>l'</i>	16.7	10.0	33.3	20.0	12.5	15.0	23.3	16.9	18.5
25	<i>h'</i>	0.0	30.0	6.7	12.2	8.3	20.0	10.0	12.8	12.5
26	<i>w'</i>	0.0	10.0	0.0	3.3	25.0	10.0	6.7	13.9	8.6
27	<i>i'</i>	25.0	40.0	40.0	35.0	25.0	50.0	33.3	36.1	35.6
28	m.size	14.6	18.8	19.2	17.5	21.9	21.9	21.7	21.8	19.7
29	<i>H/W</i>	16.7	30.0	0.0	15.6	16.7	20.0	10.0	15.6	15.6
30	<i>H/I</i>	58.3	50.0	40.0	49.4	33.3	35.0	36.7	35.0	42.2
31	<i>w'/h'</i>	0.0	0.0	33.3	11.1	16.7	0.0	16.7	11.1	11.1
32	<i>l'/i'</i>	0.0	30.0	13.3	14.4	29.2	5.0	43.3	25.8	20.1
33	<i>l'/h'</i>	50.0	30.0	46.7	42.2	37.5	25.0	30.0	30.8	36.5
34	<i>l'/w'</i>	0.0	0.0	20.0	6.7	25.0	0.0	10.0	11.7	9.2
35	m. shape	20.8	23.3	25.6	23.2	26.4	14.2	24.4	21.7	22.5
36	m. var.	17.3	20.7	21.9	20.0	23.8	18.6	22.9	21.7	20.9
37	<i>Z tests</i>	chalk	b'dry	marl	m. int.	c-m	c-b	m-b	m. ext.	m. all
38	<i>H/W</i>	33.3	0.0	13.3	15.6	12.5	20.0	26.7	19.7	17.6
39	<i>H/I</i>	0.0	0.0	20.0	6.7	8.3	0.0	0.0	2.8	4.7
40	<i>w'/h'</i>	0.0	0.0	20.0	6.7	12.5	5.0	20.0	12.5	9.6
41	<i>l'/i'</i>	0.0	0.0	26.7	8.9	8.3	0.0	13.3	7.2	8.1
42	<i>l'/h'</i>	0.0	10.0	6.7	5.6	12.5	5.0	10.0	9.2	7.4
43	<i>l'/w'</i>	0.0	0.0	60.0	20.0	16.7	0.0	20.0	12.2	16.1
44	m. exp. a	5.6	1.7	24.4	10.6	11.8	5.0	15.0	10.6	10.6
45	m. all	13.0	16.2	21.2	16.8	26.3	16.9	21.2	21.5	19.1

Text Figure 8.10 Summary of statistical tests for lithological sub-regions of the 2 kyr transect.

The transect is split into fields representing the chalk (c - samples 8, 9, 10 & 11), the marl (m - samples 1, 2, 3, 4, 5 & 6), or the boundary areas (b - samples 0, 6, 7, 8 & 12). Note that there is overlap between the designated regions such that some horizons are used more than once; it is also important to recognise that some of these fields are very small (e.g. the chalk field has only 6 possible combinations ($4 \times 4 - 4 = 12$, divided by 2 for repetitions) and will thus be quite susceptible to statistical noise.

The chart examines the percentage of sample pairings per designated region which differ significantly from one another (to a 95% confidence) in terms of the characters involved or the type of test used. For example, entry b2 shows that for *t* tests of mean shift in the character *H* there are no significantly different pairings within the chalk (i.e. between samples 8, 9, 10 & 11 - compare with Appdx. Table 3.2.1.i for confirmation); entry d2 shows that 13.3% (2 out of 15) of the possible pairings within the marl region are significant; while f2 and g2 show that 8.3% (2 out of 24) of the chalk and marl samples register as different from one another, while none of the chalk and boundary samples do.

Summary values (means) appear in the columns or rows bounding particular types of grouping to help pick out, for example, whether there are more differences internal (int) to particular groupings (column e) or between them (ext) (column i), or between, say, sizes (rows 10 & 28) or shapes (rows 17 & 35). var. = variation, ct = central tendency, exp.a = allometric exponent. Important features to note from this chart are discussed in the surrounding text.

		2 k	2 k	2 k	2 k	2 k	20 k	20 k	20 k	20 k	20 k
	a	b	c	d	e	f	g	h	i	j	k
1	<i>t tests</i>	U	L	m. int.	U-L	m. all	U	L	m. int.	U-L	m. all
2	<i>H</i>	0.0	14.3	7.1	16.3	10.2	14.3	46.7	30.5	61.9	41.0
3	<i>W</i>	19.0	0.0	9.5	28.6	15.9	23.8	13.3	18.6	31.0	22.7
4	<i>I</i>	0.0	42.9	21.4	55.1	32.7	42.9	26.7	34.8	42.9	37.5
5	<i>Ch</i>	19.0	0.0	9.5	16.3	11.8	0.0	20.0	10.0	16.7	12.2
6	<i>l'</i>	19.0	4.8	11.9	12.2	12.0	14.3	46.7	30.5	52.4	37.8
7	<i>h'</i>	0.0	4.8	2.4	4.1	2.9	9.5	33.3	21.4	59.5	34.1
8	<i>w'</i>	9.5	28.6	19.0	38.8	25.6	28.6	13.3	21.0	69.0	37.0
9	<i>i'</i>	14.3	4.8	9.5	42.9	20.6	19.0	20.0	19.5	23.8	20.9
10	m.size	10.1	12.5	11.3	26.8	16.5	19.1	27.5	23.3	44.7	30.4
11	<i>H/W</i>	42.9	23.8	33.3	28.6	31.7	4.8	13.3	9.1	57.1	25.1
12	<i>H/I</i>	19.0	57.1	38.1	53.1	43.1	42.9	26.7	34.8	31.0	33.5
13	<i>w'/h'</i>	4.8	33.3	19.0	36.7	24.9	14.3	20.0	17.2	19.0	17.8
14	<i>l'/i'</i>	4.8	0.0	2.4	42.9	15.9	19.0	20.0	19.5	23.8	20.9
15	<i>l'/h'</i>	28.6	0.0	14.3	16.3	15.0	28.6	0.0	14.3	11.9	13.5
16	<i>l'/w'</i>	28.6	42.9	35.7	34.7	35.4	4.8	20.0	12.4	4.8	9.9
17	m. shape	21.4	26.2	23.8	35.4	27.7	19.1	16.7	17.9	24.6	20.1
18	m. c.t.	15.0	18.4	16.7	30.5	21.3	19.1	22.9	21.0	36.1	26.0
19	<i>F tests</i>	U	L	m. int.	U-L	m. all	U	L	m. int.	U-L	m. all
20	<i>H</i>	9.5	19.0	14.3	20.4	16.3	23.8	33.3	28.6	26.2	27.8
21	<i>W</i>	47.6	0.0	23.8	34.7	27.4	28.6	0.0	14.3	14.3	14.3
22	<i>I</i>	0.0	23.8	11.9	28.6	17.5	38.1	40.0	39.1	31.0	36.4
23	<i>Ch</i>	19.0	23.8	21.4	16.3	19.7	19.0	20.0	19.5	14.3	17.8
24	<i>l'</i>	21.4	28.6	25.0	16.3	22.1	42.9	0.0	21.5	33.3	25.4
25	<i>h'</i>	23.8	4.8	14.3	9.2	12.6	28.6	33.3	31.0	33.3	31.7
26	<i>w'</i>	11.9	0.0	6.0	14.3	8.7	28.6	0.0	14.3	16.3	15.0
27	<i>i'</i>	50.0	28.6	39.3	38.8	39.1	28.6	6.7	17.7	14.3	16.5
28	m.size	22.9	16.1	19.5	22.3	20.4	29.8	16.7	23.2	22.9	23.1
29	<i>H/W</i>	28.6	0.0	14.3	14.3	14.3	33.3	33.3	33.3	31.0	32.5
30	<i>H/I</i>	40.5	28.6	34.5	37.8	35.6	33.3	46.7	40.0	31.0	37.0
31	<i>w'/h'</i>	0.0	28.6	14.3	14.3	14.3	28.6	13.3	21.0	26.2	22.7
32	<i>l'/i'</i>	4.8	9.5	7.1	35.7	16.7	47.6	40.0	43.8	38.1	41.9
33	<i>l'/h'</i>	33.3	42.9	38.1	33.7	36.6	52.4	20.0	36.2	33.3	35.2
34	<i>l'/w'</i>	0.0	14.3	7.1	14.3	9.5	47.6	6.7	27.2	35.7	30.0
35	m. shape	17.9	20.6	19.2	25.0	21.2	40.5	26.7	33.6	32.6	33.2
36	m. var.	20.7	18.0	19.4	23.5	20.7	34.4	21.0	27.7	27.0	27.4
37	<i>Z tests</i>	U	L	m. int.	U-L	m. all	U	L	m. int.	U-L	m. all
38	<i>H/W</i>	19.0	9.5	14.3	16.3	15.0	0.0	13.3	6.7	9.5	7.6
39	<i>H/I</i>	0.0	14.3	7.1	4.1	6.1	23.8	0.0	11.9	23.8	15.9
40	<i>w'/h'</i>	4.8	19.0	11.9	14.3	12.7	0.0	0.0	0.0	0.0	0.0
41	<i>l'/i'</i>	0.0	23.8	11.9	10.2	11.3	9.5	0.0	4.8	4.8	4.8
42	<i>l'/h'</i>	4.8	4.8	4.8	6.1	5.2	9.5	6.7	8.1	7.1	7.8
43	<i>l'/w'</i>	0.0	47.6	23.8	16.3	21.3	19.0	0.0	9.5	9.5	9.5
44	m. exp. a	4.8	19.8	12.3	11.2	11.9	10.3	3.3	6.8	9.1	7.6
45	m. all	15.5	18.5	17.0	24.2	19.4	23.8	18.6	21.2	27.6	23.3

Text Table 8.11 Summary of statistical tests for sub-regions of the 2 kyr and 20 kyr transects.

The table shows the percentage of sample pairings per designated region which differ significantly from one another (to a 95% confidence) in terms of the characters involved or the type of test. Each transect is split into two halves representing the upper and lower portions, U and L, respectively. In the 2 kyr transect, the upper half consists of the chalk and most boundary values, while the lower half includes the marl and the lowermost transition from the previous couplet. In this breakdown, the space of possible combinations per field is higher than when the section is split on the basis of lithology (Text Table 8.10), making it more statistically robust but less discriminating. The 20 kyr transect is split around C15 which is included in both upper and lower fields. Details of the splitting procedure for both transects are given in Section 8.1.4.ii.

As with Text Table 8.10, summary values (means) appear in the columns or rows bounding particular types of grouping to help identify regular patterns. Columns e and j compare differences between upper and lower halves, rather than within those zones. Important features to note from this chart are discussed in the adjacent text.

much the same again: the marl and/or the lower half of the cycle tends to house a higher proportion of significant differences than the chalk and boundary, or the upper portion as a whole.

The *t* tests for both sizes and shapes show a much higher proportion of differences *between* divisions than *internal to* a division (e.g. Text Table 8.10 cells i10 & i17 vs. e10 & e17), but for variances and trajectories the pattern is mixed (e.g. Text Table 8.10 cells i28 i35 & i44 vs. e28, e35 & e44). To put these findings into a broader context, notice that Text Table 8.11 shows *t* tests for *size* averaging 10.1% (b10) in the upper half against 12.5% (c10) in the lower, but *t* tests for *shape* averaging 21.4% (b17) in the upper against 26.2% (c17) in the lower. The difference between couplet halves (upper versus lower) is therefore clearly small in comparison to the distinction between parameter types (sizes versus shapes), which here involves a doubling of the figures rather than just a percentage or two increase. It seems that the ‘external’ influences of changing lithology and associated sedimentary factors were overshadowed by ‘internal’ elements controlling the relationship between size and shape, with shape being more malleable than size in the 2 kyr transect despite the environmental circumstances.

One final consideration: *F* tests help us to identify genuine *changes* in variance but do not address the issue of absolute *magnitude*. The *Plus ça change* model predicts that variation will increase when environments settle down, and so we might expect to see an

Size	<i>H</i>	<i>W</i>	<i>I</i>	<i>Ch</i>	<i>l'</i>	<i>h'</i>	<i>w'</i>	<i>i'</i>	Total
Upper	88.6	46.6	56.5	1.9	39.9	22.2	30.3	26.7	1
Lower	101.4	47.2	70.8	2.0	38.7	22.7	34.2	28.4	7
Shape		<i>H/W</i>	<i>H/I</i>	<i>w'/h'</i>	<i>l'/i'</i>	<i>l'/h'</i>	<i>l'/w'</i>		Total
Upper		0.20	0.18	0.22	0.49	0.20	0.11		3
Lower		0.19	0.15	0.25	0.39	0.21	0.16		3
Size	<i>H</i>	<i>W</i>	<i>I</i>	<i>Ch</i>	<i>l'</i>	<i>h'</i>	<i>w'</i>	<i>i'</i>	Total
Chalk	87.5	41.6	54.3	2.0	37.1	19.7	27.6	22.5	0
Boundary	87.9	52.3	59.8	1.7	42.8	23.5	31.8	31.1	4
Marl	102.2	46.7	71.5	2.0	38.4	22.7	34.9	28.0	4
Shape		<i>H/W</i>	<i>H/I</i>	<i>w'/h'</i>	<i>l'/i'</i>	<i>l'/h'</i>	<i>l'/w'</i>		Total
Chalk		0.21	0.18	0.21	0.48	0.20	0.19		3
Boundary		0.19	0.16	0.23	0.50	0.22	0.17		2
Marl		0.19	0.15	0.25	0.39	0.21	0.16		1

Text Table 8.12 Averages for standard deviation scores in each of the size and shape characters within restricted fields of the 2 kyr resolution transect. Largest values are marked in bold and totalled in the end column. See text for discussion.

increase in standard deviation at those points. To investigate this possibility, mean values from the usual sub-zones of C13 are presented in Text Table 8.12. We see that there was more variation in size during the lower (geologically stable) portion, although the difference between many average values is not striking. Otherwise, the signal is pretty equal no matter how the bed or characters are split.

8.2.2 20 kyr Resolution

The 20 kyr transect bridges a gap between the fine resolution survey of C13 and the coarser scale of the three main sections; it provides a valuable glimpse within an otherwise invisible timeframe. Recall that samples from this transect were taken only from the marly portion of each couplet, and in this they correspond to the 100 kyr samples more closely than to those from C13, which also included the chalk.

Charts	Contents	Location
Size	mean, standard deviation, rate	Appdx. Figs. 5.2.1.i-viii
Shape	mean, standard deviation, rate	Appdx. Figs. 5.2.2.i-vi
Trajectory	<i>a</i> and <i>b</i> values	Appdx. Figs. 5.2.3.i-vi
Categoricals	area, % similarity, diversity	Appdx. Figs. 5.2.4.i-vii
Tables	Contents	Location
Size	<i>t</i> tests	Appdx. Tabs. 3.2.1.i-viii
Size	<i>F</i> tests	Appdx. Tabs. 3.2.2.i-viii
Size	<i>haldanes</i>	Appdx. Tabs. 3.5.1.a
Shape	<i>t</i> tests	Appdx. Tabs. 3.2.3.i-vi
Shape	<i>F</i> tests	Appdx. Tabs. 3.2.4.i-vi
Shape	<i>haldanes</i>	Appdx. Tabs. 3.5.1b
Trajectory	<i>Z</i> tests	Appdx. Tabs. 3.2.5.i-vi
Categoricals	% similarity	Appdx. Tabs. 3.6.1
Categoricals	diversity	Appdx. Tabs. 3.6.2

Text Table 8.13 *Location of morphometric data for the 20 kyr scale transect.*

8.2.2.i Individual Patterns

8.2.2.i.a Size

Overall, 31.5% of the timeseries combinations show a significant correlation, only

20 kyr Folkestone — Size																			
<u>x</u>	<i>H</i>	<i>W</i>	<i>I</i>	<i>Ch</i>	<i>l'</i>	<i>h'</i>	<i>w'</i>	<i>i'</i>	<i>sd</i>		<i>H</i>	<i>W</i>	<i>I</i>	<i>Ch</i>	<i>l'</i>	<i>h'</i>	<i>w'</i>	<i>i'</i>	
<i>H</i>	<u>0</u>	0	1	1	1	1	0	0	<i>H</i>	<i>H</i>									<i>H</i>
<i>W</i>	1	<u>0</u>	1	0	1	0	0	0	<i>W</i>	<i>W</i>	0								<i>W</i>
<i>I</i>	1	1	<u>0</u>	1	1	1	0	1	<i>I</i>	<i>I</i>	0	0							<i>I</i>
<i>Ch</i>	0	0	0	<u>0</u>	1	1	0	0	<i>Ch</i>	<i>Ch</i>	0	0	1						<i>Ch</i>
<i>l'</i>	0	0	0	0	<u>0</u>	1	0	0	<i>l'</i>	<i>l'</i>	0	0	0	0					<i>l'</i>
<i>h'</i>	1	1	1	0	0	<u>0</u>	0	0	<i>h'</i>	<i>h'</i>	0	0	0	0	1				<i>h'</i>
<i>w'</i>	0	0	0	0	1	0	<u>0</u>	1	<i>w'</i>	<i>w'</i>	-1	0	0	0	0	0			<i>w'</i>
<i>i'</i>	0	1	1	0	0	0	0	<u>0</u>	<i>i'</i>	<i>i'</i>	0	1	1	1	0	0	0		<i>i'</i>
<i>m</i>	<i>H</i>	<i>W</i>	<i>I</i>	<i>Ch</i>	<i>l'</i>	<i>h'</i>	<i>w'</i>	<i>i'</i>		<i>r</i>	<i>H</i>	<i>W</i>	<i>I</i>	<i>Ch</i>	<i>l'</i>	<i>h'</i>	<i>w'</i>	<i>i'</i>	

actual & possible	9	28	0	8	14	28	6	28	29	92
% significant	<i>m</i>	32.1	<u><i>x</i></u>	0.0	<i>sd</i>	50.0	<i>r</i>	21.4	all	31.5

Text Table 8.14 *Timeseries correlations for size parameters in the 20 kyr transect. Results in bold are significant at the 95% confidence level. See Text Table 8.13 (above) for the chart locations and Section 8.1.5.iv for a discussion of the correlations and correlation grid layout. The lowermost strip summarises actual significant values as a percentage of the total number possible for each of five fields: means with means (m), standard deviations with standard deviations (sd), means with standard deviations (x), rates with rates (r), and all these fields collectively (all).*

one of which is negative. The largest proportion of these correlations occur in the standard deviation field where the seesawing behaviour of *H* and *I* (Appdx. Figs. 5.2.1.i & 5.2.1.iii) finds a resonance in many of the other characters.

All the size means show a similar pattern, rising steadily from smaller values at the sequence’s lower end (C10-C13 [0-60]) to a peak at around couplet C17 [140], and then declining somewhat towards the top (especially C20); about half of them register a net change. As one would expect for developmentally linked characters, the sequence of positive and negative steps is co-ordinated for many mean values (32.1% of them), suggesting relatively minor changes in shape for a given change in size. As with the 2 kyr transect, chamber number (*Ch*) is the exception, exhibiting a gentle zig-zag pattern composed of a series of short trends that reverse after four or five steps.

Changes in standard deviation bear some resemblance to changes in the means, but only weakly and none of them correlate significantly. Most characters do show a significant difference in the range of variation between the upper and lower half of the sequence, especially in the final chamber measurements and *W*, where the values remain low and stable for the earlier parts and then rise steadily in the upper reaches.

Rates of change show fewer correlations and less discernible regularity than either the mean or standard deviation values from which they were calculated.

8.2.2.i.b Shape

20 kyr Folkestone — Shape														
<u>x</u>	<i>H/W</i>	<i>H/I</i>	<i>w'/h'</i>	<i>l'/i'</i>	<i>l'/h'</i>	<i>l'/w'</i>	sd		<i>H/W</i>	<i>H/I</i>	<i>w'/h'</i>	<i>l'/i'</i>	<i>l'/h'</i>	<i>l'/w'</i>
<i>H/W</i>	<u>0</u>	1	1	0	1	0	<i>H/W</i>	<i>H/W</i>						<i>H/W</i>
<i>H/I</i>	0	<u>0</u>	0	0	0	0	<i>H/I</i>	<i>H/I</i>	0					<i>H/I</i>
<i>w'/h'</i>	0	0	<u>0</u>	0	1	0	<i>w'/h'</i>	<i>w'/h'</i>	0	0				<i>w'/h'</i>
<i>l'/i'</i>	0	0	0	<u>0</u>	0	0	<i>l'/i'</i>	<i>l'/i'</i>	0	0	0			<i>l'/i'</i>
<i>l'/h'</i>	0	0	1	0	<u>0</u>	1	<i>l'/h'</i>	<i>l'/h'</i>	0	0	1	0		<i>l'/h'</i>
<i>l'/w'</i>	0	0	-1	0	0	<u>0</u>	<i>l'/w'</i>	<i>l'/w'</i>	-1	0	0	0	0	<i>l'/w'</i>
m	<i>H/W</i>	<i>H/I</i>	<i>w'/h'</i>	<i>l'/i'</i>	<i>l'/h'</i>	<i>l'/w'</i>		r	<i>H/W</i>	<i>H/I</i>	<i>w'/h'</i>	<i>l'/i'</i>	<i>l'/h'</i>	<i>l'/w'</i>

actual & possible	2	15	0	6	5	15	2	15	9	51
% significant	m	13.3	<u>x</u>	0.0	sd	33.3	r	13.3	all	17.6

Text Table 8.15 *Timeseries correlations for shape parameters in the 20 kyr transect. Results in bold are significant at the 95% confidence level. See Text Table 8.13 (above) for the chart locations and Section 8.1.5.iv for a discussion of the correlations and correlation grid layout. The lowermost strip summarises actual significant values as a percentage of the total number possible for each of five fields: means with means (m), standard deviations with standard deviations (sd), means with standard deviations (x), rates with rates (r), and all these fields collectively (all).*

17.6% of the possible shape parameter combinations reveal significant correlations. In two instances the correlations are negative. As with the sizes, the majority of correlations lie within the standard deviation field, largely because of two peaks in variance at horizons C15 [100] and C19 [180] which are correlated across a wide range of shape characters.

Only one of the shape measurements, the *H/W* ratio, shows a net change across the section. *H/W* exhibits a significant shift between relatively equidimensional specimen populations in the lower portion, to narrower ones in the upper; there is no sharp boundary between these zones but rather a meandering series of steps which achieves the transition quite gradually. Timeseries for every other shape parameter consist of brief episodes in which extreme values from either end of the total range register as significant against one another, but there is never any overall and convincing style or irreversible direction to change. More or less the same can be said of differences in variance for all shape characters, despite their relatively high correlation.

8.2.2.i.c Trajectory

20 kyr Folkestone — Trajectory							
\underline{x}	H/W	H/I	w'/h'	l'/i'	l'/h'	l'/w'	b
H/W	-1	0	0	0	-1	0	H/W
H/I	0	-1	0	1	0	0	H/I
w'/h'	0	0	-1	0	0	0	w'/h'
l'/i'	0	0	0	-1	0	1	l'/i'
l'/h'	-1	0	0	0	-1	1	l'/h'
l'/w'	0	0	-1	1	0	-1	l'/w'
a	H/W	H/I	w'/h'	l'/i'	l'/h'	l'/w'	

actual & possible	3	15	6	6	4	15	13	36
% significant	a	20.0	\underline{x}	100.0	b	26.7	all	36.1

Text Table 8.16 *Timeseries correlations for trajectory parameters in the 20 kyr transect. Results in bold are significant at the 95% confidence level. See Text Table 8.13 (above) for the chart locations and Section 8.1.5.iv for a discussion of the correlations and correlation grid layout. The lowermost strip summarises actual significant values as a percentage of the total number possible for each of four fields: a values with a values (a), b values with b values (b), a values with b values (\underline{x}), and all these fields collectively (all).*

The correlations between timeseries of *a* and *b* again reveal a perfect set of negative relationships, although it should be recalled that the statistical parameters for *b* are not perfect. *a* values themselves show 20.0% correlation and *b* values show 26.6%. As with the shape ratios, there are a mixture of positive and negative cases for both *as* and *bs*, which is what we should expect from vector metrics.

On the whole, trajectory values show even less regularity than the shape ratios, oscillating rapidly back and forth with few sequences that might even be considered as trends. There are certainly some significant differences, although not many, and again these are normally either between values at each end of the total range (e.g. the *H/W* plot), or between a majority of samples and the odd outlier (e.g. *l'/w'*).

8.2.2.i.d Categorical

Three out of thirty examples of potential correlation is 10%, so despite the paucity of significant cases compared with the continuous variables, there is still more pattern here than we might expect by chance alone. As usual, however, it is hard to generalise about the categorical characters. Some, such as *ind*, *g%*, *g.dist* and *chir* show rather jerky but

20 kyr Folkestone — Categorical							
	<i>ind</i>	<i>twist</i>	<i>g%</i>	<i>dist</i>	<i>chir</i>	<i>type</i>	H
<i>ind</i>		0	0	0	0	0	<i>ind</i>
<i>tw</i>	0		0	0	0	0	<i>tw</i>
<i>g%</i>	0	0		1	0	0	<i>g%</i>
<i>dist</i>	0	0	1		0	0	<i>dist</i>
<i>chi</i>	0	0	0	0		0	<i>chi</i>
<i>type</i>	-1	0	0	0	0		<i>type</i>
%	<i>ind</i>	<i>tw</i>	<i>g%</i>	<i>dist</i>	<i>chi</i>	<i>type</i>	

actual & possible	1	15	2	15	3	30
% significant	H	6.7	%	13.3	all	10.0

Text Table 8.17 *Timeseries correlations for category parameters in the 20 kyr transect. Results in bold are significant at the 95% confidence level. See Text Table 8.13 (above) for the chart locations and Section 8.1.5.iv for a discussion of the correlations and correlation grid layout. The lowermost strip summarises actual significant values as a percentage of the total number possible for each of three fields: H values with H values (H), percentage similarity values with percentage similarity values (s %), and both these fields collectively (all).*

basically stable behaviour, whereas *tw* and *type* exhibit what appear to be gentle but consistent trends. As with the 2 kyr transect, *g.dist* is the most erratic character, with some adjacent sample populations differing by over 50%; *ind* and *g%* tend to shift by around 25% between adjacent horizons making them a little more changeable than they were at the 2 kyr scale. *type* and *tw* provide by far the most tantalising patterns. Both show a steady increase in the proportion of rare categories across the section, with diversity rising and percentage similarity (%) falling accordingly.

8.2.2.ii Systematic Patterns

In the 20 kyr transect there are a larger proportion of significant differences to be found in mean sizes (35.8%) than in shapes (22.2%)—the opposite of the pattern found in C13—with *a* values once again being the most stable features of all (only 8.6%). Shifts in variation throughout the section are more common in shapes (31.6%) than in sizes (25.6%), both scores being higher than they were at the finer resolution of 2 kyr. Text Table 8.37 (p 407) and also Text Table 8.18 (below) summarise these findings.

Size	<i>H</i>	<i>W</i>	<i>I</i>	<i>Ch</i>	<i>l'</i>	<i>h'</i>	<i>w'</i>	<i>i'</i>	Mean
% sig <i>t</i> test	47.0	25.8	42.4	13.6	42.4	43.9	48.5	22.7	35.8
% sig <i>F</i> test	28.8	16.7	33.3	18.2	31.8	33.3	24.2	18.2	25.6
Shape		<i>H/W</i>	<i>H/I</i>	<i>w'/h'</i>	<i>l'/i'</i>	<i>l'/h'</i>	<i>l'/w'</i>		
% sig <i>t</i> test		37.9	36.4	16.7	19.7	16.7	6.1		22.3
% sig <i>F</i> test		24.2	28.8	24.2	40.9	36.4	34.8		31.6
Trajectory		<i>H/W</i>	<i>H/I</i>	<i>w'/h'</i>	<i>l'/i'</i>	<i>l'/h'</i>	<i>l'/w'</i>		
% sig. <i>Z</i> test		7.6	19.7	0.0	6.1	7.6	10.6		8.6

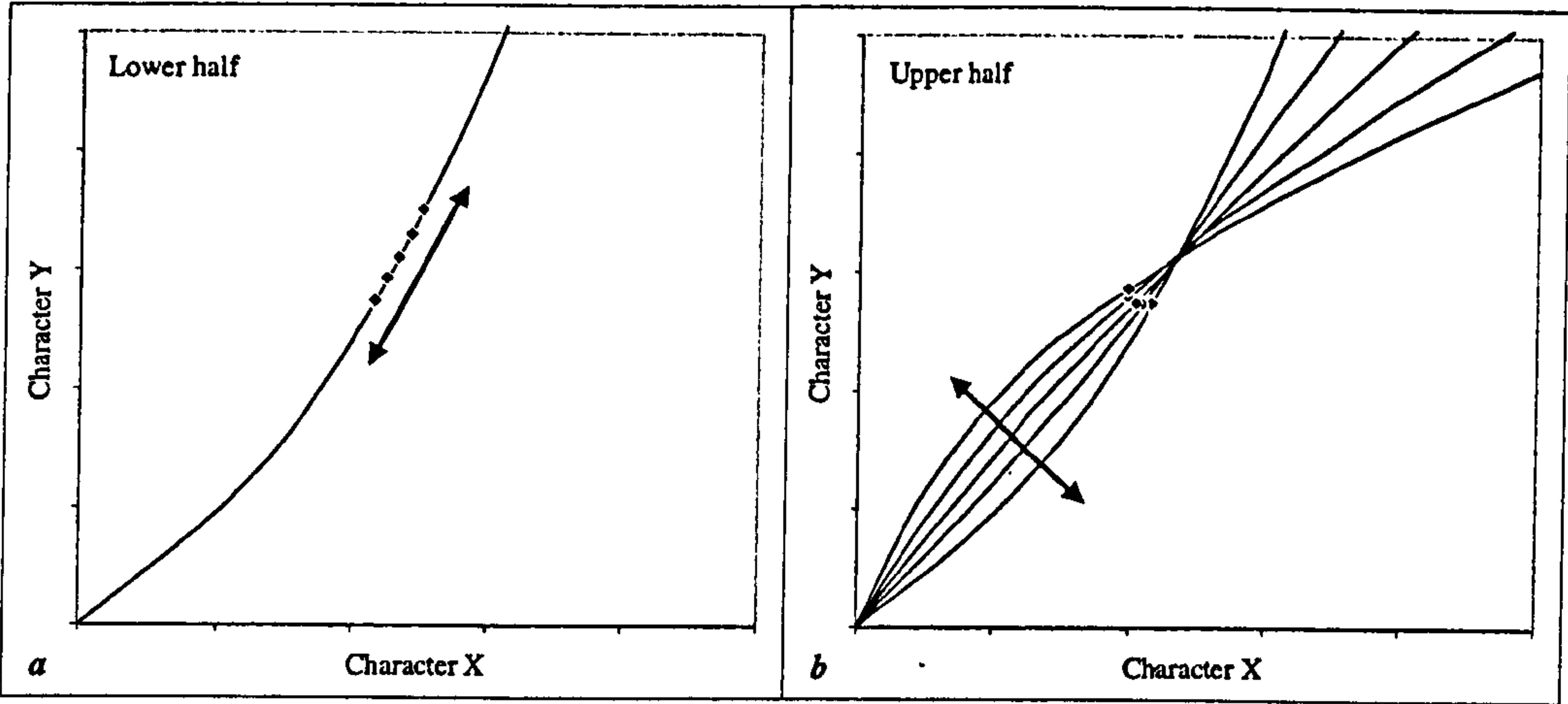
Text Table 8.18 *Significant differences as a percentage of those possible between central tendency and variation values in the 2 kyr resolution transect: size and shape, t and F tests at 95% confidence for means and standard deviation, trajectory Z tests at 95% confidence for values of the allometric exponent, ‘a’.*

8.2.2.iii Environmental Patterns

The 20 kyr resolution transect was split into upper and lower portions, which roughly correspond to more chalky and more marly, or, with regards to the strength of cyclicity, to relatively stable and relatively unstable halves, respectively (Section 3.3.2.i; Appdx. Fig. 3.2.i). Text Table 8.11 (p. 373) summarises the results of this division and shows that for most of the parameters there was more change going on within the upper portion than the lower (cells g17, g28, g35 & g44 vs. h17, h28, h35 & h44), the exception being *t* tests for sizes (g10 vs. h10). For measures of central tendency, there are often also a higher proportion of differences *between* upper and lower halves than *within* either one (i10, i17, i44 vs. j10, j17, j44 – though not i28, i35 vs. j28, j35, by a tiny amount), suggesting that the section can sensibly be split into two distinct regimes of morphological behaviour.

On examination, that suggestion turns out to be correct: a curious reverse pattern occurs between size, shape and trajectory behaviour in the upper versus lower halves of the sequence. Comparing values from Text Table 8.11 boxes g10, g17 & g44 with h10, h17 & h44, we see that the lower portion shows frequent fluctuations in size, rarer fluctuations in shape and almost no fluctuations in trajectory; the upper portion, by contrast, shows fewer fluctuations in size but more fluctuations in shape and many more in trajectory. Accompanying this behaviour is the magnitude of variation, which displays far more frequent fluctuations in the upper half than in the lower. This suggests that changes in the lower section are mostly a case of character means sliding up and down along a single

trajectory, whereas in the upper half the changes are accomplished by oscillating trajectories that nevertheless result in relatively stable average products. These features are summarised in Text Figure 8.5 below.



Text Figure 8.5 *Different relationships between size, shape and trajectory in the 20 kyr resolution transect at Folkestone. The curves represent trajectories and the diamonds show mean size on each axis; shape changes are differences in the ratio of Y to X. Double headed arrows show the dominant element of fluctuation in each half of the sequence. In the lower part (a), size changes are common, shapes less so and changes in trajectory least of all, implying that mean character values slid up and down on isometric to mildly allometric developmental pathways. In the upper part (b), size varies little, shape more so, and trajectory allometry values quite a lot, suggesting that the developmental pathways were changing but that the differences did not necessarily produce shifts in size.*

Note, incidentally, that the panels above can be used to further illustrate Text Figure 8.3 (p 352). If the shifts in the evolutionary trajectory of Text Figure 8.3 are shifts in shape, then they roughly correspond to the situation shown here, with panel a illustrating the lower half and panel b the upper. They also draw attention to the fact that there must be an equivalent evolutionary timeseries for shifts in size, which looks roughly like the one from Text Figure 8.3 turned upside down and twisted at right angles to run the length of the developmental trajectory. This ‘fishtank’ conception of looking down an evolutionary trajectory through a stack of developmental ones (as panel b, above, clearly suggests) is a useful one to bear in mind when considering any of the evolutionary timeseries.

Average magnitudes for standard deviation of the size and shape parameters in each of the section halves shows that variation was almost always greater in the upper portion than it was in the lower.

Size	<i>H</i>	<i>W</i>	<i>I</i>	<i>Ch</i>	<i>l'</i>	<i>h'</i>	<i>w'</i>	<i>i'</i>	Total
Upper	120.4	59.5	80.0	2.0	49.8	26.1	41.2	32.3	7
Lower	106.0	51.2	79.0	2.1	42.5	21.8	33.3	30.5	1
Shape		<i>H/W</i>	<i>H/I</i>	<i>w'/h'</i>	<i>l'/i'</i>	<i>l'/h'</i>	<i>l'/w'</i>		Total
Upper		0.23	0.19	0.25	0.46	0.25	0.20		6
Lower		0.21	0.19	0.22	0.43	0.22	0.15		0

Text Table 8.19 *Averages for standard deviation scores in each of the size and shape characters within restricted fields of the 20 kyr resolution transect. Largest values are marked in bold and totalled in the end column. See text for discussion.*

9.2.3. 100 kyr Resolution

The *Plus ça change* model concerns environmental stability on a geological timeframe of tens to hundreds of millennia. The 100 kyr transects represent just such a timeframe and they are the main focus of this project. Half a million years of relatively unstable environment in the lower half of the sequence give way to half a million years' worth of greater stability later on (Section 4.3), thus effecting exactly the kind of transition Sheldon's model demands (Section 1.2). With the Milankovitch cyclicity itself providing ideal calibration for scaling purposes, the three long sections also introduce a spatial dimension, thus adding an extra layer of complexity to the questions we can tackle.

Charts	Contents	Location
Size	means, standard deviation, rate	Appdx. Figs. 5.3.1i-viii
Shape	means, standard deviation, rate	Appdx. Figs. 5.3.2i-vi
Trajectory	<i>a</i> and <i>b</i> values	Appdx. Figs. 5.3.3.i-vi
Categoricals	area, % similarity, diversity	Appdx. Figs. 5.3.3.i-vii
Tables	Contents	Location
Size	<i>t</i> tests	Appdx. Tabs. 3.3.1.i-viii
Size	<i>F</i> tests	Appdx. Tabs. 3.3.1.i-viii
Size	<i>haldanes</i>	Appdx. Tabs. 3.5.2.a, 3.5.3.a
Shape	<i>t</i> tests	Appdx. Tabs. 3.3.3.i-vi
Shape	<i>F</i> tests	Appdx. Tabs. 3.3.4.i-vi
Shape	<i>haldanes</i>	Appdx. Tabs. 3.5.2.b, 3.5.3.b
Trajectory	<i>Z</i> tests	Appdx. Tabs. 3.3.5.i-vi
Categoricals	% similarity	Appdx. Tabs. 3.6.1
Categoricals	diversity	Appdx. Tabs. 3.6.3

Text Table 8.20 *Location of morphometric information for the 100 kyr scale transect.*

8.2.3.i Individual Patterns

8.2.3.i.a Size

The most immediate and striking feature of the 100 kyr plots for size is that almost everything seems to correlate with everything else. Text Table 8.21.a & b (below) quantify this intuition: out of the 348 boxes available, 128 (36.8%) of them are filled with a significant correlation; and in every single case that correlation is positive. Splitting this bulk assessment into its component parts, we discover that the means show by far the highest

100 kyr Southerham — Size																			
<u>x</u>	<i>H</i>	<i>W</i>	<i>I</i>	<i>Ch</i>	<i>l'</i>	<i>h'</i>	<i>w'</i>	<i>i'</i>	<i>sd</i>		<i>H</i>	<i>W</i>	<i>I</i>	<i>Ch</i>	<i>l'</i>	<i>h'</i>	<i>w'</i>	<i>i'</i>	
<i>H</i>	<u>1</u>	0	1	1	1	1	0	0	<i>H</i>	<i>H</i>									<i>H</i>
<i>W</i>	1	<u>0</u>	0	0	1	0	0	1	<i>W</i>	<i>W</i>	0								<i>W</i>
<i>I</i>	1	1	<u>0</u>	1	0	1	1	0	<i>I</i>	<i>I</i>	1	1							<i>I</i>
<i>Ch</i>	0	0	0	<u>0</u>	0	0	1	0	<i>Ch</i>	<i>Ch</i>	1	0	0						<i>Ch</i>
<i>l'</i>	1	1	1	0	<u>0</u>	1	0	0	<i>l'</i>	<i>l'</i>	0	0	0	0					<i>l'</i>
<i>h'</i>	1	1	1	0	1	<u>0</u>	0	0	<i>h'</i>	<i>h'</i>	1	0	0	0	1				<i>h'</i>
<i>w'</i>	1	1	1	0	1	1	<u>0</u>	0	<i>w'</i>	<i>w'</i>	1	0	0	0	0	0			<i>w'</i>
<i>i'</i>	1	1	1	0	1	0	1	<u>0</u>	<i>i'</i>	<i>i'</i>	0	0	0	0	0	0	0		<i>i'</i>
<i>m</i>	<i>H</i>	<i>W</i>	<i>I</i>	<i>Ch</i>	<i>l'</i>	<i>h'</i>	<i>w'</i>	<i>i'</i>		<i>r</i>	<i>H</i>	<i>W</i>	<i>I</i>	<i>Ch</i>	<i>l'</i>	<i>h'</i>	<i>w'</i>	<i>i'</i>	

actual & possible	20	28	1	8	11	28	6	28	38	92
% significant	<i>m</i>	71.4	<u><i>x</i></u>	12.5	<i>sd</i>	39.3	<i>r</i>	21.4	all	41.3

100 kyr Folkestone — Size																			
<u>x</u>	<i>H</i>	<i>W</i>	<i>I</i>	<i>Ch</i>	<i>l'</i>	<i>h'</i>	<i>w'</i>	<i>i'</i>	<i>sd</i>		<i>H</i>	<i>W</i>	<i>I</i>	<i>Ch</i>	<i>l'</i>	<i>h'</i>	<i>w'</i>	<i>i'</i>	
<i>H</i>	<u>1</u>	0	1	1	0	0	1	0	<i>H</i>	<i>H</i>									<i>H</i>
<i>W</i>	1	<u>0</u>	0	0	1	0	0	0	<i>W</i>	<i>W</i>	0								<i>W</i>
<i>I</i>	1	1	<u>1</u>	1	0	0	0	0	<i>I</i>	<i>I</i>	1	0							<i>I</i>
<i>Ch</i>	1	0	0	<u>1</u>	0	1	0	0	<i>Ch</i>	<i>Ch</i>	0	0	0						<i>Ch</i>
<i>l'</i>	1	1	0	0	<u>0</u>	0	0	1	<i>l'</i>	<i>l'</i>	0	1	0	0					<i>l'</i>
<i>h'</i>	0	1	0	0	1	<u>0</u>	0	0	<i>h'</i>	<i>h'</i>	0	0	0	0	0				<i>h'</i>
<i>w'</i>	1	1	1	0	1	1	<u>0</u>	0	<i>w'</i>	<i>w'</i>	0	0	0	0	1	0			<i>w'</i>
<i>i'</i>	0	1	0	0	0	0	0	<u>0</u>	<i>i'</i>	<i>i'</i>	0	0	0	0	0	0	0		<i>i'</i>
<i>m</i>	<i>H</i>	<i>W</i>	<i>I</i>	<i>Ch</i>	<i>l'</i>	<i>h'</i>	<i>w'</i>	<i>i'</i>		<i>r</i>	<i>H</i>	<i>W</i>	<i>I</i>	<i>Ch</i>	<i>l'</i>	<i>h'</i>	<i>w'</i>	<i>i'</i>	

actual & possible	14	28	3	8	7	28	3	28	27	92
% significant	<i>m</i>	50.0	<u><i>x</i></u>	37.5	<i>sd</i>	25.0	<i>r</i>	10.7	all	29.3

100 kyr Escalles — Size																			
<u>x</u>	<i>H</i>	<i>W</i>	<i>I</i>	<i>Ch</i>	<i>l'</i>	<i>h'</i>	<i>w'</i>	<i>i'</i>	<i>sd</i>		<i>H</i>	<i>W</i>	<i>I</i>	<i>Ch</i>	<i>l'</i>	<i>h'</i>	<i>w'</i>	<i>i'</i>	
<i>H</i>	<u>1</u>	1	1	0	1	0	1	0	<i>H</i>	<i>H</i>									<i>H</i>
<i>W</i>	1	<u>1</u>	1	1	1	0	1	0	<i>W</i>	<i>W</i>	0								<i>W</i>
<i>I</i>	1	1	<u>1</u>	0	1	1	1	0	<i>I</i>	<i>I</i>	1	1							<i>I</i>
<i>Ch</i>	0	0	0	<u>0</u>	1	0	0	0	<i>Ch</i>	<i>Ch</i>	0	0	0						<i>Ch</i>
<i>l'</i>	1	1	1	0	<u>1</u>	0	1	0	<i>l'</i>	<i>l'</i>	0	1	0	0					<i>l'</i>
<i>h'</i>	1	1	1	0	1	<u>0</u>	1	1	<i>h'</i>	<i>h'</i>	0	0	0	0	0				<i>h'</i>
<i>w'</i>	0	1	0	0	1	1	<u>1</u>	1	<i>w'</i>	<i>w'</i>	0	1	0	0	0	0			<i>w'</i>
<i>i'</i>	0	1	0	0	0	0	0	<u>0</u>	<i>i'</i>	<i>i'</i>	0	0	0	0	0	0	0		<i>i'</i>
<i>m</i>	<i>H</i>	<i>W</i>	<i>I</i>	<i>Ch</i>	<i>l'</i>	<i>h'</i>	<i>w'</i>	<i>i'</i>		<i>r</i>	<i>H</i>	<i>W</i>	<i>I</i>	<i>Ch</i>	<i>l'</i>	<i>h'</i>	<i>w'</i>	<i>i'</i>	

actual & possible	14	28	5	8	16	28	4	28	39	92
% significant	<i>m</i>	50.0	<u><i>x</i></u>	62.5	<i>sd</i>	57.1	<i>r</i>	14.3	all	42.4

Text Table 8.21.a (previous page) *Timeseries correlations for size parameters in the 100 kyr transects. Results in bold are significant at the 95% confidence level. See Text Table 8.20 (above) for the chart locations and Section 8.1.5.iv for a discussion of the correlations and correlation grid layout. The lowermost strip of each table summarises actual significant values as a percentage of the total number possible for each of five fields: means with means (m), standard deviations with standard deviations (sd), means with standard deviations (x), rates with rates (r), and all these fields collectively (all).*

100 kyr Between-Site — Size											
	<i>H</i>	<i>W</i>	<i>I</i>	<i>Ch</i>	<i>l'</i>	<i>h'</i>	<i>w'</i>	<i>i'</i>		% sig	
SF	1	0	1	1	1	1	0	0	m	62.5	m
FE	1	1	1	1	1	1	1	0	m	87.5	m
ES	1	0	1	1	1	1	0	0	m	62.5	m
SF	0	0	0	0	0	1	1	0	sd	25.0	sd
FE	1	0	0	0	0	0	0	0	sd	12.5	sd
ES	1	0	0	0	0	0	0	0	sd	12.5	sd
SF	1	0	1	1	0	0	0	0	r	37.5	r
FE	0	0	0	0	0	0	0	0	r	0.0	r
ES	0	0	0	0	0	0	0	0	r	0.0	r
	<i>H</i>	<i>W</i>	<i>I</i>	<i>Ch</i>	<i>l'</i>	<i>h'</i>	<i>w'</i>	<i>i'</i>		% sig	

Text Table 8.21.b *Between-site timeseries correlations for size characters in the 100 kyr transects. See Text Table 8.20 (above) for the chart locations. Results in bold are significant at the 95% confidence level, and actual-as-a-proportion-of-possible values appear as percentages in the ‘% sig’ column on the left.*

density of correlations at 60.1%, with standard deviation coming next at 35.2%, and rates in last place at only 14.8%.

Overall, the most spectacular element in these timeseries plots is the co-ordinated and statistically significant lurch between sampling points B41, C5, C10 and C15 [time horizons 200-500] which is found in most characters (*H*, *W*, *I*, *l'*, *h'* and *w'*) and at all three sites. What makes this particular feature so impressive is not so much its correlated direction of steps, but rather the fact that the values are always so close together, especially at C5 [300] where the variance of the three populations is also very high. The exceptions to this pattern are final chamber *h'*-*l'* intersect (*i'*) and the number of chambers (*Ch*), both of which have higher values at B41 [200] than at C5 [300] and share fewer correlations with the other characters accordingly.

The mean values of the populations at each of the three sites tend to drift apart from one another beyond horizon C10 [400], but they still preserve a highly co-ordinated between-site pattern. Just over half of all within site cases (13/24) register a significant net change between the earliest and latest sampling points, but the style and distribution of these transformations bears an additional theme. Although the whole test characters, *H*, *W*, *I* and

Ch, show a pattern of progressive *divergence* up-section, with mean values moving in different directions at different sites, the *directions* of change balance out to give a kind of basin-wide stasis on average. Normally, Folkestone samples show larger mean values, Escalles samples show smaller ones, and Southerham samples hang somewhere in between. Although not all of these shifts are statistically significant, the pattern is clear nonetheless. By contrast, final chamber characters, *l'*, *h'* and *w'* (but not *i'*), show what appear to be trends of increasing magnitude up-section at all three sites, generating statistically significant shifts in 8 out of 9 cases (*l'* at Escalles is the exception). Even though the final chamber values show such consistency in their direction of change, however, they still have a tendency to spread out with time, just as the whole test parameters do. This extensive between-site divergence is captured below in Text Table 8.22 showing that it happened in 19 out of 24 cases, of which 13 register, via the *t*-tests, as significant differences.

character	S	F	E	S-F	F-E	S-E
<i>H</i>	+	+	+	d	d	d
<i>W</i>	+	+	-	d	d	d
<i>I</i>	-	+	-	d	d	c
<i>Ch</i>	-	+	-	d	d	d
<i>l'</i>	+	+	+	d	d	d
<i>h'</i>	+	+	+	d	d	d
<i>w'</i>	+	+	+	d	d	c
<i>i'</i>	+	+	-	c	c	c

Text Table 8.22 *Directions of change in mean value of size parameters for within and between site relationships. '+' denotes increases in magnitude, '-' denotes decreases; 'd' denotes divergence between means at different sites, whereas 'c' is convergence. These results concern relationships between lowest and highest values only; they do not reflect intermediate states, which are very variable (see the Appdx. Figs. 5.1.3.i-viii). Results in bold are significant at the 95% confidence level.*

Standard deviation timeseries for character sizes also show a large number of correlations, including cases of correlation between a variance and its mean (i.e. \bar{x}); however, the synchronous swing between horizons B41 and C10 [200-400] is generally *less* well co-ordinated than it was for central tendency. There also appears to be an odd pattern in the marginal sites around levels C21-C29 [600-700], manifested either as a synchronous peak at both Folkestone and Escalles (e.g. *W*, *l'*, *i'*), or as a disjunct one in which Folkestone peaks a sampling point earlier (e.g. *H*, *I*, *h'*, *w'*). This positive shift in variation is not associated with any obvious change in central tendency, and, intriguingly, the characters which show it best (*W*, *l'*, *i'*) are also the ones which exhibit the B41-C10 [200-400] signal *least* well.

Overall, the *magnitude* of standard deviation scores tends to increase up-section, with 17 out of 24 cases showing a net positive change, 5 of which are significant. Most of these come from Folkestone where all 8 of the characters become more variable over time; Escalles and Southerham, by contrast, show positive shifts in only about half of their characters (Text Table 8.23).

When it comes to a comparison *between* sites, the standard deviations again exhibit rather less correspondence in their timeseries patterns than did the means. As with the means, however, there is a tendency for standard deviation values to diverge with time, so that sites which had relatively similar scores at their lowest point are likely to have less similar values by the end (we might say that variation itself becomes more variegated). This pattern is found in 15 out of 24 cases (Text Table 8.23), but populations from Southerham and Escalles are actually more likely to converge than to diverge; it is Folkestone which tends to part company by developing such broadly varying populations. Indeed, the difference in magnitude of standard deviation between Folkestone and Escalles is a consistent feature of these plots.

character	S	F	E	S-F	F-E	S-E
<i>H</i>	-	+	+	d	d	c
<i>W</i>	+	+	+	d	d	c
<i>I</i>	-	+	+	d	d	c
<i>Ch</i>	-	+	+	d	d	c
<i>l'</i>	+	+	-	d	d	c
<i>h'</i>	-	+	+	d	c	d
<i>w'</i>	+	+	-	c	d	d
<i>i'</i>	+	+	-	c	d	d

Text Table 8.23 *Directions of change in standard deviation of size parameters for within and between site relationships. + denotes increases in magnitude, - denotes decreases; d denotes divergence between standard deviation at different sites, whereas c is convergence. These results concern relationships between lowest and highest values only; they do not reflect intermediate states, which are very variable (see Appdx. Figs. 5.3.1.i-viii). Results in bold are significant at the 95% confidence level.*

As with variance and central tendency, rates of change for character sizes are more correlated than one would expect from chance alone (under a null hypothesis of zero correlation), but far less so than for the other two parameters. High rates tend to be concentrated in the lower half of the section, in association with the B41-C10 [200-400] shift.

8.2.3.i.b Shape

There are far fewer correlations among the plots for shape than there were for sizes: over the entire space of 225 possible correlations, only 26 cases are significant, coming to

100 kyr Southerham — Shape															
<u>x</u>	H/W	H/I	w'/h'	l'/i'	l'/h'	l'/w'	sd		H/W	H/I	w'/h'	l'/i'	l'/h'	l'/w'	
H/W	<u>0</u>	0	0	0	0	1	H/W	H/W							H/W
H/I	0	<u>0</u>	0	0	0	0	H/I	H/I	0						H/I
w'/h'	0	0	<u>0</u>	0	1	0	w'/h'	w'/h'	0	0					w'/h'
l'/i'	0	0	-1	<u>1</u>	0	0	l'/i'	l'/i'	0	0	0				l'/i'
l'/h'	-1	0	0	0	<u>1</u>	0	l'/h'	l'/h'	0	0	0	0			l'/h'
l'/w'	0	0	-1	0	0	<u>0</u>	l'/w'	l'/w'	0	0	0	0	0		l'/w'
m	H/W	H/I	w'/h'	l'/i'	l'/h'	l'/w'		r	H/W	H/I	w'/h'	l'/i'	l'/h'	l'/w'	

actual & possible	3	15	2	6	2	15	0	15	7	51
% significant	m	20.0	<u>x</u>	33.3	sd	13.3	r	0.0	all	13.7

100 kyr Folkestone — Shape															
<u>x</u>	H/W	H/I	w'/h'	l'/i'	l'/h'	l'/w'	sd		H/W	H/I	w'/h'	l'/i'	l'/h'	l'/w'	
H/W	<u>1</u>	0	0	0	0	0	H/W	H/W							H/W
H/I	0	<u>1</u>	0	0	0	0	H/I	H/I	0						H/I
w'/h'	1	0	<u>0</u>	0	0	0	w'/h'	w'/h'	0	0					w'/h'
l'/i'	0	0	0	<u>0</u>	0	0	l'/i'	l'/i'	0	0	0				l'/i'
l'/h'	0	0	1	0	<u>1</u>	0	l'/h'	l'/h'	0	0	1	0			l'/h'
l'/w'	0	0	0	0	0	<u>0</u>	l'/w'	l'/w'	0	0	0	0	0		l'/w'
m	H/W	H/I	w'/h'	l'/i'	l'/h'	l'/w'		r	H/W	H/I	w'/h'	l'/i'	l'/h'	l'/w'	

actual & possible	2	15	3	6	0	15	1	15	6	51
% significant	m	13.3	<u>x</u>	50.0	sd	0.0	r	6.7	all	11.8

100 kyr Escalles — Shape															
<u>x</u>	H/W	H/I	w'/h'	l'/i'	l'/h'	l'/w'	sd		H/W	H/I	w'/h'	l'/i'	l'/h'	l'/w'	
H/W	<u>1</u>	0	0	0	0	0	H/W	H/W							H/W
H/I	0	<u>0</u>	0	0	0	0	H/I	H/I	0						H/I
w'/h'	0	0	<u>0</u>	0	0	0	w'/h'	w'/h'	0	0					w'/h'
l'/i'	0	0	-1	<u>1</u>	0	0	l'/i'	l'/i'	0	0	0				l'/i'
l'/h'	0	0	1	-1	<u>1</u>	0	l'/h'	l'/h'	1	0	1	1			l'/h'
l'/w'	0	0	-1	0	0	<u>0</u>	l'/w'	l'/w'	0	0	0	0	0		l'/w'
m	H/W	H/I	w'/h'	l'/i'	l'/h'	l'/w'		r	H/W	H/I	w'/h'	l'/i'	l'/h'	l'/w'	

actual & possible	4	15	3	6	0	15	3	15	10	51
% significant	m	26.7	<u>x</u>	50.0	sd	0.0	r	20.0	all	19.6

Text Table 8.24.a (previous page) *Timeseries correlations for shape parameters in the 100 kyr transect. Results in bold are significant at the 95% confidence level. See Text Table 8.20 (above) for the chart locations and Section 8.1.5.iv for a discussion of the correlations and correlation grid layout. The lowermost strip summarises actual significant values as a percentage of the total number possible for each of five fields: means with means (m), standard deviations with standard deviations (sd), means with standard deviations (\bar{x}), rates with rates (r), and all these fields collectively (all).*

100 kyr Between-Site — Shape									
	<i>H/W</i>	<i>H/I</i>	<i>w'/h'</i>	<i>l'/i'</i>	<i>l'/h'</i>	<i>l'/w'</i>		% sig	
SF	0	0	0	0	0	0	m	0.0	m
FE	1	1	0	0	0	0	m	33.3	m
ES	0	0	0	0	0	0	m	0.0	m
SF	0	0	0	0	0	0	sd	0.0	sd
FE	0	0	0	0	0	0	sd	0.0	sd
ES	0	0	0	0	0	0	sd	0.0	sd
SF	0	0	0	0	0	0	r	0.0	r
FE	0	0	0	0	0	1	r	16.7	r
ES	0	0	0	0	0	0	r	0.0	r
	<i>H/W</i>	<i>H/I</i>	<i>w'/h'</i>	<i>l'/i'</i>	<i>l'/h'</i>	<i>l'/w'</i>		% sig	

Text Table 8.24.b *Between site timeseries correlations for shape parameters in the 100 kyr transects. See Text Table 8.20 (above) for the chart locations. Results in bold are significant at the 95% confidence level, and actual-as-a-proportion-of-possible values appear as percentages in the ‘% sig’ column on the left.*

just 11.6%; as with the higher resolution surveys, this includes both negative and positive relationships. Of these, the distributions are as follows: means $11/69 = 15.9\%$, standard deviations $2/69 = 2.9\%$, rates $5/69 = 7.2\%$ and \bar{x} , the timeseries correlation between an individual character’s own mean and standard deviation, $8/18 = 44.4\%$. (Regarding this latter value, it is worth highlighting that the significance of the \bar{x} correlations for shapes is far from straightforward since mean shape is a ‘vector’ quantity while standard deviation is ‘scalar’.) There are also far fewer between-site correlations than there were for the size parameters.

Only the mean *H/W* ratio shows anything like the pattern so clearly found with the character sizes—a co-ordinated kink of close values below the mid-point of the sequence followed by a divergence of values above. This time, however, the kink is smaller and the means in closest proximity begin and end a sample point higher at C5 [300] and C15 [500], respectively. Of the other shape characters, the *H/I* and *l'/h'* ratios show consistent and significant trends across the section as a whole, indicating, in combination with *l'/i'*, a

transition from top-heavy specimens with long, low final chambers early in the sequence, to specimens with a low centre of gravity and high, stubby final chambers in the upper half. This is comparable to the pattern of shape changes seen across C13 and indicates an increase in exotic growth types in the upper reaches of the sections. The w'/h' ratio remains impressively constant throughout, registering very few significant changes; and, by looking back at the size plots, one can deduce that changes in final chamber shape occurred because both h' and w' were increasing in magnitude faster than l' .

As the Text Table 8.24.a \underline{x} field shows, standard deviation timeseries often exhibit a similarity to the means, but, as with sizes, the most striking feature is the way in which values from Folkestone are so consistently greater than those from Escalles, especially for the final chamber ratios. Rates of change for shape seem to provide no discernible regularity whatsoever.

8.2.3.i.c Trajectory

The run of significant negative correlations between a and b values (the \underline{x} category) remains unbroken across all three 100 kyr transects. Apart from that, the a and b correlations themselves stand at $10/69 = 14.5\%$ for the a s and $6/69 = 8.7\%$ for the b s, with a majority of positive correlations, but none at all occurring in the between-site cases.

Trajectory a values for the H/W allometric exponent somewhat resemble the H/W shape component by having a co-ordinated kink between C5-C15 [300-500] and also by diverging markedly in the upper portion.

100 kyr Between-Site — Trajectory									
	H/W	H/I	w'/h'	l'/i'	l'/h'	l'/w'		% sig	
SF	0	0	0	0	0	0	a	0.0	a
FE	0	0	0	0	0	0	a	0.0	a
ES	0	0	0	0	0	0	a	0.0	a
SF	0	0	0	0	0	0	b	0.0	b
FE	0	0	0	0	0	0	b	0.0	b
ES	0	0	0	0	0	0	b	0.0	b
	H/W	H/I	w'/h'	l'/i'	l'/h'	l'/w'		% sig	

Text Table 8.25.b *Between site timeseries correlations for trajectory parameters in the 100 kyr transects. See Text Table 8.20 (above) for the chart locations. Results in bold (there are none) are significant at the 95% confidence level, and actual-as-a-proportion-of-possible values appear as percentages in the ‘% sig’ column on the left.*

100 kyr Southerham — Trajectory							
\underline{x}	H/W	H/I	w'/h'	l'/i'	l'/h'	l'/w'	b
H/W	<u>-1</u>	0	0	0	0	0	H/W
H/I	0	<u>-1</u>	0	0	1	0	H/I
w'/h'	0	0	<u>-1</u>	0	0	0	w'/h'
l'/i'	0	1	0	<u>-1</u>	0	0	l'/i'
l'/h'	0	1	0	0	<u>-1</u>	0	l'/h'
l'/w'	0	1	-1	1	0	<u>-1</u>	l'/w'
a	H/W	H/I	w'/h'	l'/i'	l'/h'	l'/w'	

actual & possible	5	15	6	6	1	15	12	36
% significant	a	33.3	\underline{x}	100.0	b	6.7	all	33.3

100 kyr Folkestone — Trajectory							
\underline{x}	H/W	H/I	w'/h'	l'/i'	l'/h'	l'/w'	b
H/W	<u>-1</u>	0	0	0	0	<u>-1</u>	H/W
H/I	0	<u>-1</u>	0	0	0	0	H/I
w'/h'	0	1	<u>-1</u>	0	0	0	w'/h'
l'/i'	0	0	0	<u>-1</u>	0	0	l'/i'
l'/h'	0	0	0	0	<u>-1</u>	0	l'/h'
l'/w'	-1	0	-1	0	0	<u>-1</u>	l'/w'
a	H/W	H/I	w'/h'	l'/i'	l'/h'	l'/w'	

actual & possible	3	15	6	6	1	15	10	36
% significant	a	20.0	\underline{x}	100.0	b	6.7	all	27.8

100 kyr Escalles — Trajectory							
\underline{x}	H/W	H/I	w'/h'	l'/i'	l'/h'	l'/w'	b
H/W	<u>-1</u>	1	1	0	0	0	H/W
H/I	0	<u>-1</u>	1	0	0	0	H/I
w'/h'	0	1	<u>-1</u>	0	0	0	w'/h'
l'/i'	0	0	0	<u>-1</u>	0	0	l'/i'
l'/h'	0	0	1	0	<u>-1</u>	1	l'/h'
l'/w'	0	0	0	0	0	<u>-1</u>	l'/w'
a	H/W	H/I	w'/h'	l'/i'	l'/h'	l'/w'	

actual & possible	2	15	6	6	4	15	12	36
% significant	a	13.3	\underline{x}	100.0	b	26.7	all	33.3

Text Table 8.25.a Timeseries correlations for trajectory parameters in the 100 kyr transect. Results in bold are significant at the 95% confidence level. See Text Table 8.20 (above) for the chart locations and Section 8.1.5.iv for a discussion of the correlations and correlation grid layout. The lowermost strip summarises actual significant values as a percentage of the total number possible for each of four fields: a values with a values (a), b values with b values (b), a values with b values (\underline{x}), and all these fields collectively (all).

With respect to trajectory values for final chamber characters, note that the w'/h' trajectory exponent oscillates around isometry at all three sites, in keeping with observations in the last section that the w'/h' shape ratio fails to change, despite size increases in both characters. Both l'/h' and l'/w' hover around a negative allometry of 0.9, corroborating the notion mooted in the section above that h' and w' tend to increase in size faster than l' . In this light, parallel trends in the size of both h' and w' would be the natural accompaniment of minor and perhaps statistically insignificant trends in l' (or vice versa), under conditions in which the trajectory relationships between each character remained roughly stable.

Beyond these observations it is hard to generalise about the trajectory plots, which have a rather disordered arrangement with even the normally well developed correlation between Folkestone and Escalles hard to pick out. As a general rule, significant differences are present only between erratic outliers which lie at either end of the total range.

8.2.3.i.d Categorical

Overall, the bulk metrics for the categorical characters show just 10 significant correlations from a total of 126 (7.9%), which is hardly more than chance alone would impose on a null expectation of zero correlation.

Four of the characters, *ind*, *tw*, *g%* and *type*, exhibit systematic differences in the distribution of their various categories across the 100 kyr succession (Appdx. Figs. 5.3.4.i, ii, iii & vi). *ind* shows a change in the proportion of highly indented specimens, the blade edged forms of the lower reaches tending to be replaced by more robust, prism-shaped individuals later on. The effect is subtle but measurable: it manifests itself as itself as lower

	<i>ind</i>	<i>tw</i>	<i>g%</i>	<i>dist</i>	<i>chi</i>	<i>type</i>		% sig	
SF	0	0	0	0	0	0	%	0.0	%
FE	0	0	0	0	0	0	%	0.0	%
ES	0	0	0	0	0	1	%	16.6	%
SF	0	0	0	0	0	0	H	0.0	H
FE	0	0	0	0	0	0	H	0.0	H
ES	0	0	0	0	0	0	H	0.0	H
	<i>ind</i>	<i>tw</i>	<i>g%</i>	<i>dist</i>	<i>chi</i>	<i>type</i>		% sig	

Text Table 8.26.b Between site timeseries correlations for categorical characters in the 100 kyr transects. See Text Table 8.20 (above) for the chart locations and Section 8.1.5.iv for a discussion of the correlations and correlation grid layout. Results in bold are significant at the 95% confidence level, and actual-as-a-proportion-of-possible values appear as percentages in the ‘% sig’ column on the left.

100 kyr Southerham — Categorical							
	<i>ind</i>	<i>tw</i>	<i>g%</i>	<i>dist</i>	<i>chi</i>	<i>type</i>	H
<i>ind</i>		0	0	0	0	0	<i>ind</i>
<i>tw</i>	0		0	0	0	0	<i>tw</i>
<i>g%</i>	0	0		1	0	1	<i>g%</i>
<i>dist</i>	0	0	0		0	0	<i>dist</i>
<i>chi</i>	0	0	0	0		0	<i>chi</i>
<i>type</i>	1	0	0	0	0		<i>type</i>
%	<i>ind</i>	<i>tw</i>	<i>g%</i>	<i>dist</i>	<i>chi</i>	<i>type</i>	

actual & possible	2	15	1	15	3	30
% significant	H	13.3	%	6.7	all	10.0

100 kyr Folkestone — Categorical							
	<i>ind</i>	<i>tw</i>	<i>g%</i>	<i>dist</i>	<i>chi</i>	<i>type</i>	H
<i>ind</i>		0	0	0	0	0	<i>ind</i>
<i>tw</i>	0		0	0	0	1	<i>tw</i>
<i>g%</i>	0	0		1	0	0	<i>g%</i>
<i>dist</i>	0	0	1		0	0	<i>dist</i>
<i>chi</i>	0	-1	0	0		0	<i>chi</i>
<i>type</i>	0	0	0	0	0		<i>type</i>
%	<i>ind</i>	<i>tw</i>	<i>g%</i>	<i>dist</i>	<i>chi</i>	<i>type</i>	

actual & possible	2	15	2	15	4	30
% significant	H	13.3	%	13.3	all	13.3

100 kyr Escalles — Categorical							
	<i>ind</i>	<i>tw</i>	<i>g%</i>	<i>dist</i>	<i>chi</i>	<i>type</i>	H
<i>ind</i>		0	0	0	0	0	<i>ind</i>
<i>tw</i>	0		0	0	0	0	<i>tw</i>
<i>g%</i>	0	0		0	0	0	<i>g%</i>
<i>dist</i>	1	0	0		0	0	<i>dist</i>
<i>chi</i>	0	0	0	0		0	<i>chi</i>
<i>type</i>	0	-1	0	0	0		<i>type</i>
%	<i>ind</i>	<i>tw</i>	<i>g%</i>	<i>dist</i>	<i>chi</i>	<i>type</i>	

actual & possible	0	15	2	15	2	30
% significant	H	0.0	%	13.3	all	6.7

Text Table 8.26.a Timeseries correlations for category parameters in the 100 kyr transect. Results in bold are significant at the 95% confidence level. See Text Table 8.20 (above) for the chart locations. The lowermost strip summarises actual significant values as a percentage of the total number possible for each of three fields: H values with H values (H), percentage similarity values with percentage similarity values (s %), and both these fields collectively (all).

diversity values where the rarer, high indentation categories are absent. The other three characters (*tw*, *type* and *g%*) undergo an equivalent but opposite modification, resulting in their rarer categories becoming more common in the upper half, and once again this is captured by their diversity rating.

The distribution of glauconite (*g.dist*) is not so easy to summarise although there is certainly regularity present in the plots. More specifically, there is an increase in the proportion of category 1 glauconite distribution patterns in the upper horizons at all three sites, especially in horizon C35 [800]; there is also a similar but broader increase in category 5 patterns, this time peaking at C40 [900]; there appears to be a regular alternation between categories 2 and 3 which is roughly correlated at all three sites (compare this to the behaviour of the same categories at 2 kyr and 20 kyr resolutions); and, finally, category 4 remains rare throughout. These patterns should also be considered relative to the percentage glauconite (*g%*) count with which they are linked.

All taken together, the data suggest a transition from deeply indented and straightforwardly triserial specimens in the lower half, to specimens in the upper horizons that were more solidly triangular but often somewhat twisted, and with a high glauconite content plus a range of exotic, non-triserial growth patterns. Chirality remained roughly equal throughout with a 50:50 split between sinistral and dextral forms.

8.2.3.ii Patterns Between Morphological Parameters

When it comes to statistical tests and their space of possible combinations, we can see from Text Table 8.27 that, as in the 20 kyr transect, size means are more likely to show significant differences than are shapes (34.4% vs. 28.1% - cells e10 & e17), and trajectories least likely of all (10.3% - e44). By contrast, although they are less liable to change than are the mean values for either, there are more significant differences in standard deviation for shapes than for sizes (26.0% vs. 22.3% - e35 & e28). These are average values and do not always correspond perfectly to the signals from individual sites, but they certainly reflect the general patterns. Other cells in rows 10, 17, 28, 35 and 44 of Text Table 8.27 give a fuller picture. This sequence—sizes > shapes > trajectories—has a regularity that hints at a common cause; we will investigate it further, along with similar regularities among the correlations, in due course.

	a	b	c	d	e	f	g	h	i	j
1	<i>t</i> tests	S	F	E	m. int.	S-F	S-E	F-E	m. ext.	m. all
2	<i>H</i>	16.4	40.0	31.1	29.2	45.5	25.5	57.3	42.8	36.0
3	<i>W</i>	32.7	32.7	53.3	39.6	33.9	36.4	48.2	39.5	39.5
4	<i>I</i>	38.2	34.5	28.9	33.9	43.0	32.7	50.9	42.2	38.0
5	<i>Ch</i>	34.5	43.6	33.3	37.1	44.6	34.5	38.2	39.1	38.1
6	<i>l'</i>	16.4	29.1	31.1	25.5	28.1	27.3	32.7	29.4	27.5
7	<i>h'</i>	47.3	49.1	44.4	46.9	49.6	40.0	46.4	45.3	46.1
8	<i>w'</i>	34.5	50.9	44.4	43.3	43.8	35.5	43.6	41.0	42.1
9	<i>i'</i>	30.9	16.4	11.1	19.5	19.8	22.7	12.7	18.4	18.9
10	m. size	31.4	37.0	34.7	34.4	38.5	31.8	41.3	37.2	35.8
11	<i>H/W</i>	20.0	43.6	33.3	32.3	47.9	22.7	43.6	38.1	35.2
12	<i>H/I</i>	40.0	25.5	26.7	30.7	24.8	28.2	21.8	24.9	27.8
13	<i>w'/h'</i>	9.1	9.2	22.2	13.5	16.5	14.5	13.6	14.9	14.2
14	<i>l'/i'</i>	34.5	36.4	13.3	28.1	25.6	26.4	27.3	26.4	27.3
15	<i>l'/h'</i>	38.2	36.4	35.6	36.7	31.4	30.9	34.5	32.3	34.5
16	<i>l'/w'</i>	25.5	20.0	35.6	27.0	24.8	28.2	25.5	26.2	26.6
17	m. shape	27.9	28.5	27.8	28.1	28.5	25.2	27.7	27.1	27.6
18	m. c.t.	29.9	33.4	31.7	31.7	34.2	29.0	35.5	32.9	32.3
19	<i>F</i> tests	S	F	E	m. int.	S-F	S-E	F-E	m. ext.	m. all
20	<i>H</i>	9.1	12.7	33.3	18.4	15.7	25.5	27.3	22.8	20.6
21	<i>W</i>	29.1	32.7	13.3	25.0	27.3	29.1	35.5	30.6	27.8
22	<i>I</i>	20.0	23.6	37.8	27.1	28.9	30.9	46.4	35.4	31.3
23	<i>Ch</i>	16.4	0.0	8.9	8.4	7.4	17.3	12.7	12.5	10.5
24	<i>l'</i>	27.3	27.3	42.2	32.3	21.5	27.3	39.1	29.3	30.8
25	<i>h'</i>	10.9	9.1	33.3	17.8	24.8	21.8	36.4	27.7	22.7
26	<i>w'</i>	18.2	47.3	37.8	34.4	33.1	28.2	45.5	35.6	35.0
27	<i>i'</i>	9.1	27.3	8.9	15.1	25.6	12.7	39.1	25.8	20.5
28	m. size	17.5	22.5	26.9	22.3	23.0	24.1	35.3	27.5	24.9
29	<i>H/W</i>	0.0	27.3	33.3	20.2	16.5	19.1	30.0	21.9	21.0
30	<i>H/I</i>	32.7	43.6	46.7	41.0	43.0	38.2	51.8	44.3	42.7
31	<i>w'/h'</i>	18.2	30.9	31.1	26.7	24.8	50.0	64.5	46.4	36.6
32	<i>l'/i'</i>	40.0	32.7	26.7	33.1	37.2	37.3	48.2	40.9	37.0
33	<i>l'/h'</i>	3.6	21.8	15.6	13.7	22.3	18.2	50.0	30.2	21.9
34	<i>l'/w'</i>	9.1	23.6	31.1	21.3	23.1	25.5	44.5	31.0	26.2
35	m. shape	17.3	30.0	30.8	26.0	27.8	31.4	48.2	35.8	30.9
36	m. var.	17.4	25.7	28.6	23.9	25.1	27.2	40.8	31.0	27.5
37	<i>Z</i> tests	S	F	E	m. int.	S-F	S-E	F-E	m. ext.	m. all
38	<i>H/W</i>	1.8	12.7	0.0	4.8	7.4	2.7	10.0	6.7	5.8
39	<i>H/I</i>	5.5	0.0	6.7	4.1	0.0	10.0	10.0	6.7	5.4
40	<i>w'/h'</i>	14.5	21.8	20.0	18.8	19.0	16.4	16.4	17.3	18.0
41	<i>l'/i'</i>	12.7	0.0	0.0	4.2	9.1	6.4	1.8	5.8	5.0
42	<i>l'/h'</i>	9.1	10.9	28.9	16.3	9.9	16.4	18.2	14.8	15.6
43	<i>l'/w'</i>	12.7	14.5	13.3	13.5	6.6	11.8	8.2	8.9	11.2
44	m. exp. a	9.4	10.0	11.5	10.3	8.7	10.6	10.8	10.0	10.2
45	m. all	21.1	26.1	26.9	24.7	26.0	25.0	33.3	28.1	26.4

Text Table 8.27 Summary of statistical tests for the 100 kyr resolution transects.

Italicised values show the proportions—as percentages—of various fields of possible sample pairings from Appendix Tables 3.3.1 - 3.3.5 which register as significantly different at the 95% confidence level. All fields correspond to entire site transects (S, F, E) without differentiation into upper and lower halves. Columns b, c & d show within site comparisons, columns f, g & h show between site comparisons. Results are split between characters and tests performed as listed; other columns and rows show summaries of the italicised fields and are mean values (m. = mean) of the percentages displayed in the rows to the left or the columns above them. Bolder or bigger values represent ever more inclusive sets so that e10, for example, is the mean for all differences in variance for size characters found in the within site fields (i.e. within S, F and E rather than between them e.g. S-F). Column j summarises both within and between site values whereas rows 18 and 36 capture both size and shape for central tendency (c.t.) and variance (var.), respectively, and 44 is for trajectory values. Row 45 is for all tests, all sites. See text adjacent text for discussion

Between-site comparisons show that Folkestone and Escalles generally have more significant differences between them than either one does with Southerham; this is true for F tests of standard deviations for size and shape (rows 28 & 35), t tests for mean size (although not for shapes—compare rows 10 & 17) and for Z tests (α values - row 44). Interestingly, this situation suggests exactly the opposite relationship to the one we saw in the timeseries patterns themselves, where Folkestone and Escalles showed the most similarity: in other words, Folkestone and Escalles differ *most* in terms of magnitude, but *least* in terms of pattern.

8.2.3.iii Patterns And Environmental Parameters

The 100 kyr transects were designed to address the question of degrees and rates of morphological change in environments of varying stability, and the sedimentary sequence is usefully divided into a changeable lower half and more stable upper one for exactly that purpose. The procedure for this analysis is similar to that used in the finer resolution transects (the method is outlined in Section 8.1.4.ii) except that three different sites are also available for cross-comparison.

Each site-to-site pairing on the statistical test grids (self with self, S-S, F-F, E-E, and self with other, S-F, F-E, S-E) was split into lower (B31-C15 [0-500]) and upper (C15-C45 [500-1000]) halves, and the relationships between various combinations of ‘internal’ (within-site) and ‘external’ (between-site) pairings were examined to see which ones tended to produce a higher percentage of statistical differences. There are 30 possible cross-comparisons which might be applied before repetitions occur, but for brevity only the most informative half-dozen of these are considered (Text Table 8.28 below).

For each of the three *within* site comparisons we can ask, “Do samples in the upper half show more differences ‘internally’ than samples from the lower half?” (e.g. “Was mean H at Folkestone shifting more in the upper or the lower half of that succession?”)—this combination of fields is shown in the three central diagonal boxes of Text Figure 8.6. Similarly, for each of the three relationships *between* sites, we can ask, “Do samples in the upper halves of sites A and B show more differences between themselves than equivalent sample pairings from their lower halves?” (e.g. “Were there more differences between mean H in populations from Folkestone and Southerham in the

S.U. vs S.U.	S.U. vs S.L.	S.U. vs F.U.	S.U. vs F.L.	S.U. vs E.U.	S.U. vs E.L.
S.L. vs S.U.	S.L. vs S.L.	S.L. vs F.U.	S.L. vs F.L.	S.L. vs E.U.	S.L. vs E.L.
F.U. vs S.U.	F.U. vs S.L.	F.U. vs F.U.	F.U. vs F.L.	F.U. vs E.U.	F.U. vs E.L.
F.L. vs S.U.	F.L. vs S.L.	F.L. vs F.U.	F.L. vs F.L.	F.L. vs E.U.	F.L. vs E.L.
E.U. vs S.U.	E.U. vs S.L.	E.U. vs F.U.	E.U. vs F.L.	E.U. vs E.U.	E.U. vs E.L.
E.L. vs S.U.	E.L. vs S.L.	E.L. vs F.U.	E.L. vs F.L.	E.L. vs E.U.	E.L. vs E.L.

Text Figure 8.6 Based on the layout of the statistical grids (Appdx. Tabs. 3.2 & 3.3), this figure shows the combination of sites and segments compared when the 100 kyr transects at Southerham, Folkestone and Escalles are split into upper and lower halves. Arrows between the grey fields denote comparisons actually made, so that ‘S.U. vs. S.U. ⇔ S.L. vs. S.L.’ is an assessment of whether there are more significant differences ‘internally’ within the Southerham upper half or more in the Southerham lower half. In the figure, these comparisons run diagonally across the middle. By contrast, the three sets of pairings in the upper right hand corner denote situations such as ‘S.U. vs. F.U. ⇔ S.L. vs. F.L.’, which is an assessment of whether or not there are more significant differences between the Southerham and Folkestone upper halves, or between Southerham and Folkestone lower halves.

upper or lower halves of those sequences?”)—this combination of fields is shown in the three boxes clustered in the top right hand part of Text Figure 8.6.

Actual numerical values for these combinations are hard to present in an easily accessible fashion (that is, they are easy to present but difficult to glean anything from), so the summary chart addressing these questions is limited to presenting a U or L per category, depending on whether it was the upper or lower half that registered a *higher* proportion of significant differences.

Text Table 8.28 documents these results, clearly revealing the pattern we anticipated from the morphometric timeseries graphs. *t* tests for mean size and shape (b10 – e10 & b17 – e17), and *Z* tests for *a* values (b44 – e44), tend to show that for *within* site cases there were more significant differences in the lower half of each site than in the upper; *F* tests for standard deviation in both sizes and shapes also give this general result (e28 & e35),

	a	b	c	d	e	f	g	h	i	j
1	<i>t</i> tests	S	F	E	sum	S-F	S-E	F-E	sum	sum.all
2	<i>H</i>	x	L	L	U0:L2	U	L	U	U2:L1	U2:L3
3	<i>W</i>	L	L	L	U0:L3	U	L	U	U2:L1	U2:L4
4	<i>I</i>	L	L	L	U0:L3	U	L	U	U2:L1	U2:L4
5	<i>Ch</i>	L	U	U	U2:L1	U	U	U	U3:L0	U5:L1
6	<i>l'</i>	L	L	L	U0:L3	x	L	U	U1:L1	U1:L4
7	<i>h'</i>	L	x	L	U0:L2	x	L	U	U1:L1	U1:L3
8	<i>w'</i>	L	L	L	U0:L3	L	L	U	U1:L2	U1:L5
9	<i>i'</i>	U	L	L	U1:L2	L	L	L	U0:L3	U1:L5
10	sum.size.c.t.	U1:L6	U1:L6	U1:L7	U3:L19	U4:L2	U1:L7	U7:L1	U12:L10	U15:L29
11	<i>H/W</i>	L	L	L	U0:L3	U	L	U	U2:L1	U2:L4
12	<i>H/I</i>	L	U	U	U2:L1	L	U	U	U2:L1	U4:L2
13	<i>w/h'</i>	L	U	L	U1:L2	L	L	U	U1:L2	U2:L4
14	<i>l'/i'</i>	x	U	L	U1:L1	U	U	U	U3:L0	U4:L1
15	<i>l'/h'</i>	L	L	L	U0:L3	L	L	L	U0:L3	U0:L6
16	<i>l'/w'</i>	L	L	U	U1:L2	L	L	U	U1:L2	U2:L4
17	sum.shape.c.t.	U0:L5	U3:L3	U2:L4	U5:L12	U2:L4	U2:L4	U5:L1	U9:L9	U14:L21
18	sum. t	U1:L11	U4:L9	U3:L11	U8:L31	U6:L6	U3:L11	U12:L2	U21:L19	U29:L50
19	<i>F</i> tests	S	F	E	sum	S-F	S-E	F-E	sum	sum.all
20	<i>H</i>	L	L	L	U0:L3	x	L	L	U0:L2	U0:L5
21	<i>W</i>	U	U	L	U2:L1	U	L	U	U2:L1	U4:L2
22	<i>I</i>	x	L	L	U0:L2	U	L	U	U2:L1	U2:L3
23	<i>Ch</i>	U	x	L	U1:L1	U	L	U	U2:L1	U3:L2
24	<i>l'</i>	L	U	x	U1:L1	U	L	U	U2:L1	U3:L2
25	<i>h'</i>	L	x	L	U0:L2	U	L	U	U2:L1	U2:L3
26	<i>w'</i>	U	L	L	U1:L2	U	L	x	U1:L1	U2:L3
27	<i>i'</i>	U	U	U	U3:L0	U	U	U	U3:L0	U6:L0
28	sum.size.var.	U4:L3	U3:L3	U1:L6	U8:L12	U7:L0	U1:L7	U6:L1	U14:L8	U22:L20
29	<i>H/W</i>	x	L	U	U1:L1	L	U	L	U1:L2	U2:L3
30	<i>H/I</i>	x	L	U	U1:L1	L	U	L	U1:L2	U2:L3
31	<i>w/h'</i>	L	L	U	U1:L2	L	U	U	U2:L1	U3:L3
32	<i>l'/i'</i>	U	U	L	U2:L1	U	U	U	U3:L0	U5:L1
33	<i>l'/h'</i>	x	U	L	U1:L1	U	L	L	U1:L2	U2:L3
34	<i>l'/w'</i>	L	L	U	U1:L2	L	U	U	U2:L1	U3:L3
35	sum.shape.var.	U1:L2	U2:L4	U4:L2	U7:L8	U2:L4	U5:L1	U3:L3	U10:L8	U17:L16
36	sum. F	U5:L5	U5:L7	U5:L8	U15:L20	U9:L4	U6:L8	U9:L4	U24:L16	U39:L36
37	<i>Z</i> tests	S	F	E	sum	S-F	S-E	F-E	sum	sum.all
38	<i>H/W</i>	x	x	x	U0:L0	U	L	U	U2:L1	U2:L1
39	<i>H/I</i>	L	x	L	U0:L2	x	L	U	U1:L1	U1:L3
40	<i>w/h'</i>	L	L	L	U0:L3	L	x	x	U0:L1	U0:L4
41	<i>l'/i'</i>	L	x	x	U0:L1	L	L	U	U1:L2	U1:L3
42	<i>l'/h'</i>	L	U	U	U2:L1	L	L	U	U1:L2	U3:L3
43	<i>l'/w'</i>	L	x	L	U0:L2	U	L	L	U1:L2	U1:L4
44	sum.exp. a	U0:L5	U1:L1	U1:L3	U2:L9	U2:L3	U0:L5	U4:L1	U6:L9	U8:L18
45	sum.all	U6:L21	U10:L17	U9:L22	U25:L60	U17:L13	U9:L24	U25:L7	U51:L44	U76:L104
46	sum. Z and t	U1:L16	U5:L10	U4:L14	U10:L40	U8:L9	U3:L16	U14:L3	U27:L28	U37:L68

Text Table 8.28 Summary of the proportion of significant differences found throughout the 100 kyr resolution transects partitioned into upper and lower halves.

The chart shows differences in the percentages of significant values appearing in the Upper or Lower halves of the fields of various combinations of sites from Appendix Tables 3.3.1 - 3.3.5.

In order to clarify the results and make patterns stand out, U and L have been used in place of actual percentage values to simply denote cases in which there is a larger proportion of significant differences found in the upper or lower portions of the specified fields. x is used for cases where there is a tie.

For example, the appearance of L in the *Ch* category of the *S t* test field (b5) means that there were more significantly differences *t* tests at S in the lower half of the succession than in the upper; the appearance of U in the *S-F t* test category (f5) records the fact that there were more significant differences between *Ch* at S and F in the upper part of the 100 kyr sequence than in the lower.

As with other charts, the fields are grouped by character and style of test while summary columns and rows appear around the edge. Further details and discussion of these results can be found in the adjacent text.

although the signal is more mixed at individual localities (b28 – d28 & b35 – d35).

When it comes to comparisons *between* sites, there are slightly more differences between the upper halves than the lower, which we should have anticipated from the widespread tendency for divergence, as noted above. The effect is most clearly seen in Folkestone and Escalles, with relationships between either of these and Southerham having a more variable pattern.

Overall, from 102 possible sets of internal patterns and 102 sets of external ones (both *F* and *t* tests for 3x8 sizes and 3x6 shapes, plus *Z* tests for 3x6 trajectories), the *within-site* assessments score 25 cases of more significant difference within the upper half against 60 cases of more in the lower (U25:L60, box e45 —with 17 ties), while the *between-site* assessments score 51 cases of greater difference between upper halves against 44 cases between the lower (U51:L44, box i45 -with 7 ties).

Furthermore, average rates of change also are generally greater *within* the lower halves of each of the sections (Appdx. Tabs. 3.5.2.a & b); but, that for size parameters at least, there are larger differences *between sites* in the upper half of the succession (Appdx. Tabs. 3.5.3.a & b).

These results are of sufficient significance to the *Plus ça change* model that they are replicated and summarised in Text Table 8.29, below.

	within site differences				between site differences			
	S	F	E	sum	S-F	S-E	F-E	sum
<i>t</i> test size	U1:L6	U1:L6	U1:L7	<i>U3:L19</i>	U4:L2	U1:L7	U7:L1	<i>U12:L10</i>
<i>t</i> test shape	U0:L5	U3:L3	U2:L4	<i>U5:L12</i>	U2:L4	U2:L4	U5:L1	<i>U9:L9</i>
<i>F</i> test size	U4:L3	U3:L3	U1:L6	<i>U8:L12</i>	U7:L0	U1:L7	U6:L1	<i>U14:L8</i>
<i>F</i> test shape	U1:L2	U2:L4	U4:L2	<i>U7:L8</i>	U2:L4	U5:L1	U3:L3	<i>U10:U8</i>
<i>Z</i> test traj	U0:L5	U1:L1	U1:L3	<i>U2:L9</i>	U2:L3	U0:L5	U4:L1	<i>U6:L9</i>
total tests	U6:L21	U10:17	U9:L22	<i>U25:L60</i>	U15:L13	U9:L24	U25:L7	<i>U51:L44</i>
size rates	U1:L7	U1:L7	U0:L8	<i>U2:L22</i>	U7:L1	U6:L2	U8:L0	<i>U21:L3</i>
shape rates	U1:L5	U3:L3	U2:L4	<i>U6:L12</i>	U3:L3	U2:L4	U3:L3	<i>U8:L10</i>
total rates	U2:L12	U4:L12	U2:L12	<i>U8:L34</i>	U10:L4	U8:L6	U11:L3	<i>U29:L13</i>

Text Table 8.29 Summary chart showing the distribution of rates and statistical shifts among the upper and lower halves of the three long sections. U and L designate Upper or Lower, respectively, and record the balance of significant differences or rate magnitudes per individual timeseries for within-site cases, or between pairs of timeseries for between-site cases. The results are broadly similar throughout: there are more shifts and higher rates within the lower half of each transect, and more shifts and larger differences between transects in the upper half. See text for discussion.

We have already seen that for size parameters there are net increases in standard deviation across the 100 kyr sections: at Folkestone all 8/8 characters show more variation in the final sampling horizon than they did in the lowermost; at Escalles there were 5/8 increases; at Southerham 4/8. More relevantly at this stage, we can ask whether there were *general*, i.e. average, differences in the magnitude of standard deviation between each half of the succession. Once again, this is not the same as applying *F* tests, which tell us whether standard deviation itself is likely to differ between pairs of samples—a case of assessing how variegated through time and space the variation is: what we are interested in here, by contrast, is simply an overall magnitude.

Text Table 8.30 (below) shows average (mean) standard deviation scores for the upper and lower half of the 100 kyr resolution sections when broken into sites and characters. Of the size parameters, three quarters (18/24) show a higher standard deviation in the upper half of the section than the lower; with shapes the proportion is two thirds (12/18). There is an unambiguous tendency for higher variation to be found in the upper, relatively stable half of the succession.

Size	<i>H</i>	<i>W</i>	<i>I</i>	<i>Ch</i>	<i>l'</i>	<i>h'</i>	<i>w'</i>	<i>i'</i>	Total
S upper	118.0	55.9	73.9	2.1	46.0	23.9	44.4	32.2	2
S lower	123.0	60.4	82.7	2.3	47.4	25.4	39.9	31.9	6
F upper	138.0	71.6	99.6	2.3	56.8	31.9	48.6	40.1	8
F lower	122.1	54.3	86.0	2.2	46.6	26.7	37.2	35.4	0
E upper	124.0	50.8	76.5	2.0	42.4	25.7	37.7	29.8	8
E lower	105.1	48.5	70.8	1.9	41.6	24.2	35.5	28.9	0
Shape		<i>H/W</i>	<i>H/I</i>	<i>w'/h'</i>	<i>l'/i'</i>	<i>l'/h'</i>	<i>l'/w'</i>		Total
S upper		0.23	0.25	0.29	0.52	0.25	0.20		5
S lower		0.23	0.20	0.27	0.46	0.27	0.19		1
F upper		0.28	0.30	0.32	0.60	0.29	0.22		5
F lower		0.25	0.26	0.31	0.53	0.30	0.19		1
E upper		0.26	0.28	0.20	0.38	0.22	0.15		2
E lower		0.20	0.19	0.22	0.42	0.23	0.18		4

Text Table 8.30 *Averages for standard deviation scores (in microns and micron ratios) in each of the size and shape characters within restricted fields of the 100 kyr resolution transect. Largest values are marked in bold and totalled in the end column. See text for discussion.*

8.2.4 Combined Scales

The Combined Scales section presents all three sampling resolutions from Folkestone calibrated to the same temporal dimension. It helps to highlight some otherwise obscure relationships between the magnitude of changes in morphology at each sampling scale. Since that is the main purpose of this section, the discussion will be fairly abbreviated.

The timeseries for this section contain no new sampling points, but they do employ larger sample numbers and are therefore more statistically robust. The correlation grids thus serve to amplify consistent patterns or dampen inconsistent ones across the three nested transects.

Charts	Contents	Location
Size	means, standard deviation, rate	Appdx. Figs. 5.4.1i-viii
Shape	means, standard deviation, rate	Appdx. Figs. 5.4.2i-vi
Trajectory	<i>a</i> and <i>b</i> values	Appdx. Figs. 5.4.3.i-vi
Categoricals	area, % similarity, diversity	Appdx. Figs. 5.4.3.i-vii
Tables	Contents	Location
Size	<i>t</i> tests	Appdx. Tabs. 3.2.1.i-viii
Size	<i>F</i> tests	Appdx. Tabs. 3.2.1.i-viii
Size	<i>haldanes</i>	Appdx. Tabs. 3.5.1.a
Shape	<i>t</i> tests	Appdx. Tabs. 3.2.3.i-vi
Shape	<i>F</i> tests	Appdx. Tabs. 3.2.4.i-vi
Shape	<i>haldanes</i>	Appdx. Tabs. 3.5.1.b
Trajectory	<i>Z</i> tests	Appdx. Tabs. 3.2.5.i-vi
Categoricals	% similarity	Appdx. Tabs. 3.6.1
Categoricals	diversity	Appdx. Tabs. 3.6.2 & 3.6.3

Text Table 8.31 *Location of morphometric information for the Combined Scales transect.*

8.2.4.i Individual Patterns

8.2.4.i.a Size

Combining the scales has magnified the frequency of positive correlation found between size characters in the earlier sections; with the exception of the x category, there are more significant values present in this extended series than for any of its individual

component transects. A pair of helpful summary charts can also be found in Section 8.2.4.ii, below. Correlations between timeseries plots for mean values now stand at 78.6%, with *i'* and especially *Ch* as the only size parameters still showing independent behaviour.

Combined Scales Folkestone — Size																			
<u>x</u>	<i>H</i>	<i>W</i>	<i>I</i>	<i>Ch</i>	<i>l'</i>	<i>h'</i>	<i>w'</i>	<i>i'</i>	sd		<i>H</i>	<i>W</i>	<i>I</i>	<i>Ch</i>	<i>l'</i>	<i>h'</i>	<i>w'</i>	<i>i'</i>	
<i>H</i>	<u>1</u>	<u>1</u>	<u>1</u>	<u>1</u>	<u>1</u>	<u>1</u>	<u>1</u>	<u>0</u>	<i>H</i>	<i>H</i>									<i>H</i>
<i>W</i>	<u>1</u>	<u>0</u>	<u>1</u>	<u>1</u>	<u>1</u>	<u>0</u>	<u>0</u>	<u>1</u>	<i>W</i>	<i>W</i>	<u>0</u>								<i>W</i>
<i>I</i>	<u>1</u>	<u>1</u>	<u>1</u>	<u>1</u>	<u>1</u>	<u>1</u>	<u>1</u>	<u>0</u>	<i>I</i>	<i>I</i>	<u>0</u>	<u>0</u>							<i>I</i>
<i>Ch</i>	<u>1</u>	<u>0</u>	<u>1</u>	<u>1</u>	<u>0</u>	<u>1</u>	<u>1</u>	<u>0</u>	<i>Ch</i>	<i>Ch</i>	<u>1</u>	<u>0</u>	<u>0</u>						<i>Ch</i>
<i>l'</i>	<u>1</u>	<u>1</u>	<u>1</u>	<u>0</u>	<u>0</u>	<u>1</u>	<u>0</u>	<u>1</u>	<i>l'</i>	<i>l'</i>	<u>1</u>	<u>0</u>	<u>0</u>	<u>0</u>					<i>l'</i>
<i>h'</i>	<u>1</u>	<u>1</u>	<u>1</u>	<u>0</u>	<u>1</u>	<u>0</u>	<u>0</u>	<u>0</u>	<i>h'</i>	<i>h'</i>	<u>0</u>	<u>0</u>	<u>1</u>	<u>0</u>	<u>1</u>				<i>h'</i>
<i>w'</i>	<u>1</u>	<u>1</u>	<u>1</u>	<u>0</u>	<u>1</u>	<u>1</u>	<u>0</u>	<u>0</u>	<i>w'</i>	<i>w'</i>	<u>0</u>	<u>0</u>	<u>0</u>	<u>0</u>	<u>0</u>	<u>1</u>			<i>w'</i>
<i>i'</i>	<u>0</u>	<u>1</u>	<u>1</u>	<u>0</u>	<u>1</u>	<u>1</u>	<u>1</u>	<u>0</u>	<i>i'</i>	<i>i'</i>	<u>0</u>	<u>1</u>	<u>1</u>	<u>0</u>	<u>0</u>	<u>0</u>	<u>0</u>		<i>i'</i>
m	<i>H</i>	<i>W</i>	<i>I</i>	<i>Ch</i>	<i>l'</i>	<i>h'</i>	<i>w'</i>	<i>i'</i>		r	<i>H</i>	<i>W</i>	<i>I</i>	<i>Ch</i>	<i>l'</i>	<i>h'</i>	<i>w'</i>	<i>i'</i>	

actual & possible	22	28	3	8	18	28	7	28	50	92
% significant	m	78.6	x	37.5	sd	64.3	r	25.0	all	54.3

Text Table 8.32 Timeseries correlations for size parameters in the Combined Scales transect. Results in bold are significant at the 95% confidence level. See Text Table 8.31 (above) for the chart locations and Section 8.1.5.iv for a discussion of the correlations and correlation grid layout. The lowermost strip summarises actual significant values as a percentage of the total number possible for each of five fields: means with means (*m*), standard deviations with standard deviations (*sd*), means with standard deviations (*x*), rates with rates (*r*), and all these fields collectively (*all*).

Plots for the size variables (Appdx. Figs. 5.4.1.i-viii) show that the tight cluster of points representing C13 almost always includes some members which are smaller than *any* of the points from the coarser resolutions; this observation holds for both mean values and standard deviations. A glance back to the fully expanded 2 kyr survey shows that it is primarily because the C13 transect contains specimens from the chalk and chalk-marl boundary zones. Specimens from C13 tend to be small anyway, and Appendix Tables 3.2.1.i-viii indicate that they are often significantly different from whole swathes of the upper halves of both the 20 kyr and 100 kyr transects, but also that those from the marl of C13 tend to be within a range set by adjacent marl-derived sampling populations in the 20 kyr transect, such as C10 [0], C11 [20], C12 [40] and C14 [80] (these square brackets refer to time horizons on the statistical grids and the 20 kyr plot). It is thus the specimens from the chalk and boundary zones of the single couplet that produce the unusually low spike on a composite plot. Apart from that, however, the shifts in size from all sampling scales are of a remarkably similar magnitude.

It is no surprise to find that rates appear fast at high sampling resolutions since reversals of direction must necessarily cancel out over extended periods, and also because the magnitude of any net change becomes ever more diluted as it is smeared across an increasing number of lifecycles (i.e. generation times). This is what we expected, and what the scaling indices ($h_{3,3}$, $h_{4,3}$, h_5) exist to account for. Nevertheless, seeing this relationship as a pictorial representation, rather than as a stark numerical value, certainly brings home how large a difference the sampling resolution can make to a perceived evolutionary rate.

8.2.4.i.b Shape

Combined Scales Folkestone — Shape															
<u>x</u>	H/W	H/I	w'/h'	l'/i'	l'/h'	l'/w'	sd		H/W	H/I	w'/h'	l'/i'	l'/h'	l'/w'	
H/W	<u>1</u>	0	1	0	1	1	H/W	H/W							H/W
H/I	0	<u>1</u>	0	0	1	0	H/I	H/I	0						H/I
w'/h'	0	0	<u>1</u>	0	1	1	w'/h'	w'/h'	0	1					w'/h'
l'/i'	0	0	0	<u>0</u>	1	0	l'/i'	l'/i'	1	1	1				l'/i'
l'/h'	0	0	1	1	<u>0</u>	1	l'/h'	l'/h'	-1	0	0	0			l'/h'
l'/w'	0	0	-1	0	0	<u>0</u>	l'/w'	l'/w'	0	0	1	1	0		l'/w'
m	H/W	H/I	w'/h'	l'/i'	l'/h'	l'/w'		r	H/W	H/I	w'/h'	l'/i'	l'/h'	l'/w'	

actual & possible	3	15	3	6	8	15	7	15	21	51
% significant	m	20.0	<u>x</u>	50.0	sd	53.3	r	46.7	all	41.2

Text Table 8.33 *Timeseries correlations for shape parameters in the Combined Scales transect. Results in bold are significant at the 95% confidence level. See Text Table 8.31 (above) for the chart locations. The lowermost strip summarises actual significant values as a percentage of the total number possible for each of five fields: means with means (m), standard deviations with standard deviations (sd), means with standard deviations (\underline{x}), rates with rates (r), and all these fields collectively (all).*

As with the sizes, there are also more significant correlations throughout the combined-scales plots for shape than were present on any of its component transects. Again, this implies that correlations between character pairs at different sampling resolutions tend agree with, rather than contradict, one another, and that the larger spread of data has permitted genuine features to be identified with greater confidence.

Mean values for the H/W ratio to some extent match the pattern we saw for the sizes wherein a portion of the tight 2 kyr cluster lies beyond the range set by any other sampling scale; this probably reflects the fact that this shape parameter changes so rapidly during growth (recall the chamber cohort trajectories of Text Figure 7.1) that small specimens from C13 translate quite literally as low values for the ratios of H/W and H/I . For the other

shape components, both means and standard deviation generally lie comfortably within the range of more widely spaced samples. As with the sizes, there is little aside from sample spacing to distinguish between the shape timeseries generated at different scales.

8.2.4.i.c Trajectory

Combined Scales Folkestone — Trajectory							
<u>x</u>	H/W	H/I	w'/h'	l'/i'	l'/h'	l'/w'	b
H/W	-1	0	0	0	-1	0	H/W
H/I	0	-1	0	1	0	0	H/I
w'/h'	0	0	-1	0	0	-1	w'/h'
l'/i'	0	1	-1	-1	0	1	l'/i'
l'/h'	-1	0	0	0	-1	1	l'/h'
l'/w'	0	0	-1	1	0	-1	l'/w'
a	H/W	H/I	w'/h'	l'/i'	l'/h'	l'/w'	

actual & possible	5	15	6	6	5	15	15	36
% significant	a	33.3	<u>x</u>	100.0	b	33.3	all	41.7

Text Table 8.34 Timeseries correlations for trajectory parameters in the Combined Scales transect. Results in bold are significant at the 95% confidence level. See Text Table 8.31 (above) for the chart locations. The lowermost strip summarises actual significant values as a percentage of the total number possible for each of four fields: a values with a values (a), b values with b values (b), a values with b values (x), and all these fields collectively (all).

Trajectories draw much the same commentary as the shapes: there are generally a higher proportion of significant correlations, but apart from that the behaviour of the two parameters is essentially the same at all scales. As ever, the *a* and *b* values match each other in perfect negative correlation, while outside the x field correlations for each of the two components occur with an equal frequency.

8.2.4.i.d Categorical

In stark contrast to the trend seen in the other measurements, the diversity and similarity plots for categorical features have scarcely more correlations among them than we would predict by chance alone. On an individual basis, however, several of these metrics, in conjunction with their proportional area plots, do show intriguing features.

Combined Scales Folkestone — Categorical							
	<i>ind</i>	<i>tw</i>	<i>g%</i>	<i>dist</i>	<i>chi</i>	<i>type</i>	H
<i>ind</i>		0	0	0	0	0	<i>ind</i>
<i>tw</i>	0		0	0	0	1	<i>tw</i>
<i>g%</i>	0	0		0	0	0	<i>g%</i>
<i>dist</i>	0	0	0		0	0	<i>dist</i>
<i>chi</i>	0	-1	0	0		0	<i>chi</i>
<i>type</i>	0	0	0	0	0		<i>type</i>
%	<i>ind</i>	<i>tw</i>	<i>g%</i>	<i>dist</i>	<i>chi</i>	<i>type</i>	

actual & possible	1	15	1	15	2	30
% significant	H	6.7	s %	6.7	all	6.7

Text Table 8.35 *Timeseries correlations for category parameters in the Combined Scales transect. Results in bold are significant at the 95% confidence level. See Text Table 8.31 (above) for the chart locations. The lowermost strip summarises actual significant values as a percentage of the total number possible for each of three fields: H values with H values (H), percentage similarity values with percentage similarity values (s %), and both these fields collectively (all).*

The percentage similarity plot for twist (*tw*) appears to exhibit a pattern which is strikingly similar to that predicted by the *Plus ça change* model, with stasis for the first half giving way to gradually increasing amounts of change later on, and finally producing a series of rapid bursts from horizon C21 [590] onwards (Appdx. Fig. 5.4.4.ii). Unfortunately, a glance back at the original 100 kyr plots for this character (Appdx. Fig. 5.4.3.ii) shows that despite an apparent general co-ordination between the three *scales* at Folkestone, neither of the other 100 kyr *sites* plays host to the same pattern, and so from that broader perspective it appears to be something of a fluke.

By way of contrast, the percentage glauconite category (*g%*) appears to behave fairly randomly at all scales in terms of rate (i.e. % similarity) and variation (Shannon's H), even though we know from the 100 kyr plots that broad correspondences do in fact occur between all three sites (Appdx. Figs. 5.4.4.iii & 5.4.3.iii).

Meanwhile, the *type* category exhibits patterns both between scales *and* between sites. The amount of change remains approximately constant throughout all three sampling resolutions, but from horizon C10 [400] onwards, diversity climbs steadily. This increase in variation can be picked out in the proportional area chart too, and, as we saw from the 100 kyr charts, it extends to all three sites (Appdx. Figs. 5.4.4.vi & 5.4.3.vi).

None of the other categorical characters has any really noteworthy feature except that all of them display roughly equivalent amounts of change no matter what the observation scale.

8.2.4.ii Systematic Patterns

<i>n</i>	Size	<i>m</i>	<i>x</i>	<i>sd</i>	<i>r</i>	all
12	F 2 kyr	7.1	0.0	17.9	0.0	7.6
11	F 20 kyr	32.1	0.0	50.0	21.4	31.5
10	S 100 kyr	71.4	12.5	39.3	21.4	41.3
10	F 100 kyr	50.0	37.5	25.0	10.7	29.3
9	E 100 kyr	50.0	62.5	57.1	14.3	42.4
33	F 2, 20, 100 kyr	78.6	37.5	64.3	25.0	54.3
<i>n</i>	Shape	<i>m</i>	<i>x</i>	<i>sd</i>	<i>r</i>	all
12	F 2 kyr	6.7	0.0	6.7	20.0	9.8
11	F 20 kyr	13.3	0.0	33.3	13.3	17.6
10	S 100 kyr	20.0	33.3	13.3	0.0	13.7
10	F 100 kyr	13.3	50.0	0.0	6.7	11.8
9	E 100 kyr	26.7	50.0	0.0	20.0	19.6
33	F 2, 20, 100 kyr	20.0	50.0	53.3	46.7	41.2
<i>n</i>	Trajectory	<i>a</i>	<i>x</i>	<i>b</i>	—	all
12	F 2 kyr	13.3	100.0	13.3		27.8
11	F 20 kyr	20.0	100.0	26.7		36.1
10	S 100 kyr	33.3	100.0	6.7		33.3
10	F 100 kyr	20.0	100.0	6.7		27.8
9	E 100 kyr	13.3	100.0	26.7		33.3
33	F 2, 20, 100 kyr	26.7	100.0	33.3		41.7
<i>n</i>	Categorical	—	—	<i>H</i>	<i>S%</i>	all
12	F 2 kyr			0.0	6.7	3.3
11	F 20 kyr			6.7	13.3	10.0
10	S 100 kyr			13.3	6.7	10.0
10	F 100 kyr			13.3	13.3	13.3
9	E 100 kyr			0.0	13.3	6.7
33	F 2, 20, 100 kyr			6.7	6.7	6.7

Text Table 8.36 Summary table showing the density of correlations for morphological measurement parameters from each transect represented in the text. All data are collected from the lowermost grids of previously shown tables. The leftmost column shows the sample number ‘*n*’ for the timeseries strings under consideration (e.g. *E* has 9 because there are 10 samples in that transect and therefore 9 instances of shifting between vertically adjacent horizons).

Text Table 8.36 shows the correlation grid summaries for all sites and scales assembled together. With the exception of the categorical parameters, which are uniformly low throughout, the combined-scales timeseries tend to reveal a higher percentage of significant correlations than most of their less inclusive, individual-scale components. This strongly suggests that an absence of significant correlation between smaller timeseries might

often be due to the signal being overwhelmed by noise, rather than it being absent entirely; nevertheless, there is likely to be some difference between the character pairings in terms of noise resistance, and this matter will be investigated in the next chapter. In those cases where the extra sample size has failed to disclose any further correlation (especially for *Ch*) it is a solid confirmation that these characters behave independently. In fact, in many cases it is satisfying to see just how little difference a tripling of the sample size actually makes. The percentage values in the table above can be perceived, in admittedly broad terms, to tell a fairly consistent story.

Indeed, there are several areas of subtle consistency in Text Table 8.36. The fact that the categorical parameters never deviate very far from the 5% significance is one. In the case of trajectories and shapes (though not trajectory χ values), the proportions wander around anywhere in the broad zone between 0-50%, but not much higher. And, regardless of scale, the sizes often show much more correlation than either shapes or trajectories, sometimes reaching well in excess of 50%. It is also evident that the 2 kyr transect always hosts rather fewer correlations than any of the coarser or more inclusive data sets.

Turning to Text Table 8.37, the occupied space of possible significant shifts (compiled from Appendix Figures 3.2.1 – 3.2.5), we see a similar story unfold. t tests for shifts in size (b10 – d10) show that the 2 kyr transect hosted less than two thirds the number of significant differences seen across broader transects; t tests for changes in shape, by contrast, were actually more frequent in C13 (cell d17), as were shifts in the allometric exponent (cell d44), in both cases perhaps partly because shifts in shape variance (cell d35) were so low.

Looking at differences *between* scales, cells f10 – h10 and f17 – h17 again show that the 2 kyr series is distinct from the others, accumulating more significant differences in both size and shape between it and them, than the coarse transects have with one another: C13 really did host specimen populations with unusual size and shape parameters, and Appendix Tables 3.2.1 – 3.2.5 show that many of these are associated with the couplet chalk and boundary zones. Aside from the peculiarities of C13, the summary rows of Text Table 8.37, in conjunction with those from Text Table 8.27 (page 394), serve to show how consistent the relationships between different parameters of size shape and trajectory were as a bulk measure.

	a	b	c	d	e	f	g	h	i	j
	<i>t</i>	100	20	2	mean	100k-	20k-	2k-	mean	mean
1	tests	kyr	kyr	kyr	within	20k	2k	100k	between	all
2	<i>H</i>	40.0	47.0	10.3	32.4	45.5	66.1	76.9	62.8	47.6
3	<i>W</i>	32.7	25.8	21.8	26.8	38.6	38.7	64.3	47.2	37.0
4	<i>I</i>	34.5	42.4	39.7	38.9	32.6	59.4	63.6	51.9	45.4
5	<i>Ch</i>	43.6	13.6	11.5	22.9	46.2	12.0	42.7	33.6	28.3
6	<i>l'</i>	29.1	42.4	11.5	27.7	34.1	54.1	44.1	44.1	35.9
7	<i>h'</i>	49.1	43.9	3.8	32.3	44.7	64.8	57.3	55.6	43.9
8	<i>w'</i>	50.9	48.5	30.8	43.4	44.7	66.1	55.2	55.3	49.4
9	<i>i'</i>	16.4	22.7	28.2	22.4	16.7	40.1	34.3	30.3	26.4
10	m. size	37.0	35.8	19.7	30.9	37.9	50.2	54.8	47.6	39.2
11	<i>H/W</i>	43.6	37.9	26.9	36.1	39.4	59.4	53.1	50.7	43.4
12	<i>H/I</i>	25.5	36.4	47.4	36.4	33.3	42.7	41.3	39.1	37.8
13	<i>w'/h'</i>	9.1	16.7	28.2	18.0	14.4	23.4	15.4	17.7	17.9
14	<i>l'/i'</i>	36.4	19.7	26.9	27.7	27.3	21.4	25.2	24.6	26.1
15	<i>l'/h'</i>	32.7	16.7	16.7	22.0	22.7	24.0	30.8	25.8	23.9
16	<i>l'/w'</i>	20.0	6.1	32.1	19.4	14.4	25.4	22.4	20.7	20.0
17	m. shape	27.9	22.2	29.7	26.6	25.3	32.7	31.4	29.8	28.2
18	m. c.f.	33.1	30.0	24.0	29.0	32.5	42.7	44.8	40.0	34.5
	<i>F</i>	100	20	2	mean	100k-	20k-	2k-	mean	mean
19	tests	kyr	kyr	kyr	within	20k	2k	100k	between	all
20	<i>H</i>	12.7	28.8	14.1	18.5	32.6	26.7	44.8	34.7	26.6
21	<i>W</i>	32.7	16.7	33.3	27.6	29.5	27.4	46.2	34.4	31.0
22	<i>I</i>	23.6	33.3	20.5	25.8	43.2	35.1	64.0	47.4	36.6
23	<i>Ch</i>	0.0	18.2	15.4	11.2	17.4	12.3	19.6	16.4	13.8
24	<i>l'</i>	27.3	31.8	21.2	26.7	31.1	33.4	41.3	35.2	31.0
25	<i>h'</i>	9.1	33.3	12.2	18.2	42.4	26.1	47.2	38.6	28.4
26	<i>w'</i>	47.3	24.2	12.2	27.9	40.9	21.0	49.3	37.1	32.5
27	<i>i'</i>	27.3	18.2	35.3	26.9	36.4	37.1	62.9	45.5	36.2
28	m. size	22.5	25.6	20.5	22.9	34.2	27.4	46.9	36.2	29.5
29	<i>H/W</i>	27.3	24.2	14.1	21.9	36.4	22.7	45.1	34.7	28.3
30	<i>H/I</i>	43.6	28.8	37.2	36.5	66.7	36.4	77.3	60.1	48.3
31	<i>w'/h'</i>	30.9	24.2	15.4	23.5	52.3	21.7	52.4	42.1	32.8
32	<i>l'/i'</i>	32.7	40.9	23.7	32.5	51.5	31.0	37.1	39.9	36.2
33	<i>l'/h'</i>	21.8	36.4	35.3	31.1	50.8	31.7	58.7	47.1	39.1
34	<i>l'/w'</i>	23.6	34.8	11.5	23.3	49.2	24.0	38.1	37.1	30.2
35	m. shape	30.0	31.6	22.9	28.1	51.1	27.9	51.5	43.5	35.8
36	m. var.	25.7	28.1	21.5	25.1	41.5	27.6	48.9	39.3	32.2
	<i>Z</i>	100	20	2	mean	100k-	20k-	2k-	mean	mean
37	tests	kyr	kyr	kyr	within	20k	2k	100k	between	all
38	<i>H/W</i>	10.9	7.6	15.4	11.3	7.6	10.7	11.2	9.8	10.6
39	<i>H/I</i>	0.0	19.7	6.4	8.7	6.1	7.3	0.0	4.5	6.6
40	<i>w'/h'</i>	16.4	0.0	14.1	10.2	12.9	17.4	16.1	15.4	12.8
41	<i>l'/i'</i>	0.0	6.1	10.3	5.4	2.3	6.0	5.6	4.6	5.0
42	<i>l'/h'</i>	10.9	7.6	6.4	8.3	9.8	16.0	9.8	11.9	10.1
43	<i>l'/w'</i>	14.5	10.6	20.5	15.2	11.4	15.4	14.7	13.8	14.5
44	m. exp. a	8.8	8.6	12.2	9.9	8.3	12.1	9.6	10.0	9.9
45	m. all	25.8	25.4	20.9	24.0	31.9	31.1	40.2	34.4	29.2
49	m. t & Z	25.8	23.6	20.4	23.3	25.2	33.5	34.2	31.0	27.1

Text Table 8.37 Summary of statistical tests for between resolution comparisons.

Italicised values show the proportions—as percentages—of various fields of possible sample pairings from Appendix Tables 3.2.1 - 3.2.5 which register as significantly different at the 95% confidence level. All fields correspond to entire transects (2, 20, 100 kyr) without differentiation into upper and lower halves. Columns b, c & d show within transect comparisons, columns f, g & h show between transect and thus between scale comparisons. Results are split between characters and tests performed as listed; other columns and rows show summaries of the italicised fields and are mean values (m. = mean) of the percentages displayed in the rows to the left or the columns above them. Bolder or bigger values represent ever more inclusive sets. See text Sections 8.2.1, 8.2.2 & 8.2.4 for details and discussion.

8.2.3.iii Patterns And Environmental Parameters

It is not immediately clear what the combination of scales will offer to a consideration of environmental effects, but one way to think about it comes from recognising that the three nested transects were set up to sample across *self-affine* lithological patterns (in what is often characterised as being a ‘fractal’ arrangement). In each case, the sequence goes from a marly lower half to a chalky upper half, even though a deeper consideration of the changes taking place makes it quite evident that the lithological link is a tenuous one. Should we really be contrasting an orbitally forced pattern of sedimentary change across a 20 kiloyear couplet with one caused by a transgressive pulse operating over a million year span? Whatever the answer is, a casual inspection of the data is easy enough without committing too much to the justification behind it.

<i>t</i> tests - size	<i>H</i>	<i>W</i>	<i>I</i>	<i>Ch</i>	<i>l'</i>	<i>h'</i>	<i>w'</i>	<i>i'</i>	
100 kyr	L	L	L	U	L	x	L	L	U1:L6
20 kyr	L	U	U	L	L	L	U	L	U3:L5
2 kyr	L	U	L	U	U	L	L	U	U4:L4
<i>t</i> tests - shape		<i>H/W</i>	<i>H/I</i>	<i>w'/h'</i>	<i>l'/i'</i>	<i>l'/h'</i>	<i>l'/w'</i>		
100 kyr		L	U	U	U	L	L		U3:L3
20 kyr		L	U	L	L	U	L		U2:L4
2 kyr		U	L	L	U	U	L		U3:L3
<i>F</i> tests - size	<i>H</i>	<i>W</i>	<i>I</i>	<i>Ch</i>	<i>l'</i>	<i>h'</i>	<i>w'</i>	<i>i'</i>	
100 kyr	L	U	L	x	U	x	L	U	U3:L3
20 kyr	L	U	L	L	U	L	U	U	U4:L4
2 kyr	L	U	L	L	L	U	U	U	U4:L4
<i>F</i> tests - shape		<i>H/W</i>	<i>H/I</i>	<i>w'/h'</i>	<i>l'/i'</i>	<i>l'/h'</i>	<i>l'/w'</i>		
100 kyr		L	L	L	U	U	L		U2:L4
20 kyr		x	L	U	U	U	U		U4:L1
2 kyr		U	U	L	L	L	L		U2:L4
<i>Z</i> tests - trajectory		<i>H/W</i>	<i>H/I</i>	<i>w'/h'</i>	<i>l'/i'</i>	<i>l'/h'</i>	<i>l'/w'</i>		
100 kyr		x	x	L	x	U	x		U1:L1
20 kyr		L	U	x	U	U	U		U4:L1
2 kyr		U	L	L	L	x	L		U1:L4

Text Table 8.38 Summary table of results for the combined scale of all statistically measurable parameters split into upper and lower halves. *L* denotes a predominance of change in the lower half of each section; *U* denotes a predominance of change in the upper half of each section; *x* denotes a tie.

Text Table 8.38 shows the statistical tests reorganised on the basis of percentage occurrence per space of possibility. The data were collected from Text Tables 8.11 and

8.28, with cells labelled U or L to indicate whether a higher percentage of significant change was found in the upper or lower (chalky or marly) halves of each transect, respectively. No clear pattern emerges from this data concerning either the parameter under consideration (e.g. means versus standard deviation, size versus shape or trajectory), the scale under consideration, or the lithology under consideration (represented here as U vs. L rather than chalk vs. marl). Despite the lithological appearance of self-affine environmental conditions, there is no evidence of a self-affine evolutionary response in the statistically verifiable characters.

There does, however, seem to be a weak tendency for fractal-like behaviour in some of the categorical features; these have already been mentioned in Section 8.2.4.i.d (above). The most convincing case is that of *type* which exhibits an increase in the proportion of exotic specimens in chalky sediments, a pattern not only reproduced at each of the three scales, but also at each of the three sites.

Summary

Chapter 8 has reviewed a vast data set (Appdx. Tables 2.1 – 2.3 will demonstrate just how vast) that was also carved into different sites, different scales, different morphometric parameters and tests to be performed on them, and different questions to focus upon—hopefully, without losing track of it all. Since it is the sole function of the next chapter to summarise all this material, there is little point in attempting to do so here. However, there are a number of findings that might usefully be highlighted in preparation.

A regular pattern exists between different character parameters and the incidence of significant change, with sizes changing more often than shapes, and shapes more than trajectories. There is also a similar pattern with regards to the strength of correlation, such that character sizes correlate better with one another than do shapes or trajectories. These regularities seem quite robust, and, where deviation does occur, it seems to be associated with populations drawn from C13.

C13 typically plays host to somewhat smaller specimens than are found elsewhere in the data set, particularly in association with its chalk and chalk-marl boundary zones. Indeed, these peculiarities of C13 serve to draw attention to how similar the populations from elsewhere in the data set can be, all of them coming, as they do, from mid-marl

sampling points. In this sense, proximal association to a particular lithology (chalk or marl) predicts the overall form of a sample population better than, for instance, where it comes from on a million year scale: if someone in the lab had switched the 20 kyr and 100 kyr sample bags with one another, I doubt it would be obvious from the pattern inversion (until it was compared with material from other sites, of course).

As with the ecological data set of Part II, we find a between-site correlation that is stronger between Folkestone and Escalles than either of them is with Southerham. The 100 kyr timeseries for size changes also show other really striking regularities, including a strong co-ordinated kick just below the middle of the sequence and a pattern of steady between-site divergence above. Shapes and trajectories are less well co-ordinated (although there is a perfect mirror pattern present between the timeseries for trajectory parameters 'a' and 'b'), but there are many intriguing regularities among the categorical features. There are also differences in behaviour among the standard metric characters, with *Ch* showing much more independent behaviour than any of the others.

All of these features receive a thorough treatment in Chapter 9.

Chapter 9 Flexibility and the Fabric of Morphospace

Introduction

The last chapter presented a wide and rather overwhelming variety of charts and tables, documenting the frequency and distribution of statistically significant change, of rates of change, and of significant correlations between the various characters, sampling scales and sites. This chapter aims to weave those findings into a more condensed story about *Tritaxia*'s mid-Cenomanian history. We start with a holistic look at growth curves and consider what they can tell us about the regular differences between parameters of morphological size, shape and trajectory. Having thus charted the broad contours of morphological change, we next consider the strengths and weaknesses of correlation between specific pairs and groups of characters, with a view to revealing the invisible contours of morphospace. Then we tackle the issue of scaling across both time and space. Finally, touching briefly on the problem of age dependency once again, we will sum up with a general sketch of *Tritaxia*'s morphological behaviour over evolutionary time.

Section 9.1 A Summary of Morphological Change

9.1.1 Growth Curves Reconsidered

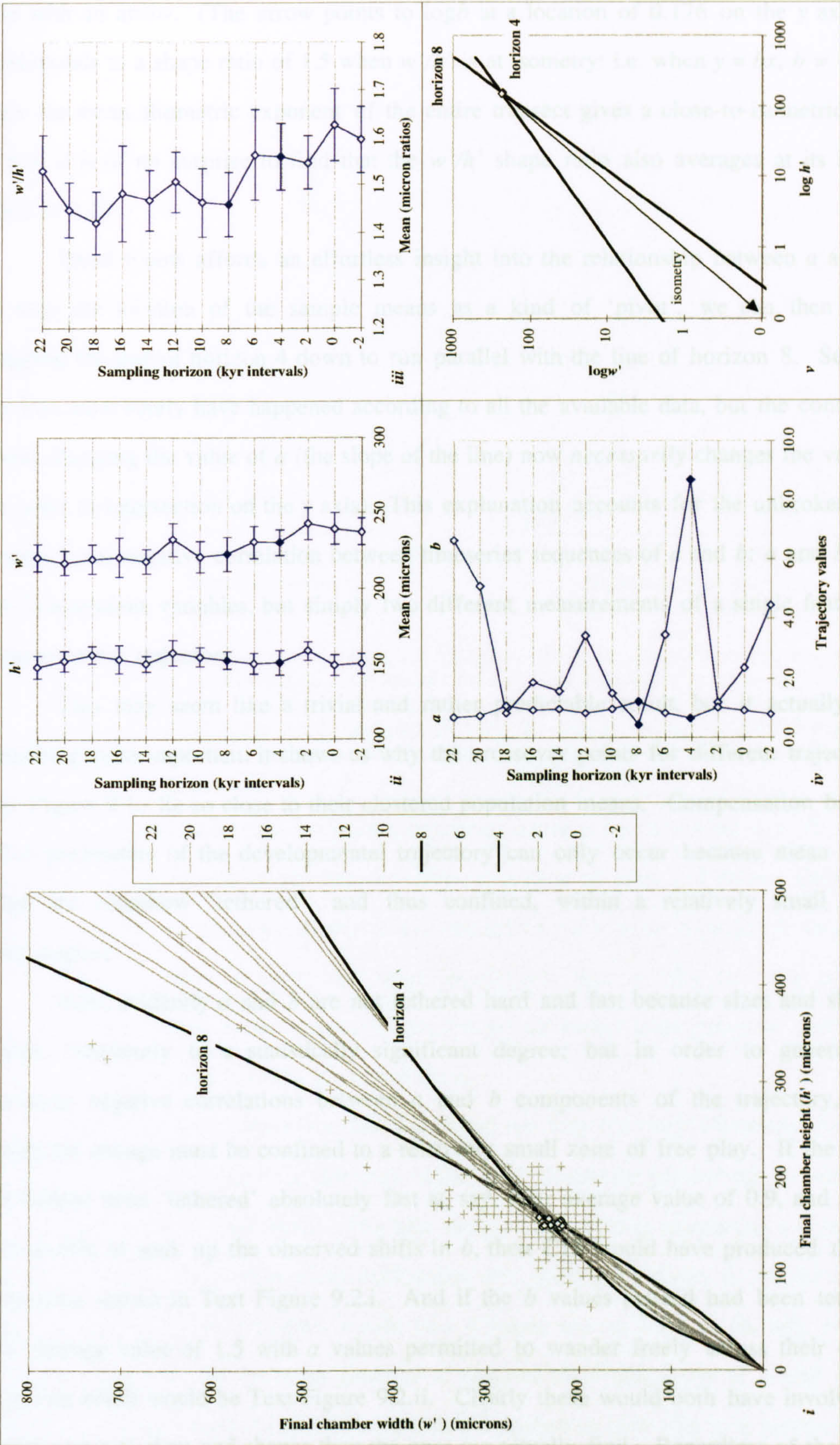
Sheldon's *Plus ça change* model concerns the rate and incidence of evolutionary change in environments of varying stability on a geological timeframe. But it is also a major goal of this thesis to unite both structural and functional approaches to biology under the information-theoretic paradigm, and to understand the phenomena we observe as continuous between timeframes, rather than disjunct. The principle reason for investigating timeseries correlation was to look for evidence of independent behaviour between morphological variables over their evolutionary trajectories. This independent behaviour, it was suggested, can be used to identify heterochrony and heterotopy, and thus will give us an insight into the mechanisms underlying evolution.

In Section 6.2.4, I suggested that the parameters of the bivariate developmental trajectories should be of particular interest because they provide an insight into the workings of the ‘developmental program’. The values of a and b , however, are only half the story: they tell us about the *route* of an average growth sequence, but they do not tell us *how far along it* the average individual travelled. For that we need to know the mean size of the characters involved. And, if the trajectory under scrutiny is significantly allometric, we can expect that any change in size will also involve a change in shape.

Text Figure 9.1.i-v shows all these components of a developmental trajectory for the characters w' and h' from the entire set of samples in C13. The w'/h' relationship from C13 was chosen for this task because it straddles the line of isometry and thus demonstrates a transition from positive through neutral to negative values of a . Panels *ii* and *iii* show changes in size and shape, corresponding to motion along the growth trajectory for sizes, or at right angles to it for shapes. To keep track of all the variables, I like to imagine panels *ii* and *iii* with their y axes extending upward, out of the page from panel *i*. The x axis of panel *ii* then runs along either the x or y axis of panel *i*, but if the pair of characters are thought of in combination they can be imagined collectively pulsing up and down the growth curves, expanding out from, or contracting back towards, the origin. Meanwhile, the shape values from panel *iii* cross the trajectory axis at right angles, with the high values pointing towards the width axis (the ratio is w'/h' so that any increase indicates that w' has gone up or h' has gone down). This act of imagination utilises the methods proposed in Section 8.1.5.i (Text Figure 8.3) for thinking about timeseries plots and allows us to move easily between conceptions of developmental and evolutionary trajectories.

For the point I wish to make it is not particularly helpful to keep track of every single sample, and so most lines and mean values on panel *i* are not labelled. Only two specific curves, shown in bold and traced by the filled diamonds on other panels, are singled out for attention; these represent a value end-points of the C13 transect. The downward curving line is C13-3 [time horizon 4] and the upward curving one is C13-5 [time horizon 8]; they have a values at either end of the C13 spectrum and b values to match (panel *iv*). Note that on panel *i* they cross one another very close to, but just after, the cluster of diamonds marking the sample means.

Panel *v* shows the same two curves plotted on a logarithmic axis; all the other unlabelled (and for simplicity, omitted) curves from the first panel occupy a position



Text Figure 9.1 Showing the relationships between size, shape and allometric trajectory with reference to the w'/h' relationship in C13. Panel **i** shows the growth curves for every population in the transect, only two of which are identified. The grey crosses mark individual specimens and the diamonds the population means. Panels **ii** and **iii** show evolutionary timeseries for size and shape, respectively. Panel **iv** shows the 'a' and 'b' parameters. Panel **v** shows the two most allometric growth curves plotted on a log-log scale. See adjacent text for a full discussion.

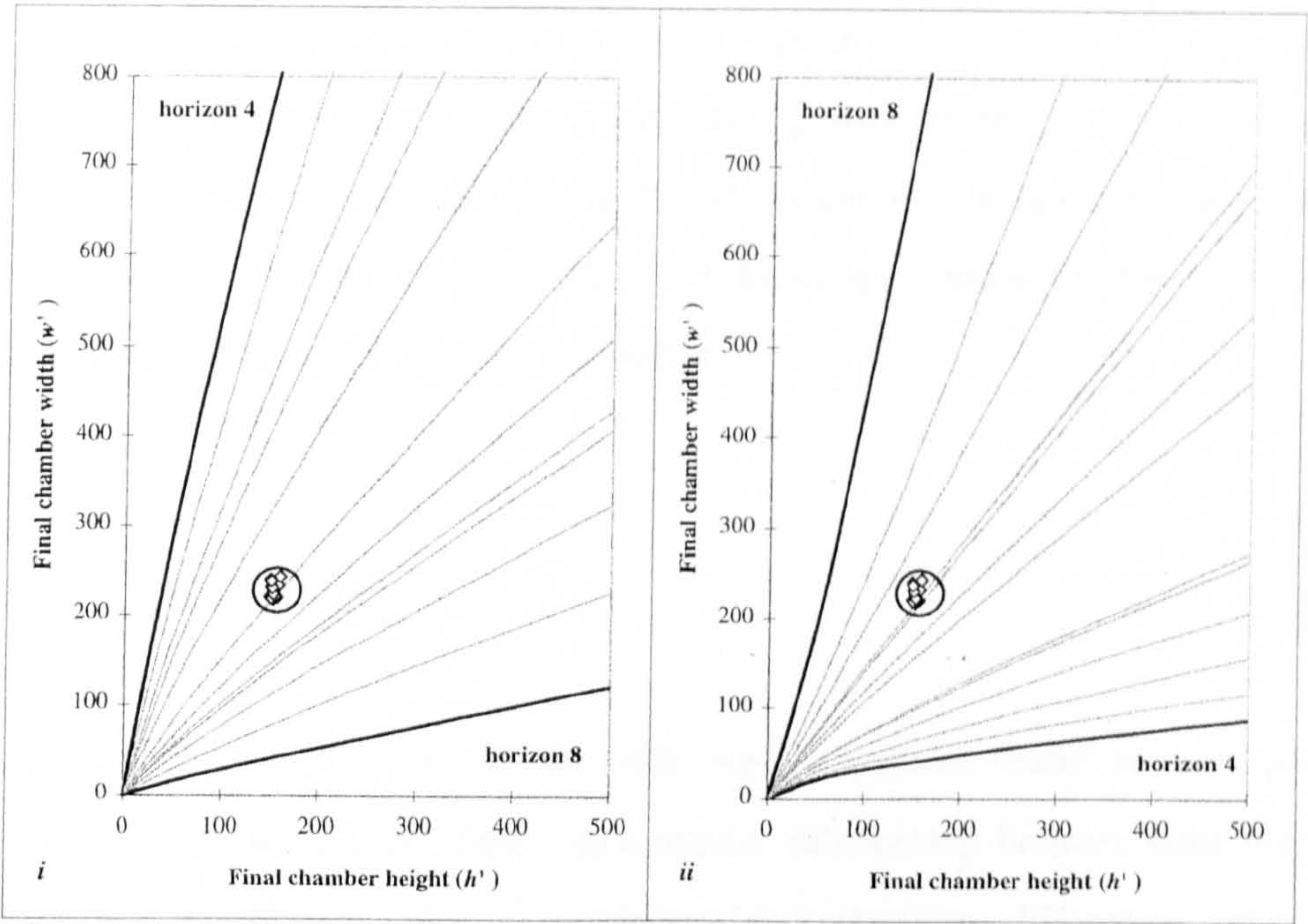
somewhere in between these two lines. We can easily see that the transition from horizon 4 to horizon 8 must have included movement *across* the line of isometry, which is marked here with an arrow. (The arrow points to $\log b$ at a location of 0.176 on the y axis, which corresponds to a shape ratio of 1.5 when w'/h' is at isometry: i.e. when $y = bx$, $b = 1.5$; and, since the mean allometric exponent of the entire transect gives a close-to-isometric a value of 0.9, it is of no surprise to find that the w'/h' shape ratio also averages at its isometric value of 1.5).

Panel v now affords an effortless insight into the relationship between a and b . If we treat the location of the sample means as a kind of 'pivot', we can then imagine dragging the line of horizon 4 down to run parallel with the line of horizon 8. Something like this must surely have happened according to all the available data, but the consequence is that changing the value of a (the slope of the line) now *necessarily* changes the value of b (its point of intersection on the y axis). This explanation accounts for the unbroken record of significant negative correlation between timeseries sequences of a and b : a and b are not two independent variables, but simply two different measurements of a single feature—the developmental trajectory.

This may seem like a trivial and rather predictable result, but it actually reveals something quite important: it shows us why the crossover points for different trajectories in Text Figure 9.1.i lie so close to their clustered population means. Compensation between a and b parameters of the developmental trajectory can only occur because mean size and shape are somehow 'tethered', and thus confined, within a relatively small zone of morphospace.

Now, evidently a and b are not tethered hard and fast because sizes and shapes *do* change, frequently to a statistically significant degree; but in order to generate such consistent negative correlations between a and b components of the trajectory, all that significant change must be confined to a relatively small zone of free play. If the a values had instead been 'tethered' absolutely fast at, say, their average value of 0.9, and had thus been unable to soak up the observed shifts in b , then C13 would have produced the range trajectories shown in Text Figure 9.2.i. And if the b values instead had been tethered at their average value of 1.5 with a values permitted to wander freely across their observed range, the result would be Text Figure 9.2.ii. Clearly these would both have involved a far greater range of sizes and shapes than the ones we actually find. Regardless of the a and b values they generate, therefore, trajectories seem to 'oscillate' or 'vibrate' between a pair of

relatively set points: they are fixed by the origin at one end, and by a restricted zone of free-play for mean shape and size at the other.



Text Figure 9.2.i & ii Trajectories for C13 ‘cut free’ from the restriction of constraints to mean size and shape, and redrawn constrained by only one allometric parameter instead. **i.** with ‘a’ values ‘tethered’ at 0.9 (the mean for the population) and the trajectories freely expressing the observed range of ‘b’ values. **ii.** with ‘b’ values ‘tethered’ at 1.5 (the mean of the population) and the trajectories freely expressing the observed range of ‘a’ values.

I should emphasise that the pattern described above is *not* restricted to w'/h' in C13: it is seen across the board, in all character pairings and at all sites and scales, albeit to an extent that depends on the zone of movement explored by the mean population shapes and sizes (see Appdx. Figs. 6.1.i-vi, for some examples); that is why the two trajectory parameters always show perfect negative correlations no matter what character pairings we look at or which samples the data are drawn from.

One further point: Peter Sheldon has asked me why for very allometric cases like H/W , there are not oppositely (in this case negatively) allometric growth curves which still reach the same mean size and shape. The best answer I can offer is to reiterate a point made in Section 7.1—that the mathematical description of a growth trajectory is subject to fewer constraints than any real organism would be. *Tritaxia* has an axis of coiling; H grows cumulatively along it. In order to generate a negative H/W allometry, H would need to somehow shoot ahead early on and then slow down enough to give way to a greater growth along W instead. The only way I can realistically envisage this happening in a foram is if

earlier chambers were progressively nested inside later ones, with a great deal of lateral spread to the sides but much less along the coiling axis. Some foraminifera *do* grow this way: *Eggerellina*, also from the Lower Chalk and an agglutinated cousin of *Tritaxia*, is a case in point (Appdx. Fig. 2.2.1.v). But given the regular triserial spiral so characteristic of *Tritaxia*, a fairly radical departure from the standard growth sequence would have to occur before we found a negative allometry for *H/W*, and one can well imagine that any early and partial steps in that direction would rapidly shift the sample means far from their present zone of developmental and/or ecological stability.

9.1.2 Parameter Malleability

Let us next consider some of the other regular features found between parameter types. For instance, we saw that there was a regular relationship between sizes, shapes and trajectories in terms of the number of correlations and significant differences generated by each. Text Table 9.1 summarises these regularities.

% sig	central tendency			variation	% sig	central tendency			variation
<u>shifts</u>	size	shape	traj	size shape	<u>correlations</u>	size	shape	traj	size shape
2 kyr	19.7	< 29.7	> 12.2	20.5 < 22.9	2 kyr	7.1	> 6.7	< 13.3	17.9 > 6.7
20 kyr	35.8	> 22.2	> 8.6	25.6 < 31.6	20 kyr	32.1	> 13.3	< 20.0	50.0 > 33.3
S 100 kyr	31.4	> 27.9	> 9.4	17.5 > 17.3	S 100 kyr	71.4	> 20.0	< 22.2	39.3 > 13.3
F 100 kyr	37.0	> 28.5	> 10.0	22.5 < 30.0	F 100 kyr	50.0	> 13.3	< 20.0	25.0 > 0.0
E 100 kyr	34.7	> 27.8	> 11.5	26.9 < 30.8	E 100 kyr	50.0	> 26.7	> 13.3	57.1 > 0.0

Text Table 9.1 *Summary of significant differences and correlations as a percentage of those possible for various parameter types. Data collected from Text Tables 8.27 and 8.37 (rows 10, 17, 28, 35 & 44), and from the correlation grids found throughout Chapter 8.*

Focusing on the inequality symbols alone (< & >), rather than the magnitude of any percentage values, there certainly seems to be a non-random association between parameter types. By assuming that there is an equal probability of the percentage value for any category being greater or less than any other, we can assign a binomial significance to these patterns by treating the five transects as separate trials in a coin-tossing run. The probability of scoring five heads or tails in a row is 2 in 32, meaning that the second, fourth and sixth columns of chevrons, all of which sport five similar cases, have a significance of 93.8%—not quite the coveted 95%, but close enough to be interesting. And when we are

dealing with *sets* of parameters, as with the central tendency trio of size, shape and trajectory *a* values, we can sensibly treat them as *sets* of trials, too. The probability of tossing two heads in a row, or a head followed by a tail etc., is 0.25; the probability of tossing two heads in a row in each of five sets of equivalent trials is thus $0.25 \times 0.25 \times 0.25 \times 0.25 \times 0.25 = 0.000976$, a little less than one in a thousand. Unfortunately, we can't quite claim this level of significance here because in each of the cases above one of the ten chevrons breaks the expected pattern. But if we restrict ourselves to $0.25 \times 0.25 \times 0.25 \times 0.25 \times 1$ (meaning that for one of the sets we will accept *any* result), the figure is still 0.004, or 1 in 256. Whatever reasoning we use, these patterns are intriguing enough to warrant an explanation, and become even more so when the actual magnitude of the percentages is also taken into account.

One feature that stands out prominently is just how consistently low the percentages of statistical shifts in trajectory *a* values are compared with everything else. In the discussion above we reasoned that specific *a* or *b* values are not particularly important so long as they jointly conspire to place the average individual in a restricted zone of morphospace. Now we see that only a small proportion of the *a* value shifts actually register as significant at all. On average, significant change *must* reflect a genuine phenomenon—that's the whole point of applying statistical tests. Even a 10% frequency, although not very high, is still double what we would expect from chance alone. But, on the whole, the proportion of these shifts was fairly small; so what the results in Text Table 9.1 seem to be telling us, is that most of the differences in *a* value are indistinguishable from random factors, and consequently that the developmental trajectories basically show almost (but not quite) complete stasis across all five transects. Generalising from this argument we can say that *trajectories show the most stasis, the shapes a little less and the sizes least of all*.

This conclusion may initially seem to contradict the argument given above where sizes rather than trajectory values were confined to a narrow zone, but it is important to remember that statistical tests measure the magnitude of change in central tendency *relative to the background scatter of variation in a pair of samples*. What we were actually discussing in Section 9.1.1 was the *potential* exploratory power of trajectory parameters in circumstances where they are not reigned in by a need to create specific end-products. Considering the range of *a* and *b* values available as raw material for trajectories, the sizes and shapes produced are indeed clearly confined to restricted zones of morphospace. But

relative to the *variation* in size and shape shown by the sample populations, small though their shifts in central tendency are, they often turn out to be statistically significant.

On examining the correlations we find a similar picture. Once more, sizes show the most correlation, with shapes and trajectories coming lower down the scale. It would have been gratifying to find exactly the same sequence as before, but alas we do not; this time it is the shapes which show least correlation, with the trajectories occupying a middle position (although there is very little in it). In line with the account given above, it seems likely that the size shifts correlate well because they were real. Unlike the shape and trajectory shifts, changes in size were substantial enough to fight their way free of background variation so as to give a well defined picture. By contrast, much of the movement we see in the shape and trajectory metrics is better thought of as noise.

Finally, *variation* also seems to differ systematically between the parameters of size and shape. Text Table 9.1 shows that in general shapes exhibited more shifts in their standard deviation than did the sizes, but that those shifts tended to correlate less well with one another than did the changes in variation of size. Recalling that size change involves motion along the growth trajectory whereas shape change requires orthogonal translation, and given what we know about free play in the trajectory parameters, one can imagine that although the expansion and contraction of variation along the length of the growth curves was being held in check, the trajectories themselves were whipping about back and forth *behind* that point, smearing the shapes through morphospace as they did so (this same situation was depicted in Text Figure 8.5.b of Section 8.2.2.iii). Interestingly, the smearing evidently happened in different directions at different times, so that *Tritaxia*'s shape was more of a wobbling multidimensional cloud than a co-ordinated pulse of expansion and contraction in shape (whatever that would mean for a vector parameter measurement!). By contrast, increases and decreases of variation in size *were* pulse-like, affecting many characters simultaneously, which is why they correlate well.

To summarise, all this adds up to the conclusion that shifts and correlations in size are more meaningful, more important, and (literally) *more significant* than equivalent shifts in either shape or trajectory parameters. And consequently it indicates that the sizes showed more morphological malleability (relative to the range of variation) than did the shapes, with trajectories being least malleable of all.

That size seems to be the most tightly controlled parameter in terms of both coordinated shifts in central tendency and the size of those shifts relative to the variance, makes perfect ecological sense. Although we often have little idea of the adaptive significance of foraminiferal shapes, we presume that they are functional in some manner; that alone is sufficient to limit the range of trajectory pathways through shape space. Sizes, however, are doubly important because not only do they contribute to shape, they also involve economic considerations in their own right. Two foraminifera can be the same shape and might thus function equally well so far as that shape is adaptive, but if one of them is twice the size of the other, it will (ignoring economies of scale) have required double the amount of energy and material to construct. Of course, it might also incur different functional constraints on its shape because of the difference in size, but that is a separate argument.

Section 9.2 Morphometric Correlations

9.2.1 Signal or Noise?

Having built up a good general understanding of the shifting parameters on a developmental trajectory, we can now move on to consider the specific form of various character relationships as they relate to the geometry of morphospace. We are looking for evidence of heterochrony and heterotopy. We already know that most characters are correlated with, and are thus somehow ‘bound to’, most of the others during the course of development; what we are searching for next is the distribution of looseness and tightness in those bindings—for regularities in the way the various parameters slip and slide past one another over evolutionary timescales.

For the purposes of revealing recurrent associations between our character variables, we can fruitfully adopt an approach that involves treating the five transects as though they were five *different* sampling tests, or independent trials. In order to generate a significant value on any one of the individual correlation grids of Chapter 8, a pair of timeseries patterns has to correlate with a confidence of 0.05. If we are looking at a large number of potential correlations we should expect 1 in 20 of them to correlate significantly for no

reason at all; equally, however, if we find the *same pair* of timeseries correlating over and over again, they will be doing so with a probability of $0.05 \times 0.05 \times 0.05 \dots$ etc.

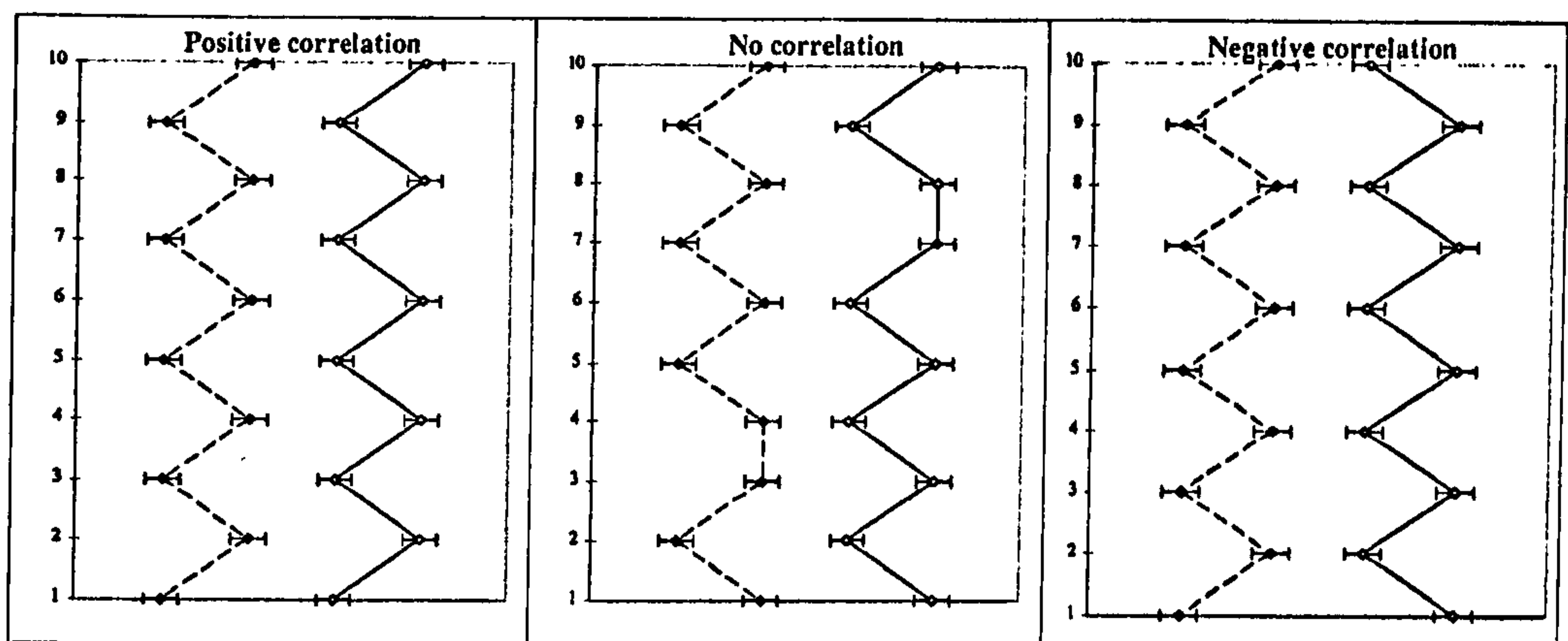
Text Tables 9.2.a-e (overleaf) show a new range of correlation grids, constructed by overlapping the original data for each of the five individual transects. Should a particular pair of timeseries, say mean *H* versus mean *W*, turn out to be positively correlated in all five original transects, then the value for this pairing on the new correlation grids (*a*, *c*, *d* & *e*, but not *b*) will be 5; if, however, there are no correlations to be found on any of the originals, then the new value will be 0. To emphasise patterns of regular association, these new values are also coded by shading. I must stress that this procedure is a tool for allowing recurrent tendencies to fight their way free of noise, and the five transects are only 'independent' in that respect; otherwise, the three long sections are linked by common time horizons, the three nested scales by a common location.

In an earlier draft of this chapter I analysed these patterns in considerable depth, differentiating, for instance, between positive and negative correlations, between the correlations for mean values, standard deviations, rates, etc., along with the significance of each parameter for particular cases of size, shape, trajectory or categorical character. Space limitation precludes such an in-depth discussion now, so this account will be restricted to correlated pairings in general (rather than segregating them by sign and so forth), and to picking out only the most salient features.

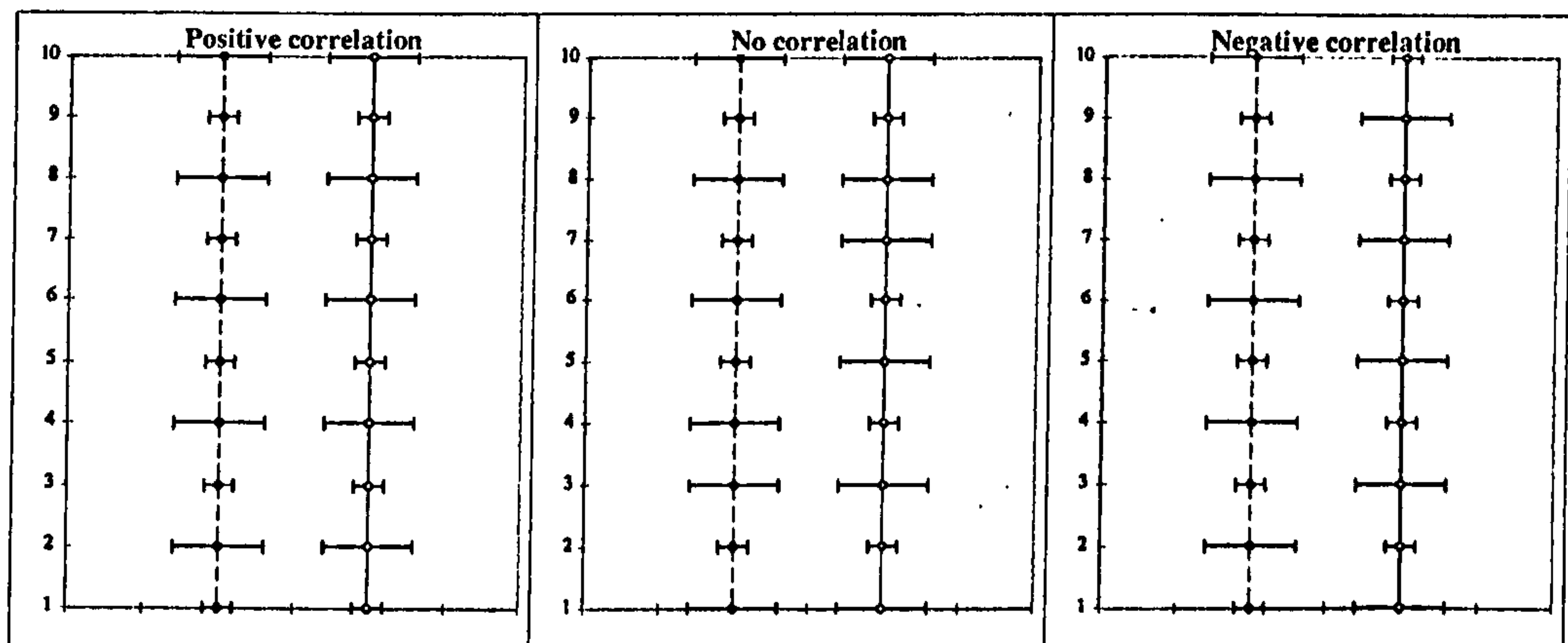
For an *evolutionary* trajectory, we have two end-point null hypotheses to entertain: that through the generations *all* characters in a *developmental* trajectory are correlated with all the others, showing no deviation from the standard developmental sequence, or that *no* characters are correlated with any of the others, showing complete independence from one another in the long-run. In practice, neither case occurs. What we find instead is a variegated pattern with some pairings correlating strongly and consistently, and some correlating far less frequently, if at all. This is exactly what one might expect to find in a system full of short-term developmental associations that were being tugged and twisted away from 100% regularity by having their relationships constantly re-set across evolutionary time. It is a prime candidate for the heterochrony and heterotopy we are searching for.

Unfortunately, it is also a prime candidate for the effects of noise generated at any point during the last 95 million years, especially in light of the fact that the Combined

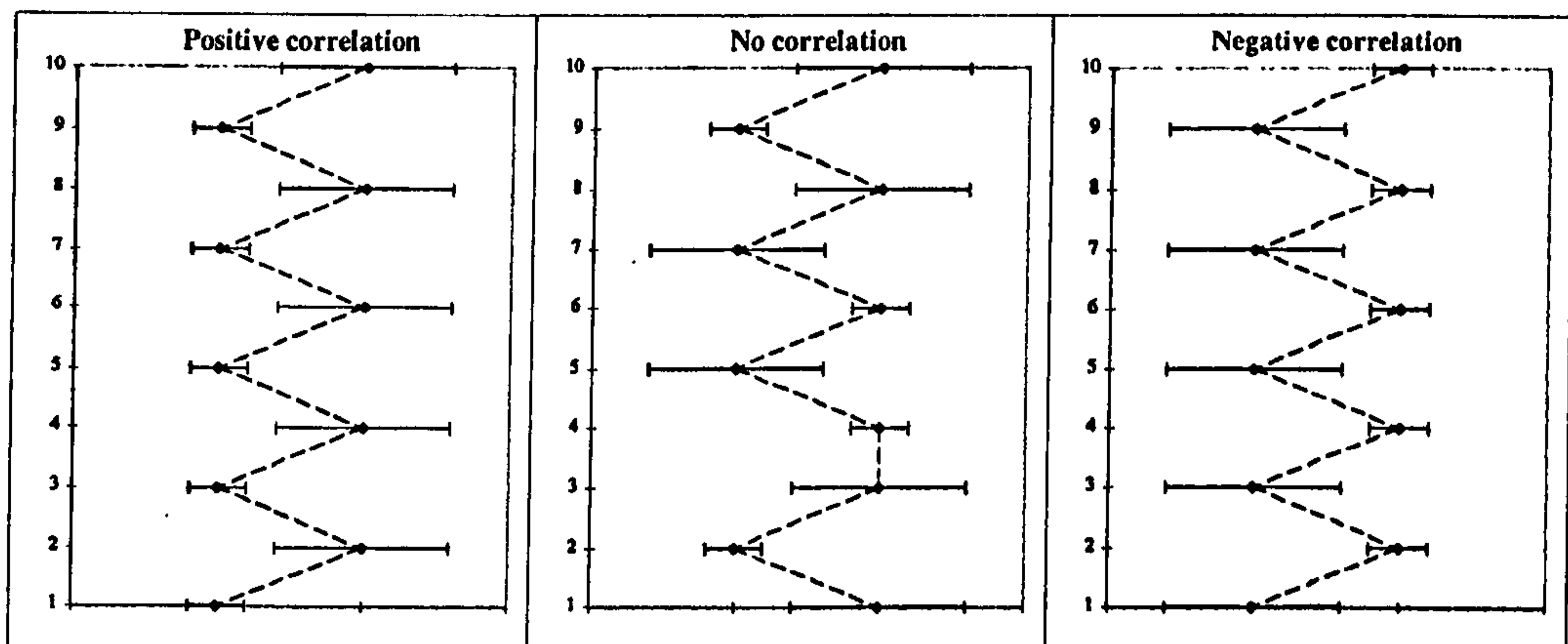
	H	W	I	Ch	l'	h'	w'	i'		H	W	I	Ch	l'	h'	w'	i'	
H	<u>3</u>	1	4	4	3	3	2	0	H									H
W	4	<u>1</u>	2	1	5	1	1	1	W	0								W
I	4	4	<u>2</u>	3	2	3	2	1	I	3	2							I
Ch	2	0	0	<u>1</u>	2	2	1	0	Ch	1	0	1						Ch
l'	3	3	2	0	<u>1</u>	3	1	1	l'	0	2	0	0					l'
h'	3	4	3	0	3	0	1	1	h'	1	0	0	0	2				h'
w'	2	3	2	0	4	4	<u>1</u>	2	w'	2	1	0	0	1	0			w'
i'	1	4	2	0	1	0	1	0	i'	0	1	1	1	0	0	0		i'
	H	W	I	Ch	l'	h'	w'	i'		H	W	I	Ch	l'	h'	w'	i'	
a Correlation grid overlay for character sizes																		
	H	W	I	Ch	l'	h'	w'	i'		H	W	I	Ch	l'	h'	w'	i'	
H	<u>3</u>								H									H
W	5	<u>1</u>							W	0								W
I	8	6	<u>2</u>						I	3	2							I
Ch	6	1	3	<u>1</u>					Ch	1	0	1						Ch
l'	6	8	4	2	<u>1</u>				l'	0	2	0	0					l'
h'	6	5	6	2	6	0			h'	1	0	0	0	2				h'
w'	4	4	4	1	5	5	<u>1</u>		w'	2	1	0	0	1	0			w'
i'	1	5	3	0	2	1	3	0	i'	0	1	1	1	0	0	0		i'
	H	W	I	Ch	l'	h'	w'	i'		H	W	I	Ch	l'	h'	w'	i'	
b Modified correlation grid overlay for character sizes (merged means and st.dev.)																		
	H/W	H/I	w'/h'	l'/i'	l'/h'	l'/w'		H/W	H/I	w'/h'	l'/i'	l'/h'	l'/w'					
H/W	<u>2</u>	1	1	0	1	1	H/W							H/W				
H/I	0	<u>1</u>	0	0	0	0	H/I	0						H/I				
w'/h'	1	0	0	0	3	0	w'/h'	0	1					w'/h'				
l'/i'	0	0	2	<u>2</u>	0	0	l'/i'	0	1	1				l'/i'				
l'/h'	1	0	3	1	<u>3</u>	1	l'/h'	1	0	3	1			l'/h'				
l'/w'	0	0	3	0	1	0	l'/w'	1	0	0	0	0		l'/w'				
	H/W	H/I	w'/h'	l'/i'	l'/h'	l'/w'		H/W	H/I	w'/h'	l'/i'	l'/h'	l'/w'					
c Correlation grid overlay for trajectory character shape ratios																		
	H/W	H/I	w'/h'	l'/i'	l'/h'	l'/w'			ind.	tw	g%	g.dist	chir	type				
H/W	<u>5</u>	1	1	0	1	1	H/W		ind.	0	0	0	0	0	ind.			
H/I	0	<u>5</u>	1	1	1	0	H/I		tw	0	0	0	0	1	tw			
w'/h'	0	2	<u>5</u>	0	0	0	w'/h'		g%	0	1	3	0	1	g%			
l'/i'	0	1	1	<u>5</u>	0	2	l'/i'		g.dist	1	0	2	0	0	g.dist			
l'/h'	1	1	1	0	<u>5</u>	3	l'/h'		chir	0	1	0	0	0	chir			
l'/w'	1	1	4	3	0	<u>5</u>	l'/w'		type	2	1	0	0	0	type			
	H/W	H/I	w'/h'	l'/i'	l'/h'	l'/w'			ind.	tw	g%	g.dist	chir	type				
d & e Correlation grid overlay for trajectories and for categorical characters.																		
Text Table 9.2 Correlation grid overlay for the morphometric parameters. See adjacent text Section 9.2.1 & 9.2.2.i-iv for details.																		



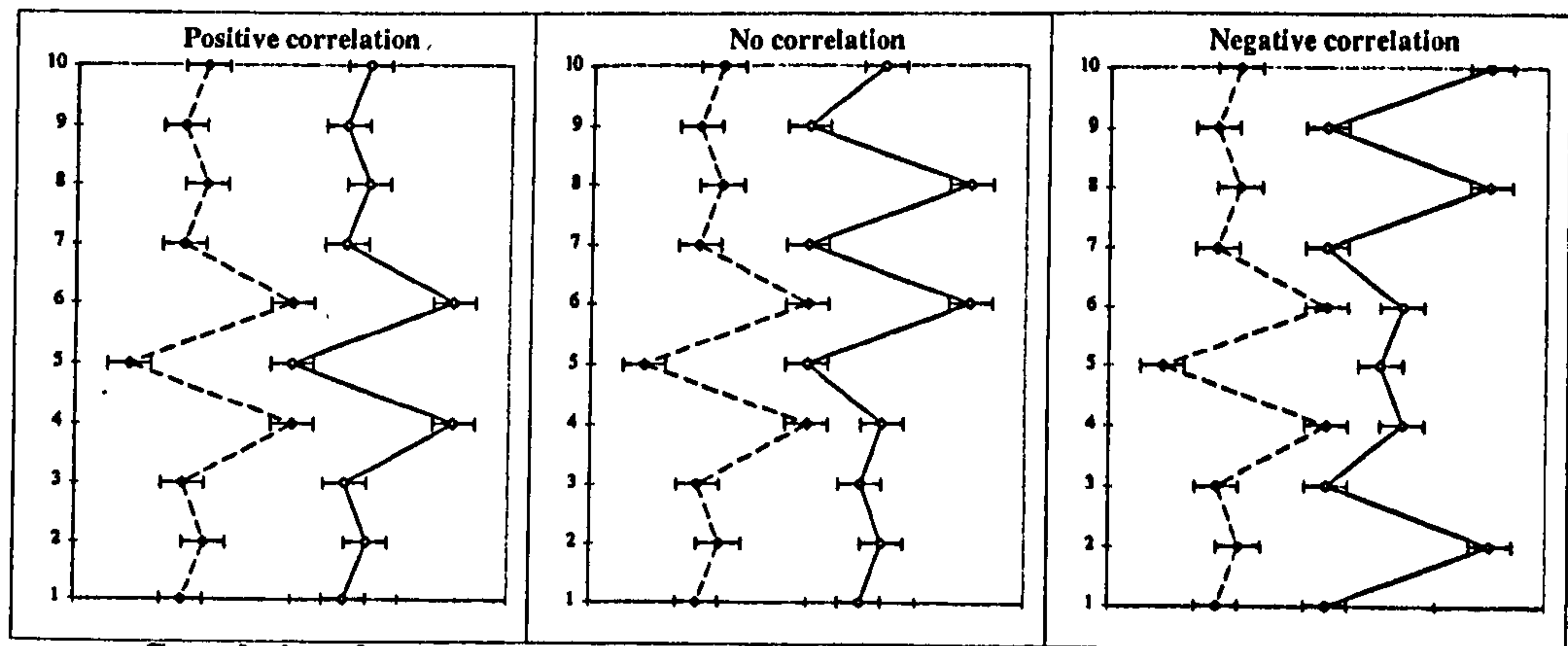
Correlations between timeseries shifts in the *mean* values of two characters



Correlations between timeseries shifts in the *standard deviations* of two characters



Correlations between the shifts in standard deviation and mean for a *single* character



Correlations between timeseries shifts in the *rates of change* for two characters

Text Figure 9.3 Idealised illustrations of the types of correlation between pairs of timeseries.

Scales section of Chapter 8 revealed that an increase in sample size also tends to improve correlations in most parameters.

There are at least three types of 'noise' to be considered here: one is the error brought about by fuzzy character definitions and measurement granularity (e.g. graticule spacing relative to character magnitude); another is due to taphonomic interference. But the final one is genuinely biological in nature: either genetic variation or the result of differing environmental influences, both of which are interesting because they constitute the raw material on which selection can act. This type of 'noise' is actually the signal we are searching for.

There are good reasons for believing that neither taphonomy nor measuring error are solely accountable for producing the patterns we see. Consider, for instance, that far from being reduced by taphonomic interference, characters like *H*, *W*, *l'* and *h'* which define the edges of the test and are therefore most susceptible to being worn away, often host the strongest correlations of all; or the fact that *Ch*, the character showing most independence, is actually a discrete categorical feature and is thus immune to the effects of fuzzy definition and measurement granularity. There is insufficient space to discuss each character in turn, so, for the sake of brevity, I shall have to simply assert that a good case can be made for most instances, and that whether there are exceptions or not (e.g. *i'* might be a genuine candidate for measuring error being a small character with a coarse measuring interval), the patterns *predominantly* tell a story about the strengths and weaknesses of developmental correlations over a series of evolutionary trajectories. With this in mind, many of the correlation patterns can be readily interpreted.

Text Figure 9.3 is a reminder of what the correlation data are telling us about the relationships between various timeseries.

9.2.2 Heterochrony and Heterotopy

9.2.2.i Size Shifts

Looking first at the field of mean (m) correlations for size we can see that it is unevenly populated with high and low values, and that these are clustered into fairly distinct

fields (Text Figure 9.2.a). In the top corner we have correlations between the three whole test parameters, H , W and I , which all show 4 out of 5 cases as significant positive correlation. We also have the other triangular field of final chamber parameters l' , h' and w' (but not i'), which record 4s and 3s. Then there is the field of overlap between final chamber and whole test parameters, centred on the 4 at W vs. h' and ringed by 2s and 3s. Finally, there is a barren zone between these fields associated with Ch , almost all of which is 0s, and also the bordering case of i' which shows a generally low occurrence of significant correlation as well.

Examining next the accompanying standard deviation (sd) field we see that these are much less clearly segregated than the means. Shifts in variance for the whole test parameters (H , W & I) sometimes correlate well, both with one another and with the final chamber dimensions, but the final chamber characters do not correlate well with one another at all. Given that the elements of the final chamber are smaller in magnitude than those of the whole test, the poorness of their correlations may have something to do with measuring noise; if this is so, we can either accept 'no pattern' or 'no data', or we can try to boost the existing data in order to uncover a pattern.

An obvious method of amplification is to compare the standard deviation field with the incidence of correlation seen in the means. Obviously, the \underline{x} category performs exactly this kind of trick for *individual* characters, but we can examine the behaviour of character *pairs*, too, by adding the number of correlations between character means to those of standard deviations for the same pair. Text Table 9.2.b shows the results of this addition: the maximum number of correlations is now 10 rather than 5, while the minimum remains at zero.

Low correlation values for Ch and i' are still generally preserved, although the relationship between Ch and H is strengthened somewhat. Relationships between H vs. I , and W vs. l' are now particularly emphatic. H also correlates well with most of the other characters (although perhaps less well with W than one might expect), and there appear to be fairly strong associations between W vs. I , h' vs. I , and h' vs. l' . We can also see that while correlations in the rate of change field (r) are far less frequent, where they do occur they also tend to cluster around these same dominant pairings. In light of the fact that rates of change are measured in *haldanes*, and therefore incorporate elements of both variance and central tendency, we can hardly be surprised by this.

As noted above, these patterns reveal something *like* the relationships shown in the x field in the standard correlation grids, except involving a pair of characters, and with a presence that gradually emerges from an overlay of numerous different transects rather than just a single timeseries snapshot. With reference to H/I , for example, it suggests that when mean H increases, the variance of H increases too; and that when mean H increases, mean I also increases, as does the variance of I ; the same holds for any other equivalently correlated character pairing: W vs. l' , h' vs. I and h' vs. l' , etc. In terms of a typical bivariate plot like Text Figure 6.13 (page 287), such correlations reveal a movement along the growth trajectory, from close to the origin where both size and variation are restricted, out toward the nether regions where the population feathers wider and the spread of variation is high. It is reminiscent of what McShea (1994) has termed a 'passive' process, where the emphasis is on 'release' followed by 'diffusion' (in contrast to an 'active' process where the average is propelled along and any trailing variation is mopped up behind it).

It should be stressed how well, in general, all characters correlate with one another—even a single value in a single grid is (95% of the time) significant. Equally, if we do not find a correlation in a particular case there may be multiple reasons for it: all it takes for a signal to be lost is for one of the timeseries patterns to be noisy enough that it fails to correlate with its counterpart. What we are observing in the overlaid correlation grids, therefore, are very subtle differences in morphological flexibility. One can imagine an axis of correlation running from 0% at one extreme to 100% at the other, with the various pairings strung out along it. Combinations like Ch vs. w' sit close to the zero end, apparently exhibiting almost complete independence from one another; those such as H vs. I cluster towards the other pole; and the likes of W vs. w' and I vs. l' lie somewhere in between.

We already know from our earlier examination of *Tritaxia*'s morphology and developmental sequence that characters like H and I or W and l' are practically joined at the hip, so to speak, and it should be of no surprise to find them correlating as spectacularly well as they do. A similar account could be given for each individual pairing— H and h' , or w' and l' etc.—relating them to general morphology and the mechanism of growth. But rather than a piecemeal evaluation, I want to take a broad-brush approach and return to the initial field of mean values in the lower left hand corner of Text Table 9.2.a. As noted above, the region is split into whole test and final chamber blocks that are extremely well-correlated internally, but which are separated from a less well-correlated block of final

chamber versus whole test pairings by the character *Ch*. We detected more or less the same pattern when looking at the timeseries charts themselves (see especially Section 8.2.4), and without getting into the details of individual character pairings, there is a straightforward explanation for it: we should *expect* the final chamber parameters to be well correlated with one another because we imagine them to perform as a coherent unit, both functionally and structurally during the course of development. The same argument extends to the parameters defining the whole test. To a lesser extent it also applies to the relationship *between* the whole test and final chamber parameters, although in this case the slightly weaker correlation plausibly arises because of an element of free play.

What, then, should we make of the *absence of correlation* between *Ch* and all the other characters? In a sense, *Ch* is the character *mediating between* final chamber dimensions and the whole test—the whole test (*H, W, I*) is built up from a particular number of chambers (*Ch*), each of which had a specific set of dimensions (*l', h', w', i'*); thus, it is tempting to suppose that variable and independent behaviour in chamber number *accounts for* the slightly lower correlation between whole test and final chamber parameters. Given the requirements of a test with a certain overall size, either the chamber number or the chamber size could vary; given the requirements of a certain number of chambers, either the whole test or the chamber size could vary; given the requirements of a particular final chamber size, either the whole test or the number of chambers in it could vary. There is a wealth of developmental plasticity to be had with this arrangement. If this is true it is interesting, but it becomes much more interesting when we also pause to consider that *Ch* is being used as a proxy for ‘age’ or ‘stage of development’, because changes in the relationship between *Ch* and other characters can then be classified and understood as a form of heterochrony.

I suspect the independent behaviour of *Ch* is highly significant in terms of the dynamics of *Tritaxia*’s microevolutionary behaviour. It suggests a flexibility and looseness of coupling between the formation of individual chambers and the overall configuration of the whole test; and, moreover, it provides a method for regulating, exploring and exploiting that flexibility—a mechanism which has been documented many times before in fossil lineages (McKinney and McNamarra, 1991). Neotony and hypermorphosis could plausibly be fast and efficient ways of switching between different developmental trajectories in response to environmental demands on the configuration of the test. And, in situations where environmental stability refuses to settle into a long term stable or unstable

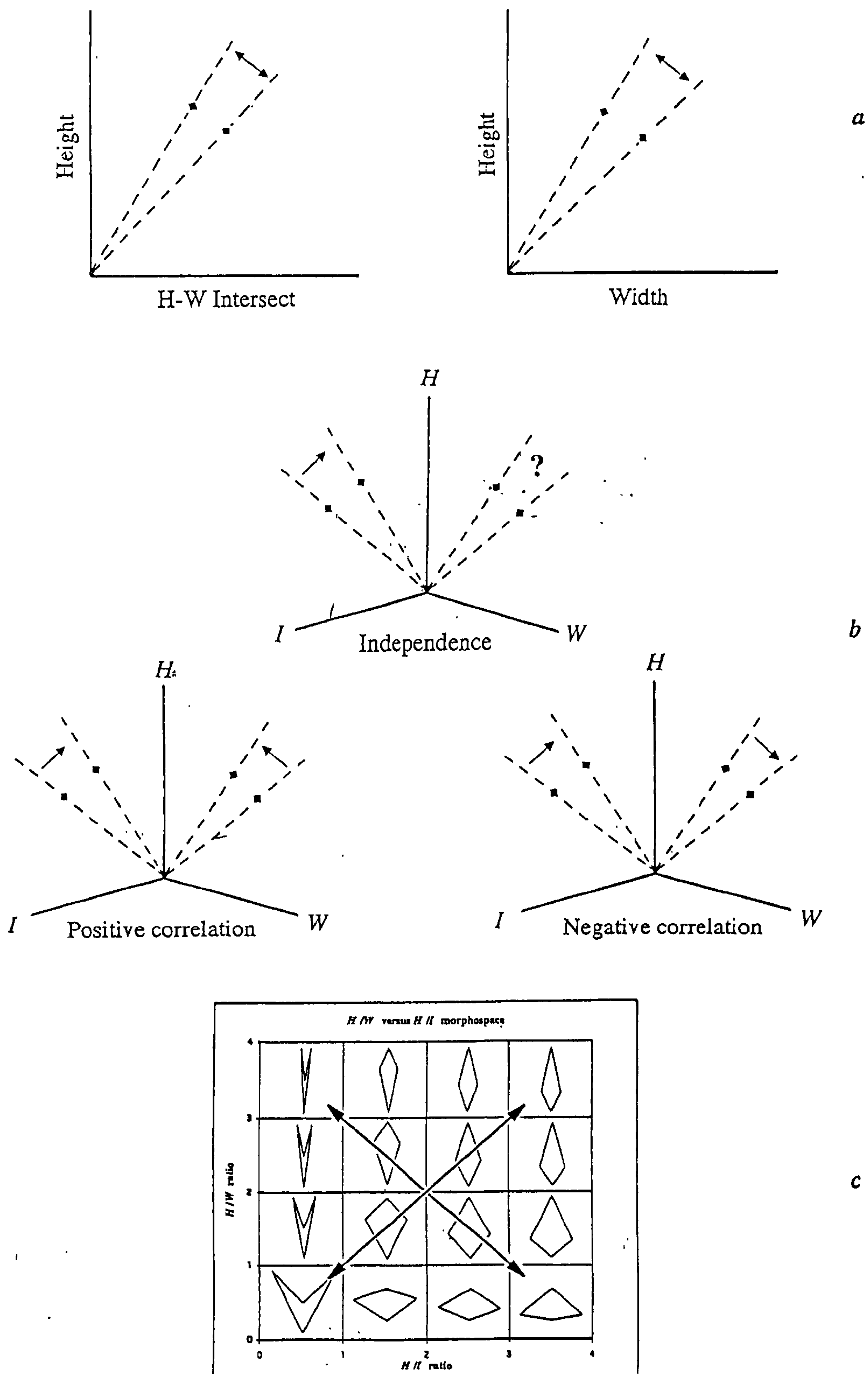
pattern (as seems to be the case in the Lower Chalk), it would also make sense to keep generation times uncoupled from other forms of adaptation, allowing rapid transitions between the K and r selected ends of a life history axis.

9.2.2.ii Shape Shifts

Turning next to a brief examination of the shapes, which we already know to be generally less well correlated than the sizes, we can immediately see that there are rather more significant cases of correlation among the final chamber ratios than among those associated with the whole test, and that this pattern would be amplified if we once again conflated variance with central tendency. We can also see echoes of these same dominant pairings appearing among the rates.

These are cases of shapes correlating with other shapes, not characters correlating with other characters, and, since it is not at all easy to imagine what it means for a shape to correlate with another shape, a visual aid is crucial here. Size shifts are, on the whole, shape preserving (most obviously so in cases of isometry, but also for modest transitions along weakly allometric trajectories); shape shifts, by their very nature, are quite different. In terms of a bivariate plot, shape changes are shifts in directions running orthogonal to the developmental trajectory (they are actually tangential movements radially centred on the origin, as demonstrated by the ratio lines on Text Figure 6.16 and Appendix Figures 4.2.1i-vi). In cases of isometry, shape shifts can only be achieved by changes in the value of b ; in cases of allometry they can be achieved by changes in either b or a , or even simply by transitions along the trajectory itself. But the precise mechanism underlying a transformation is not important at this point: we are simply attempting to track the shape relationships throughout an evolutionary timeseries. For simplicity, Text Figure 9.4 (below) uses only isometric trajectories.

Positive correlations between pairs of shapes are synchronised shifts in the 'same direction' and negative ones are synchronised shifts in 'opposite directions', recalling that in a shape ratio these 'directions' are set by the artificially chosen roles for each variable (i.e. which one functions as denominator). A lack of correlation, by contrast, implies that the behaviour of one shape parameter was largely independent of the other: it shifts in the same direction sometimes, in the other direction at others, and sometimes it fails to shift at



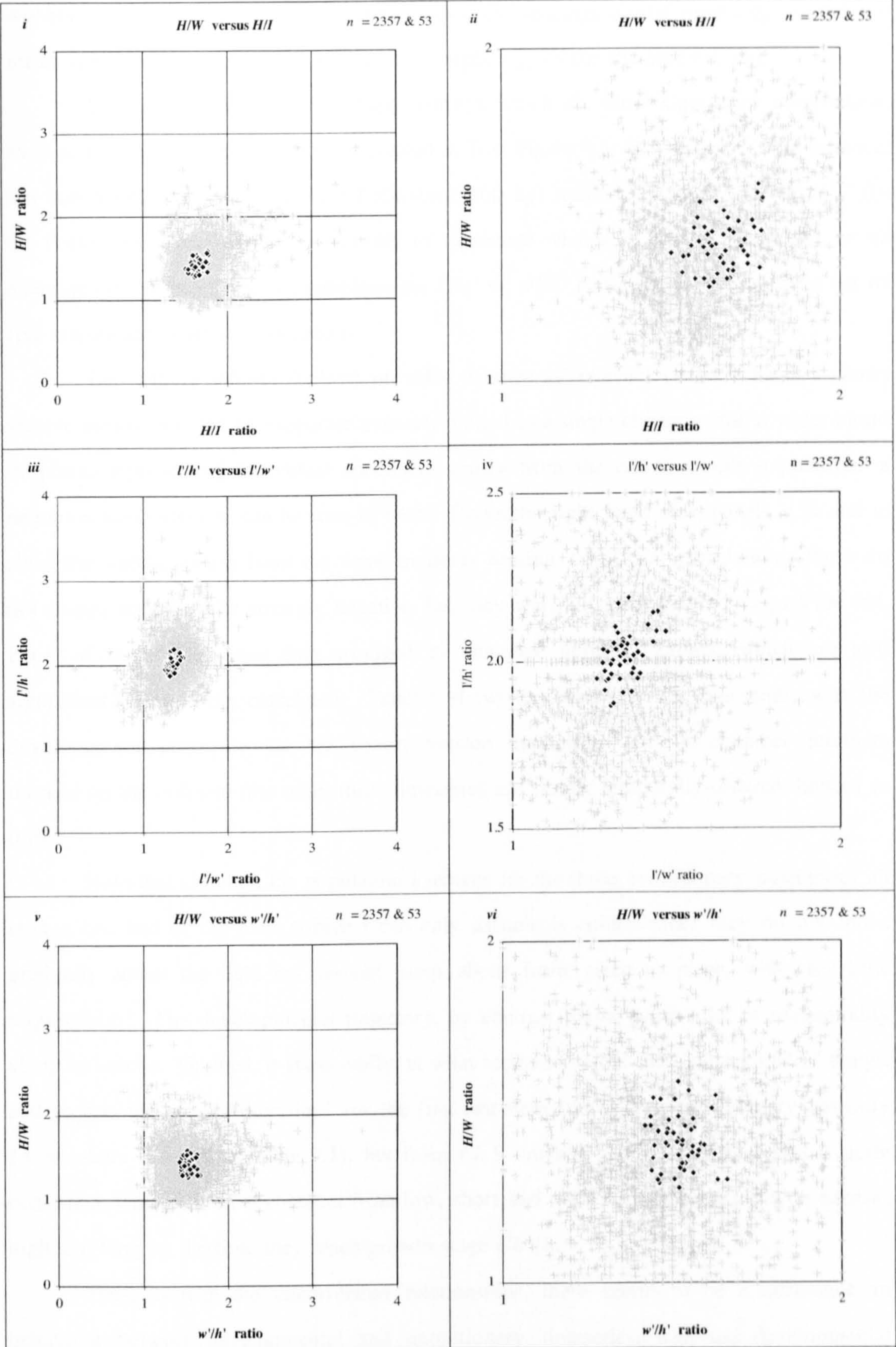
Text Figure 9.4 Mapping shape correlations from bivariate plots to higher dimensional morphospace. *a.* The kind of orthogonal movement involved in shape shifts; *b.* the range of options in terms of correlation – note that in this case it has been possible to organise the two bivariate plots back to back because they share a common axis; *c.* a translation of these shape correlations into higher dimensional morphospace, where they are show as pictures.

all. In cases of correlative independence, knowing something about changes in one variable will tell you nothing at all about changes in the other. Text Figure 9.4.a illustrates the kinds of orthogonal movements we are talking about for the H/W and H/I shape ratio; 9.4.b then shows the two plots back to back, sharing the common axis of H , and illustrating the three possible alternatives.

Having established a method for visualising shape-shift correlations on a bivariate plot, the sensible next step is to transfer the discussion wholesale into shape space itself. Text Figure 9.4.c shows the same H/W vs. H/I morphospace employed in Part III, this time with arrows marked on to show where the axes of positive or negative correlation lie. As suggested in Section 6.2.4, in order to really grasp the nature of this transition one must imagine teasing apart the origin of each individual bivariate plot, until the converging isometry lines shown in Text Figure 6.16 (and Appdx. Figs. 4.2.1.i-vi) become parallel; only then can the plots be ‘glued together’ at their new common origins to form the kind of space shown in Text Figure 9.4.c. This is not an intuitively obvious procedure, and it took me a long time to work out what was going on, but it is what we need to do in order to keep track of things.

Now, if H/W and H/I *had* been highly correlated, the sequence of mean values from at least some of our five transects would have clustered into one of the diagonal routes across the H/W vs. H/I morphospace. As it is, the correlation table (Text Table 9.2.b) tells us they were *not* well correlated, so we expect them to show no particular orientation and instead to take up a roughly circular distribution, which they do. Text Figures 9.5.i demonstrates this arrangement (9.5.ii in close up), and provides equivalent charts for the other two key pairings in the higher dimensional morphospace series (Text Figs. 9.5.iii-vi).

Such figures also provide a striking illustration of the difference between evolutionary trajectories and developmental ones. When these morphospaces were used in Chapters 7 to track *Tritaxia*’s developmental sequence according to cohorts of equivalent growth stage (Ch), the trail of mean values for H/W vs. H/I traced an inverse S-shaped route across the region (Text Figure 7.4.i, page 306). If heterochrony is thought of as the extension or retraction over a period of evolution of trends occurring during the course of development, then there is little evidence of it here. What we find instead is that in each of our five ‘independent trials’, the evolutionary trajectories show no tendency for preferential channelling along developmental pathways whatsoever; rather, in line with a model of



Text Figure 9.5 Distribution of evolutionary trajectories in higher dimensional morphospace. Multivariate plots showing mean values for each sample population ($n = 53$) against a background of specimens in the entire data set ($n = 2357$). See text for discussion. Panels **i** & **ii** H/W vs H/I ; Panels **iii** & **iv** l'/h' vs l'/w' ; Panels **v** & **vi** H/W vs w'/h' .

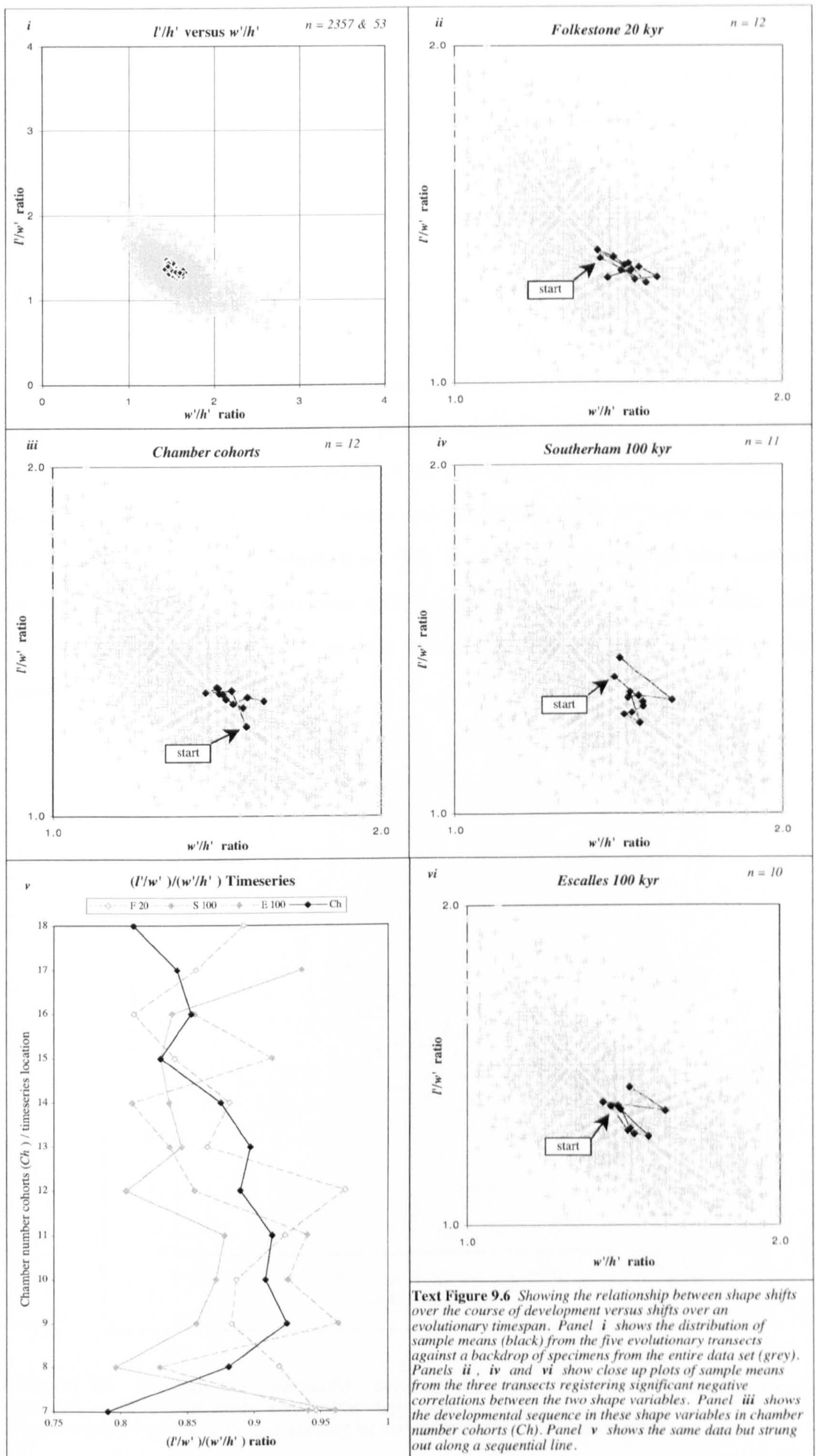
wobbly stasis, the mean values for different temporal spacings cluster randomly around the mean value for the entire database (i.e. the morphology of the Platonic Foram).

There are, however, other shape pairings which *do* show significant correlations, even some hidden within the series presented in Text Figure 9.5: H/W vs. w'/h' , for instance, has one positive correlation (in the Folkestone 100 kyr transect), as does l'/h' vs. l'/w' (in the Folkestone 2 kyr transect). In order to appreciate what such correlations entail, let us examine one of the strongest examples—the l'/w' vs. w'/h' pairing which scores three out of five significant negative correlations.

Text Figure 9.6.i-vi (below) provides a range of relevant charts. Panel *i* shows sample means from the five separate transects plotted as a single cluster within a wider cloud of points representing individual specimens drawn from the entire sample population; a negative, linear element can be seen in both. Down the right hand side, panels *ii*, *iv* and *vi* show the sample means from the three transects hosting significant correlations; these do not always appear to be strongly negative, but they were all linear enough to pass the test. Panel *iii* shows the shape data arranged as chamber number cohorts, which are also significantly negatively correlated. Panel *v* shows the same data as timeseries, with the developmental sequence/chamber cohort version uppermost and its chamber numbers marked on the ordinate (the other three timeseries are simply temporally-ordered, bottom to top).

Note that although the population averages for the three evolutionary trajectories all start at one end of the scale (which I can only assume is coincidence) they do not move gradually across the field but instead jump about from place to place, with very little sequentiality. The developmental trajectory, by contrast, shows quite a lot of sequentiality along its course. Granted, it starts oddly, at what seems to be the 'destination' end of things, and goes in the 'wrong direction' for the first two steps (the 7 chamber category has only 14 members – see Text Table 7.1); but from *Ch* 9 onwards its direction of travel is quite consistent, taking the final chamber from low, short and wide in young tritaxiids to narrow, high and long by the time they reach growth stage *Ch* 18.

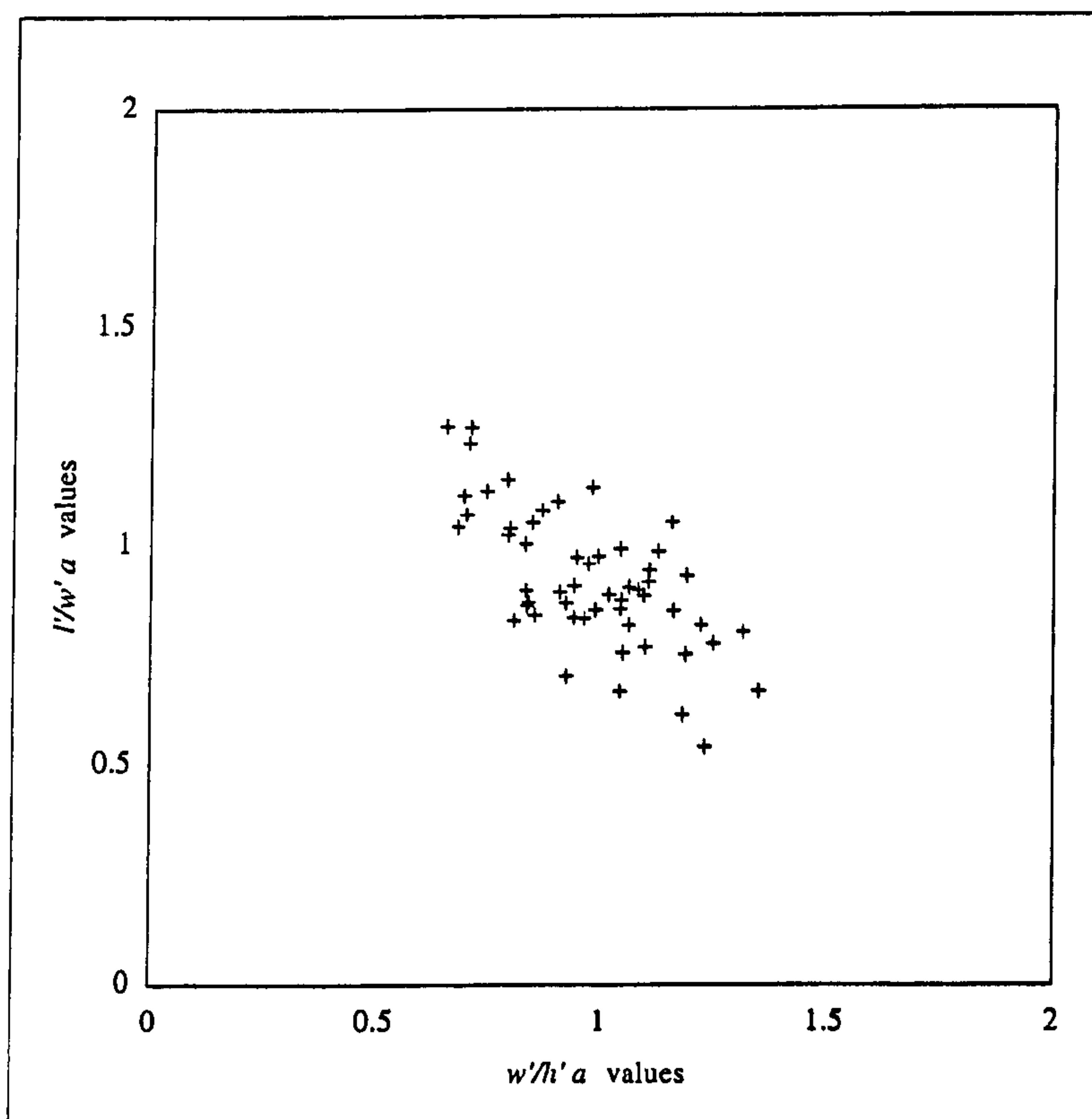
Thus, as with the uncorrelated relationships, there seems to be a difference in behaviour between developmental and evolutionary timeseries, with the developmental version being more orderly than that occurring over the course of evolution. Given the ubiquity of reversals in the fossil record we can hardly be surprised by this. Even if there is a narrow developmental channel of some sort (either structural or functional in nature) to



guide the course of evolution, there is no reason why selection should necessarily push a lineage relentlessly along it in only one direction. What we seem to be seeing here, therefore, is some sort of channel along with morphology sloshed back and forth throughout evolutionary time.

9.2.2.iii Trajectory Shifts

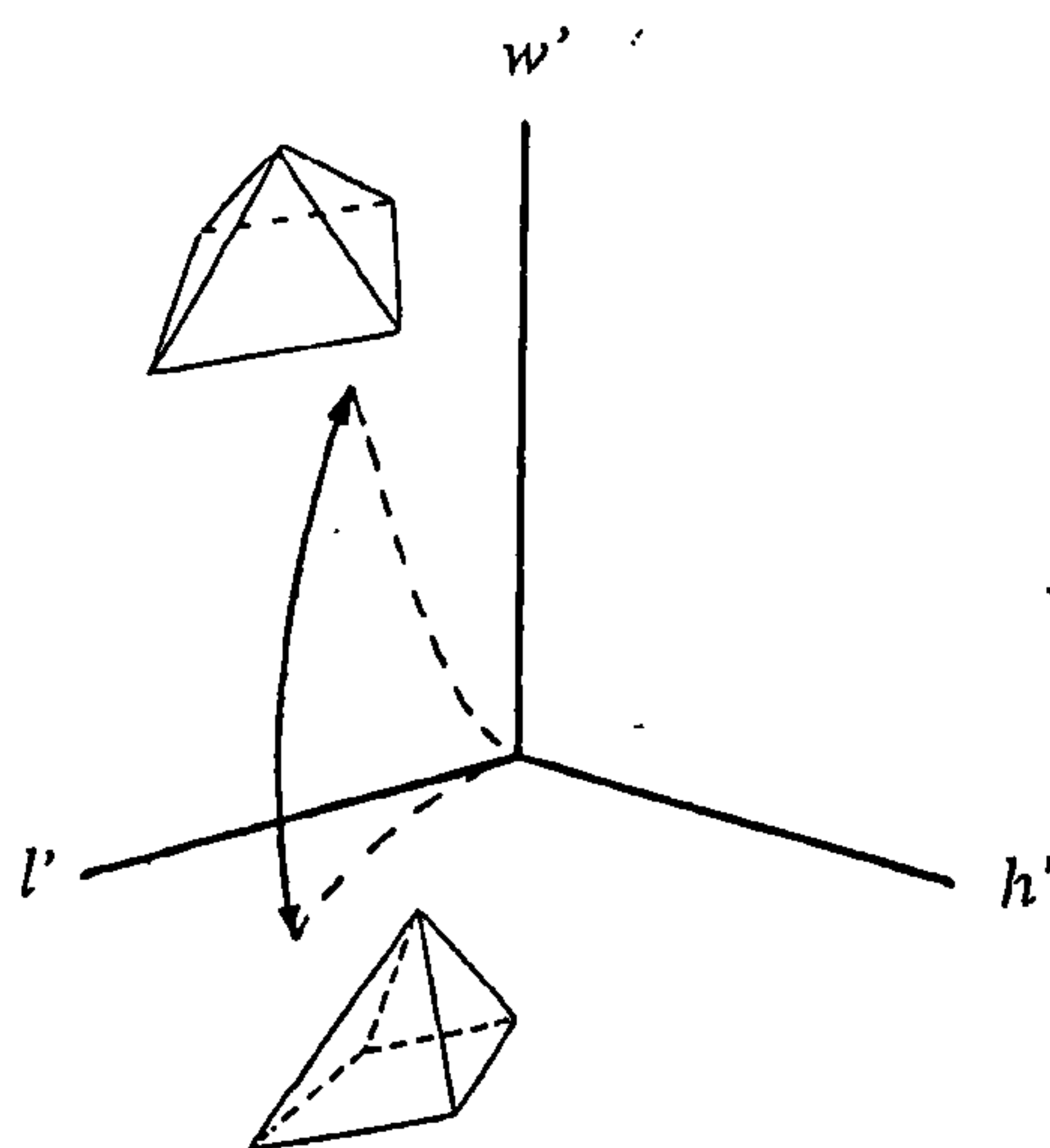
Turning next to the trajectory parameters (Text Table 9.2.d, page 421), we find they harbour a similar pattern. Apart from the perfect negative relationship between a and b values (discussed in Section 9.1.1, above), there are relatively few significant correlations to be found among the trajectories, and, where they do occur, most of them are isolated instances rather than clumps of multiple hits. Only the final chamber pairings have multiple correlations, and the thickest cluster once again occurs between l'/w' and w'/h' , which has significant correlations for a values in four out of the five transects (Escalles is the exception this time).



Text Figure 9.7 *The negative correlation between trajectory 'a' values for the pairings l'/w' v. w'/h' . Note that these are points representing entire specimen populations, not single specimens (trajectory values cannot be calculated for single specimens).*

Rendering this correlation as a bivariate plot (Text Figure 9.7) lets us see that when the a values for w'/h' shift from a negative allometry of 0.5 to a positive one of 1.5, those for l'/w' mirror them, moving from a positive allometry of 1.5 to a negative one of 0.5.

As always, the key to understanding what these patterns are telling us is to translate them back to the more familiar terms of motion along a growth curve. As with the shape relationships we saw above, the negative relationship between l'/w' and w'/h' clearly arises because w' is acting as a numerator in one case and denominator in the other, so if we are to arrange all three characters in a single connected plot we are going to have to juggle the axes somewhat. Text Figure 9.8 shows the character dimensions set up with w' , the shared feature of our two trajectories, as the vertical axis. This leaves l' lying on its back rather than upright as a traditional ordinate should be, but it is still playing the role of y-axis for the l'/w' trajectory and thus gives 'upside down' allometries as well. The solid curve in the middle traces the correlated channel in *Tritaxia*'s evolutionary trajectory within the three dimensional morphospace of the three principal final chamber axes.



Text Figure 9.8 Showing the relationship between the three principal final chamber dimensions as implied by the negative correlation in Text Figure 9.7: the final chamber can be either high, narrow and long, or it can be short, wide and stubby.

This discovery neatly complements the story from the shape correlations, but adds a twist. The trajectory parameters are calculated according to the spread of data points along each axis. In this case, a population smeared preferentially along the w' axis results in a trajectory drawn away from the axes of either h' or l' . A glance back at Appendix Figures 4.2.1.iii & 4.2.1.vi shows that the effect is very likely to occur because a population hosts a high proportion of exotic specimens. According to the chamber cohort description seen in

the last section, however, chambers that are low, short and wide are *also* characteristic of relatively young specimens, and tend to be lost progressively as growth continues. So there are evidently two different ways to achieve the same effect: one is to fill a population with juvenile specimens; the other is to fill it with much older specimens that have passed the point of no return. Plots as generalised as the ones we have been considering here cannot decide between those two alternatives, but the fact that they even *are* alternatives lends weight to the idea that exotic chamber formation occurs when the developing chamber is pushed past a structural threshold of some sort—most plausibly because it is too narrow and high—after which the default solution (in non-triserial growth) is to sag widthways (w') and recapture the characteristics of the more stable juvenile form.

Obviously there are other stories to be told about this database—the trajectory correlations are almost as strong between l'/w' and l'/i' , for instance—but we have spent long enough with the correlations to at least have a feel for what they can tell us about the fabric of *Tritaxia*'s morphospace.

9.2.2.iv Category Shifts

For the categorical characters, the combined grids present very few significant correlations (Text Table 9.2.e). Where correlations do occur they are normally isolated instances rather than multiple cases, the one notable exception being *g.dist* vs. *g%*. The other 8 cases of one-off correlation include both positive and negative examples and comprise 5.3% of the available space, suggesting that they could well be Type I events of no genuine significance. The two glauconite categories probably correlate for artifactual reasons associated with the character definitions themselves, but it seems safe to assume that the remaining characters were acting fairly independently of one another across evolutionary timescales.

Section 9.3 Timeframes

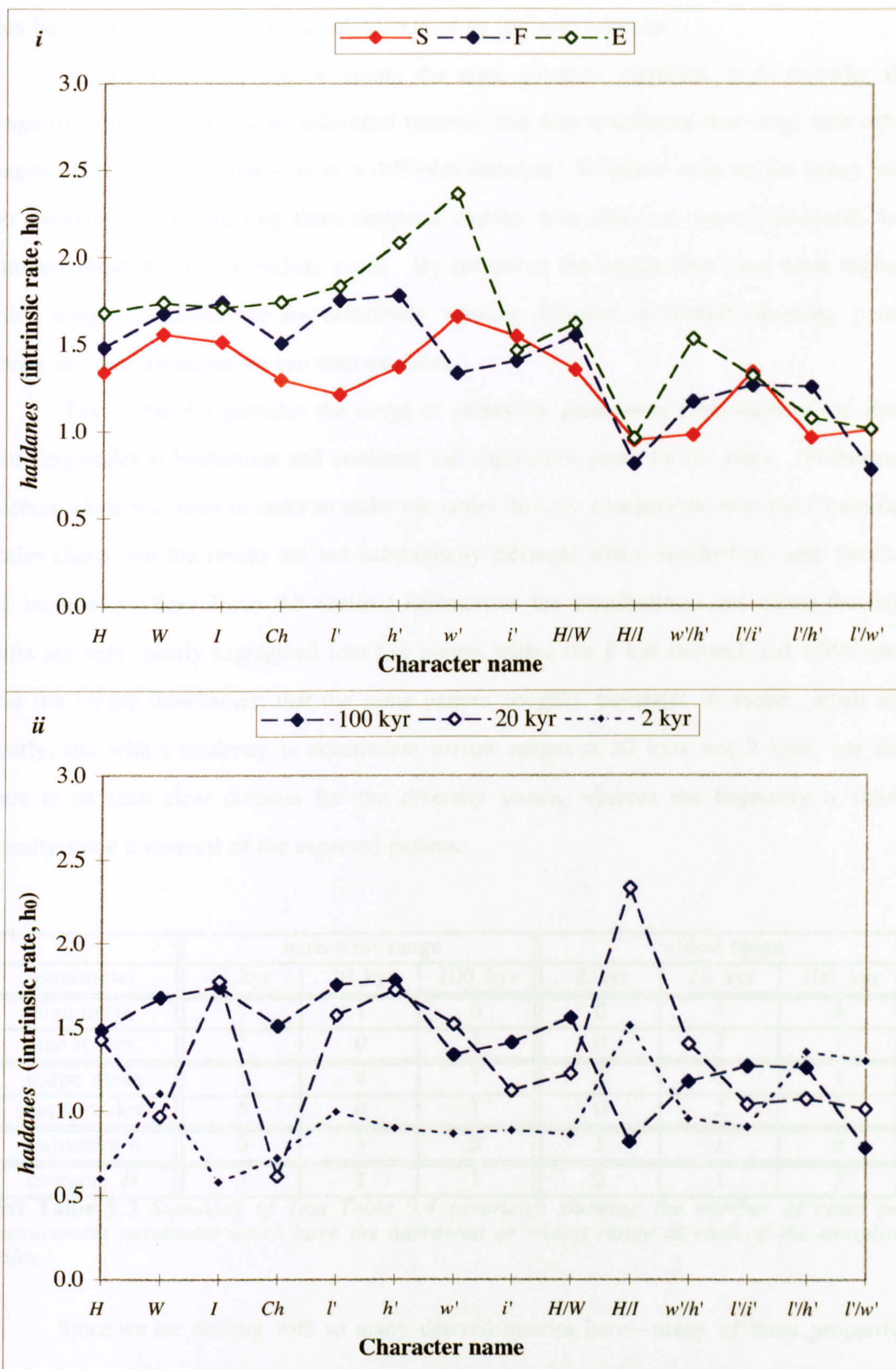
9.3.1 Magnitude of Change at Different Scales

Let us next consider how these patterns of morphological transformation were distributed over time. Straightforward extrapolationist reasoning might lead one to expect that longer observational timeframes beget greater magnitudes of change (Section 1.1.3). To a certain extent, Appendix Figures 5.4.1 – 5.4.4 seem to confirm this expectation, and a simple modification to the rate measurements can be used to quantify our intuitions.

Recall that rate measurements are defined as ‘a change in central tendency by a factor of one standard deviation per generation’ (Section 8.1.3.i.c), the basic quantities being calculated first and then divided through an assumed number of generations to give a metric in *haldanes*; and that if we ignore the elapse of generations, this basic quantity becomes an ‘intrinsic rate’, the amount of change accumulating over a single generation, which can then be used to assess *magnitudes* of morphometric shift (we have already employed the same method to quantify geographical differences between the three locations).

Text Figures 9.9.i & ii show the mean intrinsic rates for shapes and sizes from each of the transects. At the 100 kyr scale, all three sites give results that are closely comparable to one another, even to the point of highlighting regular differences between particular characters, such as the consistently low values for *H/I*. Comparing between scales instead of sites, however, we see that the 100 kyr and 20 kyr transects have almost identical magnitudes, but that the 2 kyr data tend to lie a little way below at only two-thirds the value, and thus represent lower magnitudes of change between adjacent samples within the single couplet (9.9.ii).

There is, however, a complication with this method concerning sample zone duration. In order to fit a large number of sampling points into a single couplet, specimens from the 2 kyr transect were taken from a 7 cm thickness of sediment rather than the typical 15 cm thickness used for all other scales. Since 7 cms of sediment from a highly expanded couplet (and C13 is 90 cm thick) must represent far less time than, say, 15 cms taken from a thin couplet like C10 (which is only 35 cm thick at Folkestone), this difference in accumulation time almost certainly affects the range of variation *within* a sample and can



Text Figure 9.9 Panel *i* shows the mean intrinsic rate of change per character for each of the three 100 kyr transects. Note that rates are broadly comparable between sites and show considerable regularity between characters (e.g. H/I which is always low). Panel *ii* shows the intrinsic rate of change per character for each of the three scales. Note that values are again fairly regular and close in magnitude with the 2 kyr scale being somewhat lower, and with a peak instead of a trough for H/I rates at the finer sampling scales. See text for discussion.

thus be expected to influence the calculation of an intrinsic rate, too.

An alternative method of asking the same question, therefore, is to consider the *range* of values seen across an individual transect, and then to compare that range with other ranges observed across transects of a different duration. In effect what we are doing with this procedure is contrasting three temporal chunks with spans of twenty thousand, two hundred thousand and a million years. By reviewing the oscillations over these higher-order temporal chunks we are effectively working *between* individual sampling points whose *internal* durations we can then overlook.

Text Table 9.4 provides the range of values for parameters from each of the three sampling scales at Folkestone and confirms the impression given by the rates. (Folkestone material alone was used in order to make the tables directly comparable with the Combined Scales charts, but the results are not substantially different when Southerham and Escalles are included.) Text Table 9.3 (below) summarises the distributions and shows that size shifts are very clearly segregated into low ranges within the 2 kyr transect and wider ones over the longer timeframes; that the same pattern roughly translates to shapes, albeit less clearly, and with a tendency to accumulate narrow ranges at 20 kyrs not 2 kyrs; but that there is no such clear division for the diversity scores, whereas the trajectory *a* values actually show a reversal of the expected pattern.

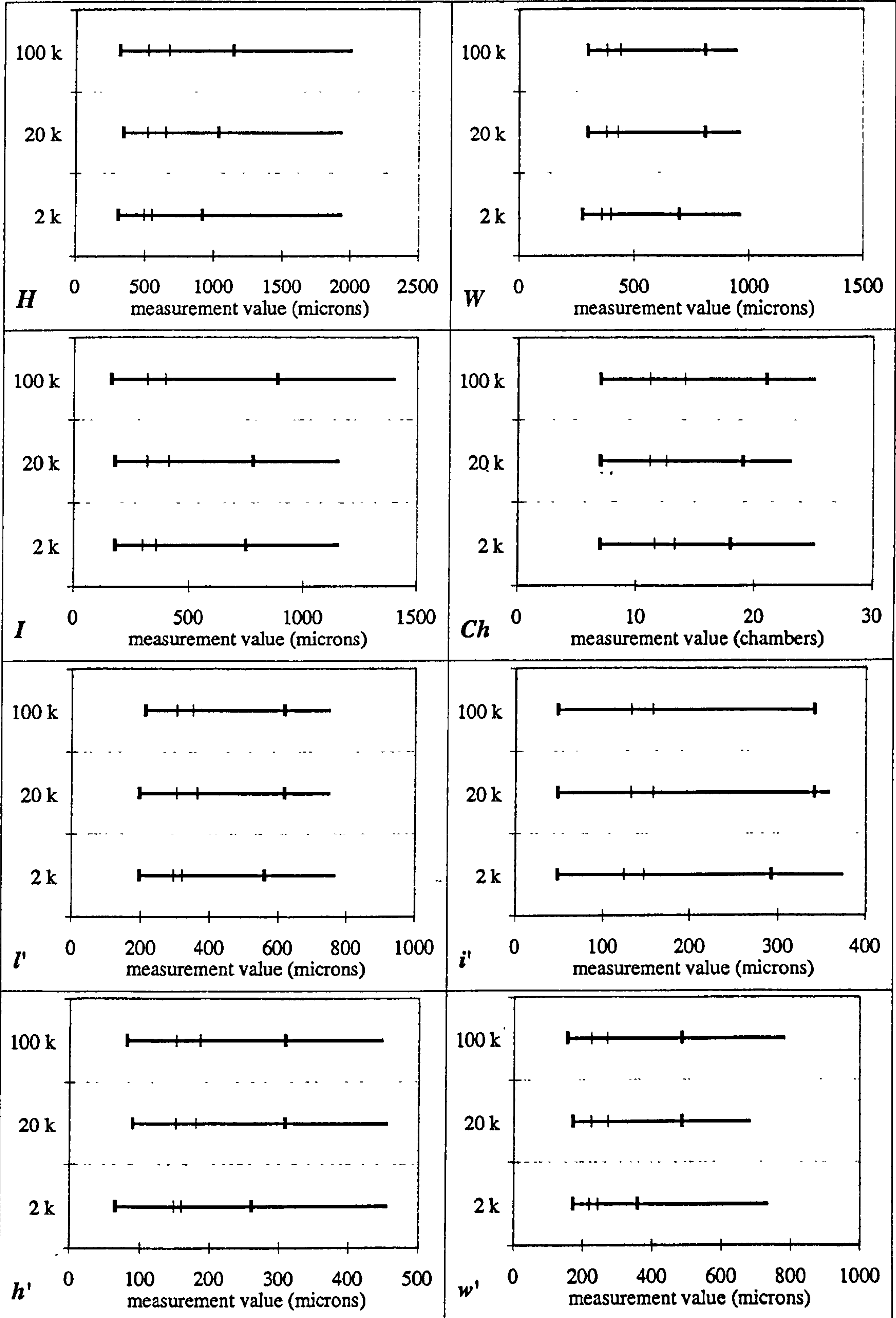
	narrowest range			widest range		
parameter	2 kyr	20 kyr	100 kyr	2 kyr	20 kyr	100 kyr
size mean	7	1	0	0	4	4
size st. dev.	7	0	1	0	7	1
shape mean	1	4	1	2	0	4
shape st. dev.	5	0	1	0	2	4
trajectory <i>a</i>	0	3	3	5	1	0
category <i>H</i>	3	2	1	2	1	3

Text Table 9.3 Summary of Text Table 9.4 (overleaf) showing the number of cases per measurement parameter which have the narrowest or widest range at each of the sampling scales.

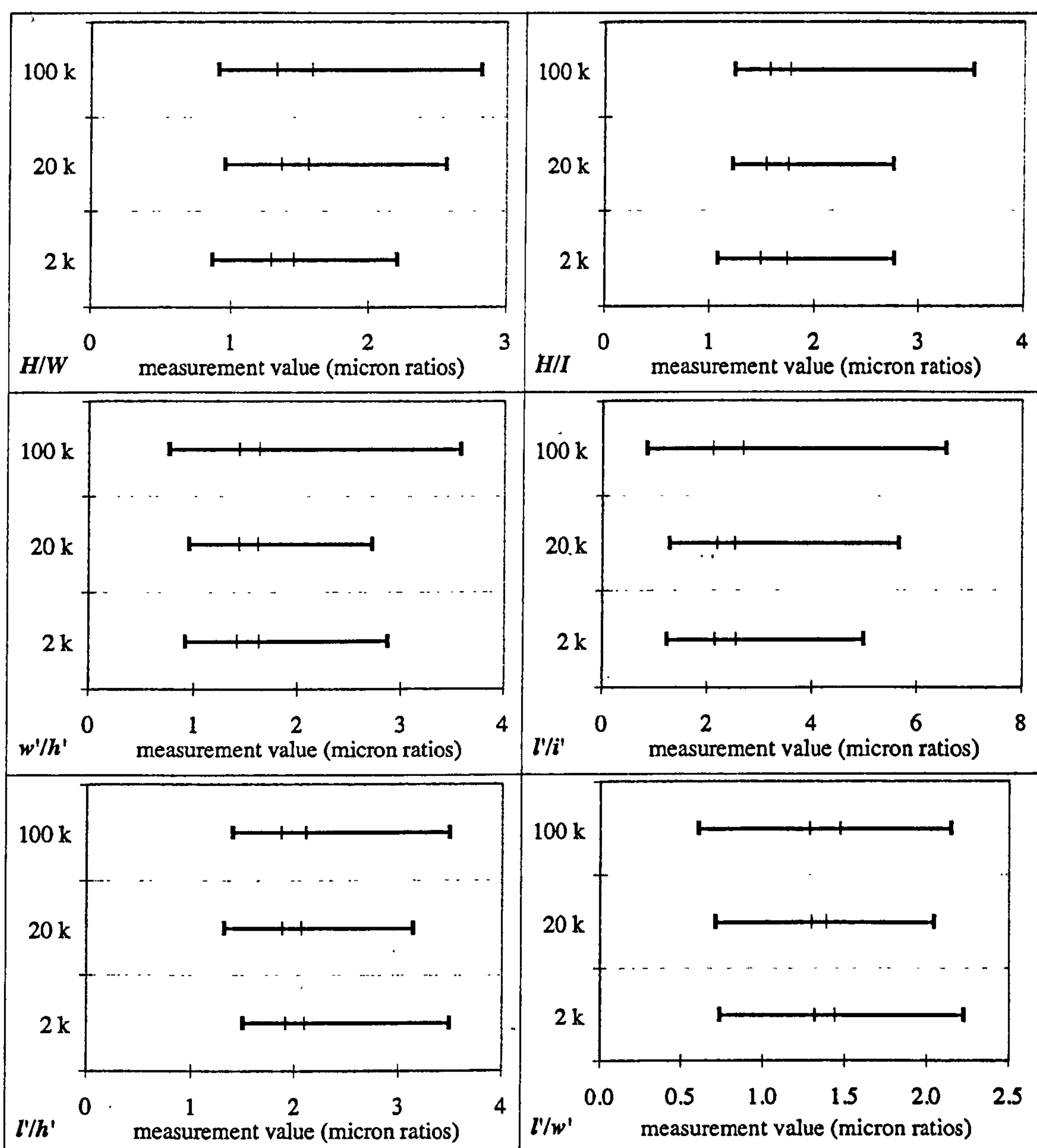
Since we are dealing with so many derived metrics here—many of them properties of populations rather than individuals—it would be helpful at this stage if we had a way of relating the features we are discussing to the raw data of the specimen populations from which they originally came. Appendix Figures 6.1.i-vi present much of the relevant information in an accessible format. The figures show standard bivariate plots of the six basic character pairings, with (for simplicity’s sake, unlabelled) growth trajectories and

Char-	Parameter	F 2 kyr	F 20 kyr	F 100 kyr	ratio of	Char-	Parameter	F 2 kyr	F 20 kyr	F 100 kyr	ratio of
acter	Size	range	range	range	high to low	acter	Size	range	range	range	high to low
<i>H</i>	mean	54.2	129.5	151.9	2.8	<i>H</i>	st. dev.	50.3	66.2	60.7	1.3
<i>W</i>	mean	40.5	48.6	60.7	1.5	<i>W</i>	st. dev.	37.4	45.7	43.3	1.2
<i>I</i>	mean	56.5	96.3	79.3	1.7	<i>I</i>	st. dev.	44.3	56.3	44.6	1.3
<i>Ch</i>	mean	1.7	1.4	3.0	2.1	<i>Ch</i>	st. dev.	0.9	1.0	0.6	1.5
<i>h'</i>	mean	10.7	29.4	34.5	3.2	<i>h'</i>	st. dev.	11.2	15.6	11.5	1.4
<i>l'</i>	mean	25.1	59.8	46.1	2.4	<i>l'</i>	st. dev.	26.1	38.8	29.9	1.5
<i>w'</i>	mean	25.7	47.5	44.8	1.9	<i>w'</i>	st. dev.	12.3	26.5	28.0	2.3
<i>i'</i>	mean	22.4	25.7	24.7	1.1	<i>i'</i>	st. dev.	19.4	25.3	22.7	1.3
	Shape	range	range	range	high to low		Shape	range	range	range	
<i>H/W</i>	mean	0.167	0.197	0.261	1.6	<i>H/W</i>	st. dev.	0.101	0.130	0.143	1.4
<i>H/I</i>	mean	0.243	0.203	0.192	1.3	<i>H/I</i>	st. dev.	0.119	0.124	0.166	1.4
<i>w'/h'</i>	mean	0.206	0.182	0.193	1.1	<i>w'/h'</i>	st. dev.	0.147	0.165	0.218	1.5
<i>l'/i'</i>	mean	0.391	0.323	0.577	1.8	<i>l'/i'</i>	st. dev.	0.285	0.458	0.493	1.7
<i>l'/h'</i>	mean	0.194	0.191	0.240	1.3	<i>l'/h'</i>	st. dev.	0.167	0.228	0.155	1.5
<i>l'/w'</i>	mean	0.125	0.097	0.191	2.0	<i>l'/w'</i>	st. dev.	0.074	0.177	0.135	2.4
	Trajectory	range	range	range	high to low		Category	range	range	range	
<i>H/W</i>	a values	0.830	0.649	0.652	1.3	<i>ind</i>	H values	0.711	0.696	0.410	1.7
<i>H/I</i>	a values	0.321	0.304	0.116	2.8	<i>tw</i>	H values	0.535	1.122	1.381	2.6
<i>w'/h'</i>	a values	0.581	0.399	0.572	1.5	<i>g%</i>	H values	0.662	1.184	1.127	1.8
<i>l'/i'</i>	a values	0.366	0.366	0.195	1.9	<i>g dist</i>	H values	0.969	0.678	0.705	1.4
<i>l'/h'</i>	a values	0.444	0.385	0.411	1.2	<i>chir</i>	H values	0.082	0.050	0.089	1.8
<i>l'/w'</i>	a values	0.732	0.537	0.448	1.6	<i>type</i>	H values	1.169	1.324	1.634	1.4

Text Table 9A Range of values for various morphometric parameters exhibited by the three transects at Folkestone. Ranges are in units appropriate to the parameter under consideration (microns for sizes, micron ratios for shapes, a values for trajectories, H values for categories). In each case, the widest instances are marked in bold and the narrowest in italics. Ratios of highest to lowest value are summarised in the end columns of each transect series. See the adjacent text for full discussion.



Text Figure 9.10.i Range of values in size shown by individuals and populations at the three sampling scales. All material is from Folkestone. The two thin inner vertical markers show upper and lower bounds for character means across the three transects. The two thick outer vertical markers show the upper and lower bounds for individuals in the statistical sample populations (i.e. the set which excludes the outliers). The total length of each line shows the full range of specimen values with outliers included.



Text Figure 9.10.ii Range of values in shape shown by individuals and populations at the three sampling scales. All material is from Folkestone. The two thin inner vertical markers show upper and lower bounds for character means across the three transects. The two thick outer vertical markers show the upper and lower bounds for individuals in the whole sample populations, including the outliers (unlike the sizes, endpoints on these ranges are not occupied by the outliers, which normally have rather average shapes).

population means, and also with reference lines drawn on to mark four important boundaries. For each sampling scale, the outermost pair of dashed lines show the limits of individual specimens in the statistical data set (i.e. all specimens apart from the outliers), while the innermost solid lines mark the limits of the sample means for populations in that transect. The three scales of observation are arranged side by side for contrast.

Text Figure 9.10.i summarises the size relationships between the range of specimens in the sample pool and the range of locations for the sample means as shown by the

appendix figures; Text Figure 9.10.ii summarises the same values for shapes (it proved too difficult to plot the shape ranges on the bivariate charts themselves but they would follow the same kind of pattern we see for the sizes, except running diagonally from upper left to lower right). Note that the size charts also include the magnitude of the outlier specimens whereas the outliers are not necessarily at the ends of shape ranges and thus do not require any special mode of presentation. Neither the categorical features nor the trajectories are depicted in this summarised form, but some idea of the trajectory α values can be gleaned from the growth curves of Appendix Figures 6.1.i-vi (see for instance how widely the 2 kyr series tend to splay relative to the two longer transects).

9.3.2 The Tension Between Stasis and Change

One major conclusion would seem to be inevitable irrespective of how the data are presented: while it is certainly the case that longer timeframes beget an increase in morphological exploration, the extent of that exploration is strictly limited. Text Table 9.4 (above) assesses the magnitude of morphological change in the three Folkestone transects as a ratio of the longest to the shortest ranges of exploration (irrespective of the scale on which they were observed). The average turns out to be 1.7, and only a single parameter, mean h' , exceeds a ratio of 3—that is, *on average, the longest range is less than twice as wide as the shortest* (in whatever units are appropriate), and only on one occasion out of forty is it more than three times as wide.

Such limitations apply equally to central tendency, standard deviation, α values, and categorical diversity scores alike. All of them oscillate within restricted domains such that a fifty-fold increase in surveillance time (from 20 000 to 1 000 000 years) does little more than double the observed breadth of morphological exploration: to put it starkly, it appears that roughly half of *Tritaxia*'s available malleability was quite readily accessed (or exhausted) within the duration of a single couplet! (And recall also that C13 specimens are very small anyway—I suspect many other couplets host a range of exploration fully equivalent to that of a million year span.)

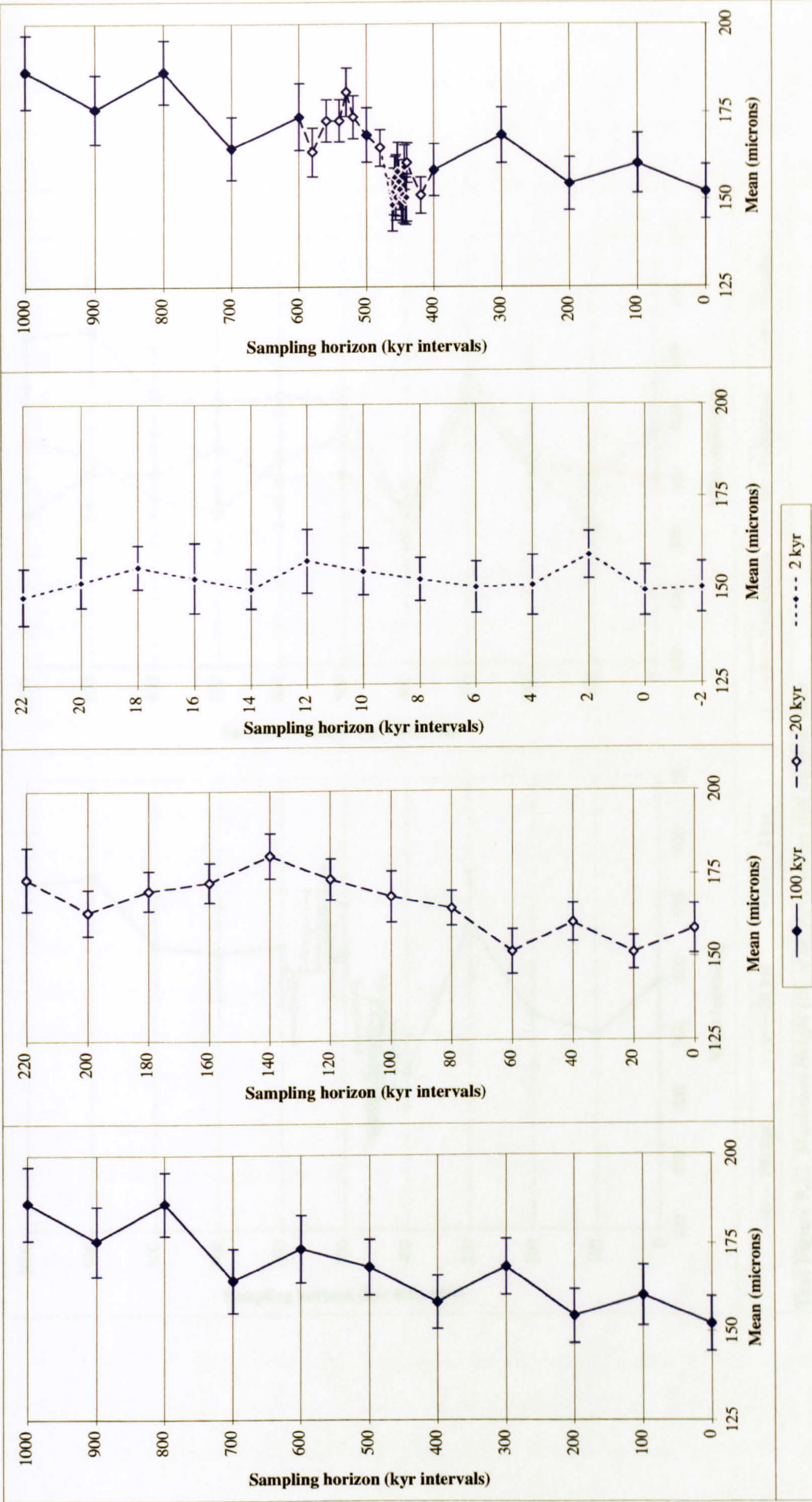
Mean h' shows the largest difference in mobility, with shifts across a 10.7 micron range in C13 against a 34.5 micron range in the Folkestone 100 kyr transect. Text Figure

9.11 confirms that the character holds a good approximation to stasis in the single couplet against a good approximation to unidirectional change over the long transect. But most other characters show neither substantial unidirectional change nor anything approaching perfect stasis: instead, they wander endlessly, and apparently aimlessly, over their restricted domains.

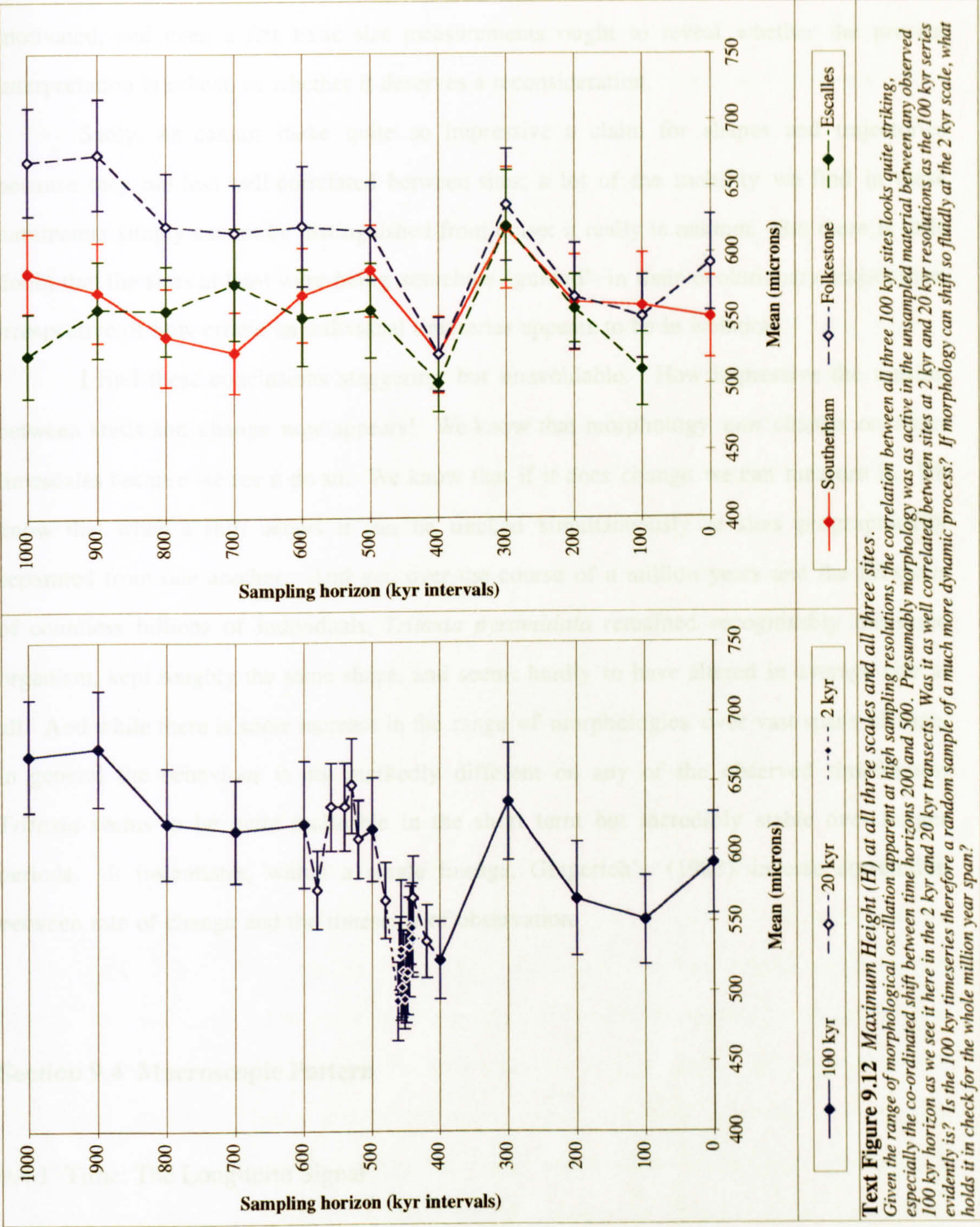
This latter phenomenon is reminiscent of the ecological patterns discussed in Section 4.2.4 where the relative abundance of various species in an ecological mix oscillated around an average value, generally producing a normal distribution whenever the species was common enough to avoid frequent zero counts. There, as here, the effect was relatively independent of time scale. It had the superficial appearance of a completely random signal; but in that case we could see from the between-site correspondences that there were common causes underlying the sequence of erratic shifts. And so it is with morphology—despite a chaotic and superficially random signal, there appears to be a deep regularity behind the patterns we observe.

Let us take mean *H* to illustrate this next point. Text Figure 9.12 is reproduced from Appdx. Figs 5.4.1.i, and 5.3.1.i. The combined-scale format provides a context which serves to remind us that the kind of morphological fluctuation seen here at 2 kyr and 20 kyr resolutions was probably typical of what was happening throughout the unsampled stretches between *any other pair* of 100 kyr horizons. With this juxtaposition of scales the hefty jump in size at B41-C10 [200-400], which completely dominates the 100 kyr plots, still obviously remains significant, but its magnitude no longer looks anywhere near as imposing as it originally did. Instead, what now stands out as quite astonishing is the fact that this character is so well correlated between the three 100 kyr sites.

Given the rate and extent of transformation apparent at the higher resolutions, it is hard to comprehend how morphology at each of the three 100 kyr locations could have wandered in *different directions* at different sites *between* the horizons sampled, and then miraculously converged back just in time to give the pattern we observe, or any pattern even half so striking. In order to generate such obviously non-random and highly co-ordinated 100 kyr timeseries, therefore, the kinds of oscillations we find at 2 kyr and 20 kyr resolution *couldn't* have been wholly random either; they must therefore have been occurring, presumably in correlated fashion, at a similar rate and magnitude behind the scenes throughout!



Text Figure 9.11 The widest difference in morphological change in any character or parameter is seen in the final chamber height (h') between the 100 kyr and 2 kyr transects at Folkestone. Transects for this character are plotted here at each of the three sampling scales and also shown in the combined scales plot. Over the million year span of the entire 100 kyr transect, mean h' shifts across a range of 34.5 microns, and at this resolution approximates unidirectional change; over the twenty thousand year span of the single couplet, the same character shifts by just 10.7 microns and gives a good approximation to stasis, although even a shift as small as this one is sufficient to register as significant at the 0.05 level (see Appdx. Tab. 3.2.1.vi for details).



While there is insufficient data in this survey to demonstrate conclusively that morphology was to some extent correlated between sites at the 2 kyr and 20 kyr scales, an empirical demonstration would be easy enough to come by. Sampling the missing material from Southerham and Escalles should be straightforward enough for anyone sufficiently motivated, and even a few basic size measurements ought to reveal whether the present interpretation is robust, or whether it deserves a reconsideration.

Sadly, we cannot make quite so impressive a claim for shapes and trajectories because they are less well correlated between sites; a lot of the mobility we find in these parameters simply cannot be distinguished from noise: it really is random. But there is little doubt that the sizes at least were being somehow ‘guided’ in their evolutionary trajectories, irrespective of how erratic an individual timeseries appears to be in isolation.

I find these conclusions staggering but unavoidable. How impressive the tension between stasis and change now appears! We know that morphology *can* change on short timescales because we see it do so. We know that if it does change we can measure it. We know that when a shift occurs it can be tracked simultaneously at sites geographically separated from one another. And yet, over the course of a million years and the lifespans of countless billions of individuals, *Tritaxia pyramidata* remained recognisably the same organism, kept roughly the same shape, and seems hardly to have altered in average size at all. And while there is some increase in the range of morphologies over vast spans of time, in general the behaviour is not markedly different on any of the observed timeframes. *Tritaxia* seems to be quite malleable in the short term but incredibly stable over longer periods. It instantiates, within a single lineage, Gingerich’s (1983) inverse correlation between rate of change and the timescale of observation.

Section 9.4 Macroscopic Pattern

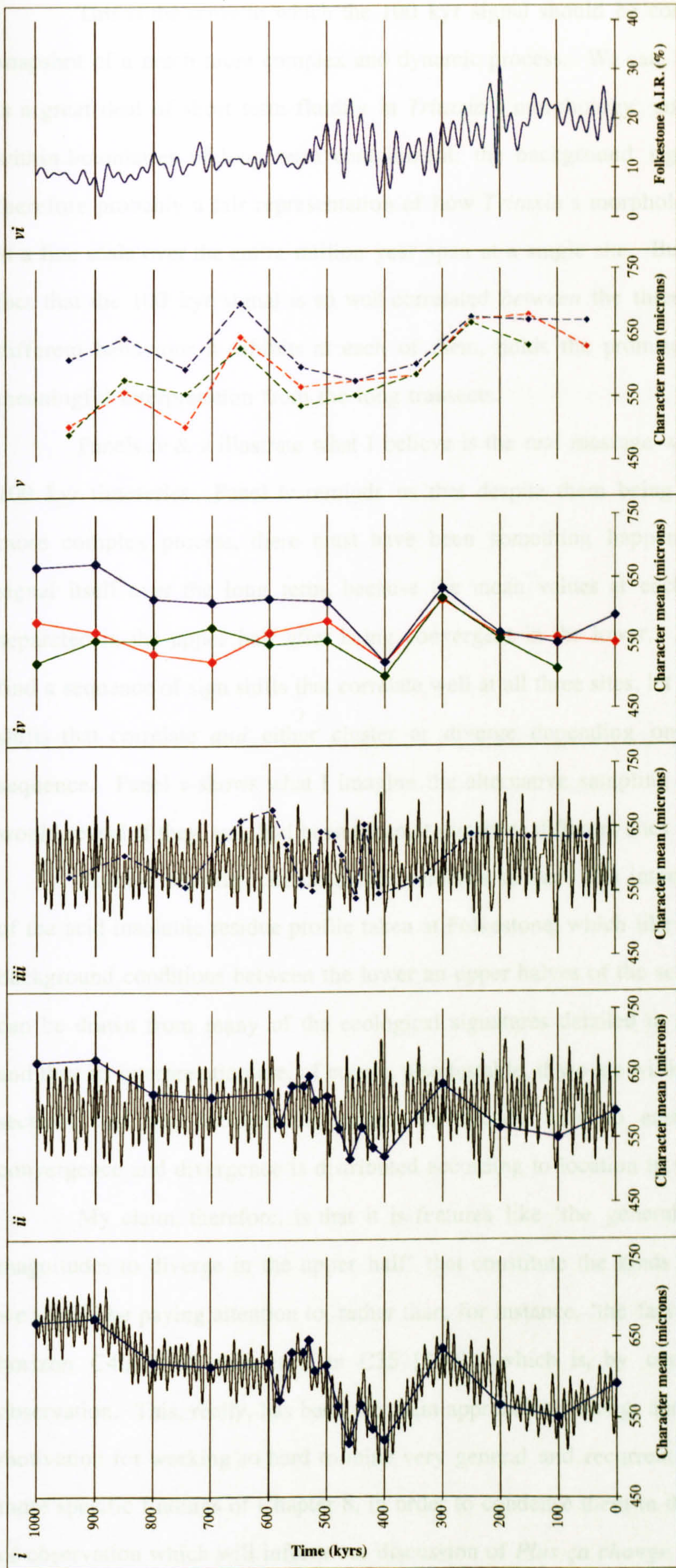
9.4.1 Time: The Long-term Signal

This brings us to a very important question concerning temporal scaling, one that has been put off since it was first raised in Part II (Sections 3.3.4.ii & 4.2.4). As we now have evidence that morphological shifts (and patterns of relative abundance) at 2 kyr and

20 kyr resolution were of almost the same magnitude as those seen at 100 kyr resolution, what is to stop the 100 kyr transects from being merely a random sample of this finer-grained process? In a sense, the answer has to be, “nothing”; but here we must be careful because it depends very much on what we think we have sampled, and also on what we are actually looking for. Text Figure 9.13.i-vi illustrates some of the various scenarios we might consider, and should help to refine our ideas about what counts as signal rather than noise.

Panel *i* illustrates (for the sake of convenience, using only 20 kyr and 100 kyr values for mean H at Folkestone) what we might like the data to be telling us in an ideal world. Although morphology oscillates somewhat around a local average, that average is itself moving, and because our samples are taken from the middle of the range, they give us a good idea of its location. This higher-order signal is what we are really interested in. That is the assumption implicit in taking a bulk sample from a piece of ancient sea-bed whose mixed and jumbled contents represent thousands of years of generation by generation evolution: we hope that despite the short term oscillation, larger scale processes are also at work, and that these can be discerned through the average values of a blended fossil population. In the case of panel *i*, however, it is abundantly clear that there might be as much oscillation going on between any unexamined 100 kyr blocks as there is within those which have been examined; and, given the data from C13 (which is not shown in the figure), it looks like we could subdivide the process even further to yield a situation somewhat like that shown in panel *ii*.

The background signal of panels *ii* and *iii* represents a basic high-resolution cyclicity with a random perturbation. In the figures shown, the cyclicity sits at around the 10 kyr mark because that is as fine a resolution as I could plot, but it could well be much higher. At a sufficiently fine scale the basic signal is locally directional, but sampling it at any resolution much beyond that of the basic cycle, or amalgamating any temporal chunk of a larger granularity than that of the basic cycle, will tend to result in a normal distribution. To this extent, the background signal approximates white noise. Sampling it at the points shown in panel *ii* would yield the pattern of shifts seen in mean H at Folkestone, while if we were to sample midway between those points, as shown in panel *iii*, a totally different pattern would be found. If a histogram was drawn with either of these timeseries, the result would be a normal distribution.



Text Figure 9.13 Showing various interpretations of how the observed morphological signal relates to the background phenomenon from which it was sampled.

Panel i. In an ideal world, sample shifts (here, mean H at Folkestone) would be representative of events in the background average of the morphological signal (thinner line with no markers); however, because the range of sample values is very similar at each of the observed timeframes, it seems more likely that they represent a randomly sampled white noise signal which has a similar structure at all scales.

Panel ii. The situation outlined above is illustrated here with a background signal as Panel ii is sampled at points between those in Panel ii, yielding a totally different pattern. Neither this sample signature nor 100 kyr and 20 kyr scales are shown here). **Panel iii.** The same background signal as Panel ii is sampled at points between those in Panel ii, yielding a totally different pattern. Neither this sample signature nor that from Panel ii can be assumed to be telling us much in terms of its detail because there are a vast range of available patterns hidden in the background series, all of which are essentially random (since they have been caused by an idiosyncratic mixture of events) and all of which are as meaningful or meaningless as any of the others. **Panel iv.** If we take a broader approach to analysing the sample signature, there are other features we can concentrate on beside the specific detail that might prove more meaningful. In Panel iv the sample signatures from all three sites show convergence of value in the lower half of the section against general divergence in the upper. Although the particular series of positive and negative steps may itself be 'random', the elements of convergence and divergence are likely to be more robust, suggesting that they would have been encountered even if we had sampled elsewhere; an argument to this effect is given in the text. **Panel v** suggests how the hypothetical alternative transect shown in Panel iii might look at all three sites if the convergence and divergence are real and persistent features. **Panel vi** provides backup evidence for a general change in circumstances between the upper and lower halves of the succession in the form of the only signal we can realistically trace on a bed by bed basis, the Acid Insoluble Residue profile for Folkestone. See main text for a full discussion.

This is the sense in which the 100 kyr signal should be considered to be a random snapshot of a much more complex and dynamic process. We can, I think, accept that there is a great deal of short term fluidity in *Tritaxia*'s morphology, and that this fluidity exists within boundaries of long term containment; the background signal of panels *ii* & *iii* is therefore probably a fair representation of how *Tritaxia*'s morphology really was behaving at a fine scale over the entire million year span at a single site. But, as I argued above, the fact that the 100 kyr signal is so well correlated *between* the three sites, coupled with the different behaviour it exhibits at each of them, holds the promise of a different kind of meaningful interpretation from the long transects.

Panels *iv* & *v* illustrate what I believe is the real message we should glean from the 100 kyr timeseries. Panel *iv* reminds us that despite them being random snapshots of a more complex process, there must have been something happening to the background signal itself over the long term, because the mean values at each of the three sites are separated in the upper half after being convergent in the lower. It is unlikely enough to find a sequence of sign shifts that correlate well at all three sites, let alone a sequence of sign shifts that correlate *and* either cluster or diverge depending on where they are in the sequence. Panel *v* shows what I imagine the alternative sampling horizons from panel *iii* would reveal if they, too, had been taken at our three different sites.

Panel *vi* provides circumstantial evidence to back this interpretation up in the form of the acid insoluble residue profile taken at Folkestone, which likewise records a change in background conditions between the lower and upper halves of the sequence. Similar support can be drawn from many of the ecological signatures detailed in Part II. (The prediction and thus its interpretation are, of course, also testable, if we are willing to re-sample the three sections half way between the points we already have to ensure that the pattern of convergence and divergence is distributed according to location in the succession.)

My claim, therefore, is that it is features like 'the general tendency for character magnitudes to diverge in the upper half' that constitute the kinds of morphological signal we should be paying attention to, rather than, for instance, 'the fact that mean *H* is larger at horizon C40 [900] than it is in C35 [800]', which is, by contrast, a fairly arbitrary observation. This, really, has been the main approach all along, and it is a large part of the motivation for working so hard to mine very general and recurrent features from the much more specific findings of Chapter 8, in order to condense them in this chapter into the kinds of observation which will inform our discussion of *Plus ça change*.

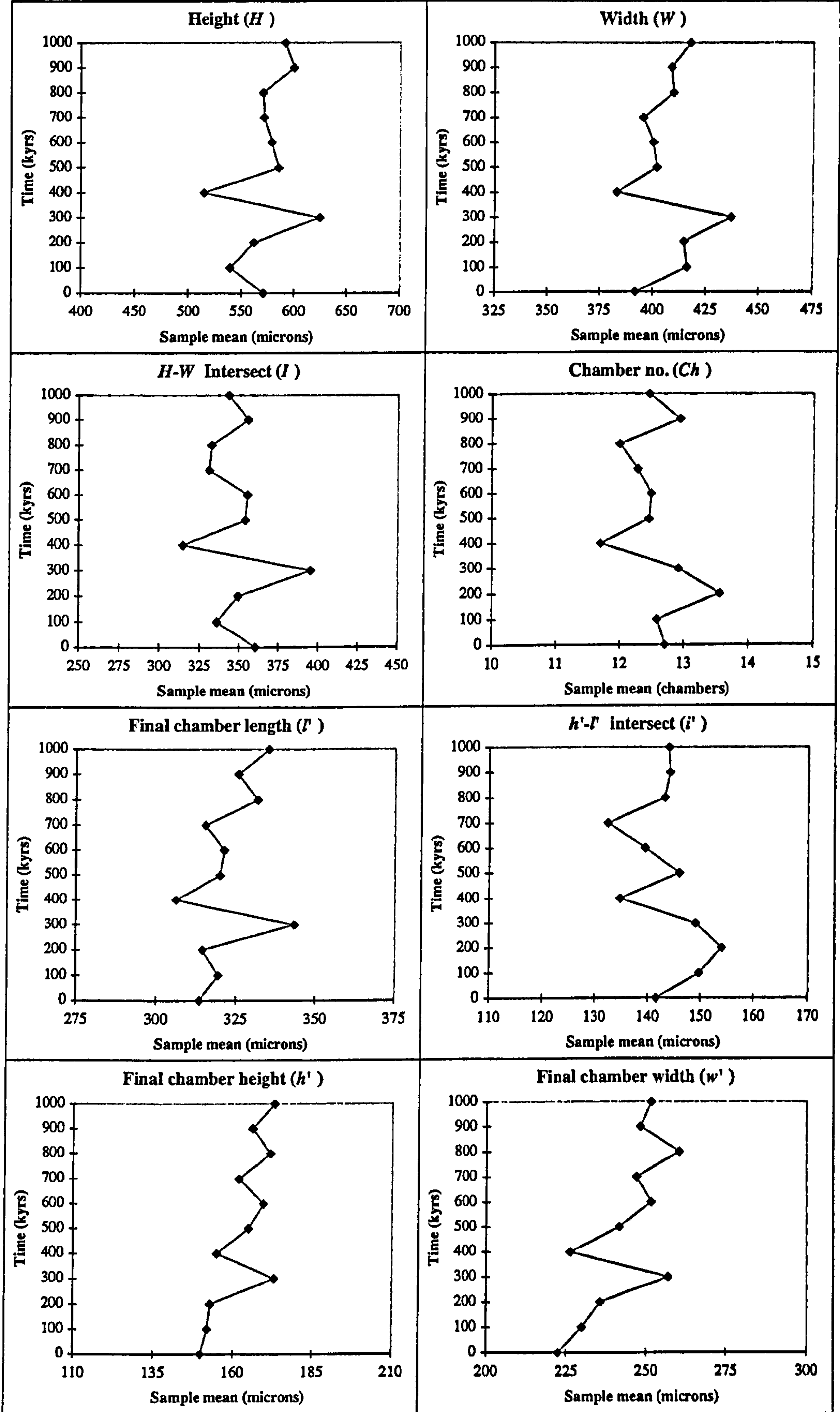
To the character divergences listed above I would add to the list of meaningful signals, ‘any persistent, trend-like tendencies to change preferentially in certain directions’. Some of these will be discussed in Sections 9.4.2 and 9.5.2, below; they include magnitude increases in the final chamber characters (l' , w' , h'), recurrent directions of shape shifting (e.g. in l'/h' and H/I), plus the tendency for *Tritaxia* to uncoil (which is pivotal to all the above). Even though these features can occur as readily on short timescales as over the longer ones, the fact that they *are* ‘tendencies’, and that they are general enough to reveal themselves in multiple or composite characters, places them firmly in the territory of *Plus ça change*. And we should not overlook the fact that ‘short term fluidity within boundaries of long term containment’ is *itself* an appropriate observation to take with us into the interpretation sections to come.

9.4.2 Space: The Basin-wide Signal

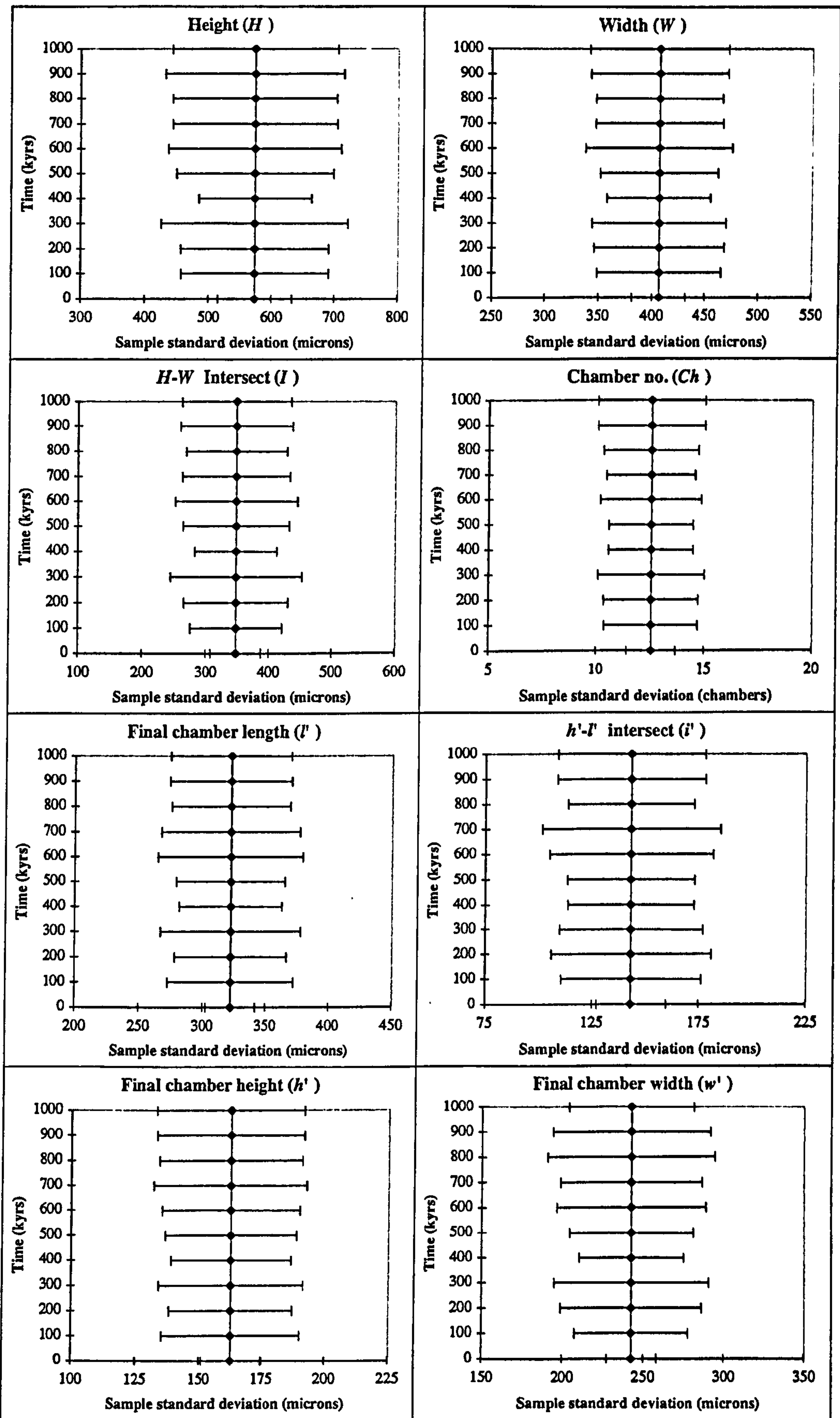
For the purposes of testing Sheldon’s *Plus ça change* model, it is the longer timeframe we are most interested in, higher resolution transects merely providing a way for us to see how processes scale up from the near-biological to the fully palaeontological. The next section aims to weave the three long sections into a single strand, to tell a more general story about *Tritaxia*’s evolution in the Anglo Paris Basin. In a sense, this is a case of ‘seeing past’ the meaningful pattern of character divergence at individual sites, but we are doing so in order to ‘tune-in’ to more deeply buried regularities.

We saw in Section 8.2.3 that the divergence effect in the upper parts of the 100 kyr transects was absent or far less marked in either the shape or trajectory parameters, but that so too was any sense of correlation between the signals from different sites, with timeseries for these parameters tending to contradict or cancel one another out. Partly as a consequence, I suggested earlier in this chapter that a large portion of the shape and trajectory signal should be considered noise rather than pattern. Let us see whether there is any more pattern forthcoming when the 100 kyr material is grouped together instead of split on the basis of sampling location.

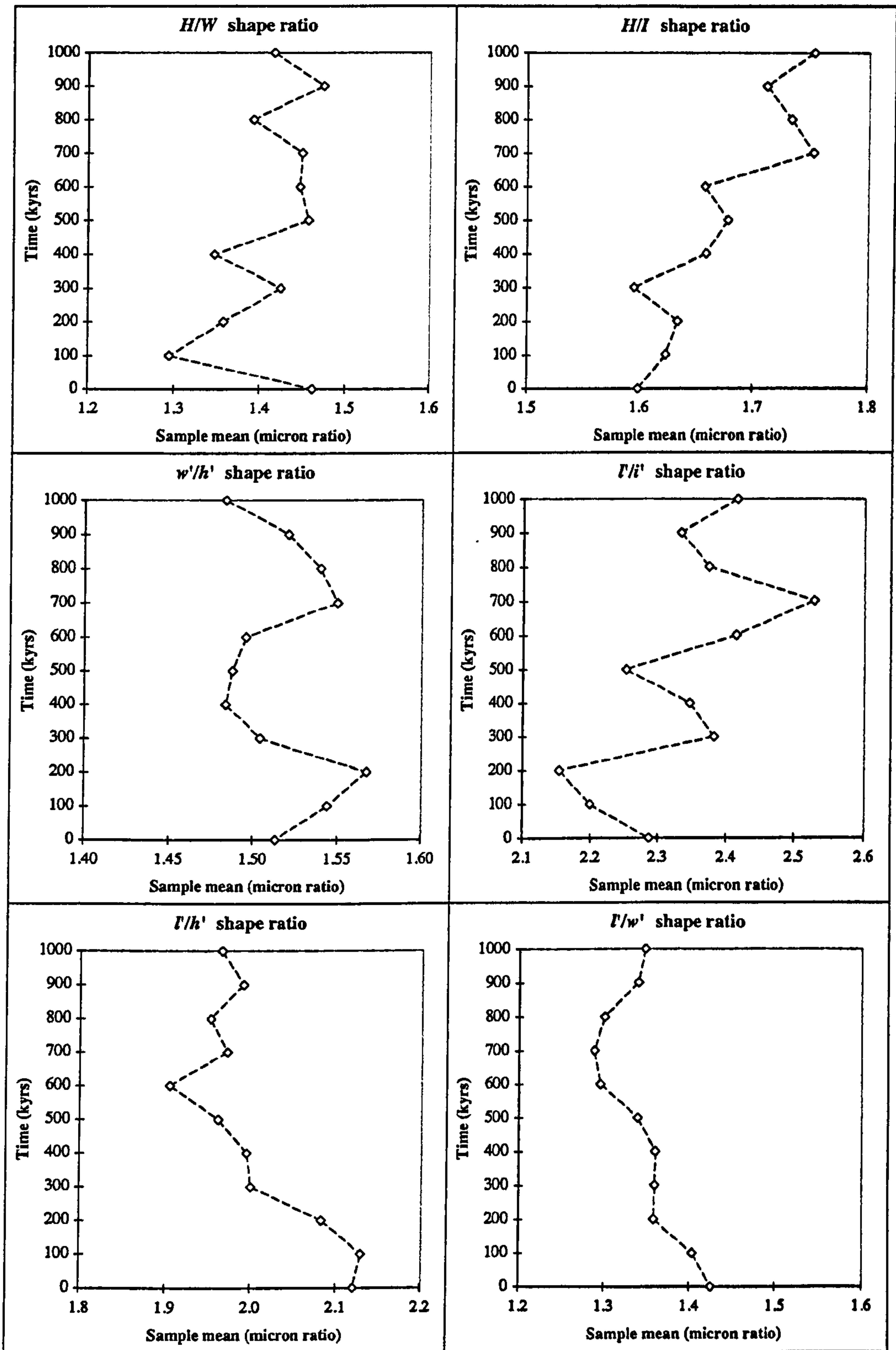
Text Figures 9.14.i-ii, 9.15.i-ii, 9.16 and 9.17 show new timeseries of data amalgamated from each of the three long transects. All values were recalculated from pooled samples, *not* simply taken as a mean of the values from each of the three sites.



Text Figure 9.14.i Basin-wide (amalgamated) 100 kyr data series for mean character sizes.
Values were recalculated from the pooled 100 kyr samples. Population sizes are $n = 135$ for every horizon except B41 [200] where $n = 100$, and B31 [0] where $n = 90$. See text for discussion.

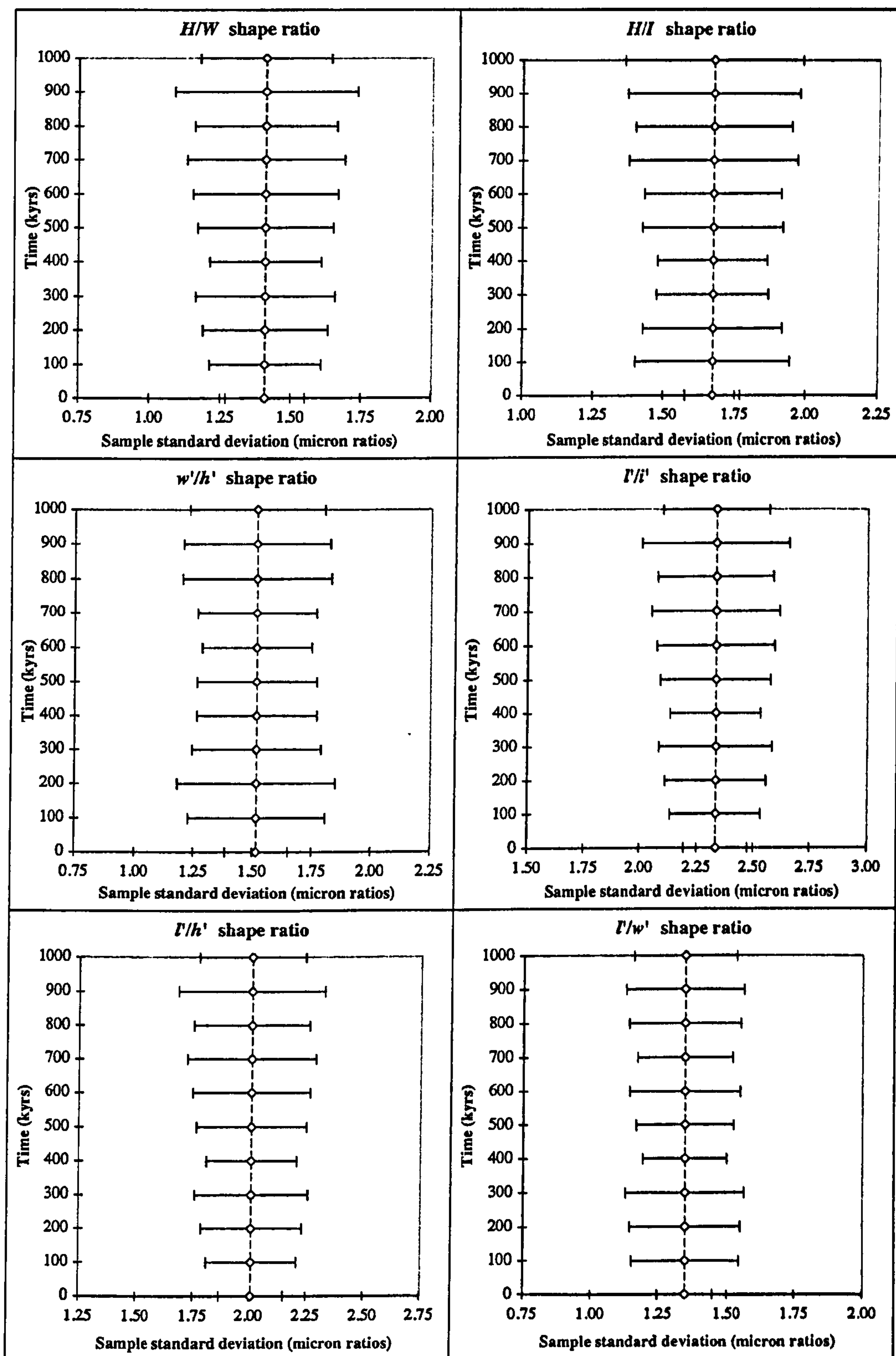


Text Figure 9.14.ii Basin-wide (amalgamated) 100 kyr data series for character standard deviation: the total width of each bar is one standard deviation. Values were recalculated from the pooled 100 kyr samples. Population sizes are $n = 135$ for every horizon except B41 [200] where $n = 100$, and B31 [0] where $n = 90$. See text for discussion.

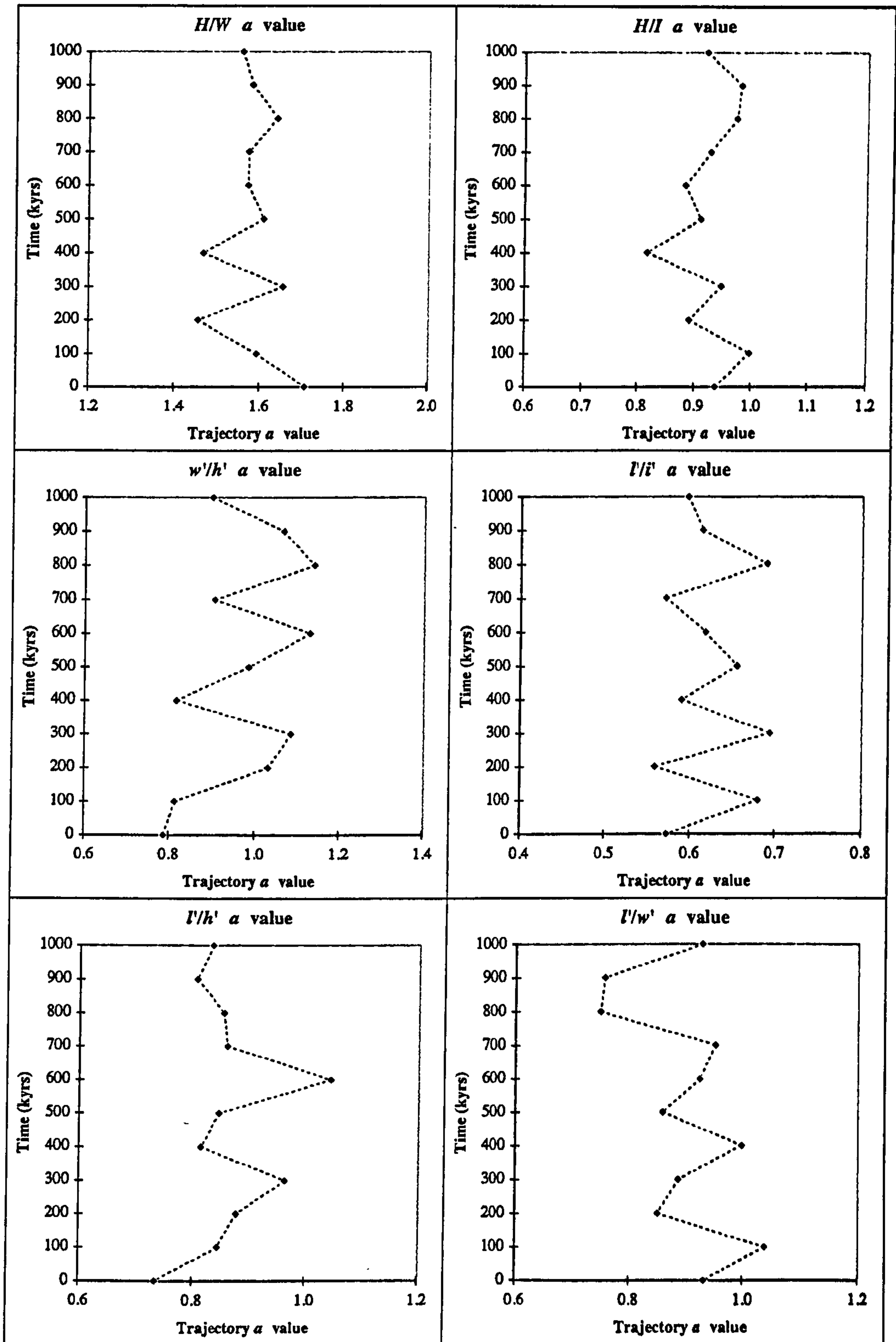


Text Figure 9.15j Basin-wide (amalgamated) 100 kyr data series for mean character shape.

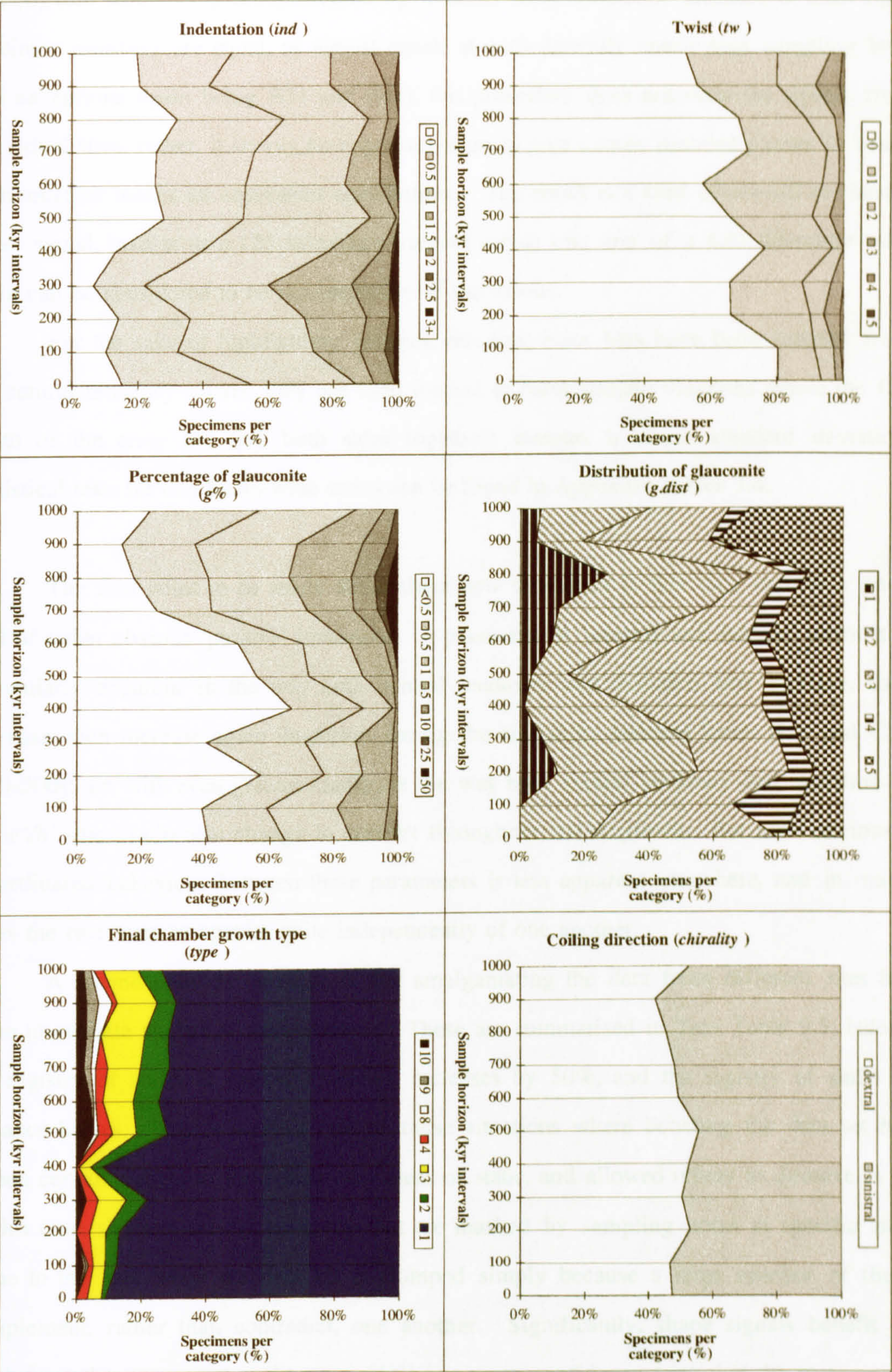
Values were recalculated from the pooled 100 kyr samples. Population sizes are $n = 135$ for every horizon except B41 [200] where $n = 100$, and B31 [0] where $n = 90$. See text for discussion.



Text Figure 9.15.ii Basin-wide (amalgamated) 100 kyr data series for character shape standard deviation: the total width of each bar is one standard deviation. Values were recalculated from the pooled 100 kyr samples. Population sizes are $n = 135$ for every horizon except B41 [200] where $n = 100$, and B31 [0] where $n = 90$. See text for discussion.



Text Figure 9.16 Basin-wide (amalgamated) 100 kyr series for trajectory 'a' values
 Values were recalculated from the pooled 100 kyr samples. Population sizes are $n = 135$ for every horizon except B41 [200] where $n = 100$, and B31 [0] where $n = 90$. See text for discussion.



Text Figure 9.17 Basin-wide (amalgamated) 100 kyr proportional area charts for the categorical characters. Values are recalculated from the pooled 100 kyr samples. For every character except g.dist, population sizes are $n = 135$ for every horizon except B41 [200] where $n = 100$, and B31 [0] where $n = 90$. For g.dist see Text Table 8.3. See adjacent text for discussion.

Sample numbers thus range from 135 for most horizons to 100 for B41 [200] and 90 for B31 [0] (the latter being unrepresented by material from Escalles). Because in most cases specimen numbers are equal, or almost equal, at each laterally continuous sampling level (the exceptions again being B31 and B41), this procedure does not skew the signals from individual sites; rather, it simply homogenises them to give a more rounded picture in which each location makes an equivalent contribution. The result is a kind of *overall* or 'basin-wide' signal, insofar as a 125 kilometre transect across one end of a 650 kilometre wide basin can be considered to be representative of the whole.

For the sake of highlighting patterns, this time error bars have been omitted from the central tendency charts; they are used instead to form spindle diagrams where the full width of the error bar (i.e. both sides together) denotes a single standard deviation. Statistical tests for this Basin-wide series can be found in Appendix Tables 3.4.

The first point to be made about these new timeseries is that they exhibit a good deal of rather obvious 'passive' behaviour. A passive style 'contain and release' element is particularly apparent in the way both central tendency and variation first increase, then decrease, then increase again in unison during the size shifts between levels B41 and C15 [200-500]; or, with even greater clarity, in the way both central tendency and variation in the w'/h' shape ratio also change in concert throughout the sequence. But such obviously co-ordinated behaviour between these parameters is less apparent elsewhere, and in many cases the two seem to operate quite independently of one another.

A second point to be made is that amalgamating the data from different sites has some immediate statistical consequences. These are summarised in Text Table 9.5, below: the registry of shifts in central tendency increases by 50%, and the registry of shifts in variance halves. This is another one of those situations where boosting the data set has helped certain signals to fight their way clear of static, and allowed others to dissolve in it. In this case, shifts in central tendency that are masked by sampling noise at specific sites come to the fore when the data set is clumped simply because a large number of them complement, rather than contradict, one another. Significantly, shape signals benefit as much from the manoeuvre as the sizes, giving us more confidence here that the patterns we observe constitute real phenomena. By contrast, shifts in variance drop dramatically, presumably because although local populations show different breadths of variation at different sites, at almost every 100 kyr horizon there is a similar range of morphological

expression found *somewhere* across the region. Z tests for the allometric exponent hardly change at all.

Test	<i>t</i> test - size	<i>t</i> test - shape	<i>F</i> test - size	<i>F</i> test - shape	Z test - traj
Split by site	34.4%	28.1%	22.3%	26.0%	10.3%
Amalgamated	49.5%	42.7%	10.9%	13.6%	11.8%

Text Table 9.5 *Regular changes in the proportion of significant differences depending on how the 100 kyr data set is organised. See text for discussion and Appendix Tables 3.3 and 3.4 for material (also Text Table 8.27).*

It is clear that for the sizes, a large portion of the significant change in both central tendency and variation is associated with the kink between B41 and C15 [200-500], principally due to the fact that C5 and C10 [300 & 400] constitute outliers significantly beyond the range of most middling character values. As discussed in the section above, we have no way of telling how much of a fluke this signal is, since it looks impressive on the 100 kyr plots but far more average when compared with the higher resolution material. For *W* and the suite of associated final chamber dimensions (*l'*, *w'* & *h'*), an element of trending also makes its presence felt, causing large portions of the succession's upper half to register as significantly different from large portions of the lower. We recognised this trending tendency in the three individual transects (Section 8.2.3), and it comes through very clearly in this basin-wide version too; it forms a striking contrast to the pattern of overall stasis seen in *H*, *I*, *Ch* and *i'*. Indeed, a fair way to summarise the shifts in character size is to break them down into those exhibiting a form of interrupted stasis versus those exhibiting an interrupted trend; such groupings tend to agree with one another not only in the overall form of their timeseries but also in the details (for instance the stasis group increase in magnitude at C40 [900] while the trending group decrease). Like the pattern of character divergence between the three sites, this distinction between the characters is probably persistent enough to constitute a meaningful signal.

With the exception of *Ch* and *i'*, and notwithstanding a partition into trend-like or static behaviour, shifts in mean size are generally very well correlated with one another; but in their minutia they give rise to numerous significant changes in shape. The most impressive of these is the strong and consistent trend in *H/I* ratio, which is almost imperceptible when looking at the size profiles themselves, but which nevertheless results in a statistically significant and (over the timescale documented) apparently permanent shift, from 'top-heavy' specimens low down in the sequence to 'bottom-heavy' specimens in the

upper reaches. Similar trends occur in the final chamber ratios, l'/h' and l'/w' , both of which start with long, virtually unidirectional stretches that peak around horizon C21 [600] and then either reverse, or plateau as a series of short term reversals. These two cases document a change from final chambers low and narrow for a given length, to ones rather higher and wider; and we know from previous discussion (e.g. 7.5, 8.2.1.i.b, 8.2.3.i.b, 9.2.2.iii) that this kind of morphological change, along with a transition to bottom heavy specimens, is characteristic of partially unwound tritaxiids displaying exotic, non-triserial final chamber types.

By contrast, note that the major shift in size between C5 and C10 [300-400] is not associated with any equally dramatic changes in shape: granted, there are significant shifts in both H/W and H/I , but in neither case is the jump any larger than jumps found in other parts of the sequence. We saw in Chapter 7 that H/W and H/I are the most rapidly altering shape ratios during development (Section 7.1), so the transformation seen between C5 and C10 [300-400] stands as a trial case for estimating the contribution made by shifts *along* the developmental trajectory. One can only conclude that such contributions were relatively minor. Despite a shift in mean chamber number from $Ch = \sim 13$ to $Ch = \sim 11.5$ between C5 and C10, plus the largest leap in magnitude for every single character size, only the two most sensitive shape ratios register any significant difference at all, and even here the amount of change in both cases is smaller than at many other parts of the series. Most of the time, therefore, it seems unlikely that shape shifts were caused by movement *along* a trajectory; where they are notable they must instead have involved an orthogonal displacement of some sort, presumably due to a shift in the growth trajectory itself.

Apart from H/I and the final chamber pairings, l'/h' and l'/w' , none of the other shape ratios produce significant changes between the lowermost horizon (B31 [0]) and the uppermost (C45 [1000]); instead, values from either end of the total range tend to register as statistically different from one another, or from the mid-range majority. Like their size-parameter counterparts, such evolutionary trajectories are probably best thought of as cases of wobbly or interrupted stasis, although there does appear to be an element of trending in l'/i' . w'/h' is especially stable, registering only 10% significant difference throughout; it stands in marked contrast to all the other final chamber ratios (Appdx. Tables 3.4).

Text Figure 9.17 shows basin-wide relative abundance charts for the categorical characters. These are drawn from the amalgamated data set and in most cases have sample

numbers of 135; again, the exceptions are B31 and B41 where the numbers are 90 and 100, respectively, but also the plot of *g.dist* where the exclusion of a zero category means that sample sizes are very variable and must be determined piecemeal from Text Table 8.3.

In almost every case, this new presentation manages to emphasise patterns that were more obscure when the data appeared split on a site-by-site basis: in fact, the most convincing insights of all come from cross-referencing the amalgamated, 'basin-wide' charts back to the original three-site versions (Appdx. Figs. 5.3.4.i-vii.a). This is fortunate because with no formal statistical tests, our interpretation of the categorical characters relies primarily on intuition. The shift from deeply indented, razor-edged specimens in the lower succession more toward solid prisms in the upper is readily apparent in the amalgamated signal for *ind*, as is the accompanying surge of glauconite in those tests (*g%*), along with the steady increase of twisted individuals (*tw*) and exotic growth types (*type*); we even get to see how the messy *g.dist* categories are connected to an increase in glauconite content, as was suggested by the correlation tests in this chapter (Section 9.2.2.iv).

All these factors, coupled with the tendency for mean sizes to diverge up-section, collectively make a strong case for concluding that morphological behaviour is markedly different in the two halves of the sequence; and this, in turn, has significant implications for the *Plus ça change* model.

Section 9.5 Summing Up

9.5.1 Age (or Stage) Dependency Again

Having decided which morphological patterns are persistent and relevant enough to grab our attention, we have almost arrived at a point where we can begin reaching out for some solid interpretations. But before we do so, there is one more important issue to clarify: the problem of differentiating between genuine shifts in morphology versus shifts in population age-structure. This matter was broached in Section 6.2.1 but never settled. To reiterate, the problem is that since morphology changes along with age as each specimen grows, differences in the average age of individuals in a population (due to varying neonate mortality rates, for example) can cause differences in the average population morphotype

without reflecting evolution *per se*. Having subsequently discovered that shifts in size constitute the bulk of morphological change over the five sampled transects, the problem has become acute—at least potentially.

I say potentially because I confess that I am deeply sceptical about the prospect of perceiving shifts of population age structure, or any other such transient phenomenon, in fossil material as time-averaged as that from the Lower Chalk. While one might find effects of this kind in life-assemblages preserved under catastrophic circumstances (mussel beds overwhelmed by sediment, say) statistically significant differences in apparent age-structure (i.e. chamber number) between pairs of samples whose *internal* durations are measured in millennia, almost certainly reflects evolutionary change in life history strategy itself. A similar line of argument will be pursued on the subject of ecophenotypy in Section 10.1.1 (to come); but for the sake of completeness, and for the peace of mind of readers who do not share my scepticism, a brief assessment of the age-character relationship is presented here.

Of course, we are not really in a position to query age as such, anyway; rather, the model developed in Chapter 7 works on the basis of ‘developmental stage’ as revealed by the number of chambers in the test. It is a fair assumption for an organism which grows by discrete chamber addition that developmental maturity, age and the number of chambers it bears will all be intimately related; but while the linkages between these factors are clear enough for each individual foraminiferan (chamber 13 cannot but be built after chamber 12, both temporally and strategically), the relationships are less clear when we are talking about the average values of populations. It is quite possible, for instance, to have a population whose 12 chambered tests took, on average, longer to construct than those of the 13 chambered population a few miles away. So the simple fact of the matter is that any attempt to constrain age and morphology in terms of one another is guaranteed to be something of a hatchet job (although we do at least have the advantage of dealing with an organism that grows in discrete phases). The flip side of this difficulty, however, is that if we do accept a case for the homogenisation of age-structured populations in the jumbled microfaunal assemblages of the Lower Chalk, then rather than talking about average age, we can instead interpret any chamber number variation between populations as subtle differences in life history strategy itself, which is what the discussion was steering towards with the interpretation of heterochrony given in Section 9.2.2.i.

This kind of analysis also has the potential to offer a more 'subjective' insight to the test building process, from the point of view which really matters—that of the foraminiferan itself. Thus far we have been treating morphological shifts 'objectively', by simply stating that the average size of this character or that character has increased or decreased by whatever amount, and that the shape ratios have changed accordingly. But this resolutely external perspective does not really frame things in terms of a growth sequence: that is, *it tells us about a result rather than a process*. I am not suggesting that we can really gain the foram's eye view (or that of its developmental program), but at least by using the growth sequence itself as the standard by which to calibrate change, we are taking a step in the right direction.

Having said that, the method is extremely clumsy. Text Figures 9.18.a-d show plots of mean character values divided by the mean number of chambers, for each of the four standard transect types (2 kyr, 20 kyr, 100 kyr and Combined Scales). The panel showing chamber number itself (*Ch*) is left in place to emphasise the crudeness of the procedure. We are simply measuring 'how much' of each character average there was per chamber. This is an extremely unrealistic quantity and should not be taken too literally. As we saw when we split the Platonic Foram into separate chamber cohorts back in Chapter 7, foraminiferal tests appear to grow in a sigmoidal fashion, so the real distribution of character magnitude throughout the whole structure is a fairly complex issue. Unfortunately, we cannot use the methodology adopted in Chapter 7 for the present purposes because there are too few specimens per cohort in a sample to generate meaningful growth sequences; and in any case what we ideally want is a succinct single value to compare between horizons. The only alternative method I can think of is to plot bivariate curves of each character/chamber relationship (e.g. *H/Ch*) and use the allometric exponent to summarise whatever shifts there are between sampling points. Having tentatively followed this route far enough to have viewed the results, my intuition is that it would tell us nothing at all. I didn't bother to calculate any statistics and the timeseries plots themselves are not presented here, although one isolated pairing, *H/Ch*, does appear as a sequence of bivariate plots in Appendix Figure 6.1.7.i.

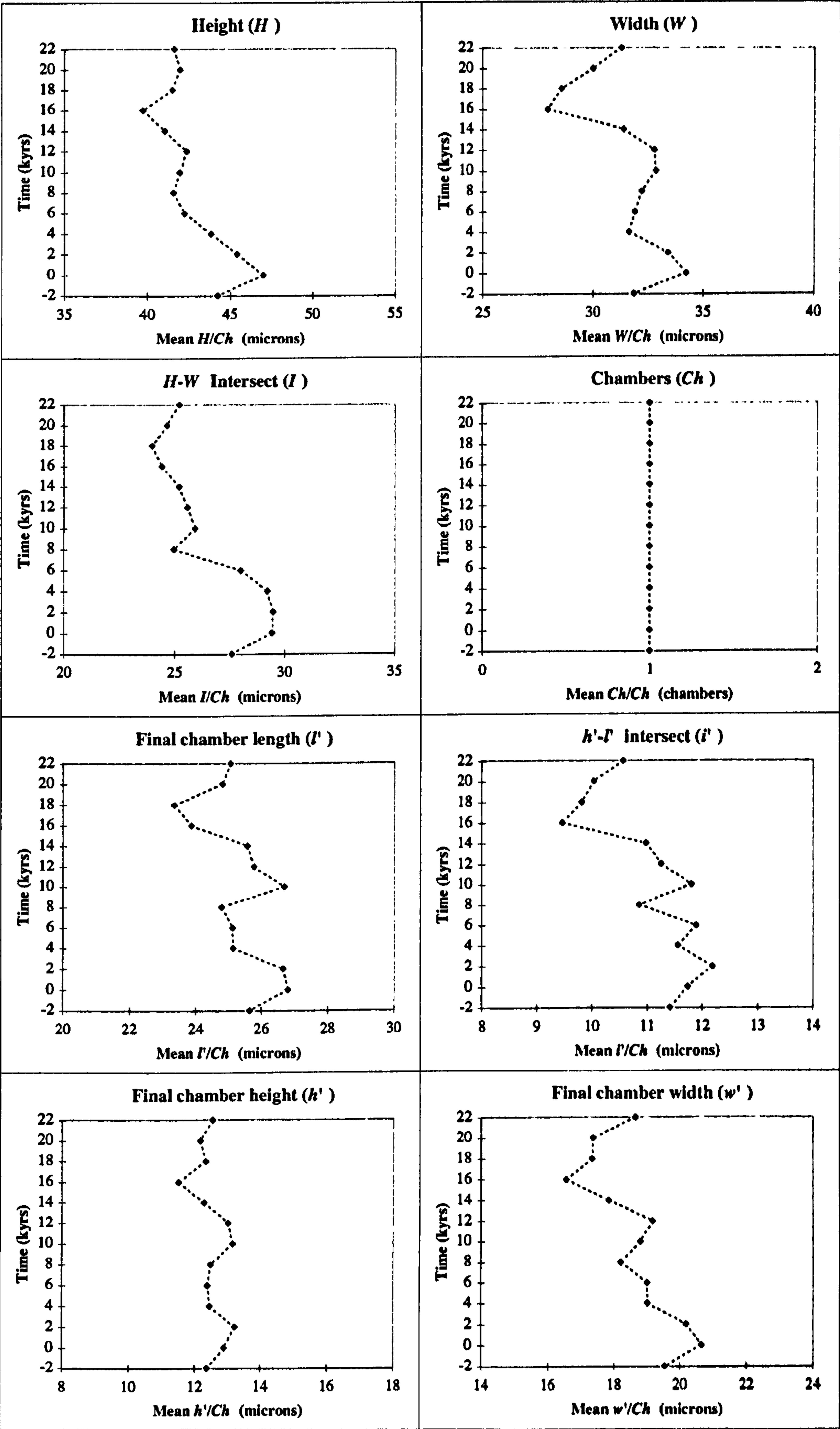
So, instead, what we have available shows simply the mean magnitude for each character divided by the mean number of chambers for the average foraminiferal test in a

sample population. Only sizes are presented in this way because there is no sense whatsoever to be made of dividing a shape ratio by a number of chambers. Quite predictably, since we already know that most character sizes correlate with one another, the results tend to show a suite of similar patterns. Equally predictably, and trivially since Ch is the locus of comparison, commonalities between the plots are due to the influence of Ch while differences are due to whatever way each particular character *fails* to correlate with the others.

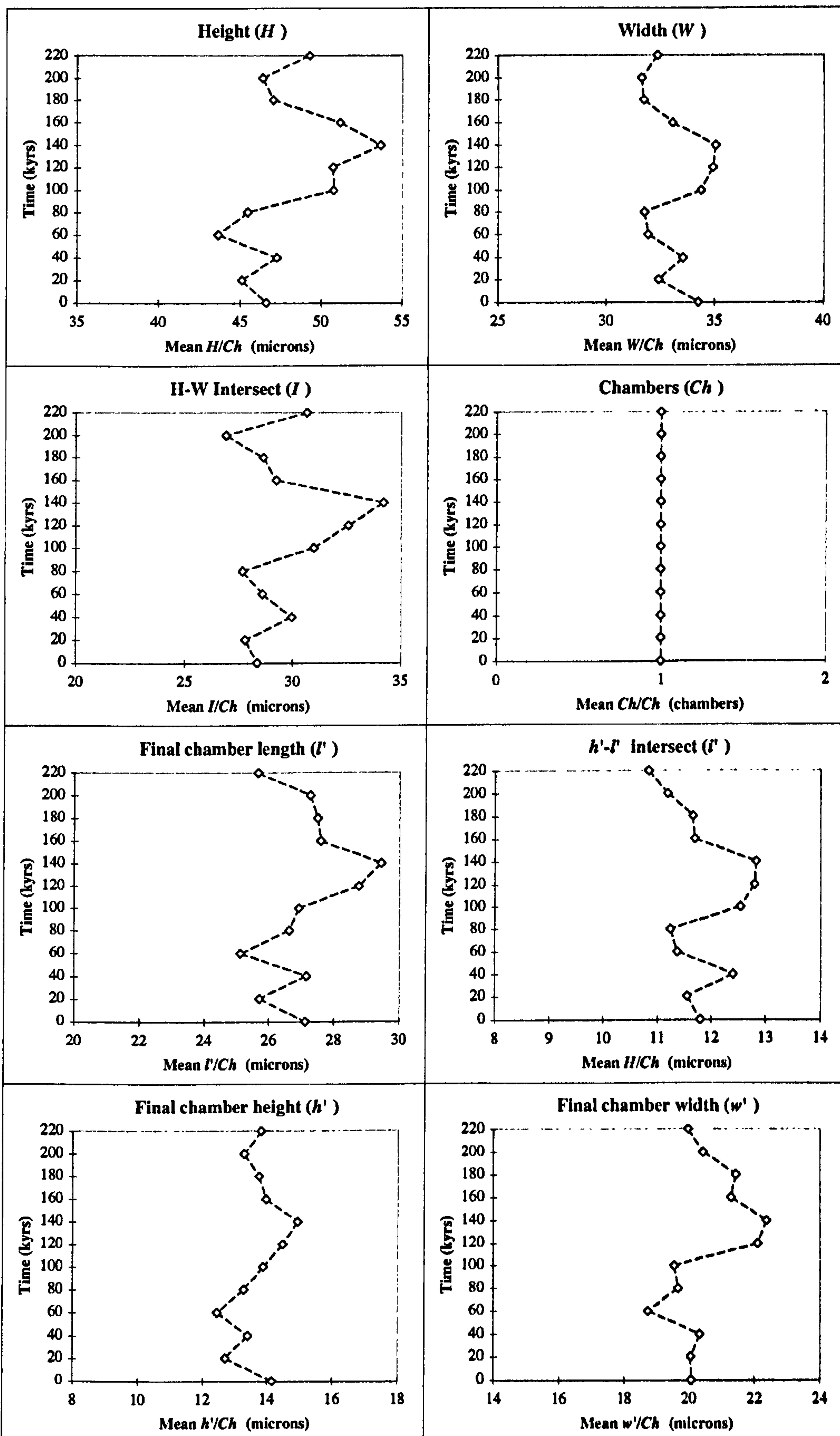
In Text Figures 9.18.a-d, shifts upward along the x axis correspond to character magnitudes smeared out among a relatively small number of chambers, while shifts down the axis point to populations in which mean chamber number was high for a given character magnitude. In Text Figure 9.18.a, for instance, H/Ch drops from a maximum of around 47 microns per chamber at horizon C13-1 [0] to a minimum of just less than 40 microns per chamber in the mid-chalk sample, C13-9 [16]. Referring back to Appendix Figures 5.1.1.i and 5.1.1.iv we can readily see where this pattern comes from.

Interestingly, in C13 there is a case to be made for the chamber-based version corresponding more closely with many of the ecological patterns than the raw character magnitudes themselves. Look at the match between H/Ch and the diversity metric in C13, for example (Appdx. Fig. 3.1.iii); or the relationship between curves for l'/Ch , h'/Ch and w'/Ch and the incidence of boundary peaking species like *Textularia* and *Pseudotextulariella* (Appdx. Figs. 3.1.iv.e & 3.1.iv.b); or the fact that the absolute abundance of *Tritaxia* rises steadily, as does that of most of the fauna, towards a mid-chalk crescendo at horizon 9 [16], while the chamber mediated character values follow the same pattern but in reverse (Appdx. Fig. 3.1.iv.a vs. Text Figure 9.18.a).

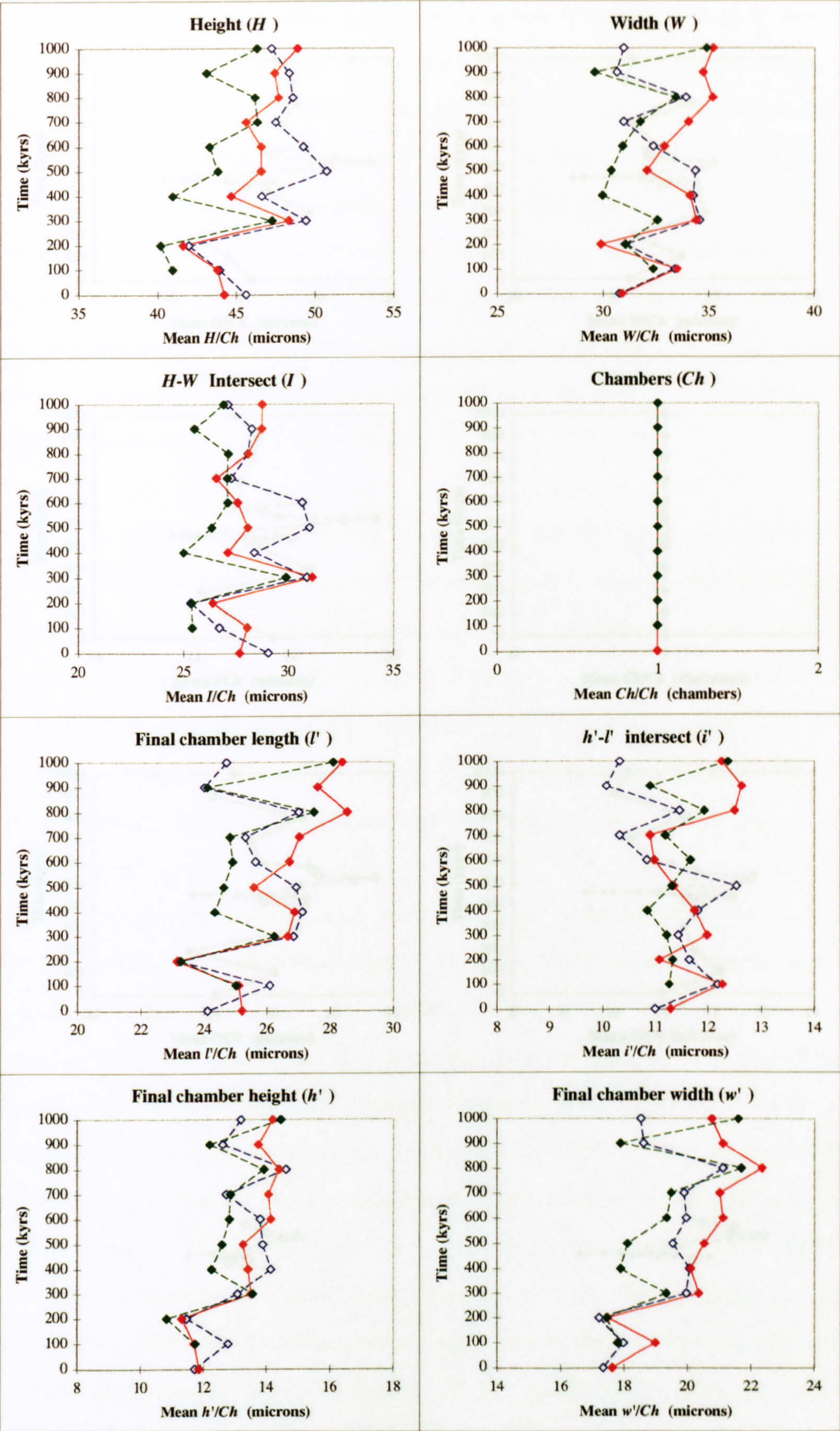
If the relationship between chamber number and character magnitude had been entirely stable throughout the single couplet, the charts of Text Figure 9.18.a would all have been perfectly flat, just like the plot for Ch/Ch . This is what we would ideally expect when shifts in characters simply reflect a change in the average age (growth stage) of the population. The fact that differences are present across the transect certainly tells us something—but what? The mid-chalk spike seems to show that chambers were generally smaller at that point: not only were the specimens themselves diminutive (Section 8.2.1.i.a), but each chamber (on average) was small enough that the dwarf tritaxiids went through more than their usual allotment of developmental stages.



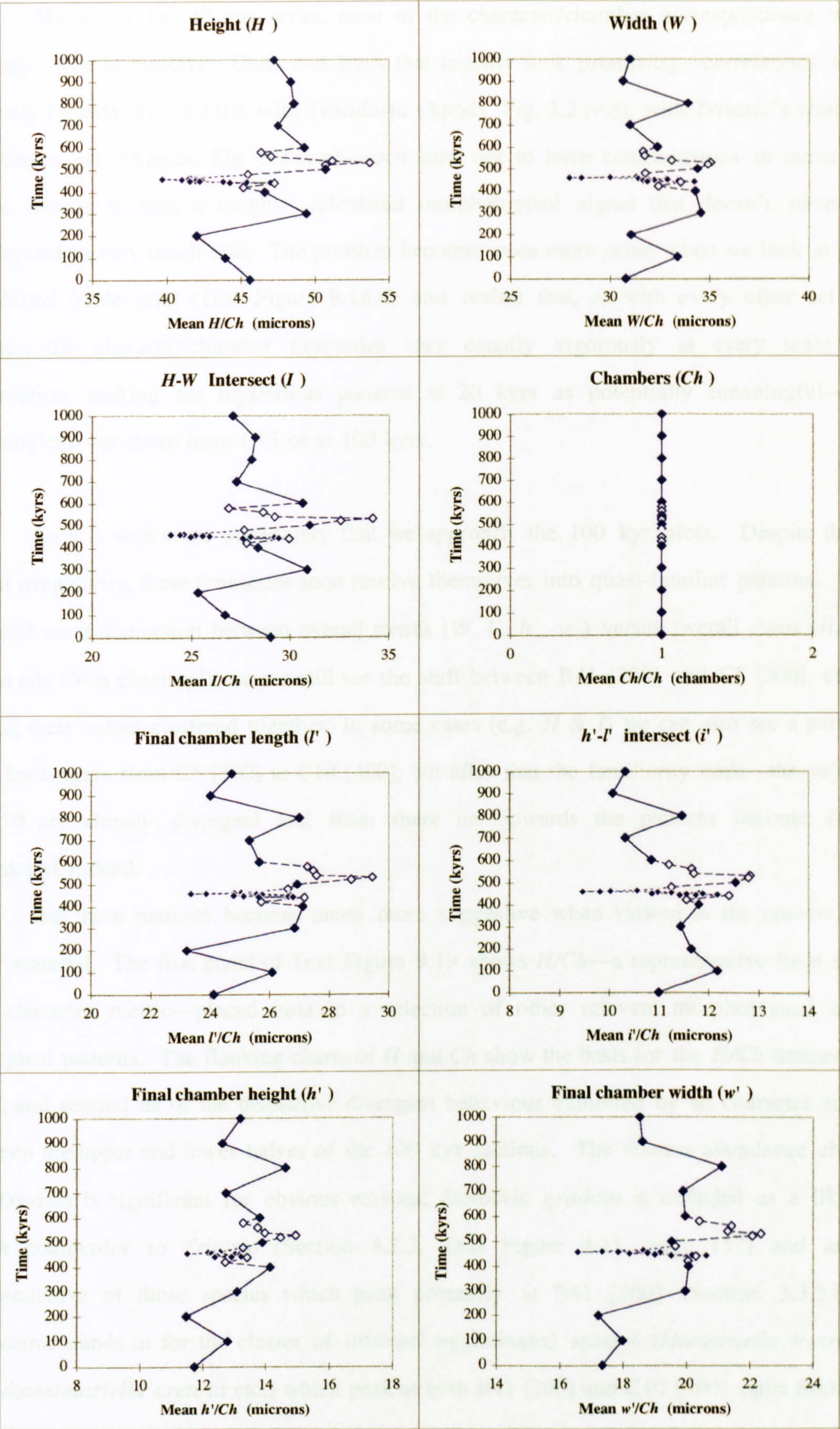
Text Figure 9.18.a Character size/chamber number ratios for the 2 kyr transects. The plots show a crude method of tracking the relationship between character magnitudes and the growth stage/population age structure. Values are obtained simply by dividing each character magnitude by the number of chambers of the individual from which it came, and then taking the mean. The result is a rough estimate and should be treated with caution. See text for a full discussion. Markers as per appendix figures.



Text Figure 9.18.b Character size/chamber number ratios for the 20 kyr transects. The plots show a crude method of tracking the relationship between character magnitudes and the growth stage/ population age structure. Values are obtained simply by dividing each character magnitude by the number of chambers of the individual from which it came, and then taking the mean. The result is a rough estimate and should be treated with caution. See text for a full discussion. Markers as per appendix figures.



Text Figure 9.18.c Character size/chamber number ratios for the 100 kyr transects. The plots show a crude method of tracking the relationship between character magnitudes and the growth stage/population age structure. Values are obtained simply by dividing each character magnitude by the number of chambers of the individual from which it came, and then taking the mean. The result is a rough estimate and should be treated with caution. See text for a full discussion. Markers as per appendix figures.

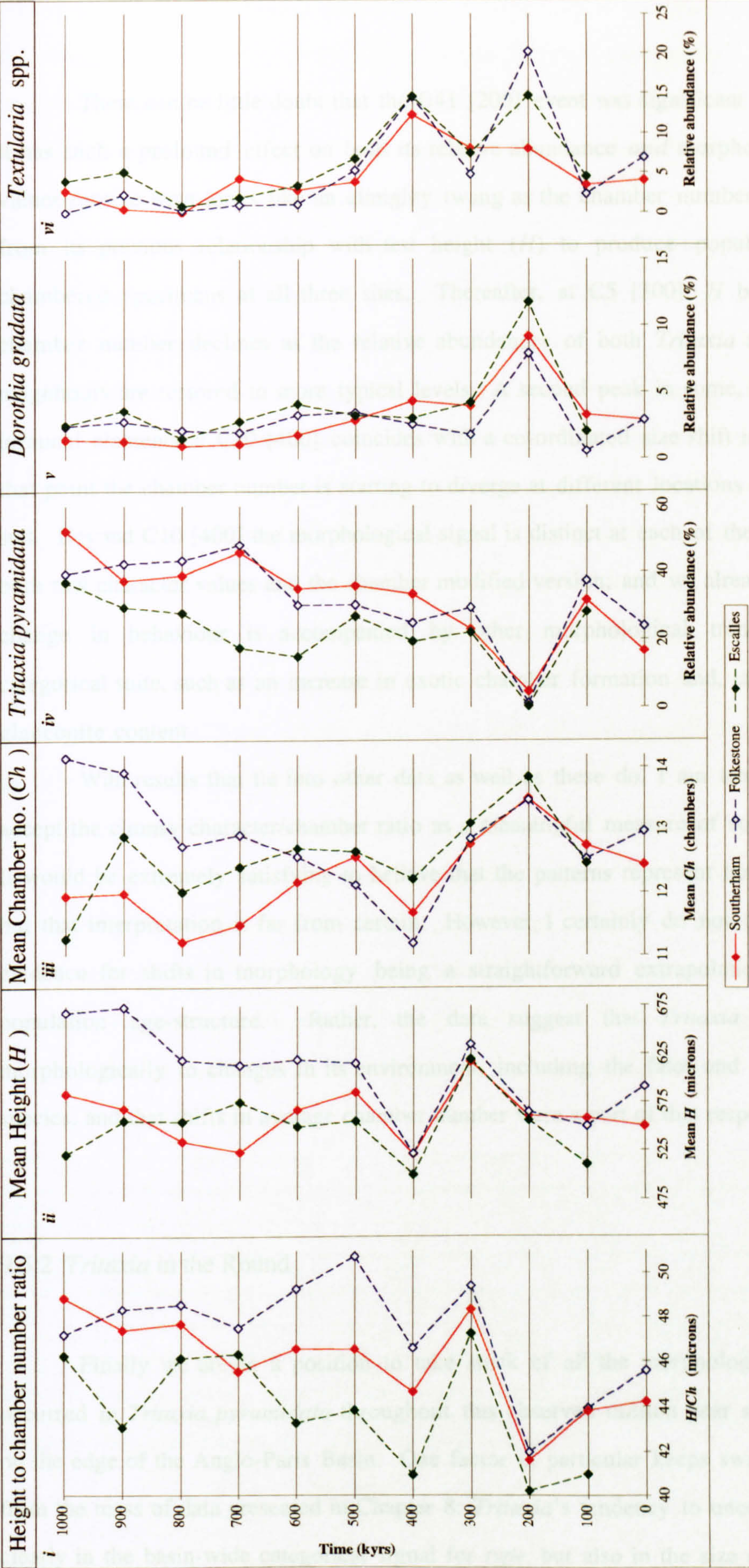


Text Figure 9.18.d Character size/chamber number ratios for the Combined Scales transects. The plots show a crude method of tracking the relationship between character magnitudes and the growth stage/ population age structure. Values are obtained simply by dividing each character magnitude by the number of chambers of the individual from which it came, and then taking the mean. The result is a rough estimate and should be treated with caution. See text for a full discussion. Markers as per appendix figures.

Moving to the 20 kyr series, most of the character/chamber correspondence with ecology seem to dissolve. Clues and leads that initially look promising—correlations with diversity (Appdx. Fig. 3.2.iii), with *Textularia* (Appdx. Fig. 3.2.iv.e), with *Tritaxia*'s relative abundance, etc. (Appdx. Fig. 3.2.iv.a)—each turn out to have contradictions in terms of detail, leaving us with a roughly calculated morphological signal that doesn't seem to correspond to very much else. The problem becomes even more acute when we look at the Combined Scales plot (Text Figure 9.18.d) and realise that, as with every other set of metrics, the character/chamber timeseries vary equally vigorously at every scale of observation, making the mysterious patterns at 20 kyrs as potentially meaningful—or meaningless—as those from C13 or at 100 kyrs.

So it is with some uncertainty that we approach the 100 kyr plots. Despite their initial irregularity, these timeseries soon resolve themselves into quasi-familiar patterns. We can still see a distinction between overall trends (W , l' , h' , w') versus overall stasis (H , I , i' —to cite *Ch* is cheating!); we can still see the shift between B41 [200] and C5 [300], each having their values clustered together; in some cases (e.g. H & I) we can also see a partial shift back again from C5 [300] to C10 [400]; but after that the familiarity ends—the values at C10 are already divergent and from there on upwards the patterns become very disordered indeed.

But these patterns become much more suggestive when viewed in the context of other material. The first panel of Text Figure 9.19 shows H/Ch —a representative from our new character metric—placed next to a selection of other relevant morphological and ecological patterns. The flanking charts of H and Ch show the basis for the H/Ch timeseries itself, and remind us of the distinctive divergent behaviour exhibited by all character sizes between the upper and lower halves of the 100 kyr sections. The relative abundance chart for *Tritaxia* is significant for obvious reasons; *Dorothia gradata* is included as a likely major competitor to *Tritaxia* (Section 4.2.3, Text Figure 4.11, page 157) and as a representative of those species which peak primarily at B41 [200] (Section 3.3.3.iv); *Textularia* stands in for the cluster of infaunal agglutinated species (*Marssonella trochus*, *Pseudotextulariella cretosa* etc.) which peak at both B41 [200] and C10 [400] (also Section 3.3.3.iv).



Text Figure 9.19 The relationship between some aspects of *Tritaxia*'s morphology and ecology.

Panel i shows the H/Ch ratio at each of the three sites. Character/chamber number relationships provide an insight into either the population age structure or the average life history strategy of a population, against which morphological change can be assessed. Panels ii & iii show the basic character components of the H/Ch ratio, demonstrating the timing and magnitude of various morphological phenomena, notably the proximity of values at each of the three sites in different parts of the sequence, and also the significant shifts between B41 [200] and C15 [500]. Panels iv, v & vi show the relative abundance of the total benthic forams of the ecological database: *Tritaxia* which crashes at level B41 [200] but is otherwise common throughout; *Dorothia gradata*, which is likely to be a main competitor of *Tritaxia* (see Section 4.2.3) and which also represents that portion of the fauna (there are many others) peaking at B41 [200]; and the genus *Textularia*, representing a small group of twice-peaking species (including *Pseudotextulariella cretosa* and *Marssonella trochus*, which, like *Tritaxia*, are infaunal agglutinating types. See main text for a full discussion.

There can be little doubt that the B41 [200] event was significant for *Tritaxia* since it has such a profound effect on both its relative abundance *and* morphology. The *H/Ch* values receive what looks like an almighty twang as the chamber number is plucked away from its previous relationship with test height (*H*) to produce populations of many-chambered specimens at all three sites. Thereafter, at C5 [300], *H* bounces back and chamber number declines as the relative abundances of both *Tritaxia* and its ecological neighbours are restored to more typical levels. A second peak in some, but not all, of the infaunal elements at C10 [400] coincides with a co-ordinated size shift in *Tritaxia*; but by that point the chamber number is starting to diverge at different locations and *H/Ch* follows suit. Beyond C10 [400] the morphological signal is distinct at each of the sites, in terms of both raw character values and the chamber modified version; and we already know that this change in behaviour is accompanied by other morphological transitions from the categorical suite, such as an increase in exotic chamber formation and, later, an increase in glauconite content.

With results that tie into other data as well as these do, I am tentatively willing to accept the clumsy character/chamber ratio as a meaningful measure of something or other. It would be extremely satisfying to believe that the patterns represent heterochronic shifts, but that interpretation is far from certain. However, I certainly do not think there is any evidence for shifts in morphology being a straightforward extrapolation of changes in population age-structure. Rather, the data suggest that *Tritaxia* was responding morphologically to changes in its environment, including the fates and fortunes of other species, and that shifts in average chamber number were a part of that responsiveness.

9.5.2 *Tritaxia* in the Round

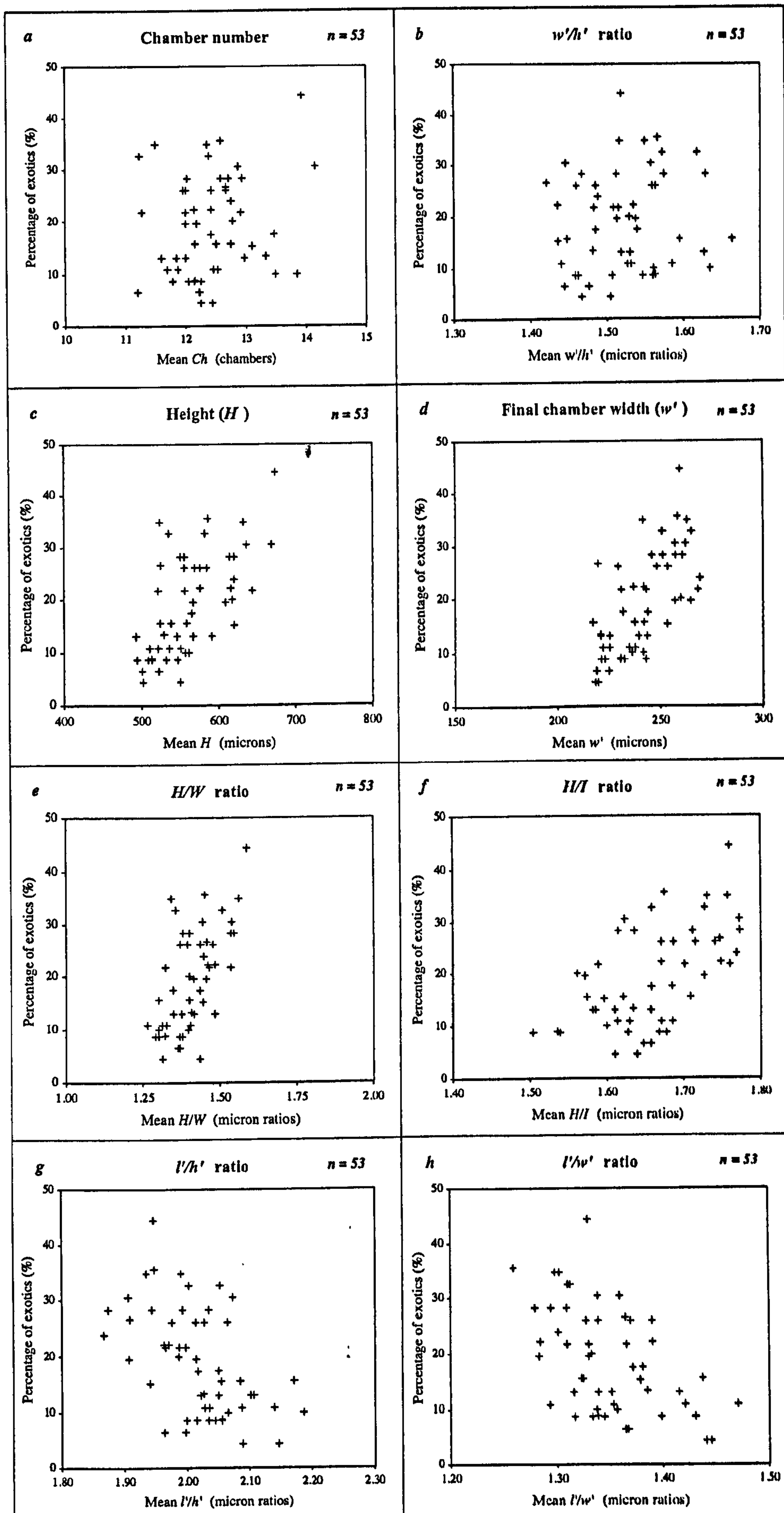
Finally we are in a position to take stock of all the morphological changes that occurred in *Tritaxia pyramidata* throughout this observed million year span of its history on the edge of the Anglo-Paris Basin. One factor in particular keeps swimming into focus from the mass of data presented in Chapter 8: *Tritaxia*'s tendency to uncoil. We can see it clearly in the basin-wide categorical signal for *type*, but also in the size and shape metrics,

too. Sometimes this tendency reveals itself as a constant preference by certain characters for changing more readily or frequently in one direction than another, of which the H/I shape ratio and the degree of *twist* are likely examples (recall the discussion in Section 7.5 in which twist was hypothesised to indicate an increase in mutation and error); and also the shifts in magnitude of several final chamber dimensions (l' , w' , h'). On other occasions the expression seems more episodic. Apart from the spike at C5 [300], for instance, exotic growth *type* itself is predominantly concentrated in the upper half of the succession; and looking at the basin-wide shape profiles for l'/h' and l'/w' (Text Figure 9.15.i), one wonders whether this is a result of shape trends in the lower part of the succession that passed some kind of threshold at around C15 [500]. The degree of indentation (*ind*) and the percentage of glauconite (*g%*) also show intriguingly sharp transitions between the two halves of the sequence, although their connection to the uncoiling is not so obvious.

To demonstrate just how central the formation of exotic chamber types were to the overall changes in morphology, Text Table 9.6 (below) and Text Figure 9.20 show the strength of correlations between various salient features. Text Table 9.6 provides values of the correlation coefficient (*r*) for correlations between the overall percentage of exotic growth types in a sample population and the population mean for various size and shape parameters. Levels of significance are given in the row below. Populations from every sample were used to generate these correlations so $n = 53$. Note that there is an impressively clear separation between those variables which *do* correlate with the exotic chambers and those which *do not*: those that do invariably correlate to better than 99%, frequently having significance levels so high they are off the scale on my statistical tables. Text Figure 9.20 presents a selection of these patterns in visual format.

character	H	W	I	Ch	l'	i'	w'	h'
correlation (<i>r</i>)	0.617	0.320	0.329	0.183	0.499	0.069	0.683	0.655
significance	>0.001	0.01	0.01	not sig	>0.001	not sig	>0.001	>0.001
character		H/W	H/I	w'/h'	l'/i'	l'/w'	l'/h'	
correlation (<i>r</i>)		0.621	0.582	0.103	0.385	-0.527	-0.519	
significance		>0.001	>0.001	not sig	0.01	>0.001	>0.001	

Text Table 9.6 *Strengths of correlation and their statistical significance for relationships between size and shape parameters and the percentage of exotic chamber types in a sample population. Note that where present the correlations are highly significant. All sample horizons were used and so for each correlation $n = 53$.*



Text Figure 9.20 Strengths of correlation between various morphological parameters and the percentage of exotic chamber types in a sample population. The entire data set is used. See main text for discussion. See Text Table 9.6 for statistical significance.

As we noted in previous sections, w'/h' is the shape characteristic which correlates least well with other shapes; here we see that it does not correlate with exotic chamber formation either: clearly it follows different rules to the other shape parameters (my guess is that these reflect the self-organizing structural properties of cytoplasm—probably its tendency to form low, equidimensional hemispherical blobs when touching a substrate). But by far the most important of these pairings is the lack of correlation between high *type* categories and *Ch*. In a sense, this is quite an astonishing discovery because we saw in Chapter 7 that there most certainly *is* a correlation between *Ch* and *type*—no doubt about it. What we have uncovered once again, therefore, is the difference between an evolutionary trajectory and a developmental one. Non-triserial growth almost never occurs earlier than the 12 chambered stage; after that it becomes increasingly common until by 16 chambers over a third of specimens show some form of exotic developmental pattern. Bivariate plots for H/Ch (Appdx. Fig. 6.1.7.i) also demonstrate very clearly that exotic chambers express themselves only after the average number of chambers is reached.

But that has nothing to do with shifts in the average chamber number of a sample population. Compare mean *Ch* with the number of non-triserial types in C29 and C35 [700 & 800] at Southerham (Appdx. Figs. 5.3.1.iv & 5.3.4.vi.a) where chamber number is at its lowest and the exotic count is almost at a peak. In other places, by contrast, *Ch* and *type* *do* shift in parallel, just as their developmental profile suggests (e.g. from C10 to C40 [400 - 900] at Folkestone). But overall, in terms of evolutionary trajectory, there is no consistent correlation between *Ch* and non-triserial growth whatsoever (Text Figure 9.20.a).

This is an important result. It relies on the crucial difference between evolutionary and developmental trajectories to even make any sense. It adds weight to our suspicions that while chamber number is a key developmental factor (growth stage), it is also an evolutionary variable. And it serves to highlight, by comparison, the extent to which exotic chamber formation *does* underlie so many of the *other* shifts in shape and size.

All the other characters in Text Figure 9.20 are easily comprehensible as manifestations of this deep underlying influence: *H* increases more rapidly when non-triserial growth rockets new chambers out along the coiling axis; w' increases in accordance with fewer chambers per whorl (typically only two) during non-triserial growth; H/I increases because *W* is always at a maximum in the triserial phase, resulting in the characteristic bottom heavy shape of uncoiled specimens; l'/h' decreases because whenever the final chamber long axis springs back from the carinate edge of the test, chamber height

takes up the slack. A good deal of the long-term morphological change we witness, therefore, is associated with exotic development, even though it manifests this common theme through the shifting montage of much subtler relationships we saw in Section 8.2. Appendix Figures 6.1 and 6.2 are intended to summarise a huge amount of the data presented in the previous sections: the relationships between size, shape and trajectory; the relationship between variation and central tendency; the up-sequence divergence of the character means; and the place of exotic specimens in the overall sample population.

This, then, is *Tritaxia pyramidata* in the round. I suggest it is best to think of *Tritaxia*'s evolutionary behaviour as 'layered', with a tendency for exotic chamber formation providing the deep, underlying influence behind a myriad of small scale shifts and tendencies that were often negotiated through the flexible intermediary of *Ch*. The nature of these influences forms the subject of the next section. If they turn out to be external and caused by environmental selection, then we can think of them as 'sculptings'; if, instead, they turn out to be 'internal' features, constrained by the contours of developmental channelling, it might be better to think of them as the 'grain' with which that sculptor has worked.

Summary

This chapter has identified several important aspects of morphological change within *Tritaxia*'s evolutionary trajectory. Specifically, we have seen that morphology is held in relatively confined zones of morphospace, with much of the oscillation in shape and trajectory parameters indistinguishable from random noise. Where change does occur, it is mostly in terms of size, with a good deal of this size shift being manifest even within the narrow temporal confines of a single couplet.

Rapid shifts in morphology add up to very little across the whole million year span, giving an impression of *Tritaxia* as a short-term fluid entity wedged within long-term boundaries of confinement. And yet there are certainly differences across the succession as a whole. In particular, the upper half of the sequence hosts populations differentiated (principally by size again) into local morphotypes; and there is also an increase in the expression of exotic, non-triserial growth forms present at all three sites.

The habit of exploring exotic zones of morphospace by uncoiling seems to be a persistent tendency for *Tritaxia*—one that often manifests itself subtly in a myriad of small scale shifts of shape and size. Many of the individual size and shape parameters can be understood as responding to this tendency, but not all. In particular, chamber number (C/h) seems to be an independent variable, as does the final chamber w'/h' shape ratio. Most plausibly, *Tritaxia* can be understood as developmentally modular to the extent that individual chambers are component parts, with chamber number as a variable; the w'/h' component of final chamber morphology is probably best understood as a structural influence.

On the whole, ecology seems to have controlled development by juggling these modular components. Frequent shifts in size are accommodated by free play between the number of individual chambers and their principal dimensions, the former very likely being an expression of heterochrony. But the deep underlying structural influences of the developmental system ensured that change beyond the bounds of simple shifts in size tended to result in channelling through habitual zones of morphospace, specifically, those concerned with uncoiled growth patterns.

Chapter 10 The Mechanics of Morphological Change

Introduction

Chapter 9 was mostly an exercise in straightening out exactly *what* was happening to *Tritaxia* in the mid-Cenomanian; this chapter is a more integrated attempt to understand *why*. The strategy to be adopted will involve specifying a well understood biological mechanism and then searching through the data for patterns which tend to either confirm or contradict it. To make things a little tidier, the mechanisms are broken into those accounting for morphological change versus those accounting for its absence. In the concluding section of the thesis, the balance of evidence and range of mechanisms are consolidated to provide a more coherent account of the processes involved before outlining what I consider to be the prospects for Sheldon's *Plus ça change* model.

Section 10.1 Causes of Change

10.1.1 Ecophenotypic change

Short term environmental influence on morphology is a perennial problem for the evolutionary palaeobiologist: how do we determine whether an observed shift in morphology is a genuine case of evolution rather than merely the product of a flexible developmental system responding to a variable environment? A first step on the road to untangling this issue is to understand what ecophenotypy is actually *for*.

As suggested in Section 5.4.3, ecophenotypy is fundamentally a method of offloading an information burden. Specifically, it is a way for genetic systems to cope with environmental fluctuation occurring on timescales close to, or perhaps an order of magnitude or so longer than, the span of a single lifecycle. Longer or shorter period changes require alternative adaptive mechanisms. For very short term changes, of which there are likely to be many instances within the span of a single lifecycle, the solution has to be a cybernetic system capable of rapidly restoring the organism to an equilibrium state.

Here we are talking about any kind of homeostasis, along with foraging and predator avoidance behaviours, the simple tropisms of plants, and so forth. For very long term changes which persist over the course of many tens to hundreds of generations, the response is likely to be evolutionary: not only does the phenotype respond to a change in environmental conditions but so, too, do the genetic instructions, with salient gene combinations strengthening and specialising and those no longer relevant to the prevailing circumstances mutating out of existence once selection pressure is removed. It is variation between these two extremes that finds ecophenotypy as its appropriate countermeasure. (Note the implicit reasoning behind this argument that lineages do not want to change, and that genetic stasis is the adaptive goal rather than an unfortunate side effect.)

Ecophenotypic reaction norms are basically fixed developmental routines chosen from a limited genetic menu by environmental prompting of an appropriate type. Such options are often available only within narrow developmental windows, and once a decision has been made the system normally remains set for an individual's whole lifespan. It is vitally important to appreciate that although environmental prompting plays a crucial role in determining phenotypic form, reaction norms are adaptations just like any other; and, like other adaptations, they require genetic coding, which is costly to store, as information always is. Thus, even ecophenotypic machinery designed to cope with impermanence and environmental unpredictability exists on a use-it-or-lose-it basis.

This latter point is actually the crux of my argument about ecophenotypic influence in the kind of fossil populations one can gather from the Chalk: I seriously doubt whether something as short-term as ecophenotypy can be observed, except as a time-averaged effect. Even in the single couplet, sample populations had an average 'internal' duration of around 2 000 years: that is, there are at least two thousand generations (and probably 20 000) congealed and homogenised in every bulk sample (taking the deposition rate compensation method of Section 3.2.2 into account, the mid-chalk sample has an expanded time bracket of around 300 years, but for a foram even that is many more generations of environmental exposure than ecophenotypic behaviour is tailored to). My guess is that in order to warrant a flexible developmental routine, the kinds of fluctuation it must be tailored to will switch back and forth many times *within* a bulk sample. The ensuing developmental flexibility may thus be manifest as an increase in morphological variance over that which would have been observed in any given extant population, but shifts in average value *between* such bulk samples are probably indicative of longer scale environmental trends—trends which would

be quite capable of reaching behind the ecophenotypic buffer to tweak the genetic foundation itself.

Unless the conditions for something like an ecophenotypic cline are met (a possibility explored in the next section), the only timescale holding even a glimmer of hope for observing ecophenotypy directly is the 2 kyr transect. Consider, for instance, the evidence for change along the K - r niche axis over the course of a single Milankovitch cycle. We saw in Sections 4.1.1 and 4.3.4 that the entire ecology of the Lower Chalk microfauna can be interpreted as pitching towards the r end of its ecological axis during precessional summers, with a resulting surge in the proportion of generalists and opportunists. There is also some evidence for associated changes in *Tritaxia*'s morphology. In Section 8.2.1.i.a we saw that specimens from the C13 chalk are generally somewhat smaller than specimens from the marl; and while the evidence from this study is not particularly compelling, it is at least backed up by the more robust findings of Leary and Hart (1992). This observation dovetails neatly with the ecological story: it suggests that a transition from K to r - style selective regimes orchestrated both an ecological shift and a morphological one—the problem is that we do not know whether the morphological shift was a case of evolution or ecophenotypy.

It is not impossible to imagine that *Tritaxia* came equipped with a variable developmental program causing it to reproduce more rapidly when food was abundant. The reproductive signal might, for instance, be a fast or slow burning chemical 'fuse' connected to the metabolism in such a way that it burned faster in circumstances where metabolic rate never dropped beyond a certain point. It would make sense for a system like that to exist, and we have evidence from the observations in Sections 9.2.2.i and 9.5.1 that the growth stage (chamber number) was disconnected from other aspects of morphology. Equally, however, given that the shifts we are talking about took place over the course of several thousand generations, it is quite possible for natural selection to have changed the fuse itself, altering the settings that governed the rate at which it burned, such that the state of the environment was taken for granted, and reproduction took place competitively soon *even if a given individual was not exposed* to the relevant environmental circumstances. That, too, would make sense.

The point is that there is no conclusive way to tell from the fossil record. But there is a further strand of evidence which may help to shed light on the matter. An increase in the proportion of exotic growth forms appears in the upper part of the C13 chalk, peaking

at horizon 10 [18]. The phenomenon is a modest event and shows up best in the categorical data, although it can also be traced in the metric character signals for shape, as discussed in Section 8.2.1.i.b. Supposing, for the sake of argument, that specimens in the mid-chalk really *had* been *r*-selected, with a concomitant shortening of their lifecycle; then the increase in deformed specimens in the sediments immediately above can be given an appealingly ingenious explanation. Referring back to Text Figure 7.5 (page 318), a lowering of the average lifespan would result in a lowering of the reproductive threshold behind which bad genes could lie hidden. Several thousand generations with such a lowered threshold is ample time to accumulate substantial mutation in genes which were not being actively selected. Consequently, it is plausible that when conditions started to drift back towards *K*-selection once again, with lifespans and the number of growth stages increasing, the first thing to be unveiled by the shifting reproductive barrier would be the mass of mutation beyond it, and this would immediately manifest itself as exotic growth patterns. If this explanation is correct, the fossil evidence for genetic change implies that even the *r*-strategic size shifts over precessional timescales are cases of evolution rather than ecophenotypy.

Sadly, data from the mid-chalk sample immediately below at horizon C13-9 [16] somewhat contradicts this neat story. Mean chamber number (*Ch*) actually peaks at that point, suggesting that the specimens were going through longer and more elaborate growth sequences rather than the shorter and simpler ones predicted. The veracity of this mid-chalk signal is somewhat uncertain because the sample numbers are so exceptionally low ($n = 15$), but the character/chamber number plots of Section 9.5.1 (Text Figs. 9.18.a) confirm that signal as the culmination of a trend. Easily the simplest way to investigate further would be to examine the specimens of Leary and Hart (presuming they have been retained) to see if they show the same evidence of post-chalk deformity.

Despite these difficulties, on the present balance of evidence I am inclined to say that the case for ecophenotypy as an explanation of changes over time is pretty sparse.

10.1.2 Cline Shifts

From the perspective of a genealogical actor, space and time are interchangeable; this applies equally to both evolutionary and developmental trajectories. If an organism

moves around in its own lifetime, or, equally, if a gene lineage moves around between successive generations, then the effect will be exactly the same as if the entity itself had stayed put and the environment changed around it. To a certain extent, therefore, ecophenotypic reaction norms exist to cope not only with changes over time, but also changes through space. This is an important point to consider, especially if *Tritaxia* occupied the kind of generalist-opportunist niche suggested in Section 4.1.4, because it is precisely in such circumstances that a flexible developmental routine would pay dividends.

But just as sufficiently durable change over time can end up manipulating the genes directly, so too can a permanent environmental gradient. *Clines* are continuous geographical transitions in any measurable character, whether morphological, physiological or genetic; to make a clear distinction from the effects of ecophenotypy, however, we should really limit ourselves to genetic differences.

Genetic differences, within the same species and occurring over spatially separated populations, can exist for a variety of reasons. They may simply be present because gene flow is sufficiently sluggish that mutations arising in one region take a long time to spread elsewhere; this will depend on population structure and density, dispersal tactics and reproductive strategy, not to mention the sheer size of the space over which a species is distributed (and the rate at which its phenotypes can move!). But most of these considerations are to do with factors internal to the species itself—the viscosity of its gene pool, if you will—rather than with any external forcing from a heterogeneous environment. More relevant to the long temporal framework of the 100 kyr transects (which constitute our only geographical control) are those environmental variations of a kind persistent enough that they are capable of imposing equally variable selection pressures on *Tritaxia*, and are thus potentially able to force its otherwise homogeneous lineage into a series of local *ecotypes*.

The land-sea axis is easily the most obvious instance of such a large scale environmental gradient: it persists indefinitely wherever there is variable topography, although its precise location may change, and it causes the kinds of correlated environmental regularity—sediment and water current interaction, pressure and temperature etc.—to which biological agents are often observed to be tuned. Could it be that *Tritaxia* was strung out as a cline running parallel to the land-sea axis, or to an environmental gradient of a similar kind? Something of this nature certainly seems to exist for the ecology of the chalk microfauna, with the slightly shallower locations of Folkestone and

Escalles generally having a similar profile to one another while the signal from Southerham is often quite distinct. If so, then the shifts we observe in *Tritaxia*'s morphology might simply be caused by shifting environmental gradients, like the ceaseless encroach and retreat of the sea on the land.

Let us take the co-ordinated size shifts between B41 and C15 [200-500] as a possible example. If there was a geographic gradient with, say, large individuals close to the shore and smaller ones out in the basin, then the kink in the transect between B41 and C15 might record a sequence of shallowing, then deepening, then shallowing again. No change in gene frequency would be necessary to create this pattern: it would simply arise from an established cline shifting around in concert with an environmental facies to which it was locally adapted.

Although we know from the sedimentary and fossil record (for example, Carter and Hart's P-B break - see Section 2.1.6) that the main transition to deep water occurred only once at around C10 [400], if we only had a single 100 kyr transect to work with this hypothesis would be difficult to test, simply because we would have no idea *how steep* the clinal gradient was; if it was very steep then even minor shifts in depth might translate to dramatic morphological signals. Fortunately, the three long transects are distributed so as to form a flattened triangle, with corners separated by several tens of kilometres and an areal coverage of around 1200 km². Because mean values at each of the three sites are almost identical during the B41 to C15 event, we know that the gradient of any hypothetical cline must have been extremely shallow; and unless it was also quite uneven, with some kind of sharp transition just beyond the range we can observe, then migration episodes must have involved moving populations into the region from very much further afield; this, in turn, suggests depth fluctuations of a magnitude for which there is no sedimentary evidence.

But the morphological event between B41 and C15 [200-500] does have *some* supporting ecological correlates, even if they are not directly depth related. *Pseudotextulariella cretosa*, *Marssonella trochus* and *Textularia* sp. C (Appdx. Figs. 3.4.iv.b, c & e) all show rapid fluctuations in abundance around the same level, although none of their patterns quite match up perfectly with *Tritaxia*'s shift in size. Despite erratic behaviour between C5 and C15 [300 & 500], the peak of ecological activity for all of these is quite obviously at B41 [200], while for *Tritaxia*, morphology in every character other than *Ch* is actually rather subdued up to and including that point. No abundance profile shows this distinction clearer than that of *Tritaxia* itself: ecologically speaking, in terms of

relative abundance, B41 [200] is the only truly significant event; the zone from C5 to C15 [300-500], by contrast, is actually the most stable (Appdx. Fig. 3.4.iv.a). In fact, it could quite reasonably be said that both the ecological and morphological signatures for *Tritaxia* show their *most consistent* behaviour between B41 and C15 [200-500], with values from all three sites clustering and shifting in unison.

So, according to a comparison between the three sites, evidence for a cline around B41 to C15 [200-500] is minimal, and consequently the shifts in morphology at that level are likely to be caused by something other than a migrating morphological gradient. What, then, of the situation in the upper half of the succession where mean size values from each of the three sites diverge? Here, one can envisage a rather steep morphological gradient, perhaps running from the high ground of the London-Brabant Platform and thus separating Folkestone with its larger specimens from the smaller ones at Southerham and Escalles. If this hypothetical cline was maintained until the end of the sequence at C45 [1000], then quite gentle shifts, for which there might be no sedimentary evidence, would be sufficient to orchestrate the between-site correlations.

I find parts of this scenario quite plausible; indeed, it is hard to see what else *could* account for the regularity we observe in the different values at our geographically separated sites. While the gentle, correlated fluctuations might equally be a case of selection instead of cline shift, there certainly seems to be some pervasive influence forcing the values from Folkestone to be consistently higher than those from the other two sites.

It is far harder to fathom exactly what this influence might be, however. Between C15 and C45 [500 & 1000] Southerham accumulated about 3m less (admittedly now condensed) sediment than either Folkestone or Escalles; but the two basinal sites themselves are almost lithologically identical. They also show the most similarity in terms of ecology: their sedimentary and fossil signals support one another in that respect. So while the London-Brabant Platform was a long-term, geologically meaningful entity, it does not seem to have made its presence strongly felt in terms of depth control in the upper half of the 100 kyr transects, and thus does not adequately account for the separation of Folkestone tritaxiid morphology from that of the other two sites.

The only other factor I can think of which *might* account for the morphological differences, especially given that most of them are differences in average size, is some sort of current sorting. The coast at Folkestone is presently scoured clean by Channel currents whereas that at Escalles is bordered by miles of sand flat. If the currents swept the same way

around the basin back in the Cenomanian, then perhaps they took material from the Folkestone region and deposited it at Escalles, much as the sand is deposited there today. It seems very odd that this would occur in the upper half of the succession when we know from all other evidence that the water was deeper at that point, and certainly deeper than it was around the sequence boundary between B block and C block; but there is some support from the fact that Escalles has a far higher proportion of broken specimens in the upper part of the sequence (Text Figure 3.4, page 94). Of course, the deep water issue is only a problem if we imagine the migration of benthic foraminiferal tests took place post mortem. If, instead, we imagine the surface water currents accumulating phytoplankton preferentially in some areas, in great gyres and eddies, then it might be that the rain of life-giving nutrients was greater in those areas, too, in which case the differences in size could be differences in life-history strategy again linked to *r*- versus *K*- selective regimes (and the differences in breakage due to bioturbation by a swollen macro fauna—which at least makes a testable prediction about the abundance of macrofossils at Escalles relative to Folkestone).

But this is all supposition. The important point is that we can imagine situations which would encourage local ecotypes, even if we have to resort to blatant *Just So* storytelling to bring them to life. The differences in morphological behaviour between the three sites in the upper half of the sequence are persistent enough to require some kind of explanation, and clinal variation is a solid candidate, as is developmental plasticity designed to cope with environmental variation on a scale of tens of kilometres.

10.1.3 Directional Selection

Directional selection is the mechanism of morphological change most relevant to a project concerned with evolution. The problem is, as we saw in the last two sections, that it is not the sole agent of such change. Instead, directional selection lies at one end of a temporally scaled spectrum of responses to environmental fluctuation, with reflexes and tropisms at the other end and reaction norms somewhere in between. It also lies along the temporal axis of a four dimensional continuum in which the environmentally correlated genetic variation of clines and local ecotypes take up the three spatial dimensions. Having seen how difficult it is to disentangle these interrelated factors, it should be obvious that an

unambiguous demonstration of directional selection is hard to find. However, there are some telltale characteristics which are unlikely to manifest themselves in either of the other two mechanisms.

Long term, persistent, unidirectional trending is one of them: processes which take hundreds of thousands of years to unfold are too long term to be ecophenotypic in nature, unless they are part of a migrating ecophenotypic cline. A second characteristic, therefore, is for a trend to be uncoupled from the kind of environmental signature which picks out those spatially variable characteristics, like depth or temperature gradients, that are likely to force a cline in the first place. If the pattern is not part of a cline-causing geographic gradient, and occurs over altogether too long a timeframe to be ecophenotypic, then it is probably directional selection. The only problem then is that with the pattern disconnected from the kinds of environmental variable to which selection might be responding, it falls prey to the possibility of being random drift.

The issue of drift is considered below; for now the focus remains on directional selection. Let us start by collecting together all the trend-like and large-scaled morphological shifts we have seen. Among the basic size parameters there are long-term trend-like patterns in three of the final chamber characters, l' , h' and w' , and in the whole test character, W (Text Fig. 9.14.a, page 451). For shapes, the best example is the H/I ratio (which, incidentally, demonstrates that there must have been some kind of trending behaviour in at least one of its components, even though it is virtually invisible in that timeseries). In all these cases the directional bias shows up in both the basin-wide version and often also in the timeseries from individual sites. In no case, however, is there a genuine episode of sustained unidirectional change; rather, the values pass gradually from one side of a character axis to the other, executing numerous short term reversals as they go.

Are these really trends? I used the term 'trend-like' instead of 'trend' itself because by many statistical standards the patterns we see here would fail a proof of directionality. As an example, if the basin-wide sequence for h' were treated as a simple binomial coin tossing run of 10 trials, it would score 7 heads (increases) against 3 tails (decreases), an outcome with a probability of only 0.117 (88.3%). And h' is the best of the bunch; every other pattern would score a lower significance via the same argument. Even so, there is no doubt that *something* has happened across the basin-wide transect for h' , because with the exception of the C5 [300] excursion, all samples below C15 [500] are significantly different from all samples above. This is the case for most of the examples

cited above, and it occurs largely because in spite of the number of steps involved, shifts in one direction tend to push the population mean further than those pushing it back the other way. Despite the difficulty with formal description, then, there is something 'trend-like' about this behaviour, and it *does* result in significant change.

As we saw in the last chapter, it also seems that a whole suite of morphological transitions are connected together through the common medium of *Tritaxia*'s tendency to uncoil. The increase in magnitude of several characters is part of a global pattern linking the biased slide of the *H/I* ratio towards bottom heavy specimens, with an increase in the proportion of twisted individuals, and also with more discrete transitions like the shifts in final chamber ratio (l'/h' & l'/w') which seem likely to reflect the burgeoning exotic growth types of the upper sequence. Do the more discrete transitions also count as sufficiently 'trend-like' tendencies? They probably do if we want them to since one man's punctuation is indeed another's phyletic gradualism. The point is that all these phenomena occur over too long a period to be counted as ecophenotypic, and that actually brings us to the core of the issue.

Whether or not we count something as a case of selection or as some other process depends fundamentally on how persuaded we can be that the other process was not in operation. I can think of no knockdown proof that what we see in the Lower Chalk was selection rather than developmental plasticity or habitat tracking and cline shift. I suspect that there *are* cases of ecophenotypy but that they are concealed within the jumbled mass of an individual sample. I also suspect that there are cases of habitat tracking (the migrating pulse faunas mentioned in Section 2.2.6 are a case in point, as are some of the foram patterns discussed in 4.2.2). We may even be seeing the development of local ecotypes in those size divergences between the three sites. But, on the whole, I think that what we are finding, most of the time, in a standard morphometric timeseries is probably short term directional selection, even for shifts at the highest available resolution.

Whenever natural populations are monitored for any period, they oscillate furiously within restricted morphological boundaries—Darwin's finches of the Galapagos are a perfect case in point (Weiner, 1995). According to a wealth of observational evidence, short term directional selection is going on all the time. So given the fact that plasticity is designed to cope with shorter-term change than we can observe in the bulk samples, and given what evidence we have of the scope and extent of geographical differentiation, I can think of no good reason why virtually all the significant differences in morphology at all

three sampling resolutions should not be considered cases of directional selection. In fact it is my belief that the predominant challenge to directional selection comes not from either ecophenotypy or cline-shift but from an altogether different source—*drift*.

10.1.4 Neutral Drift

Random or neutral drift is a term usually synonymous with genetic drift, the change in frequency of neutral alleles via stochastic processes of non-selective sorting. Here, I am using it to mean something similar, except that it is a change in the frequency of neutral features of morphology. Presumably the phenomenon is underlain by genetic changes also, but we cannot observe those directly.

Random drift is normally considered to be important only in small populations where the chances that a neutral allele will drift to fixation are relatively high; but for the kind of process I am envisaging there need be no fixation (which is fortunate because the population size of *Tritaxia* was probably typically vast). Instead, neutral alleles can happily float around in Hardy-Weinberg equilibrium for as long as they like; the crucial feature is the size of the space (genetic or morphological) in which such floating occurs. In genetic terms this depends on the number of loci hosting alternative neutral alleles. In morphological terms it depends on the volume of neutral morphospace available. If the volume of neutral morphospace increases, then mutations causing phenotypic expressions within that range will also be selectively neutral, and will thus drift around on their own Hardy-Weinberg plateaus until they fall off the edge into fixation or extinction; the only contribution made by population size will be in determining how long, on average, this takes.

As pointed out in Section 9.5.2 at the end of the last chapter, many of the main instances of morphological change can be linked together into a single scheme: *Tritaxia* has a tendency to uncoil. The model accounting for this tendency was presented in Chapter 7. It argued that because non-triserial growth phases occur predominantly after the average life expectancy (as measured by chamber number), they therefore represent developmental errors concealed behind the reproductive barrier, rather than truly functional features.

But function and malfunction are categories cast entirely in terms of selection—one of them is, by definition, selectively advantageous, the other disadvantageous (Section

5.2.2). What, then, of neutrality? If an ecological space were opened up in which unusual morphotypes could be expressed without selective interference, the expression of those morphotypes would constitute an *exploration of neutral territory* rather than a case of either function or malfunction. Could it be that the uncoiling effect was malfunctional only under certain circumstances, and that when those circumstances were relaxed it became neutral? There are good reasons to think so. We have already seen (Sections 4.1.3, 4.2.3; Text Figures 4.11, 9.19) what appears to be an antagonistic ecological relationship between *Tritaxia* and several other benthic forams. *Dorothia gradata*, in particular, stands out as a candidate for the role of direct competitor, not only because of its ecological behaviour (Text Fig. 4.11) but because it has a morphology similar that of *Tritaxia* in many respects, with an early triserial phase that gives way to a biserial one as development unfolds (Appdx. Fig. 2.3.10). It seems highly plausible that the presence or absence of such competitive elements in the environment might make a crucial difference as to how selectively disadvantageous *Tritaxia*'s uncoiling actually was.

Species name	morphotype	value of <i>r</i>	sign	significance
<i>Tritaxia pyramidata</i>	infaunal	0.353	+	0.01
<i>Pseudotextulariella cretosa</i>	infaunal	-0.282	-	0.025
<i>Textularia</i> sp. A	infaunal	-0.452	-	>0.001
<i>Textularia</i> sp. B	infaunal	-0.323	-	0.01
<i>Textularia</i> sp. C	infaunal	-0.438	-	>0.001
<i>Dorothia gradata</i>	infaunal	-0.272	-	0.025
<i>Flourensina intermedia</i>	infaunal	0.498	+	>0.001
<i>Gavelinella cenomanica</i>	epifaunal	0.376	+	0.005
<i>Gavelinella reussi</i>	epifaunal	-0.331	-	0.01
<i>Lenticulina rotulata</i>	epifaunal	-0.241	-	0.05

Text Table 10.1 Significant correlations between the relative abundance of various benthic foraminiferal species and the percentage of exotic tritaxiid specimens the same sample (*n* = 53).

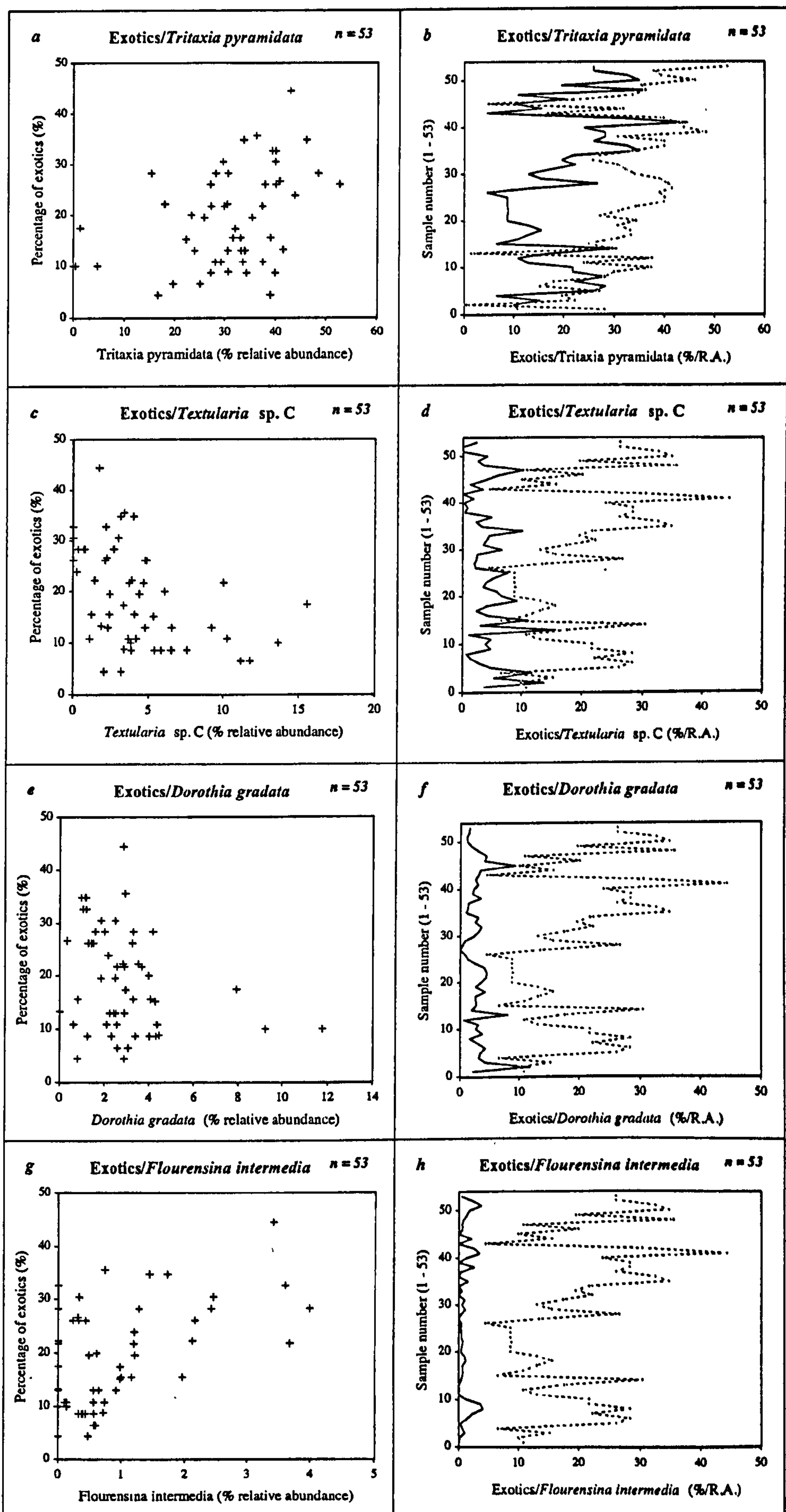
Text Table 10.1 shows every significant correlation so far found to exist between the percentage of exotic tritaxiid specimens and the relative abundance of various species in the same sample. Note that *Tritaxia* correlates positively with its *own* tendency to uncoil: in samples where there are a high proportion of individuals showing non-triserial growth, *Tritaxia*'s relative abundance also tends to be high. Rather disappointingly, *Dorothia gradata* is one of the least significantly correlating species at only 97.5% confidence; but two species of *Textularia*, A and C, and *Flourensina intermedia* correlate exceptionally well, having significance levels that register well off the available scale at better than 99.9%.

Of the infaunal agglutinated morphotypes, only *Flourensina* correlates positively, and it is worth a brief glance back at Text Figure 4.7 (page 142) to review the abundance relationships between *Tritaxia*, *Flourensina* and *Textularia* spp. A & C. There appears to be a kind of ecological see-saw mediating this quartet, with the textulariids as a pivot for the ‘virtual’ positive relationship between *Tritaxia* and *Flourensina*, neither of which correlates directly with the other.

Bear in mind that we are not just talking about ecology here, but about correlations between the *morphometric characters* of one species and relative abundance of others! Nor could the patterns be a passive fall out from the fact that *Tritaxia*’s uncoiling correlates well with its own relative abundance: there are many other species that correlate with *Tritaxia* but that do not correlate with its tendency to uncoil (*Arenobulimina advena*, for example – see Text Fig. 4.7). What seems a more likely scenario is that an increase in the abundance of *Flourensina* permitted *Tritaxia* to unwind by getting rid of unwelcome pressure from the likes of *Textularia*; it is hard to see what else could account for the data. Certainly the negative correlation between *Textularia* and *Tritaxia*’s uncoiling is staggeringly regular (Text Figure 10.1), far more so than the uncoiling is with *Tritaxia* itself, for instance.

Nor is there anything in this evidence to suggest that uncoiling was actually functional. It is possible that it constituted some kind of co-adaptation with *Flourensina*, but hard to imagine what kind it might be. Far more likely is the interpretation already given: that the uncoiling was a developmental error which was more or less heavily penalised depending on the environmental context. But if that is the case then evidence of uncoiling is evidence for a *lack* of selection, and evidence instead for neutral morphological drift (conversely, of course, evidence for a lack of uncoiling becomes evidence *for* selection, although in this case it is probably better thought of as stabilizing selection than directional selection, as we shall see below).

There is another interesting possibility we might consider with regards to drift. In Section 9.5.1 (Text Fig. 9.19) we saw that the crash in *Tritaxia*’s relative abundance at B41 [200] was associated with a number of disparate but apparently related morphological phenomena. There was the first real incidence of size convergence at all three sites, plus an unusual spike in *Ch*, and a corresponding kink in the character/chamber ratios; furthermore, these phenomena seemed to disappear only slowly, taking at least another 200 000 years to



Text Figure 10.1 Strengths of correlation between the relative abundance of various benthic foraminiferal species and the percentage of exotic tritaxiid specimens in the same sample. Panels a, c, e, & g show bivariate scatters with exotic specimens on the ordinate. Panels b, d, f & g show line charts with exotic specimens marked by dots. Sample numbering is arbitrary and simply reflects the 5 transects stacked. The sample sequence is arbitrary. See Text Table 10.1 for statistical significance.

diminish. Note that the end of this diminishing was marked by mean size values spreading out into what was, in Section 10.2, above, argued to be a cline-like structure; and that this morphological diversification was associated, after C10 [400], with a rise in proportion of non-triserial growth forms.

But what caused the homogenisation of morphology at B41 in the first place? One possibility is that it could have been the result of a genetic bottleneck brought on by plummeting population sizes as shown by *Tritaxia*'s relative abundance. If the gene pool was homogeneous simply because it was drawn from a few surviving populations, then that would explain why morphology at all three sites was also responding so uniformly to whatever environmental influence was causing the shifts in size. I suggested in Section 9.5.1 that the size increase at C5 [300] might be *Tritaxia*'s expansion into some ecological hole left by competitors like *Textularia*; but when those competitors return in C10 [400], they return with a vengeance. The effect is apparently severe: there is a co-ordinated crash in both *Tritaxia*'s absolute size and in its expression of exotic growth styles (Text Figure 9.17, page 456)—exactly what one might expect of a homogeneous and thus 'brittle' genome that was only just beginning to re-explore the space of alternative (and thus redundant and perhaps buffered) ways to encode its phenotype. If this interpretation is correct, then it could also be that the supposed cline is nothing more than drift-like exploration along the growth trajectory (rather than adaptation, which, by comparison, is drift accompanied by selection).

Section 10.2 Causes of Stasis

10.2.1 Developmental Constraint

The persistent tendency shown by *Tritaxia* in switching from triserial growth to the closely related biserial and uniserial growth patterns simply cries out for an interpretation of developmental constraint. The fact that this tendency occurs repeatedly, and even at the smallest observable timescale, strongly suggests that it is a phenomenon latent in the organism itself, not something forced by a particular suite of environmental circumstances.

The non-functional interpretation given in Section 7.3.ii backs this position up. But what exactly is the constraint? Is it the historical fact that *Tritaxia* is triserial to begin with? Is it some fabrication aspect of the developmental process, like the chemical attributes of the cytoplasm or the physics of membrane tension? Or is it an algorithmic consequence of the developmental program being organised around some particular genetic configuration?

In their 1985 paper on the nature of developmental constraint, Maynard Smith et al. suggested a primary dimension of classification ranging from *local* to *universal*, depending on how broadly applicable a given constraint might be (Section 1.1.5). They then subdivided this axis and introduced a five-fold taxonomy of types: 1) phenotypes accessible or not given *a particular* developmental mechanism; 2) phenotypes accessible or not given *any* developmental mechanism; 3) phenotypes accessible or not for selective reasons; 4) constraints resulting from canalizing selection; and 5) genotypes accessible or not given the present genetic system. Since it provides such an excellent bridge between the biological reasoning of the constraints paper and the information-based approach I championed in Chapter 5, let me organise these categories in terms of Seilacher's Triangle (Text Fig. 5.11). Classes 1 and 5 clearly fall under the banner of local constraints and can be placed in the phylogenetic corner, as artefacts of history. Class 2 is universal and sits in the fabrication corner. Classes 3 and 4 are selective and should therefore live in the functional corner.

What caused *Tritaxia* to uncoil? I argued in Chapter 7 that triserial growth was a case of rather precise engineering and that almost any deviation from such precision would result in a spontaneous switch to biserial or uniserial translation along the coiling axis. One part of the reasoning was that the elongate form of a normal triserial chamber is itself a highly unnatural shape for cytoplasm to be in: it relies on membrane adhesion to the surrounding substrate preferentially stretching the nascent chamber in one direction (the *l'* axis) more than the others, and that this factor is set against the intrinsic tendency for cytoplasm to spontaneously organise into more symmetrical hemispherical blobs. When adhesion fails, the final chamber springs back into a hemisphere and the triserial pattern is lost from there on. A natural tendency to form hemispherical blobs is shown by droplets of all sorts (Thompson, 1917); it is, I believe, the reason why *Tritaxia*'s *w'/h'* ratio was so uniformly stable and isometric throughout. It is a universal constraint. It belongs in the fabrication corner of Seilacher's Triangle.

Why does *Tritaxia* not exhibit tendencies other than uncoiling? In some character dimensions it does. Look at the $(H/W)/(H/I)$ morphospace template again (Text Fig. 6.17,

page 295). There are clearly regions which correspond to the shapes of different species of foraminifera. Below the $H/W = 1$ boundary, for instance, are discoidal forms like *Lenticulina rotulata* with no translation along the coiling axis at all. *Tritaxia* has plenty of variation in that direction in the form of short, fat specimens; perhaps it could be pushed over the isometric threshold if selection was strong enough. Meanwhile, on the other side of the $H/I = 1$ boundary are low to high trochospiral morphologies with an umbilicus not unlike that of *Gavelinella cenomanica*. *Tritaxia* actually has very little variation in that direction, and certainly appears to be constrained. The H/I axis has a sharp cut-off point because growth occurs in a closed spiral form with no translation out from the coiling axis (e.g. Appdx. Fig. 4.2.1.ii). It is not impossible to imagine tritaxiid specimens shifting in this direction, however: the first step, I should think, would be for the final chamber to have an aperture which opened in a direction tangential to the coiling axis instead of radially inward towards it. In a sense, a step like that would establish an umbilicus in a single move. The orientation of the aperture was not measured so I have no idea whether there is variation in this character dimension or not. I suspect there is very little because I suspect the building procedure was more or less like that described in Section 7.4: *Tritaxia* used the gaps between earlier chambers to position its next chamber in a way that depended crucially on its emerging from the existing structure as close as possible to the coiling axis. It probably did so for reasons of informational economy. That is a functional feature and it deserves to be placed in the functional corner of the Seilacher's Triangle.

But the tendency to uncoil is very definitely *Tritaxia*'s major morphological channel for exploration. By taking this route, it can, in time, reach the morphospace of any other foraminiferan. Remember that almost all foraminiferal tests vary around a common theme: they are really just a string of tiny boxes glued end to end, with the foramen of the one behind leading into directly into the one in front, and ending with a special foramen called the aperture (I am aware that this is quite a simplification but it does have a truthful core). The simplest arrangement of all is a uniserial line of chambers, like those of *Nodosaria* and *Dentalina* (Appdx. Figs. 2.2.3.vi & viii). From this arrangement can be reached any planispiral form simply by having the sequence coil around itself; and after that to any trochospire by coiling around itself while translating at right angles to the coiling axis. Involute forms can be made by having minimal translation along the growth sequence itself, and by simply allowing successive chambers to engulf their predecessors.

If *Tritaxia* flowed all the way down its most readily accessible channel for exploration, it would eventually uncoil entirely into a uniserial sequence of chambers—and from there the options are numerous. In other words, there is nothing to stop it from getting to positions on the other side of the $H/W = 1$ and $H/I = 1$ boundaries, it just has to take the long way around.

I imagine the same argument applies to the genotype. There must be *some* DNA pattern in the space of all possible genomes which could start off with a bit of cytoplasm and turn it into *Gavelinella cenomanica*, *Lenticulina rotulata* or *Dorothia gradata*: we know that, because these species exist. Presumably there is some pattern of mutations which could turn a standard piece of tritaxiid DNA into just such a sequence, but the probability of its occurring in a one-step move, by chance alone, is infinitesimally small. All of the likely mutations result in the uncoiling sequence we have documented. It isn't impossible to turn *Tritaxia* into a gavelinellid morphotype, but some routes are easier than others, and the easiest ones of all go the long way around. Like the Irishman's sage advice on the best road to Tipperary, "You wouldn't be wantin' to start from here".

This kind of constraint is local. It arises because of the specific nature of the starting point. The starting point is a consequence of *Tritaxia*'s history, so this constraint lies in the phylogenetic corner of Seilacher's Triangle.

10.2.2 Stabilizing Selection

Tritaxia has a tendency to melt out of its triserial state and trickle down the narrow developmental channel of experimental uncoiling. But it never gets very far. Certainly, when there are competitors in the vicinity, the extent of any uncoiling is strictly limited. Appendix Figures 2.3.9 and 2.3.10 show an unusually advanced case of tritaxiid uncoiling next to a young and thus relatively triserial specimen of *Dorothia gradata* (young in the sense of having a small number of chambers and relatively triserial in the sense that the early triserial portion therefore makes up a large-ish part of the test). A more typical dorothiid appears in Appendix Figure 2.2.1.x; clearly *Tritaxia* has a long way to go before it exhibits that much biseriality.

I argued in Chapter 7 that *Tritaxia*'s tendency to uncoil was not a case of directional selection because the exotic growth forms are probably not functional; rather, it is a case of

neutral morphological exploration. One very good reason why the exploration does not proceed further is because it is exploration into territory already inhabited by *Dorothia*, as the SEM images make abundantly clear. But given the negative correlations between non-triserial growth and many species other than *Dorothia*, it seems likely that virtually any source of competition was enough to keep *Tritaxia* in check.

This is stabilizing selection. *Tritaxia* is already triserial and already has a niche of its own—a niche within which it is phenomenally successful. It has a tendency to explore when the opportunity arises, but as soon as any competitive element turns up to rob it of its share of the resources, *Tritaxia*'s evolutionary response is to coil back up again, wedging itself into that portion of morphospace which most closely corresponds to the local optimum of its realised niche.

I should point out that in terms of the theme of Chapter 5, the growth form of *Tritaxia*'s test represents information *about* the competitors in its environment: triseriality is about their presence, exotic growth about their absence. It is easy to see how a heavy reliance on structural offloading, as argued in Chapter 7, makes *Tritaxia*'s test a very blunt 'instrument of perception' indeed. *Tritaxia* cannot clearly tell *which* of the surrounding specialists it is interacting with (Text Figure 4.7), although some trigger a more marked response than others. Insofar as the growth form of the interactor is a 'sense organ' for the encoder within, *Tritaxia* is almost blind. Through a striking analogy with the pseudopods themselves, we can imagine the bunched, triserial test uncoiling tentatively into the unknown until it discerns something unpleasant and (literally) re-coils in disgust! I make this point here because it illustrates very clearly what I had in mind when claiming that generalists simply cannot 'see' their environment changing because (for reasons of organisational economy) they view it through such a sparse array of coarse-grained developmental modules.

Evidently, *Tritaxia*'s options were not so tightly bound as to make small scale change impossible; quite plausibly, short, constantly reversing episodes of directional selection were occurring all the time. But they never really accomplished anything because exotic chamber formation was the major channel of exploration. Let us linger on that statement for a moment. What does it mean to say that there was a *major* channel for exploration? *Tritaxia* was clearly capable of executing shifts of size, shape and trajectory within its mode of triserial growth. Size shifts were frequent and significant, shape shifts less so, and trajectory shifts showed the most stability of all. But all of these had a limited

capacity to move *Tritaxia* around in morphospace. Exotic growth, by contrast, resulted in radical changes. Just look how the non-triserial specimens spray away from the developmental trajectory in Appendix Figure 4.2.1.i.b, or how they rocket across morphospace in Text Figure 7.9.i (page 328). The shift to exotic chamber formation was not just one of degree but of kind. Non-triserial growth is a major discontinuity. It suggests some kind of developmental threshold like that described in Section 7.5 (Text Fig. 7.8, page 326). This is what stabilizing selection was selecting *against*.

We might say that stabilizing selection was selecting *for* a broad developmental feature: triseriality; or, with *Tritaxia*'s generalist niche interpretation in mind (Section 4.1.4), perhaps for a broad functional feature. Minor shifts within the triserial mode, however, were far more specific. They were cases of fine tuning and were left to directional selection to accomplish on a much more dynamic, short term basis. The image this conjures is very similar to that deduced from the scaling patterns in Sections 4.2.4 and 9.4.1 where a lot of fluid oscillation surrounds a stable core morphology. Text Figure 9.13 (page 448) argued for an interpretation of white noise oscillation within broadly stable boundaries; exotic chamber formation in the upper half of the sequence occurred because those boundaries had been overstepped. That this is evolution on a range of fitness landscapes hardly needs to be said: the small scale fine-tuning represents a smooth topography, the exotic growth patterns an extremely rugged one.

This is one way to interpret the evidence, but of course there is another: constraint. Early in the 1985 paper of Maynard Smith et al. we find the following passage:

When the morphology of a species remains virtually unchanged for millions of years, we would like to know whether this reflects developmental constraints limiting the possibility of change or, conversely, the maintenance of uniformity by stabilizing selection.

Note that the interpretations of stabilizing selection versus developmental constraint are cast as mutually exclusive alternatives: we can choose one of them "or, conversely," we can choose the other.

In my opinion this is exactly the wrong way to approach the issue of long term stasis. The image I would opt for is one of 'figure and ground', conceptually equivalent to those black and white images of two faces in profile "or, conversely," a vase. An organism is always simultaneously a product of both constraint *and* selection; of structure *and*

function; of self-organization *and* evolution. It is held as a creative tension between these opposing forces. It makes no sense whatsoever to speak of such influences as alternatives—they are simply two different facets of, or two different ways of talking about, the same thing. I'm not the only one to have seen this. As long ago as 1983, Dan Dennett, in a paper partly entitled "The 'Panglossian Paradigm' Defended", remarked: "The optimist declares this the best of all worlds, the pessimist sighs and agrees." As usual he hit the nail squarely on its head.

The entity we call *Tritaxia pyramidata* existed in its billions and billions across a vast area of shelf sea (almost certainly far beyond the confines of the Anglo-Paris Basin); it did so for at least a million years and evidently took the lion's share of whatever resources were available to the benthic foram community. But it remained broadly in stasis for all that time, boxed into a small zone of morphological space by the twin influences of a specific and limited developmental procedure, plus furious competition from other benthic foraminifera. Both facets of this story are equally true. The difference between a verdict of constraint versus optimization, therefore, depends only on whether one's glass is half empty or half full.

10.2.3 Co-ordinated Stasis

Given that the morphology of *Tritaxia* was evidently held in check by a mixture of developmental channelling and ecological regulation, might the same not be true for the rest of the benthic foraminiferal fauna? It is easy to imagine that each species existed in its own narrow morphological zone, hemmed in by the intersecting demands of structure and function. The very simplicity of the foraminiferal test lends itself to this kind of evolutionary congestion. Might we not broaden our assessment of *Tritaxia*'s reasons for stasis to include the congealed nature of the surrounding ecosystem?

We saw in Part II that the relative abundances of microfossil species in the Lower Chalk are strikingly regular. I argued there that they were held together in a quasi-stable network by the twin attractors of their individual ecologies and a self-organizing component that collectively arose between them. Can we say something similar about the stability of their morphologies, too?

The first issue to address is whether or not the other faunal elements actually *were* morphologically stable. The answer, I think, is a qualified 'yes'. Before settling on *Tritaxia* as the subject of this survey I measured small numbers of several other species from the 100 kyr sample horizons at Folkestone: *Lenticulina rotulata*, *Gavelinella cenomanica*, *Gavelinella baltica*, *Marssonella trochus*, *Pseudotextulariella cretosa* and *Plectina mariae* all received some attention. (They all have in common the fact that they will lie flat on a slide—unlike others such as *Arenobulimina advena*, *Eggerellina mariae* and *Ataxophragmium depressum*—although admittedly *Pseudotextulariella* had to be positioned on its apertural end to do so). Most of these species could not be found in sufficient density to generate good statistical populations. Most of them did not have a sufficiently large number of obvious characters to measure. Even so, the measurements I was able to take showed very little fluctuation in morphology (although there were no statistical tests performed). In part, the reason I eventually chose to focus on *Tritaxia* was because it *did* exhibit at least some obvious signs of morphological change across the sequence. (If I recall rightly, I was, at that stage, concentrating primarily on the more subjective character evaluations such as the obvious increase in glauconite content in the upper sequence, and perhaps on changes in the degree of indentation; I certainly had not recognised the mode of uncoiling for what it was).

Apart from *Tritaxia*, the species receiving the most treatment was *Lenticulina rotulata*. 30-45 specimens of this species were measured at every 100 kyr horizon from Folkestone, apart from bed C15 [500] in which there was a large study incorporating 135 individuals. *Lenticulina* could well be a bucket category, or an 'anastamosing morphological plexus' as I have heard such things called. But, if so, even this was quite stable in terms of its principal dimensions. Test length and height (measured diametrically from the terminal aperture across the hub to the other side, and across the hub at right angles to that measurement, respectively), plus the ratio of these, stayed remarkably constant across the entire transect in every horizon except for B41. In B41 the rate of chamber size increase was unusually high in *Lenticulina* (and other species) so specimens there tended to have elongate final chambers and thus to be longer overall. There were also differences between the two halves of the succession, but mostly in fairly superficial characteristics. Specimens from the lower half were smooth, for instance, with chamber perimeters sunken inward between the septal walls to give the test a kind of webbed appearance; specimens

from the upper half were more circular, often having a small keel. But otherwise the form of the test was comparable throughout.

And so it was, I think, with the rest of the fauna. I doubt very much whether even an extremely experienced Lower Chalk micropalaeontologist could look at the photos in Appendix Figures 2.2 and tell from where in the succession those specimens were taken (they might if they saw the specimens themselves because there are certainly differences in the style of preservation; but as for morphology, I doubt it). The *arlesiensis* bed (B41) was the only horizon in which marked morphological changes were apparent, and there they were apparent in many species simultaneously. Specimens from B41 tend to be bigger than usual, often with bloated, globose chambers; but their general form is always similar enough that there is rarely a problem with identification. If I had to locate serious morphological diversity in the Lower Chalk forams it would be within the minor nodosarian group. These often showed quite dramatic shifts in ornamentation and form, though whether or not this represented change in a single lineage, or the temporary creation or incursion of a rare species, was never very clear to me (they are labelled sp. A, sp. B, sp. C etc. in Appendix Tables 1.1 but even these groupings could be artificial and include multiple morphotypes).

10.2.4 Ecological Locking

My overall impression is that both the foraminiferal and ostracod faunas of the Lower Chalk conform very closely, both morphologically and ecologically, to the pattern described by Brett & Baird (1995) and Brett, Ivany & Schopf (1996; see other papers in the same volume) as ‘co-ordinated stasis’ with ‘ecological locking’ (see also Section 1.1.5). (Note that the classic version of this pattern includes rapid turnover as well as within-fauna stability; see Jarvis et al., 1988, for documentation of the Cenomanian-Turonian turnover event.)

We should be clear about exactly what this pattern is and what its advocates think causes it. In part, the pattern is an artefact of the spotty fossil record. Boucot (1996 and references therein) has long recognised an inverse correlation between relative abundance and the long-term rate of morphological change. Sterelny (2001) summarises it thus:

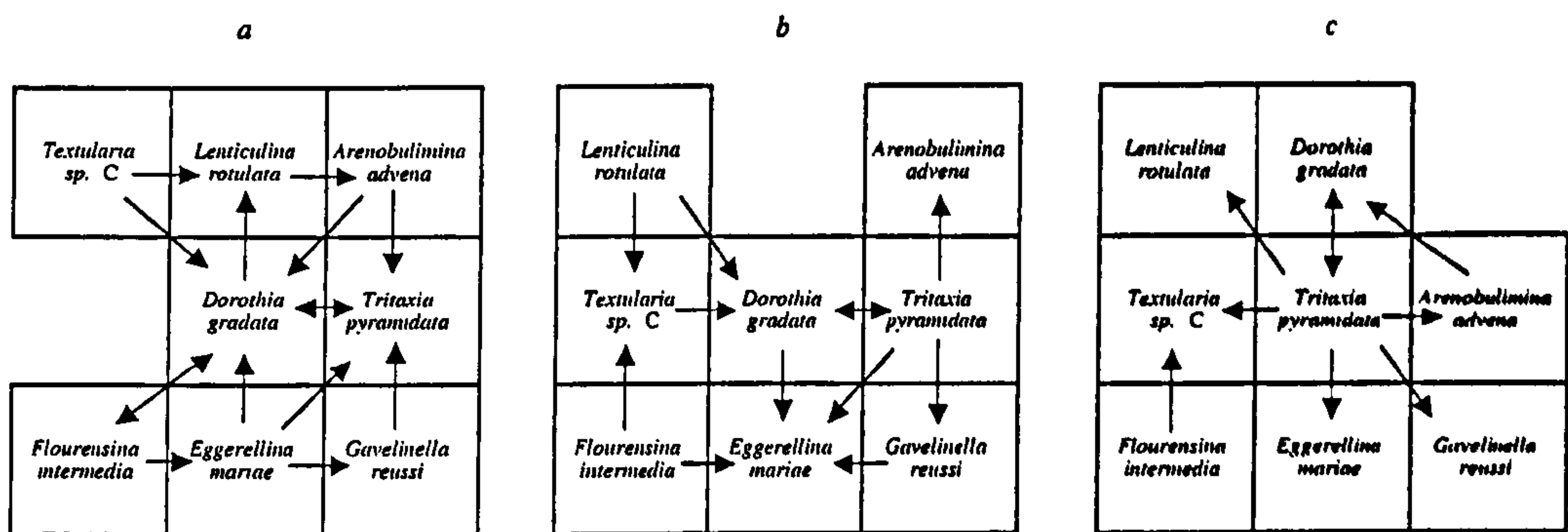
Generalist species have extensive ranges and are common within that range. As species they are long-lived and often morphologically stable. In contrast, specialist species have restricted geographic ranges and tend to be rarer even within those ranges. Moreover, they turn over more rapidly than generalist species, and they may show more morphological change while they exist. Rare species are less likely to manifest evolutionary and ecological stability. But equally, they are less likely to leave a record of their evolutionary and ecological change in biofacies. On this view, co-ordinated stasis biofacies record a real phenomenon, but also conceal one: evolutionary and ecological change in evolutionary specialists.

I think this describes the situation perfectly, both from my own experience and from what I understand of the processes involved. However, I would add a few embellishments. Firstly, I think the framework of the niche axis described in Section 4.1.4 and 5.5.2 needs to be incorporated; this, as I suggested earlier, is a universal. Secondly, I think that a structural component needs to be added, too. As organisms go, foraminifera are not well endowed with modular components. The individual chamber dimensions might vary independently (although in *Tritaxia* h' and w' in particular seem to perform as a single unit), and, through the variable medium of chamber number, these can have a flexible relationship with the rest of the test. Then there is rate of translation along the coiling axis and the rate of final chamber expansion, degrees of involution, keel and spine formation, occasionally striation and other forms of 'ornamentation', and so forth. On the whole, however, foraminifera have relatively few morphological parameters to play with; certainly far fewer than a metazoan like an ostracod.

In Chapter 5 and in the section above I argued that structure and function need to be understood holistically, and that a niche is created as much by the organism filling it as by any features of the environment itself, because regular environmental structure is only 'informative' to a developmental reading system poised to interpret it. In the case of the Lower Chalk microfauna, it is easy to imagine that the majority of the common species were so developmentally viscous that they sat firmly in their broad ecological sockets and were stable for no other reason than that. But we saw evidence in Part II that the various components of the fauna *did* interact with one another, and we now have a wealth of data on the effect some of these had on *Tritaxia*'s morphology. It seems entirely plausible (to me at least) that the whole fauna was collectively holding itself in check, both ecologically and morphologically.

Taking *Tritaxia* and *Dorothia* as the most obvious pairing, *Dorothia* seems to have been blocking *Tritaxia*'s developmental channel in the uncoiling direction; was *Tritaxia*

blocking *Dorothia*'s option of coiling tighter? Generalising, it is possible to imagine the whole fauna, so arranged, each impeding one another's evolutionary exit route so as to hold the whole in collective stasis. The arrangement reminds me of nothing so much as the kind of child's picture puzzle in which a jumbled image is to be re-constructed by sliding panels around in a frame, often in a laboriously long-handed way. If, on top of this we suppose the coveted 'image' to correspond to a 'lowest energy' configuration of some sort—perhaps the minimum amount of ecological overlap—and that the Lower Chalk micro-fauna had found its optimum solution, or at least an un-perturbable, evolutionarily stable version, long before we tune into it in horizon B31, then we have reasons for stability indeed.



Text Figure 10.2 The sliding panel puzzle as an illustration of ecological locking and coordinated stasis. The system begins at a random point fairly well out of equilibrium, with most species interfering with one another to some extent. It would ideally like to settle into a more stable configuration (one with fewer direct interactions, represented here by arrows) but finds that it has to obey the rules of the game. The panels representing different morphologies and, by extension, ecologies can only slide to a new location when there is room available in morphospace. Eventually, after a good deal of shuffling the system finds its equilibrium point at configuration c (as we find it in the mid-Cenomanian; see Text Figure 4.7) and is happy to remain there for at least a million years. Note, incidentally, that when *Tritaxia* was removed from its central keystone position during the B41 event, it left a gap to be filled in the ecosystem. This depiction invites that conclusion with particular clarity. See adjacent text for discussion.

I think the Lower Chalk benthic microfauna constituted an extreme version of this pattern. The forams were just so developmentally simple, and inhabiting *such* a monochrome environmental setting with its yearly phytodetrital 'on-off' switch, that the hub structure of their ecology was sculpted to perfection. They were also so developmentally crystalline that the same structure stayed in place for the whole million year span, allowing it to be tracked by my sampling and analysis procedure. It will probably take a lot more effort to find a similar example elsewhere, especially where there is more complexity to the ecology, or more developmental modularity to the organisms.

Nevertheless, I think the hub-centred situation depicted in Text Figure 4.9 (page 147) is a natural phenomenon, for all the reasons given in Chapters 4 and 5. I expect it to be expressed time and time again, in different settings. In fact a good alternative way to look for it might be to take a series of clades (branches on a genealogical hierarchy) and see whether they are broken up into groups and sub-groups each having the geometry of Text Figure 4.9: the species involved will probably be components in totally disparate ecosystems but on average their fates will even out to give the pattern predicted, and at least there would be good control on the structural and historical component (I should also add that there might be interesting insights into the contribution made by developmental modularity if some method of measuring that could be found).

Section 10.3 Plus ça change

10.3.1 Whither *Plus ça change*?

At last we have reached the point where we can consider all the evidence for *Plus ça change* together. Since we now know the Lower Chalk benthic environment well enough to have a fantastic grasp of the ecological factors involved, and we know *Tritaxia* better than it ever knew itself, we can analyse the model at a variety of depths. For instance, we can simply take the data at face value and ask whether the morphological patterns seen in the Lower Chalk correspond to the predictions of the *Plus ça change* model listed in Text Table 2.1. Or we can be a little more sophisticated and ask whether the mechanisms involved are in the spirit of *Plus ça change*, even if the patterns thus generated are not.

First things first. The standard criteria for the *Plus ça change* patterns were presented in Chapter II. We can deal with them systematically as follows:

Effect no. 1: Was there stasis (irrespective of reversals) in the unstable lower half of the succession and net change (irrespective of reversals) in the geologically stable upper half? The answer is found in Text Table 10.2 (below) and in general it is *no*. Assuming that what we mean by net change is simply that the lowermost and uppermost of a series of samples are significantly different from one another, there are very few cases where this condition is

met, and in those in which it is seem to be fairly trivial to the overall patterns. At the very least they are balanced out by just as many diametrically opposite results.

Size	net change?	<i>H</i>	<i>W</i>	<i>I</i>	<i>Ch</i>	<i>l'</i>	<i>i'</i>	<i>w'</i>	<i>h'</i>
Size	Upper	NO	YES	NO	NO	YES	NO	YES	YES
Size	Lower	NO	NO	NO	NO	NO	NO	YES	YES
Shape	net change?		<i>H/W</i>	<i>H/I</i>	<i>w'/h'</i>	<i>l'/i'</i>	<i>l'/w'</i>	<i>l'/h'</i>	
Shape	Upper		NO	YES	NO	YES	NO	NO	
Shape	Lower		NO	YES	NO	NO	YES	YES	
Traj	net change?		<i>H/W</i>	<i>H/I</i>	<i>w'/h'</i>	<i>l'/i'</i>	<i>l'/w'</i>	<i>l'/h'</i>	
Traj	Upper		NO	NO	NO	NO	NO	NO	
Traj	Lower		NO	NO	NO	NO	NO	NO	
Cats	net change?		<i>ind</i>	<i>tw</i>	<i>g%</i>	<i>g.dist</i>	<i>type</i>	<i>chir</i>	
Cats	Upper		NO	YES	YES	YES	NO	NO	
Cats	Lower		YES	YES	YES	NO	YES	NO	

Text Table 10.2 *Number of cases of timeseries showing the predicted pattern for the Plus ça change model. Data taken from the basin-wide timeseries statistical tests using C15 [500] as the midpoint, B31 [0] as the lowest and C45 [1000] as the highest. The categoricals were judged subjectively. Cases that match the model predictions are in bold.*

Effect no. 2: Was there evidence of increasingly strong response to even the smallest scale events in the upper, stable half, versus a diminishing response to any but the most extreme events in the lower? This is a difficult one to judge. Consider the between-site divergence of the mean size values in the upper half of the succession. Does that count as an increasingly strong response to even the smallest events? One of the most plausible interpretations for it is that the *Tritaxia* was settling into a series of local ecotypes. Equally, there is also a way of viewing the zone between B41 [200] and C15 [500] as a time of morphological *un*-responsiveness, despite the major size oscillations, simply because the mean values from each of the three sites are so close together. And the interpretation to the B41 event given in Section 9.5.1 would certainly count as a response to the most extreme event. Alternatively, however, one could play exactly the same argument back the opposite way. The extreme event at B41 actually made the lineage more responsive to small scale events, like the small surge in a handful of competitors at C10 [400], whereas the divergence of the morphotypes after C15 [500] seems to have damped their behaviour such that all the shifts from then on are relatively minor in terms of magnitude. The verdict on this one might have to be ‘no verdict’.

Effect no. 3: Was there evidence for low rates of change (irrespective of reversals) in the geologically unstable lower half versus high rates of change (irrespective of reversals) in the geologically stable upper? This one is easy. It is a resounding *no*! Rates of change were *almost always* higher in the unstable lower half of the section (Text Table 8.29, page 398). And they were higher for both sizes and shapes. However, in defence of *Plus ça change*, I should point out that the relatively minor shifts of size and shape involved in the rate calculations are almost beside the point when compared to the major feature of morphological change, *Tritaxia*'s tendency to uncoil. Plus, it is actually quite plausible that the rate of high resolution background oscillation was fairly consistent throughout, in accordance with the model presented in Text Figure 9.13 (page 448), and despite the way it appears in the 100 kyr transects.

Effect no. 4: Was there evidence of decreasing variation in morphology in any one sample in the unstable lower half versus increasing variation in the stable upper? This time I think the answer is yes. For many characters of both size and shape there are markedly higher standard deviations found in the upper half of the 100 kyr sequences, often at all three sites. In the basin-wide signal a similar pattern is found, and it is found in the categorical characters also. And, of course, the fact that most character sizes diverge in the upper half provides a different way to argue the same point, which again backs up the predictions of the *Plus ça change* model. Furthermore, if we are prepared to accept the frequency of deformed specimens as the main evidence of morphological exploration, then there was definitely more going on in the stable upper half of the succession.

To summarise these results I would say that overall the picture is one of decreased variation but possibly increased rate and magnitude of peripheral change in the lower half, against increased variation and possibly decreased rate and magnitude of peripheral change in the upper; but, adding that where such change did occur in the upper half it was often change in different directions, thus introducing a kind of second-order variation. Furthermore, if we take a tendency to uncoil to be the major example of evolutionary change, rather than the relatively trivial shifts in size and shape (i.e. change at the core rather than the periphery – see Text Figure 5.12, page 238), then there is no doubt that such change occurred preferentially in the upper half, when the environment was stable on a

geological timeframe. If this is *Plus ça change*, then it is *Plus ça change* with a twist. But I think we can do better still at this point and offer a more sophisticated conclusion by assessing the situation through the interpretations already made.

The major problem I have with accepting these patterns as a confirmation of the *Plus ça change* model is that the environmental factors involved seem to be operating at the wrong timescales. Let me compile two contradictory sets of interpretations to show what I mean, and what I think can be salvaged and what cannot.

Over the sequence observed, B41 [200] unquestionably constituted *the* big ecological 'event' for *Tritaxia*. The B41 event was most plausibly brought about by sea-level lowstand conditions, massive, continuous algal blooms and ensuing anoxia (Section 4.3.4). It seems to have lasted at least 20 000 years and qualifies as a geological scale phenomenon by anyone's definition. If the conditions associated with B41 in the Lower Chalk were widespread (and there is every indication that they were - see Paul et al. 1994), then they seem likely to have decimated *Tritaxia*'s standing population across the basin, plausibly causing a genetic bottleneck that lead afterwards to a homogenised gene pool (as shown by the clustered mean values at different sites) requiring a considerable time (hundreds of thousands of years) to recover its variability (Section 9.5.1).

This, in a sense, is what *Plus ça change* predicted: the event imposes a loss of variation and this in turn has a persistent effect on morphology, even after the population has recovered; the only problem is that the loss of variation actually seems, between B41 [200] and C15 [500], to have made morphology *more* sensitive to minor environmental fluctuations, not less. If there is any truth in this story (and I am happy to admit that it involves a lot of supposition), then it actually turns the standard *Plus ça change* pattern on its head. So let us try a different version.

Let us imagine that the minor fluctuations in size and shape are actually a distraction from the major features of morphological change, which are instead to be found in *Tritaxia*'s uncoiling. Exotic growth patterns are rarer in the first half of the succession, and where they do occur they are normally Stage II developments in which only a single deviant chamber is added before the individual expires. It is unlikely that this had anything to do with the B41 [200] event because exotic growth patterns are also relatively rare in the horizons below, for at least 200 000 years before B41 occurred (see Text Fig. 9.17, page 456).

Instead, what seems to be keeping *Tritaxia*'s expression of non-triserial growth in check is the presence of competitors like *Textularia* and *Dorothia* (Section 10.2.2, Text Fig. 10.1). And, in turn, what seems to be encouraging the presence of these competitors, if my interpretation is correct, is the fact that the environment was ecologically stable with a relatively continuous influx of phytoplankton that permitted the *K*-selected end of the fauna to flourish (Chapter 5). Conversely, in the upper part of the sequence, after the PB break at C10 [400], when the water was deep and the land far away (Sections 2.1.6 & 4.3.1), and when a corresponding lack of terrestrial nutrients made the phytoplankton input irregular and slim, *r*-selected *Tritaxia* both flourished and exploratively uncoiled in an environment blissfully free from the likes of *Textularia* and *Dorothia*. In terms of the hub model of ecological locking, we can imagine the outer rim of the fauna—the specialists—skimmed off to leave only the hub; and the hub responding to its new found freedom with a burst of morphological innovation.

This is my favoured interpretation of what went on in the Lower Chalk, and in many respects it bodes well for *Plus ça change*. The problem is that the environmental stability is at entirely the wrong scale; it has nothing to do with Milankovitch scale oscillations at all. *Tritaxia*, along with the rest of the fauna, was responding to the onset of environmental instability on an *ecological* timeframe, not on the geological timeframe demanded by *Plus ça change*. Therein lies the rub.

10.3.2 A Suggestion

Despite its promise, I am unconvinced of the validity of the *Plus ça change* model in its present form. At issue is the matter of scale, and whether or not the model works for microevolution *within* a species lineage. The lifecycle—the span of time from conception to re-birth—is the natural unit with which organisms 'view' the world, monitoring it in generation-length snapshots. *Plus ça change* is cast as a pattern of evolvability against a backdrop of geological-scale stability, and within-species evolvability is measured on far too short a timeframe for that.

When *Tritaxia* 'reads' the Milankovitch cyclicity like a laser scanner reading a bar code, it is reading it with the fluid outer periphery of its developmental system. Changes in size associated with the onset of chalky conditions are probably achieved through

heterochronic juggling of the chamber number (*Ch*). *Tritaxia* slides from the *K*- to the *r*-end of its broad ecological socket, and back again, in concert with the strength of cyclicity, mostly tracking something like the circumstances shown in Text Figure 4.17 (page 176). If a demonstration (and prediction) of its behaviour are wanted, compare the C13 relative abundance spike in Appdx. Figs. 3.4.ii.d and 3.4.iv.a with the size crash in 5.4.1.i, and imagine that repeated time and time again up the stratigraphic sections of the Lower Chalk. This is *Tritaxia* reading environmental change with the 'soft end' of its lifecycle, a developmental zone that has been winnowed into loose modules precisely *in order* to deal with such variability, and to protect the crystalline triserial core within. But on this level the *Plus ça change* model would make precisely the wrong prediction: *Tritaxia*'s size shifts would be stronger in the lower half if tracked across several well-developed chalk marl cycles than they would be if tracked across several hazy cycles in the upper reaches. All the action, however, is going on elsewhere. *Tritaxia*'s crystalline core is melting in the upper reaches not because of geological scale shifts, but because ecological scale events have skimmed a layer of *K*-strategic competitors out of its environment. Since triseriality is 'about' being surrounded by competitors, it has lost its meaning (its function) in this part of the sequence.

If *Plus ça change* is to work (and I believe that there is more than a kernel of truth to it) then it has to either scale down the environmental factor from the geological to the ecological, or scale up the genealogical factor from the micro- to the macroevolutionary. In fact, I think Sheldon should be bold enough to do both, and to maintain similar predictions for each scale. The hub model outlined in Sections 4.1.4 and 5.5.2 should be the fundamental geometry in each case, and should incorporate both structural and functional (ecological) components. A complete account would also require the inclusion of a genealogical hierarchy (Section 5.5.2).

For the within-species version, something like Williams's 'normalising clade selection' is probably valid (Section 1.1.5), but tailored so that the generalist hub spits out mainly structurally coarse grained sub-species experiments; this, I think, is what we are probably seeing in *Tritaxia*. The specialist sub branches, by contrast should generate progressively more structurally complex experiments, and also more subtle ones that blend imperceptibly into the kind of multi-dimensional oscillation we routinely witness on microevolutionary scales. In short, I envisage a whole ecosystem or clade 'melting' at its

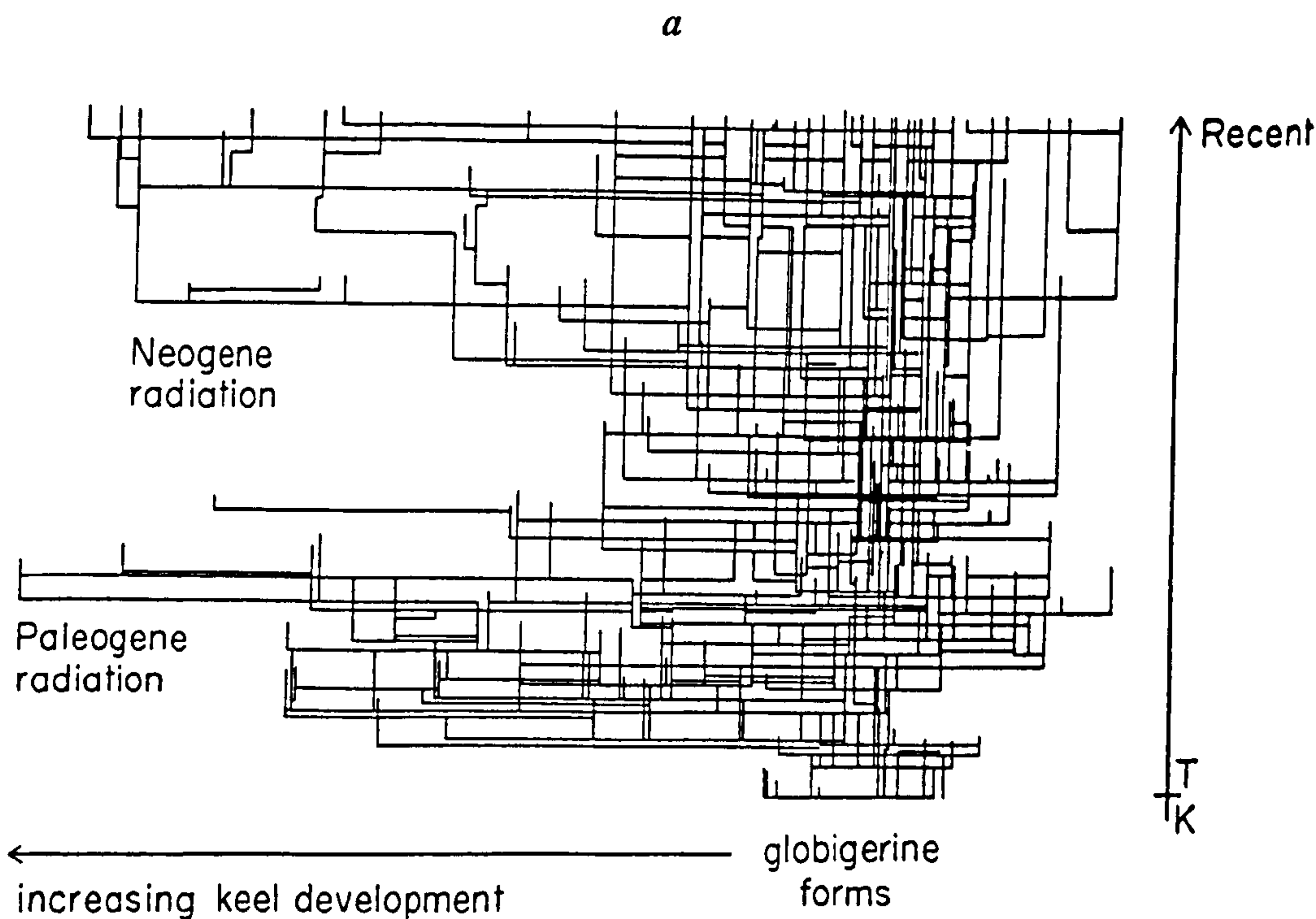


FIGURE 6—Dendrogram of Cenozoic species of planktonic foraminifera showing the two major excursions into keeled shape space. Placement of the species on the horizontal axis represents scores on a factor analysis axis which reflects size-independent development of “keeledness.”

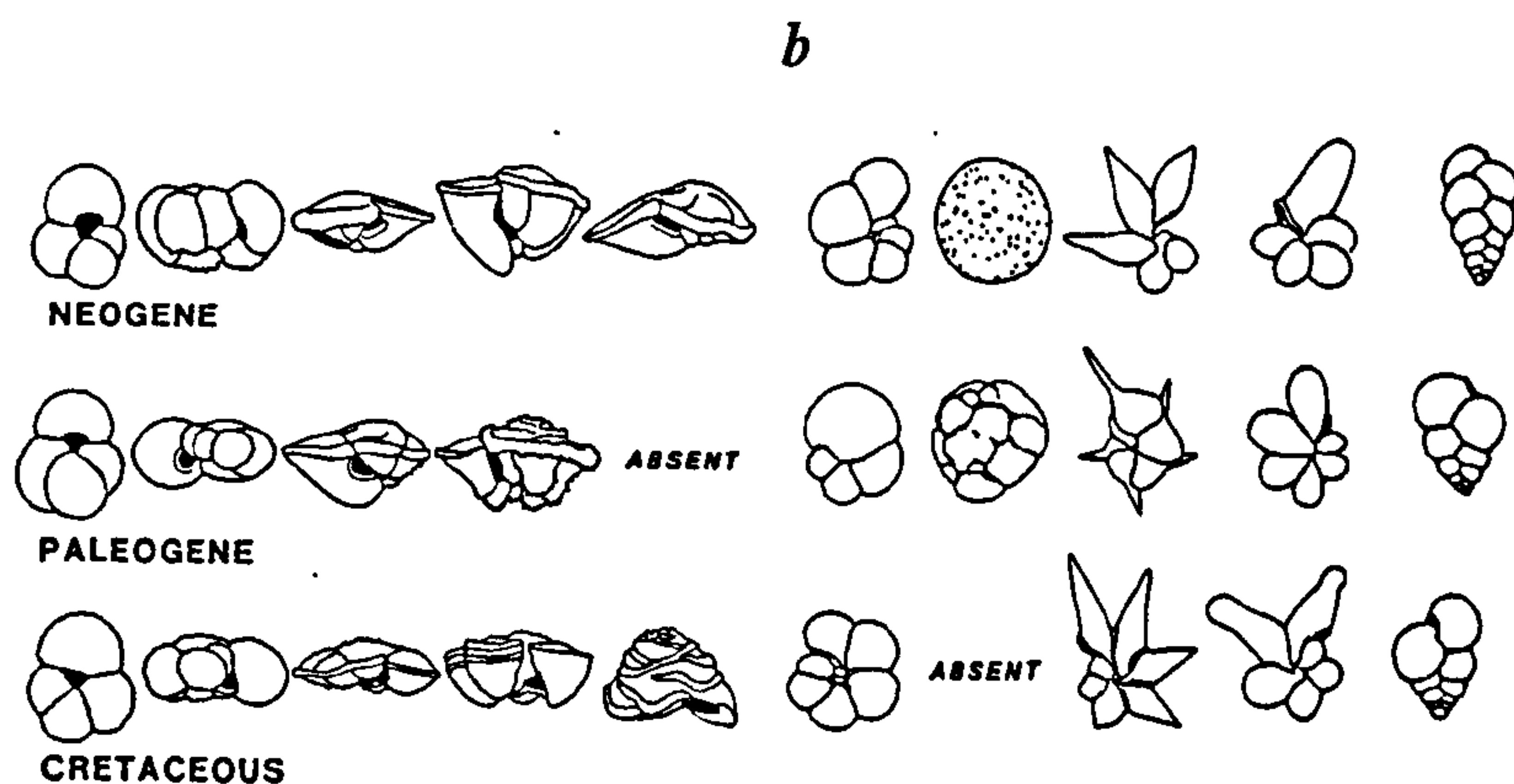


FIGURE 2. Representative homeomorphs from each of the three major radiations of planktonic foraminifera. Species not drawn to the same scale. Note the close correspondence in gross morphology between species in each radiation. Keeled species are the third, fourth, and fifth shapes from the left in each row. Some morphotypes are not represented in all the radiations (e.g., spiral-convex forms in the Paleogene, and spherical shapes in the Cretaceous).

Text Figure 10.3 *Two samples of the kind of large scale pattern Plus ça change might be able to elucidate if explicitly developed in macroevolutionary form. The first (a) taken unmodified from Arnold et al. (1995) shows more complex and keeled foram species lineages budding off from central stock through successive waves of radiation. Note that the ‘core’ is morphologically simple and thus, I would guess, generalised in function, and that it persists through the extinction events to provide a new source of innovation thereafter. The second (b), from Norris (1991) shows selected morphotypes from the same series of radiations. Note that the basic globose structural foundation has differentiated into the same complex specialists on three different occasions. If it is tempting to ask whether this is a repeated discovery of the same structure or a repeated discovery of the same niche, that temptation should be avoided: it is almost certainly both. (Note that the original captions from both publications have been retained for reference purposes.)*

fluid edges, with varying degrees of viscosity and lumpiness depending on location within the ensemble, and for the component parts of that ensemble to basically be doing the same thing in fractal form. For very stable settings and very modular organisms (like insects in the tropics), I expect Red Queen dynamics to take over, and for arms races of epistemic hostility to spiral out of control in a never-ending turbulence of evolving information; the chances of seeing something like this in the fossil record, however, are probably slim.

For the macroevolutionary, between-species version, Sheldon's suggestion of lineage selection is the best way forward. This is obviously a huge topic with a very broad literature, and cannot be pursued in any depth here. Suffice it to say that I believe species *are* higher level genealogical actors, admittedly composed (in sexual cases) of sub-specific genealogical actors such as genes and gene complexes. Where these higher level genealogical individuals correspond to the groupings we see in the fossil record (and mostly they do), we can expect to see relatively discrete morphotype lineages displaying the kind of clade normalising behaviour characteristic of Williams's within species pattern, but on an altogether different scale. Text Figure 10.3.a and b, taken from fairly recent reports on foram palaeobiology are tantalising glimpses of the kinds of pattern I think Sheldon's model could help to explain if it were properly scaled-up to a macroevolutionary version. Note that there is evidently both a structural and ecological component to the figure, and that the simple, generalist hub persists indefinitely, budding off complex specialist species when the environment is stable enough—and that this time the environmental stability really *is stability on a geological timeframe*.

Summary

The discussion has travelled a long way since Chapter 1. Part II presented a palaeoecological reconstruction of the Cenomanian Lower Chalk microfauna, providing an environmental context for the focus lineage, *Tritaxia pyramidata*. Part III presented a model of *Tritaxia*'s developmental sequence, showing both what happened when growth proceeded normally and abnormally. And Part IV documented *Tritaxia*'s morphological change over a period of a million years, at three different sites and three different timescales, as an interaction between ecology and development.

In Chapter 10 it has been possible to discuss, with evidence, a whole range of mechanisms accounting for morphological change or its absence. Many of these mechanisms are fairly standard models drawn upon by the wider biological fraternity to account for morphological behaviour; all of them find some support in the empirical material presented here. Throughout this discussion, the information-theoretic paradigm outlined in Chapter 5 has played an important role: it has provided a timescale independent framework for understanding organism-environment interactions. In particular, the hub-centred geometry outlined in Sections 4.1.4 and 5.5.2 has given us a way to 'orient' the relationship between ecology, development and evolution.

Although not all the empirical predictions of Sheldon's *Plus ça change* model are met, much of its core reasoning seems both sound and empirically valid. The final recommendation of the thesis is that *Plus ça change* needs to be expanded to explicitly incorporate micro- and macroevolutionary versions: the microevolutionary ones should be tailored to environmental change on an ecological timescale because that is what a developmental reading system operating on generation-length snapshots will perceive; the macroevolutionary one will be valid for environmental change on a geological timeframe where the engine of creativity is not developmental modularity, but those modules we call species.

References

- Alberch, P. 1982. 'Ontogenesis and morphological diversification.' *American Zoologist*, 20, 653-667.
- Allen, T. F. H. & Hoekstra, T. W. 1992. '*Toward A Unified Ecology*'. Columbia University Press, New York, 1-381.
- Anders, M. H., Krueger, S. W. & Sadler, P. M. 1987. 'A new look at sedimentation rates and the completeness of the stratigraphic record.' *Journal of Geology*, 95, 1-14.
- Anderton, R., Bridges, P. H., Leeder, M. R. & Sellwood, B. W. 1990 - (sixth edition). *A Dynamic Stratigraphy of the British Isles*. Unwin Hyman, London.
- Arnold, A. J. and Fristrup, K. 1982. 'The theory of evolution by natural selection: a hierarchical expansion.' *Paleobiology*, 8, 113-129.
- Arnold, A. J., Kelley, D. C. and Parker, W. C. 1995. 'Causality and Cope's Rule: evidence from the planktonic foraminifera.' *Journal of Palaeontology*, 69 (2), 203-210.
- Arthur, M. A., Bottjer, D. J., Dean, W. J., Fischer, A. G., Hattin, D. E., Kauffman, E. G., Pratt, L. M. & Scholle, P. A. 1986. 'Rhythmic bedding in Upper Cretaceous pelagic carbonate sequences: Varying sedimentary response to climatic forcing.' *Geology*, 14, 153-156.
- Antonovics, J. and van Tienderen, P. H. 1991. 'Ontoecogenophyloconstraints? The chaos of constraint terminology.' *Trends in Ecology and Evolution*, 6, 166-168.
- Bateson, G. 1972. *Steps to an Ecology of Mind*. University of Chicago Press, Chicago, USA.
- Bell, M. A., Baumgartner, J. V. and Olson, E. C. 1985. 'Patterns of temporal change in single morphological characters of a Miocene stickleback fish.' *Paleobiology*, 11, 258-271.
- Bennett, K. D. 1997. *Evolution and Ecology: The Pace of Life*. Cambridge Studies in Ecology Series, Cambridge University Press, Cambridge, England.
- Bernhard, J. M. 1986. 'Characteristic assemblages and morphologies of benthic foraminifera from anoxic organic-rich deposits: Jurassic through Holocene.' *Journal of Foraminiferal Research*, 16 (3), 207-215.
- Bilyard, G. R. 1974. 'The feeding habits and ecology of *Dentalium entale stimpsoni* (Henderson).' *Veliger*, 17, 126-138.
- Boney, A. D. 1989. '*Phytoplankton*.' New Studies in Biology Series, Routledge, Chapman and Hall Ltd., New York, 1-118.
- Bonner, J. T. 1988. *The Evolution of Complexity by Means of Natural Selection*. Princeton University Press, Princeton.
- Bradshaw, A. D. 1991. 'Genostasis and the limits to evolution.' *Philosophical Transactions of the Royal Society of London*, ser. B., 333, 289-305.
- Brandon, R. N. 1988. 'The levels of selection: a hierarchy of interactors.' In, Plotkin, H. (ed.) *The Role of Behaviour in Evolution*, MIT Press, Cambridge, Mass, 51-71.

- Brasier, M. D. 1979. *'Microfossils.'* George Allen and Unwin, London.
- Brett, C. E. & Baird, G. C. 1995. 'Co-ordinated Stasis and Evolutionary Ecology of Silurian to Middle Devonian Faunas in the Appalachian Basin.' *In* Erwin, D. H. & Anstey, R. L. (eds.): *New Approaches to Speciation in the Fossil Record*. Columbia University Press, New York, 285-315.
- Bristow, R., Mortimore, R. & Wood, C.J. 1998. 'Lithostratigraphy for mapping the Chalk of southern England.' *Proceedings of the Geologists' Association*, **109**, 293-315.
- Bromley, R. G. 1990. *'Trace Fossils: Biology and Taphonomy.'* Special Topics in Palaeontology, Unwin-Hyman, London.
- Buzas, M. A. & Culver, S. J. 1994. 'Species Pool and Dynamics of Marine Palaeocommunities.' *Science*, **264**, 1439-1441.
- Carter, D. J. and Hart, M. B. 1977. 'Aspects of mid-Cretaceous stratigraphical micropalaeontology.' *Bulletin of the British Museum, Natural History (Geology)* **29**, 1-135.
- Chalmers, D. J. 1996. *The Conscious Mind*. Oxford University Press, Oxford.
- Charlesworth, B., Lande, R. and Slatkin, M. 1982. 'A neo-Darwinian commentary on macroevolution.' *Evolution*, **36**, 474-498.
- Chaitin, G. 1975. 'Randomness and Mathematical Proof.' *Scientific American*, **232**.
- Cheetham, A. H. 1986. 'Tempo of evolution in a Neogene bryozoan: rates of morphologic change within and across species boundaries.' *Paleobiology*, **12** (2), 190-202.
- Cheetham, A. H. and Jackson, J. B. C. 1995. 'Process from pattern: tests for selection versus random change in punctuated bryozoan speciation.' *In* D. H. Erwin and R. L. Anstey (eds) *New Approaches to Speciation in the Fossil Record*. Columbia University Press, New York, 184- 207.
- Chiba, S. 1996. 'A 40,000-year record of discontinuous evolution of island snails.' *Paleobiology*, **22**, 177-188.
- Chiba, S. 1998. 'Synchronized evolution in lineages of land snails in oceanic islands.' *Paleobiology*, **24**, 99-108.
- Cisne, J. L. 1974. 'Evolution of the world fauna of aquatic free-living arthropods.' *Evolution*, **28**, 337-366.
- Coope, G. R. 1994. 'The response of insect faunas to glacial-interglacial climatic fluctuations.' *Philosophical Transactions of the Royal Society of London*, ser. B, **344**, 19-26.
- Corliss, B. H. 1985. 'Microhabitats of benthic foraminifera within deep-sea sediments.' *Nature*, **314**, 435-438.
- Corliss, B. H. & Chen, C. 1988. 'Morphotype patterns of Norwegian Sea deep-sea benthic foraminifera and ecological implication.' *Geology*, **16**, 716-719.
- Cottle, R. A. 1990. *Orbitally Induced Climatic Cycles from the Chalk of Southern England: Potential for High Resolution Stratigraphic Correlation and Palaeoenvironmental Studies*. Unpublished Ph.D., University of Exeter.

- Crame, J. A. 1990 'Trophic structure.' *In* Briggs, D. E. G. & Crowther, P. R. (eds.) *Palaeobiology - a synthesis*. Blackwell, London, 385-391.
- Crick, F. H. C. 1968. 'The Origin of the Genetic Code.' *Journal of Molecular Biology*, vol. 38, 367.
- Cronin, T. M. 1985. 'Speciation and stasis in marine Ostracoda: climatic modulation of evolution.' *Science*, 227, 60-63.
- Dawkins, R. 1976. *The Selfish Gene*. Oxford University Press, Oxford.
- Dawkins, R. 1982a. *The Extended Phenotype*. Oxford University Press, Oxford.
- Dawkins, R. 1982b. 'Replicators and Vehicles.' *In*, Kings College Sociobiology Group (ed.) *Current Problems in Sociobiology*, Cambridge University Press, Cambridge, 45-64.
- Dawkins, R. 1986. *The Blind Watchmaker*. Longmans, London.
- Dawkins, R. 1989. 'The Evolution of Evolvability.' *In*, Langton, C. (ed.), *Artificial Life*, Addison-Wesley, Reading, Mass. 201-220.
- Dawkins, R. 1996. *Climbing Mount Improbable*. Viking, Bath Press, Somerset.
- Dennett, D. C. 1991. *Consciousness Explained*. Little Brown, Boston, USA.
- Dennett, D. C. 1995. *Darwin's Dangerous Idea*. Penguin, London.
- Dennett, D. C. 1996. *Kinds of Minds: Towards an Understanding of Consciousness*. Weidenfield & Nicolson, London.
- Dennett, D. C. 1998. 'Do-It-Yourself Understanding.' *In* Dennett, D. C. 1998. *Brainchildren*. Penguin, London.
- DiMichele, W. A. 1994. 'Ecological patterns in time and space.' *Paleobiology*, 20 (2), 89-92.
- Ditchfield, P. W. 1990. *Milankovitch cycles in the Cenomanian chalks of the Anglo-Paris Basin*. Unpublished Ph.D thesis, University of Liverpool, 1-215.
- Ditchfield, P. & Marshall, J. D. 1989. 'Isotopic variation in rhythmically bedded chalks: Palaeotemperature variation in the Upper Cretaceous.' *Geology*, 17, no. 9 842-845.
- Dobzhansky, T. 1937; reprint 1982. *Genetics and the Origin of Species*. Columbia University Press, New York.
- Drake, J. A. 1990. 'Communities as assembled structures: Do rules govern pattern?' *Trends in Ecology and Evolution*, 5 (5), 159-164.
- Drake, J. A. 1991. 'Community-assembly mechanics and the structure of an experimental species ensemble.' *Am. Nat.*, 137 (1), 1-26.
- Drake, J. A. *et al.* (9 others) 1993. 'The construction and assembly of an ecological landscape.' *Journal of Animal Ecology*, 62, 117-130.
- Dretske, F. 1981. *Knowledge and the Flow of Information*. Bradford Books/MIT Press, Cambridge, MA.

- Drummond, P. V. O. 1970. 'The Mid-Dorset Swell: Evidence of Albian-Cenomanian Movements in Wessex.' *Proceedings of the Geologists' Association*, **81**, 679-714.
- Eble, G. T. 1999. 'On the dual nature of chance in evolutionary biology and palaeobiology.' *Palaeobiology*, **25**, 75-87.
- Edelman, G. M. and Tononi, G. 2000. *Consciousness: How Matter Becomes Imagination*. Penguin, London.
- Ehrlich, P. R. and Raven, P. H. 1969. 'Differentiation of populations.' *Science*, **165**, 1228-1232.
- Eigen, M. and Schuster, P. 1977. 'The Hypercycle: A Principle of Natural Self-Organization.' Part A: Emergence of the Hypercycle.' *Naturwissenschaften*, **64**, 541-565.
- Einsele, G. 1982. 'Limestone-Marl Cycles (Periodites): Diagnosis, Significance, Causes - A Review.' In Einsele, G. and Seilacher, A. (eds.): *Cyclic and Event Stratification*. Springer-Verlag, Berlin. 8-53.
- Ekdale, A. A. & Bromley, R. G. 1984. 'Comparative ichnology of shelf-sea and deep-sea chalk. *Journal of Palaeontology*, **58**, (2), 322-332.
- Eldredge, N. 1985. *Unfinished Synthesis: Biological Hierarchies and Modern Evolutionary Thought*. Oxford University Press, New York.
- Eldredge, N. 1995a. 'Species, speciation and the context of adaptive change in evolution.' In D. H. Erwin and R. L. Anstey (eds) *New Approaches to Speciation in the Fossil Record*. Columbia University Press, New York, 39-63.
- Eldredge, N. 1995b. *Reinventing Darwin*. John Wiley and Sons, New York, 244pp.
- Eldredge, N. and Gould, S. J. 1972. 'Punctuated equilibria: an alternative to phyletic gradualism.' In Schopf, T. J. M. (ed.) *Models in Palaeobiology*. Freeman Cooper, San Francisco, 82-115.
- Eldredge, N. and Gould, S. J. 1988. 'Punctuated equilibrium prevails.' *Nature*, **332**, 211-212.
- Erwin, D. H. and Anstey, R. L. 1995. 'Speciation in the fossil record.' In: D. H. Erwin and R. L. Anstey (eds) *New Approaches to Speciation in the Fossil Record*. Columbia University Press, New York, 11-38.
- Fischer, A. G. 1986. 'Climatic rhythms recorded in strata.' *Annual Review of Earth and Planetary Science*, **14**, 351-376.
- Fortey, R. A. 1985. 'Gradualism and punctuated equilibria as competing and complementary theories.' In Cope, J. C. W. and Skelton, P. W. (eds), *Evolutionary Case Histories from the Fossil Record, Spec. Pap. Palaeont.*, **33**, 17-28.
- Gale, A. S. 1989. 'Field meeting at Folkestone Warren, 29 Nov., 1987.' *Proceedings of the Geologists' Association*, **100**, (pp 73-82).
- Gale, A. S. 1990. 'A Milankovitch scale for Cenomanian time.' *Terra Nova*, **1**, 420-425.
- Gale, A. S. 1995. 'Cyclostratigraphy and correlation of the Cenomanian Stage in Western Europe.' In House, M. R. & Gale, A. S. (eds): *Orbital Forcing Timescales and Cyclostratigraphy*. Geological Society Special Publication

- Geary, D. H. 1990. 'Patterns of evolutionary tempo and mode in the radiation of *Melanopsis* (Gastropoda; Melanopsidae).' *Paleobiology*, **16**, 492-511.
- Geary, D. H. 1992. 'An unusual pattern of divergence between two fossil gastropods: ecophenotypy, dimorphism, or hybridization?' *Paleobiology*, **18** (1), 93-109.
- Ghiselin, M. 1974. 'A radical solution to the species problem', *Systematic Zoology*, **23**, 127-143.
- Gingerich, P. D. 1974. 'Stratigraphic record of early Eocene *Hyopsodus* and the geometry of mammalian phylogeny.' *Nature*, **248**, 107-109.
- Gingerich, P. D. 1976. 'Paleontology and phylogeny: patterns of evolution of Early Tertiary mammals.' *American Journal of Science*, **276**, 1-28.
- Gingerich, P. D. 1983. 'Rates of evolution: Effects of time and temporal scaling.' *Science*, **222**, 159-161.
- Gingerich, P. D. 1985. 'Species in the fossil record: concepts, trends and transitions.' *Paleobiology*, **11**, 27-41.
- Gingerich, P. D. 1987. 'Evolution and the fossil record: patterns, rates, and processes.' *Can. Jour. Zool.* **65**, 1053-1060.
- Godfrey Smith, P. 2000. 'Information, arbitrariness and selection: comments on Maynard Smith.' *Philosophy of Science*, **67**, 202-207
- Gooday, A. J. 1988. 'A response by benthic Foraminifera to the deposition of phytodetritus in the deep sea.' *Nature*, **332**, 70-73.
- Gooday, A. J. & Lamshead, P. J. D. 1989. 'Influence of seasonally deposited phytodetritus on benthic foraminiferal populations in the bathyal northeast Atlantic: the species response.' *Mar. Ecol. Prog. Ser.*, **58**, 53-67.
- Gooday, A. J., Levin, L. A., Linke, P. & Heeger, T. 1992. 'The role of benthic foraminifera in deep-sea food webs and carbon cycling.' In Rowe, G. T. & Pariente, V. (eds.): *Deep-Sea Food Chains and the Global Carbon Cycle*, Kluwer Academic Publishers, Printed in the Netherlands, 63-91.
- Gooday, A. J. & Turley, C. M. 1990. 'Responses by benthic organisms to inputs of organic material to the ocean floor: a review.' *Phil. Trans. R. Soc. Lond.*, **331**, 119-138.
- Goodwin, B. C. 1972. 'Biology and Meaning.' In Waddington, H. C. (ed.) *Towards a Theoretical Biology*, 4, Edinburgh University Press.
- Goodwin, B. 1982. 'Development and evolution.' *Journal of Theoretical Biology*, **97**, 43-55.
- Goodwin, B. 1984. 'A relational or field theory of reproduction and its evolutionary implications.' In Ho, M. and Saunders, P. (eds) *Beyond Neo-Darwinism*, Academic Press Inc. London, 219-241.
- Goodwin, B. C. 1994. *How the Leopard Changed Its Spots*. Phoenix, Weidenfield & Nicolson, London.
- Gould, S. J. 1980a. 'Is a new and general theory of evolution emerging?' *Paleobiology*, **6**, 119-130.

- Gould, S. J. 1980b. 'The evolutionary biology of constraint.' *Daedalus*, 109, 39-52.
- Gould, S. J. 1982. 'The meaning of punctuated equilibrium and its role in validating a hierarchical approach to macroevolution.' In Milkman, R. (ed) *Perspectives on evolution*. Sunderland, Massachusetts, 83-104.
- Gould, S. J. 1984a. 'Smooth curve of evolutionary rate: a psychological and mathematical artifact.' *Science*, 226, 994-995.
- Gould, S. J. 1984b. 'Morphological channeling by structural constraint: convergence in styles of dwarfing and gigantism in *Cerion*, with a description of two new fossil species and a report on the discovery of the largest *Cerion*.' *Paleobiology*, 10, 172-194.
- Gould, S. J. 1984c. 'Covariance sets and ordered geographic variation in *Cerion* from Aruba, Bonaire and Cruacao: a way of studying nonadaptation.' *Systematic Zoology*, 33, 217-237.
- Gould, S. J. 1988b. 'On Replacing the Idea of Progress with an Operational Notion of Directionality.' In H. Nitecki (ed.), *Evolutionary Progress*, University of Chicago Press, Chicago, 319-338.
- Gould, S. J. 1988b. 'Prolonged stability in local populations of *Cerion agassizi* (Pleistocene-Recent) on Great Bahama Bank.' *Paleobiology*, 14, 1-18.
- Gould, S. J. 1988c. 'Trends as changes in variance: a new slant on progress and directionality in evolution.' *Journal of Paleontology*, 62, 319-329.
- Gould, S. J. 1989. 'A developmental constraint in *Cerion*, with comments on the definition and interpretation of constraints in evolution.' *Evolution*, 43, 516-539.
- Gould, S. J. 1992. 'Constraint and the square snail: life at the limits of a covariance set. The normal teratology of *Cerion disforme*.' *Biological Journal of the Linnean Society of London*, 47, 407-437.
- Gould, S. J. 1996. *Life's Grandeur: the Spread of Excellence from Plato to Darwin*. Cape, London.
- Gould, S. J. 2000. 'More Things in Heaven and Earth.' In Rose, H. & Rose, S. (eds.) *Alas Poor Darwin*. Jonathan Cape, London, 85-105.
- Gould, S. J. 2002. *The Structure of Evolutionary Theory*. Harvard University Press, Cambridge, MA, USA.
- Gould, S. J. and Eldredge, N. 1977. 'Punctuated equilibria: the tempo and mode of evolution reconsidered.' *Paleobiology*, 3, 115-151.
- Gould, S. J. and Eldredge, N. 1988. 'Species selection: its range and power.' *Nature*, 334, 19.
- Gould, S. J. and Eldredge, N. 1993. 'Punctuated equilibrium comes of age.' *Nature*, 366, 223-227.
- Gould, S. J., Gilinsky, N. L. and German, R. Z. 1987. 'Asymmetry of Lineages and the Direction of Evolutionary Time.' *Science*, 236, 1437-1441.

- Gould, S. J. and Lewontin, R. C. 1979. 'The spandrels of San Marco and the Panglossian paradigm: a critique of the adaptationist programme.' *Proceedings of the Royal Society of London*, ser. B., 205, 581-598.
- Gould, S. J., Raup, D. M., Sepkoski, J. J., Schopf, T. J. M. and Simberloff, D. S. 1977. 'The shape of evolution: a comparison of real and random clades.' *Paleobiology*, 3, 23-40.
- Gould, S. J. & Woodruff, D. S. 1990. 'History as a cause of area effects: an illustration from *Cerion* on Great Inagua, Bahamas.' *Biological Journal of the Linnean Society of London*, 40, 67-98.
- Gould, S. J., Young, N. D. & Kasson, B. 1985. 'The consequences of being different: sinistral coiling in *Cerion*.' *Evolution*, 39, 1364-1379.
- Graf, G. 1989. 'Benthic-pelagic coupling in a deep-sea benthic community.' *Nature*, 341, 437-439.
- Grafe, K-U. 1999. 'Foraminiferal evidence for Cenomanian sequence stratigraphy and palaeoceanography of the Boulonnais (Paris Basin, Northern France).' *Palaeogeography, Palaeoclimatology, Palaeoecology*, 153, 41-70.
- Graham, W. R. & Grimm, E. C. 1990. 'Effects of Global Climate Change on the Patterns of Terrestrial Biological Communities.' *Trends in Ecology and Evolution*, 5 (9), 289-292.
- Gregory, R. L. (ed) 1987. *The Oxford Companion to The Mind*. Oxford University Press, Oxford, England.
- Griffiths, P. E. and Gray, R. D. 1994. 'Developmental Systems and Evolutionary Explanation.' *Journal of Philosophy*, 91, 6, 277-304.
- Griffiths, P. E. 2001. 'Genetic Information: A Metaphor In Search of a Theory.' *Philosophy of Science*, 68, 394-412.
- Hallam, A. 1972. 'Models involving population dynamics.' In Schopf, T. J. M. (ed.): *Models in Paleobiology*. Freeman, Cooper., San Francisco, 62-80.
- Hallam, A., Hancock, J. M., Labrecque, J. L., Lowrie, W. & Channell, J. E. T. 1985. 'Jurassic to Paleogene: Part 2, Jurassic and Cretaceous geochronology and Jurassic to Paleogene magnetostratigraphy.' In Snelling, N. J. (ed.) 1985: *The Chronology of the Geological Record*. Members of the Geological Society, London, 10, 118-140.
- Hancock, J. M. 1960. 'Les ammonites du Cenomanian de la Sarthe.' *Comptes rendu Congres Societes Savantes - Dijon 1959: Colloque sur le Cretace Superieur francais*, 249-252.
- Hancock, J. M. 1969. 'Transgression of the Cretaceous sea in south-west England.' *Proceedings of the Ussher Society*, 2, 61-83.
- Hancock, J. M. 1975. 'The petrology of the Chalk.' *Proceedings of the Geologists' Association*, 86, 499-535.
- Hancock, J. M. 1989. 'Sea level changes in the British region during the Late Cretaceous.' *Proceedings of the Geologist's Association*, 100, 565-594.
- Hanski, I. & Gilpin, M. 1991. 'Metapopulation dynamics: brief history and conceptual domain.' *Biological Journal of the Linnean Society*, 42 (1&2), 3-16.

- Hardin, G. 1960. 'The Competitive Exclusion Principle.' *Science*, **131**, 1292-1297.
- Harris, G. P. 1986. '*Phytoplankton Ecology: Structure, Function and Fluctuation*.' Chapman and Hall Ltd, London.
- Hart, M. B. 1980. 'The recognition of Mid-Cretaceous sea-level changes by means of foraminifera.' *Cretaceous Research*, **1**, 289-297.
- Hart, M. B. 1987. 'Orbitally induced cycles in the Mesozoic sediments of S.W. England.' *Proceedings of the Ussher Society*, **6**, 483-490.
- Hart, M. B. 1996. 'Recovery of the food chain after the Late Cenomanian extinction event.' In Hart, M. B. (ed.): *Biotic Recovery from Mass Extinction Events*. Geological Society Special Publication No. **102**, Geological Society, London, 265-278.
- Hart, M. B. & Bailey, H. W. 1979. 'The distribution of planktonic Foraminifera in the Mid-Cretaceous of N. W. Europe.' In Wiedmann, J. (ed.) (1979) *Aspekte der Kreide Europas*. IUGS Series A, **6**, 527-542.
- Hart, M. B. & Tarling, D. H. 1973. 'Cenomanian palaeogeography of the North Atlantic and possible Mid-Cenomanian eustatic movements and their implications.' *Palaeogeography, Palaeoclimatology, Palaeoecology*, **15**, 95-108.
- Haynes, J. R. 1981. *Foraminifera*. Wiley, New York.
- Hofstadter, D. R. 2000. 'Analogy as the Core of Cognition.' In Gleick, J. (ed) *Best American Science Writing 2000*. HarperCollins, New York.
- House, M. R. 1995. 'Orbital forcing timescales: an introduction.' In House, M. R. & Gale, A. S. (eds.) (1995): *Orbital Forcing Timescales and Cyclostratigraphy*. Geological Society Special Publication **85**, 1-18.
- Hull, D. 1980. 'Individuality and Selection.' *Annual Review of Ecology and Systematics*, **11**, 311-332.
- Hull, D. L. 1998. 'A clash of paradigms or the sound of one hand clapping?' *Biology and Philosophy*, **13**, 587-595.
- Ito, M., Asako, I., Nishikawa, T. & Saito, T. 2001. 'Temporal variation in the wavelength of hummocky cross-stratification: Implications for storm intensity through Mesozoic and Cenozoic.' *Geology*, **29** (1), 87-89.
- Ivany, L. C., 1996. 'Co-ordinated stasis or co-ordinated turnover? Intrinsic vs. extrinsic controls on pattern.' *Palaeogeography, Palaeoclimatology, Palaeoecology*, **127**, 239-256.
- Jablonski, D. & Sepkoski, J. J. Jr. 1996. 'Paleobiology, community ecology, and scales of ecological pattern.' *Ecology*, **77** (5), 1367-1378.
- Jackson, J. B. C. 1994. 'Community Unity?' *Science*, **264**, 1412-1413.
- Jackson, J. B. C. and Cheetham, A. H. 1994. 'Phylogeny reconstruction and the tempo of speciation in cheilostome Bryozoa.' *Paleobiology*, **20** (4), 407-423.
- Jackson, J. B. C. and Cheetham, A. H. 1999. 'Tempo and mode of speciation in the sea.' *Trends in Ecology and Evolution*, **14** (2), 72-77.

- Jarvis, I., Carson, G. A., Cooper, M. K. E., Hart, M. B., Leary, P. N., Tocher, B. A., Horne, D. & Rosenfeld, A. 1988. 'Microfossil Assemblages and the Cenomanian-Turonian (late Cretaceous) Oceanic Anoxia Event. *Cretaceous Research*, 9, 3-103.
- Jaynes, J. 1976. *The Origins of Consciousness in the Breakdown of the Bicameral Mind*. Houghton Mifflin, Boston.
- Jenkyns, H. C., Gale, A. S. & Corfield, R. M. 1994. 'Carbon- and oxygen-isotope stratigraphy of the English Chalk and Italian Scaglia and its palaeoclimatic significance.' *Geol. Mag.*, 131, 1-34.
- J Jeans, C. V. 1968. 'The origin of montmorillonite in European Chalk with special reference to the Lower Chalk of England. *Clay Mineralogy*, 7, 311-329.
- Jefferies, R. P. S. 1962. 'The Palaeoecology of the *Actinocamax plenus* Subzone (Lowest Turonian) in the Anglo-Paris Basin.' *Palaeontology*, 4 (4), 609-47.
- Jefferies, R. P. S. 1963. 'The Stratigraphy of the *Actinocamax plenus* Subzone (Lowest Turonian) in the Anglo-Paris Basin.' *Proc. Geol. Assoc.* 74, 1-30.
- Jenkyns, H. C., Gale, A. S. & Corfield, R. M. 1994. 'Carbon- and oxygen-isotope stratigraphy of the English Chalk and Italian Scaglia and its palaeoclimatic significance.' *Geological Magazine*, 131, 1-34.
- Johnson, G. 1995. *Fire in the Mind: Science, Faith and the Search for Order*. Penguin, London.
- Johnson, J. G. 1982. 'Occurrence of phyletic gradualism and punctuated equilibria through geologic time.' *Journal of Paleontology*, 56, 1329-1331.
- Johnson, P. E. 1996. 'Is genetic information irreducible?' *Biology and Philosophy*, 11, 4, 535-538.
- Jones, J. S. 1981. 'An uncensored page of fossil history.' *Nature*, 300, 109-110.
- Jones, R. W. & Charnock, M. A. 1985. "Morphogroups" of agglutinating foraminifera. Their life positions and feeding habits and potential applicability in (paleo)ecological studies.' *Revue de Paléobiologie*, 4, 311-320.
- Kauffman, S. A. 1993. *The Origins of Order: Self-Organization and Selection in Evolution*. Oxford University Press, New York.
- Kauffman, S. A. 1995. *At Home in the Universe*. Penguin, London.
- Kauffman, S. A. 2000. *Investigations*. Oxford University Press, New York.
- Kellogg, D. E. 1983. 'Phenology of morphologic change in radiolarian lineages from deep-sea cores: Implications for macroevolution.' *Paleobiology*, 9, 355-362.
- Kennedy, W. J. 1969. 'The correlation of the Lower Chalk of South-East England.' *Proceedings of the Geologists' Association*, 80, 459-560.
- Kirschner, M. and Gerhart, J. 1998. 'Evolvability.' *Proceedings of the National Academy of Science*, 95, 15, 8420-8427.
- Kitazato, H. 1984. 'Microhabitats of benthic foraminifera and their application to fossil assemblages.' In *2nd International Symposium of Benthic Foraminifera* (Pau April 1983), 339-344.

- Koutsoukos, E. A. M. & Hart, M. B. 1990. 'Cretaceous foraminiferal morphogroup distribution patterns, palaeocommunities and trophic structures: a case study from the Sergipe Basin, Brazil.' *Transactions of the Royal Society of Edinburgh: Earth Sciences*, **81**, 221-246.
- Koutsoukos, E. A. M., Leary, P. N. & Hart, M. B. 1990. 'Latest Cenomanian-earliest Turonian low-oxygen tolerant benthonic foraminifera: a case-study from the Sergipe basin (N.E. Brazil) and the western Anglo-Paris basin (southern England).' *Palaeogeography, Palaeoclimatology, Palaeoecology*, **77**, 145-177.
- Kowalewski, M., Goodfriend, G. A. & Flessa, K. W. 1998. 'High-resolution estimates of temporal mixing within shell beds: the evils and virtues of time-averaging.' *Paleobiology*, **24** (3), 287-304.
- Krebs, C. J. 1994. '*Ecology: The Experimental Analysis of Distribution and Abundance*.' 4th ed. Harper Collins, New York.
- Lake, S. D. & Karner, G. D. 1987. 'The structure and evolution of the Wessex Basin, Southern England: an example of inversion tectonics.' *Tectonophysics*, **137**, 347-378.
- Lakoff, G. and Johnson, M. *Metaphors We Live By*. University of Chicago Press, Chicago.
- Lamshead, P. J. D. & Gooday, A. J. 1990. 'The impact of seasonally deposited phytodetritus on epifaunal and shallow infaunal benthic foraminiferal populations in the bathyal northeast Atlantic: the assemblage response.' *Deep Sea Research*, **37** (8), 1263-1283.
- Lande, R. 1976. 'Natural selection and random genetic drift in phenotypic evolution.' *Evolution*, **30**, 314-334.
- Lazarus, B. D. 1986. 'Tempo and mode of morphologic evolution near the origin of the radiolarian lineage *Pterocanium prismatium*.' *Paleobiology*, **12**, 175-189.
- Leary, P. N., Cottle, R. A. & Ditchfield, P. 1990. 'Milankovitch control of foraminiferal assemblages from the Cenomanian of southern England.' *Terra Nova*, **1**, 416-419.
- Leary, P. N. & Hart, M. B. 1992. 'The Benthonic foraminiferal response to changing substrate in Cenomanian (Cretaceous) rhythms induced by orbitally -forced surface water productivity.' *Journal of Micropalaeontology*, **11**, (2), 107- 111.
- Lee, J. J. & Muller, W. A. 1973. 'Trophic dynamics and niches of salt marsh foraminifera.' *American Zoologist*, **13**, 215-225.
- Leiberman, B. S. and Dudgeon, S. 1996. 'An evaluation of stabilizing selection as an explanation for stasis.' *Palaeogeography, Palaeoclimatology, Palaeoecology*, **127**, 229-238.
- Lerner, I. M. 1954. *Genetic Homeostasis*. John Wiley, New York.
- Levin, S. A. 1992. 'The Problem of Pattern and Scale in Ecology.' *Ecology*, **73** (6), 1943-1967.
- Levins, R. 1969. 'Some demographic and genetic consequences of environmental heterogeneity for biological control.' *Bulletin of the Entomological Society of America*, **15**, 237-340.

- Levinton, J. S. 2001. *Genetics, Paleontology, and Macroevolution*. (2nd Ed.) Cambridge University Press, Cambridge, UK.
- Lieberman, B. S., Allmon, W. D. & Eldredge, N. 1995. 'Levels of selection and macroevolutionary patterns in the turritellid gastropods.' *Paleobiology*, **19** (2), 205-215.
- Lieberman, B. S., Brett, C. E. and Eldredge, N. 1995. 'A study of stasis and change in two species lineages from the Middle Devonian of New York state.' *Paleobiology*, **21** (2), 15-27.
- Lipps, J. H. 1981. 'What, if anything, is micropaleontology?' *Paleobiology*, **7**, 167-199.
- Lipps, J. H. 1983. 'Biotic interactions in benthic foraminifera.' In Trevesz, M.J.S, McCall, P.L. (eds.): *Biotic Interactions in Recent and Fossil Benthic Communities*. Plenum Press, New York, 331-76.
- Lipps, J. H. & Valentine, J. W. 1970. 'The role of foraminifera in the trophic structure of marine communities.' *Lethaia*, **3**, 279-286.
- Lister, A. 1984. 'Evolutionary case histories from the fossil record.' *Nature*, **309**, 114-115.
- Lochte, K. & Turley, C. M. 1988. 'Bacteria and cyanobacteria associated with phytodetritus in the deep sea.' *Nature*, **333**, 67-69.
- Loeblich, A. R. Jnr. & Tappan, H. 1987. *Foraminiferal genera and their classification*. Van Nostrand Reinhold Company, New York (2 vols.).
- Malmgren, B. A., Berggren, W. A. and Lohman, G. P. 1983. 'Evidence for punctuated gradualism in the Late Neogene *Globorotalia tumida* lineage of planktonic foraminifera.' *Paleobiology*, **9**, 377-389.
- Malmgren, B. A. and Kennett, J. P. 1981. 'Phyletic gradualism in a Late Cenozoic planktonic foraminiferan lineage: DSDP Site 284, southwest Pacific.' *Paleobiology*, **7**, 230-240.
- Maynard Smith, J. 1978. 'Optimization Theory in Evolution.' *Annual Review of Ecology and Systematics*, **9**, 31-56.
- Maynard Smith, J. 1984. 'Palaeontology at the high table.' *Nature*, **309**, 401-402.
- Maynard Smith, J. 1987. 'Darwinism stays unpunctured.' *Nature*, **330**, 516.
- Maynard Smith, J. 1988a. 'Evolutionary progress and levels of selection.' In Nitecki (ed.) *Evolutionary Progress*, Chicago University Press, Chicago, 219-230.
- Maynard Smith, J. 1988b. 'Punctuation in perspective.' *Nature*, **332**, 311-312.
- Maynard Smith, J., Burian, R., Kauffman, S., Alberch, P., Campbell, J., Goodwin, B., Lande, R., Raup, D. and Wolpert, L. (1985). 'Developmental constraints and evolution.' *Quarterly Review of Biology*, **60**, 265-287.
- Maynard Smith, J. and Szathmary, E. 1995. *The Major Transitions in Evolution*. W. H. Freeman, New York.
- Maynard Smith, J. 2000. 'The Concept of Information in Biology.' *Philosophy of Science*, **67**, 177-194.

- Mayr, E. 1963. *Animal Species and Evolution*. Harvard University Press, Cambridge, Massachusetts.
- Mayr, E. 1982. 'Questions concerning speciation.' *Nature*, 296, 609.
- Mayr, E. 1983. 'How to carry out the Adaptationist Program.' *American Naturalist*, 121, 324-334
- Mayr, E. 1988. 'The Why and How of Species.' *Biology and Philosophy*, 3, 431-441.
- McKinney, M. L. & Allmon, W. D. 1995. 'Metapopulations and Disturbance: From Patch Dynamics to Biodiversity Dynamics.' In Erwin, D. H. & Anstey, R. L. (eds.) *New Approaches to Speciation in the Fossil Record*. Columbia University Press, New York, 1-337.
- McKinney, M. L. and McNamara, K. J. 1991. *Heterochrony: The Evolution of Ontogeny*. Plenum Press.
- McShea, D. W. 1991. 'Complexity and evolution: What everybody knows.' *Biology and Philosophy*, 6, 303-324.
- McShea, D. W. 1992. 'A metric for the study of evolutionary trends in the complexity of serial structures.' *Biological Journal of the Linnean Society*, 45, 39-55.
- McShea, D. W. 1993. 'Evolutionary change in the morphological complexity of the mammalian vertebral column.' *Evolution*, 47 (3), 730-740.
- McShea, D. W. 1994. 'Mechanisms of large-scale evolutionary trends.' *Evolution*, 48 (6), 1774-1763.
- Miller III, W. M. 1996. 'Ecology of co-ordinated stasis.' *Palaeogeography, Palaeoclimatology, Palaeoecology*, 127, 117-190.
- Millikan, R. G. 1984. *Language, Thought and Other Biological Categories*. MIT Press, Cambridge, Mass.
- Millikan, R. G. 1989. 'In Defence of Proper Functions' *Philosophy of Science*, 56, 288-302.
- Mitchell, S. F., Ball, J. D., Crowley, S. F., Marshall, J. D., Paul, C. R. C., Veltkamp, C. J. & Samir, A. 1997. 'Isotope data from Cretaceous chalks and foraminifera: Environmental or diagenetic signals?' *Geology*, 25, no. 8, 691-694.
- Mitchell, S. F. & Carr, I. T. 1998. 'Foraminiferal response to mid-Cenomanian (Upper Cretaceous) palaeoceanographic events in the Anglo-Paris Basin (Northwest Europe).' *Palaeogeography, Palaeoclimatology, Palaeoecology*, 137, 103-125.
- Mitchison, G. J. 1977. 'Phyllotaxis and the Fibonacci Series.' *Science*, 196, 270-275.
- Moghadam, H. V. & Paul, C. R. C. 2000. 'Micropalaeontology of the Cenomanian at Chinnor, Oxfordshire, and comparison with the Dover-Folkestone succession.' *Proceedings of the Geologists' Association*, 111, 17-39.
- Monod, J. 1971. *Chance and Necessity*. Knopf, New York.
- Morris, P. J., Ivany, L. C. and Schopf, K. M. 1992. 'Paleoecological stasis in evolutionary theory.' *Geological Society of America, Abstracts with Programs*, 24:7, A313.

- Mortimore, R. N. 1983. 'The stratigraphy and sedimentation of the Turonian-Campanian in the Southern Province of England.' *Zitteliana*, **10**, 27-41.
- Murray, J. W. 1991. *Ecology and Palaeoecology of Benthic Foraminifera*. Longman Group, UK.
- Neander, K. 1991. 'Functions as Selected Effects: The Conceptual Analyst's Defence.' *Philosophy of Science*, **58**, 168-184.
- Norris, R. D. 1991. 'Biased extinction and evolutionary trends.' *Paleobiology*, **17** (4), 388-399.
- Oster, G. and Alberch, P. 1982. 'Evolution and bifurcation of developmental programs.' *Evolution*, **36**, 444-459.
- Otte, D. and Williams, K. 1972. 'Environmentally induced colour dimorphisms in grasshoppers, *Syrbula admirabilis*, *Dicromorpha viridis*, and *Chortophaga virigifasciata*.' *Annals of the Entomological Society of America*, **65**, 1154-1161.
- Overpeck, J. T., Webb, R. S. & Webb, T. 1992. 'Mapping eastern North American vegetation change of the past 18 ka: No-analogs and the future.' *Geology*, **20**, 1071-1074.
- Owen, D. 1996. 'Interbasinal correlation of the Cenomanian Stage; testing the lateral continuity of sequence boundaries.' In Howell, J. A. & Aitken, J. F. (eds.) (1996): *High Resolution Sequence Stratigraphy: innovations and applications*. Geological Society, London, Special Publications, **104**, 269-293.
- Owen, E. and Smith, A. B. 'Fossils of the Chalk: Palaeontological Association Field Guides to Fossils: No. 2.' The Palaeontological Association, London.
- Oyama, S. 1985. *The Ontogeny of Information: Developmental Systems and Evolution*. Cambridge University Press, New York.
- Ozawa, T. 1975. 'Evolution of *Lepidolina multiseptata* (Permian foraminifera) in East Asia.' *Memoir of the Faculty of Science, Kyushu University, Geology*, **D23**, 117-164.
- Parsons, P. A. 1991. 'Stress and evolution.' *Nature*, **351**, 356-357.
- Parsons, P. A. 1994. 'Morphological stasis: an energetic and ecological perspective incorporating stress.' *Journal of Theoretical Biology*, **171**, 409-414.
- Paterson, H. 1985. 'The Recognition Concept of Species', In Vrba, E. (ed.), *Species and Speciation*, Transvaal Museum Press, Pretoria, 21-29.
- Paul, C. R. C. 1992. 'Milankovitch and microfossils: principles and practice of palaeoecological analysis illustrated by Cenomanian chalk-marl rhythms.' *Journal of Micropalaeontology*, **11**, 95-105.
- Paul, C. R. C., Mitchell, S. F., Marshall, J. D., Leary, P. N., Gale, A. S., Duane, A. M. & Ditchfield, P. W. 1994. 'Palaeoceanographic events in the Middle Cenomanian of Northwest Europe.' *Cretaceous Research*, **15**, 707-738.
- Pearson, P. N. 1998. 'Speciation and extinction asymmetries in palaeontological phylogenies: evidence for evolutionary progress.' *Paleobiology*, **24**, 305-335.
- Pinker, S. and Bloom, P. 1990. 'Natural Language and Natural Selection.' *Behavioural and Brain Sciences*, vol. **13**, 707-784.

- Platt, H. M. 1981. 'Meiofaunal dynamics and the origin of the metazoa.' *In* Forey, P. L. (ed.): *The Evolving Biosphere*, British Museum of Natural History, Cambridge University Press, 207-216.
- Popper, K. R. 1959. '*The Logic of Scientific Discovery*.' Reprint, 1992, Routledge, London.
- Prell, W. L. *et al.* (27 others) 1988. 'Milankovitch and Monsoons.' *Nature*, 331, 663-664.
- Prigogine, I. 1980. *From Being to Becoming*. Freeman, San Francisco.
- Raup, D. M. 1966. Geometric analysis of shell coiling: general problems. *Journal of Paleontology*, 40, 1178-1190.
- Raup, D. M. and Crick, R. 1981. 'Evolution of single characters in the Jurassic ammonite *Kosmoceras*.' *Paleobiology*, 7, 200-215.
- Raup, D. M., Gould, S. J., Schopf, T. J. M. and Simberloff, D. S. 1973. 'Stochastic models of phylogeny and the evolution of diversity.' *Journal of Geology*, 81, 525-542.
- Reyment, R. A. 1982a. 'Phenotypic evolution in a Cretaceous foraminifer.' *Evolution*, 36, 1182-1199.
- Reyment, R. A. 1982b. 'Analysis of trans-specific evolution in Cretaceous ostracods.' *Paleobiology*, 8, 293-306.
- Reyment, R. A. 1985. 'Phenotypic evolution in a lineage of the Eocene ostracod *Echinocythereis*.' *Paleobiology*, 11, 174-194.
- Rhodes, F. H. T. 1983. 'Gradualism, punctuated equilibrium and the *Origin of Species*.' *Nature*, 305, 269-272.
- Ricklefs, R. E. & Miller, G. L. 2000. '*Ecology*.' 4th ed. W. H. Freeman and Co., New York.
- Ridley, M. 1993. *Evolution*. Blackwell Science, London.
- Ridley, M. (ed) 1997. *Evolution*. Oxford University Press, Oxford.
- Robaszynski, F. 1981. 'Moderation of Cretaceous Transgressions by Block Tectonics: An Example from the North and North-west of the Paris Basin.' *Cretaceous Research*, 2, 197-213.
- Robaszynski, F. & Caron, M. 1995. 'Foraminifères planctoniques du Crétacé: commentaire de la zonation Europe-Méditerranée.' *Bulletin de la Société géologique de France*, 166, 681-692.
- Robaszynski, F., Gale, A. S., Juignet, P., Amedro, F. & Hardenbol, J. 1998. 'Sequence stratigraphy in the Upper Cretaceous series of the Anglo-Paris Basin: Exemplified by the Cenomanian Stage.' *In: Mesozoic and Cenozoic Sequence Stratigraphy of European Basins*, SEPM Special Publication No. 60, 363-386.
- Roopnarine, P. D. 1995. 'A re-evaluation of evolutionary stasis between the bivalve species *Chione erosa* and *Chione cancellata* (Bivalvia: Veneridae).' *Journal of Palaeontology*, 69, 280-287.
- Rose, S. 1997. *Lifelines*. Allen Lane, London.

- Rossignol-Strick, M., Nesteroff, W., Olive, P. & Vergnaud-Grazzini, C. 1983. 'African monsoons an immediate climatic response to orbital insolation.' *Nature*, **304**, 46-49.
- Ruelle, D. 1991. *Chance and Chaos*. Penguin, London.
- Schindel, D. E. 1980. 'Microstratigraphic sampling and the limits of paleontologic resolution'. *Paleobiology*, **6** (4), 408-426.
- Schindel, D. E. 1982. 'Resolution analysis: a new approach to gaps in the fossil record.' *Paleobiology*, **8** (4), 340-353.
- Schlanger, S. O. & Jenkyns, H. C. 1976. 'Cretaceous oceanic anoxic events: causes and consequences.' *Geologie en Mijnbouw*, **55**, 179-184.
- Schneider, C. E. and Kennett, J. P. 1996. 'Isotopic evidence for interspecies habitat differences during evolution of the Neogene planktonic foraminiferal clade *Globoconella*.' *Paleobiology*, **22**, 282-303.
- Schrodinger, E. 1944. *What is Life?* Cambridge University Press, Cambridge, England.
- Schopf, K. M. 1996. 'Co-ordinated stasis: biofacies revisited and the conceptual modeling of whole-fauna dynamics.' In Ivany, L. C. & Schopf, K. M. (eds.): 'New Perspectives on Faunal Stability in the Fossil Record.' *Palaeogeography, Palaeoclimatology, Palaeoecology*, **127**, 239-256.
- Schopf, T. J. M. 1982. 'A critical assessment of punctuated equilibria: 1. Duration of taxa.' *Evolution*, **36**, 1144-1157.
- Scott, R. W. 1978. 'Approaches to trophic analysis of paleocommunities'. *Lethaia*, **11**, 1-14.
- Seilacher, A. 1970. 'Arbeitskonzept zur Konstruktionsmorphologie.' *Lethaia*, **3**, 393-396.
- Sepkoski, J. J. 1978. 'A kinetic model of Phanerozoic taxonomic diversity. I. Analysis of marine orders.' *Paleobiology*, **4**, 223-251.
- Sepkoski, J. J. 1981. 'A factor analytic description of the Phanerozoic marine fossil record.' *Paleobiology*, **7**, 36-53.
- Sepkoski, J. J. 1984. 'A kinetic model of Phanerozoic taxonomic diversity. III. Post-Paleozoic families and mass extinctions.' *Paleobiology*, **10**, 246-267.
- Sepkoski, J. J. Jr. 1986. 'Phanerozoic overview of mass extinctions.' In Raup, D. M. & Jablonski, D. (eds) (1986): *Patterns and processes in the history of life*. Dahlem Konferenzen: Life Science Research Report, **36**, 277-295.
- Severin, K. P. 1983. 'Test morphology in benthic foraminifera as a discriminator of biofacies.' *Marine Micropalaeontology*, **8**, 65-76.
- Shannon, C. 1948. 'A Mathematical Theory of Communication.' *Bell Systems Technical Journal*, **27**, 379-423.
- Shannon, C. E. and Weaver, W. 1949. *The Mathematical Theory of Communication*. University of Illinois Press, Urbana.
- Sheldon, P. R. 1987. 'Parallel gradualistic evolution of Ordovician trilobites.' *Nature*, **330**, 561-563.

- Sheldon, P. R. 1993. 'Making sense of microevolutionary patterns.' *In* Lees, D. R. and Edwards, D. (eds) *Evolutionary Patterns and Processes*, vol 14, Linnean Society Symposium. Academic Press, London, 19-31.
- Sheldon, P. R. 1996. 'Plus ca change - a model for stasis and evolution in different environments.' *Palaeogeography, Palaeoclimatology, Palaeoecology*, **127**, 209-227.
- Simpson, G. G. 1944. *Tempo and Mode in Evolution*. New York: Columbia University.
- Sliter, W. V. 1989. 'Biostratigraphic zonation for Cretaceous planktonic foraminifers examined in thin section.' *Journal of Foraminiferal Research*, **19**, 1-19.
- Smith, A. B. Ed. 1987 *Fossils of the Chalk*. The Palaeontological Association, London, 1-306.
- Smith, K. C. 1992. 'Neo-rationalism versus neo-Darwinism: integrating development and evolution.' *Biology and Philosophy*, **7**, 431-451.
- Stanley, S. M. 1973. 'An explanation for Cope's Rule.' *Evolution*, **27**, 1-26.
- Stanley, S. M. 1975. 'A theory of evolution above the species level.' *Proceedings of the National Academy of Science*, **72**, 646-650.
- Stanley, S. M. 1979. *Macroevolution: Pattern and Process*. W. H. Freeman, San Francisco.
- Stanley, S. M., Signor, P. W. Lidgard, S. and Karr, A. F. 1981. 'Natural clades differ from "random" clades: simulations and analyses.' *Paleobiology*, **7**, 115-127.
- Stanley, S. M. and Yang, S. 1987. 'Approximate evolutionary stasis for bivalve morphology over millions of years: A multivariate, multil lineage study.' *Paleobiology*, **13**, 113-139.
- Stenseth, N. C. 1985. 'Darwinian evolution in ecosystems: the Red Queen view.' *In* Greenwood, P. J., Harvey, P. H. & Slatkin, M. (eds.) *Evolution: Essays in honour of John Maynard Smith*. Cambridge University Press, Cambridge, 55-72.
- Stenseth, N. C. and Maynard Smith, J. 1984. 'Coevolution in ecosystems: Red Queen evolution or stasis?' *Evolution*, **38**, 870-880.
- Sterelny, K. 2000. 'The "Genetic Program" Program: A Commentary on Maynard Smith on Information in Biology.' *Philosophy of Science*, **67**, 195-201.
- Sterelny, K. 2001. 'The Reality of Ecological Assemblages: A Palaeoecological Puzzle.' *Biology and Philosophy*, **16**, 437-461.
- Summerhayes, C. P. 1987. 'Organic-rich Cretaceous sediments from the North Atlantic.' *In* Brooks, J. & Fleet, A.J.(eds): *Marine Petroleum Source Rocks*, Geological Society Special Publication, **26**, 301-316.
- Tappan, H. and Loeblich, A. R. 1988. 'Foraminiferal evolution, diversification and extinction.' *J. Palaeont.* **62** (5), 695-714.
- Thompson, D. W. 1917. *On Growth and Form*. Cambridge University Press, Cambridge UK.

- Turner, J. R. G. 1986. 'The genetics of adaptive radiation: a neo-Darwinian theory of punctuational evolution.' *In* Raup, D. M. & Jablonski, D. (eds) *Patterns and Processes in the History of Life*. Springer Verlag, Berlin, 183-209.
- Van Valen, L. 1973. 'A new evolutionary law.' *Evolutionary Biology*, **1**, 1-30.
- Von Bayer, H. C. 2003. *Information: The New Language of Science*. Weidenfield and Nicolson, London.
- Vrba, E. S. 1985. 'Environment and evolution: alternative causes of the temporal distribution of evolutionary events.' *South African Journal of Science*, **81**, 229-236.
- Vrba, E. and Eldredge, N. 1984. 'Individuals, hierarchies and processes: towards a more complete evolutionary theory.' *Paleobiology*, **10**, 146-171.
- Vrba, E. S. and Gould, S. J. 1986. 'The hierarchical expansion of sorting and selection: Sorting and selection can not be equated.' *Paleobiology*, **12**, 217-228.
- Waddington, C. H. 1957. *The Strategy of the Genes*. Allen & Unwin, London.
- Wagner, G. P. and Altenberg, L. 1996. 'Complex Adaptations and the Evolution of Evolvability.' *Evolution*, **50**, 967-976.
- Weaver, P. P. E. 1982. 'Ostracoda from the British Lower Chalk and Plenus Marls.' *Monograph of the Palaeontographical Society*, **135**, 1-127.
- Webster, G. and Goodwin, B. 1996. *Form and Transformation*. Cambridge University Press, Cambridge, 1-271.
- Wei, K. 1994a. 'Stratophenetic tracing of phylogeny using SIMCA pattern recognition technique: a case study of the late Neogene planktic foraminifera *Globoconella* clade.' *Paleobiology*, **20**, 52-65.
- Wei, K. 1994b. 'Allometric heterochrony in the Pliocene-Pleistocene planktic foraminiferal clade *Globoconella*.' *Paleobiology*, **22**, 66-84.
- Wei, K. and Kennett, J. P. 1988. 'Phyletic gradualism and punctuated equilibrium in the late Neogene planktonic foraminiferal clade *Globoconella*.' *Paleobiology*, **14**, 345-363.
- Weiner, J. 1995. *The Beak of the Finch*. Vintage Books, New York.
- Williams, G. C. 1992. *Natural Selection: Domains, Levels and Challenges*. Oxford University Press, Oxford.
- Williamson, P. G. 1981. 'Palaeontological documentation of speciation in Cenozoic molluscs from Turkana Basin.' *Nature*, **293**, 214-215.
- Winnie, J. A. 2000. 'Information and Structure in Molecular Biology: Comments on Maynard Smith.' *Philosophy of Science*, **67**, 517-526.
- Wright, C. W. & Kennedy, W. J. 1984. 'The Ammonoidean of the Lower Chalk.' *Palaeontographical Society Monographs*, 1-8.
- Wright, L. 1973. 'Functions', *Philosophical Review*, **82**, 139-168.
- Wright, S. 1931. Evolution in Mendelian populations. *Genetics*, **16**, 97-159.